



The logo for The Society for Pediatric Radiology was designed by Tamar Kahane Oestreich of Cincinnati, Ohio in 1985.

**Founded in 1959
The Society for Pediatric Radiology
55th Annual Meeting & Postgraduate Course**

Presented by
The Society for Pediatric Radiology

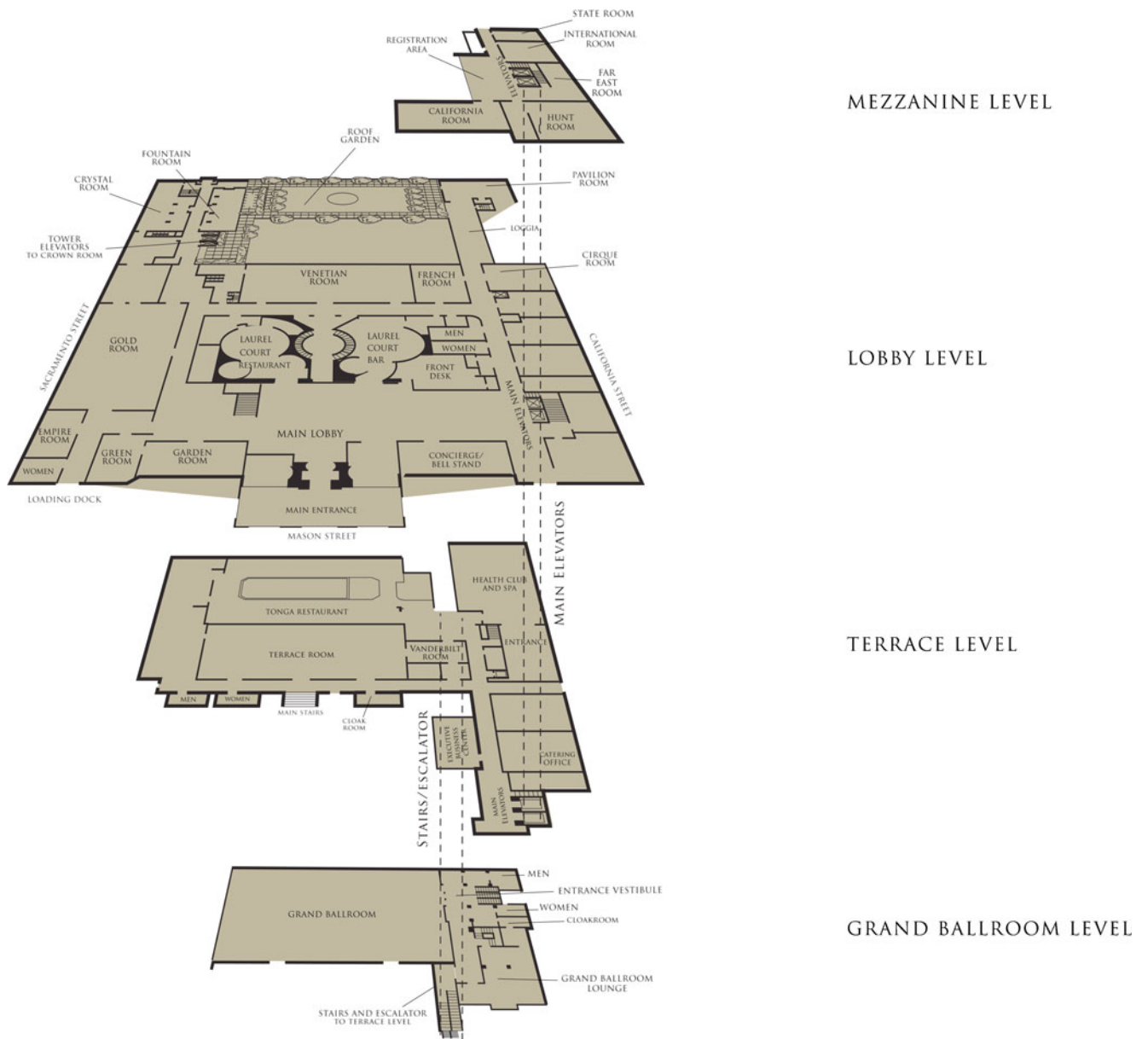
**The Fairmont Hotel
San Francisco, California**

**Postgraduate Course
April 16-17, 2012**

**Annual Meeting
April 17-20, 2012**

Jointly sponsored by the American College of Radiology

This supplement was not sponsored by outside commercial interests; it was funded entirely by the society's own resources.

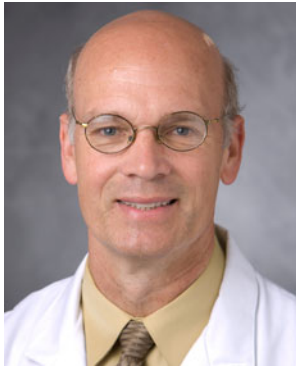


The Society for Pediatric Radiology 2012 Fairmont, San Francisco
Program At-A-Glance

		Postgraduate Course April Monday 16-Tuesday 17			Annual Meeting April Tuesday 18-Friday 20		
	Sunday 4/15	Monday 4/16	Tuesday 4/17	Wednesday 4/18	Thursday 4/19	Friday 4/20	
7:00	Board Mtg Registration	Continental Breakfast (7-8 am)	Continental Breakfast (7-8 am)	Continental Breakfast 6:45 - 8 AM		Continental Breakfast (7-8 am)	
7:30				Sunrise Sessions (7-8:25 am) Shoulder, Onc, GU	Sunrise Sessions (7-8:25 am) Fetal, GI, Iron, IG		
8:00		Thoracic Imaging (8-9:55 am)	Neuroimaging (8-9:55 am)	Concurrent Sessions III Neuro/Cardiovascular (8:30-10:30 am)		Concurrent Sessions VII IR-ALARA/Fetal-Other (8:30-10:30 am)	Concurrent Sessions Cardiac IR Neuro Nuclear Education (8 am-12 pm)
8:30							
9:00							
9:30		Break (9:55-10:10 am)	Break (9:55-10:20 am)				
10:00					Break (10:30-11:00)	Break (10:30-11:00)	
10:30		Abdominal Imaging (10:10 am-12:05 pm)	Infectious Diseases (10:20 an-12:05 pm)	Concurrent Sessions IV - GU/Public Policy (11 am-12 pm)		Concurrent Sessions VII Fetal-ALARA/Public-ALARA (11 am-12:30 pm)	
11:00							
11:30							
12:00 PM			Lunch On Own	Lunch On Own OR 3D RWE OR MR Protocols (12:05-1:30 pm)	Lunch On Own 12-1:30 pm jSPR, CBPR and AAWR Lunches (Adv. Reg. Req.)	Business Meeting/Lunch (12:30-1:45)	
12:30							
1:00							
1:30			IR (1:30-3 pm)	Welcome Neuhauser Lecture Session I -Onc/Nuc (2:30-3:30 pm)	Concurrent Sessions V GI-Neuro/Chest (1:30-3:45 pm)	Concurrent Sessions IX MSK/Onc-Neuro (1:45-4:00 pm)	
2:00							
2:30		Break (3-3:30 pm)					
3:00			Break (3:30-3:50)	Break (3:45-4:00)			
3:30		MSK (3:30-5:05 pm)	Session II-GI (3:50-5:10 pm)	Concurrent Sessions VI Neuro/GU (4-5:30 pm)	Break (4:00-4:20)		
4:00							
4:30				Awards Ceremony 5:10-5:45 pm		Concurrent Sessions X MSK/IR (4:20-5:30 pm)	
5:00							
5:30				Protocol Session - Chest/Abd/Pelvis-CT 5:30-6:45 pm	Reception and Annual Banquet (6:30-11 pm)		
6:00			Welcome Reception (6:00-7:30 pm)				
6:30							
7:00							
7:30							

Table of contents

Welcome from SPR President, Donald P. Frush, MD
SPR 2012 Organization
Continuing Medical Education
Maintenance of Certification
Objectives
Disclosure
Program Schedule
Scientific Exhibits
General Information
 Mission Statement
 Sites of Previous Meetings
 Future Meetings
 Officers, Directors and Committees
 Gold Medalists
 Pioneer Honorees
 Presidential Recognition Award
 Honorary Members
 Past Presidents
 Singleton-Taybi Award
 John A. Kirkpatrick Young Investigator Award
 Walter E. Berdon Awards
 The SPR Research and Education Foundation Awards
Social Events
SPR 2012 Gold Medalist
SPR 2012 Pioneer Honoree
SPR 2012 Presidential Recognition Awards
SPR 2012 Honorary Member
SPR 2012 Singleton-Taybi Award
John Caffey Awards
Edward B. Neuhauser Lecturers
Postgraduate Course Abstracts
Scientific Papers
Scientific Exhibits
Author Index by Abstract
Keyword Index by Abstract



WELCOME ADDRESS

Dear Colleagues,

I confess I haven't read many "Welcome Letters" at the beginning of the SPR program book over the years. Perhaps the only defensible benefit of this is that there is no preconception about the content of this message...or the length. I will be brief.

This meeting is about building bridges...bridges from our past to the future and bridges between all of us who believe fundamentally in maintaining or improving the health of our children.

The content, which is detailed on subsequent pages, speaks for itself. This material will be presented during the sessions with an appreciative look back at past accomplishments—the legacy of our subspecialty—with a vision to the future of pediatric imaging. We can only measure how broad and deep our successes have been by connecting with these beginnings. Looking beyond the titles (and the speakers), I think you will see that the material is not only about techniques and tactics but about ideas, insights, energy, all conspiring in the creative process ... an aggregate for excellence in pediatric imaging.

The content is also punctuated by a strong presence of our clinical colleagues. Again, this builds bridges. How can we maintain and expand these relationships? Moreover, the connections between science and clinical practice are evident in the structured blending of scientific papers and topical presentations by both imaging and clinical experts. This blending is also "fraternal" in that there will sometimes be disagreement and critical commentary, but this is essential in the advancement of medicine. Support and criticism make a stronger mortar. In the end, this gathering is about fostering a connected community, including technologists, nurses, physicists and other allied health experts including industry experts.

Finally, the emblem of pediatric radiology has always been embossed by cooperation, passion, commitment, and humanistic care. I believe the program content, the presenters and you, the participants, all embrace this. I hope that you will feel the spirit and the passion of the meeting and all of us will in many ways be better able to care for children because of this—even if you never read this message!

Donald P. Frush, MD

A handwritten signature in blue ink that reads "D P Frush". The signature is fluid and cursive, with the first letters of the first and last names being capitalized and prominent.

President, The Society for Pediatric Radiology

SPR 2012 ORGANIZATION**2012 MEETING CURRICULUM COMMITTEE**

Donald P. Frush, MD, Chair
Dorothy I. Bulas, MD (Education Session)
Brian D. Coley, MD (Postgraduate Course)
Marilyn J. Goske, MD (Education Session)
Jeffrey C. Hellinger, MD (3D Session)
Edward Y. Lee, MD, MPH (Postgraduate Course)
Marguerite T. Parisi, MD, MS Ed (Nuclear Medicine Session)
Tina I. Young Poussaint, MD (Neuroradiology Session)
Cynthia K. Rigsby, MD (Workshops)
Laureen M. Sena, MD (Cardiovascular Course)
Michael J. Temple, MD (Interventional Session)
Alexander J. Towbin, MD (Workshops)

ABSTRACT REVIEW COMMITTEE—PAPERS

Donald P. Frush, MD, Chair
Richard A. Barth, MD
Brian D. Coley, MD
James S. Donaldson, MD
Lynn A. Fordham, MD
Gary L. Hedlund, DO
Sue C. Kaste, DO
David B. Larson, MD
Marguerite T. Parisi, MD, MS
Tina I. Young Poussaint, MD
Thomas L. Slovis, MD
Shreyas S. Vasawala, MD, PhD

ABSTRACT REVIEW COMMITTEE—SCIENTIFIC EXHIBITS

M. Beth McCarville, MD, Chair
Michael J. Callahan, MD
Maria A. Calvo-Garcia, MD
Michael P. D'Alessandro, MD
Kassa Darge, MD, PhD
Steven Don, MD
R. Paul Guillerman, MD
Fredric A. Hoffer, MD
Thierry A.G.M. Huisman, MD
Douglas H. Jamieson, MD
Nadja Kadom, MD
J. Herman Kan, MD
Geetika Khanna, MD
Beth M. Kline-Fath, MD
Joshua Q. Knowlton, MD
Maria F. Ladino Torres, MD

Craig S. Mitchell, DO, MA
Helen R. Nadel, MD, FRCPC
Daniel J. Podberesky, MD
Janet R. Reid, MD
Douglas C. Rivard, DO
Susan E. Sharp, MD
Manrita K. Sidhu, MD
Stephen F. Simoneaux, MD
Keith J. Strauss, MS
Alexander J. Towbin, MD

CASE OF THE DAY

Debra L. Pennington, MD, Chair, Community Hospital Based Pediatric Radiologists Committee

jSPR

Ryan W. Arnold, MD

CONTINUING MEDICAL EDUCATION

Accreditation Statement

This activity has been planned and implemented in accordance with the Essential Areas and Policies of the Accreditation Council for Continuing Medical Education through the joint sponsorship of the American College of Radiology and The Society for Pediatric Radiology. The American College of Radiology is accredited by the ACCME to provide continuing medical education for physicians.

Credit Designation Statement

The American College of Radiology designates this live educational activity for a maximum of 33 *AMA PRA Category 1 Credits*.TM (10.25 Postgraduate Course/ 22.75 Annual Meeting). Physicians should claim only the credit commensurate with the extent of their participation in the activity.

This Educational Activity has been approved by CAMPEP for 69.04 MPCEC credits.

The ACR designates this educational activity as meeting the criteria for up to 30.5 Category A credit hours of the ARRT.

The American Medical Association has determined that physicians not licensed in the U.S. who participate in this CME activity are eligible for AMA PRA category 1 credit.

MAINTENANCE OF CERTIFICATION

The Postgraduate Course as well as the Friday Cardiac, Interventional, Neuroradiology and Nuclear Medicine sessions have been submitted to be qualified by the American Board of Radiology in meeting the criteria for self-assessment (SAM) toward the purpose of fulfilling requirements in the ABR Maintenance of Certification Program. Final information on the status of these applications will be provided at the meeting.

OBJECTIVES

The Society for Pediatric Radiology Annual Meeting and Postgraduate Course will provide pediatric and general radiologists with an opportunity to do the following:

1. Summarize the most current information on state-of-the-art pediatric imaging and the practice of pediatric radiology.
2. Describe and apply new technologies for pediatric imaging.
3. Discuss common challenges facing pediatric radiologists, and possible solutions.
4. Evaluate and apply means of minimizing radiation exposure during diagnostic imaging and image-guided therapy.

At the conclusion of the experience, participants should have an improved understanding of the technologies discussed, increasing awareness of the costs and benefits of diagnostic imaging in children and of ways to minimize risks, and an improved general knowledge of pediatric radiology, especially as it interfaces with clinical decision making.

DISCLOSURE

The scientific presenters of the 2012 Annual Meeting have indicated their applicable disclosures at the end of their abstracts. No statement indicates the authors have nothing to disclose.

The faculty members listed below have indicated they have no relevant financial relationships or potential conflicts of interest related to the material presented. They also do not intend to discuss the use of a medical device or pharmaceutical that is classified by the FDA as investigational for the intended use or that is “off-label” e.g. a use not described on the product’s label.

Ida Abbott	Michael J. Gelfand	Els Nijs
Joao G. Amaral	Orit A. Glenn	Hugh O’Brodivich
Sudha A. Anupindi	Marilyn J. Goske	Sarah M. O’Hara
Omolola M. Atalabi	Henry T. Greely	Robert C. Orth
Fred E. Avni, Jr.	Leslie E. Grissom	Catherine M. Owens
Paul S. Babyn	Richard B. Gunderman	Esperanza Pacheco-Jacome
A. James Barkovich	William R. Hendee	Susan Palasis
Carol E. Barnewolt	Manraj Heran	Ashok Panigrahy
Jane E. Benson	Marta Hernanz-Schulman	Marguerite T. Parisi
Ellen C. Benya	Caroline L. Hollingsworth	Manish N. Patel
George S. Bisset	Diego Jaramillo	Avrum N. Pollock
Sarah D. Bixby	Nadja Kadom	John M. Racadio
M. Ines Boechat	J. Herman Kan	Ricardo Restrepo
Barbara Botelho	Marc S. Keller	Lawrence A. Rinsky
Dorothy I. Bulas	Geetika Khanna	Richard Robertson
Anne Marie Cahill	In-One Kim	Andrea Rossi
Timothy M. Cain	Stanley T. Kim	Eva I. Rubio
Michael J. Callahan	Beth M. Kline-Fath	Yutaka Sato
Christopher I. Cassidy	Bernadette L. Koch	Lauren M. Sena
Winnie C.W. Chu	Supika Kritsaneepai boon	Susan E. Sharp
Taylor Chung	Thomas Kwee	Thomas L. Slovis
Jamie L. Coleman	Wendy Lam	Rebecca Smith-Bindman
Jesse Courtier	Tal Laor	Gloria Soto Giordani
Pedro A. Daltro	Bernard F. Laya	Stephanie E. Spottswood
Alan Daneman	Edward Y. Lee	Keith J. Strauss
Jonathan R. Dillman	Lisa H. Lowe	Peter J. Strouse
James S. Donaldson	Tippi MacKenzie	George A. Taylor
Josee Dubois	John D. MacKenzie	Alexander J. Towbin
Jerry R. Dwek	Richard I. Markowitz	Richard B. Towbin
Kirsten Ecklund	William H. McAlister	S. Ted Treves
Kathleen H. Emery	M. Beth McCarville	Beverly P. Wood
Monica Epelman	Robert C. McKinstry	Duan Xu
Judy A. Estroff	L. Santiago Medina	Benjamin M. Yeh
Eric N. Faerber	Doug Miniati	Ali Yikilmaz
Nancy Fefferman	Helen R. Nadel	Tina Young Poussaint
Robert J. Fleck	Beverley Newman	David K. Yousefzadeh
Laurent Garel	Jennifer L. Nicholas	Andrew M. Zbojnicwicz

The faculty members listed below have disclosed the following relevant financial relationships or potential conflicts of interest. Potential conflicts have been resolved.

<u>Name</u>	<u>Disclosure</u>
Richard A. Barth	GE Medical Systems, Medical Advisory Board, Honoraria received
Patricia E. Burrows	Orfagen, Inc., Research Consultant, Consulting fee; Guerbet, Research Consultant, Consulting fee
Ronald A. Cohen	Biomarin, Consultant
Heike E. Daldrup-Link	GE Healthcare, Grant Recipient, pre-clinical contrast studies
Donald P. Frush	GE Healthcare, Principal Investigator, Research support received
Michael R. Harrison	Magnets-n-Me, Inc., Founder, Ownership interest
Steven J. Kraus	Amirsys, Inc., Author, Royalties received; Elsevier Publishing, Author, Royalties received
Rajesh Krishnamurthy	Koninklijke Philips Electronics NV, Principal Investigator, Research support received; Vital Images Toshiba, Scientific Advisory Board Member, Honoraria received
David B. Larson	Patent application in process through CCHMC for CT radiation dose reduction
R.A.J. Nievelstein	Bayer B.V., Advisory Board Member, Consulting fee received
Daniel J. Podberesky	Toshiba America Medical Systems, Speaker's Bureau, Honoraria, Travel reimbursement, Research support received; Amirsys, Inc., Co-Author, Royalties received
Caroline D. Robson	Amirsys, Inc., Author, Consulting fees received
Shreyas S. Vasawala	GE Healthcare, Investigator, Research support received
Edward Weinberger	Clario Medical Imaging Inc., Medical advisor, Educational grant received
Pratik Mukherjee	GE Healthcare, Research contractor, Salaried

The following faculty members have disclosed that they will discuss use of a medical device or pharmaceutical that is classified by the Food and Drug Administration as investigational for the intended use:

Brent H. Adler	Blaise V. Jones
Talissa Altes	Sue C. Kaste
David Bloom	Rajesh Krishnamurthy
Lorna P. Browne	Kamlesh U. Kukreja
Patricia E. Burrows	Katherine K. Matthay
Heike E. Daldrup-Link	Daniel J. Podberesky
Kassa Darge	Cynthia K. Rigsby
Hyun Woo Goo	Lisa J. States
J. Damien Grattan-Smith	Michael J. Temple
R. Paul Guillerman	Shreyas S. Vasawala
Michael R. Harrison	Elliott Vichinsky
David M. Hovsepian	Stephan D. Voss

CME committee reviewers for this activity have disclosed any relevant financial relationships. No conflicts of interest exist.

ACKNOWLEDGEMENTS

The Society for Pediatric Radiology gratefully acknowledges the support of the following companies in presenting the 55th Annual Meeting and Postgraduate Course:

Platinum

GE Healthcare
Philips Healthcare
Siemens Healthcare
Toshiba America Medical Systems

Bronze

Bayer HealthCare Pharmaceuticals

Exhibitors

Agfa HealthCare
*ChiRho*Clin
Kubtec X-Ray
LMT Lammers Medical Technology
lifeIMAGE
Lippincott Williams & Wilkins
TeraRecon
Vital Images
Zonare

As of January 12, 2012

PROGRAM SCHEDULE

The Society for Pediatric Radiology

Postgraduate Course 2012

Diagnostic Pediatric Imaging in 2012: Bridging Horizons; Connecting Past, Present, and Future

Brian D. Coley, MD and Edward Y. Lee, MD, MPH, Course Directors

Supported in part by an educational grant from Bayer HealthCare Pharmaceuticals, Inc.

Monday, April 16, 2012

7:00–8:00 AM	Continental Breakfast
7:00 AM–5:00 PM	Registration
7:50–8:00 AM	Welcome and Introduction Brian D. Coley, MD and Edward Y. Lee, MD, MPH

Thoracic Imaging: From Interstitium to Airways

Richard I. Markowitz, MD and Beverley Newman, MD, FACR, Moderators

8:00–8:25 AM	Interstitial Lung Disease in Infants: New Classifications, Imaging Findings, and Pathological Correlation Edward Y. Lee, MD, MPH
8:25–8:50 AM	Large Airway Disease in Pediatric Patients: Impact of Advanced Post-processing Techniques Catherine M Owens, BSc MBBS MRCP FRCR
8:50–9:15 AM	Pediatric Thoracic Neoplasms: Review and Updates Sue C. Kaste, DO
9:15–9:45 AM	MRI of Pediatric Lungs and Airways: Current Status and Future Direction Talissa Altes, MD
9:45–9:55 AM	Question and Answer
9:55–10:10 AM	Break

Abdominal Imaging: From Asking to Answers

David K. Yousefzadeh, MD and William H. McAlister, MD, Moderators

10:10–10:35 AM	Bowel Sounds and Music: Malrotation, Intussusception, Appendicitis, Inflammatory Bowel Disease, Imperforate Anus Laurent A. Garel, MD
10:35–11:00 AM	Update on MDCT and MRI of Hepatobiliary Disease in Children: What's New Lisa H. Lowe, MD
11:00–11:25 AM	Diagnostic Errors in Pediatric Abdominal Imaging: Diagnostic Pearls and Pitfalls George A. Taylor, MD
11:25–11:50 AM	Neonatal Congenital Abdominal Masses: Clues to Reach a Diagnosis Marta Hernanz-Schulman, MD, FAAP, FACR
11:50 AM–12:05 PM	Question and Answer
12:05–1:30 PM	Lunch Break (on your own)

Pediatric Procedures: From Imaging to Intervention

James S. Donaldson MD and John M. Racadio, MD, Moderators

- 1:30–1:55 PM **The Spectrum of Vascular Anomalies in Pediatric Patients: Multimodality Imaging Evaluation and Current Treatment**
Patricia E. Burrows, MD
- 1:55–2:20 PM **Vascular Interventional Procedures in Children: Tips to Optimal Management**
Manraj Heran, MD
- 2:20–2:45 PM **Non-vascular Interventional Procedures in Pediatric Patients: What is New?**
Joao G. Amaral, MD
- 2:45–3:00 PM **Question and Answer**
- 3:00–3:30 PM **Break**

Musculoskeletal Imaging: From Planning to Performance

Paul S. Babyn, MD and Ricardo Restrepo, MD, Moderators

- 3:30–3:50 PM **Imaging of Pediatric Bone and Soft Tissue Tumors: Techniques and Advances**
Kirsten Ecklund MD
- 3:50–4:10 PM **Imaging of Congenital and Developmental Abnormalities of Early Childhood**
Tal Laor, MD
- 4:10–4:30 PM **Multimodality Imaging of Skeletal Trauma in Children: Using All of the Tools**
Peter J. Strouse, MD
- 4:30–4:50 PM **Cartilage Imaging: Indications and Techniques**
Diego Jaramillo, MD, MPH
- 4:50–5:05 PM **Question and Answer**

Tuesday, April 17, 2012

- 7:00–8:00 AM **Continental Breakfast**
- 7:00 AM–5:00 PM **Registration**
- 7:50–8:00 AM **Introduction and Announcements**
Brian D. Coley, MD and Edward Y. Lee, MD, MPH

Neuroimaging: From “What” to “How”

Richard L. Robertson, MD and Yutaka Sato, MD, PhD, Moderators

- 8:00–8:25 AM **Imaging of Stroke in Children: What do We Need to Know for Optimal Management?**
Avrum N. Pollock, MD, FRCPC
- 8:25–8:50 AM **Advanced Imaging Techniques for Neuroimaging in Pediatric Patients: Where Are We Now?**
Blaise V. Jones, MD
- 8:50–9:15 AM **A Spectrum of Abnormality in Pediatric Neck: Practical Imaging Choices and Interpretation**
Caroline D. Robson, MBChB

9:15–9:40 AM **Embryology and Diagnostic Approach in Spinal Dysraphism**
L. Santiago Medina, MD, MPH and Esperanza Pacheco-Jacome, MD

9:40–9:55 AM **Question and Answer**

9:55–10:20 AM **Break**

Infectious Diseases of the World: From Review to Updates in Imaging

Timothy M. Cain, MBBS, MD (ANZSPR), M. Ines Boechat, MD, FACR (SPR), Rutger A.J. Nievelein, MD (ESPR), In-One Kim, MD (AOSPR), Moderators

10:20–10:45 AM **Viral Infections in Children: Beyond SARS and H1N1**
Winnie C.W. Chu, MD, FRCR (AOSPR)

10:45–11:10 AM **Pediatric TB Infection: Current Status and Updates**
Bernard F. Laya, DO (AOSPR)

11:10–11:35 AM **The World of Parasites: Overview of Imaging Findings**
Pedro A. Daltro, MD (SLARP)

11:35–11:50 AM **Infectious Diseases of Africa: Facing the Challenge**
Omolola M. Atalabi, MD (ASR)

11:50 AM–12:05 PM **Question and Answer**

The Society for Pediatric Radiology

Annual Meeting Program 2012

Donald P. Frush, MD, Program Director

Cynthia K. Rigsby, MD and Alexander J. Towbin, MD, Workshop Directors

Tuesday, April 17, 2012

12:05–1:30 PM Lunch (on your own)

12:05–1:30 PM **3D Read with the Experts Lunch** (*advance registration required*)
Supported by Philips Healthcare, Siemens Healthcare, TeraRecon, Vital Images

Protocol Lunch Sessions (*advance registration required*)
Supported by GE Healthcare, Philips Healthcare, Siemens Healthcare, Toshiba America Medical Systems

Session 1: Neuro-Brain/Spine MR
Session 2: Body-ABD/MSK MR

1:30 PM **Welcome**
Donald P. Frush, MD

1:45–2:30 PM **Edward B. Neuhauser Lecture**
Present and Future Patient Benefits of Radiologist/Physicist Collaboration
William R. Hendee, PhD
Distinguished Professor of Radiology, Radiation Oncology, Biophysics and Bioethics
Medical College of Wisconsin
Milwaukee, Wisconsin

2:30–3:30 PM		Scientific Session I—Oncology & Nuclear Medicine Sue C. Kaste, DO and Geetika Khanna, MD, Moderators	
2:30–2:50 PM		Oncologic Interventions: New Hope in Cancer War Kamlesh U. Kukreja, MD	
2:50–3:30 PM		Scientific Papers—Nuclear Medicine	
PA-001	2:50	Bagrosky	FDG PET/CT Imaging in Pediatric Patients with Spinal Hardware for FUO or Suspected Spinal Infection
PA-002	2:58	McCarville	The Role of PET-CT in the Evaluation of Pulmonary Nodules in Children with Solid Malignancies: A Pilot Study
PA-003	3:06	Mandell	Twenty-Four Hour Imaging and SPECT for Increased Accuracy of Biliary Scintigraphy for Detection of Biliary Atresia
PA-004	3:14	Mhlanga	Comparison of Postoperative Radioactive Iodine Ablation of Thyroid Remnants Between Pediatric and Adult Patients with Thyroid Carcinoma
3:30–3:50 PM		Break	
3:50–5:10 PM		Scientific Session II—GI Nancy Fefferman, MD and Daniel J. Podberesky, MD, Moderators	
3:50–4:10 PM		Fetal and Postnatal Management of Abdominal Wall Defects Tippi MacKenzie, MD	
4:10–5:10 PM		Scientific Papers—GI	
PA-005	4:10	Youssfi	Ultrasound as First Modality to Evaluate for Midgut Volvulus
PA-006	4:18	Cavanaugh	Feeding Intolerance in Premature Infants After Medically Managed Necrotizing Enterocolitis (NEC): Are Findings on Abdominal Radiographs Predictive of Findings on Contrast Enemas?
PA-007	4:26	Winfeld	Relative Anatomic Distribution of Pertinent Findings on Neonatal Portable Abdominal Radiographs: Can We Shield the Gonads?
PA-008	4:34	Fierke	Prediction of Appendicitis on Ultrasound Using Three Diagnostic Categories: Positive, Negative, and Equivocal
PA-009	4:42	Herliczek	MRI of Right Lower Quadrant Pain in Pediatric Patients with Inconclusive Appendix US: Initial Experience
PA-010	4:50	Strain	Impact of Substituting US for CT in the Initial Evaluation of Appendicitis: A Quantitative Assessment
PA-011	4:58	Je	Intraluminal Pressure Monitoring and Demonstration of Pressure Curves During Pneumatic and Hydrostatic Reduction of Intussusception: Preliminary Study
5:10–5:45 PM		Awards Ceremony	
		<ul style="list-style-type: none"> • Gold Medalist • Pioneer Honoree • Presidential Recognition Award • Honorary Member • Singleton-Taybi Award 	

6:00–7:30 PM **Welcome Reception**

Wednesday, April 18, 2012

6:45–8:00 AM **Continental Breakfast**

6:30 AM–5:00 PM **Registration**

7:00–8:25 AM **Sunrise Sessions (concurrent)**

State of the Art Shoulder Imaging

Kathleen H. Emery, MD, Moderator

Normal Shoulder Anatomy and Protocols

Andrew M. Zbojniewicz, MD

Imaging Techniques and Protocols—Ultrasound

Leslie E. Grissom, MD

Benign and Malignant Neoplasms

Robert C. Orth, MD, PhD

MR Arthrography

Jerry R. Dwek, MD

Congenital and Developmental Abnormalities

Sarah D. Bixby, MD

Trauma

Kathleen H. Emery, MD

Oncology Imaging Synopsis

Stephan D. Voss, MD, PhD, Moderator

RECIST Criteria

Geetika Khanna, MD

PET CT: When is it Most Helpful?

Jamie L. Coleman, MD

PET CT: Decreasing Dose

Susan E. Sharp, MD

Tumor Diffusion-Weighted Imaging Concepts and Protocols

Thomas C. Kwee, MD, PhD

Dynamic Contrast-Enhanced MR for Tumor Imaging

Stephan D. Voss, MD, PhD

Genitourinary Imaging Update

Kassa Darge, MD, PhD, Moderator

MR Urography Imaging Protocol and Post Processing: How I Do It

J. Damien Grattan-Smith, MBBS

MR Urography Imaging Protocol and Post Processing: More Variations—Simplifications or Complications?

Kassa Darge, MD, PhD

Kidney Scintigraphy Update

Helen R. Nadel, MD, FRCPC

Modern Sonographic Techniques for GU Imaging

Sarah M. O'Hara, MD

Fluoroscopic GU Update

Steven J. Kraus, MD, MS

8:30–10:30 AM

Scientific Session III-A—Neuroradiology (concurrent)

Eric N. Faerber, MD and Ashok Panigrahy, MD, Moderators

8:30–8:50 AM

Pediatric Neuroimaging

A. James Barkovich, MD

8:50–10:30 AM

Scientific Papers—Neuroradiology

PA-012	8:50	Lober	Arterial Spin Labeling Cerebral Blood Flow as a Correlate of Clinically Significant Hydrocephalus in Children with Brain Tumors
PA-013	8:58	Maloney	Comparison of Immediate Versus Delayed Post-Contrast Imaging in Pediatric Brain Tumors
PA-014	9:06	Lober	Prognostic Role of Diffusion-Weighted MRI in Pediatric Optic Pathway Glioma
PA-015	9:14	Richards	Specific Sites of Spinal Drop Metastases in Children with Brain Tumor and its Potential Impact on Imaging Strategies
PA-016	9:22	Yong	How Specific is the MRI Appearance of Supratentorial Atypical Teratoid Rhabdoid Tumours?
PA-017	9:30	Lober	Application of Diffusion Tensor Tractography in Pediatric Optic Pathway Glioma
PA-018	9:38	Aw	Clinical Applications for Fast Brain MRI in Children
PA-019	9:46	Mortilla	Clinical Relevance of Susceptibility Weighted Imaging (SWI) in the Pediatric Population
PA-020	9:54	Rao	Radiographic Techniques Used for Performing Pediatric Head CT Examinations at an Academic Medical Center: A Snapshot
PA-021	10:02	Holdsworth	Diffusion Tensor Imaging (DTI) with Retrospective Motion Correction for Large-Scale Pediatric Imaging
PA-022	10:10	Soman	Evaluating Pediatric Neuropathologies Using Multiple TE Weighted Susceptibility Images Using Multi Shot EPI Sequence
PA-023	10:18	Rollins	Assessment of Diffusion Images Acquired Using the ACR Phantom: A Comparison of 3 Vendors

8:30–10:30 AM

Scientific Session III-B—Cardiovascular (concurrent)

George S. Bisset, III, MD and Wendy Lam, MB.BS, FRCR, FHKCR, FHKAM, Moderators

8:30–8:50 AM

Dual Source and Dual Energy CT, Optimized for Patients with Congenital Heart Disease

Hyun Woo Goo, MD, PhD

8:50–10:30 AM

Scientific Papers—Cardiovascular

PA-024	8:50	Bravo	Carotid Intima-Media Thickness in Children with Familial Hypercholesterolemia, Diabetes Type 1 and Obesity, Compared to Healthy Children
PA-025	8:58	Tariq	4-D Phase-Contrast MRI: Venous Flow Quantification is as Accurate as Arterial Flow Quantification
PA-026	9:06	Boechat	Neonatal Congenital Heart Disease: Initial Results with High-Resolution Contrast-Enhanced MR Angiography at 3.0 Tesla
PA-027	9:14	Madan	Early Signs of Iron-Mediated Cardiomyopathy in Transfusion-Dependent Children: Evaluation Using Cardiovascular Magnetic Resonance Technique of Myocardial Tagging
PA-028	9:22	Hilpipre	Analysis of a Novel Background Correction Method for Cardiac MR Phase Contrast Imaging
PA-029	9:30	Chung	Initial Clinical Experience of Congenital Heart Disease Cardiac MR Examinations with Radio Frequency (RF) Multi-Transmit Technology on 3 T MR
PA-030	9:38	Morani	Non-Cardiac Findings in Pediatric Cardiac MRI
PA-031	9:46	Meehan	Initial Experiences: Contrast-Enhanced MR Angiography (CEMRA) in Pediatric Organ Transplantation at 3.0 T
PA-032	9:54	Masand	Dynamic Contrast-Enhanced MR Venography for Evaluation of Central Venous Obstruction in Pediatric Patients
PA-033	10:02	Masand	Analysis of Optimal Phase Interval for Prospective EKG-Triggered Cardiac CT in Children
PA-034	10:10	Ralhan	Diagnostic Accuracy of CT Angiography Versus Echocardiography in Diagnosis of Aberrant Patent Ductus Arteriosus in Patients with Ductal Dependent Pulmonary Circulation
PA-035	10:18	Chau	Comparing Image Quality and Radiation Dose in Retrospective Versus Prospective ECG-Gated Cardiac MDCT in Pediatric Patients with Congenital Heart Disease Less Than One Year of Age

10:30–11:00 AM

Break

11:00 AM–12:00 PM

Scientific Session IV-A—Public Policy, Healthcare, Education, Technology (concurrent)

Jennifer L. Nicholas, MD and Edward Weinberger, MD, Moderators

11:00–11:20 AM

Children and Neuroimaging: Ethical (and Legal) Issues

Henry T. Greely, JD

11:20 AM–12:00 PM

Scientific Papers—Public Policy, Healthcare, Education, Technology

PA-036 11:20

Shah

Improving Radiology Resident Education of Pediatric Neuroradiology Using On-Line Streaming Video with Live Case Conferences

PA-037 11:28

Strain

MR Utilization Defined and Enhanced Through Process Improvement

PA-038 11:36

Strain

Indication Driven Decision Support for Order Entry in Pediatric Imaging

PA-039 11:44

Traipe

Cost-Effectiveness of Routine Neonatal Renal Ultrasound in Non-Syndromic Complex Congenital Heart Disease

11:00 AM–12:00 PM

Scientific Session IV-B—Genitourinary (concurrent)

Caroline L. Hollingsworth, MD, MPH and Supika Kritsaneepaiboon, MD, Moderators

11:00–11:20 AM

State-of-the-art Imaging—Kidney US

Alan Daneman, MD

11:20 AM–12:00 PM		Scientific Papers—Genitourinary	
PA-040	11:20	Darge	A Meta-Analysis of the Diagnostic Performance of Contrast-Enhanced Voiding Urosonography (ceVUS)
PA-041	11:28	Babikian	The Sonographic Evaluation of Hydronephrosis in the Pediatric Population: Is a Well-Tempered Ultrasound Necessary?
PA-042	11:36	Lee	Renal Elasticity Evaluation by Acoustic Radiation Force Impulse (ARFI) Measurement in Young Children with Normal Kidney vs. Hydronephrosis
PA-043	11:44	Chow	Patient and Family Impact of Pediatric Genito-Urinary Diagnostic Imaging Tests
12:00–1:30 PM		Lunch (on your own)	
jSPR Business Meeting and Lunch (<i>by invitation</i>)			
Manuscript Preparation—Thomas L. Slovis, MD			
Creating Effective Presentations—George S. Bisset, III, MD			
Community Based Pediatric Radiologists Lunch (<i>advance registration required</i>)			
AAWR 30th Anniversary Lunch			
Reflections and Prognostications by Pediatric Radiology’s Wise and Wonderful Women			
Lynn Fordham, MD, Moderator			
1:30–3:45 PM		Scientific Session V-A—Gastrointestinal (concurrent)	
Michael J. Callahan, MD and Jesse Courtier, MD, Moderators			
1:30–1:50 PM		Practical Approach to Pediatric Liver MRI	
Jesse Courtier, MD			
1:50–3:45 PM		Scientific Papers—Gastrointestinal and Neuroradiology	
PA-044	1:50	Chowdhury	Performance and Diagnostic Value of MRI for Pediatric Liver Transplant Complications
PA-045	1:58	Bittman	Diffusion-Weighted Imaging (DWI) Biomarkers for the Evaluation of Crohn’s Ileitis
PA-046	2:06	Boyd	MRE Scoring of Crohn’s Disease
PA-047	2:14	Jaju	MR Enterography: Can Diffusion-Weighted Imaging Replace the Need for Intravenous Contrast Administration?
PA-048	2:22	Ullberg	Diagnostic Accuracy and Clinical Significance of Magnetic Resonance Enterography of the Small Intestine in Comparison with Ileocolonoscopy in Pediatric Inflammatory Bowel Disease
PA-049	2:30	Brandon	CT Findings in Pediatric Eosinophilic Colitis, A Differential Diagnosis for Inflammatory Bowel Disease
PA-050	2:38	Domina	Imaging Trends and Radiation Exposure in Pediatric Inflammatory Bowel Disease Patients at a Large Academic Children’s Hospital
PA-051	2:46	Fenton	Development of a Pediatric Stroke Alert System
PA-052	2:54	Dent	Neonatal Deep White Matter Venous infarction and Liquefaction: A Pseudo-Abscess Lesion

PA-053	3:02	Stence	Recurrent Stroke in Children with Dissecting Aneurysms of the Vertebral Artery: Failure of Antithrombotic Therapies
PA-054	3:10	Barnes	Magnetic Resonance Imaging (MRI) and Ultrasonography (US) of the Extreme Preterm Brain
PA-055	3:18	Shaw	Functional Connectivity Analysis Reveals Disrupted Interhemispheric Connectivity in Unilateral Diffuse Hemispheric Disease
PA-056	3:26	Aukland	Dilated Cerebral Ventricles in Ex-Prematures: Just an Illusion? MRI-Based Normative Standards for 19-year-old Ex-Prematures
1:30–3:45 PM		Scientific Session V-B—Chest (concurrent) Catherine M. Owens, MD and Ali Yikilmaz, MD, Moderators	
1:30–1:50 PM		A Population and Genomic Based Approach to Understanding BPD Hugh O’Brodivich, MD	
1:50–3:45 PM		Scientific Papers—Chest	
PA-057	1:50	Ferguson	Best Practice for Reproducibility When Measuring T2*: Implications for Liver and Cardiac Iron Assessment
PA-058	1:58	Guillerman	Diagnostic Efficacy of Chest CT for Diffuse Lung Disease in Childhood Related to Genetic Surfactant Disorders
PA-059	2:06	Atweh	Limited Z-Axis Coverage Strategy for Reducing Radiation Dose of CT Pulmonary Angiography for the Diagnosis of Pulmonary Embolism in Children
PA-060	2:14	Lee	Multidetector CT Pulmonary Angiography in Children with Suspected Pulmonary Embolism: Thromboembolic Risk Factors and Implications for Appropriate Use
PA-061	2:22	Lee	Multidetector CT Pulmonary Angiography: Value of Multiplanar Reformation Images in Detecting Pulmonary Embolism in Children
PA-062	2:30	Newman	Chest CT in Children, Anesthesia and Atelectasis
PA-063	2:38	Jung	Comparison of Dexmedetomidine with Propofol for Airway Intervention in MRI Sleep Studies
PA-064	2:46	Fleck	MRI of Full Face Mask CPAP Causing Narrowing of the Retroglossal Airway
PA-065	2:54	Ayyala	The Contribution of Advanced Imaging in Pre- & Post-Surgical Evaluation of Children Requiring a Rex Shunt
PA-066	3:02	Ghaghada	Advantages of a Nanoparticle Blood Pool Contrast Agent Over Conventional intravascular Glomerular-Filtered Contrast Agents for Pulmonary Vascular Imaging
PA-067	3:10	Krishnamurthy	Cardiovascular Image Quality Using a Nanoparticle CT Contrast Agent: Preliminary Studies in a Pig Model
PA-068	3:18	Bell	Theoretical Cost and X-Ray Dose Reduction in Pediatric Congenital Heart Disease Imaging by the Use of a Nanoparticle Contrast Agent
PA-069	3:26	Boe	Frequencies and Patterns of Situs Discordance in Chest and Abdomen
3:45–4:00 PM		Break	

- 4:00–5:30 PM **Scientific Session VI-A—Neuroradiology (concurrent)**
Winnie Chu, MD and Robert C. McKinstry, MD, PhD, Moderators
- 4:00–4:20 PM DWI/DTI of Pediatric Congenital Brain Malformations
Pratik Mukherjee, MD, PhD
- 4:20–5:30 PM Scientific Papers—Neuroradiology
- | | | | |
|--------|------|----------|--|
| PA-070 | 4:20 | Yeom | Diminished ASL Intracranial Perfusion in Children with Neurofibromatosis Type 1 |
| PA-071 | 4:28 | Kadom | Cingulate Gyrus MRI Sign in Pediatric NF1 Patients: A Novel Imaging Marker |
| PA-072 | 4:36 | Friedman | Tract-Based Spatial Statistical Analysis of Diffusion Tensor Imaging in Pediatric Patients with Mitochondrial Disease |
| PA-073 | 4:44 | Laukka | Pelizaeus-Merzbacher Disease: White Matter Atrophy Correlates to Clinical Disability |
| PA-074 | 4:52 | Palasis | Maturational Effects on Language Localization in Children Demonstrated By fMRI |
| PA-075 | 5:00 | Sato | SLC26A4 Mutation Sensory Neuronal Hearing Loss: Genetic and Phenotypic Analysis |
| PA-076 | 5:08 | Barnes | Magnetic Resonance Imaging (MRI) in a Trial of Therapeutic Hypothermia for Term Hypoxic-Ischemic Encephalopathy (HIE) |
| PA-077 | 5:16 | Merlini | The ‘Red Dot’ on FA Color Maps: Clinical/Anatomical Correlation in Malformations of the Mid-Hindbrain Using DTI MR in Children |
- 4:00–5:30 PM **Scientific Session VI-B—Genitourinary (concurrent)**
Ronald A. Cohen, MD and Gloria Soto Giordani, MD, Moderators
- 4:00–4:20 PM Autosomal Dominant Polycystic Kidney Disease
Barbara B. Botelho, MD
- 4:20–5:30 PM Scientific Papers—Genitourinary
- | | | | |
|--------|------|---------------|--|
| PA-078 | 4:20 | Williams | Sonographic Predictors of Intermittent Testicular Torsion in the Pediatric Patient |
| PA-079 | 4:28 | Liang | Retrospective Review of Diagnosis of Testicular Torsion in Boys Presenting to Pediatric Emergency Department with Acute Scrotal Pain |
| PA-080 | 4:36 | Narayanan | Diagnostic Twists of Tubal Torsion |
| PA-081 | 4:44 | Bodmer | Adjusted Renal Length in Pediatric Bone Marrow Transplant Recipients |
| PA-082 | 4:52 | Chowdhury | Pediatric Renal Function Evaluation with a New High Spatio-Temporal Resolution Technique |
| PA-083 | 5:00 | Khanna | CT Detection of Pre-Operative Wilms Tumor Rupture |
| PA-084 | 5:08 | Grattan-Smith | The Failed Pyeloplasty: Evaluation with MR Urography |
| PA-085 | 5:16 | LeCompte | Functional Findings of Unilateral High-Grade Pelvicalyceal Dilatation in MR Urography |
- 5:30–6:45 PM **Protocol Session & Reception** (*advance registration required*)
Supported by GE Healthcare, Philips Healthcare, Siemens Healthcare, Toshiba America Medical Systems
- Session Topics: Chest/ABD/Pelvis CT

Thursday, April 19, 2012

6:45–8:00 AM

Continental Breakfast

6:30 AM–5:00 PM

Registration

7:00–8:25 AM

Sunrise Sessions (concurrent)

Fetal Imaging Overview

Richard A. Barth, MD, Moderator

Fetal Imaging Protocols

Carol E. Barnewolt, MD

Fetal GU Anomalies and Interventions

Judy A. Estroff, MD

Fetal Brain Abnormalities

Dorothy I. Bulas, MD

Fetal Chest Abnormalities, Pre and Postnatal Correlation

Richard A. Barth, MD

Postnatal Imaging of the Premature Infant

Beth M. Kline-Fath, MD

Contemporary GI Protocols and Imaging

Daniel J. Podberesky, MD, Moderator

MRE Protocol

Sudha A. Anupindi, MD

MRE Interpretation and Pathology Correlation

Jonathan R. Dillman, MD

Hepatocyte Sensitive MRI Contrast Agents

Alexander J. Towbin, MD

Liver Elastography

Daniel J. Podberesky, MD

MRCP Imaging Protocol and Image Evaluation

David A. Bloom, MD

Cardiac and Liver Iron Imaging: A Practical Approach

M. Beth McCarville, MD and Shreyas S. Vasanawala, MD, PhD, Moderators

Clinical Aspects of Iron Overload: Causes, Diagnosis, Complications, Treatment, Outcomes

Elliott Vichinsky, MD

MRI Sequences and Post-Processing Techniques for Measuring Liver and Cardiac R2 and R2*: How to Do It

Shreyas S. Vasanawala, MD, PhD

Clinical Applications of MRI R2 and R2*

M. Beth McCarville, MD

Dual Energy CT for Iron Quantification
Benjamin M. Yeh, MD

Image Gently/ALARA Forum on New Concepts in CT Radiation Dose

Marilyn J. Goske, MD, Moderator

CT—Controlling Dose: Lessons Learned from the Past
Thomas L. Slovis, MD

CT Dose Optimization: How I Do It
Beverley Newman, MD, FACR

CT Dose Optimization: The Future is Now
R. Paul Guillerman, MD

Current CT Dose Estimates in Children and Associated Risk
Rebecca Smith-Bindman, MD

A Better Pediatric CT Dose Estimate: How to Use Size Specific Dose Estimate (SSDE) in Your Practice
Keith J. Strauss, MS

Diagnostic Reference Levels and Dose Registries: Why We Need Them
Marilyn J. Goske, MD

8:30–10:30 AM

Scientific Session VII-A—IR (concurrent)

Josee Dubois, MD and Stanley T. Kim, MD, Moderators

8:30–8:50 AM

Vascular Malformations: Diagnosis and Treatment
David M. Hovsepian, MD

8:50–10:30 AM

Scientific Papers—IR and ALARA

PA-086	8:50	Obi	Venous Thrombosis in Paget Schroetter Syndrome: A Single Pediatric Institutional Experience
PA-087	8:58	Nachabe	Combined 3D Fluoroscopy Image Guided Percutaneous Intervention with Real-Time Optical Sensing at the Tip of a Needle for Tissue Characterization
PA-088	9:06	Crowley	Hepatocyte Transplant Procedure in A Children’s Hospital - Technique and Pitfalls
PA-089	9:14	Furey	Enteric Tube Placement Under Fluoroscopic Guidance: What Do We Do Right? What Do We Do Wrong?
PA-090	9:22	Raver	Doxycycline/Albumin in Vitro Drug Elution Dynamics with Clinical Correlation
PA-091	9:30	Crowley	Successful Interventional Radiologic Management of Paget Schroetter Syndrome in an Adolescent Population
PA-092	9:38	Goske	Quality Improvement Registry in CT Scans in Children (QuIRCC): Proposed Pediatric Abdominal CT Dose Reference Level Ranges Based On Image Quality Analysis
PA-093	9:46	Don	Image Gently: A Survey of Technique Factors for CR-DR Users
PA-094	9:54	Spinning	Follow-Up of 10-Year International Initiative to Reduce Pediatric Body CT Radiation Dose: A Study of Effectiveness in the U.S. at the Community Level

PA-095	10:02	Karmazyn	Optimization of Tube Voltage and Current in Size-Based Pediatric CT Imaging: A Phantom Study
PA-096	10:10	Johnston	Comparison of Radiation Dose Estimates, Image Noise, and Scan Duration in Pediatric Body Imaging Using 320-Row and 64-Row CT
8:30–10:30 AM		Scientific Session VII-B—Fetal (concurrent) Judy A. Estroff, MD and Eva I. Rubio, MD, Moderators	
8:30–8:50 AM		CDH Repair and Management Doug Miniati, MD	
8:50–10:30 AM		Scientific Papers—Fetal and Other	
PA-097	8:50	Stenhouse	The Observed to Expected Total Fetal Lung Volume as a Predictor of Short- and Long-Term Morbidity in Surviving Infants with Congenital Diaphragmatic Hernia
PA-098	8:58	Tkach	Characterization of the Inherent Acoustic Noise of a Dedicated NICU MRI System
PA-099	9:06	Guevara	Late Neurologic Events in Extremely Premature Infants
PA-100	9:14	Boe	Prenatal and Postnatal Imaging Evaluation of Pulmonary Artery, Airway and Pulmonary Findings in Tetralogy of Fallot with Absent Pulmonic Valve (TOF/APV)
PA101	9:22	Rubio	Craniosynostosis Syndromes: Prenatal Findings by US and MRI
PA-102	9:30	MacKenzie	Hyperpolarized Carbon-13 MRSI for Pediatric Disease
PA-103	9:38	Murati	Kaposiform Hemangioendothelioma: A Spectrum of MRI Features
PA-104	9:46	Tuna	Is Dedicated Chest CT Needed in Addition to PET CT for Evaluation of Pediatric Oncology Patients?
PA-105	9:54	Abdulhadi	The Role of Low Dose 64-Channel CT Angiography (CTA) to Assess Pediatric Vascular Trauma
PA-106	10:02	Lee	Elasticity Measurement by Acoustic Radiation force Impulse (ARFI) Technique of Normal Liver, Kidney and Spleen in Healthy Children
PA-107	10:10	Doshi	Continuous Quality Improvement Using a Data Mining Tool for Reducing Radiation Exposure in Pediatric Bedside Chest Radiography
10:30–11:00 AM		Break	
11:00 AM–12:30 PM		Scientific Session VIII-A—Public Policy, Healthcare, Education, Technology Ellen C. Benya, MD and David B. Larson, MD, Moderators	
11:00–11:20 AM		Helping People Learn Beverly P. Wood, MD, MS, Ed, PhD	
11:20 AM–12:30 PM		Scientific Papers—Public Policy, Healthcare, Education, Technology and ALARA	
PA-108	11:20	Goske	8 interactive Web-Based Modules with Vendor Specific Instructions to Teach Radiation Protection for Children to CT Technologists
PA-109	11:28	Gebhard	Health Literacy for Parents Regarding Fluoroscopy: Is there a Problem?
PA-110	11:36	Minhas	Compendium of Resources for Radiation Safety in Medical Imaging
PA-111	11:44	Linam	Inappropriate and Cloned Histories in Children: How Big a Problem is It?
PA-112	11:52	Westra	In vivo Validation of Size-Specific Dose Estimates (SSDE) Through Breast Entrance Skin Dosimetry (ESD) During Pediatric Chest CT Angiography

PA-113	12:00	Larson	Automated System for Slice-By-Slice CT Image Quality and Radiation Dose Monitoring and Optimization Based on Patient Size
PA-114	12:08	Goske	Body Width Predicted From Age and Weight is Not the Best Choice for Generating Protocols for Pediatric Abdominal CT Scans
PA-115	12:16	Christianson	Automated Size-Adjusted Dose Monitoring for Pediatric CT Dosimetry
11:00 AM–12:30 PM			Scientific Session VIII-B—Fetal Dorothy I. Bulas, MD and Monica Epelman, MD, Moderators
11:00–11:20 AM			Fetal Surgery Michael R. Harrison, MD
11:20 AM–12:30 PM			Scientific Papers—Fetal and ALARA
PA-116	11:20	Vaccha	Is There an Increase in Respiratory Morbidity During the Time Prior to Elective Resection of Prenatally Diagnosed Lung Masses?
PA-117	11:28	Carpineta	Clinical Utility and Impact of Fetal MRI. The McGill Experience
PA-118	11:36	Chetty	Localizing Fetal Bowel Obstruction: The Role of Fetal MRI
PA-119	11:44	Epelman	Spectrum of Imaging Appearances of Neonates and Survivors of Portal Vein Thrombosis: Correlation with Clinical Findings and Outcome
PA-120	11:52	Eslamy	Fetal MRI in Arthrogyposis
PA-121	12:00	Pettersson	Pediatric CT Radiation Dose Reduction: How Does Iterative Reconstruction Technique Affect Image Quality Metrics in Child-Sized Anthropomorphic Phantoms and Patient Images When kV is Reduced?
PA-122	12:08	Hellinger	Adaptive Iterative Dose Reduction in Evaluation of the Pediatric Abdomen with Ultra-Helical 320-Channel MDCT
PA-123	12:16	Panigrahy	The Use of Adaptive Statistical Iterative Reconstruction (ASIR) in Pediatric Head CT: A Pilot Study
12:30–1:45 PM			SPR Members' Business Meeting & Lunch <i>(Those attending may enter a drawing to win 3 nights free at the Fairmont San Francisco to be applied to a current or future stay.)</i>
1:45–4:00 PM			Scientific Session IX-A—Musculoskeletal Brent H. Adler, MD and J. Herman Kan, MD, Moderators
1:45–2:05 PM			Pelvic Osteotomies: Why, Where, Who and How? Larry Rinsky, MD
2:05–4:00 PM			Scientific Papers—Musculoskeletal
PA-124	2:05	Johnston	MR Imaging of the Skeletal Muscles in Boys with Duchenne Muscular Dystrophy (DMD): Part 2. T2 Relaxation Time Mapping (T2 Map) as a Non-invasive Biomarker to Determine Pathologic Fatty Infiltration: Comparison Between Boys with DMD and Healthy Boys
PA-125	2:13	Wang	MR Imaging of the Skeletal Muscles in Boys with Duchenne Muscular Dystrophy (DMD): Part 1. Can Fatty Infiltration and Inflammation of the Gluteus Maximus Muscle be Used as Indicators of Clinical Assessment in Boys with DMD?
PA-126	2:21	Atweh	Utility of Contrast-Enhanced MR Imaging in Children with Osteonecrosis: Does Gadolinium Help?

PA-127	2:29	Chan	Systematic Protocol for Assessment of the Validity of BOLD MRI in a Rabbit Model of Inflammatory Arthritis At 1.5 Tesla
PA-128	2:37	Doria	Quantitative Versus Semi-Quantitative MR Imaging of Cartilage in Blood-induced Arthritic Ankles
PA-129	2:45	Chauvin	Shoulder MR Arthrography in Skeletally Immature Patients
PA-130	2:53	Serai	A Novel Multi-Channel MR Coil for Improved Pediatric Elbow Coil Imaging
PA-131	3:01	Wu	Incremental Value of Knee Radiography in the Interpretation of Pediatric Knee MRI
PA-132	3:09	Rosenberg	Sonographic Evaluation of Pediatric Skeletal Lesions: Is it Worthwhile?
PA-133	3:17	Matzinger	High Incidence of Vertebral Fractures in Children with Acute Lymphoblastic Leukemia 12 Months After the Initiation of Therapy
PA-134	3:25	Little	Evaluation of Acetabular Morphology by Volume-Rendered CT: Implications for the Characterization of Femoroacetabular Impingement
PA-135	3:33	Crowe	Mistakes in Musculoskeletal Plain Film Interpretation
PA-136	3:41	Wang	Longitudinal Assessment of Osteoporosis in a Blood-Induced Hemophilia Rabbit Model Using Quantitative Ultrasound

1:45–4:00 PM

Scientific Session IX-B—Oncology and Neuroradiology

M. Beth McCarville, MD, Raghu Ramakrishnaiah MD, FRCR and Alexander J. Towbin, MD, Moderators

1:45–2:05 PM

Norepinephrine Transporter on Neuroblastoma for Imaging and Therapy
Katherine K. Matthay, MD

2:05–4:00 PM

Scientific Papers—Oncology and Neuroradiology

PA-137	2:05	Gawande	Differentiation of Benign and Malignant Pediatric Abdominal Tumors with Diffusion-Weighted MR Imaging.
PA-138	2:13	Towbin	Creation of a Database to Evaluate Imaging Findings in Long-Term Survivors of Pediatric Malignancy
PA-139	2:21	Bueno	Imaging Follow-up of Lymphoma in Pediatric Patients: Is Pelvic CT Necessary?
PA-140	2:29	Boe	Comparison of RECIST 1.1, WHO, and COG Response Criteria in Patients with Ewing Sarcoma
PA-141	2:37	Metwalli	Imaging Recognition of Chylous Ascites Following Surgery for Abdominal Neuroblastoma
PA-142	2:45	Kadom	Cervical Spine Injuries in Patients with Suspected Physical Abuse
PA-143	2:53	Loyd	Pediatric Skull Fracture
PA-144	3:01	Al-Qassabi	Evaluation of A New Classification System for Temporal Bone Fractures in Children Aimed at Increasing Prognostic Value
PA-145	3:09	Altinok	Absence of a Causal Relationship Between MR Detected Subdural Hematomas (SDH) in Neonates with Hypoxic-Ischemic Encephalopathy (HIE)
PA-146	3:17	Cecil	Sports Related Concussion in Children: An MRI and MRS Study
PA-147	3:25	Ramakrishnaiah	Predictive Value of High Resolution MR Imaging of Brain and Sella in Children with Clinical Optic Nerve Hypoplasia for Hypopituitarism
PA-148	3:33	Narayanan	CT Imaging Pearls for Shunted Pediatric Brains
PA-149	3:41	Cecil	Successful Treatment of Mice with Creatine Transporter Deficiency

4:00–4:20 PM		Break	
4:20–5:30 PM		Scientific Session X-A—Musculoskeletal	
			Tal Laor, MD and John D. MacKenzie, MD, Moderators
4:20–4:40 PM		Ankle Imaging	
			John D. MacKenzie, MD
4:40–5:30 PM		Scientific Papers—MSK	
PA-150	4:40	Feldman	Prevalence of Abusive Injuries in Siblings and Contacts of Abused Children
PA-151	4:48	Darling	Rib Fractures in Children: A Marker for Intrathoracic Injury?
PA-152	4:56	Zingula	Pediatric Elbow Fractures: A Different Angle on an Old Topic
PA-153	5:04	Kleinman	Should Views of the Hands, Feet and Spine be Eliminated from the Initial Skeletal Survey in Cases of Suspected Child Abuse?
PA-154	5:12	Walters	Fracture Dating in Infant Abuse: A Scientific System to Improve Radiologist Performance
PA-155	5:20	Shalaby-Rana	Features of Proximal Femoral Growth Plate Injuries in Abused Children
4:20–5:30 PM		Scientific Session X-B—Interventional	
			Manish N. Patel, DO and Richard B. Towbin, MD, Moderators
4:20–4:40 PM		Treatment for Vascular Malformations	
			Manish N. Patel, DO
4:40–5:30 PM		Scientific Papers—Interventional	
PA-156	4:40	McLaren	Early Results of Bioabsorbable Airway Stenting in Children
PA-157	4:48	Shafer	Long-Term Follow-Up of Tuberous Sclerosis Complex Patients Undergoing Renal Angiomyolipoma Embolization
PA-158	4:56	Shiels	Percutaneous Salivary Gland Ablation for Treatment of Sialorrhea
PA-159	5:04	Amaral	MR-Guided Procedures in Children: Initial Experience
PA-160	5:12	DiPietro	Sonography in Planning Nerve Graft Repair of Perinatal Brachioplexopathy
6:30–11:00 PM		Reception & Annual Banquet	

Friday, April 20, 20127:00–8:00 AM **Continental Breakfast**7:00 AM–12:00 PM **Registration****Cardiac Session**

Rajesh Krishnamurthy, MD and Lauren M. Sena, MD, Moderators

8:00–8:30 AM Physics of Common MR Sequences in CHD
Taylor Chung, MD8:30–9:00 AM Evaluation of Function and Flow in CHD
Lauren M. Sena, MD

9:00–9:30 AM	Segmental Approach to Imaging of CHD Rajesh Krishnamurthy, MD
9:30–9:45 AM	Break
9:45–10:15 AM	Imaging Protocol After 2 Ventricle Repair Robert J. Fleck, MD
10:15–10:45 AM	Imaging Protocol After Single Ventricle Repair Lorna P. Browne, MBBS
10:45–11:15 AM	CT and MRI of the Coronaries in Children Cynthia K. Rigsby, MD
11:15–11:45 AM	Interesting Case Presentations

5th Annual Education Summit

Teaching and Learning for the Next Generation

Dorothy I. Bulas, MD and Marilyn J. Goske, MD, Moderators

8:00–8:05 AM	Introduction Dorothy I. Bulas, MD
8:05–8:20 AM	ABR Updates Don P. Frush, MD
8:20–9:15 AM	Mentoring Ida O. Abbot, Esq.
9:15–9:45 AM	Engaging Learners Beverly P. Wood, MD, MS, Ed, PhD
9:45–10:00 AM	Discussion
10:00–10:15 AM	Break
10:15–10:45 AM	Why We Teach: Rewards for the Educator Richard B. Gunderman, MD
10:45–10:55 AM	Entrustable Professional Activities—What are They? Nadja Kadom, MD
11:00–11:10 AM	Milestone Project—What is It? Dorothy I. Bulas, MD
11:10–11:30 AM	Latest and Greatest Educational Tools/Projects on the SPR Website Jane E. Benson, MD and Geetika Khanna, MD
11:30 AM	Closing Marilyn J. Goske, MD

Neuroradiology Session

Susan Palasis, MD and Tina Young Poussaint, MD, Moderators

Pediatric Tumors

8:00–8:30 AM	Pediatric Tumors: Brain Tina Young Poussaint, MD
8:30–9:00 AM	Pediatric Tumors: Spine Susan Palasis, MD
9:00–9:30 AM	Pediatric Tumors: Head and Neck Bernadette L. Koch, MD
8:30–9:45 AM	Discussion
9:45–10:00 AM	Break

Injury to the Immature Brain

10:00–10:30 AM	Injury to the Immature Brain: Fetal Brain Injury Orit A. Glenn, MD
10:30–11:00 AM	Fetal and Neonatal MR Sequences for Evaluation of Injury to the Immature Brain Duan Xu, PhD
11:00–11:45 AM	Injury to the Immature Brain: Premature and Term Infants A. James Barkovich, MD
11:45 AM–12:00 PM	Discussion

Nuclear Medicine Session

Marguerite T. Parisi, MD, MEd and Stephanie E. Spottswood, MD, MSPH, Moderators

8:00–8:20 AM	Dose Reduction Strategies in Pediatric Nuclear Medicine: An Update S. Ted Treves, MD
8:20–8:45 AM	FDG PET/CT of Infection: Potential Pitfall or Key Diagnostic Tool in Children with Malignancies Marguerite T. Parisi, MD, MEd
8:45–9:15 AM	FDG/PET in Therapeutic Response Monitoring of Lymphoma: Outcomes Predictors M. Beth McCarville, MD
9:15–9:40 AM	Neuroblastoma: Respective Roles of MIBG and FDG PET/CT in Therapeutic Response Monitoring Susan E. Sharp, MD
9:40–9:45 AM	Discussion
9:45–10:00 AM	Break

10:00–10:20 AM	FDG PET/CT in Diagnosis and Follow-up of LCH and Wilm's Tumors: Comparison with Conventional Imaging Michael J. Gelfand, MD
10:20–10:50 AM	Pediatric Bone Tumors and Soft Tissue Sarcomas: Therapeutic Response Monitoring and Outcomes Helen R. Nadel, MD, FRCPC
10:50–11:20 AM	Hybrid Imaging of Pediatric Brain Tumors, Neurofibromatosis and Non-Lymphomatous Head and Neck Tumors Lisa J. States, MD
11:20–11:50 AM	Multi-Modality Whole Body Imaging: Data to Date and Future Perspectives Heike E. Daldrup-Link, MD
11:50 AM–12:00 PM	Discussion

Interventional Session

Michael J. Temple, MD, Moderator

8:00–8:30 AM	G and GJ Tubes Els Nijs, MD
8:30–9:00 AM	Thoracic Duct Embolization Marc S. Keller, MD
9:00–9:30 AM	Malignant Pleural Effusions Michael J. Temple, MD
9:30–9:40 AM	Discussion
9:40–10:00 AM	Break
10:00–10:30 AM	IVC Filters João G. Amaral, MD and Kamlesh U. Kukreja, MD
10:30–11:00 AM	Thrombectomy Anne Marie Cahill, MD, MBBCh
11:00–11:15 AM	Discussion
11:15 AM–12:00 PM	Interventional Case Club

Adjourn

Scientific Exhibits

Case Reports

CR-001	Bonner	Congenital Cardiac Fibroma: A Case Report
CR-002	Reavey	Right Ventricle to Pulmonary Artery (RV-PA) Conduit Stent Fractures: What the Radiologist Needs to Know. A Presentation of 3 Cases of Stent Fracture

CR-003	Gongidi	A Case of Fetal Craniopharyngioma
CR-004	Beaumont	Pre- and Postnatal MRI of Caudal Regression Syndrome
CR-005	Menghani	Unsuspecting Tuberous Sclerosis Diagnosed on Neonatal Cranial Ultrasound
CR-006	Merrow	Pyloric Atresia with Epidermolysis Bullosa: Fetal MRI Diagnosis with Postnatal Correlation
CR-007	Schubert	Wandering Appendix
CR-008	Richer	MR Imaging Patterns of Liver Transplant Complications in the Pediatric Population
CR-009	Dobbs	Imaging of Progressive Familial Intrahepatic Cholestasis (PFIC)
CR-010	Menghani	Renal Rhabdoid Mimics Wilms Tumor
CR-011	Shih	Ectopic Ureters in Young Infants: MRU Findings
CR-012	Bellah	Acquired Polycystic Kidneys in Neuroblastoma Survivors
CR-013	Narayanam	Abnormal Migration of the Retention Anchor Suture in a Case Following Gastrostomy Tube Insertion
CR-014	Garnet	Paravertebral Malposition of Peripherally Inserted Central Catheters in Neonates: A Pictorial Review
CR-015	Aouthmany	Pediatric Retroperitoneal Synovial Sarcoma
CR-016	Jubang	Longitudinal Bracket Epiphysis
CR-017	Jalbout	Whole Body MRI in Pediatric Non Oncologic Diseases: Pictorial Review
CR-018	Nagaraj	Mobile “Cerebroliths” in Hemihydranencephaly: A Case Report
CR-019	Nagaraj	Magnetic Resonance Imaging in Neonatal Citrullinemia Type I: Report of a Unique Case and Review of the Literature
CR-020	Aouthmany	Duplicated Internal Auditory Canal: A Rare Anomaly of the Temporal Bone
CR-021	Stence	Neuroimaging in Hemiplegic Migraine: Cases and Review of the Literature
CR-022	Castro	Correlation of Neurosonographic Anatomy with Matching MR Scan Planes
CR-023	Nagaraj	Ectopic Cerebellum in the Posterior Cranial Fossa: Report of a Case and Review of the Literature
CR-024	Kao	Pediatric Isodense Acute Subdural Hemorrhage
CR-025	Daniel	Undifferentiated Sarcoma of the Esophagus in an 11-year-old Male: Case Report and Radiologic / Pathologic Correlation
CR-026	Fagen	Potential Airway Management Issues in Sedated Children
CR-027	Ahlawat	CT and MR Findings of Pulmonary Lymphangiomatosis

Educational Exhibits

EDU-001	Stanescu	Aortic Arch Congenital Anomalies: What the Radiologist Needs to Know
EDU-002	Nosaka	Cardiovascular and Mediastinal Imaging in Children with Unexpected Clinical Presentation
EDU-003	Phelps	Cardiac Embryology Made Easy: A Novel Teaching Approach Using Claymation
EDU-004	Desai	Arterial Tortuosity Syndrome: An introduction to the Clinical and Radiologic Manifestations in the Pediatric Population
EDU-005	Hegde	Dynamic Pulmonary Computed Tomography for Evaluation of Cardiopulmonary Disease
EDU-006	Kurian	The Role of Low-Dose CT Angiography in the Evaluation of Renovascular Hypertension in Children
EDU-007	Singh	Fetal MRI: Brain, Head and Neck Malformations—A Pictorial Essay
EDU-008	Basta	Peridiaphragmatic Pulmonic Sequestration: Fetal MRI Appearance and Clues to the Diagnosis
EDU-009	Jaju	MRI of the Fetal Head and Neck Masses

EDU-010	Ponisio	Neonatal Hypoxia Ischemia: Comparison Between Cranial Ultrasound and Magnetic Resonance Performed Within A 24-Hour Interval
EDU-011	Poletto	Unusual Thoracic Lesions on Fetal Magnetic Resonance Imaging
EDU-012	Kitazono	Prenatal and Postnatal Imaging Findings in Megacystis-Microcolon-Intestinal Hypoperistalsis Syndrome (MMIHS)
EDU-013	Khashoggi	A Pictorial Essay: Pediatric Gastric Mass Lesions
EDU-014	Braithwaite	Imaging Findings in Megacystic Microcolon intestinal Hypoperistalsis Syndrome, A Rare Disease
EDU-015	Bagade	Pathologies of Omphalomesenteric Duct Remnant: Radiologic-Surgical Correlation.
EDU-016	Patel	Neonatal Bowel Obstruction—A Pictorial Essay
EDU-017	Egbert	3D T2-Weighted MRCP in the Pediatric Population—A Pictorial Review
EDU-018	Granader	Role of MRI Diffusion-Weighted Imaging in Pediatric Inflammatory Bowel Disease: A Pictorial Review
EDU-019	Wang	Gastrointestinal Manifestations of Cystic Fibrosis in the Pediatric Patient: An Imaging Exhibit From the Fetus to the Young Adult
EDU-020	Dietz	Beyond Acute Appendicitis: Imaging of Additional Pathologies of the Pediatric Appendix
EDU-021	LeCompte	Abdominal Giants: More Than Wilm Tumor in Children with Beckwith-Wiedemann Syndrome
EDU-022	Kwak	Radiologic-Pathologic Review of Pancreatic Masses Encountered at a Tertiary Pediatric Hospital Over a 10-year Period
EDU-023	Meyers	Evaluation of Hepatoblastoma with Gadoxetate Disodium—Typical, Atypical, Pre and Post Treatment Evaluation
EDU-024	Mamoun	Imaging of the Gallbladder and Biliary Tree in Pediatric Age Group
EDU-025	Challa	Postnatal Work Up of Congenital Uronephropathies—A Pictorial Essay
EDU-026	Courtier	Isolated Fallopian Tubal Torsion: Causes, Imaging Findings, and How to Suggest the Diagnosis
EDU-027	Udyavar	Multimodality Imaging Characteristics of Genitourinary Rhabdomyosarcoma
EDU-028	Schmitz	The Swollen Scrotum: Ultrasound Technique and Differential Diagnosis
EDU-029	Blumer	Experiences of Starting a Functional MR Urography Program At a University Hospital: Trials and Tribulations
EDU-030	Liang	Pictorial Review of Ultrasound Findings in Boys Presenting to Emergency Department/ Urology with Acute Scrotum
EDU-031	Cortes	Primary and Secondary Amenorrhea in Pediatric Patients: From the Beginning to the End
EDU-032	Horst	Imaging of Mullerian Duct Anomalies in Children
EDU-033	Rosines	Neonatal Osteomyelitis: A Radiological Review
EDU-034	Servaes	Update on DDH (Developmental Dysplasia of the Hip) and the Role of MRI
EDU-035	Rissmiller	Pediatric Musculoskeletal Ultrasound of the Proximal Lower Extremity (Pelvis to Thigh)
EDU-036	Blanco	A Multi-Modality Pictorial Review of Lesions of the Epiphysis in Infants and Children
EDU-037	Singh	Pediatric Hip Disorders: A Systematic Approach
EDU-038	Laurence	Osteoid Osteomas: A Pain in the “Night” Diagnosis
EDU-039	Chauvin	Ultrasound of Normal Enteses in the Growing Skeleton
EDU-040	Christianson	Pediatric Musculoskeletal Ultrasound of the Distal Lower Extremity (Knee to Ankle)
EDU-041	Thawait	Role of Conventional and Dynamic Contrast-Enhanced Magnetic Resonance Imaging in Diagnosis of Hemihypertrophy Syndromes in Children
EDU-042	Doria	Correlative Ultrasound, MRI Imaging and Physical Examination of Elbows in Hemophilic Children

EDU-043	Parnell	Digital Atlas of Skeletal Surveys of Common Skeletal Dysplasias
EDU-044	Morani	Pediatric Musculoskeletal (MSK) Soft Tissue Masses
EDU-045	Guandalini	MRI Findings in a Pediatric Cohort Presenting with Elbow Instability
EDU-046	Supakul	Dynamic Ultrasound Study in Evaluation of Infants with Vertical or Oblique Talus Deformities
EDU-047	Supakul	Ultrasound Evaluation of Costal Chondral Pathologies in Children Presented as Anterior Chest Wall Mass Or Pain
EDU-048	Narayanan	Challenges in Pediatric Marrow Imaging—Boning Up on Current MR Techniques
EDU-049	Shalaby-Rana	Radiologists Beware: Unusual Imaging Manifestations in Child Abuse
EDU-050	Guandalini	The Pediatric Elbow—MRI Findings with Multimodality Correlation
EDU-051	Metwalli	Spectrum of Patellar Tendon Avulsive injury on MRI in Children: Differentiation Between Acute and Chronic Avulsive Injuries of the Inferior Patellar Pole and Tibial Tuberosity
EDU-052	Thacker	MRI Anatomy of the Hindfoot and Ankle Ligaments: An Interactive Review
EDU-053	Morani	Pediatric Ankle Ultrasound: Commonly Encountered Pathologies
EDU-054	Kim	Maximizing Time Resolved MRA for Differentiation of Hemangiomas, Vascular Malformations, and Vascularized Tumors
EDU-055	Phillips	Vertical Expandable Prosthetic Titanium Rib (VEPTR): A Review of Indications, Normal Radiographic Appearance, and Complications
EDU-056	Haverkamp	Spectrum of Pediatric Spinal Neoplasms: An Interactive Tutorial
EDU-057	Tsai	Craniosynostosis
EDU-058	Byott	Posterior Fossa Tumours: A Pictorial Review
EDU-059	Gross Kelly	3DT1 Imaging of the Pediatric Spine
EDU-060	Tuna	The Normal Pediatric Spine: A Pictorial Review of MR Anatomy and Development in the Infant, Child and Adolescent
EDU-061	Blanco	Spectrum of Intracranial Cystic Lesions in Infants and Children
EDU-062	Chandra	Pediatric Spinal Cord Tumours: A Pictorial Overview
EDU-063	Au	Multi-Modality Imaging of Pediatric Head and Neck Lesions
EDU-064	Strauchler	Imaging of Congenital Spinal Malformations with MRI and Ultrasound: A Case-Based Review
EDU-065	Desai	Hypoxic Ischemic Injury: An Overview of Clinical and Radiological Manifestations From Premie To Adult
EDU-066	Chandra	Craniosynostosis: Looking Beyond the Sutures
EDU-067	Dorai Raju	The Perinatal Brain and Spinal Cord—Imaging Across a Life Border: a Case-Based Approach
EDU-068	Narayanan	Overview of Imaging of Pediatric Extraocular Orbital Tumors
EDU-069	Chandra	Pediatric Spinal Ultrasound: Pearls and Pitfalls
EDU-070	Naidu	Pediatric Brain PET-CT: An Atlas of Imaging Findings of C11 Methionine and F18 Deoxyglucose Studies for the Evaluation of Seizures and Brain Tumors
EDU-071	Jaju	Pediatric Head and Neck Neoplasms: A Multimodality Pictorial Review
EDU-072	Jacob	Pediatric Sinusitis: Spectrum of Imaging Findings with Clinicopathologic Correlation
EDU-073	Radhakrishnan	CNS Imaging Findings in Hemophagocytic Lymphohistiocytic Syndrome
EDU-074	Morani	Role of Ultrasound in the Evaluation of Palpable Head Lesions in Children: A Pictorial Review
EDU-075	Santos	Posterior Fossa Malformations—A Pictorial Review
EDU-076	Kocaoglu	Imaging of Petrous Apex in Children: Variants, Pitfalls and Pathologic Conditions
EDU-077	Khanna	Imaging of Bithalamic Lesions in the Pediatric Brain: Demystifying A Diagnostic Conundrum

EDU-078	Tuna	Cortical Developmental Abnormalities in Pediatric Seizure Patients
EDU-079	Pirkle	Cystic Neonatal Lesions Associated with the Spinal Cord : Discussion and Differential Diagnosis for these Uncommon Lesions
EDU-080	Soares	Brain MRI in Peroxisomal Disorders: A Pictorial Essay
EDU-081	Abdullah	Clots in Tots: Role of Imaging in Diagnosis of Acute Stroke and Its Causes in Children
EDU-082	Tuna	Extracranial Head and Neck Vascular Malformations: Diagnosis and Management
EDU-083	Mamoun	Isolated Cortical Diffusion Restriction in Pediatric Brain MRI
EDU-084	Singh	Inner Ear Malformations: Classification System and Embryologic Basis
EDU-085	Ellis	Modern Imaging of Pediatric Hydrocephalus
EDU-086	Bennett	Effective Imaging and Diagnosis of Congenital Cranial Nerve Anomalies: What Radiologists Should Know
EDU-87	McLellan	Pediatric Brain PET-CT Atlas and Technical Manual for Combination C11 Methionine and F18 Deoxyglucose Studies to Evaluate Seizures and Brain Tumors
EDU-088	Tuna	The Pediatric Cerebellum: A Pictorial Review of Normal Anatomy Using MRI and Diffusion Tensor Imaging
EDU-089	Menghani	Gastroesophageal Reflux Scintigraphy: A Low Radiation Alternative To GERD Evaluation in Children
EDU-090	Lukse	The Pediatric Kidney—A Review of Common and Uncommon Renal Anomalies
EDU-091	Krausz	Pediatric Hydronephrosis—The Utility of the Renal Scan in the Evaluation of Pediatric Hydronephrosis
EDU-092	Smith	The Pediatric Bone Scan—A Review of Neoplastic Pathology
EDU-093	Kwatra	The Many Faces of Duplex Kidneys on DMSA Scans—A Pictorial Essay
EDU-094	States	18 F-FDG PET/CT Imaging of Pediatric Brain Tumors, Neurofibromatosis 1(NF1) and Non-Lymphomatous Head and Neck Tumors
EDU-095	Morey	The Pediatric Bone Scan—A Review of Non-Malignant Pathology
EDU-096		WITHDRAWN
EDU-097	Gawande	Diffusion-Weighted Imaging Features of Pediatric Abdominal Masses
EDU-098	Mong	Radiology of Diesel Exposure
EDU-099	Markowitz	Pediatric Radiology in the Philadelphia Region: A Historical Review
EDU-100	Rosenberg	Superficial Lumps and Bumps
EDU-101	Radhakrishnan	Present Day Imaging of Down Syndrome
EDU-102	Schapiro	Imaging the Spectrum of Lymphatic Malformations in the Pediatric Patient
EDU-103	Mehta	'You're So VEIN'—Unusual Causes and Complications of Abdominal and Pelvic Large Vein Thrombosis in Children and Adolescents
EDU-104	Nguyen	Imaging Evaluation of Toddlers with Abnormal Gait
EDU-105	Bhat	Use of MR and CT Contrast Media in Children: Indications, Injection Protocols and FDA Approval Status
EDU-106	Hindson	A Pictorial Essay and Literature Review of the Spleen in Sickle Cell Disease
EDU-107	Miller	Cystic Fibrosis: Not Just for Children
EDU-108	Cakmakci	Imaging Pulmonary Tuberculosis in infants: What are the Most Useful Diagnostic Radiological Findings?
EDU-109	Mokashi	The Ductus Bump: Radiographic Findings of this Normal Variant and Differential Diagnoses
EDU-110	Kurian	The Contribution of 3D Imaging for Evaluation of the Pediatric Central Airways
EDU-111	Horst	Congenital Pulmonary Airway Malformation—Common and Uncommon Appearances Using a Multi-Modality Radiologic Approach

EDU-112	Caplan	The Imaging Evaluation of Cystic Lung Disease in Children: An Evidence-Based Approach
EDU-113	West	Pediatric interstitial Lung Disease (ILD): A Pictorial Review with Radiologic and Pathologic Correlation

Scientific Exhibits

SCI-001	Little	CT Radiation Dose Delivered by Community Hospitals and Imaging Centers
SCI-002	Thomas	The Impact of Adaptive Statistical Iterative Reconstruction on CT Image Quality Parameters—A Phantom Study
SCI-003	Chung	Pictorial Essay on Cardiac MR for Congenital Heart Disease on 3 T MR Scanner with RF Multi-Transmit Technology (Tx)
SCI-004	Adamu	Revisiting the Relationship Between Anthropometric Parameters and Left Ventricular Mass
SCI-005	Nguyen	Cardiac MRI in Pediatric Patients with Congenital Heart Disease: Comparison at 1.5 T and At 3.0 T
SCI-006	Huynh	Color Coded 3D Cardiac CTA of Congenital Heart Disease: A Five-Year Experience
SCI-007	Araque	Neuroimaging in the Evaluation of HIE in Term Neonates Post Hypothermia Therapy
SCI-008	Aguirre-Pascual	Prenatal Evaluation of Limb Body Wall Complex with Emphasis on MRI
SCI-009	Ream	Diffusion-Weighted Imaging in Pediatric Small Bowel Crohn Disease: MRI and Clinical Correlation
SCI-010	Huynh	Quantification of Blood Flow Into and Out of the Liver with 4D Phase Contrast MRI in the Pediatric Patient
SCI-011	Alazraki	MRI Findings in Post-Fontan Hepatopathy
SCI-012		WITHDRAWN
SCI-013	Dillon	Complications Within the Interventional Radiology Division of a Tertiary Care Children's Hospital: Initiatives for Ongoing Quality and Practice Improvement
SCI-014	McAlister	Dysosteosclerosis Presents as an 'Osteoclast-Poor' Form of Osteopetrosis: Comprehensive Investigation of a 3-Year-Old Girl
SCI-015	Okabe	Anomalous Cervical Arteries in Chondrodysplasia Punctata Brachytelephalangi Type
SCI-016	McAlister	Severe Skeletal Toxicity from Prolonged Etidronate Therapy for Generalized Arterial Calcification of Infancy
SCI-017	Araque	Magnetic Resonance Imaging in the Evaluation Of Infants with Hypoxic Ischemic Encephalopathy
SCI-018	Gupta	Posterior Fossa Abnormalities In Children
SCI-019	Khanna	Imaging Of Oculoauriculofrontonasal Syndrome with Low-Dose 3-Dimensional Computed Tomography
SCI-020	Tekes	Can Time Resolved Contrast-Enhanced MRA (TWIST) Classify Soft Tissue Vascular Anomalies in the Head and Neck In Children Accurately?
SCI-021	Poliakov	Functional Connectivity MRI in Pediatric Brain Tumor Patients with and Without Epilepsy
SCI-022	Kadom	Corpus Callosum DTI Measurements in Neurofibromatosis Type 1 and Normal Controls
SCI-023	Kain	Screening for Vitamin D Deficiency in Children with Suspected Non-Accidental Fracture
SCI-024	Edelstein	Comet Tails and Dirty Shadows: The Secrets Behind Artifacts in Pediatric Ultrasound
SCI-025	Huynh	Cardiac CTA: Non-Vascular Ring Tracheobronchial Compression Secondary to Enlarged Patent Ductus Arteriosus in Infants with Congenital Heart Disease
SCI-026	Serai	Pediatric Liver MR Elastography: A Primer
SCI-027	Gupta	Spectrum of Tuberculosis in Children

GENERAL INFORMATION

Thomas L. Slovis, MD
Shreyas S. Vasanawala, MD, PhD

MISSION STATEMENT

The Society for Pediatric Radiology is dedicated to fostering excellence in pediatric health care through imaging and image-guided care.

SITES OF PREVIOUS MEETINGS

1991 & IPR'91	Stockholm, Sweden
1992	Orlando, Florida
1993	Seattle, Washington
1994	Colorado Springs, Colorado
1995	Washington, D.C.
1996 & IPR'96	Boston, Massachusetts
1997	St. Louis, Missouri
1998	Tucson, Arizona
1999	Vancouver, British Columbia
2000	Naples, Florida
2001 & IPR'01	Paris, France
2002	Philadelphia, Pennsylvania
2003	San Francisco, California
2004	Savannah, Georgia
2005	New Orleans, Louisiana
2006 & IPR '06	Montreal, Quebec, Canada
2007	Miami, Florida
2008	Scottsdale, Arizona
2009	Carlsbad, California
2010	Boston, Massachusetts
2011 & IPR '11	London, England

FUTURE MEETINGS

2012	April 17–21, 2012	San Francisco, California
2013	May 14–18, 2013	San Antonio, Texas
2014	May 13–17, 2014	Washington, DC

OFFICERS, DIRECTORS AND COMMITTEES 2011–2012**ABSTRACT REVIEW COMMITTEE—PAPERS**

Donald P. Frush, MD, Chair
Richard A. Barth, MD
Brian D. Coley, MD
James S. Donaldson, MD
Lynn A. Fordham, MD
Gary L. Hedlund, DO
Sue C. Kaste, DO
David B Larson, MD
Marguerite T. Parisi, MD, MS
Tina Young Poussaint, MD

ABSTRACT REVIEW COMMITTEE—EXHIBITS

M. Beth McCarville, MD, Chair
Michael J. Callahan, MD
Maria A. Calvo-Garcia, MD
Michael P. D'Alessandro, MD
Kassa Darge, MD, PhD
Steven Don, MD
R. Paul Guillerman, MD
Fredric A. Hoffer, MD
Thierry A.G.M. Huisman, MD
Douglas H. Jamieson, MD
Nadja Kadom, MD
J. Herman Kan, MD
Geetika Khanna, MD
Beth M. Kline-Fath, MD
Joshua Q. Knowlton, MD
Maria F. Ladino Torres, MD
Craig S. Mitchell, DO, MA
Helen R. Nadel, MD, FRCPC
Daniel J. Podberesky, MD
Janet R. Reid, MD
Douglas C. Rivard, DO
Susan E. Sharp, MD
Manrita K. Sidhu, MD
Stephen F. Simoneaux, MD
Keith J. Strauss, MS
Alexander J. Towbin, MD

BOARD OF DIRECTORS

Dorothy I. Bulas, MD, Chair
Donald P. Frush, MD, President
Sue C. Kaste, DO, President-Elect
Richard A. Barth, MD, 1st Vice President
Brian D. Coley, MD, 2nd Vice President
James S. Donaldson, MD, Secretary
Brent H. Adler, MD, Treasurer
Paul S. Babyn, MD
Harris L. Cohen, MD
Heike E. Daldrup-Link, MD
Lisa H. Lowe, MD
Rafael Rivera, MD
Peter J. Strouse, MD
Mary R. Board Wyers, MD, ex officio
M. Ines Boechat, MD, FACR, ex officio
Christopher I. Cassady, MD, ex officio
Marilyn J. Goske, MD, ex officio
Marta Hernanz-Schulman, MD, ex officio
Neil D. Johnson, MD, ex officio
Thomas L. Slovis, MD, ex officio

BYLAWS

Dorothy I. Bulas, MD, Chair
 Paul S. Babyn, MD
 Harris L. Cohen, MD

CARDIAC IMAGING COMMITTEE

Rajesh Krishnamurthy, MD, Chair
 Dianna M. E. Bardo, MD
 Kerry A. Bron, MD
 Lorna P. Browne, MB BS
 Maryam Ghadimi-Mahani, MD
 S. Bruce Greenberg, MD
 Prakash M. Masand, MD
 Randolph K. Otto, MD
 Andrada R. Popescu, MD
 Cynthia K. Rigsby, MD
 Lauren M. Sena, MD
 Shreyas S. Vasanawala, MD, PhD

CHILD ABUSE COMMITTEE

Jeannette Perez-Rossello, MD, Chair
 Stephen Brown, MD
 Judith A. Craychee, MD
 Stephen L. Done, MD
 Jerry R. Dwek, MD
 P. Ellen Grant, MD, MSc
 Laura L. Hayes, MD
 Thaddeus W. Herliczek, MD, MS
 Vesna M. Kriss, MD
 Tal Laor, MD
 Kenneth L. Mendelson, MD
 Joelle Moreno
 Daniel M. Schwartz, MD
 Sabah Servaes, MD
 Andy Tsai, MD
 Terry J. Vaccaro, MD
 Matthew R. Wanner, MD
 Ingrid Holm, MD, consultant
 Carole Jenny, MD, consultant
 Paul K. Kleinman, MD, consultant

CLINICAL PRACTICES STEERING COMMITTEE

Sue C. Kaste, DO, Chair
 Christopher I. Cassady, MD
 Judy A. Estroff, MD
 Lynn A. Fordham, MD
 Blaise V. Jones, MD
 Rajesh Krishnamurthy, MD
 Edward Y. Lee, MD, MPH
 Marguerite T. Parisi, MD, MS
 Jeannette M. Perez-Rossello, MD
 Daniel J. Podberesky, MD
 Dennis W. Shaw, MD

Michael J. Temple, MD
 Shreyas S. Vasanawala, MD, PhD
 Sjirk J. Westra, MD

COMMUNITY HOSPITAL-BASED PEDIATRIC RADIOLOGISTS

Debra J. Pennington, MD, Chair
 Amaya Ormazabal, MD, Vice Chair
 Christopher E. Dory, MD
 Maria B. Mata, MD
 Maria-Gisela Mercado-Deane, MD
 Linnea J. Priest, MD
 Michael D. Rubin, MD

CONTRAST-ENHANCED ULTRASOUND TASK FORCE

Frank M. Volberg, MD, Chair
 Dorothy I. Bulas, MD
 Lynn A. Fordham, MD
 M. Beth McCarville, MD
 Kassa Darge, MD, PhD
 Harriet J. Paltiel, MD

CT COMMITTEE

Sjirk J. Westra, MD, Chair
 Jonathan R. Dillman, MD
 Donald P. Frush, MD
 Thaddeus W. Herliczek, MD, MS
 Edward Y. Lee, MD, MPH
 Grace S. Phillips, MD
 Sabah Servaes, MD
 Alexander J. Towbin, MD

CURRICULUM—RESOURCES TASK FORCE

Peter J. Strouse, MD, Chair
 Brent H. Adler, MD
 Richard A. Barth, MD
 Dorothy I. Bulas, MD
 Taylor Chung, MD
 Harris L. Cohen, MD
 Stuart A. Royal, MS, MD

DIAGNOSTICS

Daniel J. Podberesky, MD, Chair
 Karen M. Ayotte, MD
 Karen Blumberg, MD
 Marcus M. Kessler, MD
 Leann E. Linam, MD
 Arthur B. Meyers, MD
 Jeffrey S. Prince, MD
 Eva I. Rubio, MD
 Ethan A. Smith, MD
 Linda P. Thomas, MD
 Anthony I. Zarka, DO

EDITOR SEARCH COMMITTEE

Dorothy I. Bulas, MD, Chair
 Paul S. Babyn, MD
 Donald P. Frush, MD
 Marta Hernanz-Schulman, MD
 Edward Y. Lee, MD, MPH
 Ashok Panigrahy, MD
 Thomas L. Slovis, MD
 Alexander J. Towbin, MD

FELLOWSHIP PROGRAM DIRECTORS

Jane E. Benson, MD, Chair

FETAL IMAGING

Christopher I. Cassady, MD, Chair
 Stephen D. Brown, MD
 Dorothy I. Bulas, MD
 Maria A. Calvo-Garcia, MD
 Lucia Carpineta, MD, CM
 Lisa R. Delaney, MD
 Judy A. Estroff, MD
 Hollie A. Jackson, MD
 Beth M. Kline-Fath, MD
 Ashley J. Robinson, MBChB
 Teresa Victoria, MD

FINANCE

Molly E. Dempsey-Robertson, MD, Chair
 Brent H. Adler, MD
 Richard A. Barth, MD
 Brian D. Coley, MD
 Donald P. Frush, MD
 Sue C. Kaste, DO
 Randheer Shailam, MD

HONORS

Marta Hernanz-Schulman, MD, Chair
 M. Ines Boechat, MD, FACR
 Neil D. Johnson, MD

INFORMATICS

Alexander J. Towbin, MD, Chair
 R. Paul Guillerman, MD
 James D. Ingram, MD
 Neil D. Johnson, MD
 Edward Y. Lee, MD, MPH
 Janet R. Reid, MD
 Mahesh M. Thapa, MD, BS
 Keith S. White, MD

INTERNATIONAL TASK FORCE

M. Ines Boechat, MD, FACR, Chair
 Dorothy I. Bulas, MD

Ronald A. Cohen, MD
 James S. Donaldson, MD
 Charles A. Gooding, MD
 Neil D. Johnson, MD
 Stuart A. Royal, MS, MD

INTERVENTIONAL

Michael J. Temple, MD, Chair
 Mark A. Bittles, MD
 G. Peter Feola, MD
 Marc S. Keller, MD
 Els Nijs, MD
 John M. Racadio, MD
 Ashley J. Robinson, MBChB
 Dennis W. Shaw, MD
 Manrita K. Sidhu, MD
 Nghia (Jack) Vo, MD

JUDICIARY

Richard B. Gunderman, MD, Chair
 Stephen D. Brown, MD
 Neil D. Johnson, MD
 Charles D. Williams, MD

MR COMMITTEE

Shreyas S. Vasanawala, MD, PhD, Chair
 Adina L. Alazraki, MD
 Sudha A. Anupindi, MD
 Lauren W. Averill, MD
 Kiery A. Braithwaite, MD
 Govind B. Chavhan, MD DNB
 Ramesh S. Iyer, MD
 Sabiha P. Karakas, MD
 Hee-Kyung Kim, MD
 Arzu Kovanlikaya, MD
 Jeannie K. Kwon, MD
 Prakash M. Masand, MD
 Kassa Darge, MD, PhD
 Mahesh M. Thapa, MD, BS
 Neil Vachhani, MD

NEURORADIOLOGY

Blaise V. Jones, MD, Chair
 Thierry A.G.M. Huisman, MD
 Nadja Kadom, MD
 Paritosh C. Khanna, MD, DMRE
 Arzu Kovanlikaya, MD
 Gaurav Saigal, MD
 Unni K. Udayasankar, MD

NEWBORN

Judy A. Estroff, MD, Chair
 Dorothy I. Bulas, MD

Christopher I. Cassady, MD
 Teresa Chapman, MD MA
 Monica Epelman, MD
 Maria F. Ladino Torres, MD
 Edward Y. Lee, MD, MPH
 Kathleen M. McCarten, MD
 Ashok Panigrahy, MD
 Richard Parad, MD
 Eva I. Rubio, MD
 Teresa Victoria, MD
 Valerie L. Ward, MD

NOMINATING

Dorothy I. Bulas, MD, Chair
 Michael J. Callahan, MD
 Beverley Newman, MD, FACR
 Avrum N. Pollock, MD FRCPC
 Cynthia K. Rigsby, MD
 Lisa J. States, MD
 Raymond W. Sze, MD

NUCLEAR MEDICINE

Marguerite T. Parisi, MD, MS, Chair
 Lisa J. States, MD, Vice Chair
 Larry A. Binkovitz, MD
 Elizabeth A. Hingsbergen, MD
 Ruth Lim, MD, BS
 Helen R. Nadel, MD, FRCPC
 Marla B.K. Sammer, MD
 Victor J. Seghers, MD PhD
 Susan E. Sharp, MD
 Stephanie E. Spottswood, MD, MSPH
 S. Ted Treves, MD
 Pranav K. Vyas, MD
 John B. Wyly, MD

ONCOLOGY COMMITTEE

Sue C. Kaste, DO, Chair
 Peter C. Adamson, MD, ex officio
 Greg Reamon, MD, ex officio
 Heike E. Daldrup-Link, MD
 Michael J. Gelfand, MD
 M. Beth McCarville, MD
 Susan E. Sharp, MD
 Marilyn J. Siegel, MD
 Thomas L. Slovis, MD
 Alexander J. Towbin, MD
 Shreyas S. Vasawala, MD, PhD
 Stephan D. Voss, MD, PHD

PHYSICIAN RESOURCES COMMITTEE

Ellen C. Benya, MD, Chair
 Rebecca L. Hulett-Bowling, MD

Ramesh S. Iyer, MD
 Vesna M. Kriss, MD
 Sosamma T. Methratta, MD
 Eva I. Rubio, MD

PUBLIC POLICY

Richard M. Benator, MD, Chair
 Richard A. Barth, MD
 Kate A. Feinstein, MD, FACR
 Donald P. Frush, MD

PUBLICATIONS

Ashok Panigrahy, MD, Chair
 Brian D. Coley, MD, ex officio
 Cynthia K. Rigsby, MD, ex officio
 Thomas L. Slovis, MD, ex officio
 Peter Jackson Strouse, MD, ex officio
 Johan G. Blickman, MD
 Dorothy I. Bulas, MD
 Jonathan R. Dillman, MD
 James S. Donaldson, MD
 Charles M. Glasier, MD
 Ethan A. Smith, MD
 Alexander J. Towbin, MD

REPRESENTATIVES

Kimberly E. Applegate, MD, MS—ACR Council Steering Committee
 Richard M. Benator, MD—ACR Alternate Councilor
 Dorothy I. Bulas, MD—Academy of Radiology Research
 Christopher I. Cassady, MD—American Academy of Pediatrics
 Kate A. Feinstein, MD, FACR—ACR Councilor
 Donald P. Frush, MD—American Board of Radiology
 Tina Young Poussaint, MD—American Society of Pediatric Neuroradiology

RESEARCH AND EDUCATION FOUNDATION BOARD

Brian D. Coley, MD, President
 Donald P. Frush, MD, Vice President
 James S. Donaldson, MD, Secretary
 Brent H. Adler, MD, Treasurer
 Lisa H. Lowe, MD
 William H. McAlister, MD
 Kassa Darge, MD, PhD
 Ashok Panigrahy, MD
 Stuart A. Royal, MS, MD

SAFETY

Dennis W. Shaw, MD, Chair
 Sudha A. Anupindi, MD
 Einat Blumfield, MD

Thomas R. Goodman, MBChB
 Marilyn J. Goske, MD
 Ramesh S. Iyer, MD
 David B. Larson, MD
 Robert C. Orth, MD, PHD
 Grace S. Phillips, MD
 Ramon Sanchez, MD
 Thomas L. Slovis, MD, ex officio

STRUCTURED REPORT TASK FORCE

James S. Meyer, MD, Chair
 Kimberly E. Applegate, MD, MS
 Michael P. D'Alessandro, MD
 R. Paul Guillerman, MD
 Susan D. John, MD
 Neil D. Johnson, MD
 Ann M. Johnson, MD
 Edward Weinberger, MD

THORACIC IMAGING

Edward Y. Lee, MD, MPH, Chair
 Alan S. Brody, MD
 Maryam Ghadimi-Mahani, MD
 R. Paul Guillerman, MD
 Jeffrey C. Hellinger, MD
 Frederick R. Long, MD
 David A. Mong, MD
 Beverley Newman, MD, FACR
 Sjik J. Westra, MD

ULTRASOUND

Lynn A. Fordham, MD, Chair
 Jeanne S. Chow, MD
 Ellen M. Chung, MD
 Jamie L. Coleman, MD
 Monica Epelman, MD
 Boaz Karmazyn, MD
 Leann E. Linam, MD
 Martha M. Munden, MD
 Els Nijs, MD
 Sara M. O'Hara, MD
 Henrietta K. Rosenberg, MD
 Cicero T. Silva, MD
 Dayna M. Weinert, MD

WEBSITE

Mary R. Board Wyers, MD, Chair
 Benjamin H. Taragin, MD

GOLD MEDALISTS

1988 Frederic N. Silverman, MD
 1989 John L. Gwinn, MD
 1990 John F. Holt, MD

1991 John A. Kirkpatrick, Jr., MD
 1991 Bernard J. Reilly, MB, FRCP
 1992 Edward B. Singleton, MD
 1993 Hooshang Taybi, MD
 1994 Walter E. Berdon, MD
 1994 J. Scott Dunbar, MD
 1995 Guido Currarino, MD
 1995 Derek C. Harwood-Nash, MD, DSc
 1996 Andrew K. Poznanski, MD
 1996 Beverly P. Wood, MD
 1997 N. Thorne Griscom, MD
 1997 John F. O'Connor, MD
 1998 William H. McAlister, MD
 1999 E. Anthony Franken, MD
 2000 Eric L. Effmann, MD
 2001 Giulio J. D'Angio, MD
 2002 David H. Baker, MD
 2003 Brinton B. Gay, Jr., MD
 2003 William H. Northway, Jr., MD
 2004 Diane S. Babcock, MD
 2004 Virgil R. Condon, MD
 2005 Jerald P. Kuhn, MD
 2005 Thomas L. Slovis, MD
 2006 Robert L. Lebowitz, MD
 2006 John C. Leonidas, MD
 2007 Leonard E. Swischuk, MD
 2008 Barry D. Fletcher, MD
 2009 Charles A. Gooding, MD
 2010 Janet L. Strife, MD
 2011 Carol M. Rumack, MD
 2012 Marilyn J. Goske, MD

PIONEER HONOREES

1990 John Caffey, MD
 1991 M.H. Wittenborg, MD
 1992 Edward B. Singleton, MD
 1993 Frederic N. Silverman, MD
 1994 John P. Dorst, MD
 1995 E.B.D. Neuhauser, MD
 1996 Edmund A. Franken, MD
 1996 Kazimierz Kozlowski, MD
 1996 M. Arnold Lassrich, MD
 1997 Arnold Shkolnik, MD
 1998 Heidi B. Patriquin, MD
 1998 William H. Northway, Jr., MD
 2000 Jerald P. Kuhn, MD
 2001 Diane S. Babcock, MD
 2001 Fred E. Avni, MD, PhD
 2003 Walter E. Berdon, MD
 2004 G.B. Clifton Harris, MD
 2005 Rita L. Teele, MD
 2006 Robert L. Lebowitz, MD

2007 Carol M. Rumack, MD
 2008 Paul S. Babyn, MD
 2009 Kenneth E. Fellows, MD
 2010 David K. Yousefzadeh, MD
 2011 Massoud Majd, MD
 2012 George S. Bisset, III, MD

PRESIDENTIAL RECOGNITION AWARDS

1999 David C. Kushner, MD
 2000 Paul K. Kleinman, MD
 2001 Neil Johnson, MD
 2001 Christopher Johnson
 2002 Jennifer K. Boylan
 2002 Thomas L. Slovis, MD
 2003 Danielle K.B. Boal, MD
 2003 Marta Hernanz-Schulman, MD
 2004 Kenneth L. Mendelson, MD
 2005 Taylor Chung, MD
 2005 J. A. Gordon Culham, MD
 2005 Shi-Joon Yoo, MD
 2006 L. Christopher Foley, MD
 2007 Donald P. Frush, MD
 2008 Mary K. Martel, PhD
 2008 Connie L. Mitchell, MA, RT(R)(CT)
 2008 Harvey L. Neiman, MD
 2009 Karen S. Schmitt
 2010 Richard A. Barth, MD
 2011 Kimberly E. Applegate, MD, MS, FACR
 2011 Keith Strauss, MS, FACR
 2012 David C. Kushner, MD, FACR
 2012 Stuart A. Royal, MS, MD

HONORARY MEMBERS

1985 Jacques Sauvegrain, MD
 1987 Bryan J. Cremin, MD
 1987 Ole A. Eklof, MD
 1987 Clement C. Faure, MD
 1987 Andres Giedion, MD
 1987 Denis Lallemand, MD
 1987 Arnold Lassrich, MD
 1987 Ulf G. Rudhe, MD
 1998 Frederic N. Silverman, MD
 1989 John L. Gwinn, MD
 1990 John F. Holt, MD
 1990 Richard G. Lester, MD
 1991 Gabriel L. Kalifa, MD
 1991 Javier Lucaya, MD
 1991 John P. Masel, MD
 1991 Noemi Perlmutter-Cremer, MD
 1991 Hans G. Ringertz, MD
 1991 John A. Kirkpatrick, Jr., MD
 1991 Bernard J. Reilly, MB, FRCP(C)

1992 Edward B. Singleton, MD
 1992 Donald R. Kirks, MD
 1992 Beverly P. Wood, MD
 1993 Hooshang Taybi, MD
 1992/94 Walter E. Berdon, MD
 1994 Marie A. Capitanio, MD
 1994 Edmund A. Franken, Jr., MD
 1994 John C. Leonidas, MD
 1994 William H. McAlister, MD
 1994 Andrew K. Poznanski, MD
 1994 J. Scott Dunbar, MD
 1995 David H. Baker, MD
 1992/95 Derek C. Harwood-Nash, MD, DSc
 1995 N. Thorne Griscom, MD
 1995 Guido Currarino, MD
 1996 Francis O. Brunelle, MD
 1996 Lloyd L. Morris, MD
 1996 Heidi B. Patriquin, MD
 1997 John F. O'Connor, MD
 1997 Theodore E. Keats, MD
 1998 Rita L. Teele, MD
 1998 H. Ted Haecke, MD
 1999 J. Bruce Beckwith, MD
 2000 Joseph Volpe, MD
 2001 Ulrich V. Willi, MD
 2001 Henrique M. Lederman, MD
 2001 Mutsuhisa Fujioka, MD
 2002 Eric J. Hall, DSc, FACR, FRCR
 2002 Walter Huda, PhD
 2003 Michael R. Harrison, MD
 2004 Lee F. Rogers, MD
 2005 Carden Johnston, MD, FAAP, FRCP
 2006 Alan B. Retik, MD
 2007 Robert R. Hattery, MD
 2008 Professor Hassen A. Gharbi
 2009 Dolores Bustelo, MD
 2009 Pedro A. Daltro, MD
 2009 Cristian Garcia, MD
 2009 Antônio Soares de Souza, MD
 2010 Stephen Chapman, MD
 2011 Catherine M. Owens, MBBS
 2011 Madan M. Rehani, PhD
 2012 Harvey L. Neiman, MD, FACR

PAST PRESIDENTS

1958-59 Edward B. Neuhauser, MD*
 1959-60 Frederic N. Silverman, MD*
 1960-61 John F. Holt, MD*
 1961-62 Arthur S. Tucker, MD*
 1962-63 John W. Hope, MD*
 1963-64 R. Parker Allen, MD
 1964-65 Edward B. Singleton, MD

1965-66	J. Scott Dunbar, MD*
1966-67	Harvey White, MD*
1967-68	M.H. Wittenborg, MD*
1968-69	David H. Baker, MD
1969-70	John A. Kirkpatrick, Jr., MD*
1970-71	Norman M. Glazer, MD*
1971-72	Bertram R. Girdany, MD
1972-73	Donald H. Altman, MD
1973-74	Hooshang Taybi, MD*
1974-75	John L. Gwinn, MD*
1975-76	Lawrence A. Davis, MD*
1976-77	Marie A. Capitanio, MD
1977-78	John P. Dorst, MD*
1978-79	Bernard J. Reilly, MB, FRCP (C)
1979-80	Walter E. Berdon, MD
1980-81	Andrew K. Poznanski, MD
1981-82	N. Thorne Griscom, MD
1982-83	Virgil R. Condon, MD
1983-84	Jerald P. Kuhn, MD
1984-85	Lionel W. Young, MD
1985-86	John C. Leonidas, MD*
1986-87	Derek C. Harwood-Nash, MD, DSc*
IPR '87	Denis Lallemand, MD (ESPR)
1987-88	Beverly P. Wood, MD
1988-89	John F. O'Connor, MD*
1989-90	E.A. Franken, Jr., MD
1990-91	Donald R. Kirks, MD
IPR '91	Hans G. Ringertz, MD, PhD (ESPR)
1991-92	William H. McAlister, MD
1992-93	M. B. Ozonoff, MD
1993-94	Joanna J. Seibert, MD
1994-95	Eric L. Effmann, MD
1995-96	Kenneth E. Fellows, MD
IPR '96	Paul S. Thomas, MD (ESPR)
1996-97	Diane S. Babcock, MD
1997-98	Charles A. Gooding, MD
1998-99	Robert L. Lebowitz, MD
1999-00	Thomas L. Slovis, MD
2000-01	Janet L. Strife, MD
IPR '01	Francis Brunelle, MD (ESPR)
2001-02	Bruce R. Parker, MD
2002-03	Richard B. Towbin, MD
2003-04	David C. Kushner, MD, FACR
2004-05	Stuart A. Royal, MS, MD
2005-06	George A. Taylor, MD
IPR '06	Richard Fotter, MD (ESPR)
2007	Marilyn J. Goske, MD
2008	Marta Hernanz-Schulman, MD, FACR
2009	M. Ines Boechat, MD, FACR
2010	Neil D. Johnson, MBBS
2011	Dorothy I. Bulas, MD

*Deceased

SINGLETON-TAYBI AWARD

2006	Corning Benton, Jr., MD
2007	Michael P. D'Alessandro, MD
2007	Janet R. Reid, MD
2008	Dorothy I. Bulas, MD
2009	Lane F. Donnelly, MD
2010	Wilbur L. Smith, Jr., MD
2011	Ralph S. Lachman, MD, FACR
2012	Alan Daneman, MD

JOHN A. KIRKPATRICK YOUNG INVESTIGATOR AWARD

This award is given to the author of the best paper presented by a Resident or Fellow at the SPR meeting. Beginning in 1995, the award became known as the John A. Kirkpatrick Young Investigator Award.

1993	Philipp K. Lang, MD
1993	Stephanie P. Ryan, MD
1994	Sara O'Hara, MD
1995	Philipp K. Lang, MD
1996	Fergus V. Coakley, MB, FRCR
1997	Ronald A. Alberico, MD
1998	Laura J. Varich, MD
1999	A. E. Ensley, BS
1999	R.W. Sze, MD
2000	S. H. Schneider, MD
2001	Valerie L. Ward, MD
2002	Ricardo Faingold, MD
2003	Andrea Doria, MD
2004	Nina M. Menezes, PhD
2005	Lena Naffaa, MD
2006	Courtney A. Coursey, MD
2007	Ashley J. Robinson, MBChB
2008	Hee Kyung Kim, MD
2009	Conor Bogue, MD
2010	Albert Hsiao, MD, PhD
2011	Ethan A. Smith, MD

WALTER E. BERDON AWARDS

2011 recipients will be announced at the meeting.

Best Basic Science Paper 2010

Goo HW, Initial Experience of Dual Energy Lung Perfusion CT Using a Dual Source CT System in Children

Best Clinical Research Paper 2010

Raissaki M, Perisinakis K, Damilakis J, Gourtsoyiannis N, Eye-lens Bismuth Shielding in Pediatric Head CT: Artifact Evaluation and Reduction

For a list of prior recipients, please visit the SPR website.

THE SPR RESEARCH AND EDUCATION FOUNDATION AWARDS

The SPR Research and Education Foundation is dedicated to promoting research and scholarship in pediatric radiology. The SPR Board of Directors has supported research through grants since 1990. The Foundation was established in 1994 with an initial donation from the Society's reserves.

The Jack O. Haller Award for Excellence in Teaching

- 2005 Alan Daneman, MD
- 2006 William R. Cranley, MD and John F. O'Connor, MD
- 2007 Cindy R. Miller, MD
- 2008 Sara J. Abramson-Squire, MD
- 2009 Michael A. DiPietro, MD
- 2010 George A. Taylor, MD
- 2011 Paul K. Kleinman, MD
- 2012 Richard I. Markowitz, MD

The Heidi Patriquin International Fellowship

- 2005 Luy Lyda, MD, *Angkor Hospital for Children*, Siem Reap, Cambodia
- 2006 Hakima Al-Hashimi, MD *Salmaniya Medical Complex*, Manama, Bahrain
- 2006 Pannee Visrutaratna, MD, *Chiang Mai University*, Chiang Mai, Thailand
- 2006 Juana Maria Vallejo, MD, *Clinica del Country*, Bogota, Colombia
- 2007 Nathan David P. Concepcion, MD, *St. Luke's Medical Center*, Quezon City, Philippines
- 2008 Rolando Reyna Lopez, MD, *Hospital Santo Tomas*, Panama City, Panama
- 2009 Ahmed Mussa Jusabani, MD, *Kilimanjaro Christian Medical Centre*, Moshi Town, Tanzania
- 2010 Omolola Mojisola Atalabi, MD, *College of Medicine, University of Ibadan*, Nigeria
- 2011 Kushaljit Singh Sodhi, MD, *Postgraduate Institute of Medical Education and Research (PGIMER)*, Chandigarh, India

- 2012 Wambani Sidika Jeska, MBChB, *Kenyatta National Hospital*, Nairobi, Kenya
- 2012 Yocabel Gorfu, MD, *Addis Ababa University*, Addis Ababa, Ethiopia

Pilot Award

Michael Temple, MD, Development of a Prototype Database for Collaborative Pediatric Interventional Radiology Research Utilizing a Multi-institutional Review of Inferior Vena Cava Filter Placement in Children, Hospital for Sick Children, Toronto

Seed Grant

Sunhee Kim, MD, Assessing early chemotherapy response of pediatric low-grade glioma using combined quantitative PET and MR imaging, Children's Hospital of Pittsburgh

Fellow Award

Divyata Hingwala, MBBS, Functional and structural measures of early outcome in very preterm-born toddlers, Tirunal Institute for Medical Sciences and Technology and Hospital for Sick Children, Toronto

For a list of prior grant recipients, please visit the SPR website.

SOCIAL EVENTS

Welcome Reception

Thursday, April 17
6:00–7:30 p.m.
The Fairmont Hotel
Hors d'oeuvres and Refreshments
Casual Attire (this will be an outdoor event)

Reception and Awards Banquet

Thursday, April 19
6:30–11:00 p.m.
The Fairmont Hotel
Reception, Dinner and Dancing
Business/Cocktail Attire

SPR 2012 Gold Medalist

The Gold Medal of The Society for Pediatric Radiology is our most distinguished honor. The SPR Medal is awarded to pediatric radiologists who have contributed greatly to the SPR and our subspecialty of pediatric radiology as a scientist, teacher, personal mentor and leader.



Marilyn J. Goske, MD

Marilyn Goske has always wanted to make a difference—and what a difference she has made!

Her role as an educator, and her lifelong commitment to improving training for residents, fellows, faculty, medical staff and radiologic technologists has resulted in many wonderful initiatives that have benefited all in pediatric radiology. The work she is most proud of—the Cleveland Clinic Web Based Curriculum, working with the leadership of SPR's Philanthropic Campaign for Children, launching the Image Gently Campaign and the pediatric research component within the American College of Radiology's Dose Index Registry share a common theme: educating others in providing the best care possible for children.

Born in Berea, Ohio, Marilyn's father, George, was a chemical engineer. Her mother, Cornelia aka "Corky", loved writing as one of the first women journalists for the Associated Press and later teaching, passions she passed on to her daughter. While Marilyn was blessed with a strong female role model in her mother, it was her brother, James, who was her cheerleader, always pushing her to dream big. He encouraged her to follow in his footsteps first at Ohio University, then on to the Ohio State College of Medicine to pursue an MD degree during an era when nursing would have been a more conventional goal.

Marilyn met her husband Rick on a double date in college—unfortunately, they were with different dates! Luckily, they were able to get together for an actual date

with each other 18 months later. They quickly became engaged and married within a year of that first true date. When Rick started his residency in internal medicine, Marilyn transferred to the University of Connecticut School of Medicine in Farmington. It was here that she met her first pediatric radiologist—and what a giant—Mike Ozonoff! When Rick moved on to a neurology residency in Rochester, New York, Marilyn followed and met another pediatric radiology giant: Beverly Wood, at Strong Memorial Hospital. Beverly proved to be a wonderful teacher, mentor, co-researcher and lifelong friend. Marilyn describes Beverly as inspirational and "fearless" in trying new technologies. It was during her time in Rochester that Marilyn went to her first SPR meeting and, not surprisingly, won the 1984 Caffey Award for her work on "Experimental Neonatal Intraventricular Hemorrhage: Clinical, Radiographic and Pathologic Features."

By then Marilyn had two young children and moved on to the private sector, practicing part-time for several years first in Rochester, then in Cleveland, Ohio. Her years in private practice were particularly helpful in learning the importance of patient oriented service—and paved the way for her intuitive public relations strategies when designing the Image Gently campaign in later years.

Dr. Goske was asked to join the Cleveland Clinic in 1990, as the first full-time section head of pediatric radiology. It was here that she built a new section and spearheaded the web based education program for pediatric radiology residents with co-founder Janet Reid. This important free web site with 65 modules is used widely by over 200 radiology residencies nationally and internationally. Her passion for education continued, inspiring her to complete a medical education fellowship focused on professionalism within the Cleveland Clinic Lerner College of Medicine. Her work towards this fellowship has led to many creative educational initiatives including yearly educational summits at the SPR. She was named chair of the Professionalism committee of the RSNA where she along with her committee have sponsored interactive workshops on this topic dear to her heart.

Dr. Goske's energy and effective leadership skills brought her to become involved in the Society for Pediatric Radiology, first as the coordinator for SPR's first video-taped course in 1994. Mentors Diane Babcock and Carol Rumack proposed her for the Nominating Committee. This was followed by Chair of the Membership Committee, where she organized the first formal survey of the Society, then as a Board member, then as Secretary, and finally as President and Chair of the Board of Directors, completing 12 years on the SPR Board. Working together with Stuart Royal, she successfully energized the Campaign for Children raising

funds for the Research and Education Foundation of the SPR and expanded the work of prior presidents in further organizing the Corporate Support committee. Marilyn's years as President and Chairman of the Board of the SPR were highly successful with many unique strategic goals. She was instrumental in the founding of the junior SPR. She led the wonderful 2007 SPR national meeting in Miami which included the first educational summit to enhance knowledge in adult learning and resident competencies.

Most people would rest after completing their arduous year as President but as Chairman of the Board, Marilyn was just beginning! She moved to Cincinnati Children's Hospital, joining the radiology department and was named the Dr. Coming Benton Endowed Chair for Radiology Education where she got to work with Dr. Janet Strife, another influential mentor and friend.

Acknowledging SPR's long focus on reducing radiation doses in the imaging of children but concerned about the lack of change in practice by a majority of radiologists despite increasing reports of possible side effects, Marilyn developed a public relations and awareness campaign. Her goal was to inspire all to work towards decreasing radiation exposure to children when possible. With the help of many, she founded the Alliance for Radiation Safety in Pediatric Imaging and the Image Gently campaign, initially focusing on CT. Her ability to encourage numerous experts and societies to work together and get involved in "child sizing the amount of radiation used" has resulted in a groundswell of research and activity in this area. Currently 69 organizations with over 800,000 members have joined the Alliance including 24 international societies. The web site, www.imagegently.org, has been immensely successful filled with free information pamphlets in over 12 languages, PQI projects, and modules for parents, physicians, and technologists. The Image Gently Campaign has received several awards including the Associations Advance America Honor Roll, RT Image magazine group with the "most influence in radiology" and the Most Effective Philanthropy Program from Aunt Minnie. Image Gently has spawned the creation of the adult-focused Image Wisely campaign. The Alliance has been named by the Joint Commission, U.S. Food and Drug Administration, and the American Medical Association in their influential statements on radiation dose as providing much needed guidance and information. Marilyn's exceptional talent is inspiring and coordinating experts in multiple fields to work together towards common goals. She continues to work hard on the Image Gently campaign with more safety and quality messages planned for the coming years. She is also proud of her work with the ACR Dose Index Registry and Quality Improvement Registry in CT Scans in children in working toward developing diagnostic reference

levels with a talented consortium of pediatric radiologists, medical physicists and technologists. She has acted as a national and international expert in her work with the International Atomic Energy Agency, the World Health Organization and the National Council on Radiation Protection in Medicine and the FDA.

Dr. Goske's multiple committee appointments are taken seriously, and her work is always meticulous, well thought out, and brought to successful completion. She has been an active member of numerous national and international societies including the John Caffey Honorary Society, ACR, RSNA, ESPR, AAWR, and SCORCH. It is important to remember that Dr. Goske is also a successful researcher with numerous grants obtained through the SPR REF including the Thorne Griscom Education award and the RSNA Scholar grant. She has published over 80 peer-reviewed articles, 19 electronic publications, 7 chapters, and presented 26 scientific exhibits as well as given numerous scientific presentations. An articulate and engaging speaker, she has been invited to give over 130 lectures locally, nationally and internationally.

While Marilyn has been very focused on her work with the SPR, she believes that it is her amazing family and their love that really fuels her life. Her husband Rick is an internationally known neurologist and researcher in multiple sclerosis. Her adult children Jamie and Brian, both in Manhattan, remain close, and spending quality time together as a family remains the joy of her life. Whether it is relaxing together in Florida cooking or fishing, or taking an exotic vacation to India, being with Rick, Jamie and Brian makes her the happiest.

Marilyn's genius is partly refusing to take "No" as an answer. Along the way, at every turn there were those who believed that what she wanted to do couldn't be done. Her approach was to draft the nay-sayers to the team and charge ahead with their willing and enthusiastic help.

Daniel Burnham might have been talking about Marilyn and not about his plan for the city of Chicago when he said:

Make no little plans; they have no magic to stir men's blood and probably themselves will not be realized. Make big plans; aim high in hope and work, remembering that a noble, logical diagram once recorded will not die, but long after we are gone be a living thing, asserting itself with ever-growing insistence.

As an amazing change agent, inspirational leader, and wonderful role model, the SPR is proud to honor Marilyn Goske with the 2012 Gold Medal. She made big plans!

Dorothy I. Bulas, MD

SPR 2012 Pioneer Honoree

Pioneer Honorees were first acknowledged in 1990 as a means to honor certain physicians who made special contributions to the early development of our specialty.



George S. Bisset, III, MD

It is time to reevaluate the meaning of the Pioneer Honoree. The subspecialty of Pediatric Radiology has been in existence now for more than 50 years. We are beyond “the early development”; we must recognize other pioneering paths and should consider contributions to the subspecialty beyond the bounds of a modality, a technique, an observation or a change in practice. Whatever this advancement is, it must be forged with vision, innovative ideas, and the ability to enable and sustain science and application.

George S. Bisset, III, M.D.

Why George Bisset? Has he been part of the Pediatric Radiology landscape these last ten years? Been part of the dialogue that has been increasingly influential across all of Radiology, a conversation steeped in a deep tradition of excellence in diagnosis and treatment, and the safety and welfare of our children? Been a leader in science and application?

Part of the landscape? No. But he has been beyond that and has worked tirelessly within the horizon, surveying...a step before, but guiding us on towards our destiny. A conversant? Part of the dialogue? Maybe. But he has been defining thought and concept upon which such conversation is born and nurtured. Part of the science and application? Yes, as much as anyone who promotes, who facilitates and sustains discovery, then here we are. Horizons, innovation, and the gift of enabling...What else is needed to define a true pioneer?

How was this done?

Simply stated, George Bisset has devoted at least the last decade to the advancement of our specialty in truly novel ways through his leadership, especially in RSNA and the ABR. In the RSNA, as the Scientific Program Committee Chair several years ago he was instrumental in the conception, development and implementation of the integration of scientific papers and

refresher course topics. This has been a resounding success, is currently used in other categories during RSNA and is a model for other meetings, including the Annual Meeting for the Society for Pediatric Radiology over the past few years. Pediatric Radiology was first in this effort. George continued to endorse topics that were marquee for Pediatric Radiology over the year in his education role on the RSNA Board of Directors. He endorsed and implemented the Pediatric Campus concept at the 2011 RSNA. Early returns are that this was an extremely successful model to consolidate experts in pediatric radiology (and those interested in this subspecialty), pertinent science, education and administration. George is now the President of RSNA, perhaps the most widely respected scientific and educational organization for our profession across the globe...and I would argue, with more promise for our future success in Pediatric Radiology than has ever existed.

And George Bisset, who through two terms as the Pediatric Trustee for the Board of Trustees for the ABR, again, was on the horizon of a critical, sometimes perilous, and complete transformation of our certification examination process, always mindful of his constituency and colleagues, his duty as a physician, and the public and patients. This required delicate diplomacy, forward thinking, professionalism, and enlistment of a cadre of experts from within our subspecialty to assure excellence in pediatric radiology through ABR certification. He was also a leader in the development, validation and implementation of the image-rich computer based examination model (the pediatric CAQ) now the standard for the new ABR examinations.

With these successes in mind, who better to embody the concept of bridging horizons that is the theme for this entire meeting?

If you were looking for more numbers and accolades, I apologize. Here are some: more than 225 contributions to medical and scientific literature, advancing care through pediatric body CT and MR imaging research, a litany of presentations and invited lectures, Vice Chairs, Chairs, Chiefs, Boards of Directors, committee member and committee leader, clinical excellence including as a pediatric cardiologist and interventional radiologist, a superb speaker and author... all are on his CV but I believe serve really as signposts for his gifts, some of those mentioned above, that a CV simply cannot convey. He could have played it safe with all of these successes on his CV. But pioneers don't play it safe. They are on the horizon, too busy defining thought and enabling (our) advancement—building bridges.

I believe it is time to reevaluate the meaning of the Pioneer Honoree and I have the greatest honor and pleasure of introducing George S. Bisset, III for the Pioneer Award for 2012. Linked with past awardees, he continues an exceptional legacy and I don't believe his explorations and discoveries are finished...

Donald P. Frush, MD

SPR 2012 Presidential Recognition Award

The Society bestows Presidential Recognition Awards on members or other individuals whose energy and creativity have made a significant impact on the work of the Society and its service to its members.



David C. Kushner, MD, FACP

In 1999, David Kushner was recognized by the SPR with its first Presidential Recognition Award for his vision and foresight in working with both the American College of Radiology (ACR) and the Society for Pediatric Radiology (SPR) in developing an important new relationship and for his service to the SPR. In summarizing his considerable efforts for that award, I noted that he “contributed substantively to the increased visibility of the SPR within the ACR. His tenure as our Treasurer placed our organization on a firm financial foundation.” With the current award, the Society recognizes his indefatigable continuing efforts on our behalf including:

His work with the ACR:

1. Establishing a pediatric radiology caucus at the annual ACR meeting,
2. Convincing the ACR of the value of managing specialty societies by making the SPR its first successful new model for imaging society management,
3. Advocating tirelessly for pediatrics and children’s health within the ACR by serving on the Council Steering Committee and then as ACR Council Vice Speaker and Speaker,
4. Helping establish the first pediatric commission, assuring that pediatric issues will receive support of the College and its resources while serving on the Board of Chancellors of the ACR for the past five years. The SPR’s “Image Gently” campaign was a beneficiary of this pediatric commission of the Board of Chancellors,
5. Continuing to shepherd and contribute to the pediatric component of the ACR practice guideline process.

His work with the SPR:

Since his earlier award, David has served as:

1. President of the SPR’s Research and Education Foundation from 2000 to 2003, including the launch of the formal fundraising effort, “the Campaign for Children,”
2. SPR President 2003–2004, organizing and running a very successful meeting in Savannah,
3. Chair of the Board of Directors of the SPR from 2004 to 2005, including leading a strategic planning process that resulted in a new, more focused division of labor amongst Board members and defined Board responsibilities.

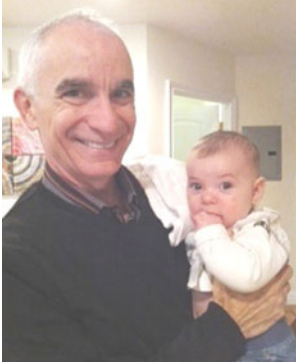
David was born in Fargo, North Dakota, received a BA from the University of Minnesota, and received his medical education at the University of Pennsylvania. This was followed by two years of training in pediatrics at Children’s Hospital, Boston. He then did a two-year fellowship at the National Institute of Health in Bethesda, performing research in embryology and teratology. He returned to Massachusetts General Hospital for training in diagnostic radiology. This was followed by a year of residency in pediatric radiology at Children’s Hospital Boston, followed by a one-year fellowship. He then became director of the pediatric radiology section at Massachusetts General Hospital, a position he held from 1979 to 1988. From 1988 to 2005, David was chief of the Division of Diagnostic Imaging and Radiology at Children’s National Medical Center in Washington, DC attracting a strong faculty, training many fellows and promoting research. During that time, he served as a volunteer radiologist and pediatrician to inner city healthcare systems aiding the indigent and homeless, and developing telemedicine capabilities linking free clinics with radiology experts.

In 2005, our man inside the beltway moved a bit outside by accepting the medical directorship of radiology at the Children’s Hospital of the King’s Daughters in Norfolk, Virginia, and Professor of Radiology and Pediatrics at the Eastern Virginia Medical School. He assures me that life there is good, being a bit more “laid back” with fishing and sailing just outside the door. He also finds time for Italian cooking and practicing jazz on his several guitars. Fortunately for all of us in the SPR, David is close enough to our central office and the ACR that he will be able to continue work on our behalf for many years to come.

Eric L. Effmann, MD

SPR 2012 Presidential Recognition Award

The Society bestows Presidential Recognition Awards on members or other individuals whose energy and creativity have made a significant impact on the work of the Society and its service to its members.



Stuart A. Royal, MS, MD

The 2012 SPR Presidential award is given in recognition of Stuart's numerous significant and outstanding contributions to the SPR over many years of service. The awardee is selected by the Honors Committee, a committee comprised of the three most recent past presidents of the Society. Dr. Royal is a proud native of Birmingham, Alabama. He is a second generation physician who came naturally to his desire to care for children as the son of a pediatrician, Arnold Royal, who took care of children in the Birmingham community until he was 79 years old. Dr. Royal attended Rice University in Houston, Texas followed by MD and MS degrees from the University of Alabama at Birmingham. He subsequently moved to San Francisco, where he completed a pediatric internship followed by a diagnostic radiology residency at the University of California, San Francisco. Dr. Royal credits Dr. Charles Gooding at UCSF for influencing his decision to pursue a career in pediatric radiology. During his internship Stuart observed Dr. Gooding make a plain film diagnosis of TAPVR, type 3 on a severely ill and perplexing newborn, and he was immediately hooked into radiology. While at UCSF Dr. Royal was also appointed as a National Institute of Health research fellow in the Department of Radiology. Following residency, Stuart completed a fellowship in pediatric radiology at The Children's Hospital Medical Center in Boston.

From Boston, Stuart returned to his roots in Birmingham, Alabama in 1980, where he was appointed as a pediatric radiologist at the University of Alabama and subsequently The Children's Hospital in Birmingham. In recognition of his outstanding leadership skills and accomplishments at The Children's Hospital, Dr. Royal was appointed as the Radiologist-in-Chief in 1987, and subsequently the Harry M. Burns endowed Chair of Pediatric Radiology. He also

holds appointments as Clinical Professor of Radiology and Pediatrics at the University of Alabama at Birmingham and serves on The Children's Hospital Board of Trustees.

At Alabama Dr. Royal has earned the high esteem of his colleagues, referring physicians, and staff for his outstanding clinical acumen as a diagnostic radiologist and for his undaunting commitment to excellent care of children. Colleagues describe Stuart as one who fosters a strong work ethic, high commitment to teaching, and sincere compassion for children. In 2006, Stuart was the recipient of the Children's Advocate award by Childcare Resources for improving the quality of care and access to radiological services for underserved children in Birmingham.

Stuart has been married to the love of his life, Barbara Royal, for the past 40 years. Stuart and Barbara are the proud parents of two very accomplished children, Jeremy a budding radiologist in training at the University of Alabama, and Rachael, who has an MBA and works as a Vice President for Moody's in New York. Stuart and Barbara are also the proud grandparents of three grandchildren. In conversation, Stuart is quick to pull out his iPhone and share the latest pictures of family members while recounting their latest activities and milestones.

Throughout his professional career, Dr. Royal has worked tirelessly to advance the mission of the Society for Pediatric Radiology. He is past president and chairman of the board of the SPR and has served on numerous SPR committees. He ran a highly successful SPR meeting in New Orleans in 2005. Those in attendance will recall the jubilant parade Stuart led through the streets of New Orleans to culminate the meeting. As President and then Chair of the SPR board, Stuart played a critical and instrumental role in bringing the SPR management contract under the umbrella of the ACR. The synergy achieved by the SPR-ACR relationship has yielded results well beyond a simple management contract. Pediatric radiology and SPR now have a voice at the "radiology table."

Stuart has also been a strong advocate for supporting translational research to advance the care of children via imaging. To help achieve this goal, he has worked aggressively to secure increased funding for the Society of Pediatric Radiology Research and Education Foundation. Following the launch of the REF's Campaign for Children in 2000, Stuart made it his personal mission to work with the leadership of the Society, both past and present, to discuss major gifts to the Foundation. Through Stuart's personal effort, the Foundation received pledges for many significant leadership gifts, including from SPR Pioneers Drs. Hooshang Taybi and Ed Singleton and from himself and Barbara.

The SPR is highly fortunate to have benefited from Stuart's numerous contributions and dedication to the care of children. The Society is very proud to bestow the 2012 President's Award on Dr. Stuart A. Royal.

Richard A. Barth, MD

SPR 2012 Honorary Member

The Society extends Honorary membership to individuals outside of pediatric radiology who have made outstanding contributions to the care of children.



Harvey L. Neiman, MD, FACR

This evening, Dr. Harvey L. Neiman, whose leadership of the American College of Radiology is resoundingly praised, is the recipient of the 2012 Honorary Member Award. For 2012, as in 2007 when his contributions were similarly recognized, Dr. Neiman's selection by the Society for Pediatric Radiology Honors Committee was made in appreciation for the strength of his efforts to further the SPR's philosophy, goals, and programs for responsible diagnosis and treatment of the young patient as embodied in the ACR and SPR's "Image Gently" campaign. *Image Gently* has succeeded not only in raising awareness of the great diagnostic benefits we can offer to pediatric patients but also directs us to acknowledge the downside of overzealous diagnostic efforts where excessive radiation becomes a risk. Importantly, the "Image Gently" campaign, an upbeat, positive program rather than a punitive one, a smile rather than a frown, makes pediatric and all radiologists aware that their best practice reflects balanced, educated, up-to-date utilization of state-of-the-art technology with exercise of responsible leadership in protecting the pediatric patient. For adults, awareness of the need for patient protection is communicated in *Image Wisely*.

Dr. Neiman's vision and successful achievements are evident on every page of his curriculum vitae. A consummate strategist in assembling teams to make forward-looking goals a reality, Harvey now stands at the top of our specialty as the first physician Executive Director of the American College of Radiology. At this time in big-business medicine, as we see the physician, leader of the patient care team, being diminished to one of many "providers," it is so important for our patients' well-being for us to recognize the obligations commanded by our training, clinical experience and commitment. Dr. Neiman's recognition of the need for physicians' leadership in improving the quality of patient

services and his development of programs in all areas of the college's activities have been just short of miraculous—*Image Wisely* for adults, Quality and Safety including the Performance Guidelines and Accreditations, Education, Government Relations, Economics, Imaging Metrix, ACRIN, and the new Radiology Leadership Institute—to name only a few. All have contributed significantly to the care of our patients and the stature of our specialty.

Dr. Neiman was born in Detroit and attended Mumford High School. From Wayne State University, he received his B.S. in 1964 and his MD in 1968. Harvey's postgraduate training was at the University of Michigan, where he was a resident in Radiology (1969–1972), Chief Resident (1971–72), and a 1972–73 fellow in Angiography (Cardiovascular Radiology), receiving ABR certification in 1973 and a CAQ in Vascular and Interventional Radiology in February 1995. Dr. Neiman often expresses his gratitude to and profound respect for his mentor and beloved chief at the University of Michigan, Dr. William Martel.

Dr. Neiman was Chief of Cardiovascular Radiology at Walter Reed Army Hospital and a lecturer in Cardiovascular Radiology at the AFIP from 1973–1975. In 1975, he joined the Northwestern Radiology faculty, rising to Professor in 1981, and for ten years he headed up the section of Angiography and Sectional Imaging, advancing its technology and honing the skills of Northwestern's radiology residents. Harvey also offered a highly sought-after fellowship in Interventional Radiology, US, and CT.

In 1985, Dr. Neiman left Northwestern to assume the Chair in Medical Imaging at the Western Pennsylvania in Pittsburgh. I was the first woman to have completed his fellowship in US, CT, and Interventional Radiology at Northwestern and accompanied him to Pittsburgh. His tenure at West Penn attests to his talent in making his visions a reality: the department became a highly respected, successful academic private practice notable in many areas including ultrasound, breast and women's imaging, and interventional radiology. Harvey instituted an excellent radiology residency program in 1988 as well as fellowship programs in 1986 in the areas of excellence noted above.

During the 40 years since Harvey received his MD, he has been awarded honors from many national, international, and specialty societies, has been an invited lecturer over 181 times on ultrasound, interventional radiologic, radiologic educational, management, turf issues, disruptive and new technology topics to name just a few. Dr. Neiman, who was a founder of the SRU (Society of Radiologists in Ultrasound), has to his credit 122 peer-reviewed articles, 69 scientific presentations and 20 exhibits, a text co-authored with Dr. James Yao, *Angiography of Vascular Disease* (1984), and 26 book chapters. He has received many honors including fellowship in the American College of Radiology, American Institute of Ultrasound in Medicine, Society of Radiologists in Ultrasound and the Society of Cardiovascular

and Interventional Radiology (now SIR). As part of his strong commitment to the future leaders of radiology, for Diagnostic Radiology he has served as a member of the Residency Review Committee of the Accreditation Council for Graduate Medical Education.

He has been a member of the American College of Radiology and its committees and commissions for many years including the Commissions on Education, Ultrasound, and Economics. He also served as chair of the Commissions on Ultrasound and Economics. From 1994 to 2002, he was a member on the ACR Board of Chancellors, serving as its chairman 2000–2002. He was President of the Radiology Advocacy Alliance from 1998 to 2000. In 2003, nine years ago, Dr. Neiman became the ACR's Executive Director. He currently serves in this position, where his excellent business skills, knowledge of health policy and economic issues, and strong administrative background have furthered our specialty. His goal, to ensure that the ACR's resources benefit all radiologists and patients across all economic strata, is evident in his actions at the College.

Harvey has a devoted, wonderful family that often included me and my youngest daughter on many Pittsburgh

occasions. His beautiful, elegant wife of many years, Ellie Neiman, is here tonight to celebrate with him the SPR's recognition of his many achievements. Dr. Neiman has two accomplished, lovely daughters, Jennifer, extremely successful in her marketing career, and Hilary, an attorney. Jennie's husband, Dr. Seth Kligerman, one of many young radiologists whom Harvey has mentored, is on the radiology staff at the University of Maryland.

How Harvey has had time between, through, and among all of these achievements to have become mentor, colleague, and friend to me and to so many others who have been inspired by his ability to see into the future and to shape it in a positive way is remarkable. Now that Dr. Neiman has taken all of radiology under his wing, not just its component parts, the future of our specialty, one of the best, can be assured but also recognized for its centrality to all of medicine. It is my honor and privilege to introduce to you Harvey L. Neiman MD, FACR as this year's Society for Pediatric Radiology Honorary Member.

Ellen B. Mendelson, MD

SPR 2012 Singleton-Taybi Award

The Singleton-Taybi Award is given in honor of Edward Singleton and Hooshang Taybi, in recognition of their personal commitment to the educational goals of the SPR. Initiated in 2006, the Award is presented annually to a senior member of the SPR whose professional lifetime dedication to the education of medical students, residents, fellows, and colleagues has brought honor to him/her and to the discipline of pediatric radiology.



Alan Daneman, MD

It comes as no surprise to those who know him that Dr. Daneman, “Dr. D” as some of us call him, has been named the 2012 recipient of the Singleton-Taybi Award in recognition of his many years of dedication to the education of residents, fellows, and colleagues.

Born in South Africa in 1947, he received his Medical Degree at the University of the Witwatersrand, Johannesburg, receiving the Harwood-Nash award for the most successful student in Surgery. Initially, Dr. D thought he would become a pediatric surgeon; but after passing the Part I examination offered by the Royal Australasian College of Surgeons, he changed his mind and began his training in diagnostic radiology. He chose a radiology residency at the Royal Prince Alfred Hospital, in Sydney, Australia. This included a year in pediatric radiology at the Royal Alexandra Hospital for Children in Sydney where his interest and love of pediatric radiology began. Dr. D then had the foresight to pursue pediatric radiology fellowship training at the Hospital for Sick Children in Toronto, Canada. After completing the fellowship, he was immediately offered a position as staff radiologist at “Sick kids.” He became Director of Body Imaging in 1984 and Radiologist-in-Chief in 1988 serving in that capacity for 7 years. His management style was simple but effective. He chose staff that were young, but smart and innovative. He nurtured them and provided them with all the tools they needed to become successful professionals, like him. But contributing to his own

department was not enough for him. He also found the time and strength to contribute, teach, train, and help pediatric radiologists in the most remote portions of the globe in every continent, which resulted in recognition from prestigious organizations in places such as South America, Israel, Europe, Taiwan and Australia: he is an Honorary member of the European Society for Pediatric Radiology and the Sociedad Latinoamericana de Radiología Pediátrica as well as other national societies.

Dr. D is an “institution” inside the great institution that is Sick Kids. His teaching is unique and praiseworthy in being enthusiastic, provocative, and fun at the same time. His lectures have been regarded as both instructive and practical by his students and trainees due to his special gift of making the most complicated things look as simple as possible. In sharing his diagnostic knowledge and know-how, he passes his own, innate teaching spirit on to his apprentices. He has earned several awards for this, including the outstanding teacher award granted by the University of Toronto fellows at Sick Kids for the past 5 consecutive years. Dr. D receives numerous invitations to present at national and international meetings and symposia and has been invited as a visiting professor to more than a hundred institutions across the globe. He does not only teach us the ins and outs of Pediatric Radiology, but he makes sure that we learn to love it and understand the importance not only of good practice but also the imperative to pass knowledge on by teaching and publishing. Dr. D is someone who inspires us to reach beyond our limits, someone we want to emulate. He shares his knowledge, his wisdom, and his advice freely. He shares with us the most incredible secrets of his own career, so we understand from his personal experience. Dr. D never tells you what to do, he suggests to you, in an incredible articulate fashion, what you want to do yourself. Dr. D has been and is for many of us, more than an educator, more than a mentor, he is our “coach.” Well before this concept was introduced into medicine by A. Gawande¹, Dr. D intuitively had the vision to “coach” his trainees, trying to get the best out of them, without pressure, but with love and passion, and especially emphasizing the importance of achieving a work-life balance in order to prevent the now so common “stress and burnout” affecting the radiology community². He warned us that many high achievers reach their goals only at the expense of their personal lives, but Dr. D has been as successful personally as he is professionally. His wonderful wife of 40 years, Louise, his two daughters and his recently newborn granddaughter serve as sources of strength and pride. He is a truthful and generous friend to many, both in and out of radiology. It is not uncommon for many of us, who came through Sick Kids, to come back and visit and be invited to his house to share a wonderful dinner with other invitees, who may be radiologists from North America or from other parts of the globe visiting Sick Kids to learn from him.

Dr. Daneman's research has widely influenced the field of Pediatric Radiology. Examples include the work of Dr. Daneman and his colleagues on intussusception, which has promulgated the use of ultrasound for diagnosis, and the use of air enema for reduction. This approach has been adopted as standard practice at many institutions in North America and across the globe. To share his research with others in the field, Dr. Daneman has authored or co-authored more than 200 publications, including peer reviewed articles and book chapters on a wide range of topics related to the imaging of children.

Dr. D is one of those rare people who are irreplaceable. He is a superb teacher, a gifted academician, a capable administrator, and a person called "friend" by so many of us. We are thrilled and proud to present our Society's Singleton-Taybi award to Dr Alan Daneman in recognition of his lifelong accomplishments and personal commitment to the educational goals of the SPR. We cannot imagine anyone more deserving of this award than Dr. D. Thank you "coach"!

Monica Epelman, MD and Oscar Navarro, MD

1. Personal Best, Top Athletes and Singers have Coaches. Should you? ; The New Yorker, http://www.newyorker.com/reporting/2011/10/03/111003fa_fact_gawande
2. Battling Burnout: Radiologists Seek Career Renewal. P. Moskowitz and M. Linzer. RSNA news, October–November 2011



John Caffey, MD 1895–1978

Dr. Caffey was regarded throughout the world as the father of pediatric radiology. His classic textbook, *Pediatric X-Ray Diagnosis*, which was first published in 1945, has become the recognized bible and authority in its field. The seventh edition of this book was completed

several months before his death in 1978. It has been among the most successful books of its kind in the medical field.

Dr. Caffey was born in Castle Gate, Utah on March 30, 1895. It is interesting that he was born in the same year that Roentgen discovered the x-ray. Dr. Caffey was graduated from University of Michigan Medical School in 1919, following which he served an internship in internal medicine at Barnes Hospital in St. Louis. He spent three years in Eastern Europe with the American Red Cross and the American Relief Administration, and returned to the United States for additional training in medicine and in pediatrics at the Universities of Michigan and Columbia, respectively.

While in the private practice of pediatrics in New York City at the old Babies Hospital of Columbia University College of Physicians and Surgeons, he became interested in radiology and was charged with developing a department of pediatric radiology in 1929. He frequently expressed appreciation and admiration for the late Ross Golden, Chairman of Radiology at Columbia Presbyterian Hospital, who allowed him to develop a separate department of diagnostic radiology without undue interference, and who was always available to help and advise him.

Dr. Caffey's keen intelligence and inquiring mind quickly established him as the leader in the fields of pediatric x-ray diagnosis, which recognition became worldwide almost instantaneously with the publication of his book in 1945.

Dr. Caffey received many awards in recognition of his achievements. Outstanding among these were the Mackenzie Davidson Medical of the British Institute of Radiology in 1956, the Distinguished Service Award of the Columbia Presbyterian Medical Center in 1962, the Outstanding Achievement Award of the University of Michigan in 1965, the Howland Award of the American Pediatric Society in 1967, the Jacobi Award of the American Medical Association in 1972, and the Gold Medal Award of the American College of Radiology in 1975. He had been a member of the American Journal of Roentgenology. He was a counselor of The Society for Pediatric Radiology and was an honorary member of the European Society of Pediatric Radiology.

Dr. Caffey's contributions to the pediatric radiologic literature were many. He was instrumental in directing attention to the fact that a prominent thymic shadow was a sign of good health and not of disease, an observation that literally spelled the end to the practice of thymic irradiation in infancy. Infantile cortical hyperostosis was described by him and is called "Caffey's Disease." Dr. Caffey in 1946 first recognized the telltale radiographic changes that characterize the battered child, and his students helped disseminate his teachings about these findings. It was Dr. Caffey who first recognized and described the characteristic bony changes in vitamin A

poisoning. He recognized and described the findings associated with prenatal bowing of the skeleton.

In 1963, three years after his retirement from Babies Hospital, he joined the staff of the Children’s Hospital of Pittsburgh as associate radiologist and as Visiting Professor of Radiology and Pediatrics at the University of Pittsburgh School of Medicine. Although Dr. Caffey came to Children’s Hospital and the University of Pittsburgh in an emeritus position, he worked daily and on weekends throughout the years he was there. In Pittsburgh, he made four major new contributions to the medical literature. He described the entity, "idiopathic familial hyperphosphatasemia." He recognized and described the earliest radiological changes in Perthes’ Disease. He called attention to the potentially serious effects of shaking children, and used this as a subject of his Jacobi Award lecture. He described, with the late Dr. Kenny, a hitherto unrecognized form of dwarfism that is now known as the Caffey-Kenny dwarf.

The John Caffey Society, which includes as its members pediatric radiologists who have been intimately associated with Dr. Caffey, or who have been trained by his students, was established in 1961. This society is now among the most prestigious in the field of radiology. His book and the society named in his honor will live on as important memorials to this great man.

His greatness was obvious to all who worked with him. He was warm, kind, stimulating, argumentative, and above all, honest in his approach to medicine and to x-ray diagnoses. His dedication to the truth was expressed in his abiding interest in the limitations of x-ray signs in pediatric diagnosis and in his interest in normal variation in the growing skeleton. He was concerned with the written and spoken word and was a skilled semanticist. His book and his articles are masterpieces of language and construction. He stimulated and was stimulated and loved by all who had the privilege of working with him. Radiology and Pediatrics have lost a great man, but they shall ever have been enriched by his presence.

Bertram R. Girdany, MD1

Caffey Award for Best Basic Science Research Paper

2004 Site-Specific Induction of Lymphatic Malformations in a Rat Model for Image-Guided Therapy. Short R, Shiels W, Sferra T, Nicol K, Schofield M, Wiet G

2005 Quantitative Measurement of Microbubble Ultrasound Contrast Agent Flow to Assess the Efficacy of Angiogenesis Inhibitors *In Vivo*. McCarville B, Streck C, Li CS, Davidoff A

2006 ⁶⁴Cu-Immuno-PET Imaging of Neuroblastoma with Bioengineered Anti-GD2 Antibodies. Voss

SD, Smith SV, DiBartolo NM, McIntosh LJ, Cyr EM, Bonab AA, et. al

2007 MR Imaging of Adenocarcinomas with Folate-Receptor Targeted Contrast Agents. Daldrup-Link HE, Wang ZJ, Meier R, Corot C

2008 Evaluation of Quality Assurance Quality Control Phantom for Digital Neonatal Chest Projection Imaging. Don S.

2009 Faster Pediatric MRI Via Compressed Sensing. Vasanawala S, Alley M, Barth R, Hargreaves B, Pauly J, Lustig M

2010 Clinical Evaluation of Readout-Segmented-EPI for Diffusion-Weighted Imaging. Bammer R, Holdsworth S, Skare S, Yeom K, Barnes P

2010 High-Resolution Motion-Corrected Diffusion-Tensor Imaging (DTI) in Infants. Skare S, Holdsworth S, Yeom K, Barnes P, Bammer R

2010 3D SAP-EPI in Motion-Corrected Fast Susceptibility Weighted Imaging (SWI). Bammer R, Holdsworth S, Skare S, Yeom K, Barnes P

2010 T1-Weighted 3D SAP-EPI for Use in Pediatric Imaging. Bammer R, Holdsworth S, Skare S, Yeom K, Barnes P

2011 An MR System for Imaging Neonates in the NICU. Tkach J, Giaquinto R, Loew W, Pratt R, Daniels B, Jones B, Donnelly L, Dumoulin C

Caffey Award for Best Clinical Research or Education Paper

2004 Feasibility of a Free-Breathing SSFP Sequence for Dynamic Cardiac Imaging in Pediatric Patients. Krishnamurthy R, Muthupillai R, Vick G, Su J, Kovalchin J, Chung T

2005 Evaluation of High Resolution Cervical Spine CT in 529 Cases of Pediatric Trauma: Value Versus Radiation Exposure. Shiran D, Jimenez R, Altman D, DuBose M, Lorenzo R

2006 Alterations in Regional O₂ Saturation (StO₂) and Capillary Blood Volume (HbT) with Brain Injuries and ECMO. Grant PE, Themelis G, Arvin K, Thaker S, Krishnamoorthy KK, Franceschini MA

2007 Evaluation of Single Functioning Kidneys Using MR Urography. Grattan-Smith D, Jones R, Little S, Kirsch A, Alazraki A

2008 Evaluating the Effects of Childhood Lead Exposure with Proton MR Spectroscopy & Diffusion Tensor Imaging Neuroradiology. Cecil KM

2009 Improving Patient Safety: Effects of a Safety Program on Performance and Culture in a Department of Radiology at a Children’s Hospital. Donnelly L, Dickerson J, Goodfriend M, Muething S

- 2010 Juvenile Osteochondritis Dissecans (JOCD): Is It a Growth Disturbance of the Secondary Physis of the Epiphysis? Laor T, Wall E, Zbojnicz A
- 2011 Quantitative Assessment of Blood Flow with 4D Phase-Contrast MRI and Autocalibrating Parallel Imaging Compressed Sensing. Hsiao A, Lustig M, Alley M, Murphy M, Vasawala S
- CAFFEY AWARD FOR SCIENTIFIC EXHIBITS**
- 2004 Outstanding Basic Science Research Poster—Imaging of the Diaphragm in Neonates and Young Infants with Special Emphasis on Diaphragmatic Motion. Epelman M, Navarro O, Miller S
- 2004 Outstanding Clinical Research Poster—The Spectrum of Renal Cystic Disease in Children. Restrepo R, Ranson M, Sookman J, Jacobson E, Daneman A, Fontalvo L
- 2005 3D MRI and CT in the Evaluation of Congenital Anomalies of the Aortic Arch. Dehkharghani S, Olson K, Richardson R
- 2006 Diffusion Weighted Imaging in Pediatric Neuro-radiology: A Primer. Sagar P, Grant PE
- 2006 Imaging of Suprarenal Fossa in Children: Radiological Approach and Clinico-Pathological Correlation. Kukreja K, Restrepo R, D’Almeida M
- 2007 Neuroimaging of Nonaccidental Trauma: Pitfalls and Controversies. Lowe L, Obaldo RE, Fickenscher KA, Walsh I
- 2008 Estimation of Cumulative Effective Doses from Diagnostic and Interventional Radiological Examinations in Pediatric Oncology Patients. Thomas KE, Ahmed BA, Shroff P, Connolly B, Chong AL, Gordon C
- 2009 *Case Report* : Multi-Modality Imaging Manifestations of the Meckel’s Diverticulum in Pediatric Patients. Kotecha MK, Bellah RD, Pena AH, Mattei P
- 2009 *Educational*: MR Urography: Functional Analysis—Made Simple! Khrichenko D, Darge K
- 2009 *Scientific*: MRI Findings in the Term Infant with Neonatal Seizures. An Etiologic Approach. Rebollo Polo M, Hurteau-Miller J, Laffan E, Tabban H, Naser H, Koujok K
- 2010 Scientific Dual Phase Intravenous Contrast Injection in Pediatric Body CT. Mann E, Alzahrani A, Padfield N, Farrell L, BenDavid G, Thomas K
- 2010 Educational Hemangiomas Revisited: The Useful, the Unusual and the New. Restrepo R, Palani R, Matapathi U, Altman N, Cervantes L, Duarte AM, Amjad I
- 2010 Case Report MRI of Congenital Urethroperineal Fistula. Mahani M, Dillman J, Pai D, Park J, DiPietro M, Ladino Torres M
- 2011 Scientific Updated Estimated Radiation Dose for Pediatric Nuclear Medicine Studies. Grant F, Drubach L, Treves ST, Fahey F
- 2011 Educational Button Battery Ingestion in Children: What the Radiologist Must Know. Kappil M, Rigsby C, Saker M, Boylan E
- 2011 Case Report MR Imaging Features of Fetal Mediastinal and Intrapericardial Teratomas. Rubio E, Kline-Fath B, Calvo-Garcia M, Guimaraes C

For a list of Caffey award papers and scientific exhibits prior to 2004, please visit the SPR website.

2012 Edward B. Neuhauser Lecture



Present and Future Patient Benefits of Radiologist/Physicist Collaboration

William R. Hendee, PhD
 Distinguished Professor of Radiology, Radiation Oncology,
 Biophysics and Bioethics
 Medical College of Wisconsin
 Milwaukee, Wisconsin

William R. Hendee received the PhD degree in physics from the University of Texas. He joined the University of Colorado, ultimately serving as Professor and Chair of Radiology for several years. In 1985 he moved to Chicago as Vice President of Science and Technology for the American Medical Association. In 1991 Dr. Hendee joined the faculty of the Medical College of Wisconsin as Senior Associate Dean and Vice President with faculty appointments as professor and vice chair of radiology with additional professorships in biophysics, radiation oncology and bioethics. He is also Professor in Bioengineering at Marquette University, Adjunct Professor of Electrical Engineering at the University of Wisconsin-Milwaukee, Clinical Professor of Radiology at the University of New Mexico, Adjunct Professor of Radiology at the University of Colorado and Adjunct Professor of Radiology at Mayo Clinic. From September through December 1994, Dr. Hendee served as Acting Executive Vice President and Dean of the Medical College. In January 1995 he assumed additional responsibilities as Dean of the Graduate School of Biomedical Sciences. In 2005 he was appointed as President of the MCW Research Foundation. He currently holds the title of Distinguished Professor of Radiology, Radiation Oncology, Biophysics and Bioethics.

Dr. Hendee is certified in Radiologic Physics by the American Board of Radiology and in Health Physics by the American Board of Health Physics. He has been a Director of the American Board of Health Physics and the Health Physics Society, chairman of the Diagnostic Physics Examination Committee for the American Board

of Radiology, and Past-President of the American Board of Radiology. He is past president of the American Association of Physicists in Medicine, the Society of Nuclear Medicine, the American Institute of Medical and Biological Engineering, the World Congress on Medical Physics and Biomedical Engineering and past vice president of the National Patient Safety Foundation. He is currently Chair of the American Board of Radiology Foundation and President and CEO of the Commission on the Accreditation of Medical Physics Graduate Programs. Dr. Hendee has authored or co-authored over 400 scientific articles and 24 books. He is the editor of *Medical Physics*, the most widely distributed and read journal in medical physics and engineering in medicine in the world. In 2010 he was awarded the American College of Radiology gold medal award. He received an honorary doctorate from Millsaps College in 1988 and from the University of Patras, Patras Greece in 2009. Other awards include the Radiological Society of North America’s gold medal, the gold medal from the American Roentgen Ray Society, the Elda Anderson Award of the Health Physics Society, and the William D. Coolidge medal from the American Association of Physicists in Medicine.

Previous Neuhauser Lecturers

- 1996 M. Judah Folkman, MD, Boston, Massachusetts.
Clinical Applications of Angiogenesis Research
- 1997 S. Steven Potter, PhD, Cincinnati, Ohio
“Homeobox Genes and Pattern Formation (Master Genes)”
- 1998 Roy A. Filly, MD, San Francisco, California
“Fetal Thoracic Surgery”
- 1999 Harold A. Richman, PhD
“Child Abuse: From a Radiologist’s Discovery to a Major Issue of Public Policy. What Have We Wrought?”
- 2000 William D. Lyman, PhD, Detroit, Michigan
“Prenatal Molecular Diagnosis and Fetal Therapy”
- 2001 Jerry R. Dwek, MD, Columbus, Ohio
“Médecins Sans Frontières/The Doctors Without Borders Experience – Afghanistan”
- 2002 Eric J. Hall, DSc, FACR, FRCR, New York, New York
“Lessons We Have Learned From Our Children: Cancer Risks From Diagnostic Radiology”
- 2003 Jeffrey A. Towbin, MD, Houston, Texas
“Molecular Cardiology: Laboratory to Bedside”
- 2004 Bruce R. Rosen, MD, PhD, Boston, Massachusetts
“New Advances in MRI: A Guide for the Practicing Pediatric Radiologist”
- 2005 Bruce R. Korf, MD, PhD, Birmingham, Alabama

	“Pathobiology and Management of NF1 in the ‘Genomic Era’”	2009	Roberta G. Williams, MD
2006	Richard M.J. Bohmer, MD, MPH		“Cardiology and Radiology: Partners in Producing Healthy Adults with Congenital Heart Disease”
	“Evolution, Innovation and the Changing Nature of Healthcare Delivery”	2010	Regina E. Herzlinger, PhD
2007	Nogah Haramati, MD		“The Economic Basis of Change in Healthcare”
	“21st Century Radiology: Growth and Development of Our Workflows and Processes”	2011	Sanjiv Gambhir, MD, PhD
2008	Emanuel Kanal, MD, FACR, FISMRRM, AANG		“Molecular Imaging”
	MR Technology: Where Are We, Where Are We Going?		

For a list of Neuhauser Lecturers prior to 1996, please visit the SPR website.

POSTGRADUATE COURSE ABSTRACTS

Monday, April 16, 2012

Thoracic Imaging: From Interstitium to Airways

Interstitial Lung Disease in Infants: New Classifications, Imaging Findings, and Pathological Correlation

Edward Y. Lee, MD, MPH

Interstitial lung disease, which is more common in infants than older children, is defined as a rare heterogeneous group of parenchymal lung conditions primarily due to underlying developmental or genetic disorders. Affected infants typically present with clinical syndromes characterized by dyspnea, tachypnea, crackles, and hypoxemia. Mainly due to a lack of evidence based information regarding underlying pathogenesis, natural history, imaging findings, and histopathologic features of interstitial lung disease, the understanding of interstitial lung disease in infants has been limited in the past. However, in recent years, the understanding of interstitial lung disease in infants has been substantially improved primarily due to: 1) advances in imaging technology for better detection; 2) improvement of thoracoscopic techniques for lung biopsy; 3) established pathologic criteria for consistent diagnosis; and 4) development of new classification system based on underlying etiology of the interstitial lung disease. In fact, several forms of interstitial lung disease in infants that exhibit distinct clinical, radiological, and pathological patterns are currently emerging. The overarching goal of this article is to review a new classification system, imaging findings, and pathological correlation of interstitial lung disease in infants. Improved understanding of this often challenging disorder can aid in early and accurate diagnosis, which in turn, will result in improved patient care.

Large Airway Disease in Pediatric Patients: Impact of Advanced Post-processing Techniques

Catherine M. Owens, BSc MBBS MRCP FRCR

The introduction of multidetector row computed tomography (MDCT) scanners has altered the approach to imaging the pediatric thorax. In an environment where the rapid acquisition of CT data allows general hospitals to image children instead of referring them to specialist pediatric centers, it is vital that general radiologists have access to protocols appropriate for pediatric applications. This lecture will focus on the main principles of volumetric CT imaging that apply generically to all MDCT scanners and in particular we describe the reconstruction techniques for imaging the pediatric thorax and the low-dose protocols used in our institution on a 64-slice dual source CT scanner. Examples of important clinical applications with the impact and added value of post processing are also given.

Pediatric Thoracic Neoplasms: Review and Updates

Sue C. Kaste, DO

Neoplasms, by definition, comprise an abnormal uncoordinated proliferation of cells that persists even after the inciting stimulus as ceased. The resulting mass may be benign or malignant and arise from any tissue that is normally found in the location where the mass develops. Thus, tumors of the chest may arise from bone, lung, pleura, lymphatics, muscle, etc. Whether benign or malignant, chest masses may be incidental findings on imaging obtained for other reasons. This presentation will focus on malignant tumors of the chest, address the imaging characteristics and staging of the most common chest malignancies and discuss characteristics that may aid in distinguishing these lesions from their corresponding benign or infectious counterparts. Included in this presentation will be the most common chest wall malignancies (Ewing family of tumors and rhabdomyosarcoma), mediastinal malignancies (lymphoma, germ cell tumors, and neurogenic malignancies) and pulmonary primary malignancies (pleuropulmonary blastoma and carcinoid). The changing appearance of selected tumors in patients treated with new targeted therapies will be introduced.

MRI of Pediatric Lungs and Airways: Current Status and Future Direction

Talissa Altes, MD

Lung disease is the most common chronic disease of childhood, but young children cannot perform the breathing maneuvers required for the most commonly used method for assessing lung function, spirometry. CT provides exquisite structure information about the lung but concerns regarding the long-term consequences of the relatively high radiation dose limit its use particularly in the pediatric population.

Magnetic resonance imaging (MRI) has the potential to provide regional information about the lung without the use of ionizing radiation. While conventional proton MRI has found widespread clinical application in most organs of the body, MRI of the lung lags behind because the lung is intrinsically difficult to image with MRI. The strength of the MR signal depends on the physical density of protons in the tissue being imaged and the local environment of the protons. The lung has a low physical density and thus a low proton density so little MR signal is generated by the lung. Furthermore, the magnetic susceptibility effects from its many air-tissue interfaces cause what little signal is generated to rapidly decay so that the lung typically appears dark on conventional proton MR images. A variety of strategies have been developed to overcome the inherent difficulties of MRI of the lung, resulting in recent substantial improvements in image quality. Additionally by administering an

inhaled gaseous contrast agent, such as the hyperpolarized noble gases helium-3 or xenon-129, direct visualization of lung airspaces in an MR image is possible. A number of unique strategies for evaluating the structure and function of the human lung using hyperpolarized gas MRI have been developed. Although the level of structure detail possible with lung MRI may never equal that of CT, MRI may nonetheless have the potential to provide clinically useful information and be a sensitive, effort independent test of pediatric lung disease.

Abdominal Imaging: From Asking to Answers

Bowel Sounds and Music: Malrotation, Intussusception, Appendicitis, Inflammatory Bowel Disease, Imperforate Anus

Laurent A. Garel, MD

Ultrasound has shown its validity and accuracy in investigating the pediatric GI tract. Mainly performed for diagnostic purposes, US features may also become prognostic predictors in some instances (e.g. pneumatic reduction failure of intussusception, bowel viability in NEC).

It is convenient to separate GI pediatric entities in 3 subgroups on the basis of US performance:

- the *classic*: hypertrophic pyloric stenosis, intussusception;
- the *useful*: inflammatory bowel diseases, occlusion, masses, NEC, imperforate anus, Meckel, trauma;
- the *controversial*: intestinal malrotation, appendicitis.

For a matter of time, we will focus in this presentation only on the following:

Intestinal malrotation

A normal visceral situs can be inferred sonographically in relation to the right-sidedness of the superior mesenteric vein, to the retromesenteric location of D3 and to the right iliac position of the ileocecal valve. Conversely, intestinal malrotation is likely when the 3 aforementioned features are reversed. In addition, CDU can display the whirlpool pattern in case of midgut volvulus or internal hernia, alleviating the need for preoperative opacification.

Intussusception

The reliability of US in diagnosing intussusception is well documented since the early 1990s. The value of US in predicting the success or failure of pneumatic reduction and/or bowel necrosis is more debatable, based upon a coexisting bowel occlusion, the presence of interloop fluid, bowel wall changes (intramural air, dilated mural vascular channels), absent blood flow at CDU.

Appendicitis

The continuous down-grading of US in comparison to CT, and the opposite conclusions of various series regarding imaging of pediatric appendicitis are based upon different prerequisites and definitions. Historically and in most USA institutions, sonography reports are either negative (entire normal appendix), positive (abnormal inflamed appendix), or equivocal (non-visualization or partial visualization of appendix). The *equivocal* group is then logically investigated by a subsequent abdominal CT.

In Europe, some USA centers, and in our practice, US reporting include 4 groups and take into account ancillary findings:

1. normal appendix (blind-ended, lamellated, compressible, <6 mm in diameter, without peristalsis);
2. appendix not depicted, no secondary signs;
3. appendix not depicted, with one of the following: hyperchoic mesenteric fat, fluid collection, local dilated small bowel loop;
4. appendix inflamed.

Group 3 represents most cases of perforated appendicitis, groups 1 and 2 the negative sonogram. CT is then indicated only in obese patients and to assess the feasibility of percutaneous interventions.

Inflammatory bowel disease

In the recent literature, MR enterography is often preferred to CT enterography. Small bowel series look prehistoric and US is rarely mentioned. Sonography however is very valuable both for screening children presenting with abdominal pain, diarrhea, weight loss, or GI bleeding and for following the course of the disease and searching for complication. Hypervascularization has been proved to parallel the disease activity.

Imperforate anus

Initially mentioned by Dr. Rita Teele, the interest of US for differentiating high-intermediate/low varieties of imperforated anus has been re-emphasized more recently. A perineal rectal cul de sac distance of 15 mm is quoted as the significant cut-off value. US can also display rectourinary fistulae outlined by air.

Update on MDCT and MRI of Hepatobiliary Disease in Children: What's New

Lisa H. Lowe, MD

A variety of disorders may affect the pediatric liver. Recent advances in histopathological knowledge and imaging techniques have led to important changes that radiologists must be aware of in order to allow for an accurate limited differential,

and in some cases, specific, diagnosis. This presentation will focus on recent developments that have led to a better understanding of the embryopathogenesis for fibropolycystic liver diseases (including choledochal cysts and Caroli disease), histopathological findings that have led to new classification systems for pediatric vascular anomalies, technological advances and contrast agents in magnetic resonance imaging that are useful to characterize and limit the differential diagnosis of hepatic masses.

Diagnostic Errors in Pediatric Abdominal Imaging: Diagnostic Pearls and Pitfalls

George A. Taylor, MD

This presentation reviews the types of diagnostic errors in abdominal imaging occurring over a 13-year period in an academic pediatric radiology practice. Radiologists engage in two interrelated processes when interpreting imaging studies: perception and analysis. Failures in perception (failure to identify an important finding) are a common source of diagnostic error in pediatric imaging, while failures in the analytic portion of the process (over- or faulty interpretation of a finding) are not as common. Under-interpretation of findings can be related to a number of perceptual and visual phenomena including visual isolation where attention is selectively focused on a main area of the image while less or no attention is given to secondary areas, and satisfaction of search which occurs when additional lesions remain undetected after detection of an initial lesion. Many analytic errors are the result of commonly used heuristics or shortcuts in reasoning. These include the availability heuristic in which likelihoods are based on memory of a similar case, the framing effect in which a different diagnosis is reached based on how the information is presented, and the anchoring heuristic in which the initial impression is difficult to change, despite conflicting new information. Another recognized pitfall is blind obedience, in which a diagnostician stops thinking when confronted by authority. This authority can be human or technical (reliance on a laboratory value). Finally, diagnostic errors can result from an attitude of overconfidence. Examples of these heuristics and strategies to minimize cognitive errors will be discussed.

Neonatal Congenital Abdominal Masses: Clues to Reach a Diagnosis

Marta Hernanz-Schulman, MD, FAAP, FACR

This session will consider abdominal masses that present in the neonatal period, spanning developmental, inflammatory and neoplastic conditions. Time constraints do not allow an exhaustive list or description, but the more important or frequent lesions are discussed. The presentation is subdivided by systems. The renal section discusses various

conditions presenting with hydronephrosis, such as ureteropelvic junction obstruction and duplication anomalies, followed by autosomal recessive polycystic kidney disease and multicystic dysplastic kidney, cystic entities commonly presenting in the perinatal period. Neoplastic renal entities include lesions with benign behavior, such as ossifying renal tumor of infancy, with the discussion extending to entities with very poor prognosis such as clear cell sarcoma and rhabdoid tumor, while discussing the congenital mesoblastic nephroma, its histologic subtypes and the differences in their presentation, imaging findings and clinical behavior. Suprarenal lesions include the adrenal hemorrhage, congenital neuroblastoma and subdiaphragmatic sequestration.

Hepatic lesions include developmental anomalies that present as mass lesions, such as choledochal cysts, vascular lesions such as congenital and infantile hemangiomas, and neoplastic lesions such as the mesenchymal hamartoma and hepatoblastoma. Differences in clinical presentation, imaging characteristics and behavior of the lesions are discussed. The section on pancreatic lesions discusses pancreatic cysts and pancreaticoblastoma. GI tract and mesenteric lesions include duplication cysts, lymphangioma, and meconium pseudocyst, and their relationship to bowel obstruction and persistent perforation.

Ovarian cysts can present as large masses in neonatal girls, and should be high in the differential diagnosis of large masses encountered in female infants; the imaging characteristics of simple and complicated cysts are described, as well as their course and potential complications.

Pediatric Procedures: From Imaging to Intervention The Spectrum of Vascular Anomalies in Pediatric Patients: Multimodality Imaging Evaluation and Current Treatment

Patricia E. Burrows, MD

Vascular anomalies are categorized into two main groups, vascular tumors and vascular malformations. Genetic and molecular regulation of vascular genesis of angiogenesis, and mutations responsible for some of the vascular malformations, have been delineated. In order to implement future targeted treatment of vascular lesions, accurate diagnosis is important. Imaging modalities that are effective in distinguishing the various types of vascular anomalies and demonstrating the extent include ultrasonography with Doppler interrogation, MRI and various forms of MR vascular flow imaging, conventional angiography and venography. Techniques used to image lymphatic channel anomalies, conventional lymphangiography, lymphoscintigraphy and infrared fluorescent lymphangiography. In this presentation, common forms of vascular anomalies will be described and rare or recently recognized anomalies will be mentioned.

Current treatment of the different forms of vascular anomalies will also be discussed, including pharmacotherapy using beta blockers, angiogenesis inhibitors and mTOR inhibitors. Endovascular techniques used in treating vascular malformations, including embolization and sclerotherapy will be presented.

References:

- Legiehn GM, Heran MK, *A Step-by-Step Practical Approach to Imaging Diagnosis and Interventional Radiologic Therapy in Vascular Malformations*. Semin Intervent Radiol, 2010. 27(2): p. 209–31.
- Burrows PE, Mason KP. Percutaneous treatment of low-flow vascular malformations. J Vasc Interv Radiol 2004; 15:431–434.
- Brouillard P, Vikkula M. Genetic causes of vascular malformations. Hum Mol Genet. 2007 Oct 15;16 Spec No. 2:R140-9.

Vascular Interventional Procedures in Children: Tips to Optimal Management

Manraj Heran, MD

Pediatric vascular disease is extremely varied, with a wide range of conditions requiring diagnostic or therapeutic intervention. Technological improvements in non-invasive imaging modalities such as MRI and CT have reduced the need for diagnostic angiography; however, with advances in interventional techniques, arteriography in the pediatric patient is now often performed for therapeutic reasons.

Pediatric arteriography presents unique issues and challenges. Tremendous variability in patient size and physical maturity limits the ability to standardize technical aspects of performing arteriography. In addition, radiation protection, sedation/anesthetic support, monitoring of fluid balance, and maintaining patient warmth must be considered. A regimented protocol for assessment of the pediatric patient must be followed, with review of the indications for the study requested, and review of patient-specific issues such as coagulation profile, concurrent medical disease, patient weight, and anesthetic concerns. Appropriate patient monitoring is imperative to ensure patient safety.

Vascular access can be quite challenging. Ultrasound and micropuncture access techniques have tremendously improved successful access while reducing associated complications. The smallest catheter that can accomplish procedure objectives should be used. For most diagnostic cases, 4 French systems can be used for children >10 kilograms, while 3 French catheters are preferred in those <10 kg. Intra-procedural heparinization (75–100 IU/kg) is also more often used, especially in children weighing less than 10–15 kg.

Rates and volumes of contrast injected for pediatric arteriography are not standardized, as in adult patients. In general, contrast dose should be limited to 6–8 mL/kg, and 4–5 mL/kg in premature infants and neonates.

References:

- MK Heran, F Marshalleck, M Temple, et al, and the members of the Standards of Practice Committee. Quality Improvement Guidelines for Pediatric Arterial Access and Arteriography. JVIR and Pediatric Radiology, 2010.

Non-vascular Interventional Procedures in Pediatric Patients: What is New?

Joao G. Amaral, MD

Pediatric interventional radiology has evolved from diagnostic angiography alone to multiple image guided minimally invasive procedures in children.

Interventional angiography, vascular access, gastrointestinal access, drainages and biopsies were the first areas that pediatric interventional radiologists (IR) adopted. New devices, better imaging equipment, new imaging modalities, research and experience allowed pediatric IR to develop new techniques and procedures.

Nowadays, some of the new non-vascular procedures offered by pediatric IR include:

- Botulin toxin injection into salivary glands (off-label use) to reduce drooling symptoms in children with cerebral palsy and significant sialorrhea;
- Use of fibrinolytics in complex and loculated pleural effusions to improve drainage, reduce hospital stay and avoid surgical intervention;
- Thoracic duct embolization in patients with severe chylothorax that does not respond to medical measures to stop drainage of chyle;
- Topical application of Mitomycin C to inhibit fibroblast proliferation and reduce scarring in recurrent esophageal strictures;
- Balloon dilatation of bowel in patients with post-surgical strictures to avoid surgical reintervention;
- Percutaneous transhepatic cholecystocholangiography (PTCC) to assess patency of the biliary tree in neonates with suspected biliary atresia;
- Cecostomy tube insertion in incontinent patients (anorectal malformations, spina bifida, etc) to provide an access for scheduled antegrade enemas and to help these patients become “socially” continent;
- Image guided steroid injections to improve precise delivery of the steroid in the target and to reduce the incidence of complications (e.g. subcutaneous fat atrophy, tendon rupture);

- Magnetic resonance (MR) guided biopsies of bone marrow lesions, soft tissue (muscle, liver, kidneys, etc) lesions identified only on MR imaging to reduce sampling errors and radiation exposure;
- Thermal therapies such as laser or radiofrequency ablation of osteoid osteomas and cryoablation of renal tumors;

All these new techniques are less invasive, improve patients' outcomes and reduce morbidity. They are also cost-effective as patients are discharged home earlier and recover faster from the intervention.

The future holds promising new technologies such as High-Intensity Focused Ultrasound (non-invasive method of thermal ablation) and nanoparticles for drug delivery. Pediatric interventional radiology will continue to be an essential part of these minimally invasive therapies.

Musculoskeletal Imaging: From Planning to Performance

Imaging of Pediatric Bone and Soft Tissue Tumors: Techniques and Advances

Kirsten Ecklund, MD

The purpose of this talk is to review advanced MR imaging techniques currently being used in the evaluation of pediatric musculoskeletal tumors. The goals of these techniques include improved image resolution and quality, lesion tissue characterization, and increased acquisition speed. Diffusion-weighted (DW) and perfusion imaging will be emphasized; however, whole body, metallic artifact mitigation, and volumetric sequences will also be discussed.

DW MRI is based upon the Brownian motion of water within extra and intra-cellular spaces which depends upon tissue cellularity. DWI can aid in the differentiation of benign from malignant lesions, which generally have restricted diffusion. There is even greater potential for DWI in the assessment of tumor response to therapy. The apparent diffusion coefficient (ADC) maps are critical to accurate interpretation of diffusion sequences. ADC maps distinguish between restricted diffusion and T2 effect, both of which appear bright on DWI. Both qualitative and quantitative tissue assessments can be made with DWI. Challenges for DWI in the pediatric musculoskeleton include susceptibility artifacts from bone, motion vulnerability, and geometric distortion at larger fields of view. Our current protocols and parameters for DWI will be presented. Contrast-enhanced (DCE) MR using one of a variety of vendor specific sequences. Qualitative and quantitative assessments of inflow and distribution of contrast have been shown to help differentiate between benign and malignant lesions and to evaluate drug efficacy during therapy. This technique is

especially promising in those patients undergoing antivasculature and antiangiogenic therapy.

Imaging of Congenital and Developmental Abnormalities of Early Childhood

Tal Laor, MD

Congenital abnormalities of the musculoskeletal system can result in alterations of limb size, configuration, and/or segmentation. These disorders often affect both the osteocartilaginous skeleton as well as the surrounding soft tissues and can be localized or diffuse. In this session, we will focus on the imaging features of several congenital abnormalities that result in a small or short limb, in altered configuration of a limb, or in abnormal segmentation. Deformities of both upper and lower limbs will be examined.

Like congenital abnormalities, developmental disorders of the pediatric musculoskeletal system can be limited to a single area or can affect numerous sites within the body. For example, neonatal brachial plexopathy is a localized disorder that produces characteristic musculoskeletal alterations about the shoulder girdle and elbow of affected children. The alterations of morphology and function of the shoulder develop over time with growth of the child and change in response to a variety of therapies. We will review the features of developmental anomalies of the pediatric musculoskeletal system and evaluate the role that imaging plays in the initial evaluation and in the subsequent assessment of these children during treatment.

Multimodality Imaging of Skeletal Trauma in Children: Using All of the Tools

Peter J. Strouse, MD

Skeletal trauma is a common indication for imaging throughout the pediatric age range. Newborns may suffer birth trauma. Infants and toddlers may be subject to abusive injury. Children of all ages may suffer accidental injury. Older children and adolescents are increasing hurt in sporting activity and vehicular accidents. Fracture patterns vary with maturation of the child. Interference with normal growth is a potential complication.

Imaging of skeletal trauma begins with radiography. Proper anatomic and age specific radiographic technique assures optimal diagnostic yield. Radiography suffices in most cases to diagnose fracture or confirm normalcy. "Clinical correlation" aids in diagnosis. Ultrasound, CT, MRI and nuclear medicine may play a role in specific instances where plain radiographs are non-diagnostic or to better delineate certain fractures. Arthrography and conventional tomography have occasionally been used in the past and tomosynthesis may

prove useful. Follow-up radiographs may be useful for diagnosis or confirmation of some fractures.

This presentation will focus on the imaging of acute skeletal injury. Technique and approach for plain radiography will be emphasized. Specific indications and roles for ancillary imaging techniques will be defined and illustrated with representative cases.

Cartilage Imaging: Indications and Techniques

Diego Jaramillo, MD, MPH

Imaging of cartilage is done both morphologically and functionally. Morphologic imaging of cartilage assesses whether the cartilage is preserved or destroyed and whether there are intracartilaginous abnormalities or associated disturbances in the adjacent bone or ligaments. Proton density images with or without fat suppression are the best way to obtain an overview of the status of cartilaginous structures. For physal cartilage imaging, increased signal intensity on water sensitive images can reveal occult trauma. 3-D gradient recalled (GRE) images demonstrate areas of transphyseal bony bridging and MIP reconstructions allow axial mapping of the bridge and quantification of the percentage of physis involved. Epiphyseal cartilage destruction due to infection, and acute or chronic trauma is best depicted with T2-weighted images. Gadolinium enhanced imaging detects transphyseal vascularity, an important predictor of growth disturbance particularly in Legg-Calve-Perthes disease. Infections limited to the epiphyseal cartilage in infants may also be best depicted after contrast administration. Articular cartilage loss is best seen on 3-D GRE images.

Functional evaluation of the cartilage is based on mapping of several MR parameters. T2 mapping reveals free water increases whenever there is breakdown of the collagen and glycosaminoglycans in the matrix.

Tuesday, April 17, 2012

Neuroimaging: From “What” to “How”

Imaging of Stroke in Children: What do We Need to Know for Optimal Management?

Avrum N. Pollock, MD, FRCPC

Although classically thought of as a disease of adulthood, stroke is much more common in the pediatric population than was once appreciated. This may be due to many factors, not the least of which is increased awareness due to the presence of subspecialty stroke teams now fairly commonplace in many children's hospitals, and the fairly recent advent of more advanced imaging technique such as diffusion-weighted imaging (DWI) and its routine use in imaging the central nervous system (CNS) in the child and adolescent.

Causes of stroke in children can be protean, and range from idiopathic on one end of the spectrum, to traumatic on the other, with many causes in between, many of which may not be intuitive to the clinician without further research. Moyamoya disease and its many causes, such as sickle cell disease (SCD), trisomy 21 and neurofibromatosis type I (NF I) can all lead to stroke in children, as can congenital clotting deficiencies such as Factor V Leiden deficiency and congenital cardiac lesions with their resultant shunting of blood between the left and right cardiac circulations.

Although usually arterial in nature, strokes may arise from the venous system in clinical scenario of venous thrombosis with resultant venous infarctions. Factors contributing to venous thrombosis in children and adolescents can be due to dehydration (especially in the very young), severe iron deficiency anemia, inflammatory bowel disease and exogenous hormone ingestion such as is seen with oral contraceptives (OCP) in young women.

Advanced Imaging Techniques for Neuroimaging in Pediatric Patients: Where Are We Now?

Blaise V. Jones, MD

The past decade has seen a large number of advanced imaging techniques introduced to the clinical armamentarium of the pediatric radiologist. From the development of multidetector CT scanners that can obtain whole head diagnostic studies in less than 2 s to the routine use of 3 T MR imaging, technical advances have dramatically changed our ability to diagnose and manage neurological disorders in children. However, all of these advances are not of equal clinical utility, and it is imperative that the pediatric radiologist be well versed in their judicious and appropriate application. This presentation will discuss the effective use of volume CT scanning, CTA, SWI, ASL, fMR, pMR, and other advanced imaging techniques in the diagnosis of neurological disorders presenting in childhood. At the conclusion of the presentation the attendee will have a better understanding of how to ideally apply these technologies in practice.

A Spectrum of Abnormality in Pediatric Neck: Practical Imaging Choices and Interpretation

Caroline D. Robson, MBChB

Learning Objectives:

1. Become familiar with an optimized imaging approach for head and neck infections
2. Recognize the complications of head and neck infections
3. Recognize the utility and interpretation of imaging for neck masses

This talk will cover the imaging approach and interpretation of findings in head and neck infection and neck masses. Infection includes acute complicated sinusitis, coalescent mastoiditis, neck infection and local and intracranial complications. Optimized imaging protocols and image interpretation for neck masses will also be discussed and illustrated.

Acute complicated sinusitis is diagnosed when acute sinusitis is accompanied by orbital symptoms (e.g. proptosis) and/or mental status changes, seizures or other neurological findings. Coalescent mastoiditis is diagnosed when otomastoiditis is accompanied by tenderness and/or swelling over the mastoid process. CT and MR provide complementary information. CT is obtained with contrast. MR sequences include fat-suppressed T2, T1, diffusion, and fat-suppressed contrast-enhanced T1 weighted images with MR venography. Intracranial complications include epidural abscess, subdural empyema, meningitis, cerebritis, brain abscess, venous thrombosis and venous infarction. The limitations and usefulness of CT in the diagnosis of neck abscess will be illustrated.

The imaging approach to masses depends on patient age, and the size and location of the mass. US, CT, MR, and nuclear medicine studies provide complementary information. As for infection, optimized imaging approaches and key imaging features for various masses will be discussed.

Embryology and Diagnostic Approach in Spinal Dysraphism

L. Santiago Medina, MD, MPH and Esperanza Pacheco-Jacome, MD

Congenital anomalies of the spine are malformations that can be confusing due to the complexity of their embryology, and to the sometimes unclear classifications and terminology.

The purpose of this review is to give a clear and basic understanding of the different stages of the embryological development of the spinal cord, starting with the bilaminar disc in the first week of gestation. During the second week, the formation of a trilaminar disc (gastrulation), the notochord, and the formation of the neural tube or neurulation. Also, a review of the development of the distal cord: conus medullaris, filum terminale, ventriculus terminalis, by a different mechanism, canalization and retrogressive differentiation.

Beside the embryological review, a case correlation will be presented using MR imaging to demonstrate these malformations.

Open spina bifida entities include meningocele and myelomeningocele. Closed or occult spinal dysraphism (OSD) is characterized by a spinal anomaly covered with skin and

hence with no exposed neural tissue. OSD spectrum includes dorsal dermal sinus, thickened filum terminale, diastematomyelia, caudal regression syndrome, intradural lipoma, lipomyelocele, lipomyelomeningocele, anterior spinal meningocele and other forms of myelodysplasia.

Several studies have shown that MRI and ultrasound have better overall diagnostic performances (i.e., sensitivity and specificity) than plain radiographs for detection of occult spinal dysraphism.

The sensitivity of spinal MRI and ultrasound has been estimated at 95.6% and 86.5% respectively. The specificity of spinal MRI and ultrasound has been estimated at 90.9% and 92.9%, respectively. Conversely, the sensitivity and specificity of plain radiographs have been estimated at 80% and 18%, respectively.

Infectious Diseases of the World: From Review to Updates in Imaging

Viral Infections in Children: Beyond SARS and H1N1 Winnie C.W. Chu, MD, FRCR

Two major outbreaks of viral infection in the last decade: Severe Acute Respiratory Syndrome (SARS) in 2003 and Swine-origin influenza A (H1N1) pandemic in 2009 are reviewed, emphasizing their impacts on pediatric population.

Both SARS and H1N1 are highly contagious febrile respiratory illnesses caused by coronavirus and influenza A virus subtype respectively. There are similarities in clinical presentation and radiological features among the two conditions.

For SARS, children of age 12 or younger had milder disease when compared with adults, while teenagers resemble adults in disease progression and may develop acute respiratory distress. No pediatric mortality has been reported. Long-term follow up showed 32% children had mild CT abnormalities (ground glass opacities, air trapping and scar) 12 months after diagnosis and suboptimal aerobic exercise capacity at 36 months.

For H1N1, most patients had mild illness but a small percentage required mechanical ventilation and ICU admission. The high risk groups include children <5 years old and those with chronic medical conditions in particular neurodevelopmental impairment. Pediatric mortality was 7.5% of all deaths associated with the pandemic reported in the U.S.

In both conditions, the most prominent radiographic and CT features were airspace disease including ground glass opacities (GGO) and consolidation, commonly with multi-focal and

bilateral involvement. Pleural effusion, adenopathy and cavities were absent. In some patients with viral infection, respiratory symptoms may be mild but are complicated by neurological manifestations. A brief review of MRI features in H1N1 related encephalopathy including acute necrotizing encephalopathy (ANE) will be given.

Pediatric TB Infection: Current Status and Updates

Bernard F. Laya, DO

Tuberculosis (TB) is a worldwide major public health problem with one-third of the world's population being infected. It is a leading cause of death and disability from infection worldwide. Children are amongst the most vulnerable group because of their immature immune status. A child usually gets TB infection after being exposed to a sputum-positive adult. Depending on many factors, the infection can lead to latency or TB disease. It can affect virtually any organ in the body and can be devastating if left untreated.

TB in children remains a diagnostic challenge. In addition to history of TB exposure, signs and symptoms, laboratory and microbiologic tests, medical imaging remains a valuable tool in its diagnosis. Although findings are nonspecific, the radiograph is the most commonly ordered initial imaging tool for screening and diagnosis of pulmonary and musculoskeletal involvement. Computed tomography and magnetic resonance imaging offer more detailed assessment especially in cranial and abdominal involvement. Medical imaging is also utilized to follow up patients during or after anti-TB treatment. Knowledge of the common imaging patterns, pitfalls and dilemma are very important in establishing the diagnosis of TB in children.

The pathophysiology of pediatric TB will be discussed as it correlates with imaging findings. The wide spectrum of imaging manifestations in various modalities will be presented. Imaging updates along with pitfalls and dilemma in the interpretation will also be discussed. TB can affect almost every organ system but the author will present cases that are more commonly encountered.

The World of Parasites: Overview of Imaging Findings

Pedro A. Daltro, MD

Parasites are living organisms that exist by obtaining the nourishment produced by other living organisms. Parasitic disease represents one of the most common types of infection in the world. It causes substantial morbidity and mortality particularly in pediatric patients living in endemic areas or developing countries. A broad spectrum of parasitic infections can affect pediatric patients including protozoa (amebiasis, malaria, trypanosomiasis), nematodes (ascariasis, strongyloidiasis, dirofilariasis), cestodes (cystic echinococcosis), and

trematodes (schistosomiasis, paragonimiasis). Early and accurate diagnosis is important for proper management of pediatric patients infected with these various parasitic infections. Imaging evaluation plays an important role for prompt diagnosis and monitoring children with parasitic disease. The overarching goal of this presentation is to review the epidemiologic, clinical, physiopathologic, and imaging characteristics of various parasitic infections that frequently affect pediatric patients. Knowledge of how these various parasitic infections can clinically present as well as how they appear on imaging studies can prevent misdiagnosis or delayed diagnosis, and thus optimize pediatric patient care.

Infectious Diseases of Africa: Facing the Challenge

Omolola M. Atalabi, MD

Despite advances in diagnosis and treatment, infectious disease continues to be the major cause of morbidity and mortality particularly in children living in Africa. Infectious disease is currently responsible for up to 68% (6 million) out of 8.8 million deaths occurring in children under the age of 5 years old globally. Approximately two-thirds of these deaths occurred in children in Africa in 2008. The top five major infections that account for these African pediatric deaths include pneumonia, HIV/AIDS, tuberculosis, malaria, and diarrhea. Early and accurate diagnosis is important for proper management of children with these infectious diseases. Imaging evaluation plays an important role. However, there are currently many challenges in Africa which include: 1) lack of both basic and advanced imaging equipment and facilities; 2) insufficient number of dedicated pediatric radiologists; and 3) limited educational opportunities for radiologists interested in taking care of children. The overarching goal of this presentation is to discuss the current status of infectious disease in the children of Africa and role of pediatric radiologists. With this background information, future plans for improving care of children with infectious disease in Africa may be hopefully and optimally established.

SCIENTIFIC PAPERS

Paper #: PA-001

FDG PET/CT Imaging in Pediatric Patients with Spinal Hardware for FUO or Suspected Spinal Infection

Brian Bagrosky, MD, MS, *Childrens Hospital Colorado - Radiology*, Brian.Bagrosky@childrenscolorado.org; Kari Hayes, Laura Z. Fenton, Franklin Chang

Purpose or Case Report: Evaluation of fever, elevated inflammatory markers and/or back pain in the pediatric patient following spinal fusion with hardware is challenging due to

inability to utilize CT or MRI secondary to hardware artifact. Purpose: To study the utility of FDG PET/CT in pediatric patients with spinal hardware and concern for infection.

Methods & Materials: FDG PET/CT scans in pediatric patients with spinal fusion hardware and suspected spinal infection or fever of unknown origin from 12/2008 through 10/2011 were performed. Results were correlated with clinical, surgical and laboratory data.

Results: A total of 23 FDG PET/CT scans in 19 patients ranging in age from 6 years to 31 years (mean 16.9 years \pm 5.5) were identified and reviewed. 10 patients were female. The patients' medical records were reviewed for presenting symptoms, inflammatory marker levels, surgical and pathology reports. A total of five patients (26%) were diagnosed with spinal hardware infection proven by positive culture and gross purulent fluid at surgery. All five of these patients had FDG PET/CT studies highly suspicious for infection with increased FDG uptake along the hardware and paraspinal muscles. Mildly increased FDG uptake was seen in two patients (11%) with proven hardware loosening, one with hardware metallosis, and other with anterior lumbar pseudoarthrosis. Other infectious etiologies diagnosed on the FDG PET/CT scans were pneumonia in 3 patients and superficial wound infection in 2. Six patients had negative FDG PET/CT scans for infection, one subsequently diagnosed with endocarditis.

Conclusions: FDG PET/CT diagnosed all 5 cases of surgically proven spinal rod infection in our series of 19 patients. Other causes of back pain including hardware loosening and superficial incision/wound infection were also reliably diagnosed. PET/CT identified an alternate infection, pneumonia, in three patients. FDG PET/CT is a reliable test in patients with spinal hardware and FUO and/or suspected spinal infection.

Paper #: PA-002

The Role of PET-CT in the Evaluation of Pulmonary Nodules in Children with Solid Malignancies: A Pilot Study

Beth McCarville, MD, St. Jude Children's Research Hospital, beth.mccarville@stjude.org; Robert Kaufman, Stephen Shochat, Catherine Billups, Jianrong Wu, Barry Shulkin

Purpose or Case Report: To assess the feasibility of performing PET-CT for evaluation of pulmonary nodules in children with solid malignancies and to obtain preliminary data regarding the accuracy of PET-CT compared to CT for distinguishing benign from malignant histology.

Methods & Materials: This IRB approved prospective study included subjects from birth to 21 years of age with solid malignancies and pulmonary nodules ≥ 0.5 and ≤ 3.0 cm.

Twenty-five subjects with 75 nodules (30 biopsied, 45 observed) underwent CT and PET-CT within 3 weeks apart. Nine radiologists and nuclear medicine physicians comprised 3 panels that reviewed CT only, PET-CT only and CT and PET-CT concurrently. Reviewers independently and then by panel consensus predicted nodule histology. Inter-reviewer agreement for each panel was assessed by Cohen's kappa coefficient. The overall accuracy and worst case sensitivity and specificity (i.e. considering indeterminate predictions as incorrect) for each panel were determined by comparing consensus predictions to histology or clinical assessment of observed nodules.

Results: There were 13 males and 12 females, median age 14.4 years (range, 2.9–21.8). Of the 75 nodules, 48 were malignant and 27 benign. Five nodules seen on CT were not visible on the attenuation correction CT obtained for PET-CT. Three additional nodules were obscured by atelectasis caused by sedation for PET-CT. There was moderate inter-reviewer agreement for the CT panel ($\kappa=0.43$) and fair agreement for the PET-CT ($\kappa=0.22$) and concurrent CT/PET-CT ($\kappa=0.33$) panels. There were more indeterminate nodule predictions by PET-CT ($n=38$ of 75; 51%) and concurrent CT/PET-CT ($n=23$; 31%) than by CT alone ($n=12$; 16%). The overall accuracy of CT alone was 71%, PET-CT alone 45% and concurrent review 60%. Worst case sensitivity and specificity were 85% and 44% for CT alone, 60% and 19% for PET-CT alone, and 67% and 48% for concurrent CT/PET-CT.

Conclusions: PET-CT assessment of pulmonary nodules in children is feasible but limited by non-diagnostic quality CT images and atelectasis caused by sedation. Subjective assessment of nodules by PET-CT does not appear to improve the ability to distinguish benign from malignant histology in children with solid malignancies. Semi-quantitative nodule assessment using the standardized uptake value may improve the performance of PET-CT in this setting and will be investigated in the future.

Paper #: PA-003

Twenty-Four Hour Imaging and SPECT for Increased Accuracy of Biliary Scintigraphy for Detection of Biliary Atresia

Gerald Mandell, MD, Radiology, Phoenix Children's Hospital, gmandell@phoenixchildrens.com; Smita S. Bailey

Purpose or Case Report: Hepatobiliary scintigraphy (HBS) is the primary tool for diagnosis of biliary atresia (BA) and its differentiation from medical causes of hyperbilirubinemia that do not require surgical intervention. This study explores whether 24 h delayed and SPECT imaging improves diagnostic accuracy for the exclusion of BA.

Methods & Materials: A retrospective analysis of 146 HBS studies on 144 patients ages 7 days to 5 months was performed following 3–5 day pretreatment with Phenobarbital. Standard HBS imaging included 30 min, 45 min, 4–9 h and 24 h (when no gastrointestinal activity [GIA] was detected) planar images. In 12 cases 24 h single photon emission computed tomography (SPECT) was also performed when discrete GIA was not seen.

Results: HBS standard imaging without 24 h or SPECT had specificity of 82% and accuracy of 83%. GIA was seen in 22 additional patients on delayed imaging at 24 h. With the addition of SPECT four additional patients with GIA were detected. 24 h imaging with SPECT showed specificity 98%, accuracy 98%; 24 h imaging without SPECT 93%, 93% and with SPECT alone specificity 88%, accuracy 92%. Sensitivity for standard, 24 h delayed and SPECT imaging was 100% (There were no false negatives).

Conclusions: The addition of 24 h imaging and SPECT to HBS significantly improves the diagnostic accuracy compared to standard imaging as well as SPECT or 24 h planar imaging alone. HBS does play a significant role in differentiating medical causes of hyperbilirubinemia from biliary atresia.

Paper #: PA-004

Comparison of Postoperative Radioactive Iodine Ablation of Thyroid Remnants Between Pediatric and Adult Patients with Thyroid Carcinoma

Joyce Mhlanga, MD, *Division of Nuclear Medicine, Johns Hopkins University Hospital, jmhlang1@jhmi.edu*; Behnaz Gourdazi, Richard Wahl, David Cooper, Paul Ladenson, Paco E. Bravo

Purpose or Case Report: Differentiated thyroid cancer (DTC) is an uncommon malignancy with usually excellent outcomes in the pediatric and young adult population following thyroidectomy and sometimes neck dissection and/or radioactive Iodine-131 ablation (RAI) therapy. We aimed to investigate the disease characteristics and ablation rates between pediatric and adult populations.

Methods & Materials: We retrospectively reviewed pediatric and adult patients with DTC who had undergone total thyroidectomy and first RAI therapy between 2001 and 2010. None had distant metastatic disease prior to RAI. Patients were prepared with either recombinant human (rh) TSH or thyroid hormone withdrawal prior to diagnostic and follow-up Iodine-123 whole body scan (I-123WBS) and RAI. Successful ablation was defined (>8 months later) as no visible thyroid bed uptake, or if visible, neck uptake <0.1% on I-123WBS and/or stimulated serum thyroglobulin (Tg) <2 ng/mL at initial follow-up.

Results: 24 pediatric patients (20 F, 4 M) mean age 16.5±6.7 years (range 8–21) were evaluated. All were stage 1 with an

average tumor size of 3±5.1 cm. 12 had conventional papillary carcinoma (PTC), 9 follicular variant, 2 follicular carcinoma, and 1 well-differentiated Hurthle cell carcinoma. 83 adult patients (49 F, 34 M), mean age at diagnosis 53.5±24 years (range 27–83) were evaluated. 55% had stage 1; 13% stage 2; 24% stage 3 and 7% stage 4 disease. Average tumor size was 2.3±3.4 cm. Pathology included 51 PTC, 19 follicular variants, 5 follicular carcinomas, 6 aggressive PTC variants and 2 Hurthle cell carcinomas. Average RAI dose was 89±73 mCi in children; and 85±63, mCi in adults (p value 0.59). The ablation failure rate was 20.8% (5/24) in children based on 4.2% with I-123 neck uptake >0.1%, and 16.7% with Tg >2 ng/ml and/or I-123 uptake. In adults, the ablation failure rate was 20.5% (17/83), based on 10.8% with I-123 neck uptake >0.1%, and 9.6% with elevated Tg and/or I-123 uptake. Successful rhTSH-stimulated ablation was achieved in 90% (9/10) children (one with residual 0.13% uptake) and 87% (20/23) adults (2 with detectable Tg, and 1 with 0.3% uptake). On follow-up median Tg was 0.2 ng/ml in children; and 0.4 ng/ml in adults (P value 0.45).

Conclusions: The post-RAI ablation rate was similar between pediatric and adult patients with DTC and no evidence of distant metastatic spread. No significant differences were found in the RAI dose and post-ablation thyroglobulin levels between children and adults.

Paper #: PA-005

Ultrasound as First Modality to Evaluate for Midgut Volvulus

Mostafa Youssfi, MD, *Radiology, Phoenix Children's Hospital, myoussfi@phoenixchildrens.com*;

Purpose or Case Report: To assess the accuracy of ultrasound in the diagnosis of midgut volvulus

Methods & Materials: 25 patients aged 2 days to 14 years with suspected midgut volvulus underwent gray scale and color Doppler ultrasound. Midgut volvulus was diagnosed when a Whirlpool sign was observed: clockwise wrapping of the bowel, mesentery and mesenteric vessels around the superior mesenteric artery when the transducer was moved in caudal direction starting at the origin of the SMA. The findings were correlated to surgery, Upper GI or both.

Results: The Whirlpool was present in 12 patients, all confirmed surgically. It was absent in 13 patients, 5 of which had elective surgery for other reasons (duodenal web, pyloric stenosis, necrotizing enterocolitis, malrotation without volvulus). 7 had Upper GI Examinations. 1 patient with negative ultrasound did not undergo UGI nor surgery. -The Sensitivity was 100%. The specificity was 100%.

Conclusions: Ultrasound is very accurate and should be considered first when midgut volvulus is suspected.

Paper #: PA-006**Feeding Intolerance in Premature Infants After Medically Managed Necrotizing Enterocolitis (NEC): Are Findings on Abdominal Radiographs Predictive of Findings on Contrast Enemas?**

Beth Anne Cavanaugh, *University of Cincinnati College of Medicine*; Steven J. Kraus

Purpose or Case Report: NEC is the most common life-threatening medical/surgical emergency of the gastrointestinal (GI) system in neonates, with an incidence up to 10% in infants weighing <1500 g. With advances in treatment of NEC, increased survival rates result in rise in post-NEC GI complications such as feeding intolerance. Development of post-NEC bowel strictures results from healing of involved bowel and can result in bowel obstruction. It has been routine to study the bowel of infants after medical treatment for NEC by contrast enema and small bowel follow-through prior to initiating feeding. However, in order to “Image Gently” we are attempting to decrease the radiation exposure to these patients. We postulate that in patients with no abnormal bowel dilation prior to initiation of feeds, the incidence of colonic stricture would be so low that routine enemas would be unnecessary and could be eliminated from the workup.

Methods & Materials: IRB exemption for retrospective study was obtained. The study population was obtained by searching the Medical Notes Search engine from our hospital database which includes radiology, pathology, and surgery reports. A list of neonates with the diagnosis of NEC was created searching from years 1995–2011. Patients were excluded if they had abdominal surgery or those with questionable NEC status. 128 neonates fit the study criterion. Radiographs and contrast enemas were reviewed by an experienced staff Pediatric Radiologist/fluoroscopist. Data collected on radiographs included presence or absence of bowel dilation, bowel thickening, gasless abdomen, soft tissue mass, and calcifications. Data on enemas included presence or absence of bowel stricture(s) and if present, the location of stricture in colon or small bowel.

Results: Preliminary data have been analyzed for the first 48 of 128 patients. Colonic strictures were seen in 16(33%) patients with medical NEC. On pre-enema radiographs: 31 patients had bowel dilation and 10 of them (32%) had colonic strictures; 17 patients had NO bowel dilation and 6 of these (35%) had colonic strictures.

Conclusions: Our preliminary results were unexpected. In patients treated for medical NEC who presented to fluoroscopy with feeding intolerance, 35% of patients with abdominal radiographs showing no sign of bowel obstruction (no dilated bowel loops) were shown to have colonic stricture by contrast enema. Despite our anecdotal experience, we will

continue to perform contrast enemas in the workup of feeding intolerance following medically treated NEC.

Disclosure: Dr. Kraus has indicated that he is an author for Amirsys and receives a royalty accordingly.

Paper #: PA-007**Relative Anatomic Distribution of Pertinent Findings on Neonatal Portable Abdominal Radiographs: Can We Shield the Gonads?**

Matthew Winfeld, *Radiology, NYU Langone Medical Center*, matthew.winfeld@nyumc.org; Nancy Fefferman, Naomi Strubel, Lynne Pinkney, Shailee Lala, James Babb

Purpose or Case Report: To assess distribution of pertinent findings on neonatal portable abdominal radiographs and their frequency in regions that would potentially be obscured by shielding.

Methods & Materials: With IRB approval, 501 portable neonatal abdominal radiographs acquired in 2010 without gonadal shielding were randomly identified using the radiology department database. Radiographs were reviewed by consensus on PACS by 4 experienced pediatric radiologists. Pertinent radiographic findings (abnormal bowel, bowel gas paucity, free air, pneumatosis, portal venous gas, calcifications, inguinal hernia, osseous abnormalities, catheter/tube tips) were recorded as present or absent in 6 anatomic abdominal regions defined as: 1 and 2—from the dome of the diaphragm to top of L2 to the right and left of midline, respectively; 3 and 4—from top of L2 to the iliac crest to the right and left of midline, respectively; 5—from the iliac crest to the top of the sacrosclatic notch; 6—below the top of the sacrosclatic notch. We assessed the frequency of findings in each region and how often findings in regions 5 and 6 were associated with findings in regions 1–4. 95% confidence intervals were calculated.

Results: The fewest pertinent findings were present in region 6 in 10.2% (51/501) (95% CI: 7.7–13.1%) of radiographs. Findings included: abnormal bowel 6% ($n=31$), bowel gas paucity 1.4% ($n=7$), pneumatosis 0.4% ($n=2$), inguinal hernia 0.8% ($n=4$) and osseous abnormalities 1.2% ($n=6$). Pertinent findings were present in region 5 in 67.7% (339/501) (95% CI: 63.4–71.8%). Findings included: abnormal bowel 43.7% ($n=219$), bowel gas paucity 19.6% ($n=98$), pneumatosis 1.6% ($n=8$), free air 0.2% ($n=1$), and abnormal bowel with pneumatosis 2.6% ($n=13$). Among 51 patients with an abnormality in region 6, 49 (96.1%) also had an abnormality within at least one of regions 1 through 4. Among the 342 patients with an abnormality in region 5 or 6, 338 (98.3%) also had an abnormality within at least one of regions 1 through 4. Catheter/tube tips were located in region 5 in 6.8% ($n=34$) and region 6 in 1.4% ($n=7$) of radiographs, respectively. Pneumatosis was present most frequently in regions 3 (5.8%), 4 (4.0%), and 5

(4.2%). Free air was present most frequently in regions 1 (1.6%), regions 2 and 3 (0.6% each).

Conclusions: Our preliminary data suggest that pertinent findings on neonatal portable abdominal radiographs are rarely isolated to the pelvis, implying that gonadal shielding of regions 5 and 6 should not compromise diagnostic accuracy.

Paper #: PA-008

Prediction of Appendicitis on Ultrasound Using Three Diagnostic Categories: Positive, Negative, and Equivocal

Shelby Fierke, MD, Cincinnati Children's Hospital Medical Center; *shelby.fierke@gmail.com*; David B. Larson, Sheila Salisbury, Alexander J. Towbin

Purpose or Case Report: The purpose of this study was to determine the sensitivity, specificity, and positive and negative predictive value of ultrasound in diagnosing appendicitis when the appendix is visualized, using three diagnostic categories: positive, negative, and equivocal. The 3-category diagnostic accuracies for appendiceal diameter and radiologist impression were compared.

Methods & Materials: A retrospective study was performed evaluating all right lower quadrant ultrasound reports dictated over a 5-month period. Included studies were interpreted as positive, negative, or equivocal for appendicitis. Report impressions that did not specify one of these categories and studies where the appendix was not seen were excluded. The pathologic diagnosis of appendicitis was considered the gold standard for a positive diagnosis. Because virtually all pediatric surgical cases in the region are referred to our hospital, it was assumed that the patient did not have appendicitis if surgery was not performed. Logistic modeling using appendiceal diameter as the independent variable established cutoff diameters of ≤ 6 mm=negative, > 8 mm=positive, and $6 < x \leq 8$ mm=equivocal. Sensitivity, specificity, and positive and negative predictive values were calculated for both methods.

Results: Of the 571 patients imaged during the study period, 255 (45%) met the inclusion criteria; 34 (6%) reports did not categorize the impression and in 282 (49%) studies the appendix was not seen. Surgery was performed on 122 (48%) subjects, of which 101 (83%) had a pathologic diagnosis of acute appendicitis. Using the radiologist impression, there were 68 true positives (TP), 2 false positives (FP), 8 false negatives (FN), and 150 true negatives (TN), for a sensitivity of 97% (95% CI=90–100%), specificity of 95% (CI=90–98%), PPV of 89% (CI=80–95%), and NPV of 99% (CI=95–100%). There were 27 (11%) cases reported as equivocal; of these, 7 (26%) had a pathologic diagnosis of appendicitis. Using appendiceal diameter, there were 46 TP, 6 FP, 2 FN, and 161 TN, for a sensitivity of 88% (CI=77–96%), specificity of 99% (CI=96–100%), PPV of 96% (CI=

86–99%), and NPV of 96% (CI=92–99%). There were 41 (16%) cases categorized as equivocal; of these, 25 (61%) had a pathologic diagnosis of appendicitis.

Conclusions: The use of diagnostic categories enables high PPV and NPV with a relatively low number of equivocal cases. Using appendiceal diameter alone results in higher PPV than that of the radiologist impression, but also yields a higher number of equivocal cases.

Paper #: PA-009

MRI of Right Lower Quadrant Pain in Pediatric Patients with Inconclusive Appendix US: Initial Experience

Thaddeus Herliczek, MD, MS, Diagnostic Imaging, Brown University; *Thaddeus_Herliczek@brown.edu*; David Swenson

Purpose or Case Report: Demonstrate the role of appendix magnetic resonance imaging (MRI) in evaluation of pediatric patients with right lower quadrant (RLQ) pain and inconclusive appendix sonography (US).

Methods & Materials: IRB approval was obtained. Appendix MRI and medical records of patients for whom appendix MRI was acquired following inconclusive appendix US were reviewed retrospectively. 36 patients (16 M: 20 F, age 7–17 yrs, ave. age 13.9 yrs) were included. MRI performed in 1.5 T or 3 T units (25 patients at 1.5 T, 11 patients at 3 T). All exams were acquired without contrast media, included a single plane short inversion time inversion recovery (STIR) sequence and included coronal T2-weighted 3-Dimensional-turbo-spin-echo sequence (SPACE) with multiplanar reconstructions and/or T2-weighted single-shot turbo-spin-echo (HASTE) without fat saturation in multiple planes. Most (28 of 36) exams included an axial true FISP sequence. FOV was from the renal inferior poles thru the urinary bladder. MRI were evaluated by two radiologists and interobserver agreement assessed. MRI findings were compared with operative notes, pathology reports and electronic medical records.

Results: The appendix was identified in 29/36 MRI (81%) by observer 1 and in 34/36 MRI (94%) by observer 2. Appendicitis was diagnosed in 7 cases by each radiologist (Kappa=1 [Pe 0.69]). Cases of acute appendicitis were verified histologically with 1 false positive. Each radiologist noted a distended appendix (> 8 mm diameter), mural edema and periappendiceal inflammatory change in the cases of acute appendicitis. Patients without acute appendicitis did not demonstrate inflammatory changes on the STIR sequence. None of the MRI was equivocal regarding acute appendicitis. No false negatives noted on review of patients' electronic medical records. MRI sensitivity / specificity for appendicitis were 100% / 97%. MRI demonstrated an alternate cause of pain in 3 patients.

Conclusions: Appendix MRI has similar sensitivity and specificity to CT for pediatric appendicitis, without the risks of ionizing radiation and intravenous contrast. Interobserver agreement for the presence of acute appendicitis on MRI is excellent. Absence of inflammatory changes on MRI excludes acute appendicitis even when the normal appendix is not identified. Appendix MRI can replace computed tomography in assessment of pediatric patients with RLQ pain and inconclusive appendix US.

Paper #: PA-010

Impact of Substituting US for CT in the Initial Evaluation of Appendicitis: A Quantitative Assessment

John Strain, MD, Children's Hospital Colorado, John.Strain@Childrenscolorado.org; Lalit Bajaj, Sara Deakne

Purpose or Case Report: This study quantifies the effect of replacing (CT) with Ultrasound (US) as the initial imaging modality for suspected acute appendicitis in children. In addition, the study tests the application of an analytic cost effective decision support model to clinical practice.

Methods & Materials: The five month pilot initiative substituted US for CT as the first imaging study for suspected appendicitis. The preceding five months served as control. A positive US resulted in surgical intervention. An equivocal US prompted surgical consultation or CT. Data analysis included CT, ultrasound and medical records. Pilot and control data were validated against imaging and clinical data from the same ten month period the previous year.

Results: ED encounters, number of patients suspected of appendicitis, percent with surgically proven appendicitis were similar. There were 490 patients in the control group and 487 in the pilot evaluated for appendicitis. The number of CTs decreased from 210 to 173 (23%). Ultrasound examinations increased from 55 in the control period to 166 (183%). Overall, cross-sectional imaging increased by 13%. There were 125 cases of path-proven appendicitis in the control group and 114 in the pilot. US was equivocal in 90 of 166 (54%). 45 of the 90 were discharged from the ED without surgical consultation and without subsequent CT. Compliance with the clinical care guidelines suggesting surgical consultation or CT following an equivocal US exam occurred in only 61%.

Conclusions: This study is unique because the defined start date for substitution of US for CT provided quantitative data on the impact of this recommendation. There was a 23% decrease in CT, a 183% increase in US and a 13% increase in cross-sectional imaging. The 61% compliance rate with the

“most cost effective imaging” recommendation from the Markov analytic model suggests the model does not transfer directly into clinical practice. In fact, the increased utilization of US would have resulted in a net increase in CT utilization over control had the recommendation been followed precisely.

Paper #: PA-011

Intraluminal Pressure Monitoring and Demonstration of Pressure Curves During Pneumotic and Hydrostatic Reduction of Intussusception: Preliminary Study

Bo-Kyung Je, Korea University Ansan Hospital, radje@korea.ac.kr; Sung-Bum Kim, Ki Yeol Lee, Sang Hoon Cha, Byung Min Choi

Purpose or Case Report: Intussusception is an obstructive condition that a segment of the bowel invaginates into adjacent bowel and is an urgency that needs to be reduced as soon as possible to prevent bowel ischemia or necrosis. When it occurs in the infants and young child, it usually develops idiopathically and reduced by the technique such as air enema under the fluoroscopic guidance or saline enema under the ultrasound guidance. The success rate of the non-surgical reduction has reported over 95%. The pneumatic reduction is to introduce air into the patients' rectum via a ballooned Foley catheter by hand pump. A mercury manometer connecting with the Foley catheter calibrates the pressure of insufflation, and the recommended maximum pressure is 120 mmHg. The hydrostatic reduction is to drip saline from a bag at the height of 3 ft that may be different according to the institute's guidelines. Until recently, in both techniques, the precise measurement of the intraluminal pressure was not possible. With the purpose of intraluminal pressure monitoring, we introduced a specific digital pressure gauge that can measure both pneumatic and hydrostatic pressure in various units and can give the collected data to our workstation. With the data, we purpose to make the curve of intraluminal pressure during the procedure and to compare the pattern and difference in both techniques of reduction, which permits suggesting the better technique for reducing the intussusception. From February 2011, we performed the intraluminal pressure monitoring in 8 children; 4 cases of pneumatic reduction and 4 cases hydrostatic reduction. The results indicated that the curves were similar in both techniques. However, the hydrostatic reduction tended to need longer time and higher pressure difference than the pneumatic reduction. We assumed that a higher flow rate and more fluctuating introduction of pressure in the pneumatic reduction made the difference between both methods.

Paper #: PA-012**Arterial Spin Labeling Cerebral Blood Flow as a Correlate of Clinically Significant Hydrocephalus in Children with Brain Tumors**

Robert Lober, *Stanford University, roblober@gmail.com*; Kristen Yeom, Allyson Alexander, Patrick Barnes, Michael Edwards

Purpose or Case Report: Hydrocephalus does not always directly correlate with ventricular size. Hydrocephalus, resulting in increased intracranial pressure (ICP), theoretically results in decreased cerebral blood flow (CBF), but this has not been previously quantified, and it is unclear whether CBF is restored when hydrocephalus is resolved. Arterial spin labeled (ASL) CBF is a magnetic resonance imaging (MRI) perfusion technique which uses inversion of proton spins in blood to quantify CBF. We hypothesized that ASL CBF would correlate with symptomatic hydrocephalus in pediatric patients with brain tumors.

Methods & Materials: Children presenting with elevated ICP from a new brain tumor diagnosis that had both baseline and follow-up ASL CBF MRI were retrospectively reviewed. ASL was performed using a pseudocontinuous labeling period of 1500 ms, followed by a 1500 ms post-label delay on 3 T MRI. Quantitative ASL CBF within each tumor was obtained by placing regions of interest (ROI) over the cerebrum. Patients were classified as symptomatic if they required surgical intervention for hydrocephalus (tumor resection or cerebrospinal fluid diversion) within seven days of the ASL MRI.

Results: Nine patients were identified (median age 6.5 years, range 0.2 to 17.3). Mean ASL CBF was significantly higher at symptomatic time points compared to asymptomatic time points in each patient (Symptomatic=25.0±10.8 ml/100 g/min, asymptomatic=35.9±10.5 ml/100 g/min, $p<0.05$).

Conclusions: ASL CBF was significantly reduced during symptomatic hydrocephalus. ASL CBF perfusion MRI may serve a future role in the evaluation of hydrocephalus, as a potential noninvasive method to follow changes in intracranial pressure.

astrocytomas, demonstrate greater enhancement on delayed post-contrast T1 weighted MR imaging compared to early post-contrast imaging. Our goal was to compare immediate post-contrast imaging with delayed post-contrast imaging in pediatric brain tumors.

Methods & Materials: The research protocol was granted exempt status by the institutional review board (COMIRB# 10–1354). Between November 2010 and March 2011, all patients for whom an MRI of the brain was ordered to follow-up known brain tumor or to evaluate new brain tumor underwent a modified protocol that included both immediate and 10 min delay post-gadolinium images. The modified protocol sequence order was DWI, T1 MPRAGE, contrast injection, immediate post-contrast T1 MPRAGE, T2, FLAIR, 10 min delayed post-contrast T1 MPRAGE. This sequence allowed both immediate and delayed post-contrast imaging to be performed without scanner downtime. A total of 67 unique patients met inclusion criteria of an enhancing primary brain tumor with the delayed imaging performed within a window of 6–19 min. These studies were evaluated independently by 2 pediatric neuroradiologists (NS and LF) and a radiology resident (JM) to compare the degree of lesion conspicuity and edge discrimination, and to determine an overall preference. In cases of discrepancy between reviewers, final grading was determined by group consensus.

Results: Delayed post-contrast images were preferred in 55/67 tumors (82%), immediate post-contrast images were not preferred in any case, and 12/67 cases were graded as equivalent (18%). Notably, delayed imaging was preferred for 19/20 pilocytic astrocytomas (95%). In 9/67 cases (13%), the improvement in conspicuity and edge discrimination on delayed imaging was felt to have a potential impact on clinical management, e.g. by extending resectable or treatable tumor margin.

Conclusions: Delayed post-contrast imaging can be performed easily by reordering existing MRI protocols, and no scanner downtime is required for this protocol change. Our results indicate that pediatric brain tumors (particularly pilocytic astrocytomas) often enhance more conspicuously on delayed imaging, that no diagnostic confidence is lost on delayed imaging, and that clinical management may be more accurately guided.

Paper #: PA-013**Comparison of Immediate Versus Delayed Post-Contrast Imaging in Pediatric Brain Tumors**

John Maloney, MD, *University of Colorado Hospital—Radiology, john.maloney@ucdenver.edu*; Monther Qandeel, Laura Z. Fenton, John Strain, Nicholas V. Stence

Purpose or Case Report: Anecdotal evidence suggests that some pediatric brain tumors, particularly pilocytic

Paper #: PA-014**Prognostic Role of Diffusion-Weighted MRI in Pediatric Optic Pathway Glioma**

Robert Lober, *Stanford University, roblober@gmail.com*; Robert Lober, Patrick Barnes, Michael Edwards

Purpose or Case Report: Magnetic Resonance Imaging (MRI) is commonly used in diagnosis and surveillance for optic pathway glioma (OPG). We investigated the role of

diffusion-weighted (DWI) MRI in assessing risk of progression and need for therapy in OPG.

Methods & Materials: Among 36 children with OPG, 13 patients (median age 3 years; range 5 months to 6 years) with tumor volume > 1 cm³ who had pre-treatment diffusion-weighted MRI (DWI) (echo planar imaging technique, $b = 1000$ sec/mm², 3-directions) were retrospectively reviewed, after IRB approval. Both sporadic ($n = 7$) and NF-1 associated optic gliomas ($n = 6$) were included. Tumors confined to intraconal optic nerve were excluded due to technical limitation of EPI DWI within the bony orbit. Apparent diffusion coefficient (ADC) of the solid portions of the tumor was measured using the region of interest method both at baseline and on follow-up MRI.

Results: For the 13 patients, 7 required treatment (surgery and/or chemotherapy) for symptomatic tumor progression (5 sporadic OPG and 2 cases of NF-1). Median follow-up interval was 3.1 years (range: 7 months to 10.5 years, SD 2.7 years). There was no difference in ADC values between sporadic and NF-1 associated OPG. OPG that required therapy had significantly higher baseline mean ADC (1589×10^{-6} mm²/s, SD 0.22), whereas OPG with low mean ADC (1255×10^{-6} mm²/s, SD 0.18) remained clinically asymptomatic or stable (Stratified Mann–Whitney test, $p = 0.0002$). An increase in mean ADC of 100×10^{-6} mm²/s doubled the odds the patient will require treatment (OR = 2.16, 95% CI: 1.51–3.10, $p < 0.0001$). Enhancement patterns did not predict tumor behavior or NF-1 status (Fisher's exact test, $p = 0.192$).

Conclusions: Significantly higher mean ADC was seen in OPG that required therapy for tumor progression. MRI may be a useful prognostic tool in further defining a subset clinically significant sporadic or NF-1 associated OPG.

Paper #: PA-015

Specific Sites of Spinal Drop Metastases in Children with Brain Tumor and Its Potential Impact on Imaging Strategies

Allyson Richards, Radiology, University of Texas Southwestern Medical Center and Children's Medical Center, allyson.richards@utsouthwestern.edu; Lynn Gargan, Daniel C. Bowers, Korgun Koral

Purpose or Case Report: To identify the specific sites of the spinal drop metastases in children with brain tumors in pursuit of improved scanning strategies.

Methods & Materials: Institutional Review Board approval was obtained for this retrospective study which was compliant with the Health Insurance Portability and Accountability Act. Institutional Neuro-Oncology database was screened from January 2000 through September 2011. One hundred children (64 male) who had pathology proven brain tumors

and underwent preoperative spine MRI at our institution were included. Spine MRI imaging was performed at 1.5 Tesla ($n = 91$) and at 3 Tesla ($n = 9$). All studies were performed following administration of intravenous gadolinium. The anonymized studies were presented to a board certified radiologist with certificate of additional qualification in neuroradiology and were evaluated with respect to the presence and absence of drop metastases. When drop metastases were present, 5 specific sites (cervical spinal cord, thoracic spinal cord, conus medullaris, cauda equina and, distal thecal sac) were assessed individually.

Results: There were 37 medulloblastomas, 30 pilocytic astrocytomas, 18 ependymomas, 8 atypical teratoid/rhabdoid tumors, and 7 other tumors. Eighteen patients (18%) had drop metastases. In 3 patients the drop metastases were present at all 5 specific sites. In 5 patients drop metastases were present only in the distal thecal sac. In 3 patients drop metastases were present only in the distal thecal sac and cauda equina. There was only one patient (5.6%) who had drop metastases at the cervical or thoracic spinal cord, but no drop metastases in the lower 3 sites (i.e. conus medullaris, cauda equina, and distal thecal sac). In the remaining 17 patients (94.4%) with drop metastases, the distal thecal sac was always involved.

Conclusions: The results of our limited retrospective study shows that, when present, the spinal drop metastases of pediatric brain tumors tend to be visualized in the caudal parts of the spinal canal (i.e. conus medullaris, cauda equina, and distal thecal sac). Therefore, MR scanner time, which is a limited resource, may be better utilized with dedicated high resolution imaging of the distal spine in addition to screening of the cervical and thoracic spine.

Paper #: PA-016

How Specific is the MRI Appearance of Supratentorial Atypical Teratoid Rhabdoid Tumours?

Kong Jung Au Yong, MBChB, MRCS, FRCR, Department of Radiology and Diagnostic Imaging, University of Alberta Hospital, kong.auyong@gmail.com; Jacob L. Jaremko, Ravi Bhargava, Lee T. Coleman, Lennart Jans, Michael R. Ditchfield

Purpose or Case Report: Atypical teratoid rhabdoid tumor (ATRT) is an aggressive tumor of young children with high potential for dissemination within the central nervous system. The recent use of specific immunohistochemical markers and genetic markers in chromosome band 22q11.2 have allowed us to differentiate ATRT from primitive neuroectodermal tumors pathologically. However, ATRT is still not confidently diagnosed pre-operatively using MRI. Accurate imaging diagnosis of ATRT could aid in preparation

for intensive therapy, which differs from the treatment of other less aggressive supratentorial tumours. We hypothesized that supratentorial ATRT has a unique appearance (thick, wavy rim of enhancement around a cystic centre) on post-gadolinium MRI, allowing ATRT to be accurately distinguished from other types of supratentorial tumours.

Methods & Materials: We performed a retrospective review of all available preoperative MRI of pediatric supratentorial tumors at two tertiary children's hospitals, and correlated imaging findings with pathologic diagnosis. We excluded juxtaseptal tumors from analysis.

Results: We had 61 supratentorial tumours in the combined two-site database, including 36 gliomas (19 low-grade, 10 high-grade, 7 indeterminate), 6 atypical teratoid rhabdoid tumours (ATRT), 6 ependymomae, 5 gangliogliomae, 4 primitive neuro-ectodermal tumours, 2 choroid plexus papillomae, and 2 meningiomae. ATRT presented in significantly younger patients than astrocytomas (mean age 2.6 yr vs 9.9 yr, $p < 0.05$). The distinctive visual pattern of a thick, wavy rim of enhancement around a cystic centre was seen in 5/6 (83%) ATRT and only 3/55 (5.4%) other tumours ($p < 0.0001$), for specificity SP=0.95, sensitivity SN=0.83, positive predictive value PPV=0.63, negative predictive value NPV=0.95.

Conclusions: A distinctive MRI appearance had 95% specificity for supratentorial ATRT in our series from two institutions. A supratentorial tumour with a thick wavy enhancing rim surrounding a central cystic region is suggestive of ATRT, especially in a child of preschool age. Image: Post-gadolinium T1 weighted axial MR image of an atypical teratoid rhabdoid tumour (ATRT) in a girl aged 2.4 yr, showing typical thick wavy enhancing rim surrounding cystic central portion.

Paper #: PA-017

Application of Diffusion Tensor Tractography in Pediatric Optic Pathway Glioma

Robert Lober, *Stanford University, roblober@gmail.com*; Michael Edwards, Patrick Barnes, Kristen Yeom

Purpose or Case Report: Magnetic resonance imaging (MRI) is commonly used in diagnosis and surveillance for optic pathway glioma (OPG). We investigated the role of diffusion tensor (DT) tractography in assessing the location of visual pathway fibers in the presence of tumor.

Methods & Materials: Data of ten children with OPG were acquired using a 3 T MRI GRAPPA DT-EPI sequence (25 isotropic directions with b 1000 s/mm², slice thickness 3 mm). Fiber tractography was performed with seed regions placed within the optic chiasm and bilateral nerves on coronal plane, including the tumor and surrounding normal-

appearing tissue. Tracking was performed with a curvature threshold 30°.

Results: OPG involved optic nerves ($n=8$) and/or optic chiasm ($n=16$). Of the 8 optic nerve lesions, fibers stopped abruptly at the tumor in 3 cases, diverged around it in 1 case, and traversed through the tumor in 4 cases. Of the 16 chiasmatic lesions, fibers were untraceable in 2 cases, diverged around the tumor in 4 cases, and either entered or completely traversed the tumor in 10 cases. For each patient, DT tractography provided additional information about visual fiber arrangement in relationship to the tumor that was not evident by conventional MRI methods. An example of unexpected superior displacement of the optic tract and corresponding visual deficit after surgical biopsy of this site will be depicted.

Conclusions: Optic pathway tractography is feasible in patients with OPG and provides new information about the arrangement of visual fibers in relationship to tumors that could be incorporated into surgical navigation for tumor biopsy or debulking.

Paper #: PA-018

Clinical Applications for Fast Brain MRI in Children

Jessie Aw, *Children's Memorial Hospital, jaw@childrensmemorial.org*; Samantha Schoeneman, Emma Boylan, Delilah Burrowes

Purpose or Case Report: Fast brain MRI imaging has recently been introduced for assessing brain ventricles in patients with ventriculo-peritoneal shunts (VPS). However, there is minimal literature on how this method could be beneficial for other indications. Compared to CT, this method reduces lifetime cumulative radiation dose and has multi-planar capabilities. It is much faster than full brain MRI, reducing exam costs and potentially reducing the need for sedation. However, fast brain MRI has lower resolution than a standard brain MRI and cannot detect hemorrhage. The goal of our study is to retrospectively assess additional clinical applications for fast brain MRI.

Methods & Materials: Patients who had undergone fast brain MRI were found in XenoBase, a database which references deidentified electronic medical records at our institution. XenoBase was then used to identify subgroups by diagnosis. One of the most common diagnoses was arachnoid cyst. After IRB approval, patients with fast brain MRI and arachnoid cyst were identified so that their fast brain MRI could be compared to any full brain MRI and to clinical outcomes. Fast brain MRI findings were excluded if there was not a full brain MRI within 1 year. Agreement with full brain MRI, and documented effect on clinical management were coded for statistical review.

Results: Between 2008 and 2011, there were 14 arachnoid cyst patients with 16 fast brain MRI exams. In 12 members of this group, fast brain MRI was used alone or in comparison with a full brain MRI in the decision to follow or discharge the patient. 2 exams failed to report a pituitary cyst and mass effect which were reported on prior exams. 6 patients had no complications in the year following their fast brain MRI. The most common complication was headache (4 cases).

Conclusions: Fast brain MRI reduces radiation exposure, time, cost, and the need for sedation in VPS patients. These benefits may cautiously be extended to other patient groups also requiring routine imaging, such as those with arachnoid cysts.

Disclosure: The authors disclose that they will discuss or describe, in the educational content, a use of a medical device or pharmaceutical that is classified by the Food and Drug Administration (FDA) as investigational for intended use.

Paper #: PA-019

Clinical Relevance of Susceptibility Weighted Imaging (SWI) in the Pediatric Population

Marzia Mortilla, *Radiology, Children's Hospital Meyer, m.mortilla@meyer.it*; Sara Savelli, Antonio Ciccarone, Claudio Fonda

Purpose or Case Report: Susceptibility-weighted imaging (SWI) is a new technique that exploits susceptibility differences in different tissues, to provide a different type of tissue contrast. SWI is a gradient echo sequence utilizing both phase and magnitude data to achieve exquisite sensitivity to tissue magnetic susceptibility effects. It is extremely sensitive to even minute amounts of paramagnetic substances and therefore for detection of blood products (hemosiderin, ferritin), deoxygenated blood, calcium, iron, and small vein depiction. It is particularly suited for vascular imaging, especially in cerebral ischemia. SWI has been shown to be more sensitive in detecting cerebral microbleeds than is conventional T2*-weighted gradient-recalled echo imaging (GRE) partly because of its inherent sensitivity, increased spatial resolution and the thinner slices acquired. Recent studies have shown that SWI detected more microbleeds in more patients, irrespective of their location and that SWI may be more sensitive in detecting traumatic lesions than CT or MRI.

Methods & Materials: Between January 2011 and October 2011 we have performed SWI on 75 pediatric patients (from 1 day to 15 yrs old) affected with different pathologies. MRI was performed using either a 3- or 1.5-T magnet (Achieva; Philips Healthcare, Best, The Netherlands). Among these patients 62 also received a classic GRE sequence.

Results: Our experience confirms a greater sensibility of SWI than GRE in detecting microbleedings and larger bleedings. SWI is much more helpful in patients younger than 1 year since it can distinguish hemorrhagic and non hemorrhagic punctuate white matter lesions detected as hyperintensities on T1-W images. It is more accurate in distinguishing petechial hemorrhages and ischemic foci in patients with germinal matrix hemorrhages. SWI can provide important diagnostic information not only in vascular pathologies but also in tumors showing the altered tumor microvasculature, the degree of intratumoral necrosis and the presence of subtle defects of the BBB within the surrounding parenchymal tissue. The technique also allows the detection of possible bleedings in infectious lesions.

Conclusions: SWI is a valuable technique in the evaluation of a wide variety of intracranial pathologies in the pediatric population and its use is advisable on a routine basis.

Paper #: PA-020

Radiographic Techniques Used for Performing Pediatric Head CT Examinations at an Academic Medical Center: A Snapshot

Anil Rao, MD, *Radiology and Radiological Science, Medical University of South Carolina, raoa@musc.edu*; Muhammad A. Naveed, Walter Huda

Purpose or Case Report: To document the radiation used to perform pediatric head CT examinations during a representative month in a radiology department at an academic medical center.

Methods & Materials: We reviewed the dose summary sheets of all pediatric patients who underwent a single head CT examination on six CT scanners installed at our institution in February 2011. There were 62 studies that qualified for this study. We obtained values of x-ray tube voltage, CT DIvol, Dose Length Product (DLP), The examination scan length was obtained by dividing the DLP by the corresponding CT DIvol. Each parameter was plotted as a function of patient age, and a linear least square fit obtained, together with the correlation coefficient (r).

Results: Age correlated with x-ray tube voltage ($r=0.73$), CT DIvol ($r=0.62$), and DLP ($r=0.61$). Increasing the patient age from 1 to 10 years increased x-ray tube voltage from 95 to 113 kV, and CT DIvol from 31 to 48 mGy. The average scan length was 16.5 ± 4.3 cm and which showed very little correlation with patient age ($r=0.22$).

Conclusions: Ten year old patients undergoing head CT examinations use about 50% more radiation than one year old patients, and use x-ray tube voltages that are about 20% higher.

Paper #: PA-021**Diffusion Tensor Imaging (DTI) with Retrospective Motion Correction for Large-Scale Pediatric Imaging**

Samantha Holdsworth, PhD, *Department of Radiology, Stanford University, sholdsworth@stanford.edu*; Kristen Yeom, Murat Aksoy, Anh Van, Roland Bammer, Stefan Skare

Purpose or Case Report: A common problem with pediatric MR imaging is motion. Diffusion-weighted imaging (DWI) is highly sensitive to the effects of both rigid-body motion and brain pulsation. The resulting motion artifacts can manifest in several ways, and include blurring (motion between volumes), slice ‘drop-outs’ (motion during the diffusion encoding), and aliasing (motion during the parallel imaging/ghost calibration scan). In order to improve image quality in pediatric DWI and avoid the potential for repeat scans, we have implemented our GRAPPA-accelerated diffusion tensor (DT)-EPI sequence on over 1,600 pediatric patients at our institution, and have developed tailored reconstruction software to correct for large motion and reduce the need for general anesthesia (GA).

Methods & Materials: GRAPPA-accelerated EPI DTI data was collected on 100 patients at 1.5 T and 1,500 patients at 3 T between the ages of 1 month and 18 years old. With these data, we investigate the use of a method to select the best GRAPPA and ghost calibration weights; 3D rigid-body realignment with importance weighting; a new volume rejection criterion for large motion; together with other procedures to lower image noise and reduce phase artifacts. All image reconstruction was performed using compiled threaded MATLAB code on the vendor's (GE) multiprocessor reconstruction hardware.

Results: Using the maximum motion detected from the 3D realignment procedure on the 1,600 DTI exams, 51% of patients did not move (either through co-operation or GA, denoted here by <1 mm of motion); 28% of patients moved between 1–3 mm; 13% between 3–5 mm; 6% between 5–10 mm; and 2% between 10–18 mm. Except for 3 patients in total, the motion correction steps employed here were extremely robust in correcting for motion. In addition, the motion correction steps employed here do not blur or negatively affect the data on non-moving patients.

Conclusions: Our proposed integrated reconstruction scheme suggests that correcting for different types of motion at different stages of the DTI acquisition is critical to provide scans of diagnostic quality. Apart from the very rare instance (0.2%) where the patient moved continuously an extensively throughout the scan, our motion correction procedures employed here are extremely robust. Using this scheme,

we show that highly diagnostic motion-corrected DTI data can routinely be read on our patient database within 10 min.

Paper #: PA-022**Evaluating Pediatric Neuropathologies Using Multiple TE Weighted Susceptibility Images Using Multi Shot EPI Sequence**

Salil Soman, MD, MS, *Lucille Packard Children's Hospital—Stanford University, salsoman@stanford.edu*;

Purpose or Case Report: Susceptibility weighted imaging has been proved clinically useful in a variety of clinical scenarios. However, for any susceptibility weighted imaging, the length of the TE will determine the extent of susceptibility effects depicted. Sequences such as susceptibility weighted imaging (SWI) regularly employ a 3D gradient sequence at a single TE value to obtain isotropic susceptibility weighted images. The multi-shot EPI sequence (3D MSME EPI) is an MRI pulse that allows for the acquisitions of images for multiple TE per each TR, and can effectively acquire images for multiple TE's in the same time as a single 3D GRE sequence. We sought to evaluate the utility of multiple TE images for evaluating pediatric pathologies compared to each other as well as against our standard 2D GRE sequence.

Methods & Materials: 50 pediatric patients imaged as part of our clinical practice had multi-shot EPI sequences and 2D GRE sequences performed under an IRB approved protocol. TE=15 (short), 25 (medium) and 60 (long) were used. Imaging of patients ranging from 1 to 21 years in age demonstrated various stages of tumors, hemorrhage, postoperative changes, or no abnormalities. A board certified pediatric neuroradiologist and a second year neuroradiology fellow reviewed all images.

Results: Numerous instances were found where long 3D TE images better-depicted pathologies (such as blood products, post operative changes, or siderosis, vessel prominence) than short or medium 3D TE images or 2D GRE images. In one case, a patient with elevated ferritin levels suspected of having hemophagocytic lymphohistiocytosis demonstrated siderosis on long TE images, while all other sequences appeared to be negative. Numerous cases also demonstrated that the extent of artifact (motion, braces, hardware) worsened with increasing TE.

Conclusions: Multi-shot EPI images can provide images that demonstrate susceptibility findings better seen on long TE 3D GRE images, can depict findings on short TE images that may be obscured by artifacts on longer TE images, and overall, often can show findings not visible on 2D GRE

images, all in the same time as standard 3D GRE sequences (such as SWI). Additionally, this method produces multiple TE images that may be useful for advanced applications such as calculating T2* values (which may be useful in characterizing neuropathologies), producing phase images or performing quantitative susceptibility mapping.

Paper #: PA-023

Assessment of Diffusion Images Acquired Using the ACR Phantom: A Comparison of 3 Vendors

Nancy Rollins, MD, *Children's Medical Center, nancy.rollins@childrens.com*; Ashok Panigrahy, Barbara Holshouser, Evelyn Babcock, Hao Huang, Zhiyue W. Wang

Purpose or Case Report: Technical differences in MR scanners may result in measurable differences in scalar metrics that could erroneously be attributed to biological differences in patients; an important issue in conducting a multi-site study using diffusion imaging. The American College of Radiology (ACR) phantom is widely available. We used the ACR phantom to compare quality measures for diffusion tensor images (DTI) acquired on different MR vendors using standardized protocols.

Methods & Materials: DTI was acquired using the ACR phantom on 3 T scanners: Siemens [TrioTim Syngo B17 ($n=2$)], GE [HDXT 15.0 and HD16.0 ($n=2$)], and Philips [Achieva R3.2-3.6 ($n=4$)]. Participating sites followed mutually agreed upon vendor-specific DTI protocols used for neonates in clinical practice: SS-EPI; $b=700$; ~ 2 mm³ voxel; 30–32 directions; TE ~ 84 msec; 1 acquisition; parallel imaging; multi-channel (8–32) head coil. Tensor data was analyzed at one site using internally developed software in IDL. B0 and eddy current distortion were assessed by analyzing grid line distortion on ACR slice 5; deviations from linearity were measured in the phase encoding direction. ACR slice 7 was used to assess SNR of the center and periphery of the $b=0$ image, and fractional anisotropy (FA) of the phantom, which should approach 0. Deviations from specified sequence parameters were recorded.

Results: Both Siemens scanners had some image degradation due to vibration subsequently corrected by the vendor. Nonlinear gridline distortion was highest on the GE followed by Philips but was corrected with the use of 2nd order shimming. Eddy current distortion was consistently smaller than acquisition voxel size after image registration. TE varied from 74–92 msec; acquisition bandwidth range was 1563–2928 Hz/pixel. The 2 mm slice thickness was problematic on clinical GE scanners resulting in non-isotropic voxels. Across vendors, SNR was consistently higher in the

image periphery than center by a factor of 1.3–2.0. SNR normalized by the voxel size was greatest at image center for GE and 14% lower on average on Siemens and Philips scanners. FA deviated from 0.07–2.4%. The highest FA values were seen on Philips scanners.

Conclusions: In the absence of an affordable widely available anisotropic phantom, the ACR phantom can be used to objectively assess quality of diffusion images across vendors and sites; knowledge of which aids both the vendors and sites.

Paper #: PA-024 SLARP Best Paper 2011

Carotid Intima-Media Thickness in Children with Familial Hypercholesterolemia, Diabetes Type 1 and Obesity, Compared to Healthy Children

Monica Bravo, *Hospital Nacional de Pediatria Juan P. Garrahan, monicabravo26@hotmail.com*; I. Collado, E. Dardanelli, M. Araujo, J. Lipsich, S. Moguillansky

Purpose or Case Report: Evaluate with ultrasonography the Intima-Media Thickness (IMT) as a marker of cardiovascular risk (CVR) in patients with early clinical and laboratory diagnosis of Familial Hypercholesterolemia (FHC), Diabetes Type 1 (DBT-1) and Obesity (OB), compared with healthy controls.

Methods & Materials: We used a descriptive, controlled and blinded cross-sectional study. We evaluate the IMT of the common carotid arteries and included in a single variable other structural alterations of the wall (atherosclerotic plaques and irregularities of the intima). We did it in a blinded fashion to the results of blood tests (as recommended by the consensus of Mannheim 2007) in 117 patients (29 FHC, 38 DBT-1 and 50 OB) and 15 controls (6 to 18 years). We excluded patients with other diseases that could alter the arterial wall. Variables analyzed with the program Statistix 8.

Results: The three groups were more IMT compared with controls were statistically significant. The Media IMT (mm) was FHC: 0.59 (0.31–2.15), $p=0.006$, CI 0.06 to 0.36. Obese: 0.48 (0.3 to 0.85), $p=0.001$, CI 0.06 to 0.14 and DBT-1: 0.46 (from 0.25 to 0.65), $p=0.0004$, CI 0.03 to 0.13. Control group: 0.37 (0.30–0.45). The greatest difference was showed in patients with FHC. No association was found between the value of LDL-C and IMT. The 62.5% received drug treatment at the time of evaluation. In DBT-1 a no association was found between the IMT and the levels of HbA1c and lipids. And in the OB group found no association between IMT and BMI Z score. FHC 31%, 8% of DBT-1 and 6% of OB showed atherosclerotic plaques and intima irregularities.

Conclusions: The IMT ultrasonography was able to demonstrate that patients with chronic diseases, with increased cardiovascular risk in adulthood, showed early alterations of carotid intima media in children. This allows clinical applications of preventive and therapeutic guidance.

Paper #: PA-025

4-D Phase-Contrast MRI: Venous Flow Quantification is as Accurate as Arterial Flow Quantification

Umar Tariq, MBBS, *Radiology, Stanford University, utariq@stanford.edu*; Albert Hsiao, Marcus Alley, Shreyas Vasanaawala

Purpose or Case Report: The accuracy of 4-D phase contrast (PC) MRI for arterial blood flow quantification has already been established; however, veins have lower velocity to noise ratio (VNR). The significance of this lower venous VNR in 4D flow has not been well evaluated in a pediatric clinical setting. Here we assess precision & accuracy of 4-D PC venous flow quantification in children with congenital heart disease (CHD). **Methods & Materials:** With IRB approval and HIPAA compliance, 22 CHD patients without shunts were identified who underwent 4-D flow. Superior vena cava, inferior vena cava, ascending aorta, descending aorta & pulmonary trunk flow rates were measured in blinded fashion. A benchmark for precision of flow assessment was determined from differences between aortic and pulmonary arterial flows, which should agree. The precision of flow when utilizing a slow flow structure (vein) and a fast flow structure (artery) was then determined, serving as an indicator of the precision of slow flow measurements. This was done in pairs for the upper body (SVC flow vs difference between ascending and descending aortic flow), lower body (IVC flow vs descending aortic flow) & total body (SVC flow+IVC flow vs ascending aortic flow). Paired t-tests were used to identify significant differences in the respective arterial and venous flow rates. With an f-test, the relative precision of the arterial flow (determined from aortic and pulmonary arterial flow) was compared against the precision of agreement between upper, lower, and total body flows, each of which has a slow flow venous component, thus assessing precision of venous flow measurement.

Results: Arterial & venous flow measurements were strongly correlated for the upper body ($r=0.89$), lower body ($r=0.96$) and total body flow ($r=0.97$); net aortic and net pulmonary trunk flow rates were also tightly correlated ($r=0.97$). Moreover, there was no significant difference in the precision of arterial & venous flow measurements (t-test, $p=0.31$). Lower

venous (200 cm/s or lower) improves the accuracy and precision associated with low velocity venous flow, a finding that tended to but it did not reach statistical significance.

Conclusions: With 4-D PC MRI, the accuracy and precision of venous flow quantification are comparable to arterial flow quantification, though venous settings may improve venous flow assessment.

Disclosure: Dr. Tariq has indicated that he will discuss or describe, in the educational content, a use of a medical device or pharmaceutical that is classified by the Food and Drug Administration (FDA) as investigational for intended use.

Paper #: PA-026

Neonatal Congenital Heart Disease: Initial Results with High-Resolution Contrast-Enhanced MR Angiography at 3.0 Tesla

M. Ines Boechat, *Radiological Sciences, UCLA Medical Center, iboechat@mednet.ucla.edu*; John Moriarty, Brian Reemtsen, Kambiz Nael, Paul J. Finn

Purpose or Case Report: Neonates with complex congenital heart disease (CCHD) frequently have associated vascular anomalies requiring detailed and urgent vascular imaging. The spatial resolution requirements for imaging tiny target vessels in neonates have so far precluded its use of CEMRA in this patient population. The purpose of our study, therefore, was to explore the potential of high resolution CEMRA at 3.0 T in neonates with suspected congenital vascular anomalies

Methods & Materials: 16 neonates (mean age 9.4 days, range 1–28 days; mean weight 2.7 kg, range 1.5 kg–4.2 kg) underwent CEMRA at 3.0 T. CEMRA was performed under controlled apnea on a 32-channel 3.0 T system using either a 12-channel head-neck coil (9 pts) or a 15-channel adult knee coil (7 pts). Gd contrast delivery was calculated based on a total dose of 0.2 mmol/kg. Parallel imaging factors of 4–6 were used, generating 0.7 x 0.5 x 0.6 mm voxels in an acquisition time of 17–22 s. Images were scored for quality and the presence of artifacts independently by two observers. The CEMRA series were evaluated to identify pulmonary arterial and venous anatomy. Extra-pulmonary vascular anatomy was divided into 12 sections for image quality assessment on MPR.

Results: The MRA data sets had high mean image quality and low mean artifact grading scores. No significant difference was evident between the two observers for scoring image quality and artifact ($p=0.9$), and there was good interobserver agreement ($k=0.66$, 95% CI: 0.26–0.81). The pulmonary arteries were confidently visualized to at least the 2nd order branches in all 16 patients, at least the 3rd order branches in 15 (93%).

Out of 176 evaluated segments, 164 (93%) were graded as the vessel “very well visualized with excellent definition of vessel” PA abnormalities were diagnosed in 10 patients and PV anomalies in 6 patients. Correlation was made with open surgical findings in 12 cases, confirming the CEMRA diagnoses with no discrepancy between the operative and imaging conclusions. **Conclusions:** The results of our study suggest that high resolution CEMRA at 3.0 T is extremely promising in neonatal CCHD and, in combination with echocardiography, may often provide comprehensive information for treatment planning. With appropriate use of physiological motion compensation, parallel imaging and coil configuration, voxel volumes less than 0.5 mm³ are routinely achievable.

Paper #: PA-027

Early Signs of Iron-Mediated Cardiomyopathy in Transfusion-Dependent Children: Evaluation Using Cardiovascular Magnetic Resonance Technique of Myocardial Tagging

Shobhit Madan, MD, MPH, *Radiology, Children’s Hospital of Pittsburgh of UPMC, madans@upmc.edu;* Soma Mandal, Sameh Tadros

Purpose or Case Report: It is not well understood whether transfusion-dependent children (mainly those who have hereditary anemias subject to excessive iron levels from regular blood transfusions) with no or mild cardiac iron overload and without signs of heart failure exhibit early changes in cardiac dysfunction. This study aims to evaluate intramyocardial deformation and subsequent cardiac dysfunction in such patients using the cardiovascular magnetic resonance technique of myocardial tagging as well as assess iron overload by another cardiovascular magnetic resonance technique of T2 star (T2*). We hypothesize that transfusion dependent children undergoing chelation therapy will be at high-risk for cardiomyopathy despite normal or slightly elevated iron levels and no signs of heart failure due to progressive myocardial deformation as assessed by myocardial tagging; that is, we expect abnormal mechanical parameters to exist despite T2* values which correspond to normal or slightly elevated myocardial iron levels.

Methods & Materials: 8 patients (mean age 15 yrs) requiring regular blood transfusions for various reasons (e.g. Thalassemia, Sickle Cell disease, other anemias) were investigated using Harmonic Phase magnetic resonance tagging and T2* imaging. Various myocardial mechanical parameters were quantified and correlated to cardiac iron levels as measured by T2*.

Results: 2 children with no overt signs of heart failure (as measured by ejection fraction and volume indices) exhibited normal T2* iron levels in combination with global circumferential abnormal myocardial strain and 4 children exhibited regional strain.

Conclusions: This preliminary data suggests that transfusion-dependent children without overt signs of heart failure exhibit early signs of cardiac dysfunction (an effect of strain as assessed by myocardial tagging) in direct relation to normal or slightly elevated myocardial iron levels (as measured by T2*). A larger sample size of children could support the idea of abnormal myocardial mechanics being a diagnostic imaging marker for the development of myocardial iron overload and eventual iron-mediated cardiomyopathy.

Paper #: PA-028

Analysis of a Novel Background Correction Method for Cardiac MR Phase Contrast Imaging

Nicholas Hilpiper, *Medical Imaging, Children’s Memorial Hospital, NHilpiper@childrensmemorial.org;* Cynthia K. Rigsby, Emma Boylan, Gang Zhang, Andreas Greiser, Gary McNeal

Purpose or Case Report: Phase contrast magnetic resonance imaging (MRI) is a powerful tool for evaluating vessel flow. Inherent errors in acquisition, such as phase offset and image noise, can cause significant inaccuracies in flow parameters. These errors can be compensated for with the use of background correction (BC) software. This background correction software automatically performs a spatially dependent background phase correction as part of image reconstruction without the need for additional scan time or use of a phantom. The objective of this study was to evaluate this automatic BC software.

Methods & Materials: A retrospective evaluation was performed of 43 patients undergoing cardiac MRI including phase contrast imaging for flow quantification in the aorta and main pulmonary artery (MPA). Standard phase contrast image reconstruction was performed then BC software was automatically applied to the phase contrast data. Non-BC and BC corrected net flow phase contrast data for the aorta and MPA were recorded and were separately compared using the Wilcoxon signed rank test. In an analysis of a subset of 35 patients expected to have a Qp:Qs of 1, a Student’s T-test was applied to determine how significantly the non-BC and BC corrected net flow data varied from 1.

Results: The mean BC aortic net flow values were significantly lower than the non-BC values ($p=0.0031$). The mean

BC MPA net flow values were also significantly lower than the non-BC values ($p=0.0001$). Neither the non-BC ($p=0.46$) nor the BC ($p=0.59$) mean Qp:Qs values were significantly different than 1.

Conclusions: There is a significant difference between BC and non-BC phase contrast values. However, in our system, the accuracy of phase contrast imaging using BC as measured by Qp:Qs is not significantly different than non BC data as both values are close to 1, implying that our original phase contrast data is relatively accurate.

Paper #: PA-029

Initial Clinical Experience of Congenital Heart Disease Cardiac MR Examinations with Radio Frequency (RF) Multi-Transmit Technology on 3T MR

Taylor Chung, MD, *Diagnostic Imaging, Children's Hospital & Research Center Oakland, taylorchung12@gmail.com*

Purpose or Case Report: To review the initial clinical experience of pediatric cardiac MR on 3 T MR scanner without and with parallel radiofrequency (RF) multi-transmit (Tx) Technology.

Methods & Materials: We retrospectively reviewed all cases of Cardiac MR performed on our 3 T MR scanner from January 2010 to October 2011. The Tx hardware upgrade occurred in March 2011. All MR examinations were reviewed specifically for whether artifacts on cine SSFP images would render the examination non-diagnostic.

Results: Prior to March 2011, there were 4 examinations performed on 2 volunteers (ages 11 years old and 35 years old) and 3 clinical examinations. From the examination of the adult volunteer, there were unpredictable banding and shading artifacts on cine SSFP sequences such that the examination was deemed non-diagnostic. From the examination of the 11-year-old volunteer, cine SSFP images were considered diagnostic. On both volunteers, images from coronary MRA with 3D fast gradient echo sequence with respiratory navigator and free-breathing cine phase contrast were considered diagnostic. Therefore, Cardiac MR service on 3 T was limited to coronary MRA for all patients and complete cardiac MR examination for small size patients. The 3 clinical examinations were performed on a 3-year-11-month-old girl for VSD shunt quantification, a 9-year-5-month-old girl for post-operative evaluation of transposition of great vessel s/p Jatene procedure, and 23-year-old male with Kawasaki disease for coronary MRA. All examinations were considered diagnostic. After the Tx upgrade and successful testing with adult volunteers, from March 2011 to October 2011, the 3 T cardiac MR service expanded to cover all cardiac MR examinations without limitations. A total of 29 clinical cardiac MR cases were performed, successfully completed, and considered to be diagnostic. There were 29 patients

with median age: 16 years 10 months (range 9 years 4 months to 25 years 5 months), median weight: 56.1 kg (range: 30–88.7 kg), median height: 163 cm (range: 132–187 cm), median BSA: 1.56 m² (range: 1.05–2.11 m²).

Conclusions: Our initial clinical experience of congenital heart disease cardiac MR examinations with radio frequency (RF) multi-transmit technology on 3 T MR suggest that the Tx technology can minimize artifacts on cine SSFP allowing successful expansion of our Cardiac MR service.

Disclosure: Dr. Chung has indicated that he will discuss or describe, in the educational content, a use of a medical device or pharmaceutical that is classified by the Food and Drug Administration (FDA) as investigational for intended use.

Paper #: PA-030

Non-Cardiac Findings in Pediatric Cardiac MRI

Ajaykumar Morani, MBBS, MD, DNB, *Department of Radiology, University of Michigan, ajaycmorani@gmail.com*; Maryam Ghadimi Mahani, Jimmy C. Liu, Adam Dorfman, Prachi Agarwal

Purpose or Case Report: To determine the prevalence and nature of non-cardiac findings (NCFs) in pediatric cardiovascular magnetic resonance imaging (MRI).

Methods & Materials: Reports of all pediatric cardiac MRIs performed in our center from January 2008 to March 2011 were reviewed. All cases had been jointly interpreted by a pediatric cardiologist and one of three radiologists each with 2–6 years of post-fellowship experience. For each case, indication of study, age, sex, and reported NCFs were extracted. All non-cardiovascular reported findings in neck, chest, and spine and NCFs in abdomen were included in NCFs. The electronic medical records of these patients were then reviewed. The NCFs which resulted in additional imaging or laboratory workup, therapy or intervention or rendered a new clinical diagnosis were considered significant.

Results: 189 NCFs were reported in 166 of 631 patients. Median age was 4 years, range 2 days to 18 years, with 46% females. Overall, 36% (69/189) of NCFs were in the abdomen, 55% (105/189) in the chest, 7% (12/189) in spine, and 1.6% (3/189) in the neck. 51 NCFs (27%) in 41 patients were already known and 12 NCFs in 8 cases were expected due to patient's underlying clinical status. 26 NCFs in 22 patients (3.4% of all pediatric cardiac MRI cases) were considered significant. These included solitary kidney, cystic renal disease, hydronephrosis, renal arterial narrowing, cirrhosis, liver lesion, asplenia, heterotaxy, ascites, mediastinal mass, and pleural effusion. The most common insignificant NCFs included atelectasis 27% (52/189), spine deformities 6% (12/189), and accessory renal arteries 4.7% (9/189).

Conclusions: NCFs can be seen in clinical pediatric cardiac MRI. While these are not common and are different in nature from those reported for adults, recognizing these findings may change patient management during or after the study.

Paper #: PA-031

Initial Experiences: Contrast Enhanced MR Angiography (CEMRA) in Pediatric Organ Transplantation at 3.0 T

Conor Meehan, UCLA; Sarah Khan, Ines Boechat, Paul J. Finn

Purpose or Case Report: Transplantation is a definitive treatment option for advanced liver and intestinal disease. Confident preoperative identification of vascular variation or pathology may preclude surgery or influence technique. CEMRA offers non-invasive, comprehensive evaluation, avoiding ionizing radiation and access complications seen with CT and conventional angiography. To our knowledge, ours is the first reported series of 3 T CEMRA in this transplant population.

Methods & Materials: We retrospectively analyzed pediatric body CEMRA performed between August 2008 and October 2011. The IRB waived informed consent for this HIPAA-compliant study. All exams used a 32-receiver channel 3.0 T MR system (Magnetom Trio, Siemens). Standard protocol imaged chest to pelvis, including multi-pass spoiled gradient echo CEMRA, and post gadolinium (0.2 mmol/kg) 2D GRE sequences. Two readers independently evaluated subtracted thin MIP coronal reconstructions (10 mm thickness, 1 mm overlap), at PACS workstations. Image quality and artifacts were graded. Variants and abnormalities were noted. SNR (signal-to-noise ratio) and CNR (contrast-to-noise ratio) were calculated for aorta and visceral branches, portal vein and tributaries, and venae cava.

Results: 21 males and 14 females were imaged, mean age 5 yrs 4 m±4 yrs 7 m, mean weight 23.5 kg±20. Indications included: exclusion of thrombosis (16), vascular mapping for surgery (11) or line placement (7). 27 patients were preoperative. 25 studies utilized anesthesia with controlled ventilation. At first pass, SNR of abdominal aorta measured mean 93.0±SD 33.4, and CNR 65.3±28.7. At second pass, SNR and CNR for portal vein measured (56.9±21.6 and 34.3±13.9) and for intrahepatic IVC, 49.2±18.5 and 39.1±17.3. At 3rd pass, mean SNR and CNR for intrahepatic IVC measured 47.7±21.3 and 38.9±19.7. When anesthesia was used, inter-reader agreement was high, Kappa=0.81, and abdominal aorta and visceral branches, portal tributaries, and central veins were invariably rated good or excellent. In smaller patients, inferior mesenteric artery was less well rated, but never lower than “good”. Associated findings were

common: organomegaly, venous occlusions, and in one child, heterotaxy. 5 patients have received transplantation to date, with concordant surgical findings.

Conclusions: 3.0 T CEMRA angiography provides high quality imaging with comprehensive diagnostic vascular evaluation in a pediatric transplant population.

Paper #: PA-032

Dynamic Contrast Enhanced MR Venography for Evaluation of Central Venous Obstruction in Pediatric Patients

Prakash Masand, MD, *Texas Children's hospital,* *drmasand@gmail.com;* Rajesh Krishnamurthy

Purpose or Case Report: Present our experience with dynamic MR venography (4D MRV) using keyhole technique (high temporal resolution without a loss of spatial resolution) and SENSE (parallel imaging), providing ultra-short dynamic times for evaluation of central venous obstruction in children.

Methods & Materials: 4D MRV studies were performed in 20 children (age range: 3 months to 12 years) with suspected central thrombosis of the upper (neck/chest) or lower (abdomen/pelvis) venous system. IRB approval was obtained for this retrospective analysis from the hospital's review board. Sedation, where necessary was provided by our anesthesiologists. The choice of coil and field of view varied according to the age and size of the patient. Imaging was performed on a 1.5 T magnet (Philips MRI system). After the cine gradient echo time of flight sequences were acquired, the dynamic keyhole MR angiographic sequence was applied in the coronal orientation. This sequence commenced 2–5 s after initiation of the first bolus administration of 2–10 mL of undiluted gadopentate dimeglumine (0.5 mmol/mL, Magnevist) at a rate of 2–3 mL/sec followed by 10–20 mL of saline at a rate of 2 mL/sec. Image acquisition was repeated multiple times without delay for 60 s during shallow breathing. Contrast material was administered through a peripheral or central venous line, and sometimes via simultaneous bilateral extremity injections. Rarely manual hand injection was performed. The parameters were as follows: CENTRA k-space filling, acquired voxel size 1–1.2 x 1–1.2 x 2–3, reconstructed voxel size 0.4–1 x 0.4–1 x 1–1.5, number of dynamics 8–20, keyhole percentage 25–38%, SENSE (parallel imaging) factor 2x1–2x2, dynamic times 1–3.6 s, and injection rate 1–3 cc/second. Image analysis was based on original contrast-enhanced data sets, MIP and volume rendering. The quality of the MRV was graded by a subjective scale from 1–5 (1=excellent, no limitations; 5=non-diagnostic). Comparison with unenhanced MR venographic sequences and Doppler ultrasound were available in all cases.

Results: 4D MRV provided diagnostic information on patency of venous segments in all cases, including the presence

of venous occlusion or stenosis, the segments involved, and collateral venous pathways.

Conclusions: 4D MR venography using the method outlined is a reliable means of estimating central venous thrombosis in children, using short dynamic scan times with high spatial and temporal resolution, creating an effect similar to conventional venography.

Paper #: PA-033

Analysis of Optimal Phase Interval for Prospective EKG-Triggered Cardiac CT in Children

Prakash Masand, MD, *Texas Children's Hospital*, Savivek Bogale, Lorna Browne, Rajesh Krishnamurthy

Purpose or Case Report: Evaluate high temporal resolution cine MRI of the heart in children to determine relationship of heart rate to the optimal motion free interval during the cardiac cycle, and to derive a chart depicting optimal reconstruction intervals across a range of heart rates which could be applied for prospective EKG triggered CT imaging of the heart.

Methods & Materials: Pediatric patients who had high temporal resolution cine Steady State Free Precession sequence (50 frames acquired across a single cardiac cycle) performed as part of a MRI/MRA of the heart from 2005–2011 were included. A single reader analyzed the high temporal resolution cine data to determine the location and duration of the motion-free phase interval in systole and diastole for heart rates ranging from 60–140 bpm. The following information was collected: age, heart rate, duration of systole and diastole, EKG phase and phase percentage of motion-free interval, and duration of motion-free interval. Heart rates were grouped in ranges of 10 (61–70, 71–80, 81–90 etc.), with at least 25 patients in each group. Wilcoxon sum rank test was performed to compare the static durations of systolic and diastolic phases for each heart rate group. Two-tailed P-values <0.05 were considered to indicate statistical significance. A chart matching heart rate range to the optimal phase of image acquisition and reconstruction was created.

Results: Optimal reconstruction intervals for motion-free imaging of the heart in systole and diastole, and single best phase for a given heart rate are as follows: (Please see Table 1) Mean duration of the motionless phase in systole and diastole for a given heart rate is as follows: (Please see Table 2)

Conclusions: This is the first time that variability in location of the motion-free interval within the cardiac cycle with respect to heart rate in children has been studied in rigorous

fashion. This chart will have immediate application in the so-called 'target scan', which uses prospective EKG triggered acquisition of data in combination with half-scan reconstruction to minimize radiation dose with respect to retrospective EKG gated imaging.

Paper #: PA-034

Diagnostic Accuracy of CT Angiography Versus Echocardiography in Diagnosis of Aberrant Patent Ductus Arteriosus in Patients with Ductal Dependent Pulmonary Circulation

Taruna Ralhan, MD, *Radiology, St. Joseph's Hospital, Phoenix*; Andrew Ligouri, Randy Richardson

Purpose or Case Report: Although patent ductus arteriosus (PDA) is a common congenital cardiovascular anomaly, aberrant PDA associated with other cardiac malformations is rare. It is important to accurately diagnose the anatomy of the PDA in patients with ductus arteriosus-dependent pulmonary circulation prior to surgery. The objective of our study was to compare CT angiography versus echocardiography in diagnosing aberrant PDA.

Methods & Materials: A retrospective study of 280 patients who underwent EKG gated cardiac CT angiography (CCTA) was done from October, 2006 to August, 2011. CCTA detection of PDAs was compared to PDAs detected by echocardiography and surgery. Patients ranged in age from 2 days to 1 year, with most cases diagnosed within the first month of life. CCTA was performed with a 64-slice MDCT, with EKG gating, using a modulation technique.

Results: A total of 10 patients were found to have aberrant PDA by CCTA. Nine patients had a PDA emanating from the brachiocephalic artery to the pulmonary arteries and one patient had PDA emanating from the carotid or the subclavian artery according to the operative report. All ten patients had echocardiography in addition to CCTA. Nine of the ten patients underwent surgery. One patient was lost to follow up. Comparison between CCTA and echocardiography to operative report showed the following: 3 out of the 10 echocardiograms agreed completely with CCTA and operative report. 7 out of the 10 echocardiograms did not report aberrant PDAs which were seen on CCTA and confirmed during surgery. In one patient, the echocardiogram reported a double aortic arch which was found to be an aberrant PDA from the LEFT brachiocephalic artery; a finding that changed the surgical management and pre-surgical planning. The results were statistically significant with a p value of <0.05.

Conclusions: Diagnostic accuracy of ductus arteriosus anatomy is important in pre-surgical planning and management

of patients with ductal dependent pulmonary circulation. Cardiac CT angiography is more accurate as compared to echocardiography in diagnosis of aberrant patent ductus arteriosus.

Paper #: PA-035

Comparing Image Quality and Radiation Dose in Retrospective Versus Prospective ECG-Gated Cardiac MDCT in Pediatric Patients with Congenital Heart Disease Less Than One Year of Age

Cam Chau, MD, *Radiology, St. Joseph Hospital and Medical Center*; Ernerio Alboliras, Karim Diab, Olga Kalinkin, Randy Richardson

Purpose or Case Report: To date, there are very few studies that have evaluated the image quality and radiation dose of the retrospective ECG-gated multi-detector computed tomographic (MDCT) versus prospective ECG-gated cardiac MDCT imaging in pediatric patients. Aim of this study is to compare the image quality and radiation dose of the retrospective ECG-gated MDCT versus prospective ECG-gated cardiac MDCT imaging in pediatric patients with congenital heart disease less than one year of age.

Methods & Materials: We retrospectively evaluated 50 thorax CT images which were obtained using two different ECG-gated cardiac MDCT protocols (retrospective helical ECG-gated [$n=22$] versus prospective non-helical ECG-triggering [$n=28$]) in patients younger than 1 year of age. The prospective ECG-gated protocol scanned 50% of the cardiac cycle with 10 msec padding in patients with heart rates greater than 100 bpm. Two experienced radiologists evaluated the image quality and course of the coronary arteries. Image quality was assessed based on the degree of homogeneity of vascular enhancement, presence of stair-step artifacts, image signal and noise as well as the overall subjective image quality based on a 4 point scale. The course of the left and right coronary arteries was also evaluated based on a 4 point scale, focusing on how well the evaluator was able to visually follow the coronary artery from its origin to its termination. Radiation dose was recorded and compared.

Results: The mean score of the homogeneity of vascular enhancement, stair step artifacts, image noise and signal, overall image quality, and score given to visualization of the course of the coronary arteries showed no significant difference ($p>0.35$) in the retrospective and prospective ECG gated groups. The mean estimated effective dose was significantly lower for the prospective ECG gated group compared to the retrospective group, (0.83 mSV vs 2.39 mSV) respectively ($p<0.0005$).

Conclusions: Prospective ECG-gated cardiac MDCT provides comparable assessment of coronary anatomy, image quality with significantly less radiation dose when compared to the retrospective ECG-gated MDCT. Prospective ECG gated cardiac MDCT is a powerful adjunct to the treatment and surgical planning of pediatric patients with congenital heart disease less than 1 yr of age with lower radiation dose.

Paper #: PA-036

Improving Radiology Resident Education of Pediatric Neuroradiology Using On-Line Streaming Video with Live Case Conferences

Chetan Shah, *Radiology, Arkansas Children's Hospital, shahchetanc@uams.edu*; Raghu H. Ramakrishnaiah, Charles M. Glasier, Shelly Lensing, Linda A. Deloney, S. Bruce Greenberg

Purpose or Case Report: Radiology resident conferences consist of live didactic lectures or case conferences. Didactic lectures require attendance at a fixed time. Case conferences assume a knowledge base prior to attending. Our premise is that radiology resident learning of pediatric neuroradiology would improve if didactic lectures were reviewed by on-line streaming video prior to a series of live case based conferences.

Methods & Materials: 3 pediatric neuroradiology lectures were recorded and made available to 29 radiology residents at a university program through on-line streaming video viewed through an internet link. Topics included brain tumors, phakomatosis, and congenital brain malformations. One lecture per week was recommended prior to case conferences that reviewed the same topic. Pre- and post-tests and a feedback survey were administered. Nonparametric paired sign test and analysis of covariance were used to evaluate changes in test scores overall and according to feedback responses. Spearman's partial rank correlation coefficient was used to evaluate the relationship between the number of viewed videos and test scores.

Results: Twenty-nine residents completed the pre-test and 28 the post-test. The means (SD) scores were 59.3% (12.0%) and 64.8% (14.2%) respectively. There was a significant improvement in test scores ($p=0.019$). Residents that agreed/strongly agreed that the streaming technology lectures were convenient had greater improvement than those who did not (14.0 vs. -3.2%, $p=0.001$). Similarly, those who agreed/strongly agreed that being able to replay a lecture was helpful had greater improvement than those who did not (10.9 vs. -6.7%, $p=0.001$). Finally, those who agreed/

strongly agreed that the streaming technology lecture format was a better teaching tool had greater improvement than those who did not (10.8 vs. -4.7%, $p=0.003$). Significant positive correlation between number of videos watched post-conference and improvement was present (Spearman's $\rho=0.48$, $p=0.013$).

Conclusions: On-line streaming video with live case conferences enhances radiology resident learning of pediatric neuroradiology.

Paper #: PA-037

MR Utilization Defined and Enhanced Through Process Improvement

John Strain, MD, *Children's Hospital Colorado, John.Strain@Childrenscolorado.org*; Linda Wright, Katie Bushur, Neta Hogestad, Kelly Kasper

Purpose or Case Report: Define a reliable metric for MR utilization. Describe aspects of a process improvement initiative that were critical to improved utilization.

Methods & Materials: Utilization was calculated as the sum of the scan times divided by elapsed time from first scan to last image of the day. Modality Perform Procedure Step (MPPS) software provided an accurate measurement of scan time. Visual charting made gaps in utilization apparent. Technologists and nursing notes correlated to gaps identified barriers and opportunities for improvement. Nursing and Anesthesiology reduced redundancies. Standardized protocols lead to more consistent scan times. Appointment access for sedated MRI was measured by the third available appointment.

Results: Manually entered data points were time consuming, inconsistent and unreliable. The process improvement was most effective when fewer more reliable data points were used to evaluate the effect of change. The program resulted in a reduction of appointment access for sedated MRI from 30 days to 2 days with no change in the hours of operation. Magnet utilization was increased from 58% to 73%. Induction outside the scan room provided the most efficient process tested. We ranked first in utilization in a Children's Healthcare Cooperation of America (CHCA) survey as measured by exams per scanner. Patient preference for a.m. scheduling was shown by survey and corroborated by scheduling data. Consistent scan times were achieved by protocol standardization augmented by indication driven decision support.

Conclusions: A concise definition of MR utilization established a metric that was used in the process cycle of Analyze–Optimize–Measure. Anesthesia induction outside the

magnet was the most efficient practice but required collaboration between nursing, MR technologists and Anesthesiology. Protocol standardization were valuable aspects of process improvement essential to optimizing parallel sedation. These adjustments reduced appointment access from 30 days to 2 days, increased utilization from 58% to 73% and produced a number one rank in utilization by CHCA survey.

Paper #: PA-038

Indication Driven Decision Support for Order Entry in Pediatric Imaging

John Strain, MD, *Children's Hospital Colorado, John.Strain@Childrenscolorado.org*; Nicholas V. Stence, Gordon Teubner, Kelly Kasper

Purpose or Case Report: Develop a process for indication driven order entry in pediatric imaging.

Methods & Materials: Order entry through Epic EMR is multifaceted with preference lists, and order sets. Best practice alerts can help direct imaging. However indication driven decision support for order entry is lacking. We exploited the synonym option in Epic order entry to translate indications into procedures mapped to specific protocols for MRI neuroimaging. The order screen allows the provider to enter an indication. That indication is linked through a synonym option to a specific exam and protocol. The recommendation is based upon institutionally created clinical care guidelines, and can be accepted with a single click to complete the order. The requesting provider retains the option to override the recommendation. An step in process development utilized an order queue established within the Epic inbasket. A Pediatric Radiologist monitored the queue and communicated with referring providers to obtain additional history and educate toward best imaging practice. These interactions facilitated development of a robust index of clinical indications used to create the synonym pool.

Results: MRI neuroimaging indications were expanded into a robust data set linked to specific MRI exams aligned with specific protocols. The synonym option within Epic created the opportunity for the requesting provider to simply enter an indication which drives the procedure and recommended protocol. Provider satisfaction has been high and concurrence with recommendations nearly universal.

Conclusions: Indication driven order entry was achieved through the synonym option in order entry within the Epic EMR. Imaging recommendations are based upon institutional clinical care guidelines developed through consensus. A

robust compilation of pediatric MRI neuroimaging indications has been created and linked to specific exams and protocols. Compliance with the indication driven recommendation has been high. Modifications of the current system are currently under development for all cross sectional modalities and organ systems.

Paper #: PA-039

Cost-Effectiveness of Routine Neonatal Renal Ultrasound in Non-Syndromic Complex Congenital Heart Disease

Elfrides Traipe, TCH, extraipe@texaschildrens.org; Jill V. Hunter, Marthe Munden

Purpose or Case Report: To assess the prevalence of abnormal renal ultrasound in non-syndromic complex congenital heart disease (CCHD) and assess the cost-effectiveness of routine renal ultrasound in this population.

Methods & Materials: We retrospectively reviewed the initial neonatal renal ultrasound and any subsequent renal imaging in 97 patients with non-syndromic CCHD. Etiologies included hypoplastic left heart syndrome (HLHS), transposition of the great vessels (TGA), coarctation of the aorta (CoA), truncus arteriosus (TA), double outlet right ventricle (DORV) with or without patent ductus arteriosus. Patients were recruited consecutively as part of a prospective trial for pre- and post-operative magnetic resonance imaging of the brain.

Results: The neonatal pre-operative renal ultrasounds were analyzed in 41 female and 56 male patients. Only 1 of the 97 patients showed any congenital renal anomaly. This patient was born with hypospadias, that would have routinely stimulated neonatal follow up.

Conclusions: Knowledge of embryology would not lead us to anticipate a high co-incidence of congenital renal and cardiac pathology. Based on this statement and our findings, our recommendation to improve cost-effectiveness is not to perform routine neonatal renal ultrasound in non-syndromic CCHD, but only if otherwise clinically indicated.

Paper #: PA-040

A Meta-Analysis of the Diagnostic Performance of Contrast Enhanced Voiding Urosonography (ceVUS)

Kassa Darge, MD, PhD, [University of Pennsylvania, Dept. of Radiology, The Children's Hospital of Philadelphia, darge@email.chop.edu](mailto:darge@email.chop.edu); Katerina Ntoulia, Vangelis Evangelou, Frederica Papadopoulou

Purpose or Case Report: To conduct a meta-analysis of the diagnostic performance of contrast enhanced voiding urosonography (ceVUS) in comparison to voiding cystourethrography (VCUG) or direct radionuclide cystography (DRNC).

Methods & Materials: A literature search was conducted for studies published on ceVUS in the pediatric age group. Studies were included if the ultrasound contrast agents (USCA) Levovist® (Bayer-Schering Pharma, Germany) or SonoVue® (Bracco, Italy) were used and enough data was available to extract 2x2 tables. If the ceVUS was compared to both VCUG and DRNC in the same patients the results for each were analyzed separately. A bivariate hierarchical model that takes into account the heterogeneity in ceVUS sensitivity and specificity in different studies was used for the assessment of the summary diagnostic metrics. The summary ROC curve was derived and presented graphically from the parameters of the model. Additionally, the 95% confidence intervals (CI) and the positive (LR+) and negative (LR-) likelihood ratios were calculated.

Results: Out of 127 publications only 30 comparative studies fulfilled the inclusion criteria. These encompassed 26 ceVUS studies in comparison with VCUG and 4 with DRNC with regards to detection of vesicoureteric reflux. In 26 studies the USCA Levovist® and in 4 SonoVue® were used. A total of 2549 children with 5078 pelvi-ureteral-units (PUUs) were included in the meta-analysis. ceVUS compared to VCUG and DRNC had a sensitivity of 90% (CI: 85–93) and a specificity of 92% (CI: 89–94) with LR+ and LR- of 11.7 and 0.11, respectively. The performance of ceVUS was better when compared to DRNC than to VCUG (sensitivity 94%, specificity 95% versus 90% and 92%, respectively). The meta-analysis of the diagnostic performance of ceVUS regarding the urethra included 880 patients (682 boys). Excellent imaging of urethral anatomy was reported in over 97% of the patients. However, currently there is only one comparative study with 146 patients available. In this study 100% sensitivity and 100% specificity were reported.

Conclusions: Sufficient evidence is available clearly demonstrating the high diagnostic performance of ceVUS compared to VCUG or DRNC regarding the detection or exclusion of VUR in children. These findings combined with the absence of radiation should be convincing reasons for promoting the widespread use of ceVUS in children.

Disclosure: Dr. Darge has indicated that he will discuss or describe, in the educational content, a use of a medical device or pharmaceutical that is classified by the Food and Drug Administration (FDA) as investigational for intended use.

Paper #: PA-041**The Sonographic Evaluation of Hydronephrosis in the Pediatric Population: Is a Well-tempered Ultrasound Necessary?**

Sarkis Babikian, MS, MD, Tripler Army Medical Center, *sarkis.babikian@amedd.army.mil*; Marc R. Walker, Michael B. Lustik, Leah P. McMann, Veronica Rooks

Purpose or Case Report: Prenatal ultrasound (US) has increased identification of infants with asymptomatic renal pelvic dilatation. Society for Fetal Urology (SFU) grading is used in the sonographic evaluation of pediatric hydronephrosis. Based on US findings, a nuclear medicine diuretic renogram may assess renal function, which could result in operative intervention. Standardized protocols for diuresis renography, the “well-tempered renogram,” already exist; however, no current study has assessed effect of intravenous hydration (IV) status with US in the evaluation of childhood hydronephrosis. Our study assesses the effect of hydration on SFU grading.

Methods & Materials: In this prospective IRB approved study, pediatric patients diagnosed with pelvicaliectasis requiring a diuretic renogram were recruited to undergo pre and post hydration renal US. A urinary catheter was placed followed by renal US pre and post IV hydration (10 ml/kg normal saline bolus). Imaging was performed by the same sonographer on the same US machine. A well-tempered renogram was then performed. All images were reviewed by two blinded radiologists, one pediatric radiologist who assigned SFU grades to each kidney.

Results: Data were collected from 34 studies, with ages ranging from 6 weeks–16 years, with an average age of 22 months. There were 28 unique patients. Of these, 23 underwent a single renogram, 4 underwent two renograms, and 1 underwent 3 renograms. One patient had a solitary kidney due to MCDK. Thus, there were 33 usable paired sonograms (67 kidneys) for analysis. SFU grades were compared in the pre- and post-hydration US for each kidney. Two-sided statistical tests were done to assess whether SFU grades changed significantly after hydration (sign test). 52 of 67 (78%) kidneys remained the same grade post hydration. When there was a difference, most demonstrated an increase (13 of 15 kidneys and $p < 0.01$). No change in SFU grade pre- and post-hydration differed by more than 1. Only 1 kidney went from grade 2 to grade 3. SFU above grade 2 is considered clinically significant. No kidney that was grade 3–4 pre-hydration became grade 0–2 post-hydration. When SFU is dichotomized grade 0–2 vs. 3–4, there was no significant change in grade from pre to post hydration ($p = 1$).

Conclusions: Hydration does not appear to have a clinically significant effect on SFU grade. Therefore, performance of a “well-tempered” US is unnecessary.

Paper #: PA-042**Renal Elasticity Evaluation by Acoustic Radiation Force Impulse (ARFI) Measurement in Young Children with Normal Kidney vs. Hydronephrosis**

Mi-Jung Lee, Radiology, Severance Children's Hospital, *mjl1213@yumc.yonsei.ac.kr*; Myung-Joon Kim

Purpose or Case Report: There are many previous studies about using acoustic radiation force impulse (ARFI) value to measure the elasticity of tissue, mainly the liver in adult patients. Also there are several trials to use the ARFI value in the adult kidney, such as evaluating of renal mass and assessment of renal allograft fibrosis. But as we know, there was no study about ARFI measurement in the pediatric kidney. The purpose of this study was to evaluate the ARFI value in the normal kidney and hydronephrosis in young children and to correlate between the ARFI value and the degree of hydronephrosis

Methods & Materials: The study prospectively enrolled 51 patients who are under 24 months old, and underwent kidney ultrasonography (US) and ARFI between July 2011 and August 2011. Degree of hydronephrosis was evaluated in both kidneys based on Onen's hydronephrosis grading. ARFI velocity measuring was performed by 4–9 MHz linear probe for pediatric patients. In 49 patients ARFI velocity was measured 3 times at each side kidney. In other 2 patients measuring was done two times due to poor patient cooperation.

Results: There were 38 boys and 13 girls with mean age of 7 months. Twenty patients had no hydronephrosis bilaterally. Four patients had right kidney hydronephrosis only. Twenty patients had left kidney hydronephrosis only. And seven patients had bilateral hydronephrosis. The mean of ARFI value measured in normal kidney was 1.85 ± 0.43 m/s at right and 1.69 ± 0.46 m/s at left. The mean of ARFI value measured in hydronephrotic right kidneys was 1.82 ± 0.55 m/s and in hydronephrotic left kidneys was 1.88 ± 0.39 m/s. ARFI velocity was not significantly different between normal and hydronephrotic kidney. The mean of ARFI velocity in severe hydronephrosis (grade III or IV) was 2.08 ± 0.50 m/s in right and 1.91 ± 0.36 m/s in left, and was not significantly different with ARFI velocity in normal group.

Conclusions: ARFI measurement of kidney is feasible in young pediatric patients. ARFI velocity of normal kidney in patients who are under 2 years old is measured 1.85 m/s at right and 1.69 m/s at left which is lower than previous adult data (2.37 m/s). Mean of ARFI velocity was not significantly different between normal and hydronephrotic kidney even in severe hydronephrosis.

Disclosure: Dr. Lee has indicated that she will discuss or describe, in the educational content, a use of a medical device or pharmaceutical that is classified by the Food and Drug Administration (FDA) as investigational for intended use.

Paper #: PA-043**Patient and Family Impact of Pediatric Genito-Urinary Diagnostic Imaging Tests**

Jeanne Chow, *Children's Hospital Boston, jeanne.chow@childrens.harvard.edu*; Caleb Nelson, Iina Rosoklija, Sonja Ziniel, Jonathan Routh, Bartley Cilento

Purpose or Case Report: The impact of diagnostic genito-urinary imaging (GUI) on patients and families is poorly understood. This study sought to measure patient and family reaction to commonly performed GUI studies, using a standardized measurement tool.

Methods & Materials: We prospectively surveyed families undergoing GUI (renal ultrasound (RUS), voiding cystourethrography (VCUG), radionuclide cystogram (RNC), static renal scintigraphy (DMSA), and diuretic renal scintigraphy (MAG3)). We developed a Likert-scaled 11-item survey instrument to assess impact of GUI across 4 domains (pain, anxiety, time, test satisfaction). Survey scores were analyzed using ANOVA and linear regression.

Results: 263 families were surveyed (61 RUS, 52 VCUG, 55 RNC, 47 MAG3, 48 DMSA). 37% <1 yr, 42% 1–3 yrs, and 22% >3 yrs. 45% were male. 77% were white. Patient age, gender, and prior GUI history varied by study type. Study type was significantly associated with both total and weighted score (both $p < 0.0001$). RUS was better and MAG3 was worse than VCUG, RNC, and DMSA, which did not differ from each other. Other factors associated with worse total scores included patient age 1–3 years ($p < 0.001$) and non-white race ($p = 0.04$). Gender, prior testing history, wait time, and parent education were not associated with total scores. In the multivariate model, RUS remained the best, MAG3 the worst, and DMSA, VCUG, and RNC in the middle ($p < 0.0001$). Compared directly, DMSA and VCUG total score did not differ ($p = 0.59$).

Conclusions: This study documents significant differences among GUI studies with respect to the patient and family experience, but there was no overall difference between DMSA and VCUG. These findings may be useful to aid decision-making when considering GUI for pediatric patients.

Paper #: PA-044**Performance and Diagnostic Value of MRI for Pediatric Liver Transplant Complications**

Shilpy Chowdhury, MD, MPH, *Stanford University School of Medicine, Department of Pediatric Radiology, drshilpy@stanford.edu*; Shreyas Vasanawala

Purpose or Case Report: The purpose of this study is to assess diagnostic value and accuracy of using MRI in detecting post liver transplant biliary and vascular complications in children.

Methods & Materials: 57 pediatric liver transplant recipients who underwent MR imaging between January 2006 and April 2011 were retrospectively identified with IRB approval and HIPAA compliance (age range: 0.13–22 years; mean \pm SD = 7.88 ± 6.12 years; 53% males and 47% females). Taken as gold standard, ERCP, catheter angiography/venography, surgical exploration and follow-up imaging were used to catalog post liver transplant complications. Relative to this gold standard, findings on MRI were used to determine sensitivity, specificity, positive predictive value, negative predictive value, and accuracy.

Results: By gold standard frequencies of biliary and vascular complications were 19% and 30%, respectively. 18% of patients undergoing MRI had biliary complications while 32% had vascular complications. For biliary complications MRI showed a sensitivity of 82%, specificity of 98%, PPV of 90%, NPV of 96% and an accuracy of 95%. MRI had a diagnostic value of 100%, specificity of 98%, PPV of 80%, NPV of 100% and 98% accuracy in detecting hepatic artery stenosis. Hepatic artery thrombosis had a diagnostic value and accuracy of 100% with MRI. Portal vein stenosis showed sensitivity of 100%, specificity of 98%, PPV of 83%, NPV of 100% and an accuracy of 98%; portal vein thrombosis showed sensitivity of 75%, specificity of 100%, PPV of 100%, NPV of 98% and an accuracy of 98% with MRI. For inferior Vena Caval complications MRI showed sensitivity of 86%, specificity of 98%, PPV of 86%, NPV of 98% and an accuracy of 96%.

Conclusions: MRI is an accurate and reliable technique to detect pediatric post liver transplant biliary and vascular complications.

Disclosure: Dr. Chowdhury has indicated that he will discuss or describe, in the educational content, a use of a medical device or pharmaceutical that is classified by the Food and Drug Administration (FDA) as investigational for intended use.

Paper #: PA-045**Diffusion-Weighted Imaging (DWI) Biomarkers for the Evaluation of Crohn's Ileitis**

Mark Bittman, *Radiology, Children's Hospital Boston, mark.bittman@childrens.harvard.edu*; Moti Freiman, Michael J. Callahan, Jeannette Perez Rossello, Simon Warfield

Purpose or Case Report: To compare the diagnostic capacity of qualitative and quantitative DWI to gadolinium

enhanced MR enterography (MRE) in the detection of ileitis in pediatric patients with Crohn's disease (CD).

Methods & Materials: We retrospectively reviewed the imaging findings of 29 consecutive patients with histologic diagnosis of CD (17 males, 12 females; mean age 14.6 years; age range 5–24 years) who underwent MRE between 1/21/2011 and 10/10/2011. The MRE was performed in a Siemens Avanto 1.5 Tesla scanner. Standard departmental volume of polyethylene glycol and fluid were administered for bowel distention. The imaging protocol included DWI with eight b values ranging between 0 sec/mm² and 800 sec/mm² and gadolinium enhanced dynamic 3D VIBE (volume interpolated breath hold exam) in the coronal plane. The studies were qualitatively evaluated in a blinded fashion by two board certified radiologists. Disease activity was defined as bowel wall thickening and enhancement in the gadolinium enhanced images. DWI abnormality was defined as bowel thickening, increase signal on DWI images and decrease signal on ADC maps of the ileum. Intra voxel incoherent motion (IVIM) DWI parameters were used as quantitative biomarkers for the analysis of slow diffusion (D) and fast diffusion fraction (f).

Results: Gadolinium enhanced VIBE images identified abnormal thickening and enhancement of the ileum in 11/29 (38%) patients. DWI identified abnormal signal in 11/29 (38%) patients. The sensitivity and specificity of the qualitative DWI for identifying ileitis, as shown by gadolinium enhanced imaging, were 82% and 89%, respectively. Quantitative analysis showed statistically significant difference in IVIM maximal values for f (fast diffusion fraction) between abnormal (mean=0.67, std=0.17) and normal (mean=0.8, std=0.14) ileum segments ($p=0.012$). There was statistically significant difference in IVIM maximal values for D (slow diffusion) between abnormal (mean=2.2 $\mu\text{m}^2/\text{ms}$, std=0.7 $\mu\text{m}^2/\text{ms}$) and normal (mean=2.7 $\mu\text{m}^2/\text{ms}$, std=0.6 $\mu\text{m}^2/\text{ms}$) ileum segments ($p=0.0084$). Abnormal loops of bowel had decreased slow and fast diffusion parameters.

Conclusions: Diffusion weighted imaging has excellent sensitivity and specificity for the detection of active ileitis in pediatric CD. Furthermore, quantitative IVIM model parameters provide effective biomarkers for this condition. IVIM DWI has the potential to assess bowel inflammation without intravenous contrast enhancement and further increase our understanding of CD.

Paper #: PA-046

MRE Scoring of Crohn's Disease

Kevin Boyd, DO, *Medical Imaging, Children's Memorial Hospital, kboyd@childrensmemorial.org*; Cynthia K. Rigby, Ellen Benya

Purpose or Case Report: To compare an MR Enterography (MRE) scoring classification of severity of Crohn's disease with a clinically utilized Short Pediatric Crohn's Disease Activity Index (SPCDAI).

Methods & Materials: MRE imaging findings of 15 pediatric subjects ages 11 to 21 years (mean 15.6 years) with pathologically proven Crohn's disease were retrospectively reviewed by 3 pediatric radiologists. An MRE imaging scoring system was devised. The small bowel and colon were divided into 6 segments and scored (0-absent, 1-present) based on the presence of bowel wall thickening, T2 bowel wall high signal intensity, bowel wall hyperenhancement, mesenteric engorgement and lymphadenopathy. Complications were scored (0-absent, 2-present) for the presence of stricture with prestenotic dilation, intraabdominal abscess, intrabdominal fistula and perineal disease. The MRE score recorded for each patient was the average of scores from the 3 readers. A retrospective chart review of each subject was performed to determine the SPCDAI prior to the MRE. SPCDAI scoring includes assessment of general well being, abdominal pain, and weight loss each scored at 20 points. Stool quality and quantity, abdominal exam and extraintestinal manifestations were each scored at 10 points. A total score <15 is considered inactive disease, 15–29 mild disease, and ≥ 30 moderate to severe disease.

Results: MRE scores ranged from 1–10 [mean (SD) of 5 (2.7)]. SPCDAI score ranged from 0–80 [mean (SD) of 32 (22.7)]. Mean (SD) MRE score in patients with a SPCDAI indicating inactive disease was 4.3 (1.5), for mild disease by SPCDAI was 6.3 (3.8), and for moderate to severe disease by SPCDAI was 5.3 (2.7). 50% of patients classified as mild disease by SPCDAI had MRE imaging findings of stricture and prestenotic dilation causing there to be higher MRE scores in these patients.

Conclusions: MRE imaging disease activity score provides an objective, supplemental tool in the assessment of the severity of Crohn's disease with utility in standardizing image evaluation and identifying patients that have more advanced disease than is clinically apparent by the SPCDAI. Ongoing data collection is in process.

Paper #: PA-047

MR Enterography: Can Diffusion-Weighted Imaging Replace the Need for Intravenous Contrast Administration?

Alok Jaju, MD, *Mallinckrodt Institute of Radiology, alokjaju@gmail.com*; Geetika Khanna, Fowler Kathryn

Purpose or Case Report: MR enterography (MRE) has become the imaging modality of choice for assessment of disease activity in pediatric inflammatory bowel disease (IBD). Preliminary data suggest that diffusion-weighted

imaging (DWI) can be used to assess IBD activity. Our study compares the diagnostic performance of non contrast MRE (NCMRE) with DWI, and contrast enhanced MRE (CEMRE) in assessing disease activity status and associated complications, using histopathology as the gold standard.

Methods & Materials: This retrospective, IRB approved, HIPAA compliant study included patients under the age of 25 years, who underwent MRE with DWI between September 2008 to June 2011, and had histological proof of disease activity status within 8 weeks of MRE. NCMRE images (HASTE and DWI) and CEMRE images (HASTE and CE gradient echo) were interpreted by two radiologists in separate sessions, six weeks apart, masked to all clinical information. The sensitivity, specificity, positive predictive value (PPV) and negative predictive value (NPV) for each of these methods was calculated using histopathology as the gold standard.

Results: 28 patients met the inclusion criteria, with median age of 18 years, and range from 5–24 years. There were 17 males and 11 females. At the bowel segmental level, 92 segments had corresponding histological proof. For observer 1, the sensitivity, specificity, PPV, NPV for NCMRE/DWI and CEMRE for detection of disease activity were 63%, 90%, 82%, 77% and 54%, 98%, 96%, 76% respectively. The corresponding values for observer 2 were 37%, 98%, 94%, 70% and 53%, 88%, 77%, 72% respectively. Abscesses were correctly identified in 3 patients by both techniques.

Conclusions: The diagnostic performance of non contrast MRE with DWI is comparable to that of contrast enhanced MRE. Both methods have high specificity but relatively lower sensitivity. Our data suggest that given comparable diagnostic performance, NCMRE with DWI can be used for surveillance of IBD. These results will be validated with future prospective studies.

Paper #: PA-048

Diagnostic Accuracy and Clinical Significance of Magnetic Resonance Enterography of the Small Intestine in Comparison with Ileocolonoscopy in Pediatric Inflammatory Bowel Disease

Ulla Ullberg, *Dept of Radiology, Astrid Lindgren's Children's Hospital, Karolinska Institute, ulla.ullberg@karolinska.se*; Ulrika Fagerberg, Michael Torkzad, Lennart Blomqvist, Hans Hildebrand, Per Hellström

Purpose or Case Report: The aims were to study the diagnostic accuracy of Magnetic resonance enterography (MRE) in paediatric inflammatory bowel disease (IBD) in diagnosing intestinal inflammation in and to evaluate the clinical significance of the MRE results on the management of pediatric IBD patients.

Methods & Materials: Forty pediatric patients (median age 13.8 years, range 10.0–17.7) with suspected ($n=35$) or confirmed IBD ($n=5$) were included and underwent gastroileocolonoscopy with biopsies followed by MRE (median interval 20 days, range 6–55). The MRE results were compared with macroscopic and microscopic assessment of the ileum. The clinical importance of the MRE results was registered.

Results: Crohn disease (CD) was diagnosed in 25 cases, ulcerative colitis (UC) in 12, and IBD unclassified (IBDU) in three. Macroscopic ileitis was detected in 15/25 (60%) of CD cases and in 2/12 (17%) of UC (backwash ileitis). Microscopic inflammation was found in another four CD cases and one IBDU patient. In total, discrepancy between macroscopic and microscopic inflammation was found in 9 CD, 2 UC and one IBDU patients. The sensitivity of MRI was 64% (against macroscopy and/or microscopy) to 71% (against macroscopy alone), while the specificity was 100% and 92%, respectively. MRE findings was decisive for diagnosis in 4/40 (10%) and led to treatment adjustments in 11/40 (28%) in the following six months.

Conclusions: MRE is a reliable method for imaging of intestinal inflammation in pediatric IBD, and can be supportive or essential for clinical treatment decisions.

Paper #: PA-049

CT Findings in Pediatric Eosinophilic Colitis, A Differential Diagnosis for Inflammatory Bowel Disease

Jonathan Brandon, MD, *Children's Hospital Colorado—Radiology, jonbra@gmail.com*; Laura Z. Fenton, Shauna Schroeder, Kelley Capocelli, Joanne Masterson, Glenn Furuta

Purpose or Case Report: Eosinophilic colitis (EC) is an idiopathic subtype of eosinophilic gastrointestinal disease. Clinical features of EC overlap with the more common inflammatory bowel disease. CT imaging features of EC have not been described in children. We report clinical, imaging, and histologic findings of seven children with eosinophilic colitis.

Methods & Materials: Consecutive children with EC were identified in a pathology database from January 2010 to September 2011. Clinical and pathologic features and CT findings were recorded.

Results: Of 15 children with EC, 7 had CT imaging of the abdomen and pelvis. These 7 children ranged in age from 15 months to 16 years (mean 10.2 years \pm 6.3) with a male predominance ($n=4$, 57%). The most common presenting symptoms were abdominal pain ($n=6$), bloody diarrhea ($n=3$), and rectal bleeding ($n=3$). EC was characterized as a dense and predominant eosinophilic inflammatory infiltrate in the lamina propria and/or epithelium without granulomas. CT

scans were abnormal in 6 (86%). No colonic luminal contrast was present in 2 patients, and in one of these, the colon appeared normal. Abnormal CT findings included cecal wall thickening ($n=5$, 71%), mucosal enhancement without colonic wall thickening, ($n=1$, 14%), mesenteric lymph node enlargement ($n=2$, 29%), terminal ileal thickening ($n=2$, 29%), jejunal and ileal thickening ($n=1$, 14%), and pneumatosis ($n=1$, 14%). Of the 5 patients with cecal involvement, 4 primarily involved the cecum with less severe or no ileal or downstream colonic involvement. Pneumatosis extended along the length of the colon with rectal predominance.

Conclusions: The predominant CT finding in our EC series was wall thickening, most severe in the cecum with variable extent downstream with mild or no involvement of the terminal ileum. Although there is overlap, these findings are different from the most common patterns encountered with ulcerative colitis or Crohn disease and should raise the possibility of EC in children presenting with abdominal pain and bloody diarrhea.

Paper #: PA-050

Imaging Trends and Radiation Exposure in Pediatric Inflammatory Bowel Disease Patients at a Large Academic Children's Hospital

Jason Domina, MD, Radiology, University of Michigan, dominaj@med.umich.edu; Jonathan R. Dillman, Jeremy Adler, Adam Dorfman, Peter J. Strouse, Shokoufeh Khalatbari

Purpose or Case Report: To define diagnostic trends in pediatric inflammatory bowel disease (IBD) patients at a large academic children's hospital between 2001 and 2010.

Methods & Materials: IBD patients ≤ 18 years of age within the BLINDED Health System during the calendar years of 2001, 2006, and 2010 were identified by searching electronic medical records. The number of abdominopelvic radiologic and endoscopic exams performed during each one-year period was recorded for each subject. The average number of exams for each diagnostic modality per subject performed during each one-year period was compared using the Wilcoxon rank sum test. The lifetime number of diagnostic studies by modality and estimated effective radiation dose for the 2010 subject cohort were calculated.

Results: Our study documents a 53% increase in the yearly number of abdominopelvic diagnostic studies obtained in pediatric IBD patients between 2001 to 2010 (1.29 ± 2.19 vs. 1.98 ± 3.46 , $p=0.004$). During the same period, there was significantly reduced utilization of most ionizing imaging studies, including contrast enema (0.06 ± 0.27 vs. 0.02 ± 0.19 , $p<0.0001$), small-bowel follow-through (SBFT) (0.23 ± 0.44 vs. 0.05 ± 0.22 , $p<0.0001$), and upper GI (UGI) series ($0.21 \pm$

0.42 vs. 0.06 ± 0.23 , $p<0.0001$). Radiography (0.22 ± 0.84 vs. 0.46 ± 1.56 , $p=0.02$), MRI (0.00 vs. 0.59 ± 1.01 , $p<0.0001$), and esophagogastroduodenoscopy (EGD) (0.13 ± 0.37 vs. 0.23 ± 0.63 , $p=0.01$) demonstrated significantly increased use. While ileocolonoscopy and CT use also increased, this change was not significant ($p>0.05$). Univariate analysis demonstrated that CD (vs. UC, $p=0.04$), female gender ($p=0.01$), younger age ($p=0.004$), and being imaged in the 2010 calendar year (opposed to 2001 or 2006, $p=0.004$) were predictors of an increased number of diagnostic studies per patient per year. The average patient in the 2010 IBD cohort (mean age = 14.9 ± 3.5 years) had undergone 1.08 CT, 0.82 MRI, 1.36 radiographic, 0.14 contrast enema, 0.52 SBFT, 0.54 UGI, 1.00 ileocolonoscopy, 0.72 EGD, and 0.014 wireless capsule endoscopy (WCE) exams during their lifetime.

Conclusions: The number of diagnostic studies performed on pediatric IBD patients per year has increased significantly over the past decade. While the use of several ionizing imaging modalities has significantly decreased over this time period, the use of radiography, MRI, and EGD has significantly increased.

Paper #: PA-051

Development of a Pediatric Stroke Alert System

Laura Fenton, MD, Children's Hospital Colorado, laura.fenton@childrenscolorado.org; Nicholas V. Stence, John Strain, Elizabeth Carroll, Meghan J. Calhoon, Timothy J. Bernard

Purpose or Case Report: Timely identification of childhood arterial ischemic stroke (AIS) is critical to development of acute treatment strategies. We present our experience prior to and following development of a pediatric stroke alert system (SAS).

Methods & Materials: Through multi-disciplinary collaboration in a tertiary care setting, a pediatric SAS was established in 2008. We describe the system, imaging protocol evolution, and impact upon the time between admission and MRI initiation (time-to-MRI) in patients with childhood AIS. Of 74 patients in our stroke database (COMIRB #05-0339), 27% met inclusion criteria for stroke alert initiation (acute focal neurological deficit within 12 h). Eleven pre-2008 and nine post-2008 patients met criteria. We compared the time-to-MRI between these two groups, utilizing a two-tailed t-test.

Results: The pediatric SAS has two phases: I—neurological evaluation and II—imaging and treatment consideration. Phase I stroke alert is initiated when a child presents with an acute focal neurologic deficit. If neurology confirms stroke symptoms and CT head is negative for an alternative etiology, a stroke alert is called prompting an emergent brain MRI. If MRI confirms an acute stroke, hyperacute therapies

are considered. Initial MRI protocol included DWI, T2, FLAIR, 3D TOF COW MRA, 2D TOF neck MRA and fat saturated T1 neck imaging. After internal quality review, T1 MPRAGE brain and contrast enhanced 3D neck MRA were added. The sequence order was also altered so diagnostic sequences were scanned first (DWI and COW MRA). There was a trend towards decreased time-to-MRI in the post-2008 group (mean=152 min, SD +/- 120) as compared to the pre-2008 group (mean 340 min, SD=+/-304; $p=0.10$).

Conclusions: Institution of a pediatric SAS improved urgent neurologic evaluation and demonstrated a trend towards shorter time-to-MRI. Ongoing quality review has enhanced imaging quality and decreased time-to-MRI. Continued refinement of Pediatric SAS's will be critical to the success of recently funded phase I clinical trials in the evaluation of hyperacute therapies.

Paper #: PA-052

Neonatal Deep White Matter Venous Infarction and Liquefaction: A Pseudo-Abscess Lesion

Carly Dent, BS, *Radiology, Nationwide Children's;* Lynne Ruess, Michelle A. Yoshida, Jerome A. Rusin

Purpose or Case Report: To characterize the MRI findings of white matter necrosis and liquefaction after hemorrhagic deep white matter venous infarction in infants to distinguish these lesions from cerebral abscesses.

Methods & Materials: An institutional review board approved retrospective review of imaging records to identify all patients with cerebral venous infarction at a children's hospital over a 10 year period. Nine infants had deep white matter hemorrhagic venous infarction with subsequent significant white matter necrosis. A diagnosis of cerebral abscess was considered in all. The imaging and laboratory findings in these patients are reviewed.

Results: There were 6 female and 3 male infants. The mean post-gestational age at presentation was 20 days (range 0–90 days), while the corrected age was less than 30 days for all patients. 7 patients presented with seizures and signs of infection; 1 presented with lethargy and later proved to have protein C deficiency. MRI was performed 0–12 days from presentation in these 8 patients. Another patient with known protein C deficiency underwent MRI at 3D for followup of screening US abnormalities. There were a total of 27 deep cerebral white matter lesions: 21 frontal, 4 parietal, 2 temporal lobe. Lesions were fluid signal cavities with restricted diffusion. Larger lesions had dependent debris. All lesions had associated hemorrhage and most lesions had evidence of adjacent small vessel venous thrombosis. Lesions imaged after Gad showed peripheral enhancement. Three lesions were seen to

increase in size on follow-up imaging. Three patients, 2 with meningitis confirmed via microbiology and 1 with presumed meningitis by CSF counts, underwent surgical aspiration of a total of 6 lesions. All specimens were sent for pathology and culture and were negative for microorganisms.

Conclusions: Recognizing the MR appearance of necrosis and liquefaction after deep white matter cerebral venous infarction in neonates can distinguish this entity from cerebral abscess and potentially avoid an unnecessary neurosurgical aspiration procedure.

Paper #: PA-053

Recurrent Stroke in Children with Dissecting Aneurysms of the Vertebral Artery: Failure of Antithrombotic Therapies

Nicholas Stence, MD, *Children's Hospital Colorado—Radiology, nicholas.stence@childrenscolorado.org;* William Colantoni, Laura Z. Fenton, David Kumpe, Joshua Seinfeld, Timothy Bernard

Purpose or Case Report: Dissecting aneurysms of the vertebral artery (DAVA) are a known complication of cervical trauma in adults, and the adult literature usually describes a benign clinical course. Few case reports of childhood DAVA or its long term outcome have been published, however. We present a series of four children with DAVA who suffered recurrent arterial ischemic stroke (AIS) despite antithrombotic therapy.

Methods & Materials: The Children's Hospital Colorado AIS database (COMIRB #05-0339) was queried for cases of DAVA from 2006–2011. A chart review was conducted for details of presentation, imaging, therapy and clinical course.

Results: Four children with DAVA were identified (3–6 years old at presentation). A history of preceding trivial trauma was elicited in all children. Presenting symptoms included headaches, ataxia, hemiparesis and visual changes. MRI demonstrated restricted diffusion compatible with AIS in the occipital lobes and cerebellum of all four children. DAVA diagnosis required catheter angiography (CA) in 3/4 children. Findings of DAVA included wall irregularity and filling defects at a segment of fusiform arterial enlargement. The left lower V3 segment was involved in 3/4 patients. All four children were initially treated with aspirin but experienced recurrent events on therapy. All four were subsequently anticoagulated. Two children have remained on warfarin for 6–7 years without recurrent events, while the other two had recurrent events despite adequate anticoagulation. These two children underwent uncomplicated

coil embolization of the affected vertebral artery segment, and they have remained symptom-free for five and 20 months since then.

Conclusions: DAVA was diagnosed by CA in 3/4 patients. All four children with DAVA in our series suffered recurrent strokes despite aspirin therapy. Two of the four experienced further strokes on anticoagulation, necessitating endovascular therapy. These findings suggest that DAVA in children may require CA to diagnose, and that it may be refractory to standard adult therapies. Ongoing multicenter efforts in childhood AIS should further evaluate the diagnostic approach and recurrence risk of childhood DAVA.

Paper #: PA-054

Magnetic Resonance Imaging (MRI) and Ultrasonography (US) of the Extreme Preterm Brain

Patrick Barnes, MD, Radiology, Lucile Packard Children's Hospital at Stanford, pbarnes@stanford.edu; Dorothy Bulas, Thomas Slovis, Lisa Wrage, Rosemary Higgins, Susan Hintz

Purpose or Case Report: To compare near-term brain MRI with early and late neonatal brain US in a large cohort of extreme preterm newborns.

Methods & Materials: A prospective secondary study was done of near-term MRI (mean PMA 37.9 wk) as compared with early (4–14 days postnatal age) and late (34–42 weeks PMA) US in 480 infants (mean 25.9 weeks EGA) as part of the multicenter NICHD Neonatal Research Network Surfactant Positive Airway Pressure and Oximetry Trial (SUPPORT). All had late US and MRI within 2 weeks of each other. Independent MRI and US central readers were masked to the clinical and other neuroimaging findings.

Results: 306 (89.5%) of 342 infants with normal late US had normal near-term MRI or only mild white matter abnormalities (WMA) on MRI. The remaining 36 (10.5%) of them had moderate-severe WMA. All 18 infants with late US findings of moderate-severe ventriculomegaly (VMG) had MRI findings of moderate-severe WMA, moderate-severe VMG, or cystic lesions. 76% of 46 infants with grade 3 or 4 hemorrhage on early US had moderate-severe WMA on MRI. On MRI, cerebellar abnormalities were present in 79 (16.5%) and cerebral gray matter abnormalities were present in 6 (1%). Posterior fossa lesions were seen on US in 1.6%, but mastoid views were included in only 50% of the centrally read US.

Conclusions: In the largest extreme preterm cohort to date with near-term MRI and serial US, 19% had mod-severe WMA on brain MRI, similar to previous reports. Cerebellar abnormalities were detected more frequently by MRI than by US.

Neurodevelopmental outcomes at 18–22 months and school age will assess the relative and combined values of MRI and US as outcome predictors.

Paper #: PA-055

Functional Connectivity Analysis Reveals Disrupted Interhemispheric Connectivity in Unilateral Diffuse Hemispheric Disease

Dennis Shaw, MD, Radiology, Seattle Children's Hospital, shawdennis@gmail.com; Andrew V. Poliakov, Seth D. Friedman, Edward Novotny, Jeff Ojemann

Purpose or Case Report: Functional connectivity MRI (fcMRI), an analysis technique based on task-free resting state fMRI recording, can be useful in assessing disruption of connectivity in certain disease states, including epilepsy. In healthy control subjects, functional connectivity reveals strong bilateral interhemispheric connectivity in such system as sensory-motor, visual, auditory as well as dorsal attention and default mode networks. In patients with epilepsy associated with unilateral diffuse hemispheric disease such data is limited. Differences in the pattern of activation would suggest alteration in connectivity in these entities. This finding would impact the typical interpretation of this data that is becoming routinely collected for epilepsy pre-surgical evaluation.

Methods & Materials: Siemens (Erlangen, Germany) system, 3-Tesla (Trio) scanner was used for imaging (EPIBOLD sequence, TE=30 ms, flip angle=90°). Resting state fMRI scan were performed in both awake and anesthetized patient. Awake patients were instructed to relax and rest while keeping their eyes open. Analysis was performed using 1000 Functional Connectomes Project scripts based on AFNI and FSL software packages. Resting state data were analyzed for connectivity with the following seeds: Somatomotor, Visual, Auditory, and Default Mode (posterior cingulate cortex (PCC)).

Results: We applied this technique to evaluate 12 patients with hemispheric seizure disorders, including Rasmussen's, neonatal infarct and migration disorders. All the subjects demonstrated some deviation from typical interhemispheric connectivity with a spectrum of findings. The figure below shows connectivity patterns in a patient with cortical dysplasia. While some interhemispheric connectivity remained in somatomotor (SM) and auditory (A1) systems, it was disrupted in Visual (V1) and default mode (PCC) networks. Variable patterns were found across the cases that corresponded to lesion side, supportive of disruption in interhemispheric connectivity as measured by fMRI.

Conclusions: Resting state functional connectivity patterns are well documented in healthy subjects. These results suggest that interhemispheric connectivity disruption is a typical

feature of unilateral diffuse hemispheric disease though variable in presentation, either being limited to select systems or demonstrating broad disconnect between the two hemispheres. These results should be carefully considered when evaluating data for pre-surgical epilepsy evaluation.

Paper #: PA-056

Dilated Cerebral Ventricles in Ex-Prematures: Just an Illusion? MRI-Based Normative Standards for 19-Year Old Ex-Prematures

Stein Magnus Aukland, MD, PhD, *Institute of Surgical Sciences, Section for Radiology, University of Bergen, stein.magnus.aukland@helse-bergen.no*; Irene B. Elgen, W.K. Kling Chong, Geir Egil Eide, Karen Rosendahl

Purpose or Case Report: Premature birth is associated with white matter injury leading to a wide ventricular system. However, normative standards for ventricular size are lacking for this particular group. **Aims:** We aimed to, in a controlled, population based Norwegian cohort of ex-prematures without major handicaps, and for men and women separately, to 1) create standards for radiological indices of ventricular dilatation, 2) investigate associations of these measurements with subjectively assessed ventricular size, 3) examine differences in ventricular size between ex-prematures and healthy controls

Methods & Materials: The initial birth cohort included 217 neonates, birth weight below 2000 g (low birth weight) born within Hordaland county, Norway, between April 1st 1986 and August 8th 1988. 113 of 174 eligible survivors (without major handicaps) underwent MR examination during the period January 2006 to May 2007. 103 of these were ex-premature (born before gestational age 37 weeks) and were included in this sub-study. Based on T2 weighted images, the ventricular size was subjectively judged as being normal, mildly, moderately or severely dilated by an experienced paediatric neuroradiologist, while objective measurements were performed in a blinded fashion, by a second observer (SMA) using an imaging software program (Nordic Ice®).

Results: The normative standards for the ventricular system in ex-premature young adults showed wide variations, in particular for the occipital horns. The agreement between subjective and objective assessment of ventricular size was good. Ex-prematures had smaller heads than those born term (control group). There was no difference in ventricular size between the two groups, even after adjusting for head size. Ex-premature males had larger ventricles than females; however, the difference disappeared after adjusting for head size.

Conclusions: Young adults born prematurely with a birth weight below 2000 g do not have larger lateral ventricles

than healthy controls born term, even after correcting for a smaller head size.

Paper #: PA-057

Best Practice for Reproducibility When Measuring T2*: Implications for Liver and Cardiac Iron Assessment

Mark Ferguson, MD, *Radiology, Seattle Children's Hospital, markferg@uw.edu*; Randolph Otto, Seth D. Friedman

Purpose or Case Report: Patients with red blood cell transfusion-dependent conditions receive high amounts of iron that can lead to abnormal iron accumulation in tissues resulting in organ damage. While the liver is the dominant excess iron storage organ, iron related cardiotoxicity is a leading cause of morbidity and mortality in patients with transfusion-dependent thalassemia. Therefore, accurate determination and tracking of tissue iron levels in both the liver and the myocardium is important for patient prognostication as well as monitoring treatment changes. While multi-echo gradient echo MRI (T2*) is widely used and validated method employed for iron assessment, less attention has been given to derived metrics. Specifically, the literature almost exclusively reports and uses the mean value for T2* from a pixel-wise (PW) map. Infrequently used is the median. The median is a potentially superior metric than the mean because it is insensitive to outliers. Outliers will always occur in data because of either noise or imperfect vessel exclusion. To compare mean versus median on reproducibility of T2* measurement, 23 subjects who had paired heart/liver measurements were examined.

Methods & Materials: The entire liver (excluding vessels) and the interventricular septum myocardium were traced on representative images from each series. Mean and median T2* values were generated from the pixel maps. R2* (1000/T2*) and coefficient of variation (CV) were computed on a patient-by-patient basis. These measures were then summarized for the group.

Results: Markedly higher R2* values were observed in both heart and liver using median summary measures (liver: $t=-2.79$, $p=.01$, heart: $t=-2.8$, $p=.01$). These findings were accompanied by lower CV's (better reproducibility) for the median approach (liver: $t=1.89$, $p=.07$; heart: $t=1.91$, $p=.07$).

Conclusions: The consistent difference in derived T2* values between the methods (median > mean) should be considered when comparing derived R2* values to established normal ranges. CV data support that using the median as the final summary metric will always outperform mean metrics for measuring change in R2*. This finding has immediate implications for the scientific literature and for guiding therapeutic management over time.

Paper #: PA-058**Diagnostic Efficacy of Chest CT for Diffuse Lung Disease in Childhood Related to Genetic Surfactant Disorders**

R. Paul Guillerman, *Department of Pediatric Radiology, Texas Children's Hospital, rpguille@texaschildrens.org*; Jennifer A. Rama, Alan S. Brody, Frederick R. Long, Edward Y. Lee, Wei Zhang

Purpose or Case Report: Genetic surfactant disorders (GSDs) are increasingly recognized as a cause of chronic diffuse lung disease (DLD) in childhood and are associated with considerable morbidity. The purpose of this study is to determine the diagnostic efficacy of chest CT in differentiating GSDs from other DLDs.

Methods & Materials: A retrospective review of pulmonary medicine consults at Texas Children's Hospital over the period 1997–2007 was conducted to identify all children with GSDs and a control group with other DLDs. Chest CT exams were independently reviewed by two pediatric chest radiologists blinded to the diagnoses, and discrepant readings were resolved by a third pediatric chest radiologist. Sensitivity and specificity of individual chest CT findings were tested for statistical significance with Fisher's exact test. Combinations of findings were evaluated with stepwise logistic regression.

Results: Twelve children (age 5mo–13yo; M:F 6:6) with GSDs (7 ABCA mutations, 4 SP-C mutations, 1 undefined mutation) and 16 children (age 2wk–18yo; M:F 10:6) with other DLDs (including pulmonary interstitial glycogenosis, neuroendocrine cell hyperplasia of infancy, lymphocytic interstitial pneumonia, lipoid pneumonia, diffuse alveolar damage, granulomatous infection, capillaritis and other pulmonary hemorrhage syndromes) were identified. CT findings with highest sensitivity for GSDs were ground glass attenuation (83%), parenchymal cysts (67%), and interstitial thickening (58%). Parenchymal cysts, honeycombing, and pectus excavatum were more specific for GSDs compared to other DLDs ($p < 0.05$). The combination of either parenchymal cysts and honeycombing or ground glass attenuation and pectus excavatum provided the highest specificity (100%) but low sensitivity (25%). The combination of parenchymal cysts and ground glass attenuation provided good specificity (81%) and modest sensitivity (50%). No combination of findings provided both high sensitivity and specificity.

Conclusions: Ground glass attenuation is the most sensitive finding for GSDs, while parenchymal cysts, honeycombing, and pectus excavatum are more specific findings for GSDs than other chronic DLDs of childhood. However, no single finding or combination of findings on chest CT is both highly sensitive and specific for GSDs, and chest CT cannot substitute for genetic testing or lung biopsy for the differentiation of GSDs from other DLDs.

Paper #: PA-059**Limited Z-axis Coverage Strategy for Reducing Radiation Dose of CT Pulmonary Angiography for the Diagnosis of Pulmonary Embolism in Children**

Lamya Atweh, MD, *Radiology, Texas Children's Hospital, laatweh@texaschildrens.org*; Robert C. Orth, Victor Seghers, Wei Zhang, R. P. Guillerman

Purpose or Case Report: Radiation dose concerns in pediatric patients suspected of having pulmonary embolism (PE) has led to recommendations for perfusion scintigraphy over CT pulmonary angiography (CTPA) for patients with a normal chest radiograph. CTPA is the preferred exam at many institutions because it is readily available, highly accurate for the diagnosis of PE, and can provide alternative diagnoses. We evaluated the anatomic distribution of PEs in children to determine if CTPA z-axis coverage length could be reduced to lower patient radiation dose while maintaining high diagnostic efficacy.

Methods & Materials: A retrospective review of a radiology report database was conducted to identify all CT exams demonstrating PEs in children at our institution from 2005–2011. The anatomic distribution of pulmonary emboli was recorded for all CT scans with the carina set as the reference point along the z-axis. The minimal z-axis scan length capturing all PEs in all scans as well as at least one PE in all scans was determined. Radiation effective doses were estimated with CT-Expo v1.6 for institutional helical CTPA protocols on GE LightSpeed scanners.

Results: PEs were noted on 45 CT exams conducted on 41 patients (M:F 20:21; age range: 0.25–25 years). A total of 90 PEs were observed in 33 scans of patients without a history of congenital heart disease (CHD), and 26 PEs in 12 scans of patients with a history of CHD. Z-axis scan lengths for the chest CT exams ranged from 10.1–33.3 cm. A z-axis scan length of 14 cm centered 3.5 cm below the carina captured all PEs in all patients, and a length of 12 cm centered 3.5–4 cm below the carina in patients with CHD. A z-axis scan length of 8 cm centered 5 cm below the carina was sufficient to capture at least one PE in all patients, and a length of 8 cm centered 4–5 cm below the carina in patients with CHD. The radiation effective dose of the chest CTPA exams ranged from 3–10 mSv. Limiting the z-axis scan length on CTPA exams to 14 cm or 8 cm would have resulted in a 20% or 40% decrease in z-axis coverage, respectively, and estimated radiation effective dose reduction of 21–42% due to less radiation exposure to the intrathoracic structures, thyroid gland and upper abdominal viscera.

Conclusions: Limiting the z-axis scan length coverage for CTPA exams based on a model of the typical anatomic distribution of PEs relative to the reference level of the carina permits a substantial reduction of radiation dose in children without reducing the sensitivity for detection of pulmonary emboli.

Paper #: PA-060**Multidetector CT Pulmonary Angiography in Children with Suspected Pulmonary Embolism: Thromboembolic Risk Factors and Implications for Appropriate Use**

Edward Lee, MD, MPH, *Department of Radiology, Children's Hospital Boston and Harvard Medical School, Edward.Lee@childrens.harvard.edu*; Sunny K. Tse, David Zurakowski, Victor M. Johnson, Tracy A. Donald, Phillip M. Boiselle

Purpose or Case Report: To evaluate thromboembolic risk factors for pulmonary embolism (PE) detected utilizing computed tomography pulmonary angiography (CTPA) in children; and to determine whether such information could be used for more appropriate use of CTPA in this patient population.

Methods & Materials: The institutional review board approved this HIPAA-compliant retrospective study and waived the need for written informed patient consent. This was a retrospective study of 227 consecutive CTPA studies from 227 pediatric patients who underwent CTPA studies for clinically suspected PE in a single, large pediatric referral hospital from July 2004 to March 2011. Age, gender, referral setting, D-dimer result as well as seven possible risk factors were compared between patients with and without PE. Multiple logistic regression modeling was used to identify the independent risk factors of PE. Receiver operating characteristic (ROC) curve analysis was applied to determine the optimal cutoff number of risk factors for predicting a CTPA positive result for PE in children.

Results: Thirty-six (16%) of 227 CTPA studies were positive for PE. Five risk factors, including immobilization ($P<.001$), hypercoagulable state ($P=.003$), excess estrogen state ($P=.002$), indwelling central venous line ($P<.001$), and prior PE and/or DVT ($P<.001$), were found to be significant independent risk factors for PE. Using 2 or more risk factors as the clinical threshold, the sensitivity for positive PE was 89% (32/36 patients) and the specificity was 94% (180/191 patients).

Conclusions: It is very unlikely for CTPA to be positive for PE in children with no thromboembolic risk factors. The use of risk factor assessment as a first-line triage tool has the potential to guide more appropriate use of CTPA in children, with associated reductions in radiation exposure and costs.

Paper #: PA-061**Multidetector CT Pulmonary Angiography: Value of Multiplanar Reformation Images in Detecting Pulmonary Embolism in Children**

Edward Lee, MD, MPH, *Department of Radiology, Children's Hospital Boston and Harvard Medical School, Edward.Lee@childrens.harvard.edu*; Evan J. Zucker, Jason Tsai, Donald A. Tracy, David Zurakowski, Phillip M. Boiselle

Purpose or Case Report: To determine whether the addition of multiplanar reformation MDCT images affects reader performance parameters and provides added diagnostic value compared to the use of axial CT MDCT images alone for diagnosing PE in children.

Methods & Materials: This was an institutional review board-approved retrospective study of 60 consecutive pediatric patients who underwent CTPA for clinically suspected PE. Two faculty pediatric radiologists and two radiology residents independently reviewed each study initially using only axial MDCT images and later using MPR MDCT images in any x-, y-, or z-axis for detecting PE. Diagnostic accuracy, confidence level, and interpretation time of MPR MDCT images were compared to axial MDCT images using McNemar's test and paired t-tests. The kappa coefficient was calculated to assess interobserver agreement. Diagnostic accuracy was compared between faculty pediatric radiologists and radiology residents by logistic regression whereas confidence level, interpretation time, and added diagnostic value were evaluated with analysis of variance (ANOVA).

Results: The final study cohort consisted of 60 CTPA studies from 60 children (28 M/32 F; mean age 14.7 years). Nine (15%) of 60 CTPA studies were found to have PE. Diagnostic accuracy in correctly detecting PE ranged from 91.7 to 100% (mean=96.7%), with no significant differences between the use of axial and MPR MDCT images. Logistic regression indicated no significant difference in diagnostic accuracy of detecting PE between faculty pediatric radiologists and radiology residents for axial MDCT images ($P=.48$) or MPR MDCT images ($P=.24$). Confidence level and interobserver agreement were significantly higher and average interpretation time was longer in evaluating PE with MPR MDCT images compared to axial MDCT images for all reviewers ($P<.001$). Compared to faculty pediatric radiologists, significantly greater increases in confidence level, interobserver agreement, interpretation time, and added diagnostic value using MPR MDCT images compared to axial MDCT images to diagnose PE were found for radiology residents ($P<0.001$).

Conclusions: Use of MPR MDCT images in diagnosing PE on CTPA in children significantly increases confidence, interobserver agreement, and interpretation time among faculty pediatric radiologists and radiology residents. Because MPR MDCT images provide significantly greater improvements in reading parameters for residents than for faculty members, their routine use should be encouraged for trainees.

Paper #: PA-062**Chest CT in Children, Anesthesia and Atelectasis**

Beverley Newman, MD, Radiology, Stanford University, bev.newman@stanford.edu; Elliot Krane, Terry E. Robinson

Purpose or Case Report: In spite of advances in CT equipment and speed, sedation/ anesthesia is required in many young children for optimal quality CT for detailed parenchymal evaluation; resultant atelectasis is a common and important quality issue. Our purpose was to evaluate the safety and effectiveness of a standardized lung recruitment technique.

Methods & Materials: With IRB approval and parental informed consent, 49 controlled ventilation, low dose, chest CT's (cooperative effort between anesthesia, pulmonology and radiology) were performed in 38 children (7 had 2–4 CTs) (21 F, 16 M; ages .02–5.13 yrs, mean 2.5 yrs). Indications included cystic fibrosis 8; ciliary dyskinesia 4; chronic or interstitial lung disease 16; evaluate pulmonary metastases 10. CT parameters were 80–100kVp, 25–80mAs, IV contrast 11. Various prior methods employed by the pediatric anesthesiologists to maintain lung inflation had unpredictable results (a brief survey showed 5/9 nonintubated anesthetized cases had problematic atelectasis). A standardized intubation technique was therefore adopted: 1. Use of a tight fitting face mask during induction and IV placement, inspiratory pressures of 20–25 and PEEP of 5. 2. Introduction as early as possible using an appropriately sized cuffed endotracheal tube. 3. Alveolar recruitment maneuvers—10–12 3 s breaths to 40 cm H₂O/5 (32–35 in 1st 6 cases). 4. Three breaths at 25/5, inspiratory breathhold followed by 25–30 cm on 4th breath for scout and inspiratory scan, and complete ventilator disconnection for expiratory scan. Recruitment breaths repeated before each scan. Two experienced readers reviewed and scored the images on a 5 point scale for overall quality and atelectasis.

Results: All studies were completed safely with no procedural complications. One child had propofol-related postoperative emergence delirium. All CT scans were diagnostically good to excellent with small subsegmental atelectasis in 8 (6/8 were the initial cases with lower recruitment pressures) and segmental atelectasis in 2. 13 cases had prior CTs, without this technique, that were suboptimal due to moderate procedural atelectasis, in spite of tracheal intubation in the majority of cases.

Conclusions: An intubation lung recruitment technique can be performed safely and consistently by different individuals using a standardized protocol. Procedural atelectasis that affects quality is reliably absent and repeat sequences are not needed.

Paper #: PA-063**Comparison of Dexmedetomidine with Propofol for Airway Intervention in MRI Sleep Studies**

Dorothy Jung, Department of Radiology, University of Cincinnati College of Medicine, Cincinnati Children's Hospital Medical Center; Mohamed Mahmoud, Shelia Salisbury, Mario Patino, Robert J. Fleck

Purpose or Case Report: Children with obstructive sleep apnea (OSA) may present for cine MR imaging of the airway. Obtaining a high-quality dynamic airway imaging study is critical for accurate interpretation and subsequent medical decision-making. The ideal MRI sleep study is one that allows successful completion while maintaining spontaneous breathing without artificial airway, which can be an anesthesia challenge. Dexmedetomidine has been shown to have sedative properties paralleling natural sleep with minimal respiratory depression. We hypothesized that dexmedetomidine compared to propofol would have less effect on upper airway tone and airway collapsibility and provide favorable conditions with less airway interventions required during dynamic MRI airway imaging in children with OSA.

Methods & Materials: In this prospective study, we examined the requirement for airway intervention for propofol (100–200 mcg/kg/m) and dexmedetomidine (1–3 mcg/kg/h) in children and adolescents with OSA. Severity of OSA was analyzed by overnight polysomnography. For children with history of mild OSA there was no intervention unless oxygen saturation decreases below 90%; while for children with history of moderate/severe OSA, an artificial airway was placed when oxygen saturation decreased below 85%.

Results: Demographics and OSA severity by polysomnography were comparable. Requirement for artificial airway by severity of OSA as documented by polysomnography will be shown. MRI sleep studies required airway intervention in 3/26 (12%) children in the dexmedetomidine group versus 7/29 (24%) children in the propofol group. MRI sleep studies were successfully completed without the use of artificial airways in 23 children (88%) in the dexmedetomidine group versus 22 children (76%) in the propofol group.

Conclusions: Safe and effective anesthetic management is a key factor in obtaining good quality MR images of the airway. Although there was no statistical significant difference in the need for airway intervention between drugs, dexmedetomidine provided acceptable sedation for MRI sleep studies with less airway intervention in children with OSA. Dexmedetomidine may be the preferred agent for sedation during MRI sleep studies in children, and may offer benefits to children with sleep disordered breathing requiring anesthesia or sedation for other diagnostic imaging studies.

Paper #: PA-064

MRI of Full Face Mask CPAP Causing Narrowing of the Retroglossal Airway

Robert Fleck, MD, Department of Radiology, University of Cincinnati College of Medicine, Cincinnati Children's Hospital Medical Center, robert.fleck@cchmc.org; Raouf S. Amin, Sally R. Shott, Mohamed Mahmoud, Ephraim Gutmark, Keith McConnell

Purpose or Case Report: To report the effect of applying positive pressure to an airway during MR imaging of the nasopharyngeal airway in 2 children with Down syndrome and sleep apnea.

Methods & Materials: Patients with obstructive sleep apnea (OSA) and Down syndrome (DS) were imaged as part of an ongoing study to dynamically model the airway with a combination of computational fluid mechanics and flow structure interaction. Subjects were sedated by anesthesia and moved into the MR scanner for static and dynamic cine imaging of the nasopharyngeal airway under atmospheric pressure and continuous positive airway pressure (CPAP) at 15 cm of water pressure by full facemask.

Results: Down syndrome patients with OSA typically sleep with the mouth open and have enlarged tongues relative to their oral compartment. An open mouth and administration of CPAP resulted in smaller AP diameter of the retroglossal airway compared to images without CPAP due to CPAP pressure pushing the tongue posteriorly. In patient 1 volume of oral cavity anterior to the tongue increased from 7.41 mL to 11.74 mL. Meanwhile, the AP diameter of the retroglossal airway decreased from 4.8 to 1.4 mm (71% decrease). In patient 2 the mouth was initially closed but parted when the pressure of CPAP was added with the oral volume increasing from 3.69 ml to 15.80 ml. The AP measure of the retroglossal airway

decreased from 8.3 mm to 2.8 mm (66% decrease). In patient 2 the mouth was then closed and CPAP reapplied resulting in an AP measurement of 11.0 mm (33% increase). The AP diameter difference between CPAP and no CPAP were tested with paired t-test, but were not statistically significant ($p=0.1475$).

Conclusions: Positive airway pressure on a patient by full facemask and an open mouth can have an adverse effect on the retroglossal airway. This adverse effect is an important consideration in the use of positive airway pressure to support airways for OSA, or during emergency resuscitation when a full facemask is used.

Paper #: PA-065

The Contribution of Advanced Imaging in Pre- and Post-Surgical Evaluation of Children Requiring a Rex Shunt

Rama Ayyala, Radiology, New York Presbyterian Hospital-Columbia, rsa9006@nyp.org; Sudha A. Anupindi, Monica Eelman

Purpose or Case Report: To illustrate clinical utility of advanced imaging techniques in pre- and post-operative assessment of children with extrahepatic portal vein obstruction (EHPVO) being evaluated for a Rex Shunt procedure.

Methods & Materials: We performed a retrospective review of the medical records and pre- and post-operative imaging of patients with EHPVO who underwent a Rex shunt. Demographics, etiology of EHPVO, presenting symptoms before and after surgery and details of the procedure were recorded. Imaging included: 2D Doppler US, 2D & 3D CTV and MRV exams. 3D imaging, such as multiplanar reconstructions, maximum intensity projections (MIP) and/or volume rendered displays, and liver volumes were performed on a dedicated 3D workstation. Pre-surgery imaging evaluated patency and size of the internal jugular vein, portal vein and branches, and superior mesenteric vein, presence or absence intrinsic liver disease. Post-operatively we evaluated patency of the Rex, flow in LPV and intrahepatic branches, decrease in size of collaterals, decrease in splenomegaly, and liver volumes.

Results: There were 5 patients identified who underwent the Rex shunt procedure. 1 patient had only preoperative US performed, and was excluded. We retrospectively evaluated 2D & 3D images of 8 CTV and 4 MRV in 4 patients (2 F:2 M, mean age 4 yr, range 2–9 yr). Indications for the surgery included portal hypertension, recurrent variceal bleeding and splenomegaly. In the preoperative setting,

CTV and MRV was performed in all patients and Doppler US in 2 patients. In the postoperative setting, 2 patients had US and all had CTV and/or MRV. In all patients, conventional 2D imaging incompletely demonstrated small portal veins and hypoplastic intrahepatic portal veins. Preoperative 3D reconstructions improved depiction of these abnormal findings critical for preoperative planning. No patient required catheter portal venography to confirm 3-D features. Pre & post Rex shunt liver volumes were calculated in 3 pts which increased by at least 30% on post op imaging confirming improved shunt function and permeability. No post-procedural complications occurred.

Conclusions: US is commonly used as first-line evaluation for pre- and post-operative evaluation of a Rex Shunt. In the author's experience CTV should be utilized when US is not feasible as it can better delineate vascular pathology. Our cases illustrate the feasibility of rendering 3D images and the clinical role of advanced imaging for the pre-procedural planning.

Paper #: PA-066

Advantages of a Nanoparticle Blood Pool Contrast Agent Over Conventional Intravascular Glomerular-Filtered Contrast Agents for Pulmonary Vascular Imaging

Ketan Ghaghada, Radiology, Texas Children's Hospital, kbghagha@texaschildrens.org; Ananth Annapragada, R. P. Guillerman, Eric Hoffman, David Kaczka, Cristian Badea

Purpose or Case Report: A nanoparticle blood pool iodinated contrast agent (NCTX) has been designed and tested in preclinical animal models. We report data in animal models exemplifying its advantages over conventional contrast in the setting of CT pulmonary angiography

Methods & Materials: NCTX blood pool nanoparticles of ~125 nm diameter with an encapsulated total iodine concentration of ~125mgI/ml were administered by intravenous injection to mice, rabbits, dogs, pigs and sheep. (These studies were actually conducted for other purposes and a review of the data revealed the similarities that motivated this paper.) Total injected volumes were ~5 ml/kg in large animals, and as high as 10 ml/kg in small animals to provide satisfactory vessel enhancement. Iohexol or iopamidol was administered for comparative studies with conventional contrast. In a subset of pigs, iatrogenic pulmonary arterial emboli were introduced prior to contrast administration. Toxicity studies were conducted in mice and monkeys.

Results: The visualization of pulmonary vessels using NCTX blood pool nanoparticles was generally at least equivalent to using conventional contrast, and superior in several cases, particularly in small veins and when bolus timing of the

conventional contrast was suboptimal. In all cases, satisfactory vessel enhancement was achieved for a duration of several hours following a single infusion of NCTX blood pool nanoparticles. There was no evidence of renal toxicity, and only transient elevation of hepatic enzymes at relevant dose levels.

Conclusions: NCTX nanoparticle blood pool agents demonstrate several advantages over conventional glomerular-filtered iodinated contrast agents for CT pulmonary angiography in animal models, including no nephrotoxicity, no dependence on bolus injection technique, superior depiction of small veins, and capability of re-imaging for follow-up studies without needing contrast re-injection. Potential applications in human pediatric subjects include the diagnostic and post-therapeutic evaluation of cardiopulmonary anomalies and pulmonary embolism, especially in patients with renal insufficiency or tenuous vascular access.

Disclosure: Dr. Annapragada has indicated that he is a stock holder and consultant for Marval Biosciences Inc.

Paper #: PA-067

Cardiovascular Image Quality Using a Nanoparticle CT Contrast Agent: Preliminary Studies in a Pig Model

Rajesh Krishnamurthy, Radiology, Texas Children's Hospital, rxkrishn@texaschildrens.org; Ketan Ghaghada, Prakash Masand, Abhay Divekar, Eric Hoffman, Ananth Annapragada

Purpose or Case Report: Image quality in a separate study using a long circulating, liposomal-based nanoscale blood pool iodinated contrast agent (NCTX) suggests clinical utility in pediatrics, potentially reducing difficulties in contrast-CT of children with congenital heart disease (CHD) including the size of intravenous cannula, need for accurate timing, inability to simultaneously opacify multiple targets of interest (requiring repeated contrast administration and/or repeated imaging).

Methods & Materials: Six pigs (average weight 30 kg) were imaged after slow intravenous infusion of NCTX (105 mg I/mL) at an iodine dose of approximately 900 mg I/kg (8.5 mL/kg). Retrospective EKG gated CT imaging was performed 3 h later using a 128-slice dual-source CT scanner at 80 and 120 kVp. Two radiologists analyzed and graded (on a 5-point scale with 1: unreadable, 5: Excellent) images aimed at anatomic structures relevant to CHD. Quality of images obtained at 80 and 120 kVp were compared. Uniformity of contrast opacification was measured using a ROI-based CT-number method at various intracardiac and extracardiac sites and mean non-uniformity was calculated.

Results: There was excellent agreement between the two readers on all counts at 120 kVp. 80 kVp images received

lower scores for coronary morphology (4/5), and aortic valve visualization (3.5/5), but were comparable in other aspects. Pulmonary artery and pulmonary vein branch visualization extended up to the 5th generation in all cases. Visualization of coronary artery branches was possible up to the second generation, with good arteriovenous separation. Subtle morphologic features including crista terminalis, Thebesian valve, foramen ovale, membranous septum, and chordae of the mitral valve were demonstrated in all cases. Automated functional analysis and myocardial mass quantitation was feasible in all cases. There was no significant difference in blood pool attenuation between the atria, ventricles, and extracardiac vasculature on quantitative assessment. No image artifacts were visible on the reconstructed images.

Conclusions: These findings suggest that NCTX promises to be superior to conventional contrast agents for CT imaging of complex congenital heart disease, due to the absence of nephrotoxicity, avoidance of repeated contrast administration, and reduced number of scans performed. Avoiding the need for accurately timed scans precludes the need for large bore intravenous access. These attributes make it a promising agent that warrants further studies.

Disclosure: Dr. Annapragada has indicated that he is a stock holder and consultant for Marval Biosciences Inc.

Paper #: PA-068

Theoretical Cost and X-Ray Dose Reduction in Pediatric Congenital Heart Disease Imaging by the Use of a Nanoparticle Contrast Agent

Robert Bell, *The University of Texas-Houston*; Rajesh Krishnamurthy, Gabriela Espinosa, Christopher Petit, Ananth Annapragada

Purpose or Case Report: The purpose of this study is to determine the effective, population averaged reduction in costs and radiation dose that can be achieved in the diagnosis of congenital heart disease by use of a nanoparticle long circulating blood pool contrast agent.

Methods & Materials: A Markov model of the decision tree followed at the Texas Children's Hospital in the image based diagnosis of congenital heart disease was constructed in TreeAge software. The model included CT Angiography, MR Angiography, cardiac catheterization, and echocardiography diagnostic modalities. Patient records, accumulated between 2003 and 2011 were examined to inform the model. The radiation dose and cost for each step were encoded as penalty functions. Markov simulations were run for two decision trees: (1) utilizing CT angiography and (2) replacing conventional CT angiography with blood-pool agent based CT angiography. The overall population X-ray dose

and accrued cost was calculated for each pass through the model.

Results: X-ray dose distributions for the example populations showed substantial reductions per CT study, as much as 50%. Averaged over the population, since a sizeable fraction of patients are diagnosed without ever being exposed to any X-ray based modality, reductions were more modest, but still substantial. Costs per CT study were slightly higher when the blood pool contrast agent was used. When the diagnostic probability using the blood pool agent increased, it led to an automatic overall cost reduction. Conversely when the diagnostic probability remained unchanged, costs rose, commensurate with the increased cost of the contrast agent.

Conclusions: The use of a blood pool contrast agent for CT angiography leads to substantial reduction in radiation dose in the setting of congenital heart disease. Cost reductions are more modest, and are driven almost completely by the reduction in the number of MR and invasive angiography procedures resulting from increased diagnostic success using blood pool based CT angiography. The model as constructed does not account for potential workflow changes that might result from the use of a new contrast agent. Actual reductions realized may therefore be higher.

Disclosure: Dr. Annapragada has indicated that he is a stock holder and consultant for Marval Biosciences Inc.

Paper #: PA-069

Frequencies and Patterns of Situs Discordance in Chest and Abdomen

Justin Boe, *Stanford*, justinj.boe@gmail.com; Beverley Newman, Shreyas Vasanawala, Frandics Chan

Purpose or Case Report: Incidence of situs anomalies, including heterotaxy and situs inversus, is estimated at 0.02% of population. As the first step in the segmental analysis of structural heart disease, the determination situs position is of fundamental importance. Abdominal situs, as defined by splenic position and morphology, and cardiac situs, as defined by atrial morphology, are usually but not always in agreement. Echocardiographers also employ the relative position of the great arteries and vein at the hiatus to determine cardiac situs. We evaluate the frequencies of discordances among abdominal, hiatal and cardiac situs.

Methods & Materials: With retrospective IRB approval, imaging records from 2001 to 2011 were reviewed for the diagnosis of cardiac situs inversus and heterotaxy. Patients who had cardiac CT or MRI were included. Images were evaluated on a 3D-processing station by a cardiac radiologist. Cardiac situs was determined by the morphology of the

atrial appendages. When an atrial appendage was not adequately visualized, cardiac situs was assessed by the relative position of the main pulmonary artery and bronchi. Hiatal situs was determined by the relative position of the aorta and the systemic venous return, and abdominal situs by the position and morphology of the spleen.

Results: Thirty-five cases were identified, with 23 cardiac CT and 12 MRI. Patients' age ranged from 1 day to 35 years old. In the abdomen, the numbers of situs inversus, asplenia, and polysplenia were 11 (32%), 12 (34%), and 12 (34%). For the heart, the numbers of situs solitus, inversus, right-isomerism, and left-isomerism were 2 (6%), 13 (37%), 11 (31%) and 9 (26%). The abdominal and cardiac situs were discordant in 5 (14%) cases. Polysplenia had the highest number of discordance with the heart. Hiatal situs was discordant with the abdomen in 5 cases (16%) and with the heart in 8 (25%) cases.

Conclusions: Situs disagreement between the abdomen and the heart is not uncommon and they should be documented separately in radiology reports. Hiatal situs, as used by echocardiographer, disagrees with the cardiac situs in a quarter of the cases. It should be used with caution in the segmental analysis.

Paper #: PA-070

Diminished ASL Intracranial Perfusion in Children with Neurofibromatosis Type 1

Kristen Yeom, MD, Stanford University, kyeom@stanford.edu; Cynthia Campen, Patrick Barnes

Purpose or Case Report: Neurofibromatosis type 1 (NF1), a neuro-cutaneous syndrome affecting 1/3500 children is associated with moyamoya syndrome (MMS). However, no comparisons of cerebral perfusion in patients with NF1 and NF1-associated MMS to healthy controls exist. We hypothesize cerebral blood flow (CBF), as measured by magnetic resonance imaging (MRI) arterial-spin-labeled (ASL), is diminished in children with NF1 compared to healthy controls, with the lowest levels seen in patients with NF1-associated MMS.

Methods & Materials: Twenty children aged 2–18 years with NF1, four with MMS, and 26 age-matched controls underwent ASL CBF on a 3 T magnet. Pseudocontinuous-spin-echo-ASL technique was used. Measurements were taken bilaterally in cerebral cortical-subcortical regions, and the deep gray nuclei. Trends in measurements as a function of disease severity were tested with the Jonckheere-Terpstra test for ordered alternatives. A Bonferroni-adjusted p-value less than 0.0013 was considered significant.

Results: We identified 6/12 areas with significantly diminished ASL CBF (ml/100 g/min) in patients with NF1 (mid-range), and NF1-associated MMS (lowest) compared to healthy controls (highest). These included the: thalami (left: $p=0.0002$, right: $p=0.0004$); superior/middle temporal lobes (left: $p=0.0012$, right: $p=0.0009$); temporo-occipital lobes (left: $p=0.0006$, right: $p=0.0003$); occipital poles (left: $p=0.0008$, right: $p=0.0001$); centrum semiovale (left: $p=0.0022$, right: $p=0.0005$); and left parietal lobe ($p=0.0012$).

Conclusions: Cerebral perfusion diminishes in a graded fashion in children with NF1 and NF1-associated MMS, particularly in the posterior circulation and the MCA-PCA posterior watershed zones. Future studies may demonstrate an important role for ASL in the presymptomatic diagnosis of cerebral vasculopathy, and the definition of NF1-related vasculopathy patterns.

Paper #: PA-071

Cingulate Gyrus MRI Sign in Pediatric NF1 Patients: A Novel Imaging Marker

Nadja Kadom, MD, Radiology, Children's National Medical Center, nkadom@childrensnational.org; Nabila Hai, Rhea Udyavar, Amir Noor, Gilbert L. Vezina, Maria T. Acosta

Purpose or Case Report: We observed a magnetic resonance imaging (MRI) signal abnormality in the anterior cingulate gyrus of pediatric patients with neurofibromatosis type 1 (NF1). The cingulate gyrus could play a role in cognitive deficits of NF1 patients. The first objective here is to document inter-rater reliability scores for visual detection of this sign. The second objective is comparing ADC values of the cingulate gyrus in areas of visually abnormal MRI signal in NF1 patients to matched normal MRIs to confirm a pathophysiological basis of the visual MRI sign.

Methods & Materials: Retrospective analysis, IRB approved, 61 NF1 patients and 38 matched controls. In the visual assessment part, two blinded neuroradiologists rated presence or absence of MRI signal abnormality in the cingulate gyrus in three different age groups of NF1 patients mixed with normal controls. Cohen's Kappa inter-rater reliability coefficients were calculated. The same blinded neuroradiologists evaluated the cohort one year later, this time by agreement at the workstation. In the ADC measurements part, two researchers, one blinded, manually placed ROI's in the anterior and posterior cingulate regions of 26 NF1 patients and their matched controls, and student t-test was used to assess for significance of differences in measured values.

Results: Cohen's Kappa for the three age groups showed very good agreement (Kappa coefficients were either 0.9 or 1.0). Rater agreement at the workstation was 100%. All subjects with a positive finding also had NF1 and the sign was not seen in any of the normal controls. The prevalence of the sign was 43%. ADC measurements showed significantly higher ADC values in the anterior cingulate gyrus of NF1 patients when compared to normal controls and also when compared to the posterior cingulate gyrus in NF1 patients.

Conclusions: Our results show that visual T2/FLAIR MRI abnormalities in the anterior cingulate gyrus are present in 43% of patients with NF1 from ages 2 to 19 years. ADC measurements confirm a pathophysiological basis for this finding. Future correlation with clinical manifestations, such as learning and behavioral manifestations in patients with NF1, are under way to further evaluate the clinical importance of this finding.

Paper #: PA-072

Tract-Based Spatial Statistical Analysis of Diffusion Tensor Imaging in Pediatric Patients with Mitochondrial Disease

Seth Friedman, PhD, *Seattle Children's*, seth.friedman@seattlechildrens.org; Andrew V. Poliakov, Sandra L. Poliachik, Dennis W. Shaw

Purpose or Case Report: Often diagnosed at birth or in early childhood, mitochondrial disease presents with a variety of clinical symptoms, particularly in organs and tissues that require high energetic demand such as brain, heart, liver, and skeletal muscles. In a group of pediatric patients identified to have complex I or I/III deficits, but with white matter tissue appearing qualitatively normal for age, we hypothesized that quantitative DTI analyses might unmask deficits in microstructural integrity.

Methods & Materials: DTI and structural MR brain imaging data were collected in 10 pediatric patients with confirmed mitochondrial disease and 10 clinical control subjects matched for age, gender, scanning parameters, and date of exam. Paired Tract-Based Spatial Statistics (TBSS) were performed to evaluate differences in fractional anisotropy (FA) and mean diffusivity (MD).

Results: In patients with mitochondrial disease, significant widespread reductions in FA values were shown in white matter tracts. MD values were significantly increased in patients, having a sparser distribution of affected regions compared to FA. Results of TBSS statistical analysis will be shown. To be shown in green is the mean FA skeleton which represents the centers of main white matter tracts. All

results $p < .05$. Red and yellow represent a significant increase, blue and light blue represent a significant decrease.

Conclusions: Despite qualitatively normal appearing white matter tissues, patients with confirmed mitochondrial disease have widespread microstructural changes measurable with quantitative DTI. This supports the evaluation of such metrics in other populations where gross imaging features may be normal.

Paper #: PA-073

Pelizaesus-Merzbacher Disease: White Matter Atrophy Correlates to Clinical Disability

Jeremy Laukka, PhD, *Radiology, Neurology and Ophthalmology, Michigan State University*, Jeremy.Laukka@radiology.msu.edu; John Kamholz

Purpose or Case Report: To determine whether quantitative measures of magnetic resonance imaging data from patients with the inherited leukodystrophy, Pelizaesus-Merzbacher disease (PMD), correlate with clinical disease severity or progression.

Methods & Materials: To extend our studies to patients with other PLP1 mutations, we analyzed the brains of 52 male PMD patients (ranging in age from 2 to 45) and 9 female carriers for whom the PLP1 genotype had been determined and analyzed by MRI. For each patient we measured, white matter volume (WMV) and the intercaudate distance (ICD). The MRI data were correlated with functional disability scores (FDS) using a system we developed for clinical evaluation of PMD patients and which was validated by assessments of 22 PMD patients. Brain volume and segmentation were measured using NIH image 1.62. The average number of coronal slices analyzed from each patients MRI was 60 slices. When gray-white contrast was not adequate, then the Intercaudate distance (ICD) and intercaudate ratio were measured as described in Caon et. al., (2003).

Results: Comparison of the MR measurements and the FDS demonstrated that white matter volume inversely correlates with functional disability, suggesting that the initial disability does correlate with the extent of myelination. The intercaudate distance also correlated with the FDS, and may usefully substitute when gray-white matter segmentation is not possible.

Conclusions: PMD is a clinically and genetically heterogeneous disease caused by mutations in the gene encoding the major CNS myelin protein, proteolipid protein (PLP). Myelin is a major target of disease pathogenesis in most cases of PMD, but how the various mutations cause clinical disability is not fully understood. Our data demonstrate that the extent

of brain white matter atrophy, measured directly by volumetric fractionation, or indirectly by analyzing the intercaudate ratio, is significantly correlated with the patient's functional disability. White matter atrophy is thus the main cause of clinical disability in patients with PMD of all ages and mutation type.

Paper #: PA-074

Maturation Effects on Language Localization in Children Demonstrated by fMRI

Susan Palasis, MD, *Children's Healthcare of Atlanta at Scottish Rite*, spalasis@yahoo.com; Binjian Sun, Laura L. Hayes, Richard A. Jones

Purpose or Case Report: Language localization is of paramount importance when contemplating surgery in children with intractable epilepsy or brain tumors. The potential risk of injury to language centers in the developing pediatric brain needs to be weighed against the potential benefits of surgery. In the past, language localization was crudely and invasively determined using the WADA test. Most institutions are now transitioning to non invasive localization using functional MRI (fMRI). The purpose of our study was to analyze language localization relative to age in children using age appropriate language paradigms and fMRI.

Methods & Materials: Forty three healthy, English speaking, right handed children underwent fMRI evaluation for language localization. The studies were performed on a 3 T system. Three novel age appropriate language block paradigms were utilized, targeted both to expressive and receptive language processing. These paradigms were the auditory category decision task (AUDCAT), the auditory description decision task (ADDT), and the Listening task. The spatial statistical maps generated by the fMRI data were fused to the 3D anatomical MRI dataset. Language areas were localized and statistical analysis was performed with age as the variable in a general linear model.

Results: Our results demonstrate a distinct trend in language localization and lateralization with brain maturation. In the young age groups (less than 12 years) the localization tended to be less focused and bilateral in the frontal and temporal regions of the brain. In the older age groups (greater than 12 years), language became more localized and lateralized to the expected left sided pattern. The findings were more robustly demonstrated with the ADDT task and were statistically significant ($p < 0.05$).

Conclusions: Our study clearly demonstrates the plasticity of language centers in the maturing pediatric brain. This observation is significant for neurosurgical planning and rehabilitation in the pediatric population.

Paper #: PA-075

SLC26A4 Mutation Sensory Neuronal Hearing Loss: Genetic and Phenotypic Analysis

T. Shawn Sato, *Radiology, U. of Iowa*, shawn-sato@uiowa.edu; Ameera Ismail, Yutaka Sato, Fatemoh Alasti, Richard Smith

Purpose or Case Report: Mutations in SLC26A4 are the most frequent cause of autosomal recessive enlarged vestibular aqueduct (EVA), vestibulo cochlear (V/C) dysplasia and goiter (Pendred syndrome). The purpose of this study is to investigate phenotypic variations of inner ear anomalies by imaging in a large group of pediatric patients with genetic data.

Methods & Materials: 82 cross-sectional temporal bone images from 75 hearing-impaired children (mean age, 2 years) referred for genetic analysis were reviewed and correlated with genetic variations.

Results: In genetic analysis, (1) double and (2) single mutation of SLC26A4 and (3) no SLC26A4 mutations were found in 16, 12 and 47 subjects, respectively. Significantly higher association with SLC26A4 mutations was found in bilateral EVA+V/C dysplasia (16/18). Double mutations of SLC26A4 is more often associated with combined EVA+V/C dysplasia, while a single mutation with EVA only. Cochlear aplasia without EVA (0/2) and SNHL with normal imaging (3/21) are less likely associated with SLC26A4 mutation.

Conclusions: SLC26A4 mutation is highly associated with EVA and V/C dysplasia. Once EVA with or without V/C dysplasia are found at imaging, genetic investigation is recommended for SLC26A4 mutation because of possible thyroid involvement.

Paper #: PA-076

Magnetic Resonance Imaging (MRI) in a Trial of Therapeutic Hypothermia for Term Hypoxic-Ischemic Encephalopathy (HIE)

Patrick Barnes, MD, *Radiology, Lucile Packard Children's Hospital at Stanford*, pbarnes@stanford.edu; Seetha Shankaran, Susan Hintz, Abbot Laptook, Rosemary Higgins, Scott McDonald

Purpose or Case Report: To correlate brain MRI findings with neurodevelopmental outcomes in a retrospective study of term neonates enrolled in a multicenter NICHD Neonatal Research Network trial of whole body hypothermia.

Methods & Materials: Brain MRI findings were obtained by 44 weeks postmenstrual age in 136 infants with

moderate-severe HIE who were randomized to cooling (33.5°C for 72 h). There were 73 in the hypothermia group and 63 in the control group. All MRIs were reviewed by a central reader masked to the clinical findings, groupings, and outcomes. The MRI findings were scored according to pattern and extent of injury, including involvement of the cerebral hemispheres, basal ganglia, thalami, internal capsules, and other structures. Brain injury scores were correlated with death or disability at 18 months postnatal age.

Results: No MRI abnormalities were observed in 38 of 73 infants (52%) in the hypothermia group and in 22 of 63 infants (35%) in the control group ($P=0.08$). Infants in the hypothermia group had fewer areas of injury (12%) as compared with the control group (22%, $P=0.02$). There were 51 of the 136 infants with death or disability at 18 months. The brain injury score correlated with outcome of death or disability ($P=0.001$) and disability among survivors ($P=0.0001$).

Conclusions: Fewer areas of brain injury on MRI were observed following whole-body hypothermia. The MRI brain injury score is a marker of death or disability at 18 months following hypothermia for term HIE.

Paper #: PA-077

The “Red Dot” on FA Color Maps: Clinical/Anatomical Correlation in Malformations of the Mid-Hindbrain Using DTI MR in Children

Laura Merlini, *University Hospital of Geneva, laura.merlini@hcuge.ch*; Joël Fluss, Mehrak Anooshiravani, Sylviane Hanquinet

Purpose or Case Report: To investigate the clinical significance of the presence or absence on Fractional Anisotropy (FA) color map of the “red dot” considered as the decussation of the Superior Cerebellar Peduncles (SCP). This structure is reported as absent in some malformations of the mid-hindbrain

Methods & Materials: We describe 8 patients (3 Joubert Syndromes (JS), 1 Horizontal Gaze Palsy and Progressive Scoliosis (HGPPS), 3 Congenital Oculomotor Apraxia (COMA), 1 Wildervanck syndrome (WVS) and fifteen age-matched controls. MRI with DTI was performed with a 1.5 T Avanto Siemens. FA and Mean diffusivity (MD) values were measured with TrackVis software. ROIs were placed on SCP, posterior columns (PC) and Pyramidal Tracts (PT). Presence or absence of the “red dot” on FA color maps was correlated to clinical (ataxia, oculomotor abnormalities etc.) and morphological data, and to FA and MD measurements.

Results: The “red dot” was absent in JS and HGPPS (genetic cross wiring impairment diseases) and present in

COMA and WVS (no reported gene abnormalities so far) as in normal controls. JS and COMA presented on MRI molar tooth appearance. HGPPS presented “split pons” appearance. JS and COMA patients presented oculomotor apraxia, WVS and HGPPS palsy of the horizontal gaze. Mirror movements were found in 2 JS and in WVS. Ipsilateral responses are present in HGPPS. WVS presented multiple cranial nerves impairment. In JS, FA and MD values of SCP, PT and PC were significantly lower than in normal controls ($p > 0.01$). In HGPPS high FA and low MD were found in PC and PT ($p > 0.01$) and normal in SCP.

Conclusions: The “red dot” absence is unrelated to morphological or clinical abnormalities. Absence of the “red dot” is associated to abnormal measurements of FA and MD in PC and PT (low in JS and high in HGPPS). These findings indicate a pivotal role for the PC in the physiopathology of these diseases. The “red dot” absence seems to be a marker of genetic cross wiring diseases. In this view, COMA and WVS should not be considered as part of these diseases.

Paper #: PA-078

Sonographic Predictors of Intermittant Testicular Torsion in the Pediatric Patient

Jennifer Williams, MD, *Pediatric Radiology, Texas Children's Hospital, jllwilli1@texaschildrens.org*; Marthe Munden

Purpose or Case Report: Intermittent testicular torsion (ITT), defined as sudden onset unilateral scrotal pain with spontaneous resolution, is difficult to confirm both clinically and sonographically. The purpose of this study was to determine if sonographic predictors exist for diagnosing ITT in the pediatric patient.

Methods & Materials: A search of the PACS data system for patients presenting with suspected intermittent testicular torsion was performed. Fifteen patients with a total of 20 episodes presenting over a 2 year period were found. A retrospective review of the medical records for clinical presentation, surgical outcome, and comorbidities was performed. Scrotal ultrasound images and reports were reviewed for testicular size and echotexture, testicular flow, epididymal appearance, vascular bundle appearance, and presence of hydrocele.

Results: An abnormal appearance of the vascular bundle was found in 85% of episodes (17/20). Initial absence of testicular flow followed by reperfusion during the scan was seen in 30% of episodes (6/20); 45% had increased flow (9/20), 10% had decreased flow (2/20), and 15% had normal flow (3/20). Nine of the 15 patients had surgery; of these 8 were found to have evidence of ITT and 1 was found to have acute testicular torsion. Of patients with ITT, 88% (7/8)

had an abnormal vascular bundle. Testicular flow was not initially visualized but returned during the exam in 50% of patients (4/8), was increased in 38% of patients (3/7) and was decreased in 13% patients (1/8).

Conclusions: ITT is a difficult diagnosis. The most reliable sonographic indicator is an abnormal spermatic cord, found in 85% of episodes and 88% of surgically proven ITT. Dedicated views of the spermatic cord must be obtained in order to differentiate an abnormal epididymis from an engorged vascular bundle (the so-called pseudomass). Attention to testicular flow is of particular importance. While visualization of a transition from no or decreased testicular flow to normal flow during the sonogram is certainly diagnostic of ITT, increased testicular flow should not lead to false reassurance.

Paper #: PA-079

Retrospective Review of Diagnosis of Testicular Torsion in Boys Presenting to Pediatric Emergency Department with Acute Scrotal Pain

Teresa Liang, BSc, *Faculty of Medicine, University of British Columbia, teresaliang86@gmail.com*; Peter Metcalfe, William Sevcik, Michelle Noga

Purpose or Case Report: Testicular torsion is a common acute condition in boys requiring prompt and accurate diagnosis. The objective was to evaluate ultrasound accuracy and findings, and clinical predictors in testicular torsion in boys presenting to the Stollery pediatric emergency department (ED) with acute scrotal pain.

Methods & Materials: Retrospective review of US, surgical and ED records for boys aged 1 month to 17 years, presenting with acute scrotum from 2008 to 2011, was performed. Age, demographics, clinical symptoms, physical findings, US and surgical techniques, findings and diagnoses were recorded. Surgical results and follow-up were used as the gold standard as all pediatric urology in our region is performed at our centre.

Results: 343 patients presented to ED with acute scrotum with the following diagnoses: 35 testicular torsion, 11 possible torsion-detorsion, 3 torsion of appendix testes, 135 epididymo-orchitis, and 159 other. Of 266 US performed, 29 boys had torsion confirmed by surgery. There were 8 inconclusive US reports, none of which had torsion at surgery or follow-up. The false positive rate of US was 1.5% (4 patients), and there were no false negatives. Six torsion patients had no US. Median time from ED to US and surgery for torsion patients was 159 and 303 min. Six patients had non-salvageable testes. Diagnostic accuracy of US compared to surgery was 96% for torsion and 67% for other. Sonographic heterogeneity was seen in 80% of patients with

testes that the surgeon felt were non-viable at surgery and 72% of patients with viable testes ($p=0.35$). Sudden-onset scrotal pain (92%), abnormal position (86%) and absent cremasteric reflex (91%), were most prevalent in torsion patients.

Conclusions: Color Doppler US is accurate and sensitive for diagnosis of torsion in the setting of acute scrotum. Despite heterogeneity on pre-operative US, many testes were felt to be salvageable at surgery. Rate of salvage of torsion was high. Common symptoms and findings of torsion were sudden onset of pain, abnormal testicular position and absent cremasteric reflex.

Paper #: PA-080

Diagnostic Twists of Tubal Torsion

Srikala Narayanan, MD, *Children's National Medical Center, snarayan@childrensnational.org*; Anjum N. Bandarkar, Dorothy Bulas

Purpose or Case Report: Fallopian tube torsion is a rare cause of acute pelvic pain in a young female and requires prompt diagnosis for immediate surgical intervention. Our purpose is to review varied imaging findings of surgically proven cases of tubal torsion.

Methods & Materials: Retrospective review of our data base from 2007 to 2011 revealed 7 cases of surgically proven fallopian tube torsion. Ages ranged from 9 to 15 years of age. All had pelvic ultrasound performed, 3 cases had additional CT performed for acute pelvic pain.

Results: US findings included thickened dilated tubular hypoechoic structure (5), cystic mass (4); adnexal (3), midline (1). Five cases had normal ovaries bilaterally (2 with paratubal cysts). CT imaging findings include dilated, fluid filled, thick-walled tube with internal hyperdensity (40HU) likely debris/hemorrhage in 1 case. Additional findings included cystic adnexal mass (3 cases), beak sign (1 case) and increased vascularity (1 case). Secondary signs included free fluid (5), peritubular fat stranding (1), vascular congestion and thickening of the broad ligament (1) and enlarged draining vein (1). Laparoscopic salpingectomy was performed in 3 cases (including 2 cases with isolated tubal torsion). Laparoscopic detorsion was performed in a total of 4 cases. In addition, laparoscopic cyst drainage was performed in 2 out of these 4 cases. Detorsion with paratubal cystectomy and hemorrhagic ovarian cystectomy was performed in 1 of the 4 cases.

Conclusions: Imaging diagnosis of tubal torsion can be difficult. It can occur in isolation with a dilated thickened tubular structure adjacent to a normal ovary or potentially mimic appendicitis, pyosalpinx, complex adnexal cyst or cystic adnexal neoplasm. Presence of normal ovaries, beaked tapered tubular structure with

intratubal fluid level and hemorrhage may help in making the diagnosis. It is important to recognize this entity in a patient with acute pelvic pain to facilitate prompt tubal sparing surgery.

Paper #: PA-081

Adjusted Renal Length in Pediatric Bone Marrow Transplant Recipients

Nicholas Bodmer, MD, *University of Washington, nbodmer@gmail.com*; Teresa Chapman, Sangeeta Hingrani, Marguerite Parisi

Purpose or Case Report: Bilateral nephromegaly has been observed in the bone marrow transplant (BMT) patients at our institution. This study aims to quantify this observation, thereby providing radiologists with an adjusted baseline age-determined renal growth curve for BMT patients.

Methods & Materials: A retrospective clinical chart and imaging review was performed on 185 patients who underwent BMT between 2006 and 2010 and who had abdominal imaging including the kidneys. Ultrasound, CT, and MRI exams were used for renal length measurement. Renal lengths were assessed for each age group, first as an average length of all the patients within that age group overall, and subsequently as an average renal length by age group divided into the following time frames after transplantation: 0–30 days, 31–90 days, 91–180 days, and 181+ days. Clinic chart information collected included BUN, creatinine, weight, and medication use.

Results: Renal length was measured using 278 imaging cases, distributed across each age group as follows: 6–12 months, $N=11$; 13 months–2.5 years, $N=30$; 2.6–4.5 years, $N=33$; 4.6–7.5 years, $N=38$; 7.6–11.5 years, $N=51$; 11.6 years and higher, $N=115$. Renal lengths were greater, on average, within every age group, compared with previously established normative age-related renal lengths (Rosenbaum et al.). The augmented renal lengths universally were observed in the 0–30 day post-transplantation time-frame. Return to normal renal lengths typically occurred by 6 months post transplant. Clinic chart review revealed that the majority (87%) of patients received nephrotoxic medication within two weeks of imaging.

Conclusions: Pediatric BMT patients have larger kidneys in the absence of known renal disease than age-matched peers. A revised, age-based renal length chart for post-BMT patients has been generated which should help prevent the misdiagnosis of nephromegaly in this population, eliminating unnecessary diagnostic evaluations. Multiple etiologies to explain renal enlargement in these patients are possible, including fluid overload, nephrotoxic medication, or direct effect of the transplant.

Paper #: PA-082

Pediatric Renal Function Evaluation with a New High Spatio-Temporal Resolution Technique

Shilpy Chowdhury, MD, MPH, *Stanford University School of Medicine, Department of Pediatric Radiology, drshilpy@stanford.edu*; Kyung Sung, Manojkumar Saranathan, Shannon Walters, Brian A. Hargreaves, Shreyas Vasanawala

Purpose or Case Report: MR urography can be a comprehensive exam for anatomical and functional pediatric renal evaluation. Quantification of renal function may benefit when dynamic contrast enhanced images can be obtained at high spatiotemporal resolution and with minimal respiratory motion artifacts. Though respiratory triggering may decrease motion artifacts, it results in loss of temporal resolution by a factor of about three.

Methods & Materials: A two-echo gradient echo sequence with segmented outer k-space sampling and view-sharing/Dixon image reconstruction (DISCO, Differential Subsampling with Cartesian Ordering) was chosen as a starting point due to its high temporal resolution. It was then modified to enable respiratory triggering while maintaining temporal resolution of one temporal frame every one to two respirations, with segments of k-space only acquired in the expiratory phase of respiration. Imaging parameters were: 12° flip angle, ± 167 kHz bandwidth, $TR \sim 3.56$, matrix 256×200 , FOV $28\text{--}34$ cm, slice thickness 4 mm, and 2×2 spatial acceleration. With IRB approval and informed patient consent 9 consecutive patients referred for MRI renal function evaluation were recruited (age range; 0.5 to 9.6 years, mean \pm SD: 3.99 ± 3.6 years; males 78% females 22%), and scanned on a GE 3 T MR using a 32-channel torso array with the respiratory-triggered high spatiotemporal resolution technique to extract regional GFR maps. Two readers by consensus assessed image qualitative SNR, motion artifacts and volumetric fat-water suppression performance.

Results: Data acquisition was obtained to completion in all subjects without triggering failure. Temporal resolution was approximately 12 s for two respiratory cycles. No case had major fat suppression failure, whereas minor fat suppression failure was seen in 11% (95% C.I. 0 to 37%). All cases had diagnostically acceptable SNR. No motion artifacts were noted in 7/9 cases, while some artifacts with ghosting in 2/9 cases. Regional GFR maps could be successfully extracted for each patient without the need for image registration. Attached figure shows image quality.

Conclusions: View-sharing offsets loss of temporal resolution from respiratory triggering. Thus, high spatiotemporal resolution renal dynamic contrast enhanced

respiratory triggered images can be obtained with minimal motion artifacts in a pediatric clinical setting to evaluate renal function.

Disclosure: Dr. Chowdhury has indicated that he will discuss or describe, in the educational content, a use of a medical device or pharmaceutical that is classified by the Food and Drug Administration (FDA) as investigational for intended use.

Paper #: PA-083

CT Detection of Pre-Operative Wilms Tumor Rupture

Geetika Khanna, *Washington University, Mallinckrodt Institute of Radiology, khannag@mir.wustl.edu*; Arlene Naranjo, Fredric A. Hoffer, Jeffrey Dome, Peter Ehrlich, Elizabeth Perlman

Purpose or Case Report: Preoperative Wilms tumor (WT) rupture is a risk factor for tumor recurrence. Diagnosis of WT rupture is based on surgical findings in North America and on baseline imaging in Europe. WT rupture implies stage III disease requiring abdominal radiation. In spite of advances in pediatric oncologic imaging, imaging signs of pre-operative WT rupture are unclear.

Methods & Materials: The study cohort was selected from the IRB approved Children's Oncology Group AREN03B2 study. Cases are evaluated for pre-operative WT rupture based on central review of surgical/pathology findings. 70 WT cases with rupture were matched to 70 WT controls by age and tumor weight (within 6 months and 50 g). CT scans were independently reviewed by 2 blinded radiologists, for presence/absence of rupture and the following CT signs: poorly circumscribed mass, perinephric fat stranding, peritumoral fat planes obscured, retroperitoneal fluid, ascites beyond cul-de-sac, peritoneal implants, ipsilateral pleural effusion, intratumor hemorrhage. Sensitivity, specificity of CT for assessing pre-operative WT rupture was determined. The relationship between CT signs and rupture was assessed by McNemar's test, and the most predictive CT signs determined by backward selection multivariate logistic regression.

Results: Sensitivity, specificity for detecting WT rupture were: reviewer 1–53.7%, 88.4%, reviewer 2–70.2%, 88.4%. Kappa coefficient for interobserver agreement was substantial: 0.76 ($p < 0.0001$). All CT signs tested, except peritoneal implants and intratumoral hemorrhage, had significant association with tumor rupture ($p < 0.01$). For reviewer 1, ascites and fat stranding around tumor were most predictive (Odds ratio 18.359 and 10.554, $P < 0.01$). For reviewer 2, ascites and retroperitoneal fluid were most predictive (OR 8.345 and 4.916, $P < 0.01$).

Conclusions: CT has high specificity but relatively low sensitivity for detecting preoperative WT rupture. The presence of ascites beyond cul-de-sac is the best indicator of pre-operative rupture, followed by fat stranding and retroperitoneal fluid.

Paper #: PA-084

The Failed Pyeloplasty: Evaluation with MR Urography

Damien Grattan-Smith, *Children's Healthcare of Atlanta, damien.grattansmith@mac.com*; Ricahrd Jones, Stephen Little, Wolfgang Cerwinka, Hal Scherz, Andrew Kirsch

Purpose or Case Report: To identify imaging characteristics associated with failed pyeloplasty seen with MR urography.

Methods & Materials: We have performed MR Urography in 142 children following pyeloplasty. From this group, 16 children had follow-up surgical intervention with repeat pyeloplasty or balloon dilatation of the UPJ. Imaging features reviewed included degree of hydronephrosis, calyceal transit times, renal transit times, signal intensity versus time curves, as well as functional analysis based on volumetric and Patlak differential function and change in the asymmetry index.

Results: All children who underwent a second surgical procedure had delayed calyceal transit times. The degree of hydronephrosis and renal transit times were either stable or worse when compared to pre-operative evaluation. Functional derangement could show stability, slight improvement or deterioration. The asymmetry index estimated the severity of the obstruction.

Conclusions: MR urography is valuable in the evaluation of children who have undergone pyeloplasty. The calyceal transit time appears to be the most reliable discriminator when comparing successful and failed pyeloplasty. Calyceal transit times may be prolonged before the hydronephrosis becomes progressive.

Disclosure: Dr. Grattan-Smith has indicated that he will discuss or describe, in the educational content, a use of a medical device or pharmaceutical that is classified by the Food and Drug Administration (FDA) as investigational for intended use.

Paper #: PA-085

Functional Findings of Unilateral High-Grade Pelvicalyceal Dilatation in MR Urography

Lesli LeCompte, MD, *Children's Hospital of Philadelphia, lecomptel@email.chop.edu*; Melkamu Adeb, Dmitry Khrichenko, Sarah Lambert, Pasquale Casale, Kassa Darge

Purpose or Case Report: Initial attempts at interpreting functional MR Urography (fMRU) can be challenging. A time intensive navigation through a multitude of both subjective and objective functional results is necessary to render a useful interpretation. This is a guided review of fMRU, noting the important functional findings in high-grade unilateral pelvicalyceal dilatation (PCD), in the absence of ureterectasis, with a contralateral normal kidney allowing for an optimal functional comparison.

Methods & Materials: A retrospective functional evaluation of 16 cases with unilateral pelvicalyceal dilatation (PCD), without prior pyeloplasty, was conducted. The fMRU studies were carried out according to a standard protocol and post-processing using the CHOP-fMRU software. This included IV hydration, bladder catheterization and IV Furosemide administration. Fifteen minutes after diuretic administration, a dynamic coronal 3D fat saturated T1 sequence was performed in a supine position over 15 min. A sagittal 3D T1 and delayed single coronal T1, both fat saturated, followed in a supine and/or prone position. The following functional features were evaluated: visualization of the ureter, the presence of a contrast-urine level and swirling of contrast in the dilated renal pelvis. The functional results included in the analysis were calyceal transit time (CTT), renal transit time (RTT), time-to-peak (TTP), parenchymal volume (PV), differential renal functions (volumetric—vDRF, Patlak—pDRF and volumetric Patlak—vpDRF) and the difference between vDRF and pDRF.

Results: 16 patients were comprised of 8 males and 8 females with an age range of 0.1–17.0 years (median 0.8 yrs). Of the kidneys with PCD, the ureter was visualized in 10, 3 during the dynamic sequence, 4/9 during supine delay and 3/7 only in prone position. A contrast-urine level was present in 14 of the dilated systems, and swirling in 6. The ureter was visualized during dynamic sequence in all contralateral normal kidneys and at no time was swirling or a contrast-urine level identified. The average functional parameters are seen in Table 1. A statistically significant ($p < 0.05$) difference between the normal and dilated pelvicalyceal systems was achieved in TTP, pDRF and vpDRF for this small sample size.

Conclusions: Awareness of multiple functional features and the range of calculated results may aid in subsequent combined interpretation of the fMRU with the morphologic analysis.

Disclosure: Dr. LeCompte has indicated that she will discuss or describe, in the educational content, a use of a medical device or pharmaceutical that is classified by the Food and Drug Administration (FDA) as investigational for intended use.

Paper #: PA-086

Venous Thrombosis in Paget Schroetter Syndrome: A Single Pediatric Institutional Experience

Chrystal Obi, BA, *Perelman School of Medicine at the University of Pennsylvania, chrystal.obi@gmail.com*; Leslie Raffini, Paul Foley, Marilyn Blumenstein, Ron Fairman, Anne Marie Cahill

Purpose or Case Report: The purpose of the study is to analyze our percutaneous endovascular techniques and clinical outcomes as compared with the literature for upper extremity deep vein thrombosis secondary to thoracic outlet obstruction (Paget Schroetter Syndrome).

Methods & Materials: Under IRB approval, a retrospective review was performed of all patients with Paget Schroetter Syndrome treated with endovascular therapy at our institution between 2007 and 2011. Demographics, clinical presentation, diagnostic studies and treatment outcomes were evaluated. Post-procedure imaging was evaluated for clot burden reduction (patency) and residual venous stenosis by two-reader consensus.

Results: Ten patients (5 male; 5 female, mean age 16 years, range 15–18) presenting with acute upper extremity swelling and pre-procedure imaging revealing 100% occlusion of the axillary and subclavian veins received successful endovascular therapy. All 10 patients underwent infusion catheter placement for thrombolysis with tissue plasminogen activator or urokinase. 6 patients received additional pharmacomechanical treatment. Angioplasty was also performed in all patients. The mean treatment duration was 33 h (range 16–62). Post-procedural imaging revealed that 9 of 10 patients achieved 75–100% patency (clot burden reduction) and 1 patient achieved 50–75% patency. The residual venous stenosis was graded: 5 patients had 0–25% stenosis, 2 patients had 25–50% stenosis and 3 patients had 75–100% stenosis. All patients were discharged on full anticoagulation therapy with low molecular weight heparin. 9 patients had surgical rib resection post-thrombolysis with an average length of time from thrombolytic therapy to surgery being 32 days (range 14–73). 3 patients had re-thrombosis events during the follow-up period (mean 10 months; range 1–34), with one re-thrombosis event occurring within one week of thrombolytic therapy, prior to surgery and the other two occurring 3–5 weeks post-rib resection. There were no procedure related complications. One patient was lost to follow-up after initial successful catheter directed therapy.

Conclusions: Percutaneous endovascular techniques such as pharmacomechanical thrombolysis and angioplasty appear to be feasible and safe options for Paget Schroetter Syndrome in otherwise healthy adolescent patients. In attempt to prevent re-thrombosis and chronic symptoms, we refer all patients for

adjunctive surgical decompression. Future larger studies are needed to address optimal strategies for these patients.

Paper #: PA-087

Combined 3D Fluoroscopy Image Guided Percutaneous Intervention with Real-Time Optical Sensing at the Tip of a Needle for Tissue Characterization

Rami Nachabe, *Philips*, rami.nachabe@philips.com; John M. Racadio, Drazenko Babic, Ross Schierling, Jasmine Hales, Benno Hendriks

Purpose or Case Report: To investigate the feasibility and potential of real-time tissue characterization at the tip of a needle with diffuse optical spectroscopy (DOS) sensing capabilities during 3D fluoroscopy guidance using cone beam CT and dedicated needle path planning software.

Methods & Materials: A C-arm X-ray system that combines fluoroscopy and 3D imaging from a cone beam CT was used to image a woodchuck with hepatocellular carcinoma (HCC). The imaging system enabled needle path planning, which was used to perform insertion and navigation of a needle toward the liver tumor. The needle was integrated with optical fibers for real-time tissue spectral sensing at its tip. Optical spectra measurements were obtained continuously as the needle passed through healthy liver tissue and then into the tumor. From the diffuse optical spectra measurements, the following clinical parameters were extracted for tissue characterization: blood volume fraction, blood oxygenation, lipid volume fraction and tissue light scattering (related to tissue density). The tissue parameters were compared for healthy liver and tumor using the Kruskal-Wallis test.

Results: The tissue density of the healthy liver was lower than that of the tumor. Higher blood and lipid volume fractions as well as oxygenation levels were observed in the healthy liver as compared to the tumor. All differences were statistically significant ($P < 0.01$). Additionally, a much wider heterogeneity in tissue density was observed in the tumor as opposed to the healthy liver.

Conclusions: Differences in tissue properties between tumor and healthy liver enable discrimination between these two types of tissues. Adding real-time optical sensing at the tip of a needle to 3D fluoroscopy image guidance is a feasible technique that complements the imaging information with relevant physiological parameters; it facilitates more precise definition of tumor boundaries despite any target motion during needle insertion.

Disclosure: Dr. Racadio has disclosed that he is a consultant for Philips Healthcare and receives travel reimbursement.

Rami Nachabe, Drazenko Babic and Benno Hendriks are employees of Philips Healthcare.

Paper #: PA-088

Hepatocyte Transplant Procedure in a Children's Hospital—Technique and Pitfalls

John Crowley, MB, *Radiology, Children's Hospital of Pittsburgh*, crowleyjj@upmc.edu; Ira Fox, Kyle Soltys, Kevin Baskin, Charles Fitz

Purpose or Case Report: To describe the technique of the hepatocyte transplant procedure, a new procedure for the treatment of liver failure in children—the central role of the interventional radiologist and the early recognition of possible complications.

Methods & Materials: Two children aged 6 months and 3 months were treated at this institution for liver failure resulting from urea cycle disorders, with a hepatocyte transplant procedure. The recipient liver was irradiated prior to transplant to facilitate engraftment. The procedure involves the injection of prepared hepatocytes from a suitably screened, compatible donor, via a main portal vein branch into the recipient liver. In both procedures access to the umbilical vein was achieved by the surgery service and a 4 French arterial sheath was placed. A 4 French angled catheter was used for diagnostic runs and to access the right and left main portal vein. A 3 French Fogarty catheter (Edwards Lifesciences, Irvine, Ca) was placed to isolate each portal vein branch in turn and hepatocytes injected using hand injections. Pressures in the main, right and left portal veins were measured and hand injections of contrast made at regular intervals. Careful attention must be paid for evidence of pruning of portal branches, indicating occlusion of small portal branches, or portal to hepatic vein shunting. If shunting is seen, infusion must be stopped as embolism of hepatocytes into pulmonary arteries may result with serious clinical sequelae

Results: In both patients, the desired number of hepatocytes were successfully delivered into the recipient liver. In both cases, mild pruning of the portal vein branches was evident at the end of the procedure. Portal vein pressures remained steady. There was no venographic or clinical evidence of pulmonary arterial embolization.

Conclusions: The interventional radiologist plays a central role in the hepatocyte transplant procedure. Familiarity with catheterizing portal branches from an umbilical vein approach, measuring venous pressures, using small occlusion catheters and recognizing venographic end points such as portal vein pruning and portal to hepatic vein shunting are necessary to the safe and successful completion of this new technique.

Paper #: PA-089**Enteric Tube Placement Under Fluoroscopic Guidance: What Do We Do Right? What Do We Do Wrong?**

Beth Furey, *Pediatric Radiology, IWK Health Centre, efurey@dal.ca*; Pierre Schmit

Purpose or Case Report: The aim of the study was to evaluate the trends in term of type of tube placed, number of procedures per year, number and age of the patients as well as the number of procedures per patient and the interval of time between two placements, and finally the irradiation burden borne by the patients.

Methods & Materials: After REB approval the radiologic files of the patients who underwent naso-duodenal-jejunal (NDJ) or gastro-jejunal (GJ) or jejunal (J) tube placement under fluoroscopy over the past five years (2006 to 2010) were extracted from the RIS and reviewed. The results were tabulated as a single batch and stratified by year.

Results: Eighty-nine patients representing 234 procedures (155 NDJ, 77, GJ, 2 J) were included. Only 38 patients underwent a single procedure. The average number of procedures per patient was 2.6 with a maximum of 12 during the study period. The average patient's age was 55.3 months (SD=74.88, median=11.43). The average fluoro time per procedure was 7.2 min (SD=8.3, median=5.0). The average interval between two procedures was 58 days (SD=108.44, median=18). The average fluoroscopy time per patient combining those having a single procedure and those having multiple ones, was 19.57 min (range 0.3 to 151.7, SD=24.36, median=12.45).

Conclusions: Fluoroscopic placement of enteric tubes delivers a significant amount of irradiation. Our data led to two interventions with respect to insertion and management of the tubes. On one hand, when the attempt pursued by a radiologist is not successful after 10 min of fluoroscopy other strategies should be considered including another operator or an alternative technique for tube positioning. On the other hand, information will be distributed toward the clinicians and nurses in order to improve the management of these tubes and avoid fortuitous displacement which was responsible of a significant amount of repeated procedures leading to undue irradiation.

Paper #: PA-090**Doxycycline/Albumin in vitro Drug Elution Dynamics with Clinical Correlation**

Emma Raver, BA, *Radiology, Nationwide Children's Hospital, emma.raver@nationwidechildrens.org*; William E. Shiels

Purpose or Case Report: To evaluate drug elution pharmacodynamics of doxycycline in an albumin-based solution, as used in percutaneous imaging-directed therapy of aneurysmal bone cyst (ABC) and microcystic lymphatic malformation (LM)

Methods & Materials: Doxycycline mixed with 25% human serum albumin (HSA), and doxycycline mixed with saline solution (both 20 mg/ml) were evaluated using a fluid diffusion chamber system over 8 h, recording pH and doxycycline concentration. Static pH and doxycycline concentrations were recorded every 5 min for the first 180 min, then every 30 min for a total of 8 h, averaged over 3 trials in each of the HSA and saline systems. Statistical analysis evaluated standard deviation and rate of change for the 3 trials in each system. Drug elution dynamics data were correlated with clinical experience in the doxycycline/albumin treatment of 49 patients (233 treatments) with aneurysmal bone cyst (ABC) and 63 patients with 1263 lymphatic malformation microcysts.

Results: Drug elution was linear in both the HSA and saline systems, with statistically significant ($p<.001$) slower elution drug release from the albumin system as compared with the doxycycline and saline solution, both over 3 and 8 h. Average differences in eluted doxycycline concentrations (ug/L) between the saline and HSA solutions, respectively, were 16.74 vs.3.67 at 60 min; 40.17 vs. 6.63 at 120 min; and 57.80 vs. 8.39 at 180 min. Average rates of change of the saline and HSA systems were 0.39 vs. 0.06 at 60 min; 0.46 vs. 0.04 at 120 min; and 0.35 vs. 0.03 at 180 min. Doxycycline/HSA was injected as a stable foam in all ABC and LM treatments, visible as a static air echogenicity or lucency on both ultrasound and fluoroscopic imaging, and visible on CT imaging after 3 days in 2 patients (1-ABC, 1-LM).

Conclusions: Doxycycline as a protein bound therapy agent, targeting tumor cells of ABC and endothelial cells of LM, is slowly eluted when mixed with an HSA drug delivery system, as demonstrated in an in-vitro elution system. Clinical correlation in 1496 injections confirms the stable foam injection and delayed foam dissipation, in both ABC and LM patients.

Paper #: PA-091**Successful Interventional Radiologic Management of Paget Schroetter Syndrome in an Adolescent Population**

John Crowley, MB, *Radiology, Children's Hospital of Pittsburgh, crowleyjj@upmc.edu*; Sabri Yilmaz, Peter Shaw, Robert Rhee

Purpose or Case Report: To describe a successful Interventional Radiologic approach to the management of Paget Schroetter Syndrome presenting as acute arm swelling in adolescent athletes.

Methods & Materials: Institutional Review board approval was obtained for this retrospective study. Five patients aged 14 to 18 years (mean 16.5 years) were treated at this Institution over a 2 year period all presenting with acute arm swelling (July 2009 - July 2011). Ultrasound confirmed subclavian vein thrombosis in all cases. All were treated with placement of an infusion catheter (EV3, Plymouth, MN), infusion of Tissue plasminogen Activator (TPA) at a rate of 1 mg/hour overnight and aspiration of remaining clot with a "Trellis" (Bacchus Vascular, Santa Clara, CA, USA) thrombectomy device.

Results: Clot was successfully removed in all five patients. Complete clearance of clot was confirmed by contrast venography in all cases. In four patients balloon angioplasty of a narrowing at the junction of the subclavian and brachiocephalic veins was carried out. In one, the thrombus recurred within 6 h. The patient was retreated the next day with aspiration of clot using the "Trellis" device and an infusion catheter placed with low dose (0.5mgs/hour) TPA commenced until surgical review; this patient was operated on within 48 h of final thrombolysis. All patients were seen by a Vascular Surgeon with an interest in this condition. All underwent surgical decompression; at end of the study period all patients were asymptomatic.

Conclusions: Interventional Radiologic management of acute axillo-subclavian thrombosis due to Paget Schroetter syndrome is safe and highly successful in the adolescent population. Early recurrence of thrombus is not uncommon and prompt surgical consultation with a view to early surgical decompression is recommended.

Paper #: PA-092

Quality Improvement Registry in CT Scans in Children (QuIRCC): Proposed Pediatric Abdominal CT Dose Reference Level Ranges Based on Image Quality Analysis

Marilyn Goske, MD, Radiology, Cincinnati Children's Hospital; Keith Strauss, Laura Coombs, Michael Callahan, Kassa Darge, Donald Frush

Purpose or Case Report: Diagnostic reference levels (DRL) or target radiation dose ranges for pediatric CT scans are needed in the U.S. The first U.S. pediatric CT dose index registry (QuIRCC) within the American College of Radiology recorded estimates of patient radiation dose using a new method (SSDE) based on body width (BW) for the purpose of developing Diagnostic Reference Levels (DRL). In addition to developing DRL at the 75th percentile, the purpose of this study was to determine the SSDEs associated with the lower range of acceptable image quality through subjective image quality evaluation.

Methods & Materials: Six children's hospitals participated in a retrospective review of abdominal CT with IV contrast on patients <18 yrs of age. From 939 exams, each site submitted de-identified images for selected cases based on SSDE and patient width. A total of 106 cases were selected from the lowest, first quartile and median SSDE. Six investigators reviewed 3 images from each case under identical viewing conditions and rated them for subjective quality according to a score sheet and reference scale of images with known quantum mottle. Cases were considered non-diagnostic if at least 3 of 6 reviewers ranked them as such.

Results: First, second, and third quartile SSDE and CTDIvol32 values from 6 sites for each BW will be shown. 6/106 cases were ranked non-diagnostic by the reviewers. 4/6 non-diagnostic cases were below the 10th percentile based on SSDE. 5/6 of "non-diagnostic" cases had SSDE less than the 25th percentile. The unacceptable case with SSDE above the 25th percentile (16 cm, SSDE 8.2 mGy) was due to subcutaneous metal implant with artifact. The QuIRCC 75th percentile using CTDIvol 32 for a 5 yr old is 7.1 mGy which is 30% lower than the ACR CT accreditation data's published 75th percentile.

Conclusions: This consortium developed target dose ranges (DRLs) for CT of the abdomen with IV contrast for routine exam indications based on evaluation of image quality that establish lower and upper ranges (25–75 percentile) of patient dose (using SSDE) associated with clinically acceptable images. This study demonstrates that pediatric radiologists in this consortium are comfortable interpreting images at or above the 25 percentile SSDE and judged all but one image within this target range as diagnostically acceptable.

Paper #: PA-093

Image Gently: A Survey of Technique Factors for CR-DR Users

Steven Don, MD, Mallinckrodt Institute of Radiology, dons@mir.wustl.edu; Marilyn J. Goske, Robert A. Uzenoff, Gail Rodriguez, Thalia T. Mills, David C. Spelic

Purpose or Case Report: The ACR-SPR Practice Guideline for General Radiography calls for technique charts tailored to a range of pediatric patient sizes. Only a single U.S. survey of pediatric radiography technique factors from 1998 exists (Nationwide Evaluation of X-ray Trends) for a single study, pediatric chest. The purpose of our study is to develop technique charts for digital x-ray equipment, categorized by detector type and manufacturer, based on selected routine radiographic exams.

Methods & Materials: An Alliance for Radiation Safety in Pediatric Radiology survey was sent to the Society of Chairmen of Radiology Departments at Children's Hospitals and vendors through the Medical Imaging & Technology Alliance. The exams included: neonatal chest; 5-year-old for two-view chest, supine abdomen, and three-view wrist; 13-year-old two-view scoliosis. The survey requested patient parameters (age, weight, or body part thickness) used to determine radiographic technique factors; use of manual technique or automatic exposure control; the exposure factors (kVp, mAs, grids, SID); and the type and range of exposure indicator (proprietary indicator or new International Electrotechnical Commission (IEC) exposure index standard).

Results: 14 centers returned 32 surveys (14 computed radiography [CR] and 18 digital radiography [DR], Table 1). With the exception of neonate chest, most used age-based techniques; only two centers reported using thickness. No survey used grids for wrist images, while 2/3 of the surveys used grids for chest and abdomen exams in 5-year-olds. At the most common SID there was up to a 60 kVp variation (5-year-old chest AP) and up to 8-fold variation in mAs (13 year old Scolio Lat). Only two surveys used equipment that displayed the new IEC exposure index.

Conclusions: Participants report variability in the techniques and methods used to acquire common radiographic studies, reflecting differences between detector types and users. Radiologists, technologists, medical physicists, manufacturers, and the FDA have an opportunity to work together to standardize the techniques based on detector type to optimize radiation exposure for pediatric radiographic exams.

Disclosure: Dr. Don has indicated that he performs contract research for Carestream and that he is on the speaker's bureau for Siemens and receives an honoraria.

Paper #: PA-094

Follow-up of 10-year International Initiative to Reduce Pediatric Body CT Radiation Dose: A Study of Effectiveness in the U.S. at the Community Level

Kristopher Spinning, Oregon Health & Science University, spinning@ohsu.edu; David Pettersson, Dianna M. Bardo, Katharine Hopkins

Purpose or Case Report: This study assesses community adoption of CT radiation dose guidelines after a 10-year international initiative to reduce medical radiation exposure in children. Size-specific dose estimates (SSDE) from community pediatric body CT scans are compared to SSDE from matched scans obtained at a children's hospital that adheres to Image Gently Campaign principles.

Methods & Materials: We reviewed 112 pediatric CT scans (14 chest (C), 80 abdomen/pelvis (AP), 18 chest/abdomen/

pelvis (CAP)) transferred from 32 community imaging centers to our university children's hospital between July 2010 and February 2011. Community scans were acquired with variable parameters and reconstructed with traditional filtered back projection (FBP). Comparison was made to 432 children's hospital CT scans, performed in accordance with principles of the Image Gently Campaign. Because iterative reconstruction (IR) software was added to our scanner during the study, enabling us to reduce CTDIvol by 60%, children's hospital scans were divided into two groups: A) 213 scans obtained with standard weight-based pediatric protocols and FBP (October 2009–October 2010; 58 C, 110 AP, 45 CAP) and B) 219 scans obtained with reduced-dose weight-based pediatric protocols and blended IR/ FBP (October 2010–April 2011; 85 C, 104 AP, 30 CAP). CTDIvol and greatest lateral dimension were recorded from each scan and were used to calculate SSDE. Mean SSDE from community scans was compared to mean SSDE from children's hospital groups A and B. Statistical analysis was performed with Student's t-test.

Results: Patient age range was 0–17 years in both community and children's hospital groups. Mean SSDE for community C, AP, and CAP scans was 1.7, 1.3, and 1.6 times higher than mean SSDE for matched scans in control group A ($p < 0.001$) and 5.0, 2.8, and 3.7 times higher than mean SSDE for matched scans in control group B ($p < 0.0001$).

Conclusions: SSDE was significantly higher for community pediatric body CT scans than for matched scans performed at a children's hospital that adheres to Image Gently Campaign principles. Results suggest that more community outreach and education are required in implementation of low-dose CT protocols outside of children's hospitals. Concurrent use of IR provides a means of achieving even greater SSDE reduction than is possible with FBP alone and should be encouraged.

Paper #: PA-095

Optimization of Tube Voltage and Current in Size-based Pediatric CT Imaging: A Phantom Study

Boaz Karmazyn, MD, Radiology, Riley Hospital for Children, bkarmazy@iupui.edu; Yun Liang, Keith Kaser, Peter Johnson, Mervyn Cohen

Purpose or Case Report: Determine the change in CT dose index (CTDIvol) required to maintain the same quantum mottle noise when using lower tube voltages (80 and 100 kVp) relative to 120 kVp in different sized cylinder water phantoms (CWP) representing a wide range of pediatric body sizes.

Methods & Materials: We performed 256 MDCT scans of 10, 20, 25, and 35 cm CWP. Thirty scans were performed for each phantom. The tube currents ranged from 50 to 500 mAs

with increments of 50 mAs, and the tube voltage levels were 80, 100, and 120 kVp. The noise (standard deviation in HU) was measured using center region of interest (ROI) that was 80% of phantom's area. Two other ROIs (each 2% of the area) were placed at the center and periphery of the phantom images to measure noise gradient.

Results: In the smallest (10 cm) CWP, approximately the same noise level was maintained with all three tube voltages without a significant change in CTDIvol. For the 20, 25, and 35 cm phantoms, the average CTDIvol needed to be increased by 2%, 4%, and 19%, respectively, to maintain same noise level when the voltage was decreased from 120 to 100 kVp. The average CTDIvol needed to be increased by 15%, 22% and 52% to maintain the same noise level in the 20, 25, and 35 cm CWP when the tube voltage was decreased from 120 to 80 kVp. The difference between central and peripheral noise increased on average by 11.1%, 19.6%, 23.7%, and 28.0% in the CWP of 10, 20, 25, and 35 cm, respectively. In each CWP, the central to peripheral noise difference was more pronounced (up to 3.7% more) with decrease in kVp from 120 to 100 or 80.

Conclusions: Noise measurements in the water phantom model indicate that tube voltage could be decreased from 120 to 80 in CWP of 10 cm without significant change in CTDIvol. It is also possible to decrease the voltage from 120 to 100 kVp with a minimal (< average 5%) increase in dose in CWPs of 10, 20, and 25 cm. The noise gradient increases with larger CWP and smaller kVp.

Paper #: PA-096

Comparison of Radiation Dose Estimates, Image Noise, and Scan Duration in Pediatric Body Imaging Using 320-Row and 64-Row CT

Jennifer Johnston, MD, *Radiology, Cincinnati Children's Hospital Medical Center, jhtai@yahoo.com*; Daniel J. Podberesky, Erin Angels, Terry T. Yoshizumi, Greta Toncheva, Donald P. Frush

Purpose or Case Report: To compare effective dose (ED) estimates, image noise, and scan duration for pediatric chest, abdomen and pelvis protocols using 320-row and 64-row CT scanners in various acquisition modes.

Methods & Materials: Organ doses were measured using 20 MOSFET dosimeters. Dose, scan duration, and noise measurements were made in a 5-year-old anthropomorphic phantom for conventional helical, 160-detector helical and volume acquisition modes for chest, abdomen and pelvis protocols on a 320-row CT, and for helical mode on a 64-row CT (Aquilion ONE and Aquilion 64, Toshiba Medical Systems, Otawara, Japan) using similar scan parameters

representing currently used clinical protocols. Mean organ doses from three runs for each protocol, in combination with ICRP 103 tissue weighting factors, were used to obtain ED for each protocol. Noise was measured as the standard deviation of Hounsfield units in 3 equivalent locations at 4 levels for each protocol with an ROI tool. ED and noise were compared with a paired T-test or sign test.

Results: Compared to helical acquisitions on the 64-row CT, ED of all tested acquisition modes on the 320-row volume CT were significantly lower for chest, abdomen/pelvis (AP) and chest/abdomen/pelvis (CAP) protocols (Table). Scan durations were lower across the board on the 320-row volume CT. Compared to acquisitions on the 64-row CT, noise was in general similar to those on 320-row CT protocols, but some acquisition protocols on the 320-row CT produced greater noise (Table), specifically volume acquisition for chest CT and 160-detector helical and volume modes for AP and CAP protocols.

Conclusions: Dose savings can be achieved for chest, AP and CAP CT examinations on a 320-row CT scanner compared to helical acquisition on a 64-row CT, with shorter scan durations. Image noise was in general comparable between protocols. Although noise differences between some modes did reach statistical significance, the impact on overall image quality will need to be studied further.

Paper #: PA-097

The Observed to Expected Total Fetal Lung Volume as a Predictor of Short- and Long-Term Morbidity in Surviving Infants with Congenital Diaphragmatic Hernia

Emily Stenhouse, *The Royal Hospital for Sick Children, emilysten@doctors.org.uk*; Neil Patel, Judith Simpson, Watt Andrew, Gregor Walker, Carl Davis

Purpose or Case Report: Observed-to-expected total fetal lung volume (O:E TFLV) is a validated MR measure which we have previously demonstrated to be significantly reduced in non-surviving infants with Congenital Diaphragmatic Hernia (CDH). Our aim was to investigate the relationship between O:E TFLV and short- and long-term morbidity outcomes in surviving infants with CDH.

Methods & Materials: A retrospective analysis of cases of isolated left-side CDH referred to our institution for fetal MR evaluation between 24–35 weeks. MR imaging studies were performed on a 1.5 T Philips system using a phased array body coil. The observed TFLV was calculated by multiplying the summed area of the region of interest by the section thickness. The expected TFLV was calculated with a formula previously described in the literature using the gestational age of the fetus. The observed TFLV was expressed as a percentage of the expected TFLV at a given gestation. Morbidity outcome data

was obtained from the case records of all surviving infants. Specific measures of illness severity relating to short-term intensive care management and long-term outpatient management were recorded. Differences in O:E TFLV between outcome groups were assessed by t-test.

Results: 18 liveborn infants with isolated left-side CDH and antenatal MR scans were identified. Scans were performed at 24–35 weeks gestation. 12 infants survived to discharge; gestation 38.5 (36.0 – 39) weeks, birth weight 3.17 (2.03–3.66) kg. Median length of admission was 38 (23–103) days, median duration of follow-up was 3.1 (0.7–5.4) years. O:E TFLV was significantly lower in non-surviving infants; 23 vs. 37%, $P=0.005$. O:E TFLV was significantly lower in infants who received High Frequency Oscillation Ventilation (HFOV) versus those who were conventionally ventilated (29% vs 41%, $P=0.05$). O:E TFLV was also significantly lower in those infants who had a length of admission greater than the median of 38 days (29% vs. 43%, $P=0.02$). O:E TFLV trended lower with other measures of increased morbidity; inhaled nitric oxide use, patch repair of diaphragm, rehospitalisation within 1 year, supplemental feeding at discharge, gastro-oesophageal reflux, and developmental delay.

Conclusions: As well as predicting survival, lung volume measurement by O:E TFLV is a promising predictor of outcome and morbidity in surviving infants with CDH. Further studies in larger populations are required to provide quantitative predictive risk data.

Paper #: PA-098

Characterization of the Inherent Acoustic Noise of a Dedicated NICU MRI System

Jean Tkach, PhD, *Cincinnati Children's Hospital Medical Center, jean.tkach@cchmc.org*; Yu Li, Ron G. Pratt, Christopher Villa, Beth M. Kline-Fath, Charles Dumoulin

Purpose or Case Report: We have developed a small footprint 1.5 T MRI scanner specifically for neonatal imaging that can be easily installed in a Neonatal Intensive Care Unit (NICU). The scanner has a maximum patient bore diameter of 21.8 cm (without RF coil), and roughly twice the gradient performance of the best conventional adult whole-body 1.5 T MR systems. It is known that sensory stimulation such as acoustic noise can elicit autonomic instability in both term and preterm neonates. The inherent noise properties of the NICU MRI system were measured as part of the initial safety evaluation of the system and compared against that of a conventional 1.5 T MRI system.

Methods & Materials: To evaluate the inherent acoustic noise characteristics of the NICU MRI scanner, Sound Pressure Level (SPL) measurements were performed on it and on a conventional adult sized whole body 1.5 T HDx GE MRI

system (GE Healthcare, Waukesha, WI). A Brüel & Kjaer model 2250 sound level meter (Brüel & Kjaer Sound & Vibration Measurement A/S, Denmark) was used to perform the SPL measurements for 6 several different MR acquisitions (spin echo, gradient echo, fast RF spoiled gradient echo, fully balanced steady state free precession, gradient echo echo planar, and diffusion weighted) using acquisition parameters consistent with clinical protocols. The MR sequences, acquisition parameters, noise measurement equipment and methodology were identical for the two MR systems. The maximum SPL in units of A weighted decibels (dBA) was recorded for each of the MR acquisition/MR system combinations evaluated.

Results: The maximum SPL values measured during each of the 6 MR acquisitions were lower for all sequences (average 11.33dBA (range=5–18dBA)) for the NICU MRI unit as compared to the conventional MRI scanner (Table 1). The average measured maximum SPL value, reported in dBA, across all 6 acquisitions was 86.2 ± 2.6 for the NICU scanner, and 97.5 ± 2.9 for the conventional MRI scanner. The highest SPL values were measured for the diffusion-weighted sequence: 85 and 103dBA, for the NICU and conventional MRI scanner respectively.

Conclusions: Because of the smaller dimensions of the gradient coils in the NICU MRI system, acoustic noise is less than that of conventional MRI scanners despite the superior gradient performance of the smaller coils. The lower inherent acoustic noise level of the NICU system provides improved safety for the neonate, and facilitates siting of the unit in the NICU.

Disclosure: Dr. Tkach has indicated that she will discuss or describe, in the educational content, a use of a medical device or pharmaceutical that is classified by the Food and Drug Administration (FDA) as investigational for intended use.

Paper #: PA-099

Late Neurologic Events in Extremely Premature Infants

Carlos Guevara, MD, *Radiology, Duke University, cjc7@duke.edu*; Brett Bartz, Caroline L. Hollingsworth, Caroline W. Carrico, Michael C. Cotten, Charles M. Maxfield

Purpose or Case Report: Germinal matrix hemorrhage (GMH) is a major complication of prematurity. Persistence of germinal matrix and immature neurovascular autonomic regulation in the premature neonate is thought to predispose to GMH. Most GMH in premature population occurs during the first 4 days of life, and yet the persistence of the germinal matrix to 32 weeks gestation may allow for post-natal GMH outside of the immediate perinatal period. To our knowledge, this is the first systematic review of late GMH (after

the first week of life) in a large population of extremely preterm neonates (less than 28 weeks of gestation).

Methods & Materials: This IRB approved retrospective review included patients weighing less than 750 g or born at less than 28 weeks of gestation from 2008 through 2010. The study population included 150 infants who had a head ultrasound (HUS) within the first week of life and at least one follow HUS after the first week of life. All HUS were reviewed by three experienced pediatric radiologists for the presence and grade of ICH or late developing hemorrhage-like lesions (HLL). Infants with and without HLL were evaluated for several clinical variables, including neurodevelopmental outcomes (Bayley scales).

Results: Average gestational age of study population was 25.1 weeks. The incidence of GMH in the first week of life was 34% Grade 1, 38.6% Grade 2, 4.9% grade 3/4, and 2.2% posterior fossa. New echogenic foci (HLL) at the caudothalamic groove were seen in 13.3% after the first week of life. 70% of these lesions were bilateral. A four-fold increase in incidence of HLL was seen in infants <750 g compared to those >750 g. Higher grade hemorrhages were not seen in this patient population, although 6% of infants had late posterior fossa hemorrhages. The clinical course of infants with HLL trended towards a higher incidence of stressors, but this was not statistically significant. The Psychomotor Development Index scores were lower than those infants without hemorrhage.

Conclusions: Small HLL at the caudothalamic groove are common in extremely preterm infants after the first week of life. Higher grade (2–4) hemorrhages were not seen. There were no cases of intraventricular extension and no direct complications. If isolated, this finding necessitates no follow-up imaging, but may be associated with poor neurodevelopmental outcome.

Disclosure: Dr. Guevara has indicated that he will discuss or describe, in the educational content, a use of a medical device or pharmaceutical that is classified by the Food and Drug Administration (FDA) as investigational for intended use.

Paper #: PA-100

Prenatal and Postnatal Imaging Evaluation of Pulmonary Artery, Airway and Pulmonary Findings in Tetralogy of Fallot with Absent Pulmonic Valve (TOF/APV)

Justin Boe, *Stanford*, justinj.boe@gmail.com; Theresa Tacy, Beverley Newman, Erika Rubesova, Shreyas Vasanawala, Richard A. Barth

Purpose or Case Report: TOF/APV is a rare congenital heart lesion in which pulmonary arteries may become aneurysmally dilated and compress adjacent airways. Pulmonary arterioplasty is often required to relieve tracheobronchial compression in addition to intracardiac repair. The purpose of this

study was to review pre and postnatal imaging findings and their impact on patient management and clinical course.

Methods & Materials: A retrospective database search identified 9 infants with TOF/APV between 2005–2011 (4 fetal diagnosed cases and 5 diagnosed postnatally). For FDC, prenatal ultrasound (US) and fetal MRI were correlated with postnatal CT for the size of the central pulmonary arteries, airway compression, and presence / distribution of air trapping/atelectasis. For all cases postnatal CT findings (between 3–9 days of age) were correlated with clinical management and outcome.

Results: Prenatal diagnosis of TOF/APV was suggested sonographically, based on dilated central PAs, between 21–28 weeks gestational age (GA). Fetal MRI, performed between 32–37 weeks GA confirmed the diagnosis and aneurysmal central PAs and demonstrated air trapping &/or atelectasis in 3/4 with normal appearing lungs in 1 fetus. Size of the PAs (4/4) and presence and distribution of lung abnormality (3/4) correlated closely between fetal MRI and postnatal CT, although detailed visualization of the central airway/vascular relationships were better defined on CT. Fetal MRI identified an unexpected diaphragmatic hernia (DH) not seen on US. For the PND cases, CT showed aneurysmal PAs and airway compression with air trapping &/or atelectasis in 4/5 infants. Seven infants with airway obstruction on CT required pulmonary arterioplasty; 1 infant with no air trapping did not have arterioplasty. 7/8 operative patients survived, one with concomitant DH died at age 22 days due to hemorrhagic shock. One FDC was inoperable due to poor cardiac function and died at age 7 days.

Conclusions: Prenatal MRI correlates well with postnatal CT for assessing pulmonary artery size and location and severity of lung abnormality in patients with TOF/APV, this allows for appropriate management planning and may negate the need for an immediate postnatal CT. CT accurately depicts the location and extent of airway compression and resultant air trapping or atelectasis, serving to guide the need for and extent of the arterioplasty procedure.

Paper #: PA-101

Craniosynostosis Syndromes: Prenatal Findings by US and MRI

Eva Rubio, MD, *CNMC*, rubioeva@yahoo.com; Anna Blask, Alexia Egloff, Dorothy Bulas

Purpose or Case Report: Craniosynostosis with associated malformations is a feature of several related syndromes resulting from a FGFR or Twist genetic mutation. Syndromes include Apert, Crouzon, Pfeiffer, and Carpenter syndromes. Our purpose was to review imaging findings which aid in suggesting the diagnosis prenatally.

Methods & Materials: We retrospectively reviewed prenatal US and MRI findings in 6 cases with prenatal (5 with postnatal/molecular) diagnosis of a craniosynostosis syndrome: 3 cases of Apert, 1 case of Carpenter, and 2 cases of Pfeiffer syndrome.

Results: 5/6 cases were correctly diagnosed prenatally. In the second trimester findings may be subtle, with mild calvarial changes; digit abnormalities, in particular, may elude the imager in unsuspected cases. Although the diagnosis could be made with either modality, the full spectrum of abnormalities was best appreciated using a combined imaging approach of MRI and US. By US many salient features were depicted: Turribrachycephaly/trigonocephaly/cloverleaf (6/6); Syndactyly (4/4); Polydactyly (1/1). Agenesis of the corpus callosum was identified by US in (2/2) cases. Conversely, MRI, performed in all cases, contributed additional observations not well seen by US: the fetal airway was well delineated in all cases (6/6); a low lying spinal cord was noted (1/1), midface hypoplasia (6/6) and migrational/sulcation abnormality (1/1). Additional findings of absent ductus venosus with biliary atresia (1/1), abdominal wall defect (1/1) and renal anomalies (1/1) were seen with both modalities. Reimaging in later pregnancy depicted important changes (2/2), including worsening hydrocephalus and resolution of suspected airway occlusion.

Conclusions: US and MRI are complementary modalities in evaluating fetuses with craniosynostosis. Airway patency, midface hypoplasia, spinal cord abnormalities and intracranial abnormalities are often better seen with MRI. Fetal activity, digits, bone detail, and cardiac anomalies are better appreciated by US. Findings may be subtle in the second trimester. Repeat imaging in later pregnancy may reveal specific information affecting delivery planning.

Paper #: PA-102 PCPRA Best Paper 2011

Hyperpolarized Carbon-13 MRSI for Pediatric Disease

John MacKenzie, MD, *Department of Radiology and Biomedical Imaging, UCSF, john.mackenzie@ucsf.edu;* Yi-Fen Yen, Linda Nguyen, Jeffrey Gu, John Kurhanewicz

Purpose or Case Report: To study the potential of carbon-13 MR spectroscopic imaging (13 C-MRSI)—a radiation free molecular imaging strategy—for the detection and treatment monitoring of pediatric disease.

Methods & Materials: The potential of 13 C-MRSI to detect pediatric disease was tested in rodent models of pediatric arthritis. Animals were induced with arthritis and subsequently given intravenous hyperpolarized 13 C-pyruvate, and imaged. The amount of 13 C-lactate produced from pyruvate in normal and arthritic joints was measured both at single points in time and dynamically at either 3 or 14 Tesla. The 13 C-MRSI data were compared with clinical

measures of arthritis, cell stimulation studies, and joint changes on conventional anatomic MRI and histology.

Results: Alterations in lactate production as measured by 13 C-MRSI appear to depict sites of arthritis and correlate with other more established but potentially less reliable or more invasive measures of disease status. Imaging robust mouse models of pediatric disease may be feasible at 14 Tesla. This method may also be translated from high-field to clinical equipment with reasonable hardware and software modifications that allow detection of hyperpolarized 13 C compounds. 13 C-MRSI depicts increased lactate production at specific regions of inflammation within arthritic joints and is confirmed by histological inspection and anatomic MRI. On average, lactate production is increased by 60% in areas affected by inflammation.

Conclusions: The intravenous injection of hyperpolarized carbon-13 compounds and subsequent imaging with 13 C-MRSI provides a unique molecular imaging strategy to non-invasively monitor pediatric disease. This non-invasive imaging strategy may eventually provide clinical utility for several pediatric diseases involving inflammation, infection and tumor.

Disclosure: Dr. MacKenzie has indicated that he will discuss or describe, in the educational content, a use of a medical device or pharmaceutical that is classified by the Food and Drug Administration (FDA) as investigational for intended use.

Paper #: PA-103

Kaposiform Hemangioendothelioma: A Spectrum of MRI Features

Michael Murati, *Cincinnati Children's, mura0071@umn.edu;* Arnold C. Merrow, Manish Patel

Purpose or Case Report: To describe the MR imaging findings of Kaposiform Hemangioendothelioma (KHE) at the time of diagnosis in the largest case series yet published.

Methods & Materials: Using the Hemangioma-Vascular Malformation Clinic registry at Cincinnati Children's Hospital, we searched for patients diagnosed with KHE whose evaluation included MRI. Twenty such patients were found, although three of the patients had no pre-therapy MRIs. The imaging studies were reviewed by the authors with assessment of the following characteristics: location, margin definition, soft tissue involvement, and pre and post contrast signal intensity.

Results: Location: Lesion location was as follows: trunk (9), extremity (3), extremity plus trunk (3), and head/neck (2). Signal: All lesions were dark on T1 weighted sequences with diffuse enhancement after contrast administration. The majority of the lesions were bright on T2 weighted sequences, but there were 3 cases that had heterogenous to low T2

signal (with all involving the retroperitoneum). Of the 17 cases, only one had both high arterial and venous flow by MRI. Margin definition: Four of the lesions had well defined borders (greater than 50% well circumscribed) with minimal to no adjacent infiltration/edema. Two of those four cases were exophytic masses. The remaining 13 cases were poorly defined lesions with adjacent infiltrative fluid signal intensity and enhancement. Tissue/Organ involvement: Tissue/organ involvement was counted if abnormal fluid-signal intensity or enhancement was identified at that site. Review of these cases showed fifteen patients with muscular involvement. Dermal and subcutaneous involvement was observed in all but 4 cases, with the uninvolved lesions being isolated and deep. Additional sites of suspected involvement included bone (3), pleura (1), penis (1), and pancreas (2).

Conclusions: KHE is a rare neoplasm of infancy with a spectrum of features by MRI. Poorly defined lesions are much more frequent than well-circumscribed masses. However, pathologic correlation of such infiltrative margins is usually not available as treatments after biopsy are primarily medical rather than surgical. Common additional MRI features include predominant involvement of muscle, subcutaneous fat, and skin over viscera and bone with lesions generally showing increased T2 signal and enhancement.

Paper #: PA-104

Is Dedicated Chest CT needed in Addition to PET CT for Evaluation of Pediatric Oncology Patients?

Ibrahim Tuna, *Montefiore Medical Center, dristuna@yahoo.com*; Jeffrey Levsky, Jeremy Rosenblum, Rosanna Ricafort, Benjamin Taragin

Purpose or Case Report: To evaluate the diagnostic accuracy of low dose CT performed during PET-CT as compared to dedicated chest CT in the assessment of pulmonary findings in children with malignancy.

Methods & Materials: The institutional review board approved this HIPAA compliant research. Pediatric oncology patients, ages between 0–21, with known solid malignant tumors who were referred to PET-CT and standard chest CT within 30 days for staging or assessment of treatment response between 01–2008 and 01–2011 were eligible for this retrospective study. Radiology reports were reviewed for potential discrepancies. Two radiologists re-evaluated the standard chest CT and low dose chest CT portion of the PET CT of the discordant cases, while comparing with the most recent prior studies. Studies were scored for pulmonary nodules, bony metastasis, adenopathy, and pleural effusions. True discrepancies were assessed by a panel of pediatric oncologists to judge whether the differences in reports might lead to a significant change in management.

Results: 120 (57 female, 63 male) patients were identified. 31 radiologic reports of 16 different patients (8 female, 8 male) had potential discrepancies based on review of the reports. The primary tumors were rhabdomyosarcoma ($n=6$), Hodgkin's lymphoma ($n=3$) and others ($n=7$). Re-evaluation of the original images showed true discrepancies in 3.3% (4/ total 120). In 2 studies, the discrepancy had no clinical significance. In 2 studies, a pulmonary nodule was identified on standard chest CT which was not described on the PET-CT. Both of these patients had rhabdomyosarcoma. One of these patients had findings that pediatric oncologists considered significant enough to alter patient management.

Conclusions: We found a low false negative rate for clinically significant findings on the low dose portion of PET-CT as compared to standard chest CT. In the future, improvements in acquisition technique and post processing of the CT portion of the PET-CT may further improve its diagnostic utility, obviating the need for a routine separate diagnostic CT, thereby minimizing radiation exposure in these young patients.

Paper #: PA-105

The Role of Low Dose 64-Channel CT Angiography (CTA) to Assess Pediatric Vascular Trauma

Mike Abdulhadi, MD, *Children's Hospital of Philadelphia*; Sabah Servaes, Jeffrey Hellinger, Arastoo Vossough, Monica Epelman

Purpose or Case Report: To assess the clinical utility of low dose multidetector-row CT (MDCT) angiography for evaluation of suspected traumatic vascular injury in pediatric patients.

Methods & Materials: 98 low-dose CTA examinations were performed in pediatric patients over a three year period to evaluate suspected vascular traumatic injury with some patients receiving scans of more than one area of the body. Areas scanned in this include the head and/or neck ($N=54$), chest ($N=17$), abdomen and/or pelvis ($N=13$), upper extremity ($N=8$) and lower extremity ($N=17$). In 80 of these patients, suspected vascular injury was due to a history of either blunt ($N=41$) or penetrating ($N=39$) trauma. 64 patients were referred directly from the emergency department, while 27 were inpatients and the remaining 7 were referred from an outpatient setting. Patients (32 F:66 M) ranged in age from 0 to 23 years old (mean age 11). Studies were performed on a 64-channel MDCT scanner with 80 or 100 kV, 40 to 200mAs, 1.0 to 1.5 mm section thickness, reconstructed with 50% overlap, and 0.8 to 1.5 pitch. Contrast medium was power-injected using weight-based protocols to optimize iodine delivery. Exams were interpreted on a workstation using advanced imaging techniques. Patient

radiation dose was calculated in all cases. Clinical outcome was assessed through a 6 month follow-up when possible.

Results: All studies were technically adequate. 76.5% ($N=78$) of studies revealed no vascular injury, while 23.5% ($N=23$) revealed acute vascular pathology. Vascular injuries included vascular occlusion ($N=12$), vasospasm ($N=3$), narrowing/dissection ($N=4$), pseudoaneurysm ($N=2$), and transection ($N=1$). Extravascular traumatic findings were demonstrated in 51.0% ($N=50$), including fractures, lung injury, soft tissue hematomas, and a ruptured Baker's cyst. Of the patients with acute vascular findings, 43.4% ($N=10$) underwent surgical management (including 6 for vascular injury), while 52.1% ($N=12$) were managed conservatively. One patient with active extravasation was managed with angiographically-guided embolization. In no case was catheter angiography required to confirm CTA findings.

Conclusions: Low dose CTA is a reliable means to screen pediatric patients emergently for acute vascular injury. Vascular and non-vascular pathology can be diagnosed non-invasively for efficient patient management.

Paper #: PA-106

Elasticity Measurement by Acoustic Radiation Force Impulse (ARFI) Technique of Normal Liver, Kidney and Spleen in Healthy Children

Mi-Jung Lee, *Radiology, Severance Children's Hospital, mj11213@yumc.yonsei.ac.kr*; Myung-Joon Kim

Purpose or Case Report: There are many previous studies about using acoustic radiation force impulse (ARFI) value to measure the elasticity of tissue, mainly the liver in adult patients. However, there was limited study about ARFI measurement in the children. The purpose of this study is to evaluate the ARFI value in the normal liver, kidney and spleen in healthy children and to evaluate the effect of sex, age, and body mass index (BMI).

Methods & Materials: The study prospectively enrolled healthy pediatric volunteers who are under 18 years old, and underwent abdominal ultrasonography and ARFI between July 2011 and August 2011. ARFI velocity measuring was performed by 4–9 MHz linear probe for children under 5 years old and 1–4 MHz convex probe for older children. ARFI velocity was measured three times at each organ. However this measurement was stopped if the child cannot tolerate.

Results: Two hundred two children ($M:F=92:110$; mean age, 8 ± 4.7 years) were enrolled. And ARFI measurement was performed only two time for some organs in three children. The mean ARFI value was 1.12 ± 0.20 m/s in liver, 2.20 ± 0.49 m/s in right kidney, 2.33 ± 0.53 m/s in left kidney, and 2.25 ± 0.41 m/s in spleen. ARFI velocity was not

different between boys and girls. However, ARFI velocity was different between right and left kidneys ($p=0.001$). The ARFI value of right kidney, left kidney and spleen was correlated with age, height, weight and BMI ($p<0.001$). However, the ARFI value of liver was not correlated with these parameters.

Conclusions: ARFI measurement is feasible in children with only three times acquisition for each abdominal organ. The mean ARFI velocity was increased according to the age, height, weight and BMI in kidney and spleen, but it was constant in liver.

Disclosure: Dr. Lee has indicated that she will discuss or describe, in the educational content, a use of a medical device or pharmaceutical that is classified by the Food and Drug Administration (FDA) as investigational for intended use.

Paper #: PA-107

Continuous Quality Improvement Using a Data Mining Tool for Reducing Radiation Exposure in Pediatric Bedside Chest Radiography

Taral Doshi, MD, *University of Chicago Medical Center, tdoshi@uchicago.edu*; Richard Davis, Neel Patel, Heber MacMahon, Seng Ong, Kate Feinstein

Purpose or Case Report: Diagnostic image quality can be achieved over a wide range of radiation exposure in digital radiography. "Exposure Factor Creep" or "Dose Creep" in which technologists tend to increase dose to avoid the appearance of noise has been well described. Using the ALARA principle, acceptable images can be achieved while minimizing dose. At our institution "dose creep" has been observed in bedside pediatric chest radiography. To address this we coupled a data mining tool with a continuous quality improvement (CQI) initiative which educates individual technologists on appropriate technique.

Methods & Materials: Radiation dose in digital radiography is estimated from an exposure index, a proprietary format that varies among manufacturers. Our institution uses a Fuji Computed Radiography system which calculates an S, or Sensitivity value, that provides an approximation of the radiation dose to the imaging plate, using an inverse scale. Overexposed bedside chest radiographs were defined by a S value less than 150. A data-mining program was developed to extract from the DICOM header the S value and other relevant information, on a monthly basis. These data were used to provide training and feedback on a one-on-one-basis.

Results: With ad hoc feedback and group training initiatives prior to implementation of this new system, approximately 16.7% (344/2057) of bedside chest radiographs were

overexposed over a four month period. After one-on-one intervention with the technologists, preliminary findings reveal a trend towards fewer overexposed radiographs with approximately 9.2% (40/435) with $S < 150$.

Conclusions: Our tool provides a simple method for systematically identifying overexposed radiographs and the corresponding responsible technologists. We anticipate that this personalized educational program will continue to reduce the proportion of overexposed radiographs and thus the radiation dose to our pediatric patients.

Paper #: PA-108

8 Interactive Web-based Modules with Vendor Specific Instructions to Teach Radiation Protection for Children to CT Technologists

Marilyn Goske, MD, *Radiology, Cincinnati Children's Hospital*; Gregory Morrison, Myke Kudlas, Elizabeth Ey, Eric Faerber, Donald Frush

Purpose or Case Report: Ensuring radiation protection for children undergoing CT scans is challenging due to rapidly changing technology, differences in CT equipment and potential lack of understanding of unique aspects of scanning children. The Joint Commission has named technologists' training as an "action" item. We developed 8 online training modules to fill potential gaps in CT technologists' education.

Methods & Materials: Four modules were created by pediatric radiologists, radiologic technologists and medical physicists; 4 were developed by education/training experts from major CT vendors (GE, Philips, Toshiba, Siemens) through the Medical Imaging Technology Alliance. 4 modules were created as Microsoft Word documents containing de-identified images and edited by education specialists at the American Society of Radiologic Technologists and the Alliance for Radiation Safety in Pediatric Imaging. They were converted to audio/video format using question/answer narration. 4 vendor modules were created in Microsoft Powerpoint format and edited. All 8 modules were converted into Adobe Captivate learning program to achieve uniformity of appearance. Modules are hosted on the ASRT server and linked to the Image Gently website. A certificate may be printed as documentation of completion.

Results: All 8 modules are available at www.imagegently.org. Two introductory modules discuss basics of CT equipment and medical physics related to radiation dose in children. The third and fourth modules discuss dose-saving strategies for neuroCT and body CT. Four vendor-produced modules address unique aspects of equipment design such as automatic exposure control and dose saving strategies for children.

Conclusions: Through collaborative efforts with medical imaging professionals and vendors, we have developed 8 free online modules addressing radiation protection for children. CT technologist training in specific dose saving strategies for children is variable and limited. These modules have the potential to improve CT technologists' understanding of equipment.

Paper #: PA-109

Health Literacy for Parents Regarding Fluoroscopy: Is There a Problem?

Robyn Gebhard, *Radiology, Cincinnati Children's Hospital Medical Center*, gebharrd@mail.uc.edu; Marilyn J. Goske, Shelia Salisbury, Dianne Hater, Catherine Leopard, Steven J. Kraus

Purpose or Case Report: In 2004, the Institute of Medicine issued its pivotal report, Health Literacy: A Prescription to End Confusion which focused attention on improving communication with patients and families. There is little research regarding health literacy (HL) in radiology. The purpose of our study was to determine if an educational intervention (brochure) improves HL for parents whose child will undergo a fluoroscopic study.

Methods & Materials: An education exemption was obtained from the IRB. A multidisciplinary team developed brochures for 5 fluoroscopic procedures. Participants were randomly selected and asked to complete a survey to assess their knowledge of the procedure and use of radiation both before and after reading a brochure. A final survey to rate and gain feedback about the brochure was completed.

Results: Median age of children whose parents participated ($n=120$) was 4 years. VCUG was most commonly performed (46%). Prior to the brochure, 92% of participants knew the name of the test their child was having. After the brochure, 99% knew the name ($p < .0001$). Prior to the brochure, 81% felt informed about the test, whereas 99% felt informed after ($p < .0001$). Test scores showed an improvement in parent knowledge about the procedure with a median increase of 20 points after the brochure (scale of 1–70; $p < .0001$). Even after reading the brochure, 23% of parents wanted more information. Prior to the brochure, 68% of parents knew the test involved radiation compared to 100% afterwards ($p < .0001$). Parents improved their understanding of the relative amount of radiation compared to background from 25% before to 79% after the brochure ($p < .0001$). Overall, 99% rated the brochure > 2 on a 3-point scale with 92% rating the brochure 3 ($p < .0001$). Written feedback was uniformly excellent.

Conclusions: Improving HL for parents is part of the mission of radiology medical professionals. Our study demonstrates that there is room for improvement in communicating with parents about fluoroscopy. Straightforward information for parents provided as a brochure improves their understanding of radiologic fluoroscopic procedures.

Paper #: PA-110

Compendium of Resources for Radiation Safety in Medical Imaging

Anum Minhas, Duke University, anum.minhas@duke.edu;
Donald Frush

Purpose or Case Report: Diagnostic imaging, including ionizing radiation modalities, maintains a foremost role in evaluation of medical disorders. There is increasing awareness and need for information across varied sectors about low level radiation and potential risks. Many medical/scientific organizations have resources discussing radiation risk and management. However, there is no one resource compiling the same available information.

Methods & Materials: Websites, including those of national and international medical organizations (e.g., ACR, “Image Gently” Alliance, IAEA) were reviewed for information on radiation dose, risk, justification, optimization, guidelines (which included general information about improvement in quality and dose reduction without specific mention of optimization techniques), appropriateness criteria, and general principles of radiation safety for radiography, fluoroscopy/angiography, and CT. This information was divided by modalities and separated into adult and pediatric populations. Information from organizations that were not arbitrarily considered to be national (e.g., subspecialty society, regional organization, individual institution/practice) was not reviewed. The resources were then organized into 8 tables, organized by modality. Websites with training modules were noted as well.

Results: 29 websites were explored. Overall, less information is available about medical radiation safety in children compared to adults. Across both, most information is available on CT, then fluoroscopy, and finally radiography. Across all groups and modalities, there is no information available for patients/parents on optimization, appropriateness, or guidelines, with the exception of adult radiography where there were some guidelines.

Conclusions: This compendium on medical imaging radiation serves as a collective resource for communities including the public and regulatory organizations. Additionally, the compendium can be used to determine redundant or

deficient areas, providing opportunities for more comprehensive and efficient efforts in medical radiation protection for patients.

Paper #: PA-111

Inappropriate and Cloned Histories in Children: How Big a Problem is It?

Leann Linam, MD, Radiology, UAMS/ACH, llinam@uams.edu; Chetan C. Shah, S Bruce Greenberg

Purpose or Case Report: ACR standards require appropriate clinical history for obtaining imaging examinations. Cloning clinical histories is a federal violation. Our purpose is to determine the frequency of inappropriate histories (IH) and/or cloning histories (CH) at a tertiary children’s hospital.

Methods & Materials: Three pediatric MOC radiologists reviewed clinical histories for radiographs obtained at a tertiary children’s hospital on 3 randomly selected dates (2 weekdays and 1 weekend day) for appropriateness and cloning. Appropriate histories have associated ICD-9 codes. Cloning is defined by identical clinical histories occurring on 3 consecutive days and could be clinically appropriate or inappropriate. Only the first patient radiograph on a day was included. χ^2 testing was performed to determine significant differences.

Results: 14% (54/388) of exams had IH. IH were significantly more common in inpatients than outpatients ($p < 0.0001$). NICU examinations accounted for 52% of all IH and were significantly more frequent than other inpatient locations ($p = .006$). The CVICU examinations accounted for 11% of all IH and was the second most common patient location for IH, but not significantly different from other inpatient locations ($p = 0.09$). The increased frequency in IH on the weekend reflects a change in patient mix with fewer outpatient examinations performed than on weekdays and was not significant ($p = 0.07$). The most common IH included: evaluate ETT or evaluate lungs (15 each). Cloning only occurs in inpatients and was combined with IH in 48% of patients with CH. The NICU accounted 63% of CH which was significantly greater than other inpatient locations ($p = 0.026$).

Conclusions: 1 in 7 radiographs had IH which can lead to misdiagnoses or nonpayment by insurance companies. Inpatients, especially the NICU were the most common patient locations. Cloning was also a common problem and was frequently combined with IH. Identifying the extent of IH allows for corrective educational measures to be instituted which should improve compliance with existing medical and legal standards for ordering radiographs.

Paper #: PA-112**In Vivo Validation of Size-Specific Dose Estimates (SSDE) Through Breast Entrance Skin Dosimetry (ESD) During Pediatric Chest CT Angiography**

Sjirk Westra, MD, Radiology, Massachusetts General Hospital, swestra@partners.org; Xinhua Li, Mannudeep Kalra, Bob Liu, Suhny Abbara

Purpose or Case Report: SSDE is a new CT dose measure that corrects scanner console CT Dose Index (CTDI) for cross-sectional body diameter, being a better estimate of absorbed dose in individual patients of varying body size. SSDE has been developed through phantom studies and computer simulations of CT dose, but has not yet been validated in vivo. The purpose of our study was to determine correlation between SSDE and measured breast entrance skin dose (ESD) for pediatric chest CTA across a variety of scanning techniques, scanner models and patient sizes.

Methods & Materials: Our study was IRB-approved, with waiver of written informed consent. During 42 consecutive chest CTA exams done on 4 different scanners over a period of 7 years, we measured mid-sternal ESD as an approximation of breast dose with skin dosimeters, which was also expressed as mammogram equivalents. For each scan, we recorded patient age, weight, effective mA, kVp, console CTDIvol-32 cm and DLP-32 cm (from which we calculated age-adjusted effective dose (ED)). We measured effective chest diameter \emptyset to convert CTDI to SSDE, and we correlated SSDE with measured breast ESD, using linear regression. We evaluated image quality with regard to answering the clinical question.

Results: Patient age was $8.4 \pm 6.1/7.9$ [0.02–19.5] yr (mean \pm SD/median [range]), weight $35 \pm 27/26$ [3.5–115] kg, \emptyset $20 \pm 7/19$ [10–35] cm. ED was $2.9 \pm 2.8/2.2$ [0.1–14.4] mSv. We observed an excellent linear correlation between SSDE ($11 \pm 11/7$ [0.5–40] mGy) and breast ESD ($12 \pm 11/7$ [0.3–44] mGy), with an R-square of 0.98 ($P < 0.005$, Graph). Measured and calculated dose values decreased significantly ($p < 0.05$) during the course of our study (Table), due to systematic introduction of automatic exposure control, low kV and high pitch scanning techniques. All studies were of diagnostic image quality to address the clinical question.

Conclusions: SSDE is a valid measure of CT dose in pediatric patients undergoing chest CTA over a wide range of scanner platforms, techniques, and patient sizes, and may be used to model breast and other organ dose, and to document results of dose reduction strategies over time.

Paper #: PA-113**Automated System for Slice-by-Slice CT Image Quality And Radiation Dose Monitoring and Optimization Based on Patient Size**

David Larson, MD, MBA, Radiology, Cincinnati Children's Hospital Medical Center, david.larson@cchmc.org; Remo Malarik, Seth Hall, Daniel J. Podberesky, Alexander J. Towbin, Marilyn J. Goske

Purpose or Case Report: The purpose of this project was to create an automated system capable of quantifying slice-by-slice CT image quality and radiation dose data based on patient size. The information generated from this system should enable size-specific optimization of CT scan parameters in order to obtain images of diagnostic quality at the lowest possible radiation doses.

Methods & Materials: A mathematical model was developed to predict CT image noise based on kVp, effective mAs, and water-equivalent diameter of the patient. A conical water phantom was used to calibrate the model on multiple scanners and accounting for different operational modes and scan parameters, including tube voltage (kVp), tube current (effective mAs), bowtie filter, and focal spot size. A software application was created to process image data from the scout topogram and incorporate DICOM metadata from the axial images. A database and data viewing application were developed to display individual and aggregate study data. All of these systems were integrated and automated to enable real-time monitoring of image quality and radiation dose as a function of patient size.

Results: Since the completion of the automated system, 565 CT exams have been processed. A search application allows the user to find an individual study or a collection of studies based on parameters such as body part imaged or study protocol. The viewing application displays slice-by-slice patient diameter, radiation dose, and image quality for each study. Radiation dose estimates are adjusted for patient size, yielding size-specific dose estimates. The application also graphs individual study data compared to those of comparative studies that are included in the search.

Conclusions: We have successfully developed an automated system that monitors CT image quality and radiation dose data based on patient size. The system enables simultaneous real-time monitoring of all studies performed on all CT scanners at our institution. Specifically, the system enables size-specific radiation dose estimates at every scan level. This system will be used to guide protocol adjustments in order to optimize CT image quality and thus optimize radiation dose.

Disclosure: Dr. Larson has disclosed that he has a patent application in process through CCHMC for CT radiation dose reduction.

Paper #: PA-114

Body Width Predicted from Age and Weight is Not the Best Choice for Generating Protocols for Pediatric Abdominal CT Scans

Marilyn Goske, MD, *Cincinnati Children's Hospital Medical Center, marilyn.goske@cchmc.org*; Laura Coombs, Keith Strauss, Kassa Darge, Donald Frush, Sjirk Westra

Purpose or Case Report: At many institutions, CT scan parameters for children are determined by patient age or weight. AAPM Task Group 204 recommends cross sectional body dimension, such as patient width to determine Size Specific Dose Estimates. The purpose of our study was to develop prediction models of body width based on patient age and weight and compare these models with actual measured body widths for children undergoing body CT.

Methods & Materials: 6 children's hospitals participated in a 3-month retrospective review of abdominal CT scans on patients <18 years of age after local IRB approval. Recorded values included patient width(cm) from an axial image at the level of the splenic vein, patient age (yrs) and patient weight (lbs). A regression model for predicting patient width as a function of age and weight was determined.

Results: 939 exams, 472 had all 3 measurements. Both age and weight were significant predictors of patient width ($p < .0001$). There was also a significant interaction between weight and age ($p < .0001$), indicating that the relationship between patient width and weight depended on the age of the patient. The R² for the regression model for predicting patient width from age and weight individually were 0.65 and 0.83 respectively. The R² for the model including both age and weight and their interaction was 0.86 leaving 14% of the variation unexplained. The regression equation for this model is: Patient width = $14.1 + 0.34 \times \text{Age (yrs)} + 0.12 \times \text{Weight (lbs)} - 0.003 \times \text{Age} \times \text{Weight}$. Despite the R² of 0.86 for the model using both age and weight, the average error (RMSE) for predicting patient width compared to a direct measurement of width was 1.9 cm. The plot of observed minus predicted values (residuals) versus predicted values indicates that the best model (combination of weight and age) results in measurable errors of predicted patient width relative to direct measurement.

Conclusions: A combination of both patient age and weight results in a more accurate patient width prediction than using age or weight alone. While age and weight can be used to

predict body width, this is not sufficiently accurate for generating CT protocols. Therefore, direct measurement of body width from either physical measurement on the patient or from the scout view or an axial image is preferred to select appropriate scan parameters for pediatric abdominal CT.

Paper #: PA-115

Automated Size-Adjusted Dose Monitoring for Pediatric CT Dosimetry

Olav Christianson, *Clinical Imaging Physics Group, olav.christianson@duke.edu*; Ehsan Samei, Donald Frush

Purpose or Case Report: The potential health risks associated with low levels of ionizing radiation have created a movement in the radiology community to minimize radiation dose during CT imaging; this is especially important for pediatric patients due to their increased sensitivity to radiation. It is thus essential to accurately assess the risks to pediatric patients undergoing CT imaging. Current efforts to monitor radiation dose, however, are limited because they do not account for differences in risk from ionizing radiation due to variability in patient size, age, and gender. In this context, we developed an automated size-adjusted dose monitoring program capable of performing patient-specific risk estimation to facilitate protocol optimization.

Methods & Materials: DICOM routing software was used to send dose reports and scout images to an image repository on a dosimetry server. Optical character recognition was used to extract dose-relevant data from dose reports; patient size was determined from corresponding scout images. Based on anatomical location, risk estimation conversion coefficients (q-factors) were determined for each series in the dose reports. The q-factors were adjusted according to patient size, age, and gender and then multiplied by the DLP to estimate the risk to each patient. This process was applied to the cohort of pediatric patients undergoing CT examination at our institution. To evaluate the impact of including patient size, age, and gender, risk estimates were obtained excluding and including the dependencies on size, age, and gender. The results were computed in units of cancer incidence per 1000 cases exposed (cpt).

Results: The average patient-generic risk estimate for a pilot group of patients undergoing body CT was 0.15 ± 0.14 cpt. By including patient size, the risk estimate was increased to $0.26 \text{ cpt} \pm 0.27$ cpt. By including patient age and gender, the average risk estimate was further increased to $1.0 \text{ cpt} \pm 0.72$ cpt.

Conclusions: We developed a new size-adjusted dose monitoring program for pediatric CT dosimetry. Comparisons between patient-generic and our new patient-specific risk

estimates show that failure to consider patient size, age, and gender resulted in risk estimates that were too low by a factor of seven. Additionally, the increase in standard deviation we observed demonstrates that our method of including patient size, age, and gender is sensitive to the inherent variability in the patient population.

Disclosure: Dr. Christianson has indicated that he will discuss or describe, in the educational content, a use of a medical device or pharmaceutical that is classified by the Food and Drug Administration (FDA) as investigational for intended use.

Paper #: PA-116

Is There an Increase in Respiratory Morbidity During the Time Prior to Elective Resection of Prenatally Diagnosed Lung Masses?

Behroze Vachha, *Advanced Fetal Care Center, Depts of Radiology and Newborn Medicine, Children's Hospital Boston, Bvachha@bidmc.harvard.edu*; Richard B. Parad, Judy A. Estroff

Purpose or Case Report: Treatment of prenatally diagnosed lung masses is controversial, with many specialists recommending elective surgical removal in the first year of life because of a reported or perceived increased risk of infection and malignancy, while other centers recommend a conservative approach to management. The natural history of unresected lung masses is not clear. In our center, our standard recommendation is prophylactic resection of asymptomatic lesions, although not all families choose this option. We asked whether respiratory morbidity increased during the time prior to elective resection of prenatally diagnosed lung masses.

Methods & Materials: Ninety-eight pregnant women carrying fetuses with chest masses were imaged by ultrasound (US) and magnetic resonance imaging (MRI). Medical records of the liveborn infants were retrospectively reviewed.

Results: Fetal diagnosis of a lung mass was made at a mean of 27 weeks gestation (range 17–32 wks). Intrauterine fetal demise was documented in 4 pregnancies. There was one elective termination of pregnancy. Three infants were lost to follow up. Thus, outcomes were available for 90 children (59% M, 41% F) with prenatally diagnosed lung masses. Significant respiratory morbidity (RM) was defined as the occurrence of pneumonia, asthma, chronic coughing or wheezing, or respiratory symptoms severe enough to require an Emergency Room visit or hospitalization. Of the 76 children who had surgical removal of their lung mass, 34 (45%) had RM prior to surgery. Fifteen out of 90 children did not have surgery but have been followed expectantly, and 3 of 14 (21%) developed some form of RM. Fifteen of 76 (20%) infants had immediate and significant RM (tachypnea, grunting, increased work of breathing, increased oxygen requirements or need for intubation) in the newborn period

leading to urgent surgery (range of age at surgery: 1–10 d; mean 2.5 d). Of the 61 initially asymptomatic infants, 17 (28%) developed RM prior to elective removal of the mass (range 6–96 weeks, mean 17 weeks). Of the lesions removed, histology revealed: cystic adenomatoid malformation (CCAM) 59%, CCAM+sequestration 21%, Sequestration 8%, congenital lobar emphysema (CLE) 7%, CCAM+CLE 1%, other 3%.

Conclusions: The risk of respiratory morbidity appears to be increased during the time prior to elective resection of prenatally diagnosed lung masses, which may be important for parents and pediatric specialists to consider when deciding whether to remove an initially asymptomatic lung mass.

Paper #: PA-117

Clinical Utility and Impact of Fetal MRI: The McGill Experience

Lucia Carpineta, MD, CM, *Medical Imaging, McGill University Health Center, luciacarpineta@gmail.com*

Purpose or Case Report: It is now accepted that fetal MRI with its superior tissue resolution can be very helpful in clarifying anomalies detected during obstetrical ultrasound. This is particularly the case with intracranial abnormalities, although indications are expanding. The current English medical literature, though, appears to be focused on evolving MRI techniques and how MRI compares to ultrasound with regards to image quality and detection of additional findings which may alter the diagnosis. However, we found no study specifically evaluating the clinical relevance and impact of the information obtained by fetal MRI to the specialists who counsel and treat these patients.

Methods & Materials: A "Satisfaction and Clinical Impact" survey was created and sent to all the members of our Fetal Diagnosis and Treatment Group, asking specifically how the clinicians rated their satisfaction with this type of imaging, its influence on their counseling and on various clinical decisions, both prenatal and postnatal.

Results: We received responses from 37 specialists in 10 different clinical disciplines. The greatest number of respondents came from our obstetricians (28%), many of whom perform their own ultrasounds, and from members of our medical geneticists/genetic counselors (27%), although 46% of respondents were from various other clinical disciplines, both medical and surgical. There was a surprisingly high degree of satisfaction overall with the quality of the images and with the type and amount of information provided. Most respondents indicated they felt fetal MRI was "moderately" or "extremely" useful for their particular clinical decisions, and most respondents agreed that fetal MRI impacted "moderately" or "significantly" on counseling

and management of these pregnancies. Impact appeared greatest on the counseling of the parents and their decision to terminate/pursue the pregnancy, and the least impact was on issues around delivery.

Conclusions: Fetal MRI, in addition to providing images of better quality, particularly in certain conditions, has clinical value in that it directly impacts on the counseling of parents and on clinical decisions.

Paper #: PA-118

Localizing Fetal Bowel Obstruction: The Role of Fetal MRI

Shilpa Chetty, MD, *Stanford University, Department of Obstetrics and Gynecology*; Mary E. Norton, Shreyas Vasanaawala, Richard A. Barth, Erika Rubesova

Purpose or Case Report: Despite increased utilization of fetal MRI to assess and describe bowel abnormalities, there are limited data demonstrating that fetal MRI can localize bowel obstruction. The purpose of our study is to evaluate the accuracy of MRI for localization of fetal bowel obstruction and to correlate the results with postnatal findings.

Methods & Materials: Our ultrasound database was queried to identify cases of bowel dilation diagnosed during the period of 2006–2011. Ultrasound reports were reviewed to determine sonographic diagnoses. Selected patients from this cohort underwent MRI using GE 1.5 Tesla magnet without contrast (Sequences included SSFSE, FIESTA, FGRE or dual echo in 3 planes). The images were reviewed and multiple characteristics were assessed for specifying the area of obstruction. The features included: presence of normal fluid-filled bowel, small rectum for gestational age, signal of meconium in the rectum, and meconium filled dilated bowel.

Results: 46 cases of sonographically suspected bowel obstruction were identified during the study period; 27 of these underwent fetal MRI. Of these 27 cases, 4 had normal MRI and postnatal outcomes, 2 cases did not have postnatal findings available, and 2 had postnatal meconium peritonitis but no obstruction. One case of congenital chloride diarrhea was diagnosed by fetal MRI. A variety of bowel abnormalities were observed amongst the remaining 18 cases. Proximal obstruction was diagnosed in 8 cases: jejunal atresia ($n=7$) and multiple atresia ($n=1$). Distal obstruction was diagnosed in 10 cases: ileal atresia ($n=3$), meconium plugging ($n=4$), closed gastroschisis ($n=1$), enteral duplication cyst ($n=1$), and imperforate anus ($n=1$). Characteristic patterns of features were identified amongst these 18 cases that specified the location of obstruction. These patterns of findings allowed accurate localization of the level of obstruction in all cases when compared to

postnatal findings. Distal obstruction was characterized by normal fluid-filled small bowel and high T1 signal in distended loops. Jejunal atresia was characterized by multiple loops of dilated bowel with high T2 signal primarily in the left upper quadrant. Small rectum for gestational age was not consistently associated with proximal or distal atresia.

Conclusions: Evaluation of fetal MRI with attention to specific features allows localization of bowel obstruction. This may aid in counseling and postnatal management, including the need and type of postnatal imaging study.

Paper #: PA-119

Spectrum of Imaging Appearances of Neonates and Survivors of Portal Vein Thrombosis: Correlation with Clinical Findings and Outcome

Monica Epelman, MD, *CHOP*, monica_epelman@hotmail.com; Alan Daneman, Iris Morag, Prakesh S. Shah, Aideen M. Moore

Purpose or Case Report: Portal vein thrombosis (PVT) is considered a major cause of childhood portal hypertension (PH). The diagnosis of neonatal PVT is frequently an incidental finding on US, as clinical symptoms are minimal. Early diagnosis and treatment of PH may prevent clinical deterioration. PVT may produce a spectrum of imaging appearances, which has not been fully recorded in the literature. The goal of this paper is to review the spectrum of imaging appearances of neonates and survivors of neonatal PVT with special emphasis on the role of US and to correlate these findings with the clinical findings including outcome.

Methods & Materials: A retrospective review of 133 consecutive neonates admitted between 1999–2003 and diagnosed with PVT was conducted. Diagnosis was established by US at a mean age of 9 days (range: 1–40). Health records, initial and follow-up (f/u) imaging were reviewed. Findings were classified as non occlusive, single branch, PVT (grade 1); occlusive PVT (grade 2) and PVT with extensive parenchymal ischemia (grade 3).

Results: PVT was diagnosed in 133 patients, 70 of whom were followed up to for 2 years or longer. Twelve patients were excluded due to liver disease, 22 expired and 29 were lost to f/u. Of the 70 in whom f/u was available, at the time of initial diagnosis, grade 1 PVT was present in 27, all were on the left. Grade 2 PVT was diagnosed in 28 and grade 3 PVT in 15. On f/u physical exam, findings were unremarkable in 68/70 patients. Liver function tests (LFT) and thrombophilia assessment were available in 25 children, mild LFT abnormalities were noted in 9 and 6 children had evidence of thrombophilia. US exams were available in 37/70 children. Among the 37 survivors of neonatal PVT, US was regarded

as normal in only 14 children; 16 showed left lobar atrophy (LLA), 5 had slowly progressive splenomegaly without other signs of PH, and 2 developed clinically significant PH requiring shunting.

Conclusions: PVT has a wide spectrum of imaging appearances, it is possibly underdiagnosed and clinically unsuspected. Varying degrees of LLA are likely a sequela of clinically silent left PVT. US is a sensitive method for the detection of disease and assessment of progression.

Paper #: PA-120

Fetal MRI in Arthrogryposis

Hedieh Eslamy, MD, Radiology, Lucile Packard Children's Hospital, hkeslamy@gmail.com; Erika Rubesova, Louanne Hudgins, Britton Rink, Richard A. Barth

Purpose or Case Report: To present the fetal MRI findings in fetuses with a prenatal diagnosis of arthrogryposis and correlate with postnatal outcome or autopsy results. Arthrogryposis refers to contractures involving more than one joint which often represent deformational changes secondary to decreased or absent fetal movement. Prognosis varies widely dependent on diagnosis, ranging from isolated contractures in amyoplasia to lethality in some cases. We hypothesized that fetal MRI may demonstrate central nervous system (CNS) pathology and muscle abnormalities which are important for predicting postnatal outcome.

Methods & Materials: We identified 6 fetuses with a diagnosis of arthrogryposis between January 2010 and October 2011. All had fetal MRI which was performed on a GE 1.5 Tesla magnet, with SSFSE, FIESTA and FGRE sequences in 3 planes. The fetal MRI's were evaluated for CNS and muscle abnormalities. The extremities were evaluated for: muscle mass, increase in subcutaneous fat (indicative of muscle atrophy), and extremity joint positioning. These findings were subsequently correlated with the clinical exam of the neonates, pathology in the abortus and karyotype when available.

Results: Results of fetal US, amniocentesis, fetal MRI and post-natal or post-termination outcomes will be summarized. Five fetuses had ≥ 2 limb joint contractures. A sixth case had neck hyperextension and lateral flexion associated with akinesia and hydrops. On MRI, no structural brain or spine abnormalities were identified. The abnormalities detected in the extremities were: severe decrease in muscle mass associated with increased subcutaneous fat (3 cases); normal muscle mass (2 cases); moderate decreased muscle mass associated with increased subcutaneous fat (1 case). In the 3 cases that delivered, the diagnoses were amyoplasia (2) and distal arthrogryposis (1). In a fourth case that underwent elective termination, autopsy was consistent with amyoplasia. Two cases are pending delivery.

Conclusions: While fetal MRI can be useful to rule out CNS anomalies, it may also provide important information on decreased muscle mass as an important prognostic sign in a fetus with arthrogryposis. In our series, severely decreased muscle mass was predictive of amyoplasia, and joint contractures limited to hands and feet with preserved proximal muscle mass was predictive of distal arthrogryposis. Both diagnoses are associated with relatively good prognosis and usually normal intelligence.

Paper #: PA-121

Pediatric CT Radiation Dose Reduction: How Does Iterative Reconstruction Technique Affect Image Quality Metrics in Child-Sized Anthropomorphic Phantoms and Patient Images When kV is Reduced?

David Pettersson, Radiology, Oregon Health and Science University; Katharine Hopkins, Donna M. Stevens, Amar C. Dhanantwari, Jeff Yanof, Dianna M. Bardo

Purpose or Case Report: The purpose of this study is to assess the effects of iterative reconstruction technique (IRT) on image quality metrics measured in child-sized anthropomorphic phantoms as kVp is changed.

Methods & Materials: CT scans were performed on anthropomorphic phantoms with sizes of 1, 5 & 10 years (ATOM Phantoms, CIRS, Norfolk Virginia) using low dose pediatric chest protocols (1.6, 3 & 6 mSv) to determine baseline noise and dose levels. Subsequently three voltage levels (120, 100 & 80 kVp) were used while adjusting mAs to maintain baseline CT DIvol and without mAs adjustment which allowed varied CT DIvol. Images were reconstructed using 100% filtered back projection (FBP) and blends FBP:IR (80:20, 60:40, & 40:60). Parameters including CT DIvol, dose length product, scan length, kVp, and mAs, were recorded for each scan. Image noise, contrast:noise (CNR), and signal:noise (SNR) data were recorded from ROIs in phantoms and dilute iodine contrast filled syringes (5, 3, 1.5%).

Results: As kV is lowered from 120 to 80, image noise is doubled if mAs is not increased to maintain CT DIvol, and CNR is increased but SNR is decreased due to the increased image noise. As kVp is lowered from 120 to 80, image noise is increased nominally (8–21%) if mAs is increased to maintain CT DIvol; therefore the increase in CNR and decrease in SNR is negligible. CT DIvol is reduced >300% in all phantom scans as kV is reduced from 120 to 80. IRT reduces image noise by up to 36% [range 10–41%] in all phantom sizes and in clinical images. As CT DIvol is maintained in patient scans, image noise, CNR, and SNR are reduced in patients ($p < 0.05$), resulting in improved image quality.

Conclusions: When lowering kVp, compensation with increases in mAs is necessary to maintain CT DIvol.

However, lower target CTDI_{vol} can be achieved when adding IRT as image noise can be decreased. For these phantoms, CNR and SNR improved using all [selected] levels of IR, even when kV was reduced, resulting in lower CTDI_{vol} in phantoms. At all kVp settings when IRT is applied, image noise is reduced, resulting in improved CNR and SNR for all phantoms.

Disclosure: Dr. Bardo has indicated she is in the speaker's bureau and receives an honorarium from Koninklijke Philips.

Paper #: PA-122

Adaptive Iterative Dose Reduction in Evaluation of the Pediatric Abdomen with Ultra-Helical 320-Channel MDCT

Jeffrey Hellinger, MD, Stony Brook University, *jeffrey.hellinger@yahoo.com*; Bernice Hoppel, Richard Mather, Monica Epelman

Purpose or Case Report: Radiation reduction is paramount for pediatric patients. Ultra-helical 320-channel MDCT allows for rapid acquisitions at low dose. We evaluated the ability of a new adaptive iterative dose reduction algorithm (AIDR) to reduce noise in low-dose ultra-helical pediatric abdominal CT scans. AIDR is an iterative algorithm that adaptively reduces noise in the raw and image domains while preserving image structure.

Methods & Materials: The raw data from 14 consecutive low-dose pediatric abdomen exams was gathered. A dose simulation tool which adds noise to raw projection data was employed to simulate tube current at 1/4 of baseline mA. Data were reconstructed with both standard filtered back projection and with AIDR. Regions of interest were drawn in the liver and lumbar musculature to determine the signal-to-noise (SNR), contrast-to-noise (CNR) and overall diagnostic quality of each data set. Statistical significance was determined using a Student's t-test. Subjective image quality was evaluated by two reader blind review using a five point scale (5=excellent, 1=unacceptable).

Results: The SNR and CNR were significantly lower for the 75% dose reduction datasets compared to the original filtered back projection reconstructions (SNR: 3.59 vs 2.20, $p < 0.001$; CNR: 1.24 vs 0.75, $p = 0.01$). When AIDR was applied to the 75% dose reduction data, the SNR and CNR improved to be superior to the native case (SNR: 3.59 vs 5.48, $p < 0.001$; CNR: 1.24 vs 1.95, $p = 0.02$). The average image quality score for the low dose datasets with AIDR was 4.2 compared to 3.4 with standard filtered back projection at the baseline mA

Conclusions: AIDR significantly improves the image quality of pediatric abdominal CT images. With a simulated 75% reduction in dose, AIDR produces images

with significantly greater SNR and CNR. The subjective image quality scores for AIDR showed dramatic improvement over standard filtered back projection. AIDR processing algorithms with ultra-helical 320 MDCT will allow 75% reduction in radiation exposure while achieving the same diagnostic quality as compared to routine pediatric abdomen MDCT radiation protocols with filtered back projection processing algorithms.

Paper #: PA-123

The Use of Adaptive Statistical Iterative Reconstruction (ASIR) in Pediatric Head CT: A Pilot Study

Ashok Panigrahy, MD, Children's Hospital of Pittsburgh, University of Pittsburgh Medical Center, ; Gregory Vorona, Giulio Zuccoli, Thomas Sutcavage, Barbara Clayton, Rafael Ceschin

Purpose or Case Report: To explore incorporating ASIR into pediatric head CT protocols, to reduce patient radiation dose while maintaining image quality.

Methods & Materials: An Alderson RANDO head phantom was estimated to approximate the size of a 7-year-old child's head, and was scanned at decreasing 10% mA intervals (100 to 50%, 150 to 75 mA) relative to this institution's age-based head CT protocols. Each of these studies was then reconstructed at 10% ASIR intervals (0% to 100%), and a 100 mm² ROI was obtained in a consistent location behind the frontal bone to estimate noise (SD). Using this phantom data, our ventriculoperitoneal (VP) shunt follow-up CT protocol was modified, and patients were scanned at 20% ASIR with approximately 20% mA reductions relative to our normal age-based mAs. These ASIR studies were then anonymously compared to older non-ASIR head CT studies from the same patients (with identical kVp/slice thickness) by two blinded attending pediatric neuroradiologists. All studies were evaluated subjectively for diagnostic utility (1–4), sharpness (1–5), noise (1–4), and artifacts (1–4). 50–100 mm² ROIs were drawn in consistent locations to estimate noise in air, bone, CSF, and white matter (WM).

Results: The phantom study suggested similar same noise levels at 100% mA/0% ASIR (3.9) and 80% mA/20% ASIR (3.7). 12 patients (average=9, range=1 to 17 years) were then scanned at approximately 20% mA reductions, with an average of 349 days (range=27 to 871 days) between the ASIR study and prior non-ASIR study. The average CTDI_{vol} and DLP values of the 20% ASIR studies were 22.4 mGy and 338.4 mGy-cm, and for the non-ASIR studies were 28.8 mGy and 444.5 mGy-cm, representing statistically significant decreases in the CTDI_{vol} (22.1%, $p = 0.00007$) and DLP (23.9%, $p = 0.0005$) values. There were no significant differences between the ASIR studies and non-ASIR studies in

respect to diagnostic acceptability ($p=0.33$), sharpness ($p=0.45$), or noise ($p=0.84$). There was a non-significant trend that the ASIR studies had a lower artifact score (1.8 vs 2.1, $p=0.06$). There was good to perfect ($\kappa=0.5$ to 1.0) agreement. The ASIR studies had statistically significant decreased CSF noise (3.0 vs 4.4, $p=0.000008$), but no noise differences were seen in air ($p=0.46$), bone ($p=0.26$), or WM ($p=0.22$).

Conclusions: Our findings suggest that ASIR can provide dose reductions in pediatric head CT without affecting image quality.

Paper #: PA-124

MR Imaging of the Skeletal Muscles in Boys with Duchenne Muscular Dystrophy (DMD): Part 2. T2 Relaxation Time Mapping (T2 Map) as a Non-Invasive Biomarker to Determine Pathologic Fatty Infiltration: Comparison Between Boys with DMD and Healthy Boys
Jennifer Johnston, MD, Radiology, Cincinnati Children's Hospital Medical Center, jhtai@yahoo.com; Hee K. Kim, Arnold C. Merrow, Tal Laor, Suraj Serai, Brenda L. Wong
Purpose or Case Report: To validate the T2 map as a noninvasive quantitative biomarker of fatty infiltration of muscles and to determine whether the T2 map can differentiate between boys with DMD and healthy boys.

Methods & Materials: Two groups of boys with similar ages (range 5–15 years) were evaluated: 42 boys with DMD (mean age 10.4 years) and 29 healthy boys (mean age 11.7 years). MR images were performed at 3 T. Fatty infiltration of the pelvic and thigh muscles on T1-weighted images (WI) was graded from 0 to 4. On T2 maps with and without fat suppression, the muscle with the greatest fatty infiltration on T1-WI was selected, and a region of interest was placed to obtain T2 values. T2 values from T2 maps with fat suppression were subtracted from values of T2 maps without fat suppression and designated as the “T2 fat value.” T2 fat values were obtained from the same muscles in all boys. Comparison was made between the T2 fat values of the two groups. The upper reference limit of the reference interval (RI) of T2 fat values was obtained from the control group to establish the normal range and applied to both groups to determine the accuracy of the T2 map.

Results: The gluteus maximus muscle had the greatest fatty infiltration on T1-WI. Median T2 fat value was 73.0 msec for DMD (95% RI 193.8, range 29.2–175.6) and 7.5 msec for the control group (95% RI 19.2, range 1.4–21.6). When applied to the two groups, the upper reference limit of the RI for control patients yielded 100% sensitivity, 93% specificity, 95% positive predictive value, and 100% negative predictive value.

Conclusions: Utilization of T2 maps for the quantitative measurement of fatty infiltration of muscles can clearly differentiate between DMD and normal control boys with a high degree of accuracy and precision. This advanced non-invasive technique may potentially replace invasive muscle biopsies currently used for diagnosis.

Paper #: PA-125

MR Imaging of the Skeletal Muscles in Boys with Duchenne Muscular Dystrophy (DMD): Part 1. Can Fatty Infiltration and Inflammation of the Gluteus Maximus Muscle be Used as Indicators of Clinical Assessment in Boys with DMD?

Lily Wang, MBBS MPH, Department of Radiology, Cincinnati Children's Hospital Medical Center, lily.wang@cchmc.org; Hee K. Kim, Arnold C. Merrow, Tal Laor, Suraj Serai, Brenda Wong

Purpose or Case Report: Prior work has shown that the gluteus maximus muscle has the greatest T2 relaxation time on MR imaging using T2 mapping in boys with Duchenne muscular dystrophy (DMD). However, an increased T2 value on T2 relaxation time mapping may reflect both fatty infiltration and inflammation of the muscle. Fatty infiltration characteristically follows inflammation in this disease process. Therefore, the purpose of this study was to determine the contribution of each component (fat and inflammation) within gluteus maximus muscles and to correlate each component to clinical assessments.

Methods & Materials: Forty-six boys with DMD (ages: 5–15 years) were recruited. MR imaging of the pelvis using T2 maps with and without fat suppression were performed. The T2 map “fat values” (T2 value calculated from the T2 map without fat suppression [FS] minus T2 map with FS) and the T2 map “inflammation value” (T2 value from the T2 map with FS) were obtained. Clinical assessments typically used to evaluate DMD patients (including clinical functional score, 30 ft run, Gower score, and 4 step-up time) were also performed. Spearman correlation coefficients between fat and inflammation values and the clinical assessments were calculated.

Results: There was a statistically significant correlation between the fat value of the gluteus maximus muscle and each clinical assessment test ($p<0.05$). However, the inflammation value of the gluteus maximus muscle did not correlate with any clinical assessment.

Conclusions: In DMD, the amount of fatty infiltration of the gluteus maximus muscle has excellent correlation with clinical assessment. The amount of inflammation of the gluteus

maximus muscle, however, does not correlate with clinical function. Therefore, further study is needed to determine whether components (fatty infiltration or muscle inflammation) of the single most involved muscle reflect the components of all the muscles of the pelvis and thighs and whether the cumulative muscle involvement of each component represents clinical disease severity.

Paper #: PA-126

Utility of Contrast-Enhanced MR Imaging in Children with Osteonecrosis: Does Gadolinium Help?

Lamya Atweh, MD, Radiology, Texas Children's Hospital, laatweh@texaschildrens.org; Robert C. Orth, Wei Zhang, R. Paul Guillerman, Herman Kan

Purpose or Case Report: At our institution, gadolinium contrast-enhanced MR sequences are often obtained to assess epiphyseal and non-epiphyseal osteonecrosis in children. Several studies have shown that dynamic contrast-enhanced sequences may provide prognostic information about long-term complications and healing of osteonecrosis. To our knowledge, no studies have determined the added value of routine post-contrast MR imaging in assessing acute complications related to chronic osteonecrosis. The purpose of this study was to evaluate the utility of intravenous gadolinium contrast in the MRI identification of complications in children with an established diagnosis of osteonecrosis.

Methods & Materials: 64 patients were retrospectively identified (age range: 1.75 years to 25.75 year; M:F=59:80) with an imaging diagnosis of chronic osteonecrosis who underwent 139 contrast-enhanced MR studies between 1/2000 and 9/2011. The pre- and post-contrast MR images were consensus reviewed by two CAQ pediatric radiologists. Pre- and post-contrast images were reviewed at separate times. The pre-contrast images were available during the review of post contrast images. Studies were assessed for: osteonecrosis location (epiphyseal, non-epiphyseal osteonecrosis, or both), joint effusion, marrow edema, and epiphyseal collapse. 95% confidence interval (CI) and Cohen's kappa coefficient(κ) was calculated to assess observed agreement.

Results: The diagnosis of osteonecrosis without complicating features was made in 49.6% (CI: 41.3–58.0%) (69/139) of pre-contrast studies and 53.2% (CI: 45.0%–61.5%) (74/139) of post-contrast studies. When chronic osteonecrosis with complicating features was identified, pre- and post-contrast images identified joint effusion in 44.9% (57/127) and 51.2% (65/127) ($\kappa=0.686$, $p<0.001$); marrow edema in 50.4% (70/139) and 46.8% (65/139) ($\kappa=0.727$, $p<0.001$);

and epiphyseal collapse in 51.2% (65/127) and 42.5% (54/127) ($\kappa=0.796$, $p<0.001$), respectively. Myositis or muscle strain was incidentally diagnosed in 12.2% (17/139) pre-contrast and 10.1% (14/139) post-contrast ($\kappa=0.674$, $P<0.001$) studies.

Conclusions: The high observed agreement between the pre- and post-contrast MR images shows that the addition of intravenous gadolinium may not be necessary in the majority of children with chronic osteonecrosis.

Paper #: PA-127

Systematic Protocol for Assessment of the Validity of BOLD MRI in a Rabbit Model of Inflammatory Arthritis at 1.5 Tesla

Michael Chan, BHSc, University of Toronto, mw.chan@utoronto.ca; Afsaneh Amirabadi, Anguo Zhong, Antonella Kis, Rahim Moineddin, Andrea S. Doria

Purpose or Case Report: Blood oxygen level-dependent (BOLD) MRI has the potential to identify regions of early hypoxic and vascular joint changes in inflammatory arthritis. At this point, there is no standard protocol for data analysis of BOLD MRI measurements in musculoskeletal disorders. Standardization of the technique is paramount to compare results between studies and assess the validity of this technique in tissues outside the blood–brain barrier. Our objective is to optimize BOLD MRI reading parameters in a rabbit model of inflammatory arthritis by determining the diagnostic accuracy of (1) statistical threshold values ($r>0.01$ vs $r>0.2$), (2) summary measures of BOLD MRI contrast [the mean of the % BOLD signal differences within the region of interest (ROI) (diff_on_off) and the percentage of suprathreshold voxels within the ROI (PT%)], and (3) voxel activation algorithm (positive, negative, and positive_negative).

Methods & Materials: Using BOLD MRI protocols with a carbogen stimulus on a 1.5 T magnet, we imaged injected and contralateral knee joints of 21 juvenile rabbits at baseline, and days 1, 14 and 28 after a unilateral intra-articular injection of carrageenin. Nine non-injected rabbits served as controls. Receiver operating characteristic (ROC) curves were plotted to determine the diagnostic accuracy of the reading parameters. The BOLD measures from [(injected knee—control knees)/control knees] were counted as positive cases, while the BOLD measures from [(contralateral knees—control knees)/control knees] were regarded as negative cases. Areas under the curve (AUCs) were calculated to determine the most accurate parameters.

Results: Using diff_on_off and positive_negative activations as constants, $r>0.01$ was found to be more accurate than $r>0.2$ ($p=0.03$ at day 28). Comparison of diff_on_off

and PT% yielded no statistically significant difference ($p > 0.05$). Finally, positive_negative activations for diff_on_off and negative activations for PT% using $r > 0.01$ were the most diagnostically accurate (AUC=0.78, $p < 0.01$ at day 28, and AUC=0.90, $p < 0.01$).

Conclusions: From the results of this study, the most diagnostically accurate and clinically relevant reading parameters included the use of a more lenient threshold of $r > 0.01$, a diff_on_off measure of BOLD contrast, and a positive_negative voxel activation algorithm. PT% may be used as an ancillary measure of BOLD contrast.

Paper #: PA-128

Quantitative versus Semi-Quantitative MR Imaging of Cartilage in Blood-Induced Arthritic Ankles

Andrea Doria, MD, PhD, *Diagnostic Imaging, The Hospital for Sick Children, andrea.doria@sickkids.ca*; Ningning Zhang, Carina Man, Pamela Hilliard, Ann Marie Stain, Victor Blanchette

Purpose or Case Report: To cross-sectionally compare the ability of a scoring system (semi-quantitative method) with a manual segmentation technique (quantitative method) to evaluate the status of the articular cartilage of growing ankles of children with blood-induced arthritis.

Methods & Materials: 12 boys, 11 with hemophilia (A, $n=9$; B, $n=2$) and 1 with von Willebrand disease, median age 13 (range, 6–17) underwent a high resolution MRI protocol at 1.5 Tesla, x-rays, and physical examination using the Hemophilia Joint Health Score (HJHS) system. Two blinded radiologists scored the MRI examinations for cartilage items (horizontal component: surface erosions, scores 0–2 and vertical component: cartilage degradation, scores 0–4) according to the semi-quantitative method (International Prophylaxis Study Group MRI scale). An experienced operator applied a validated quantitative 3D-MRI method (horizontal components: AC, VC, VCtAB, ThCtAB; vertical component: ThCcAB) to corresponding high resolution MR images of ankles.

Results: Internal correlation of the semi-quantitative method components was substantial ($r=0.72$, $P < 0.0001$, tibia) to high ($r=0.91$, $P < 0.0001$, talus) in any site of investigation, but it was site-specific with the quantitative method, being significant only in the talar trochlea ($r=0.86$, $P < 0.0001$). External correlation of corresponding components of the semi-quantitative and quantitative methods was moderate ($r=0.55$, $P=0.005$) to poor ($r=0.39$, $P=0.05$) for horizontal components, and non-existent for vertical components. Components of the semi-quantitative method highly correlated with lifetime number of previous ankle bleeds ($r=0.74$ – 0.84 , $P < 0.0001$), Pettersson x-ray ($r=0.87$ – 0.94 , $P < 0.0001$), and HJHS scores

($r=0.91$, $P < 0.0001$). This correlation was poor ($r=0.42$, $P=0.04$) to moderate ($r=-0.56$, $P=0.004$) for horizontal components of the quantitative method.

Conclusions: The biologic concepts of the semi-quantitative and quantitative MRI methods are distinct for assessment of ankles. The semi-quantitative method is valid for assessing cartilage changes in cross-sectional studies of blood-induced arthropathy, however the quantitative method is suboptimal or less powerful for this purpose.

Paper #: PA-129

Shoulder MR Arthrography In Skeletally Immature Patients

Nancy Chauvin, MD, *Department of Radiology, The Children's Hospital of Philadelphia, chauvinn@email.chop.edu*; Camilo Jaimes, Victor Ho-Fung, Diego Jaramillo

Purpose or Case Report: There has been a well documented increase in sports participation in children which has led to an increase in sports-related injuries. To date, there are no studies describing the value of shoulder MR arthrography compared with the gold standard, arthroscopy.

Methods & Materials: We retrospectively reviewed 80 MR shoulder arthrograms obtained in pediatric patients between 2004 and 2010 who underwent subsequent shoulder arthroscopy. Interpretation of the images was performed by three pediatric radiologists who were blinded to the arthroscopy findings. Images were evaluated in consensus and independently. Assessment included evaluation of the osseous structures, labral-ligamentous complex, joint space and the rotator cuff interval. The MR results were compared with reported surgical findings. Sensitivity and specificity were calculated.

Results: Nine patients were excluded due to technical reasons. Of the remaining 71 patients, 48 were boys (9.7–18.5 years, mean 15.7 years) and 23 were girls (12.7–19.3 years, mean 15.6 years). At arthroscopy, 53 patients (74%) had injury to the anterior inferior glenoid labrum. MR sensitivity was 92% for depiction of Bankart-type injuries with a specificity of 94%. 37 patients (52%) had Hill Sach lesions and MR had sensitivity of 86% with specificity of 88%. 24 Superior Labrum Anterior Posterior (SLAP) tears (33%) were identified at arthroscopy with MR sensitivity of 67% and specificity of 89%. Overall, MR arthrography had a positive predictive value of 96% for identification of a surgical lesion. Agreement between the observers was high. Interobserver reliability was calculated with an intraclass correlation coefficient (ICC) of 0.638 with a Cronbach's Alpha of 0.841.

Conclusions: MR shoulder arthrography can accurately depict labral and osseous injury and provides pertinent preoperative information.

Paper #: PA-130

A Novel Multi-Channel MR Coil for Improved Pediatric Elbow Coil Imaging

Suraj Serai, PhD, CCHMC, suraj.serai@cchmc.org; Randy Giaquinto, Kathleen Emery, Charles Dumoulin

Purpose or Case Report: Single flex coils or adult size coils are currently used for imaging the pediatric elbow. This frequently results in uncomfortable patient positioning, motion, poor fat suppression, low SNR and there is currently lack of a dedicated pediatric elbow coil in the commercial market. Our goal was to explore the usefulness of a new coil array dedicated for pediatric elbow imaging and to compare quantitative & qualitative imaging findings to commercially available coils.

Methods & Materials: An eight channel elbow coil was designed. The coil frame was designed to be rigid and lightweight. Seven identical loop coils were built into a polycarbonate frame and an eighth coil built into a paddle that fits into the top frame. The coil elements were constructed with heavy copper to provide a high Q-factor and increased SNR. The complete coil including electronics & covering, weighs only 1.4 kg. MR Imaging under IRB approval was performed on a GE 1.5 T scanner using a routine clinical elbow protocol including T1W, PDW, T2W, Fat-Sat, Non-fat-sat, 2D & 3D sequences. Subjects were positioned feet-first with the elbow on the side & were subjectively assessed for comfort level. Images obtained from the new coil & from the current commercial coils were compared for SNR.

Results: Scan positioning was reported to be comfortable. SNR was between 20–25% higher as compared to the routine coils. Fat saturation was uniform, indicating that the magnetic susceptibility of the coil is well-matched to human anatomy. Anatomical detail depiction was subjectively better for anatomic features such as trochlea. Detection & diagnostic confidence of elbow disorders were improved with the new coil & greatly decreased motion artifacts were observed.

Conclusions: The new pediatric elbow coil provided excellent image quality, patient acceptance and clinical performance improvements over existing coils. The open coil design also allows for imaging of the elbow in a partially flexed position or in a cast. The advantages provided by the new coil are expected to include shortened image acquisition times (via parallel imaging) & increased SNR.

Disclosure: Dr. Serai has indicated that he will discuss or describe, in the educational content, a use of a medical device

or pharmaceutical that is classified by the Food and Drug Administration (FDA) as investigational for intended use.

Paper #: PA-131

Incremental Value of Knee Radiography in the Interpretation of Pediatric Knee MRI

Yen-Ying Wu, Texas Children's Hospital, yxwu@texaschildrens.org; Robert C. Orth, Wei Zhang, R. P. Guillerman, Herman Kan

Purpose or Case Report: The ACR Appropriateness Criteria recommendation for the imaging work-up of knee pain is radiography followed by MRI. In many cases, MRI is performed prior to review of radiographs or the referring subspecialist does not feel radiographs add value, particularly when ligamentous injury is suspected. The purpose of this study is to determine if radiography adds incremental value in the interpretation of knee MR studies electively referred by pediatric sports medicine and orthopedic subspecialists.

Methods & Materials: Knee MRI studies referred from pediatric sports medicine physicians or pediatric orthopedic surgeons between 9/2008 and 9/2011 ($N=194$, ages 4–18 years, $M:F=87:107$) with accompanying radiographs were identified. Patients were separated into 3 groups based on MRI findings: normal, ligamentous injury, or osteochondral injury (osteochondral lesions, bone contusions/fracture, and avulsion injury). Knee radiographs were consensus reviewed by two CAQ pediatric radiologists blinded to MRI findings and categorized into the same groups. Radiograph and MRI findings were compared and categorized into 3 groups: neutral if radiograph and MRI findings were the same, misleading if findings were discordant, or helpful if radiographs improved MR interpretation. The latter group was analyzed for impact on MR diagnosis.

Results: For 194 knee radiographs, 166 were normal, 2 showed ligamentous injuries, and 26 showed osteochondral injuries. When radiographs were interpreted as normal ($N=166$), by MR 44% were normal, 33% had ligamentous injury, 10% had osteochondral injury, and 13% had both ligamentous and osteochondral injury. When radiographs were interpreted as ligamentous injury ($N=2$), by MR 50% were normal and 50% had ligamentous injury. When radiographs were interpreted as osteochondral injuries, by MR 8% had ligamentous injury, 38% had osteochondral injury, and 54% had both ligamentous and osteochondral injury. Subset analysis of true positive radiographs ($N=25$) found 56% to be helpful and 44% to be neutral in MR diagnosis. For radiographs considered helpful, 0% resulted in a change in MR diagnosis. In regards to the influence of radiographs on MR interpretation, 37% (72/194) were misleading, 56% (108/194) were neutral, and 7% (14/194) were helpful.

Conclusions: A minority of pediatric knee radiographs aided MR diagnosis, and none resulted in a change in diagnosis. Pediatric knee MRI and interpretation should not be predicated on radiologist review of knee radiographs in this subset of patients.

Paper #: PA-132

Sonographic Evaluation of Pediatric Skeletal Lesions: Is it worthwhile?

Henrietta Rosenberg, MD, Radiology, The Mt. Sinai Medical School, Henrietta.Rosenberg@mountsinai.org; Amish Patel, Neil Lester

Purpose or Case Report: The purpose of this paper is to demonstrate how ultrasound (US) may serve as a readily available, cost-effective, non-invasive, non-ionizing, practical tool for the evaluation of a variety of skeletal abnormalities in the pediatric age range.

Methods & Materials: We reviewed the clinical and imaging findings in 31 patients seen during the past 2 years in whom US demonstrated abnormalities related to the skeletal system, excluding patients with hip joint effusions or DDH.

Results: US proved useful in the following situations: evaluation hard superficial immobile mass (osteoma shin) (1), absent medial end clavicle on X-ray in region of neck mass (US showed ABC medial end clavicle)(1), to determine if soft tissue mass involves adjacent bone nodular fasciitis surrounding clavicular head (1), for diagnosis and follow-up fracture (displaced/non-displaced) in infants (4), diagnosis osteomyelitis in patients with cellulitis (4), question of fracture underlying cephalohematoma or subgaleal hematoma (4), rib mass (osteochondroma) (1) or mass costochondral junctions (contour deformities costochondral cartilage) (6), firm posterior knee mass (Baker's cyst) (1), firm anterior knee mass (septated cystic mass suprapatella region due to rheumatoid disease) (1), immobile hard scalp mass due to epidermoid cranial vault (1), painful mass occipital bone with soft tissue components extending through the skull externally and internally due to Langerhan's histiocytosis (1), indeterminate mass clavicle clinically thought to be post-traumatic sequellae, resolved on follow-up (1), assessment craniosynostosis (3), for differentiation of pathological entity from normal anatomic structure (lump on back of slender baby proved to be normal posterior spinous process) (1).

Conclusions: US is worthwhile for evaluation of wide range of pediatric skeletal abnormalities and helps to determine if the a lesion is one that is "touch" or "don't touch". To maximize diagnostic accuracy, the imager should have thorough knowledge of the clinical history, physical findings, laboratory and other imaging findings. In equivocal cases or in those patients in whom the field of view (FOV) is

insufficient for complete visualization of an obvious lesion or if malignancy is suspected, US serves to triage those patients in whom further imaging is necessary.

Paper #: PA-133

High Incidence of Vertebral Fractures in Children with Acute Lymphoblastic Leukemia 12 Months After the Initiation of Therapy

Mary Ann Matzinger, MD FRCP(C), University of Ottawa, matzinger@cheo.on.ca; Nazih Shenouda, Brian Lentle, Josée Dubois, Helen R. Nadel

Purpose or Case Report: Vertebral fractures due to osteoporosis are a potential complication of childhood acute lymphoblastic leukemia (ALL). To date, the incidence of vertebral fractures during ALL treatment has not been reported

Methods & Materials: We prospectively evaluated 155 children with ALL during the first 12 months of leukemia therapy. Lateral thoracolumbar spine radiographs were obtained at diagnosis and 12 months. Vertebral bodies were assessed for incident vertebral fractures using the Genant semi-quantitative method, and relevant clinical indices such as spine bone mineral density (BMD), back pain and the presence of vertebral fractures at diagnosis were analyzed for association with incident vertebral fractures.

Results: Of the 155 children, 25 (16%, 95% Confidence Interval [CI] 11% to 23%) had a total of 61 incident vertebral fractures, of which 32 (52%) were moderate or severe. Thirteen of the 25 children with incident vertebral fractures (52%) also had fractures at the time of diagnosis. Vertebral fractures at diagnosis increased the odds of an incident fracture at 12 months by an odds ratio of 7.3 (95% CI 2.3 to 23.1, $p=0.001$). In addition, for every 1.0 standard deviation reduction in spine BMD Z-score at diagnosis, there was 1.8-fold increased odds for incident vertebral fracture at 12 months (95% CI 1.2 to 2.7%, $p=0.006$).

Conclusions: Children with ALL have a high incidence of vertebral fractures 12 months after diagnosis, and the presence of vertebral fractures and reductions in spine BMD Z-scores at diagnosis are highly associated clinical features.

Paper #: PA-134

Evaluation of Acetabular Morphology by Volume-Rendered CT: Implications for the Characterization of Femoroacetabular Impingement

Stephen Little, Children's Healthcare of Atlanta, stephen.little@choa.org; Joseph Williams, Tim Schrader

Purpose or Case Report: To provide objective measures of acetabular morphology utilizing volume-rendered CT and to better characterize normal acetabular development in adolescents. Implications for the diagnosis of femoroacetabular impingement (FAI) will be discussed.

Methods & Materials: 146 hips in 73 consecutive patients (36 female, 37 male; ages 13–20 years) who underwent abdominal and pelvic CT for non-hip related complaints were retrospectively examined. Examinations were performed for a variety of complaints, including abdominal pain, nephrolithiasis, vomiting etc. Patients with obvious hip pathology were excluded. Pelvic rotation was eliminated, and pelvic inclination was measured and corrected to 60° utilizing a volume rendered CT model. Measurements of femoral head diameter (FHD), anterior femoral head coverage (FHCA), and posterior femoral head coverage (FHCP) were obtained. Femoral head area (FHA) was defined as $\pi(FHD/2)^2$. Percent anterior femoral head coverage (%FHCA) was defined as $(FHCA/FHA)*100$. Percent posterior femoral head coverage (%FHCP) was defined as $(FHCP/FHA)*100$. Acetabular version by volume-rendered CT (AVVR) was defined as $(FHCP/FHCA)$.

Results: Average pelvic inclination angle (sd) was 70.9 (5.6) for females and 64.8 (6.3) for males. Average (sd) %FHCA was 22.7 (4.9) for males and 18.6 (5.6) for females. Average (sd) AVVR was 2.39 (0.57) for males and 3.42 (1.19) for females. Among males, average AVVR decreased with subject age. On the other hand, there was little change in average AVVR with age among females.

Conclusions: Average AVVR is greater for females than males, and this difference becomes more striking with increasing subject age. This represents an unexpected finding given the reported increased incidence of “pincer” type FAI among females. Characterization of acetabular morphology among adolescents with clinical FAI should consider subject age and gender. In this regard, volume-rendered CT is capable of providing an objective measure of acetabular morphology.

Paper #: PA-135

Mistakes in Musculoskeletal Plain Film Interpretation

James Crowe, *Pediatric Radiology, Texas Children's Hospital, jecrowe@texaschildrens.org*; George S. Bisset

Purpose or Case Report: To evaluate the mistakes made by trained pediatric radiologists when interpreting radiographs of the extremities obtained for the evaluation of outpatient acute pain (mostly post-traumatic).

Methods & Materials: We retrospectively evaluated all radiographs and associated interpretations obtained during a 6 month period from April 15, 2011, to October

15, 2011, of the elbows, wrists, knees and ankles in pediatric outpatients who presented with acute pain in the affected area. All radiographs were previously interpreted by a CAQ-certified pediatric radiologist varying in experience from 1 year to 57 years. 745 abnormalities were identified, including 305 elbows, 168 wrists, 175 knees and 97 ankles. All radiographs were determined to be “as dictated”, missed significant finding, or overcall. Attention was focused on the missed findings and overcalls.

Results: Findings were as follows: elbow radiographs—14 missed findings and 10 overcalls, wrist radiographs—12 missed findings and 5 overcalls, knee radiographs—9 missed findings and 0 overcalls, ankle radiographs—14 missed findings and 10 overcalls. This resulted in a total of 49 missed findings (6.6% of abnormalities) and 25 overcalls (3.4% of abnormalities). Of the 49 misses, 49% were fractures. The highest mistake percentage occurred in the ankles where the combined misses and overcalls approached 25%. This was also the location where we found the highest percentage of missed fractures (9.0%)

Conclusions: When just abnormal cases were considered, fully trained pediatric radiologists have a mistake rate of approximately 9.8%, if misses and overcalls are included. From a quality improvement perspective, we will review all of the types of misses and overcalls to expose common themes.

Paper #: PA-136

Longitudinal Assessment of Osteoporosis in a Blood-Induced Hemophilia Rabbit Model Using Quantitative Ultrasound

Kuan-Chieh Wang, *University of Toronto, kc.wang@utoronto.ca*; Afsaneh Amirabadi, Anguo Zhong, Christopher Tomlinson, Andrea S. Doria

Purpose or Case Report: The reduction of physical activities in hemophilic patients may lead to bone demineralization and consequent osteoporosis. Quantitative Ultrasound (QUS) is free of ionizing-radiation, relatively inexpensive, and easy to use that making this technique suitable for follow-up of hemophilic children with clinical suspicion of osteoporosis. To our knowledge, no previous study has investigated the value of QUS for longitudinal assessment of growing bones in an animal model which is paramount for clinical translation of the technique once change in measurements could relate to either the baseline pathology or physiologic bone growth variability. The objective of this study is to investigate the intra- and inter-operator reliability of QUS over time, and its ability to discriminate bone loss in pathologic vs control knees of a rabbit model of blood induced arthritis.

Methods & Materials: Sixteen juvenile white New Zealand rabbits distributed into two groups: 8 received 8 intra-articular blood injections over 17 weeks ($n=8$ pathologic and 8 contralateral knees), and 8 non-injected rabbits were used as controls ($n=16$ knees). Midshaft tibia speed-of-sound (SOS) was measured at baseline, and weeks 8 and 17 of the experiment. Two operators scanned each site twice at each time point. QUS measurements were compared to microCT (reference standard) on week 17 to validate the study results.

Results: The SOS measured in the control group increased significantly ($P<0.001$) over the 17 week period. There was not such an increase in the arthritis SOS value ($P>0.05$). In both groups the overall intra-operator coefficient of variation of SOS measurements was 6% at baseline and decreased to 2% at week 17 likely due to increased tibia size. The inter-operator reliability was 6% at baseline and 3% at week 17. With regard to the effect of bone growth on QUS measurements for the control group ($n=16$), SOS values increased by 419.13 m/s, whereas for the pathologic group ($n=8$), they only increased by 195 m/s. Statistically significant differences in ratios of SOS between final/baseline results were noted ($P=0.016$) between the pathologic and control groups.

Conclusions: The longitudinal use of QUS has an acceptable intra- and inter-operator reliability. Even accounting for the significant impact that bone growth has on QUS measurements over time, QUS can differentiate pathologic from control knees in the proposed animal model and holds potential for clinical use in the assessment of osteoporosis in hemophilic children.

Paper #: PA-137

Differentiation of Benign and Malignant Pediatric Abdominal Tumors with Diffusion-Weighted MR Imaging

Rakhee Gawande, *Lucile Packard Childrens Hospital, rgawande@stanford.edu*; Gabriel Gonzalez, Shreyas Vasanaawala, Heike Daldrup-Link

Purpose or Case Report: To evaluate if benign and malignant pediatric abdominal tumors can be differentiated based on apparent diffusion coefficient (ADC) values.

Methods & Materials: The study was approved by the institutional review board. 68 pediatric patients with 73 abdominal tumors (34 malignant and 39 benign lesions) underwent diffusion-weighted MR imaging (DWI) on clinical 1.5 T ($n=39$) and 3 T ($n=29$) MRI scanners. ADC maps

were generated from $b=500$ DWI and ADC values were retrospectively and independently measured by two radiologists. ADC values of benign and malignant tumors were compared with the Welch two sample t-test. A p value of 0.05 was considered to indicate statistical significant differences. In addition, a receiver operating curve analysis (ROC) was performed to determine the optimal cut-off ADC value for differentiating benign and malignant tumors.

Results: The mean ADC value (mm²/sec) of benign tumors was 1.681×10^{-3} for the first reader and 1.679×10^{-3} for the second reader. The mean ADC value (mm²/sec) of malignant abdominal tumors was 1.018×10^{-3} for the first reader and 1.113×10^{-3} for the second reader. The differences between benign and malignant tumors were statistically significant ($p<0.001$ for both readers). ROC analysis revealed an optimal cut-off ADC value for differentiating malignant and solid tumors as 1.1×10^{-3} mm²/sec.

Conclusions: Diffusion-weighted imaging with ADC maps can be used to differentiate between benign and malignant pediatric abdominal tumors.

Paper #: PA-138

Creation of a Database to Evaluate Imaging Findings in Long-Term Survivors of Pediatric Malignancy

Alexander Towbin, MD, *Radiology, Cincinnati Children's Hospital Medical Center, alexander.towbin@cchmc.org*; Seth Hall

Purpose or Case Report: Over the past 20 years, there have been significant improvements in the treatment of pediatric malignancies. Improved therapy has led to an increase in the number of long-term survivors. Many of these survivors are now experiencing late effects as a result of the original disease process or its treatment. These late effects are frequently identified on imaging. The purpose of this study is to create a database of the imaging findings of long-term survivors of pediatric malignancy in an attempt to begin to classify the findings and identify associations.

Methods & Materials: After IRB approval, the institutional cancer registry was searched to identify all patients younger than 20 years of age who were diagnosed with a solid tumor between 1980 and 2005. Patients were included in the database if they survived for more than 2 years from the date of their initial diagnosis. The electronic medical record system was then used to obtain demographic and treatment information for each included patient. The dictated reports from all cross-sectional imaging studies evaluating the chest, abdomen, or pelvis performed more than two years from

the date of diagnosis were then reviewed. Each positive imaging finding was classified by the involved organ.

Results: After querying the institutional cancer registry, 909 patients were identified who met the inclusion criteria for this database. The most common neoplasms were neuroblastoma, Wilms tumor, and astrocytoma. Of the included subjects, 420 had imaging of the chest, abdomen, or pelvis. Overall, 2851 reports were evaluated and classified. Findings were most commonly identified in the lungs, musculoskeletal system, kidneys, liver, and lymph nodes.

Conclusions: A database examining the late effects in long-term survivors of pediatric malignancies was created. This database has the potential to help identify the radiologic manifestations of the complications of cancer therapy and thus help guide rationally determined long-term risk-benefit ratios in the treatment of pediatric malignancies.

Paper #: PA-139

Imaging Followup of Lymphoma in Pediatric Patients: Is Pelvic CT Necessary?

Javier Lopez Bueno, MD, *Children's Hospital of Eastern Ontario, jlopezbueno@cheo.on.ca;* Nishard Abdeen

Purpose or Case Report: Pelvic CT is often included in the imaging followup of patient with lymphoma before, during and after treatment to assess response to treatment and monitoring for relapses. While such followup is expected to improve detection of relapse, there is little objective evidence of its effectiveness in lymphoma. Anecdotally, there are few pelvic relapses in pediatric patients with lymphoma regardless of primary site. We hypothesize that pelvic CT could be avoided as part of the followup without adverse impact on survival or in the detection rate of relapses, and with subsequent significant reduction in the radiation dose, particularly to the gonads.

Methods & Materials: Research ethics board approval was obtained. Patients diagnosed with lymphoma and with at least one year of followup at our tertiary care pediatric hospital were included. Sex, age, type of lymphoma, stage, primary site, site of relapse if any as well as the number of CT scans of the head, neck, chest, abdomen and pelvis were recorded.

Results: A total of 29 patients met study criteria. There were 21 males and 8 females, with an average age of 11.9 years (range 3–17 years). Eighteen patients had Hodgkin disease (62%) and eleven had non-Hodgkin lymphoma (38%). Mean length of followup was 3.8 years (range 1–12 years). An average of 4.5 pelvic scans per patient were performed for surveillance (range 0–12). Three relapses were detected. Of these only one was in the pelvis, in a patient whose initial T

cell non-Hodgkin lymphoma was extensive and involved the neck, chest, abdomen and pelvis.

Conclusions: This study suggests a low incidence of pelvic relapse in pediatric patients with lymphoma. The routine use of pelvic CT in surveillance protocols may therefore be of little benefit while imposing a significant radiation burden. Our study is limited by small sample size and short length of followup. Further large scale studies are required.

Paper #: PA-140

Comparison of RECIST 1.1, WHO, and COG Response Criteria in Patients with Ewing Sarcoma

Justin Boe, MD, *Stanford, Radiology, justinj.boe@gmail.com;* Joshua Lee, Rakhee Gawande, Neyssa Marina, Heike Daldrup-Link

Purpose or Case Report: Assessing treatment response of Ewing sarcoma Family of Tumors (ESFT) is performed by measuring the size of the tumors before and after chemotherapy. The proposed method of measuring tumor size, however, differs amongst RECIST 1.1 (Response Evaluation Criteria in Solid Tumors), WHO (World Health Organization) and COG (Children's Oncology Group) response criteria. In our project, we assessed whether response classification differs between the three different methods.

Methods & Materials: After IRB approval, we retrospectively analyzed MRI studies of 55 patients with Ewing Sarcoma who were treated at Stanford and UCSF Medical Centers. Tumor size was assessed before and after therapy. Tumor measurements were obtained using RECIST 1.1 (longest single diameter), WHO (longest diameter and perpendicular diameter), and COG criteria (three measurements to calculate tumor volume). Tumor response was assessed by the differences in sizes of the tumors before and after treatment using four response categories: progressive disease (PD), stable disease (SD), partial response (PR), and complete response (CR). Concordance between the three response classification systems was assessed using Cohen's kappa (k) coefficient and percentage of disagreement per response category.

Results: The k statistic for concordance in COG/WHO, COG/RECIST and RECIST/WHO were 0.663, 0.210 and 0.166 respectively. Disagreement rates for RECIST/WHO, COG/WHO, and COG/RECIST were 12.73, 34.55, and 47.27% respectively. Using tumor volume, twenty-six patients were reclassified: twenty-four cases of Stable Disease coded by RECIST were reclassified as Progressive Disease by COG and two cases of Partial Response coded by RECIST were reclassified as Complete Response by COG.

Conclusions: This study demonstrates poor agreement between the RECIST 1.1 and COG response criteria in ESFT. Given the degree of discordance between response criteria in ESFT, evaluation of the prognostic impact of each of these classification systems may guide selection of the optimal system for future use in this disease.

Paper #: PA-141

Imaging Recognition of Chylous Ascites Following Surgery for Abdominal Neuroblastoma

Zeyad Metwalli, MD, *Baylor College of Medicine, metwalli@bcm.edu;* R. P. Guillerman, Heidi V. Russell, Eugene S. Kim

Purpose or Case Report: Surgical resection is a standard part of multimodality treatment of neuroblastoma, the most common abdominal malignancy of infancy and early childhood. Chylous ascites is a rarely reported complication of surgery for abdominal neuroblastoma, and is likely under-recognized, posing the risk of nutritional deterioration and sepsis. To facilitate early diagnosis and institution of appropriate therapy, we present the salient imaging findings of the largest known series of chylous ascites following surgery for abdominal neuroblastoma.

Methods & Materials: All patients with abdominal neuroblastoma complicated by post-operative chylous ascites over a five-year period at a large children's hospital were identified by a database search. A retrospective review of the imaging studies and clinical charts was conducted.

Results: Chylous ascites developed following surgical resection of abdominal neuroblastoma in 5 of 36 patients, with the diagnosis made between postoperative days 20 and 33. Four cases were high-risk neuroblastoma and one was intermediate-risk neuroblastoma. All 5 cases involved resection of an adrenal mass and dissection around the abdominal great vessels. All 5 cases manifested with abdominal distention on physical exam, and ascites was suspected clinically in 3 cases. Computed tomography (CT) in all 5 cases revealed a large volume of ascites of near-water attenuation (range of -3 to 16.5 Hounsfield units). The 3 cases imaged with ultrasound (US) showed hypoechoic or anechoic ascites without septations. The chylous ascites resolved after 1–4 months of treatment with dietary fat restriction, medium chain triglycerides, intravenous octreotide, or peritoneal catheter drainage.

Conclusions: Chylous ascites is an under-recognized complication of surgical resection for abdominal neuroblastoma, occurring in 14% of patients in this series. The diagnosis is supported by the demonstration on CT or US of a large volume of ascites causing abdominal distention 3–5 weeks post-operatively. The ascites is typically near-water in attenuation rather than fatty in attenuation and should not be

misattributed to peritonitis, hemorrhage, bowel leak, or early tumor recurrence.

Paper #: PA-142

Cervical Spine Injuries In Patients With Suspected Physical Abuse

Nadja Kadom, MD, *Radiology, Children's National Medical Center, nkadom@childrensnational.org;* Zarir P. Khademian, Tanya Hinds, Katherine Deye, Allison M. Jackson, Eglal Shalaby-Rana

Purpose or Case Report: To evaluate the incidence and nature of cervical spine injuries and relationship to posterior fossa abnormalities in children who underwent brain and cervical spine MRI as part of the clinical workup for suspected physical abuse.

Methods & Materials: Authors retrospectively analyzed records of eighty-five children less than three years of age who were documented by the Child Protective Services at a level one pediatric trauma center over a period of four years (2006–2010). Only patients who underwent both MRI imaging of the cervical spines (c-spine) in addition to brain imaging as part of the clinical workup were included. C-spine and posterior fossa of brain MRIs were independently reviewed by two pediatric neuroradiologists, both blinded to clinical details. C-spine abnormalities (bone marrow edema, cord edema, intrathecal blood, disc pathology, soft tissue/ligamentous injury, vascular injury) were documented and correlated with abnormalities seen in the posterior fossa (blood, brainstem edema, cerebellar edema).

Results: At this time, 40/82 patients have been reviewed. Twenty patients (50%) had both cervical spine injuries and posterior fossa abnormalities. There were no patients with isolated cervical spine injuries without posterior fossa abnormalities, but there were five patients (12.5%) that had posterior fossa abnormalities in the absence of c-spine injuries. Fifteen patients (37.5%) did not have any spinal or posterior fossa imaging abnormality. None of the patients had bone marrow edema, disc pathology, or intrathecal blood. One patient had vascular neck injury and cord edema.

Conclusions: Our results show that the incidence of cervical spine injury in children under investigation for abusive head trauma is as high as 50%. Our data show further that cervical spine injury predicted posterior fossa injury in all patients, while presence of posterior fossa injury predicted concomitant c-spine injury in only 75%. The incidence of c-spine trauma we found in these patients is higher than reported elsewhere in the literature and may impact whether or not routine c-spine MRI will be included in national imaging guidelines for children under investigation of abusive head trauma.

Paper #: PA-143**Pediatric Skull Fracture**

Andre Loyd, PhD, *Biomedical Engineering, Duke University, aml6@duke.edu*

Purpose or Case Report: Skull fractures are often seen in the setting of Non accidental trauma (abuse) abuse, and are usually attributed to falls from heights above 1 m. Part of the difficulty in assessing height is due to uncertainties in actual distance. Objective: To determine what types of skull fractures can occur in pediatric and adult post-mortem human specimens during controlled impacts on hard surfaces from various heights.

Methods & Materials: Skull fracture patterns in post-mortem human specimens from a unique bank of pediatric specimens (30-week gestation to 16-years-old, $n=13$) were subjected to controlled drops from both arbitrarily low heights (15 and 30 cm) and high heights (2 m) onto an aluminum platen. The specimens were dissected from the neck at the occipital condyles and intracranial were sealed inside the head using PMMA. The heads were dropped on to five different impact locations. Fractures were identified using palpation and high resolution MDCT.

Results: No specimens between 33-weeks-gestation and 24-days-old sustained fractures from the 15–30 cm drops. Three out of four (75%) specimens ages between 5- and 22-months old fractured due to the 15 or 30 cm drops. The 9- and 16-year-old specimens and all adult specimens survived the 15–30 cm drops. All specimens subjected to the 2 m drop fractured. The specimen between 11-months and 22-months sustained either a linear fractures or diastatic fractures from the 15 cm and 30 cm drops.

Conclusions: The results indicate that some aged infants and young children can sustain skull fractures by being dropped or falling from relatively low heights. Drops, as low as 15 cm, can cause linear and diastatic fractures in pediatric skulls. The presences of compliant sutures and fontanelles in neonatal heads allow the head to deform during impact. These data add very important information to mechanisms of skull fractures across ages, including ages in which child abuse is a consideration.

Paper #: PA-144**Evaluation of a New Classification System for Temporal Bone Fractures in Children Aimed at Increasing Prognostic Value**

Badriya Al-Qassabi, MD, *McGill University, albahlania1@yahoo.com*; Lucia Carpineta, Rania Ywakim, Bahar Torabi, Andrew M. Zakhari, Lily H P. Nguyen

Purpose or Case Report: To compare a new classification of temporal bone fractures which specifically evaluates

involvement of the otic capsule against the traditional classification system (transverse versus oblique versus longitudinal), to evaluate whether this new classification is able to better identify patients at risk of adverse otologic outcome and neurologic complications in the pediatric population.

Methods & Materials: A retrospective hospital chart review was performed by ENT colleagues searching for all patients with temporal bone fractures seen at our center over the past 10 years. This was followed by a blinded review of the CT heads by a resident and a trained pediatric radiologist with neuro expertise. These CTs were evaluated for petrous involvement, otic capsule involvement and any associated intracranial lesions. This information was then correlated with clinical outcome measures including post-traumatic hearing deficit, facial nerve palsy, persisting CSF leak and global neurologic sequelae. The new classification was compared to the traditional one, and specifically analysed for the ability to better predict the clinical outcomes.

Results: Expectedly, pediatric temporal bone fractures were infrequent and otic involvement even more rare. Fractures with involvement of the otic capsule (versus otic sparing) were found more frequently in boys. They were also more likely to be associated with immediate otologic signs and neurologic findings on presentation. These fractures also had the highest association with conductive hearing deficit (>60%) and were twice as likely as otic sparing fractures to be associated with immediate facial nerve palsy and with more important concomitant intracranial injuries such as midline shift.

Conclusions: While our numbers are small, our results suggest a trend that when temporal bone fractures show involvement of the otic capsule, there is higher risk of adverse otologic outcome and neurologic complications even in the pediatric population.

Paper #: PA-145**Absence of a Causal Relationship Between MR Detected Subdural Hematomas (SDH) in Neonates with Hypoxic-Ischemic Encephalopathy (HIE)**

Deniz Altinok, *Children's Hospital of Michigan*; Jay Shah, Harut Haroyan, Gulcin Altinok, Nitin Chouthai

Purpose or Case Report: The existing controversy regarding subdural hemorrhages noted in patients with HIE is an important discussion in the medical, legal and child-welfare realms. It is our goal to provide additional information to this critical debate through MR findings on patients with clinically diagnosed HIE.

Methods & Materials: All patients born with clinically diagnosed HIE, and treated at Children's Hospital of Michigan in the past 8 years were examined; those with Head MRI taken within 19 days of life were selected. In total, 41 patients fit the criteria, this included: 22 Males and 19

Females, and an age range of 2–19 days at scan (average age of 10 days at scan). All traumatic births, coagulopathies, and other pertinent clinical findings were noted. MR Imaging was reviewed and reported by a blinded pediatric neuroradiologist, these reports were then compared to the “original read”.

Results: All 41 patients were confirmed radiologically to have HIE. The causes of HIE in all cases examined were either intrauterine/delivery asphyxia, aspiration, or congenital disease. Of these 41 cases, the findings were: 6 SDH, 11 parenchymal hemorrhages, 4 intraventricular hemorrhages, 4 cephalohematomas, 3 subarachnoids, 1 large subcutaneous hemorrhage and 1 instance of MCA stroke. All 6 patients with MR Detectable SDH had 1 or more confounding factors (1 Meningitis, 3 Coagulopathies, 4 Chest Compressions, 1 Cardiac Malformation, 1 PPH, 1 Severe Pulmonary Hemorrhage requiring Transfusion of Plasma and pRBC).

Conclusions: It has been hypothesized that SDH is often found incidentally in children diagnosed with HIE, this is however a dubious conclusion considering our results. In fact, the presence of SDH and HIE concomitantly is low even when including a population with traumatic births such as ours.

Paper #: PA-146

Sports-Related Concussion in Children: An MRI and MRS Study

Kim Cecil, PhD, *Cincinnati Children's Hospital Medical Center, kim.cecil@cchmc.org*; Todd A. Maugans, James L. Leach, Mekibib Altaye

Purpose or Case Report: The pathophysiology of sports-related concussion (SRC) is poorly understood, especially for children. Following SRC and mild traumatic brain injury in adults, a few MRI and proton MRS studies have identified axonal injury with declines in the neurometabolite N-acetyl aspartate (NAA). We wanted to examine a SRC adolescent population with proton MRS, diffusion tensor imaging (DTI) and other MRI methods within 72 h of concussion and with short term followup to determine if there were differences in imaging metrics with age and sex matched healthy control participants.

Methods & Materials: Twelve children, ages 11–15 years, who experienced SRC were evaluated with ImpACT neurocognitive testing, T1-weighted MRI, susceptibility weighted imaging (SWI), DTI, proton MRS, and phase contrast angiography (PCA) at less than 72 h, 14 days and 30 days or greater post-concussion. Healthy, age and sex matched controls for each SRC participant were recruited and evaluated

at a single time point. Quantitative imaging metrics included fractional anisotropy, metabolite concentrations, and global cerebral blood flow (CBF). Group comparisons were examined by paired t-test or Wilcoxon signed rank test. Correlational data employed Spearman rank correlation.

Results: ImpACT results revealed significant differences in initial total symptom score (TSS), and reaction time (RT) for the SRC group compared with the control group, with TSS resolving by a mean of 14 days and RT at 30 days. No evidence of structural injury was observed qualitatively for either group. Analyses between groups or over time within the SRC group found no decreases in NAA or elevation of lactic acid upon MRS, and no changes in fractional anisotropy upon DTI. Within the SRC group, significant changes in the global CBF were observed. Improvement towards control values occurred by 14 days for 27% and by 30 days for 64% of SRC group participants.

Conclusions: Pediatric SRC affects global CBF without evidence of structural or metabolic injury.

Paper #: PA-147

Predictive Value of High Resolution MR Imaging of Brain and Sella in Children with Clinical Optic Nerve Hypoplasia for Hypopituitarism

Charles Glasier, *Radiology, Arkansas Childrens Hospital, glasiercharlesm@uams.edu*; Raghu H. Ramakrishnaiah, Julie Shelton, Chetan C. Shah, Paul H. Philips

Purpose or Case Report: To review the spectrum of CNS abnormalities and their incidence in children with optic nerve hypoplasia and to calculate the sensitivity and specificity of magnetic resonance imaging in predicting endocrine abnormalities.

Methods & Materials: This is an IRB approved retrospective study of 44 children with clinical optic nerve hypoplasia who underwent MRI of the brain and orbits as part of the clinical workup in a tertiary care pediatric hospital. High resolution MRI studies were performed on 1.5 Tesla scanners. MRI studies were reviewed for optic nerve hypoplasia, absent or ectopic posterior pituitary, absent pituitary infundibulum, absent septum pellucidum, migration anomalies and hemispheric injury. Radiologists were blinded to patients endocrinologic status. All patients had clinical evaluation by a pediatric Neuro-ophtalmologist and endocrinologist. A standardized panel of serologic testing that included serum cortisol, ACTH, TSH, and free T4 levels were performed on all patients. Statistical analysis was performed to determine the sensitivity and specificity of MR findings in predicting endocrinologic deficiency.

Results: Study included 44 children (26 males and 18 Females) who had clinical optic nerve hypoplasia. The mean age of the study population was 3 yr (SD:4.7 Yr). 15 children had unilateral and 29 children had bilateral optic nerve hypoplasia by MRI. 6 children had absent posterior pituitary bright spot and 9 had ectopic posterior pituitary, 7 had absent infundibulum, 1 had complete callosal agenesis, 3 partial callosal agenesis and 16 had callosal thinning. 9 had absent septum pellucidum. 2 had hypopituitarism. Of the 12 patients with Hypopituitarism 8 had abnormal abnormal pituitary on MRI, 3 had absent septum pellucidum, and 1 child had migration abnormality. None had corpus callosal abnormality. The sensitivity and specificity of MRI in predicting Hypopituitarism by demonstration of abnormal pituitary is 75% and 81% respectively. The positive predictive value and the negative predictive value is 60% and 90% respectively. Among the 32 patients with normal endocrinologic function, none had pituitary abnormalities on MRI.

Conclusions: Pituitary abnormalities are the most common intracranial abnormality in patients with optic nerve hypoplasia followed by absent septum pellucidum. Detection of pituitary abnormalities by the MRI has high specificity and high negative predictive value for endocrine abnormality.

Paper #: PA-148

CT Imaging Pearls for Shunted Pediatric Brains

Srikala Narayanan, MD, *Children's National Medical Center, snarayan@childrensnational.org;* Nadja Kadom

Purpose or Case Report: Shunted pediatric patients frequently present emergently with symptoms that could indicate shunt malfunction, such as headache and vomiting. Here, we present imaging pearls on non-contrast head CT in shunted children.

Methods & Materials: Illustration of each of the following: 1. Shunt tip and volume averaging—Consider location of side holes and use of multiplanar reformatted images. 2. Shunt at burr hole—Consider radiolucent shunt parts. 3. Shunt rupture in the neck—Remember to investigate the lower extracranial shunt parts. 4. Shunt in cyst/subdural shunt (vs dislocation)—Consider primary shunt location in a cyst rather than shunt dislocation. 5. Enlarged temporal horns—Look for it. In infants occipital horns may dilate first. 6. Enlarged 3rd ventricle—Look for bulging of lateral walls. 7. Sulcal effacement—Use the “three shades of gray” rule. 8. Small cisterns- Detecting shape distortion can help. 9. Periventricular edema—Easily overlooked because of similar low density compared to ventricular fluid. 10. Slit-ventricle—Requires cautious reporting.

Conclusions: Careful evaluation of CT images in shunted pediatric patients can reveal important clues for making

an accurate diagnosis, even when prior images are not available.

Paper #: PA-149

Successful Treatment of Mice with Creatine Transporter Deficiency

Kim Cecil, PhD, *Cincinnati Children's Hospital Medical Center, kim.cecil@cchmc.org;* Diana M. Lindquist, Matthew R. Skelton, Gail J. Pyne-Geithman, Joseph F. Clark

Purpose or Case Report: Creatine transporter deficiency (CTD) is an untreatable X-linked mental retardation syndrome with severe cognitive and speech impairment. Patients are identified by an absence of creatine in the brain on MR spectroscopy (MRS) and distinguished from two creatine synthesis deficiency syndromes with genetic testing. For CTD, the absence of the transporter (SLC6A8) prevents creatine from crossing the blood brain barrier and entering brain cells. A brain specific CTD knockout mouse was developed replicating key features of the human disease and establishing an animal model for treatment of CTD. We report the successful treatment of the CTD knockout mouse and present confirmation by MRS.

Methods & Materials: Brain specific knockout and littermate control mice were randomly assigned and treated with one of three supplements: AgentX (confidential), creatine or maltodextrin as placebo. 1H and 31P MRS data were collected on a 7 T MR system (Bruker). Mice ($N=16$) were studied with MRS after 9 weeks of supplementation. Single voxel 1H data were acquired on a 144 μ L voxel covering the cerebrum using a double spin echo sequence. 31P data were acquired with an ISIS sequence from the same voxel. Metabolite quantification was performed with jMRUI and compared between groups and over time with statistical tests for significance (t-tests, ANOVA).

Results: Creatine and phosphocreatine levels in the brain were all significantly higher after 9 weeks supplementation of AgentX in knockout mice, compared to creatine and placebo fed knockout mice (Phosphorus MRS [144 μ L brain voxel] with phosphocreatine (PCr) (0 ppm) observed only in AgentX treated knockout mice. Adenosine triphosphate (ATP) gamma (-2.5 ppm), alpha (-7.5 ppm) and beta (-17 ppm) peaks are noted in all three knockouts.

Conclusions: Successful treatment was achieved in a SLC6A8 brain specific knockout mouse for the second largest known cause of X-linked mental retardation in humans, CTD.

Disclosure: Dr. Cecil has indicated that she will discuss or describe, in the educational content, a use of a medical device or pharmaceutical that is classified by the Food and Drug Administration (FDA) as investigational for intended use.

Paper #: PA-150**Prevalence of Abusive Injuries in Siblings and Contacts of Abused Children**

Kenneth Feldman, MD, *General Pediatrics/Children's Protection Program, University of Washington/Seattle Children's, kfeldman@u.washington.edu*

Purpose or Case Report: Siblings and children who share a home with a physically abused child are thought to be at high risk for abuse. However, rates of injury in these children are unknown. Disagreements between medical and CPS professionals are common and screening is highly variable. Our objective was to measure the rates of occult abusive injuries detected in contacts of abused children using a common screening protocol.

Methods & Materials: This was a multi-center, observational cohort study of 20 child abuse teams who shared a common screening protocol. Data were collected for all children <10 years undergoing evaluation for physical abuse and their contacts. For contacts of abused children, the protocol recommended physical examination for all children <5 years, skeletal survey and physical exam for children <24 months, and physical exam, skeletal survey and neuroimaging for children <6 months old.

Results: Among 2,825 children evaluated for abuse, 618 met criteria as "physically abused" and these had 477 contacts. For each screening modality, screening was completed as recommended by the protocol in approximately 75% of cases. Of 133 contacts who met criteria for skeletal survey, new injuries were identified in 16 (12.0%). None of these fractures had associated findings on physical examination. Physical examination identified new injuries in 6.2% of 257 eligible, examined contacts. Neuroimaging failed to identify new injuries among 19 imaged, eligible contacts less than 6 months old. Twins were at significantly increased risk of fracture relative to other non-twin contacts (56.3% vs 11.9%, OR 19.9).

Conclusions: These results support physical examinations and skeletal survey, regardless of physical examination results, for contacts of abused children <24 months of age. Too few children had cranial imaging to change recommendations to image contact children less than 6 months old. Even for children where no injuries are identified, these results demonstrate that abuse is common among children who share a home with an abused child. They support including contacts in evaluations and interventions (foster care, safety planning, social support) designed to protect physically abused children. The project was supported by the Health Resources and Services Administration/Maternal

and Child Health Bureau, Emergency Medical Services for Children Program (H34MC19346-01-02).

Disclosure: Dr. Feldman indicates that he is a medical-legal consultant in child abuse.

Paper #: PA-151**Rib Fractures in Children: A Marker for Intrathoracic Injury?**

Stephen Darling, MD, *Seattle Children's Hospital, sdarling@u.washington.edu*; Stephen Done, Seth D. Friedman, Kenneth Feldman

Purpose or Case Report: Physical abuse of children is a serious health problem. Injuries, including rib fractures, often initiate abuse evaluations. Previous studies have shown that pediatric rib fractures may be a marker for significant intrathoracic injury. This information has been used to suggest that children with rib fractures and no underlying intrathoracic injury may have sustained them due to insufficient bony mineralization and minor trauma rather than inflicted injury.

Methods & Materials: IRB approval was obtained for a retrospective review of all children under 3 years of age with imaging diagnosis of rib fracture over a 6-year period at two University hospitals. Children with prior thoracotomy, previously recognized metabolic bone disease, and prematurity <36 weeks were excluded. Medical records were reviewed and children with documented abuse or accidental trauma were evaluated. Children with indeterminate injury mechanisms were excluded. Sixty-six patients with rib fractures were included in analysis, 47 due to abusive injury and 19 due to accidental trauma. Children were analyzed for associated intrathoracic, abdominal or intracranial injury, additional fractures and retinal hemorrhage.

Results: Abused children were younger (4.7+/-6.1 months) than accidentally injured children (18.9+/-11.1 months, $p < 0.001$). Children with rib fractures due to accidental trauma had a higher incidence of intrathoracic injury compared to those due to abusive injury (53% vs 13%, $p < 0.001$). There was no difference in the incidence of abdominal or intracranial injury between groups. Mortality and ICU admission rates were similar. Abused children had a higher total number of rib fractures (mean 5.5 vs 3.0, $P < 0.009$) and were more likely to sustain additional fractures outside of the thoracic cavity (77% vs 63%, $P < 0.001$).

Conclusions: Abuse is a more common cause of rib fractures in young children than accidents. Children with rib fractures due to abusive trauma are less likely to have

intrathoracic injury compared to those sustaining rib fractures due to accidental trauma. This suggests differences in mechanism of injury between groups.

Paper #: PA-152

Pediatric Elbow Fractures: A Different Angle on an Old Topic

Shannon Zingula, MD, *Pediatric Radiology, Cincinnati Children's Hospital Medical Center*; Kathleen Emery, Christopher G. Anton

Purpose or Case Report: The 3 most common elbow fractures classically reported in pediatric orthopedic texts are supracondylar (SC) (50–70%), lateral condylar (LC) (20%), and medial epicondylar (ME) fractures (10%) with fractures of the proximal radius (including but not limited to fractures of the radial neck) being relatively uncommon (5–10%). Our experience at a large children's hospital suggests a different distribution. Purpose: 1) to describe the frequency of different elbow fracture types in a large pediatric population, and 2) to determine the fracture types that were occult on initial radiographs but detected on follow-up.

Methods & Materials: Review of medical records identified 468 children, median age 6 years and interquartile range for age of 4–8 years (range, 0.8–18 years) diagnosed with elbow fractures at our institution from October 2010 through July 2011. Initial and follow-up radiographs were reviewed in blinded fashion independently by two experienced pediatric musculoskeletal radiologists to identify fracture type(s) on initial and follow up radiographs. Note was made of fractures identified on follow up only.

Results: The most common fractures included SC ($n=254$, 54%), radial neck (RN) ($n=80$, 17%), and LC fractures ($n=66$, 14%). As compared to classically referenced incidences, RN fractures were seen significantly more ($p<0.0001$) and ME fractures ($n=25$, 5%) significantly less ($p=.0008$) than would be predicted. In 26 patients without fracture seen on initial films, occult fractures were seen on follow up; SC ($n=12$, 46%) and RN fractures ($n=8$, 31%) were most common. The frequency of RN fractures compared to the overall group (31% vs. 17%) approached but did not reach statistical significance ($p=0.06$). 34 patients with one fracture had additional fractures seen on follow-up not seen initially with olecranon fractures most frequent ($n=18$, 53%). This was significantly more common than the number identified on initial radiographs ($n=33$, 7%) ($p<0.0001$).

Conclusions: SC fractures are the most frequent elbow fracture seen initially and in follow up followed by RN

and LC fractures in a distribution different than classically described. The relatively high frequency of RN and olecranon fractures detected on follow up speaks to their potentially occult nature. Careful attention to these areas is warranted in patients with initially normal radiographs.

Paper #: PA-153

Should Views of the Hands, Feet and Spine be Eliminated From the Initial Skeletal Survey in Cases of Suspected Child Abuse?

Paul Kleinman, MD, *Radiology, Children's Hospital Boston*, paul.kleinman@childrens.harvard.edu; Nicole B. Morris, Joseph Makris, Rebecca L. Moles, Patricia L. Kleinman

Purpose or Case Report: Previous studies have found that fractures involving the spine, hands and feet are rare on skeletal surveys for suspected child abuse, leading some authors to suggest eliminating views of these regions from the initial skeletal survey protocol. The purpose of this study was to assess this recommendation by performing a historical review of these injuries in a population undergoing screen-film based skeletal surveys for suspected abuse.

Methods & Materials: This cross-sectional, retrospective IRB approved study reviewed the reports of the initial skeletal surveys of all children <2 years of age with suspected abuse imaged between April, 1988 and December, 2001. Infants underwent skeletal surveys according to ACR standards acquired on a mammographic type screen-film imaging system with at least 13 line pairs per millimeter resolution. Studies in toddlers were performed using a par speed screen-film system.

Results: 62% (225/365) of all skeletal surveys demonstrated positive findings, and 44% (98/225) had >1 fracture. 5.5% (20/365) of all studies had fractures involving the spine, hands or feet. Of all positive skeletal surveys, 8.9% (20/225) had fractures involving the spine, hands or feet, and 20.4% (20/98) of all patients with >1 fracture on skeletal survey had fractures involving these regions.

Conclusions: These data, acquired in the screen-film era, suggest that fractures of the spine, hands and feet may not be rare in infants and toddlers in cases of suspected child abuse. The benefits of eliminating views of these regions from the initial skeletal survey should be carefully weighed against the cost of missing these potentially important injuries in at-risk pediatric populations.

Paper #: PA-154**Fracture Dating in Infant Abuse: A Scientific System to Improve Radiologist Performance**

Michele Walters, MD, Radiology, Children's Hospital Boston, michele.walters@childrens.harvard.edu; Peter Forbes, Sarah Bixby, Carlo Buonomo, Paul Kleinman

Purpose or Case Report: Dating fractures is critical in cases of suspected infant abuse, but there are little scientific data to guide radiologists, and dating is generally based on personal experience and conventional wisdom. We previously reported a scientific scheme for dating fractures in infants based on an analysis of subperiosteal new bone and callus formation in birth-related clavicular fractures. We hypothesize that when used as a guide this system can significantly improve the ability of radiologists to accurately date fractures in young infants.

Methods & Materials: 103 radiographs of presumed birth-related clavicular fractures in infants 0–3 months were reviewed by 2 pediatric radiologists with 2 (reader A) and 15 (reader B) years experience in two reading sessions separated by one year. For the first read, no guidelines were provided. Training was carried out prior to the second session, and readers were given the dating scheme as a guide during fracture analysis. Readers were asked to provide an estimate of the minimum and maximum fracture age in both sessions. The primary outcome was whether or not the reader's estimated range for fracture age included the actual fracture age. A secondary outcome was the width of the estimate of fracture age. These outcomes were compared across the two reading sessions.

Results: The rate of correct response significantly increased after training for each reader (reader A: 66% to 89%, $p < .0001$; reader B: 76% to 86%, $p = .041$). The width of estimated fracture age after training was significantly smaller for each reader (reader A: mean width 17 days to 13 days, $p < .0001$; reader B: 25 days to 15 days, $p = .001$).

Conclusions: Our results suggest that the ability of a radiologist to accurately date fractures can improve significantly when provided with a scientifically based system outlining patterns of fracture healing. This scheme can be applied in radiologic practice and may prove particularly useful in cases of suspected abuse, where fracture dating often has forensic implications.

Paper #: PA-155**Features of Proximal Femoral Growth Plate Injuries in Abused Children**

Eglal Shalaby-Rana, MD, Children's National Medical Center, erana@childrensnational.org; Tanya Hinds, Katherine Deye, Allison Jackson

Purpose or Case Report: To demonstrate the acute and subacute features of proximal femoral physal fractures in the abused child. Also to demonstrate how to recognize this injury in patients with unossified femoral heads.

Methods & Materials: The database of patients with suspected non-accidental trauma, accumulated over 12 years, was reviewed. 254 out of a total of 599 patients (43%) were proven to be cases of non-accidental trauma, as determined by the child abuse pediatrician. From these 254 patients, the cases of proximal femur growth plate fractures were identified.

Results: 7 patients with proximal femur growth plate fractures were identified for a prevalence of 2.8%. One patient had bilateral proximal femoral fractures, for a total of 8 fractures in 7 patients. 5 were boys, 2 were girls with ages ranging from 2.5 mos to 2 yrs 2mos. In 4 patients, the fracture was revealed on imaging performed because of refusal to bear weight; in the other 3 patients, the fracture was found during imaging for the skeletal survey. The fracture was on the left side in 7 cases and on the right side in 1 (the patient with bilateral fractures). In all of the fractures, there was lateral displacement of the femoral shaft. In 3 fractures, the femoral head was not yet ossified simulating the appearance of a dislocation. Location of the femoral head in the hip joint was verified by ultrasound or CT (CT abdomen had already been done in 1 patient) thus delineating the presence of a physal fracture. 6/8 fractures were Salter-Harris I and the other 2 were Salter-Harris II fractures. The fracture was acute in 2 cases and subacute in 6 cases. In these 6 subacute cases, periosteal reaction and/or calcifying subperiosteal hemorrhage was present in 3, and irregularity and scalloping of the metaphysis was present in the other 3.

Conclusions: Proximal femoral growth plate fractures are quite uncommon in non-accidental trauma. The injuries are typically Salter-Harris I or II fractures, seen more often in the healing phase. In the presence of an unossified femoral head, the laterally displaced femoral shaft can simulate hip dislocation; this can be clarified with hip sonogram.

Paper #: PA-156**Early Results of Bioabsorbable Airway Stenting in Children**

Clare McLaren, DCR(R), Department of Radiology, Great Ormond Street Hospital, derek.roebuck@gosh.nhs.uk; Martin J. Elliott, Derek J. Roebuck

Purpose or Case Report: In recent years, metal stents have been used to overcome airway obstruction in children for whom no better surgical option is available. These devices are not designed for use in the airway, however, and may cause significant complications. Bioabsorbable airway stents may avoid some of the problems associated with metal stents.

Methods & Materials: This is a retrospective review of all endoluminal insertions of bioabsorbable airway stents at a single institution from April 2010 to September 2011. Custom-made polydioxanone stents of various sizes (Ella DV, Ella, Czech Republic) were used.

Results: Twelve stents were inserted in the airways of seven children. Indications were: recurrent obstruction after slide tracheoplasty (2), persistent airway compression after correction of a congenital cardiac lesion (2), collapse of stem cell supported tracheal homograft, tracheomegaly following fetal balloon insertion, and syndromic tracheobronchomalacia (TBM). Eleven stents (diameters 6 to 12 mm) were placed in the trachea and one in the left main bronchus. Two stents had to be removed and replaced for technical reasons (one was too long and the other too narrow). The child with syndromic TBM died when treatment was withdrawn because she could not be weaned from the ventilator. The remaining children are alive at a median follow-up of nine months (range 1 to 17 months). The granulation tissue response was similar to that seen after placement of metal stents. The stents were observed to absorb gradually over a period of approximately three months, requiring serial stenting in two children.

Conclusions: Bioabsorbable airway stents are more difficult to insert than metal stents. They cause similar early complications, especially granulation tissue formation, but appear to avoid potential long-term complications of metal stents, including vascular erosion and growth limitation.

Disclosure: Dr. McClaren has indicated that she will discuss or describe, in the educational content, a use of a medical device or pharmaceutical that is classified by the Food and Drug Administration (FDA) as investigational for intended use.

Paper #: PA-157

Long-Term Follow-up of Tuberous Sclerosis Complex Patients Undergoing Renal Angiomyolipoma Embolization

Grant Shafer, Interventional Radiology, Cincinnati Children's Hospital Medical Center, shafergt@mail.uc.edu; John M. Racadio, John Bissler

Purpose or Case Report: Renal angiomyolipomas (AMLs) in tuberous sclerosis complex (TSC) grow at a faster rate, exhibit a wider and more problematic range of symptoms, and hemorrhage more frequently than sporadic AMLs. We examined the efficacy of prophylactic embolization of renal AMLs in TSC in decreasing tumor size, alleviating symptoms, and preventing hemorrhage while preserving renal function.

Methods & Materials: We retrospectively reviewed the charts and imaging studies of 47 consecutive patients who underwent transarterial, transcatheter embolization of 52

AMLs. Tumor volume was measured from available CT or MRI imaging before and after embolization. Pre- and post-embolization symptoms and creatinine levels were documented.

Results: 37 patients had available follow-up imaging at a mean of 63 months post-embolization. The mean pre-embolization tumor volume was 581 mL and post-embolization was 284 mL; median decrease in volume was 76%. Using the Schwartz method, the mean glomerular filtration rate before embolization was calculated to be 95.75 mL/min/1.73 m². After embolization the mean value was statistically unchanged at 101.97 mL/min/1.73 m². None of the patients experienced renal hemorrhage or symptom recurrence during the follow-up period.

Conclusions: Selective embolization of renal AMLs in patients with TSC decreases tumor volume, relieves symptoms and reduces the risk of future hemorrhage while preserving renal function.

Paper #: PA-158

Percutaneous Salivary Gland Ablation for Treatment of Sialorrhea

William Shiels, DO, Radiology, Nationwide Children's Hospital, william.shiels@nationwidechildrens.org

Purpose or Case Report: To evaluate clinical feasibility and efficacy of percutaneous and transductal salivary gland ethanol ablation in the treatment of children with sialorrhea and its complications.

Methods & Materials: Twenty-five neurologically impaired patients (age 2-22Y, mean=10.9Y) were treated for sialorrhea with percutaneous ethanol ablation (ETOH) (with sodium tetradecyl cell pretreatment) either percutaneously (submandibular gland [SMG] and sublingual glands [SLG]) or transductal (parotid). Percutaneous treatment was directed with US guidance; transductal with fluoroscopic guidance. ETOH was injected percutaneously with 25 G needle; transductal ablation performed through a 4 F micropuncture sheath. Drug volumes, technical difficulties, percentage reduction in saliva production, family reported clinical significance, and complications were recorded.

Results: Salivary gland ablation (SGA) included bilateral SMG and SLG ablation without parotid gland ablation in 20 cases, and with unilateral parotid gland ablation in 4 cases. One case of bilateral parotid gland ablation following surgical resection of bilateral SMGs. Mean ETOH dose for SMG=4.2 ml, and 3.1 ml for SLG. One case of focal skin necrosis was noted; no other complications. Patient families reported response to SGA in 24/25 cases (96%) with mean saliva production of 66%. Greatest health and family impact was reported with elimination of hospitalizations for

recurring aspiration pneumonia (2 cases), elimination of choking in bed (3 cases), and improved patient sense of self-hygiene in 8 cases. One complication occurred with temporary marginal mandibular nerve paralysis (resolution in 6 months).

Conclusions: Percutaneous and transductal SGA is feasible, safe, and effective in this small patient series, offering an alternative to surgical salivary gland resection, or treatment option following failed surgical intervention.

Paper #: PA-159

MR-Guided Procedures in Children: Initial Experience

Joao Amaral, MD, *Diagnostic Imaging, The Hospital for Sick Children, joao.amaral@sickkids.ca*; Michael Temple, Dimitri Parra, Philip John, Bairbre Connolly

Purpose or Case Report: The primary purpose of this study was to review our initial experience with MR-Guided procedures in children. Our secondary objective was to share some aspects on how to start an MR-Guided program in a tertiary pediatric center.

Methods & Materials: Patients with lesions identified only on Magnetic Resonance (MR) imaging were selected to undergo an MR-Guided procedure. Patients' demographic data, primary diagnosis, referring team's clinical suspicion, lesion's anatomical location, tissue adequacy for pathology, final diagnosis and clinical follow up were reviewed. Aspects of starting a program of MR-guided procedures, safety concerns, imaging and technical challenges, and MR compatible materials were also addressed.

Results: To date, 7 procedures (5 bone biopsies, 1 soft tissue biopsy and 1 pre-surgical needle localization) were performed in 6 patients during 9 months. There were 4 girls and 2 boys with a mean age of 10.2 years (3y5mo–17 yrs). One patient had a Nasopharyngeal Carcinoma, 1 Cardiofacial Syndrome, 1 Wilm's tumor and 3 had no previous medical issues. The clinical suspicion for 2 procedures in 2 patients was metastatic disease and for 5 procedures in 4 patients was primary malignancy or infection. Lesions were located in the tibia (2- metaphysis and diaphysis), femur (2—metaphysis and epiphysis), thigh (1—soft tissues), sacrum (1) and retroperitoneum (1). All biopsies provided adequate tissue for diagnosis. Needle localization and hook deployment was also accurate. Malignancy was excluded in all patients. Final diagnosis included 1 Chronic Recurrent Multifocal Osteomyelitis (CRMO), 3 Osteomyelitis, 1 fibrous tissue, 1 Osteoid Osteoma, and 1 scar tissue. Mean follow up was 6.6 months. No patient required a second procedure to confirm the diagnosis.

Conclusions: MR with its unique soft tissue resolution and lack of ionizing radiation is an excellent method to guide

interventions in children. One of the greatest advantages of this method is the precise target localization especially in lesions located in the bone marrow or lesions better identified on MR. Special safety measures, specific MR compatible material (needles, surgical instruments), dedicated imaging techniques to reduce or increase material/needle artifact and careful technique are paramount.

Paper #: PA-160

Sonography in Planning Nerve Graft Repair of Perinatal Brachioplexopathy

Michael DiPietro, MD, *University of Michigan—Radiology, dipietro@umich.edu*; Lynda Yang

Purpose or Case Report: To describe multi-faceted sonographic techniques.

Methods & Materials: 26 children from 2006–2011. 11 M, 15 F; 2.5–59 months, mean 8.3 months, median 5 months, mode 5 months. Sonographic approach expanded as our experience grew over 71 months. 25 studies performed by a single pediatric radiologist. Bilateral sonography included: interscalene and supraclavicular neck, nerve roots at neural foramina, cervical spinal canal, diaphragm during spontaneous respiration, rhomboid muscle, serratus anterior muscle, posterior shoulder, all performed and interpreted blind to other imaging.

Results: Interscalene and supraclavicular neck evaluated in all patients. All exhibited echogenic interscalene portion of brachial plexus. Size and extent of traction neuroma varied. Nerve roots at foramina noted in axial and coronal planes. In 11 cases enlarged root(s) noted. Cervical spinal canal studied in 19 patients: cord oscillated normally, no syrinx, cord concentric in canal. Intracanalicular traction pseudo-meningoceles on concurrent CT myelography or MRI were not apparent on US. In 2 cases a “clumped” retracted nerve root on the cervical cord was later found to correspond to a pseudo-meningocele on CT myelogram. Otherwise, cervical spinal canal US was unremarkable in 24 cases. Diaphragm motion was evaluated in 23 patients during spontaneous respiration; no phrenic nerve palsy. Rhomboid muscle was evaluated for atrophy in 16 patients; 4 had atrophy. The rhomboids are innervated by the dorsal scapular nerve which arises solely from C5, prior to C5 joining the brachial plexus. Intact rhomboid indicates that the central C5 root is intact. Serratus anterior muscle, innervated by the long thoracic nerve (C5,C6,C7), was evaluated for atrophy in 12 patients; 6 had atrophy. Dynamic evaluation of the posterior shoulder looking for posterior laxity was evaluated in 10 patients; 4 had laxity. Posterior shoulder dislocation or subluxation is a known sequela of brachioplexopathy which sometimes requires muscle transfer when the child is older.

Conclusions: Comprehensive US evaluation of perinatal brachioplexopathy detects: extent of traction neuromatofibroma from the interscalene region peripherally toward clavicles (important for neurosurgeon), thick nerve roots, phrenic nerve diaphragm palsy, muscle atrophy from denervation, and posterior shoulder subluxation. US misses: intracanalicular traction pseudomeningoceles.

ALTERNATE PAPERS

Paper #: ALT-001

Impact of the Image Gently Campaigns in Adult-Focused Hospitals: A Survey of Practice Leaders

Brett Bartz, *Duke University Medical Center*; Donald Frush, Kimberly Applegate, Michael Callahan, Laura Coombs, Marilyn Goske

Purpose or Case Report: The Alliance for Radiation Safety in Pediatric Imaging is an organization that uses social marketing to promote radiation protection for children and effect change across radiology practices. The impact of the Alliance's Image Gently campaigns on practice patterns in radiology practices has yet to be assessed, especially outside of freestanding children's hospitals. The purpose of this investigation was to assess the impact of the Image Gently campaigns on academic and private practices/institutions that treat children but primarily serve adults.

Methods & Materials: A web-based survey was emailed to leaders in radiology practices ($n=1186$) who do not practice at freestanding children's hospitals utilizing the ACR's PRED database. The survey consisted of 18 questions designed to measure the recognition and impact of the Image Gently campaigns, including the impact on practice patterns.

Results: A total of 186 practice leaders in 41 U.S. states and territories responded for a response rate of 15.7%. The majority (94%) of sites image pediatric patients in their practices. Respondents consisted of department chairs (60%), group presidents/CEOs (33%), and division chiefs (13%). The majority (52%) of respondents described their practice as a hospital-based private practice without a dedicated pediatric radiology division. The vast majority (95%) of respondents was familiar with the Image Gently campaigns; 55% of respondents reported that Image Gently had effected a change on how they imaged children. Specifically, respondents (%) reported that the campaign caused a modification to lower dose protocols for head CT (57%), chest CT (66%), and abdominal/pelvic CT (69%). Slightly more than half of respondents (55%), however, estimated that the Image Gently campaign resulted in no modification of pediatric fluoroscopy exposure.

Conclusions: To our knowledge, this is the first survey evaluating the impact of the Image Gently campaigns. There is near universal recognition of the campaigns, which have impacted practice patterns beyond the freestanding children's hospital in CT, but not in fluoroscopy.

Paper #: ALT-002

Reliability of Shear-wave Velocity Using Different Frequencies in Acoustic Radiation Force Impulse (ARFI) Elastography

Mi-Jung Lee, *Radiology, Severance Children's Hospital, mj11213@yumc.yonsei.ac.kr*; Suyon Chang, Myung-Joon Kim

Purpose or Case Report: Although there are many studies about acoustic radiation force impulse (ARFI) measurement, standard protocol has not been established. And a new probe with high frequency has been developed which can be applied for pediatric patients. The purpose of this study was to assess the reliability of shear-wave velocity (SWV) at various depths using different frequencies to suggest standard measurement in ARFI elastography.

Methods & Materials: ARFI elastography of both the elasticity phantom and normal liver was performed at different depths (2–5 cm) with convex (1–4 MHz) and linear (4–9 MHz) probes. Ten valid SWV measurements at each depth were performed. It was repeated ten times with the phantom and it was done in 8 healthy volunteers (M:F=3:5, age 20–34 years; mean 25.5). The mean value and standard deviation of SWV were calculated.

Results: In both the elasticity phantom and the liver, variability of SWV was different between the depths in both probes. The depth with lower variability in the phantom was 4 and 5 cm with the convex probe and 2 cm with the linear probe. In the liver, the depth with lower variability was 4 cm with the convex probe and 3 and 4 cm with the linear probe. In comparison of two probes, the linear probe showed lower variability at 2 and 3 cm depth in the phantom and at 3 cm depth in the liver whereas the convex probe showed it at 4 cm depth in both the phantom and the liver.

Conclusions: In ARFI elastography, measurement of depth shows different variability in both low and high frequency probes. To obtain the most reliable measurement of SWV, using high frequency probe is recommended for 2-3 cm depth and using low frequency probe is recommended for 4-5 cm depth.

Disclosure: Dr. Lee has indicated that she will discuss or describe, in the educational content, a use of a medical device or pharmaceutical that is classified by the Food and Drug Administration (FDA) as investigational for intended use.

Paper #: ALT-003**Imaging 100-Year-Old Fetuses**

Sabah Servaes, *Children's Hospital of Philadelphia*; Teresa Victoria, Ann Johnson, Sandra Kramer, Richard Markowitz, Diego Jaramillo

Purpose or Case Report: To demonstrate normal anatomy and pathology of medical museum specimens without disturbing the specimens.

Methods & Materials: Nine fetal specimens from a medical museum were imaged with CT and MRI (1.5 T and 3.0 T) when possible with the specimens in their preserving fluid and containers.

Results: The 9 fetal specimens are estimated to be approximately 100 years old. One specimen is from the first trimester, seven are from the second trimester, and one is from the third trimester. Normal anatomical structures at various stages of development including the brain (and varied sulcation pattern), lungs (lobar anatomy), and skeletal structures (several developmental features such as the ossification centers, perichondrial structures, and marrow cavitation) can be evaluated using imaging without causing harm to the specimens. Pathologic entities including anencephaly and sirenomelia are also evaluated demonstrating features of these entities.

Conclusions: Imaging historical fetal specimens provide an opportunity to evaluate normal developmental changes and pathological entities and also to gain a better understanding of the museum pieces without damaging the museum specimens.

determine if there was added value provided by the reinterpretation.

Results: CT scans from 732 patients were submitted for reinterpretation. Disagreements were found in 301/732 cases (41.1%); with 50.5% (152/301) classified as major disagreements. Among the 427 neurologic cases, major disagreements occurred in 53 patients (12.4%) and minor disagreements in 92 patients (21.5%). Among the 305 body scans, major disagreements occurred in 99 cases (32.5%) and minor disagreements in 57 cases (18.7%). In the cohort of cases reviewed for final diagnosis, the second read interpretation was more accurate in 90.2% of cases with a p-value of <0.0001 (neurologic 84.4%, $p=<0.0001$; body 95.7%, $p=<0.0001$).

Conclusions: In our review, discrepancy rates between community and tertiary care radiologists in interpretation of pediatric CT scans were substantial, with discrepancies occurring in more than 40% of cases. Further review of the cases for final diagnosis, showed that a significant number of the tertiary care interpretations were more accurate. Possibilities that may account for this discrepancy include subspecialty training and elapsed time since performance of the study, which might provide additional clinical data in some cases. Diagnostic CT scans performed at outside institutions should not be repeated considering added radiation burden to the child and additional expense. Our data indicates there is added value to the reinterpretation which impacts the accuracy of the report (as assessed by the final diagnosis), and should be recognized by payors as integral to optimal patient care.

Paper #: ALT-004**Pediatric CT Interpretations: Does a Tertiary Care Radiologist Make a Difference?**

Wendy D. Ellis, *Monroe Carell Jr. Children's Hospital at Vanderbilt University*; Sumit Pruthi, David Johnson, Christopher Eakins, Chang Yu, Marta Hernanz-Schulman

Purpose or Case Report: To determine whether a substantive difference exists between the pediatric imaging reports of community radiologists and reinterpretations by tertiary care radiologists at a free-standing children's hospital; and how those interpretations were related to the final diagnosis.

Methods & Materials: This retrospective review examined the computed tomography (CT) reports of all pediatric patients referred to our tertiary care children's hospital over a 17 month period (1/1/2009–5/31/2010). The outside reports and the requested second interpretation reports were compared and their content categorized as "agreement" vs. "disagreement: major or minor". A representative sample of 92 major disagreements in which there was reliable follow-up information was correlated with the final diagnosis to

Paper #: ALT-005**Ionizing Radiation Exposure from Radiography in the Neonatal Intensive Care Unit—Per-Patient Cumulative Effective Doses**

Amaya Basta, *Radiology and Biomedical Imaging, UCSF*; Jesse Courtier, John MacKenzie

Purpose or Case Report: To better understand the levels of exposure to ionizing radiation for infants in the neonatal intensive care unit (NICU).

Methods & Materials: We retrospectively collected the number and types of radiographs performed per infant in our NICU by searching our radiology information system database over a five-year period. We focused on the most common examinations (98% of all radiographs) and assigned each an estimated equivalent dose based on published literature: chest and abdomen=21.3 micro Sieverts (μSv), one-view chest=13.3 μSv , abdomen=13.5 μSv , two-view chest=26.6 μSv , two-view abdomen=27 μSv . We then calculated a cumulative equivalent dose (CED) for each

infant based on the number of each type of examination they received. Descriptive statistics were generated to depict the distribution of number of examinations and CED.

Results: Over five years, 2,626 infants cared for in our NICU received at least one radiograph of the chest and/or abdomen. The number of examinations obtained on these infants was 9.6, 4, 1, 137 (mean, median, minimum, maximum). The 1st quartile was 1 and the 3rd quartile was 11 examinations. The cumulative equivalent dose these infants received was 157.9, 61.2, 13.3, 2,092.2 μSv (mean, median, minimum, maximum). The 1st quartile was 21.3 and the 3rd quartile was 61.2 μSv . Two hundred infants (7.6% of the study population) received a CED of over 500 μSv .

Conclusions: Descriptive statistics provide a valuable assessment for the broad range of radiation that infants receive in the NICU. Although the distribution is skewed towards a low level of exposure, a subset of patients (7.6%) received a CED of over 500 μSv . Identification of factors that cause infants to enter this group will be important for future dose reduction strategies.

SCIENTIFIC EXHIBITS

Poster #: CR-001

Congenital Cardiac Fibroma: A Case Report

Earic Bonner, *Meharry Medical College, ebonner07@email.mmc.edu*; Seth Crapp, David Parra

Purpose or Case Report: A 5-week-old male presented to his pediatrician with a II/VI systolic ejection murmur along the left sternal border. He had mild tachypnea without cyanosis. His oral intake was adequate with no evidence of failure to thrive. He was referred to a pediatric cardiologist who performed an ECG and a transthoracic echocardiogram. The ECG showed normal sinus rhythm at 135 beats per minute with no abnormalities. The transthoracic echocardiogram showed a 25 x 25 x 14 mm homogeneous mass originating from the anterior free wall of the right ventricle, and mild dilation of the right ventricle. Mild dynamic subpulmonary stenosis and a secundum atrial septal defect were also noted. Although the murmur was significantly louder at one month follow-up, a repeat echocardiogram did not reveal any increase in the size of the mass. At 2 months of age, a cardiovascular magnetic resonance imaging (CMRI) study under general anesthesia was performed. CMRI revealed a 16 x 21 x 22 mm cardiac tumor that was causing narrowing of the right ventricular outflow tract. The tumor was hypointense on T2-weighted imaging and hyperintense on T1-weighted imaging, with positive delayed enhancement. These findings, along with the size and location of the mass,

are consistent with a diagnosis of a cardiac fibroma. Chest MRA, that was also performed, showed normal extracardiac vascular anatomy with no evidence of peripheral branch pulmonary stenosis. Cardiac fibromas do not usually increase in size; however, the concern is the child's risk of arrhythmias. Frequent Holter monitoring was recommended for this patient. Considerations were also made for an electrophysiology study in the next 1–2 years to determine the risk of ventricular ectopy. At that point, the patient can be assessed for the possibility of resection of the fibroma.

Poster #: CR-002

Right Ventricle to Pulmonary Artery (RV-PA) Conduit Stent Fractures: What the Radiologist Needs to Know. A Presentation of 3 Cases of Stent Fracture

Hamilton E. Reavey, MD, *Radiology, Emory University, hfryer@emory.edu*; Kiery Braithwaite, Kimberly Applegate

Purpose or Case Report: Treatment of pulmonary atresia is complex and demands intricate solutions. One solution is the creation of a conduit between the right ventricle and the main pulmonary artery. The lifespan of these conduits is limited by progressive occlusion over time, which can be treated with endovascular stent placement in lieu of surgical re-intervention. However, these stents are at high (40%) risk for fracture, typically at the stent waist. The radiologist should be aware of this complication, as they may be the first to identify it on chest radiograph. The purpose of this electronic poster is to familiarize radiologists with this entity by presenting 3 cases of stent fracture and migration.

Methods & Materials: Over a 6 month period, we identified three children with RV-PA stent fractures and associated stent migrations on chest radiography. Imaging analysis was focused on the appearances of these fractured stents. Patient management and outcomes were reviewed.

Results: Three children, 2 males, 1 female (ages 4, 3, and 3 years) were found to have asymptomatic RV-PA conduit stent fractures with fragment migration. One chest x-ray was performed in the ER for fever and cough; one was pre-op for GI surgery; one was done to confirm abnormal findings seen on a routine cardiac echo. The time between stent placement and fracture detection ranged from 1 to 22 months. Two patients had stent fractures and embolizations to the right ventricle that required open surgery to remove stent fragments. The third patient had embolization to both pulmonary arteries, but did not require treatment. All patients did well.

Conclusions: Stent fractures and migrations are a relatively common complication of RV-PA conduit stent placement. Pediatric radiologists need to be aware of this complication in order to provide value-added interpretations.

Poster #: CR-003**A Case of Fetal Craniopharyngioma**

Preetam Gongidi, DO, MHS, *Christiana Care Health Services, preetamgongidi@gmail.com*; Wadia Mulla, Mark Mitchell

Purpose or Case Report: We describe the case of a 23 week stillborn fetus with a 5.5 cm diameter craniopharyngioma detected by ultrasonography. A G1P0 woman in her third decade had ultrasonographic examination showing hydrocephalus, polyhydramnios and an intracerebral mass. The nature of the mass was uncertain and intracerebral hemorrhage was considered. The pregnancy was terminated at 23 weeks gestation. At postmortem examination the decedent was a 650 g male fetus with a head circumference of 24.5 cm and a crown-rump length of 21.8 cm. Anterior and posterior fontanelles appeared large. No other external abnormality was found. The placenta was unremarkable and cytogenetics on placental tissue showed a normal male karyotype. Examination of fetal viscera was remarkable for mildly underweight adrenal glands (0.75 g, expected 1.5 g) and hepatomegaly (66.4 g, expected 21.7 g). Intracranial CSF was increased in volume. There was a suprasellar 5.5 cm diameter somewhat gritty, but smooth-surfaced tumor. The brain and tumor together weighed 135 g. The floor of the cranium and sella turcica were grossly normal. Histologic examination of the tumor showed an adamantinomatous type craniopharyngioma with characteristic epithelium, stellate reticulum, focal keratinizing squamous epithelium and calcification.

Poster #: CR-004**Pre- and Postnatal MRI of Caudal Regression Syndrome**

Claire B. Beaumont, MD, *University of Arkansas for Medical Sciences, cbbeaumont@uams.edu*; Nafisa K. Dajani, Leann E. Linam

Purpose or Case Report: Caudal regression syndrome is a rare form of caudal dysplasia characterized by a spectrum of findings including agenesis of the lumbosacral vertebra, multiple orthopedic deformities in the lower limbs, as well as anomalies of the gastrointestinal and genitourinary tracts. The mechanism of caudal regression syndrome is not completely understood but is believed to be secondary to a defect in the induction of caudal elements. MRI is a valuable tool for identifying the specific anomalies involved with caudal regression syndrome on a case-by-case basis. The following is a case from our institution which includes both pre- and postnatal MRI.

Poster #: CR-005**Unsuspecting Tuberous Sclerosis Diagnosed on Neonatal Cranial Ultrasound**

Vikas Menghani, MD, *Pediatric Radiology, Women's and Children's Hospital, drvikasmenghani@gmail.com*; Puneet Gupta, Richard Thomas, Vaseem Iqbal, Jan Najdzionek.

Purpose or Case Report: Tuberous sclerosis (TS) is a rare autosomal dominant genetic disorder causing hamartomatous proliferation in number of organ systems. Because the classical triad of epilepsy, mental retardation and adenoma sebaceum is not commonly seen on clinical examination, imaging plays a central role in the diagnosis and treatment of tuberous sclerosis. Central nervous system features of TS include subependymal nodules, cortical tubers, subependymal giant cell astrocytoma, white matter bands and cysts. In patients with TS, cerebral involvement in the form of subependymal nodules is seen in 95% to 100% and white matter abnormalities are noted in 40% to 90% of cases. Knowledge of expected radiological features is thus important in making the correct diagnosis. Recent studies have indicated that earlier appearance of brain lesions indicate a greater risk of mental retardation and a more severe clinical course. We present a case of a 23-day-old neonate who was referred to us with concerns for hydrocephalus. The cranial ultrasound demonstrated multiple echogenic subependymal nodules of varying sizes and mild asymmetry of the ventricles. The differential diagnosis included TS, TORCH infections, and X-linked subependymal heterotopia. Areas of increased echogenicity were noted within the white matter of the left frontal lobe, which favored TS. Subsequently, an MRI was performed to validate these findings and assess for additional white matter lesions. The MRI showed classic manifestations of TS that included periventricular lesions and streaky, linear, wedge-shaped hyperintensities on FLAIR imaging. A noncontrast CT scan was also performed which revealed classic calcified subependymal nodules. Cardiac rhabdomyoma and renal angiomyolipoma are the other recognized manifestations of TS and were respectively excluded by subsequent echocardiogram and renal ultrasound.

Poster #: CR-006**Pyloric Atresia with Epidermolysis Bullosa: Fetal MRI Diagnosis with Postnatal Correlation**

Arnold C. Merrow, MD, *Radiology, Cincinnati Children's Hospital Medical Center, carl.merrow@cchmc.org*; Jason S. Frischer, Anne W. Lucky

Purpose or Case Report: Pyloric atresia (PA) is an uncommon disorder, accounting for 1% of congenital gastrointestinal

atresias. Up to 55% of cases have associated anomalies, the most common of which is epidermolysis bullosa (EB). Prenatal findings have been reported sonographically for each of these anomalies, both in isolation and in the rare case of association. A case of isolated PA has been reported by fetal MRI. We present the first reported case of PA with EB diagnosed by fetal MRI with corroborative postnatal imaging and surgical findings. The mother of this child was initially referred to the Fetal Care Center of Cincinnati at 21 weeks gestation for a possible myelomeningocele diagnosed by prenatal ultrasound at an outside facility. These ultrasound images were not available for review at the time of our workup. A fetal MRI was the first study to be obtained at our institution. The MRI showed no myelomeningocele or brain anomalies. The stomach was moderately enlarged throughout the exam and did not empty. Subjective polyhydramnios was also noted. No duodenal dilation was seen, and there was minimal fluid in the distal bowel loops. This constellation of findings raised concern for pyloric atresia, resulting in a careful search for any sign of epidermolysis bullosa due to a known association of these disorders. Prominent debris was seen layering dependently in the amniotic fluid and in the dilated fetal stomach, and the external ears were abnormally small and misshapen. The PA-EB association was proposed as the underlying diagnosis based on our MRI findings. It was also postulated that skin blistering over the lumbosacral spine at the time of the prior outside ultrasound could have mimicked a myelomeningocele, thus prompting the referral to our center. At delivery, the baby had numerous skin defects, and the ears were malformed. An abdominal radiograph obtained after nasogastric tube placement and air injection showed no gas beyond the stomach. A pyloric ultrasound showed a distended stomach without a patent pyloric channel to the duodenal bulb, consistent with pyloric atresia. A skin biopsy confirmed epidermolysis bullosa, and the patient underwent a resection of the PA with gastroduodenostomy. The baby subsequently expired less than two weeks later, most likely due to sepsis based on wound cultures and autopsy results. Our case demonstrates the ability of fetal MRI to diagnose this rare condition and highlights the key imaging manifestations of the PA-EB association.

Disclosure: Dr. Merrow has indicated that he is an author for Amirsys and receives a royalty accordingly.

Poster #: CR-007

Wandering Appendix

Johanna Schubert, MD, *Children's Hospital and Medical Center, Omaha;* Lincoln M. Wong, Terri L. Love, John D. Wendel, Lisa M. Wheelock, Travis D. Kruse

Purpose or Case Report: We demonstrate a case where the changing position of the contrast filled appendix lead to the

diagnosis of malrotation, with review of the embryology of intestinal rotation. A newborn preterm female presented with a golf ball sized umbilical mass, that reduced by itself, thought to represent an umbilical hernia vs omphalocele. She was unstable to undergo an upper GI exam under fluoroscopy, therefore a limited contrast study was performed at bedside and was inconclusive for malrotation. Subsequent NICU radiographs showed changing position of the appendix filled with residual contrast, visiting all quadrants of the abdomen in a random pattern over a few days period. This confirmed our suspicion for malrotation. It is well know that in malrotation the position of the cecum can be variable, most commonly located in the right upper quadrant or left lower quadrant. To our knowledge it has not been described yet that the changing position of the appendix can lead to the diagnosis of malrotation. Through this case we display the embryology of the intestinal rotation and the radiologic signs of malrotation.

Poster #: CR-008

MR Imaging Patterns of Liver Transplant Complications in the Pediatric Population

Edward Richer, MD, *Emory University, richerej@gmail.com;* Adina Alazraki, Jonathan Loewen

Purpose or Case Report: Pediatric liver transplantation is a relatively common surgery, with more than 500 transplants in the United States annually. The spectrum of post transplant complications has been previously described, primarily utilizing ultrasound. As MRI has become a more widely used technique in pediatric imaging, and ultrasound findings may be non-specific, knowledge of MR imaging patterns is an important adjunct in the post-transplant evaluation. We present a spectrum of complications, including vascular, biliary, hepatic parenchymal, and systemic complications.

Methods & Materials: Using an electronic record system, we identified pediatric patients with prior liver transplantation who subsequently underwent abdominal MRI at our institution and were found to have a post transplant complication. Patient management and outcomes were reviewed.

Results: Our review of a subset of the available patients shows vascular complications to be the most commonly encountered abnormality at our institution, including hepatic artery stenosis/thrombosis, and portal vein stenosis/thrombosis, cavernous transformation of the portal vein. Biliary complications were relatively common, including biliary stenoses and bilomas. Hepatic parenchymal and systemic complications, such as PTLT, were less common. We demonstrate the MR imaging patterns of these complications.

Conclusions: Pediatric liver transplantation is a relatively common surgery, and the MRI appearance of post-transplant complications warrants illustration as abdominal MRI becomes more widely used in pediatric imaging. We present a pictorial review of common patterns of complication.

Poster #: CR-009

Imaging of Progressive Familial Intrahepatic Cholestasis (PFIC)

Matthew D. Dobbs, MD, *Radiology, Vanderbilt University Medical Center; matthew.dobbs@vanderbilt.edu*; Sumit Pruthi, Stephanie E. Spottswood

Purpose or Case Report: Progressive familial intrahepatic cholestasis (PFIC) is a relatively rare pediatric liver disease due to a genetic mutation (ABCB11 gene on chromosome 2q24-31) in a bile salt export protein causing cholestasis leading to chronic inflammation within the biliary system. The diagnosis is made clinically with detection of a low GGT in the face of an elevated bilirubin and alkaline phosphatase. Genetic testing confirms the diagnosis. One of the 3 subtypes, Type 2, was shown in 2006 to be highly related to the development of hepatocellular carcinoma. The vast majority in children in this study developed HCC at less than 2 years of age. Radiological contribution to the management of these chronic liver disease patients is to perform surveillance imaging to detect HCC. Due to the rarity of this condition, almost no reports exist in the radiological literature describing the imaging features or management of this condition. Our presentation will review the imaging findings in our small population of PFIC Type 2 patients on US, CT, and MRI. We will also review suggested surveillance imaging techniques and imaging algorithms.

Poster #: CR-010

Renal Rhabdoid Mimics Wilms Tumor

Vikas Menghani, MD, *Pediatric Radiology, Women's and Children's Hospital, drvikasmenghani@gmail.com*; Paul Montgomery, Jan Najdzionek, Vaseem Iqbal

Purpose or Case Report: In the past most pediatric renal tumors have been classified together under the umbrella of Wilms tumor. However, over the last decade with advancement in imaging, several distinctive imaging features specific to renal tumors have been recognized which aid in their classification as being distinct pathologically. We present a case of Rhabdoid Tumor where

in the primary tumor arose from the kidney. It had classical imaging features of Wilms tumor. We want to highlight that even with the most sophisticated imaging techniques, specific renal tumors cannot always be diagnosed with preoperative imaging and how this alters the management and prognosis for child with a renal mass. In our case, the postoperative findings, pathology and immunohistochemical techniques confirmed a Rhabdoid Tumor. Differentiation of these two tumors is essential since in patients with Rhabdoid Tumor survival is poor with 4-year overall survival rates of 42% for stages I and II and 16% for stages III, IV, and V. On imaging, there are several features that suggest the diagnosis of rhabdoid tumor. These include subcapsular fluid collections, linear calcifications outlining tumor lobules, and vascular invasion. Also, a pertinent feature of rhabdoid tumor due to its aggressive nature is the presence of lung metastasis (83%) and synchronous malignant brain lesions (15%). These findings were not present on our case, which led us in formulating a diagnosis of Wilms. Our patient is unusual in the fact that the local renal findings and absence of metastasis, synchronous malignant lesions, and vascular invasion led us to an incorrect diagnosis of Wilms tumor. In conclusion, we would like to stress that diagnosis of rhabdoid tumor of the kidney on imaging presents a challenge because of its imaging similarity to Wilms tumor.

Poster #: CR-011

Ectopic Ureters in Young Infants: MRU Findings

Shin-Lin Shih, MD, *Department of Radiology, Mackay Memorial Hospital*; Yi-Fang Chen, Chun-Chao Huang, Fei-Shih Yang

Purpose or Case Report: To localize the terminations of ectopic ureters by MRI

Methods & Materials: MR urography (MRU) was conducted in four female patients with hydroureter and a suspected ectopic orifice. MR imaging was performed with a 3 T MR scanner (Achieva; Philips). The imaging protocol mainly consisted of a single-shot T2-weighted turbo spin echo sequence with a slice thickness of 4 mm and multiplanar reformations. The ages of the four patients were 1 day, 3 days and 2 months (for two). The latter two patients presented with urinary tract infection. The newborn patients presented with abnormal prenatal examination. The pertinent findings and descriptions of a variety of renal anomalies were described.

Results: The locations of the ectopic ureters were two in the vagina, one in the uterus and one in the bladder neck. The

associated renal anomalies were a right duplex kidney in four, a left duplex kidney in one, a left ectopic dysplastic kidney in one and vesicoureteral reflux in one (confirmed by VCUG).

Conclusions: MRU may demonstrate the exact point of termination of an ectopic ureter and also the associated renal anomalies.

Poster #: CR-012

Acquired Polycystic Kidneys in Neuroblastoma Survivors

Richard Bellah, *Radiology, The Children's Hospital of Philadelphia, BELLAH@email.chop.edu*; Bernard Kaplan, Camilo Jaimes, Yael P. Mosse, Jill P. Ginsberg, Kevin E. Meyers

Purpose or Case Report: Neuroblastoma (Nbl) is the most common extracranial solid malignancy of childhood. With current therapy, the prognosis and long term survival of patients affected by this condition has dramatically improved. Nevertheless, the treatment for Nbl may account for some complications further in life. In patients with neuroblastoma, acute renal failure can occur usually as a result of a thrombotic microangiopathy associated with bone marrow transplantation. In addition, end-stage renal disease has been reported in long-term survivors of Nbl. This exhibit describes and illustrates the first case series of five patients with treated Nbl in whom the imaging features of polycystic kidney disease (PKD) developed over time, and in some cases, as progressive renal failure ensued.

Methods & Materials: Medical and imaging records were reviewed (IRB approved) of patients with treated Nbl in whom PKD became apparent during the course of follow-up imaging.

Results: Five patients displayed findings of PKD on US and/or CT. Three of the five patients (where images were available) had normal renal imaging at time of Nbl diagnosis. The mean age at Nbl diagnosis was 2.4 years (range 1.3–3.3 yr). The mean age at time PKD was detected was 14.6 years (range 8–18 yrs). None of the patients had a family history of PKD, or had previously undergone dialysis. All patients received chemotherapy and total body irradiation prior to bone marrow transplantation. Four patients survived Nbl therapy but eventually developed end-stage renal disease.

Conclusions: An association between acquired PKD and Nbl has not been previously reported. The etiology of this observation is still unclear, but a toxic insult is likely to account for the renal changes. Further research is needed to establish the epidemiology, prognosis, and etiology of this association.

Poster #: CR-013

Abnormal Migration of the Retention Anchor Suture in a Case Following Gastrostomy Tube Insertion

Surendra Narayanam, MBBS, DMRD, DNB, *Division of Image Guided Therapy, Department of Diagnostic Imaging, The Hospital for Sick Children, nrssbabu@gmail.com*; Joao Amaral, Luke Toh, Bairbre Connolly, Vicente Deoliveira, Dimitri Parra

Purpose or Case Report: During percutaneous gastrostomy tube placement, retention anchor suture(s) are deployed into the stomach to tack the anterior gastric wall to the abdominal wall. In our practice the thread of the retention anchor suture is cut at 14 days and the metallic portion passes pre rectum. We report an interesting and very rare migration of the metallic portion of the retention anchor suture in post-primary gastrostomy tube insertion. An 8-month-old girl, with a mitochondrial disease and severe hypotonia underwent percutaneous gastrostomy placement. During the procedure the retention anchor suture thread snapped and the metallic portion of the suture remained within the stomach. Day 1 post procedure, the child became uncomfortable, so a gastrostomy tube check was performed. The suture was not visible in the abdomen on abdominal x-ray or fluoroscopically. On close review of the images, the suture was found projected over the distal esophagus. Initial impression was the anchor suture had refluxed into the esophageal lumen. Careful attempts were made to remove it along with the nasogastric tube, from above under fluoroscopic control. However on withdrawal of the nasogastric tube, the retention anchor suture moved en bloc with the nasogastric tube. Once removed the retention anchor suture was confirmed to be within the nasogastric tube. This case illustrates the importance of examining the chest X-ray carefully before assuming a retention anchor suture has passed.

Poster #: CR-014

Paravertebral Malposition of Peripherally Inserted Central Catheters in Neonates: A Pictorial Review

Daniel Garnet, MD, *Winthrop-University Hospital, dgarnet@winthrop.org*; Dan Barlev

Purpose or Case Report: 1. Outline the indications, importance and the technique of peripherally inserted central venous catheter placement in neonates. 2. Pictorial review of the radiographic features, relevant anatomy and embryology of the paravertebral venous plexus. 3. Case based pictorial review of the radiographic findings of malpositioned central venous catheters, the mimics and pitfalls in making the

diagnosis. 4. Discuss the reported complications of an unrecognized malpositioned catheter and the steps taken by our radiology department in collaboration with Neonatal Intensive Care Unit for timely diagnosis.

Conclusions: The major teaching points of this exhibit are: 1. To recognize the key radiographic findings in paravertebral malposition of central venous catheters in neonates. 2. To understand the appropriate post procedural radiographic workup and its technique for timely diagnosis. 3. To learn the potential complications of delayed diagnosis.

Poster #: CR-015

Pediatric Retroperitoneal Synovial Sarcoma

Ahmad Aouthmany, *University of Toledo Medical Center, ahmad.aouthmany@utoledo.edu*; Asif Abdullah

Purpose or Case Report: Pediatric synovial sarcoma most commonly affects the extremities, especially the lower thigh and knee region; other primary sites such as the retroperitoneum have been only infrequently reported. We report an extremely rare case of a retroperitoneal synovial sarcoma masquerading as retroperitoneal hematoma in a 16-year-old white female with non-traumatic back pain and non-contrast enhanced CT findings of right quadratus lumborum and psoas region presumed hematoma. Coagulation studies revealed Factor XI deficiency also known as Hemophilia C. However, on follow-up imaging, the presumed retroperitoneal bleed persisted and a subsequent MR examination revealed a solid enhancing mass. CT, MR, and FDG-PET findings as well as a brief histopathology are discussed. Our case is rare in the regards that the tumor occurred in an uncommon retroperitoneal location in a pediatric patient and was mimicking a retroperitoneal hematoma which posed a significant diagnostic challenge. Despite a rare entity, synovial sarcoma among other sarcomatous lesions maybe considered in the differential consideration of a spontaneous retroperitoneal hematoma even in hemophiliac patients.

Poster #: CR-016

Longitudinal Bracket Epiphysis

Michael Jubang, *Geisinger, mjjubang@geisinger.edu*; Farzad Sedaghat, William J. Malone, George Wu, William Miranda

Purpose or Case Report: Longitudinal bracket epiphysis is a rare anomaly with multiple synonyms such as delta bone, triangular bone, and congenital angular deformity. The purpose of this case report poster is to discuss an 11-month-old

male born with an adducted right great toe with a broad nail and a notch in the center of the distal phalanx. The review will discuss radiographic findings, the natural progression of the disease, the treatment options, the MRI findings used for pre-surgical planning, and associated pathology.

Poster #: CR-017

Whole Body MRI in Pediatric Non Oncologic Diseases: Pictorial Review

Ramy El Jalbout, MD, *Radiology, CHU Sainte Justine, ramy.jalbout@yahoo.com*; Vijay Moorjani

Purpose or Case Report: With the advances in scanning techniques and the scanning sequences, the role of WBMRI is expanding. MRI has a great role in the pediatric population owing to its inherent advantages namely lack of radiation, high tissue specificity, and high diagnostic yield at the level of the entire body under a single sedation. Unlike the application of WBMRI in the assessment of metastasis and bone marrow involvement in leukemia, its role in systemic diseases is yet to be further investigated. Certain diseases such as CRMO are very often multifocal. The extent of osteonecrosis in patients on steroids, dermatomyositis and the lesions related to child abuse are very often wide spread in the skeleton. We intend to present some of the findings of these pediatric systemic and multifocal diseases on WBMRI. Chronic Relapsing Multifocal Osteomyelitis (CRMO): CRMO can be acute or chronic and is multifocal. The abnormality manifests as high signal intensity. WBMRI can guide for the best site for biopsy and provides monitoring for response to treatment. Osteonecrosis: Only few small studies evaluated the usefulness of WBMRI in the diagnosis of both the symptomatic and asymptomatic sites of osteonecrosis in ALL patients on steroid therapy. WBMRI is more sensitive than conventional radiographs. The abnormalities are typically geographical areas of high STIR signal intensity. Myopathies: WBMRI has also the role of detecting the extent of idiopathic inflammatory myopathies such as dermatomyositis in the entire skeleton. Child abuse: WBMRI has a low sensitivity for the highly specific fractures that are pathognomonic for child abuse.

Conclusions: WBMRI is a useful examination in the pediatric patient that is radiation free, quick and allows imaging of the entire body. It is an adjunct to dedicated MRIs to look for multifocality and extent of systemic diseases such as CRMO, osteonecrosis in patients on steroids and dermatomyositis. It has a great potential as a screening examination but at the same time can detect both the symptomatic and the asymptomatic lesions in the bone marrow and muscles that are otherwise not seen on conventional radiography. It also allows guidance for biopsy and monitors response to treatment.

Poster #: CR-018**Mobile “Cerebroliths” in Hemihydranencephaly: A Case Report**

Usha D. Nagaraj, MD, *The Ohio State University Medical Center*, usha.nagaraj@osumc.edu; Brent Adler

Purpose or Case Report: Hydranencephaly is a congenital central nervous system disorder manifested by the replacement of the cerebral hemispheres with a thin membranous sac filled with cerebrospinal fluid and necrotic debris. Hemihydranencephaly is an extremely rare brain condition in which the vascular anomaly is unilateral, with fewer than 10 cases previously reported in the literature. This is a case of a 4-month-old male who presented to the ophthalmologist for evaluation of possible leukocoria of the right eye. The patient had a history of a difficult vaginal delivery that required forceps delivery with possible associated trauma to the right eye. Dilated fundoscopic exam revealed retinal calcifications. This caused a clinical concern for retinoblastoma and CT and MRI of the orbits were obtained. CT demonstrated profound dilatation of the left lateral ventricle with only a thin rim of cortex surrounding it. There was some midline shift to the right with mild dilatation of the right lateral ventricle. The thalami and brainstem were spared. There were multiple soft tissue bodies that layered in the dependent portion of the left lateral ventricle, which were isodense to grey matter. MRI revealed similar findings consistent with hemihydranencephaly involving the left cerebral hemisphere. There were multiple round soft tissue masses that measured up to 1 cm in size that layered posteriorly in the left lateral ventricle. These masses were isointense to grey matter on T2 and hyperintense on T1. When the patient was placed with his head turned to the left, these masses moved to the dependent portion of the left lateral ventricle. The orbits were normal on both CT and MR. These soft tissue collections are presumed to be mobile collections of infarcted brain tissue. This unusual appearance has not been described in the radiology literature. We review the CT and MR findings and review the relevant literature.

Poster #: CR-019**Magnetic Resonance Imaging in Neonatal Citrullinemia Type I: Report of a Unique Case and Review of the Literature**

Usha D. Nagaraj, MD, *The Ohio State University Medical Center*, usha.nagaraj@osumc.edu; Jerome Rusin, Carly M. Dent, Kim L. McBride, Lynne Ruess

Purpose or Case Report: Citrullinemia type I is a rare inborn error of urea cycle metabolism resulting in hyperammonemia. In the classic form, the newborn presents with poor feeding, vomiting, progressive lethargy and signs of increasing intracranial pressure 3–7 days after birth, rapidly progressing to apnea, coma and death if left untreated. We present a case of a term infant who presented to the hospital on the 5th day of life with a typical history of poor feeding and profound hypotonia. Upon admission he had multiple episodes of apnea and hemodynamic instability prompting intubation and intensive support. Laboratory evaluation revealed multiple abnormalities, most notably, hyperammonemia (910 $\mu\text{mol/L}$) and elevated citrulline (>800 $\mu\text{mol/L}$). MRI of the brain performed on the 7th day of life showed findings consistent with term hypoxic ischemic encephalopathy with restricted diffusion in bilateral rolandic cortex and subcortical white matter, bilateral caudate heads and lenticular nuclei, bilateral insular cortex, and bilateral cerebral peduncles. The genu of the corpus callosum, bilateral deep frontal white matter, and the left parietal white matter also demonstrated restricted diffusion suggesting infarction secondary to thrombosis of deep intramedullary veins. An area of restricted diffusion in the right parietal cortex was suspicious for superficial venous infarct. Review of the literature reveals that this case of neonatal citrullinemia has unique MRI findings. While our patient had diffusion changes with some shared similarities to the previous two cases in the literature, there are also findings consistent with deep intramedullary venous thrombosis and infarction.

Poster #: CR-020**Duplicated Internal Auditory Canal: A Rare Anomaly of the Temporal Bone**

Ahmad Aouthmany, *University of Toledo Medical Center*, ahmad.aouthmany@utoledo.edu; Asif Abdullah

Purpose or Case Report: Duplicated internal auditory canal (IAC) is a rare anomaly of the temporal bone, which is usually associated with sensorineural hearing loss. Only a few cases have been previously described in literature. We describe an extremely rare case of duplicated right internal auditory canal in a six month-old patient with a history of Down syndrome. A six month-old male with Trisomy 21 presented with profound bilateral sensorineural hearing loss. The patient failed the newborn hearing screening tests. Past medical history was unremarkable for recurrent ear infections. On focused physical examination, the auricles were normal appearing. External auditory canals were patent bilaterally revealing clear and translucent tympanic membranes. Patient did not reveal a facial palsy. Subsequently,

a high resolution computed tomography (HRCT) of the temporal bone was performed. Duplicated appearance of the right internal auditory canal with separation of facial and vestibulocochlear segments was noted. The facial nerve canal demonstrated normal caliber while there was significant narrowing of the cochlear canal near the fundus. Significant stenosis of the vestibulocochlear segment of the duplicated IAC was identified at the porus acousticus. Dehiscent right posterior semicircular canal was also seen. An enlarged right vestibule was also noted. A single IAC was identified on the contralateral side with significant stenosis at the porus acousticus. High-resolution magnetic resonance imaging of IAC was recommended which revealed normal appearance of the bilateral cochlear and vestibular nerves. Duplication of the IAC is an extremely rare anomaly involving a redundant osseous canal extending from the cerebello-pontine angle through the otic capsule bone toward the labyrinth or cochlea. A duplicated IAC may or may not be associated with congenital sensorineural hearing loss secondary to aplasia or hypoplasia of the vestibulocochlear nerve. To evaluate for structural abnormalities that may preclude cochlear implantation, it is important to evaluate pediatric patients with sensorineural hearing loss radiologically. Although HRCT is the best imaging modality for evaluation of osseous IAC, the IAC contents are best viewed on MRI in oblique sagittal planes of the IAC using a 3-D volumetric steady state sequence.

Poster #: CR-021

Neuroimaging in Hemiplegic Migraine: Cases and Review of the Literature

Nicholas V. Stence, MD, *Children's Hospital Colorado—Radiology, nicholas.stence@childrenscolorado.org*; Sita Kedia, John A. Maloney, Jennifer Armstrong-Wells, Timothy Bernard

Purpose or Case Report: Hemiplegic migraine (HM) is a rare variant of migraine with aura. It is characterized by a motor deficit lasting up to 24 h that is fully reversible. Little neuroimaging data for HM exists in the literature. We report our experience with two pediatric cases of hemiplegic migraine. We also review published cases of pediatric HM with abnormal findings on neuroimaging.

Methods & Materials: Cases 1 and 2 presented to our institution with severe headache (HA), acute right-side weakness, aphasia, and altered mental status (AMS), which did not resolve after 24 h. Magnetic resonance imaging (MRI) and genetic testing are reviewed for these cases. The literature was reviewed for pediatric cases with neuroimaging changes during HM attacks.

Results: Initial MRI, including diffusion-weighted imaging (DWI), was negative in both patients within 24 h of onset. Repeat MRIs at 93 h (Case 1) and 75 h (Case 2) were both positive for mild hyperintensity on trace diffusion images, and corresponding reduced diffusion on ADC maps, involving regions of the cortex and juxtacortical white matter in left middle cerebral artery distributions. These findings completely resolved at 3 months in both cases. MR angiograms (MRA) were negative in both cases. Case 1 had a family history of migraines and was found to have an unreported mutation in ATP1A2 gene at a highly conserved location in vertebrates. Case 2 had a family history of HM and was found to have an indeterminant mutation in the CACNA1A gene. Infectious, metabolic and hypercoagulability work up was negative. Case 1 required inpatient rehabilitation and at 1 year follow up was requiring speech therapy. Case 2 resolved completely. In the literature, 6 cases of hemiplegic migraine with neuroimaging changes were reported. All cases had prolonged hemiplegic migraines (symptoms >24 h) and showed cerebral edema with or without restricted diffusion.

Conclusions: All eight HM cases in the literature with abnormal findings on neuroimaging had prolonged attacks. MRIs for our two cases and two cases reported in the literature were initially normal at admission. Mild swelling and restricted diffusion developed in our two cases after 24 h, and resolved on follow up MRIs. Subtle findings on diffusion and T2 imaging may lag behind the clinical picture in HM, therefore serial neuroimaging may be useful in individuals with prolonged symptoms. Most cases eventually show resolution clinically and on MRI.

Poster #: CR-022

Correlation of Neurosonographic Anatomy with Matching MR Scan Planes

Denise Castro, *Hospital for Sick Children, denisecastro22@gmail.com*; Pam Rasalingham, Omar Islam, Don Soboleski

Purpose or Case Report: New high-resolution MR sequences have allowed for exquisite anatomic detail and enables reconstruction of images in any scan plane desired. This ability allows for precise matching of MR image planes with the standard oblique coronal, sagittal and axial images obtained during routine neurosonography. The purpose of this poster is to correlate the morphology demonstrated on neurosonography with the MR image, utilizing this ability in order to enhance our understanding of the neuroanatomy distinguishable on sonographic imaging. We believe this will allow a better appreciation of the subtle differences in echotexture of neuroanatomic structures which are often ignored or overlooked on neurosonography and help improve our detection of subtle sonographic abnormalities.

Poster #: CR-023**Ectopic Cerebellum in the Posterior Cranial Fossa: Report of a Case and Review of the Literature**

Usha D. Nagaraj, MD, *The Ohio State University Medical Center, usha.nagaraj@osumc.edu*; Daniel Boue, Lisa Martin

Purpose or Case Report: Cerebellar heterotopia is a common congenital anomaly frequently encountered in the form of cell rests around the fourth ventricle. However, isolated well-differentiated cerebellar ectopia is extremely rare. Of the 8 previously reported cases in the literature, only 4 have presented as a discrete, extra-axial mass and none have been described in the posterior cranial fossa. We present a case of a 5-year-old male who initially presented with persistent daily headaches. Physical exam including a detailed neurologic exam was within normal limits. Non-contrast computed tomography (CT) of the brain was initially performed, demonstrating no abnormalities. Further work-up with magnetic resonance imaging (MRI) was performed, which revealed a well-defined, extra-axial mass superior to the cerebellum and inferior to the tentorium, immediately beneath the vein of Galen. The mass was isointense to grey matter on T1 and T2 sequences and there was no significant enhancement on post-contrast images. There was mass effect on the vermis and the cerebellar tonsils were displaced 3 mm below the foramen magnum. Neurosurgery was consulted and the mass was removed for diagnosis and treatment of the patient's symptoms. The mass was easily identified intra-operatively and gross total resection was accomplished successfully. Pathologic analysis of the mass revealed well-formed cerebellar tissue without evidence of neoplasia. To the best of our knowledge this is the only case of ectopic cerebellum presenting as a discrete extra-axial mass in the posterior cranial fossa. Our case shows that an extra-axial mass that parallels grey matter on all sequences can be a presentation of ectopic cerebellum. We describe the CT and MRI findings, surgical and histopathological results and review the relevant literature.

Poster #: CR-024**Pediatric Isodense Acute Subdural Hemorrhage**

Jeffrey S. Kao, MD, MSEE, *University of Kansas—Wichita, run4boston@gmail.com*; Debbie Desilet-Dobbs

Purpose or Case Report: The density (attenuation coefficient) of subdural hemorrhage (SDH) in computed

tomography (CT) is important in assessing the acuity of SDHs. An acute SDH is traditionally described as hyperdense and then becoming isodense in approximately 3 weeks when entering the subacute phase. In this report, we document the case of a pediatric patient with the new appearance of an acute SDH within 40 h of the prior CT that was isodense. Greater than 95% of the collection was isodense, with a small focus of hyperdensity. Acute SDHs are known to be isodense to gray matter in patients with anemia (WP Smith, *Am J Neuro-radiol* 1981). However, the hemoglobin and hematocrit was within normal limits. In addition, acute SDHs that are only a few hours old can have a mixed hyperdense and hypodense appearance because of uncoagulated blood before clotting takes place (J Provenzale, *AJR* 2007). Thus, an acute SDH can have an isodense appearance in a non-anemic patient. Radiologists should consider the possibility of an acute SDH with an isodense appearance, especially in case of possible non-accidental trauma where timing of an injury is important.

Poster #: CR-025**Undifferentiated Sarcoma of the Esophagus in an 11-year-old Male: Case Report and Radiologic/Pathologic Correlation**

Michael E. Daniel, MD, *UT Southwestern / Children's Medical Center Dallas, michael.daniel@utsouthwestern.edu*; Lisa Sutton, Sandy Cope-Yokoyama, Neil J. Fernandes

Purpose or Case Report: Mesenchymal neoplasms of the gastrointestinal (GI) tract occur infrequently in the adult and are extremely rare in the pediatric population. The occurrence of these lesions in the esophagus is limited to a collection of case reports in the available literature. Most esophageal mesenchymal tumors in the pediatric GI tract are benign leiomyomas. The vast majority of malignant mesenchymal tumors in children are categorized as either sarcomas or gastrointestinal stromal tumors (GIST). We report a case of a high grade undifferentiated sarcoma of the distal esophagus in an 11-year-old male. While this tumor most closely resembles a GIST, the immunohistochemical profile of the lesion is not typical of any distinct mesenchymal neoplasm. A review of the literature demonstrates a single case report of a likely benign undifferentiated mesenchymal neoplasm of the distal esophagus in an adolescent. To our knowledge, this is the first reported case of an undifferentiated esophageal sarcoma in a pediatric patient. We provide radiologic and pathologic features of the above lesion, and review the typical imaging and pathologic characteristics of mesenchymal GI neoplasms.

Poster #: CR-026

Potential Airway Management Issues in Sedated Children
Kimberly Fagen, MD, MS, *Children's National Medical Center*; kfagen@childrensnational.org; Nadja Kadom, Ira Cohen

Purpose or Case Report: Many pediatric imaging studies require sedation. It has been shown that a variety of health care professionals other than anesthesiologists may provide sedation, including advanced practice registered nurses, nurse practitioners, physician assistants, fellow level trainees, emergency medicine physicians, intensivists, pediatricians and, last but not least, radiologists. Moderate sedation, also called “conscious sedation”, does generally not require an anesthesiologist as there is usually adequate spontaneous ventilation and no airway intervention required. However, in case of a complication during the imaging study intubation may become necessary. For patients with certain congenital or acquired conditions emergent intubation may be very difficult and should be brought to the attention of an anesthesiologist prior to inducing moderate sedation. The four “D’s” is a quick way to assess potentially difficult airways that necessitate consultation with anesthesia prior to moderate sedation: Dentition (incisor/tooth size, dental alignment, and macroglossia), Distortion (swelling from infection, tumor, or trauma), Disproportion (hyoid-chin ratio, such as with micrognathia), and Dysmobility (jaw or cervical spine movement issues, i.e. trauma or atlanto-occipital instability). Presence of some of these features may be an indication to consider general anesthesia for sedation; at the very least, anesthesiologist’s awareness of a potentially difficult intubation adds to patient safety during moderate sedation.

Methods & Materials: Case 1: Severely enlarged adenoids and tonsils (may appear to obstruct the airway, but usually not a problem). Case 2 (Dentition): a. Example of Macroglossia b. Mallampati Scale Case 3 (Distortion): a. Example of retropharyngeal abscess b. Example of large plexiform neurofibroma Case 4 (Disproportion): a. Example of micrognathia in a patient with Pierre-Robin Syndrome Case 5 (Dysmobility): a. Example of jaw trauma with hematoma b. Down’s patient with atlanto-occipital instability

Poster #: CR-027

CT and MR Findings of Pulmonary Lymphangiomas
Shivani Ahlawat, MD, *Children's National Medical Center*; ahlawash@gmail.com;

Purpose or Case Report: Lymphangiomas describes the presence of multiple lymphangiomas often with multiorgan involvement; typically bones, spleen, mediastinum and

lungs. Although lymphangiomas has been described in patients ranging from birth up to 80 years, it most frequently presents in childhood. The lesions can occur in any tissue in which lymphatics are normally found, with a predilection for neck and chest involvement. The clinical presentation is variable including pleural or pericardial effusion, hemoptysis, protein wasting enteropathy, peripheral edema, hemihypertrophy and disseminated intravascular coagulopathy. The coexistence of lytic bone lesions and chylothorax serves as an important diagnostic clue. We describe typical radiographic, CT and MRI findings in the appropriate clinical setting that narrow the differential diagnosis and raise concern for this rare entity as the etiology for the patient’s symptoms.

Methods & Materials: We report a 12-year-old girl and 2-year-old boy with pulmonary lymphangiomas with typical presentation and imaging findings.

Results: Bilateral interstitial infiltrates, pericardial and pleural effusions are evident on chest radiograph. Sampling of the pleural fluid demonstrates chylous effusion. CT scans of the thorax reveal diffuse smooth thickening of interlobular septa and bronchovascular bundles with extensive infiltrative involvement of mediastinal fat. Osseous and splenic lesions are demonstrated both on CT and MR. Differential diagnosis includes interstitial edema, lymphoma and sarcoidosis.

Conclusions: The natural history of pulmonary lymphangiomas is characterized by progressive growth and compression of adjacent structures. Therapy should aim to decrease the compressive effects, to control chylous effusions, and to maintain cosmesis. The success of surgical resection is limited by inability to separate lymph collections from normal structures. Characteristic clinical and radiographic presentation, chylothorax, and extrathoracic lymphatic dysfunction should prompt a consideration of lymphangiomas and prevent delay in diagnosis.

Poster #: EDU-001

Aortic Arch Congenital Anomalies: What the Radiologist Needs to Know

Luana Stanescu, *Radiology, Seattle Children's Hospital*, stanescu@u.washington.edu; Stephen Done

Purpose or Case Report: 1. Review classic imaging findings in congenital aortic arch anomalies which can improve detection on radiographs and barium esophagogram 2. Describe pertinent embryologic basis of the radiologic findings 3. Describe correlative imaging findings on CT and/or MRI in dedicated cases 4. Describe common diagnostic pitfalls

Methods & Materials: After obtaining institutional IRB approval we reviewed various patients presentations with this condition and analyzed images to characterize this

particular entity and its manifestations for better definition of diagnostic criteria.

Results: Radiographs and barium esophagogram: algorithmic approach in reviewing chest radiographs in order to improve detection of aortic arch anomalies; classic findings and common pitfalls. Cross-sectional imaging (CT and MRI): What the surgeons need to know before surgical repair; detection of associated cardiac anomalies. Sample cases: double aortic arch, double aortic arch with complete or partial atresia of one of the arches.

Conclusions: Major teaching points of this exhibit are: 1. Review of classic features of congenital aortic anomalies on radiographs, esophagogram, CT and MRI with pertinent embryologic basis 2. Describe the utility of various imaging modalities in congenital aortic anomalies, emphasizing common pitfalls.

Poster #: EDU-002

Cardiovascular and Mediastinal Imaging in Children with Unexpected Clinical Presentation

Shunsuke Nosaka, MD, Radiology, National Center for Child Health and Development, nosaka-s@nchd.go.jp

Purpose or Case Report: Children with cardiovascular and mediastinal diseases can be congenital or acquired in etiology. They usually present with straightforward clinical course. In certain situation, however, some of the children show unexpected clinical presentation predominantly with those of neighboring organs such as respiratory tract, hepatobiliary system, and gastrointestinal tract. These unexpected presentations can be the cause of delay in proper diagnosis and treatment. The purpose of this exhibit is demonstrate a variety of imaging findings of cardiovascular and mediastinal diseases in children with unexpected clinical presentation.

Methods & Materials: This exhibit is case based presentation of cardiovascular and mediastinal imaging in children including tips, pitfalls and lessons learned among patients presented with unexpected clinical presentation. Diagnostic imaging modalities for cardiovascular disease usually consist of various combinations of plain radiography, ultrasound, CT, MR imaging, fluoroscopy, nuclear medicine, and angiography. The general concept of ALARA—as low as reasonably achievable—should always be utilized when radiation-producing modalities are indicated in children.

Results: The diseases included will be double aortic arch found during workup for the cause of aspiration pneumonia, unilateral pulmonary vein atresia presented with recurrent episodes of pneumonia, severe mitral regurgitation secondary to chordal rupture mimicking fluminant hepatic failure, myocarditis initially present as acute abdomen, cardiomyopathy as unusual initial presentation of

neuroblastoma, and thymolipoma mimicking gradual development of cardiomegaly.

Conclusions: It is important for radiologist to be familiar with imaging findings of cardiovascular and mediastinal diseases in children with unexpected clinical presentation.

Poster #: EDU-003

Cardiac Embryology Made Easy: A Novel Teaching Approach Using Claymation

Andrew Phelps, Children's Hospital Boston, aphelpsm@gmail.com;

Purpose or Case Report: Congenital heart disease can be an intimidating subject for radiology residents, and cardiac embryology is key to its understanding. However, this can be an equally intimidating topic to teach! Various diagrams and animations are available in textbooks and online, but much like advanced origami, many of these resources suffer from being visually too complex for the first-time learner. To overcome this teaching obstacle, I created my own cardiac embryology animations using modeling clay and incorporated them into a comprehensive didactic lecture on congenital heart disease.

Methods & Materials: Cardiac embryology animations were created using modeling clay, a digital camera, and Microsoft PowerPoint. Surface and cross-sectional views were generated, depicting the key events in cardiac embryology: heart tube formation, cardiac looping, chamber division, truncus arteriosus division, and pulmonary venous connection. Example models are shown in Figure 1.

Results: In this lecture, the animations are presented alongside actual embryonic heart photographs. The lecture then uses the embryology knowledge as a basis to explain the common congenital heart diseases and their MRI appearances. Examples of septal defects, ventricular hypoplasia, and transposition of the great arteries are presented, among others.

Conclusions: Understanding cardiac embryology is required in order to approach congenital heart disease in a logical fashion. Modeling clay animations are a cheap and easy way to simplify this complex topic.

Poster #: EDU-004

Arterial Tortuosity Syndrome: An Introduction to the Clinical and Radiologic Manifestations in the Pediatric Population

Neal Desai, UMKC SOM, neal540@gmail.com; Suchit Patel, Ayushi Gupta, Marius Hubbel, Doug Rivard

Purpose or Case Report: 1. To describe the clinical findings of Arterial Tortuosity Syndrome and give a brief

discussion of the disease process. 2. To describe the radiologic manifestations of Arterial Tortuosity Syndrome. 3. To give a brief discussion of Loeys-Dietz Syndrome—a disease with similar arterial findings, but with unique molecular characteristics from Arterial Tortuosity Syndrome. 4. To use this knowledge to help establish the diagnosis and reduce mortality.

Methods & Materials: Arterial Tortuosity Syndrome Overview • Epidemiology • Molecular basis • Pathophysiology • Review of signs, symptoms and presentation • Brief discussion of treatment Differential Diagnosis of Arterial Tortuosity Syndrome • Loeys-Dietz Syndrome—similarities and differences Radiologic Findings and Discussion • Chest Radiograph • Computed Tomographic Angiography • Magnetic Resonance Angiography—Neck • Magnetic Resonance Angiography—Head • Conventional Angiography Making a Diagnosis • Sample case report • Review questions

Conclusions: Arterial Tortuosity Syndrome is a rare disease whose chief manifestation is severe cardiovascular connective tissue defects. Due to the nature of these defects and the significance of rapid intervention, it is important to be aware of and recognize the radiologic manifestations associated with Arterial Tortuosity Syndrome in the presence of appropriate clinical history to help offer a better prognosis to the patient.

Poster #: EDU-005

Dynamic Pulmonary Computed Tomography for Evaluation of Cardiopulmonary Disease

Shilpa V. Hegde, MD, *Arkansas Childrens Hospital, University of Arkansas, shilpavhegde@gmail.com*; S. Bruce Greenberg

Purpose or Case Report: Dynamic pulmonary computed tomography (DPCT) is a wide-detector CT technique that allows for continuous chest imaging during respiration. When combined with intravenous contrast, the technique is a unique tool for evaluation of cardiopulmonary abnormalities in children with cardiopulmonary abnormalities. The purpose of this poster is to illustrate the technique of DPCT for evaluation of cardiopulmonary disease in children with congenital heart disease and persistent respiratory distress.

Methods & Materials: Methods and Materials: 8 DPCT exams with intravenous contrast were performed on 5 infants with a history of congenital heart disease and palliative surgery. Four continuous 350 msec gantry rotations were obtained with respiratory rates set at 40/minute. The imaging was accomplished during the time of a single respiratory cycle. 80 kVp and low mA resulted in effective dose

of ≈ 1.5 mSv. Eight respiratory phases were reconstructed to create 3D and MPR cine loops for evaluation of cardiopulmonary abnormalities.

Results: Cardiopulmonary abnormalities were detected in all patients. Patency of Sano shunt, Blalock Tausig shunt or patent ductus arteriosus stent was established. Intimal thickening was identified in one Sano shunt. Hypoplastic branch pulmonary arteries were present in 3 infants and pulmonary vein thrombosis in 1 infant. Left bronchomalacia was identified in four of five infants and best or only identified on the expiratory phase of respiration. Left lung air trapping was present in two patients.

Conclusions: DPCT with intravenous contrast is the ideal study for evaluation of the post-operative infant with congenital heart disease and persistent respiratory distress.

Poster #: EDU-006

The Role of Low-Dose CT Angiography in the Evaluation of Renovascular Hypertension in Children

Jessica Kurian, MD, *CHOP, kurianj@email.chop.edu*; Monica Epelman, Kassa Darge, Els Nijs, Jeffrey Hellinger

Purpose or Case Report: Historically, the evaluation of renovascular hypertension has been accomplished via US and conventional angiography. Based on the reported adult experience we introduced renal CT angiography (CTA) for the evaluation of renovascular hypertension in mid-2006. Our Institution has a robust, well-established protocol, which results in reproducible, high quality images. We aim to present our imaging strategies for the evaluation of these patients and to discuss and illustrate the role of low-dose CTA with 3-D imaging as a noninvasive alternative in the evaluation of pediatric renovascular hypertension.

Methods & Materials: We used our department information system to identify pediatric patients (< 18 years of age) who had documented renovascular hypertension confirmed either by conventional angiography and/or surgery during a 5-year period. We present our protocol and discuss the indications, limitations and benefits of renal CTA. CT thin slice data, obtained employing dose reduction strategies, was reviewed and reconstructed in 2D and 3D renderings. Pertinent US and MR studies as well as demographic and clinical data were reviewed and recorded. Several causes for renovascular hypertension were documented and relevant CT angiographic findings were selected for presentation.

Results: Radiation dose ranged 0.58–4 mSv. Fibromuscular dysplasia was the most common diagnosis followed by neurofibromatosis type 1. Vascular pathology included stenoses, beading, occlusions, and aneurysms. Disease was noted in the extraparenchymal renal arteries in approximately 70% of the cases.

Conclusions: The choice of the imaging modality for the investigation of renovascular hypertension in pediatric patients remains controversial. In the authors' experience, CTA with 3-D imaging is a valuable, non-invasive diagnostic tool for the evaluation of pediatric renovascular hypertension. Low dose protocols can reduce the radiation exposure associated with CT. This method can spare patients the complications associated with conventional angiography.

Poster #: EDU-007

Fetal MRI: Brain, Head and Neck Malformations—A Pictorial Essay

Sumit Singh, MD, *Children's Hospital of Wisconsin, sumitsingh78@yahoo.com*; Mohit Maheshwari, Teresa C. Gross Kelly, Tushar Chandra, Ibrahim S. Tuna, Craig Johnson

Purpose or Case Report: The purpose of the exhibit is to illustrate various brain, head and neck masses/vascular anomalies on fetal MRI. We will also briefly discuss the normal fetal brain anatomy as seen on fetal MRI.

Methods & Materials: Major indications for fetal MRI include evaluation of inconclusive sonographic findings in cases of CNS malformations. In our institute patients are scanned on 1.5 T MR Scanner. A body surface six channel phased array coil is used to maximize signal to noise. All the scans are checked by a neuroradiologist to make sure adequate 3 plane imaging of the brain or other lesion in question were performed. 3 plane scanning of the fetal body is also performed for the laterality determination of the lesion and also screen for other congenital anomalies.

Results: Prenatal USG is frequently inconclusive for evaluation of complex fetal brain and head and neck anomalies. Most studies suggest that MRI after first trimester is safe. In addition, advent of rapid MRI sequences like single shot fast spin echo (ssFSE) have helped in reducing scan time and motion artifacts leading to availability of diagnostic quality images. These have led to increasing use of MRI as supplemental tool to further investigate inconclusive fetal sonographic findings. MRI provides better anatomical delineation of these complex abnormalities. It helps in making appropriate diagnosis with high confidence and aids in appropriate obstetric and prenatal/neonatal surgical planning or intervention. This educational exhibit will illustrate few common fetal anomalies. These will include agenesis of corpus callosum, malformation of cortical development, posterior fossa malformations, ventriculomegaly, in-utero stroke, orbital abnormalities and some fetal neck masses/vascular malformation. Correlation and confirmation with the postnatal MRI will also be provided for some cases.

Conclusions: Technical and therapeutic advances have driven the development of fetal MRI. It is an important adjunctive

tool for prenatal imaging in those instances in which a complex anomaly is suspected by sonography, when fetal surgery is contemplated, or when a definitive diagnosis cannot be determined. It has prognostic implications and may help in optimal and timely obstetric and neonatal management.

Poster #: EDU-008

Peridiaphragmatic Pulmonic Sequestration: Fetal MRI Appearance and Clues to the Diagnosis

Amaya M. Basta, *University of California, San Francisco—Department of Radiology, amaya.basta@ucsf.edu*; Jesse Courtier, Tippi Mackenzie, John D. MacKenzie, Fergus V. Coakley

Purpose or Case Report: This educational report will provide a review of the imaging appearance of intradiaphragmatic and subdiaphragmatic pulmonary sequestrations on fetal MRI. The proposed pathophysiology, review of sequestration subtypes, and surgical management options will also be described. Case examples will be provided to illustrate the fetal MR imaging findings of these variants of pulmonary sequestration that help support the diagnosis. Specifically a “triangle sign” of T2 hyperintense tissue directed toward the diaphragm will be demonstrated. Illustrative case examples will be placed in the context of a differential diagnosis for subdiaphragmatic masses seen on prenatal imaging. Imaging signs that help make a diagnosis of these pulmonary sequestration variants and separate this entity from other lesions will be emphasized.

Poster #: EDU-009

MRI of the Fetal Head and Neck Masses

Alok Jaju, MD, *Mallinckrodt Institute of Radiology, alokjaju@gmail.com*; Joshua Shimony, Per Amundson

Purpose or Case Report: Fetal magnetic resonance imaging (MRI) is a useful problem solving tool for abnormalities detected by prenatal ultrasound (US). Masses of the head and neck region can vary from benign incidental lesions to devastating neurological lesions and life threatening tumors. We share our experience in characterizing these lesions by prenatal MRI, that can have a bearing on follow up imaging, perinatal management and overall prognosis.

Methods & Materials: We did a retrospective review of all fetal MRI studies performed at our tertiary care Children's hospital between 11/2002 and 06/2011, to identify fetuses with head and neck masses. We reviewed the maternal demographic and clinical data, prenatal ultrasound, fetal outcomes and post natal imaging (when available).

Results: Out of the 351 fetal MRI studies, 20 had dominant head and neck masses. Majority were encephaloceles (9 occipital, 1 parietal). The remaining included variety of masses such as nasal glioma, teratoma (3), epidermoid cyst, hemangioma and lymphatic malformation (3). MRI played a useful role in distinguishing encephaloceles from other masses based on underlying bone defect and intracranial extension. It also helped in characterizing other masses based on location and signal characteristics. The presence and degree of airway compromise was determined. Intracranial anomalies associated with encephaloceles including callosal dysgenesis, cerebral and cerebellar hypoplasias, migrational disorders and spinal anomalies were also correctly identified.

Conclusions: We present the prenatal MR imaging findings of a spectrum of head and neck lesions, correlating with prenatal ultrasound, postnatal imaging and clinical or pathological outcomes.

Poster #: EDU-010

Neonatal Hypoxia Ischemia: Comparison Between Cranial Ultrasound and Magnetic Resonance Performed Within a 24-hour Interval

Maria R. Ponisio, MD, Mallinckrodt Institute of Radiology;
Robert McKinstry

Purpose or Case Report: The immaturity of the CNS in neonatal infants makes neurologic assessment difficult. Neuroimaging plays an essential role in the assessment of brain injury by helping to identify the injury and expected neurologic outcome. Cranial ultrasound (US) is usually the first neuroimaging modality used since the technique is portable, does not involve radiation and can be used sequentially. Magnetic resonance imaging (MRI), however, is the most sensitive imaging modality for the detection of hypoxic brain injury. The goal of this presentation is to compare the US and MRI performed within a 24-hour interval, and evaluate these findings to improve the interpretation of the US which is usually the first methodology used to evaluate these patients.

Methods & Materials: We performed a retrospective review of the neonatal imaging studies with US and MRI performed within 24-hour interval on 72 preterm and term newborns with clinical history of hypoxia-ischemia. The imaging findings of the two modalities, MRI and US, were correlated with the pattern and severity of the injury and brain maturity.

Results: Diffuse white matter abnormalities were observed in 60% of the patients by US or MRI. The ultrasound identified diffuse increased echogenicity which did not show correlation with MRI in 30% of patients. Focal white matter abnormalities were better identified by MRI on non-cavitary leukomalacia which is the most common PVL observed in premature neonates with low birth weight and the most

difficult to identify using US. Cavitary leukomalacia showed strong agreement in both methodologies. The MRI identified 6% more cases of intraventricular hemorrhage, however, the corresponding increase in hemorrhage was of minimal clinical significance. In most cases extra axial hemorrhage was better identified by MRI.

Conclusions: After viewing this exhibit, the viewer will gain a better appreciation and understanding of the neuroimaging characteristics of hypoxia-ischemia in US and MRI, and thus improving the interpretation of the US which is usually the first imaging modality used to evaluate this patient population.

Poster #: EDU-011

Unusual Thoracic Lesions on Fetal Magnetic Resonance Imaging

Erica Poletto, MD FRCPS(C), Department of Radiology, Children's Hospital of Philadelphia, eweinberg2@hotmail.com; Teresa Victoria, Sandra S. Kramer, David A. Mong, Ann Johnson

Purpose or Case Report: The most common thoracic lesions found on prenatal imaging, congenital pulmonary airway malformation (CPAM), bronchopulmonary sequestration (BPS), and congenital diaphragmatic hernia (CDH), usually have characteristic imaging findings previously described in detail. However, common entities presenting with atypical findings and rarer thoracic entities do occur and can be characterized by fetal magnetic resonance (MR) imaging. The purpose of this educational exhibit is to show examples of atypical presentations of common thoracic lesions and more unusual thoracic entities on fetal MR. When applicable, prenatal MR is compared with prenatal ultrasound, postnatal imaging, operative findings, or pathology.

Methods & Materials: Using a radiology information system database, the reports of all fetal MR exams at our institution from January 2005 through January 2011 were reviewed. When unusual thoracic findings were described in the report, all prenatal and postnatal images (when available) were evaluated. In the cases selected, medical charts were reviewed for operative findings and pathologic reports.

Results: The cases to be described, both pulmonary and extrapulmonary in location, include: hybrid lesion in a horseshoe lung, CPAM extending across the midline, bilateral BPS, BPS located within the mediastinum, BPS located within the leaves of the diaphragm, ectopia cordis and CDH as components in Pentalogy of Cantrell, CDH with herniation of liver into the pericardium, elongated esophageal duplication cyst, chest wall lymphatic malformation, and tight double aortic arch causing congenital high airway obstruction syndrome (CHAOS).

Conclusions: After studying this educational exhibit, the reader will be acquainted with a variety of unusual fetal pulmonary and extrapulmonary lesions, with emphasis on fetal MR.

Poster #: EDU-012

Prenatal and Postnatal Imaging Findings in Megacystis-Microcolon-Intestinal Hypoperistalsis Syndrome (MMIHS)

Mary Kitazono, *CHOP, mkitazono@gmail.com*; Richard Bellah

Purpose or Case Report: To review the classic constellation of findings seen in prenatal and postnatal imaging of Megacystis-Microcolon-Intestinal-Hypoperistalsis Syndrome (MMIHS), as well as to illustrate additional imaging features that are variably seen in this syndrome.

Methods & Materials: The imaging database at our children's hospital was searched for all cases of MMIHS diagnosed since 2002. All available prenatal and postnatal imaging studies were reviewed in patients with a diagnosis of MMIHS, and representative images are provided with a description of the findings.

Results: Since 2002, 6 patients (5 girls, 1 boy) have been diagnosed with MMIHS at our institution, including 4 on prenatal MRI and US. The characteristic prenatal imaging findings include marked urinary bladder distension, bilateral pelvicaliectasis, and dilated, tortuous ureters, as well as a diminutive colon containing no or minimal T1W-hyperintense meconium on MRI. Postnatal imaging studies also characteristically demonstrate a massively distended urinary bladder (with no apparent mechanical cause of obstruction) as well as a small, unused colon with dilated, hypoperistaltic small bowel seen proximal to the microcolon. Additional findings which are variably seen include intestinal malrotation, stomach and esophageal hypoperistalsis or aperistalsis, gastroesophageal reflux, and biliary stasis.

Conclusions: Although a rare syndrome, the constellation of imaging findings in MMIHS is pathognomonic, and recognition of the classic pattern of findings can allow the radiologist to make a diagnosis of MMIHS in both the in-utero and postnatal setting. Early diagnosis is essential for allowing prenatal counseling regarding this generally fatal disorder, as well as to optimize early management options.

Poster #: EDU-013

A Pictorial Essay: Pediatric Gastric Mass Lesions

Khalid Khashoggi, MD, *Radiology, British Columbia Children's Hospital, khalidkhashoggi@gmail.com*; Rui Santos, Angela T. Byrne, Heather Bray, Helen R. Nadel, Douglas Jamieson

Purpose or Case Report: Gastric mass lesions are uncommon. This presentation is an educational review of pediatric gastric mass lesions including gastro-intestinal stromal tumor (GIST), inflammatory myofibroblastic tumor (pseudotumor), Burkitt's lymphoma, squamous cell carcinoma, gastric teratoma, gastric varices, gastric hamartoma, gastric polyp and hypertrophic pyloric stenosis (HPS). Clinical presentation is varied with upper GI bleeding, feeding intolerance, pain, weight loss and fatigue manifesting. The imaging work-up might initially have been endoscopy or ultrasound. Cross section imaging (CT/MR) can be invaluable. The role and impact of FDG PET on the management, staging and follow up of the oncologic pathology will be emphasized.

Poster #: EDU-014

Imaging Findings in Megacystic Microcolon Intestinal Hypoperistalsis Syndrome, A Rare Disease

Kiery Braithwaite, *Pediatric Radiology, Emory—Egleston, kieryb@yahoo.com*; Kiery Braithwaite, Paula Dickson, Marianne M. Ballisty

Purpose or Case Report: Megacystis microcolon intestinal hypoperistalsis (MMIH) syndrome is a rare congenital form of severe functional intestinal obstruction which is more commonly found in females. The presenting clinical and imaging features of this disease can often mimic other causes of proximal bowel obstruction in the neonate. In combination with its common association with intestinal malrotation, the clinical picture of MMIH syndrome may be confusing at times. Awareness of additional imaging features characteristic of MMIH syndrome may help the radiologist suggest this diagnosis. The purpose of this study is to enhance the ability of the pediatric radiologist to suggest this rare diagnosis by recognizing this unusual constellation of imaging features.

Methods & Materials: We retrospectively reviewed the clinical data and imaging studies of four patients with MMIH syndrome at our institution. Imaging studies included plain radiography, ultrasonography, fluoroscopy, and cross sectional imaging. The initial presentation and clinical outcome was also reviewed.

Results: The clinical presentations of our patients, who were all female, were somewhat varied but typically included symptoms of intestinal obstruction. The diagnosis of MMIH syndrome was made in our patients from the first few weeks of life through early childhood. The four patients demonstrated imaging features characteristic of this disease including a very large dilated bladder, severe bilateral hydronephrosis, gaseous distention of the stomach and proximal small bowel, intestinal hypoperistalsis, and a very small colon. The clinical course of these patients that we observed was also quite variable, with some patients dying in neonatal period while

another patient continues to do reasonably well at 14 years old after a multi-organ transplant.

Conclusions: MMIH syndrome is a rare and frequently lethal disease. The ability of the pediatric radiologist to recognize this constellation of imaging findings can help the clinical team arrive at a diagnosis of MMIH syndrome. More prompt diagnosis can aid in the development of a long term management plan for the patient and in counseling the family regarding the prognostic implications of this disorder.

Poster #: EDU-015

Pathologies of Omphalomesenteric Duct Remnant: Radiologic-Surgical Correlation

Swapnil Bagade, MD, *Pediatric Radiology, Mallinckrodt Institute of Radiology, bagades@mir.wustl.edu*; Geetika Khanna, Rebecca Hulett

Purpose or Case Report: 1. To facilitate understanding of embryology of the omphalomesenteric(vitelline) duct and normal anatomy of the umbilicus. 2. Review the spectrum of omphalomesenteric duct malformations and diversity of clinical presentations of these remnants. 3. Illustrate the imaging findings of omphalomesenteric remnants, from the common such as Meckel's diverticulum to the uncommon such as the omphalomesenteric duct cyst, with surgical correlation.

Methods & Materials: Cases with complications of persistent omphalomesenteric duct were collected from the joint surgery/radiology conferences at a tertiary level children's hospital. Imaging features were correlated with intraoperative findings.

Conclusions: Preoperative diagnosis of complications related to the omphalomesenteric duct remnants can be challenging because clinical and imaging features overlap with other etiologies of acute abdomen. Knowledge of the embryologic, clinical, radiologic, and surgical characteristics of omphalomesenteric duct remnants will aid in early and accurate diagnosis.

Poster #: EDU-016

Neonatal Bowel Obstruction—A Pictorial Essay

Tanmay Patel, *University of Kentucky*; Harigovinda Challa

Purpose or Case Report: Bowel obstruction is the most common abdominal emergency in the newborn period and in most cases is secondary to a congenital anomaly requiring early surgical intervention. However not every case of abdominal distension or dilated bowel is secondary to mechanical bowel obstruction or underlying surgical condition.

Radiologic imaging forms a central role in the work up of newborns with suspected intestinal obstruction. The role of the radiologist is to identify whether or not mechanical obstruction is present; if obstruction is identified on initial radiographs, to determine the level of obstruction, and finally to identify the etiology of obstruction. Initial plain radiographic evaluation also helps to determine the subsequent diagnostic or therapeutic approach.

Methods & Materials: A retrospective review of multiple radiographic and fluoroscopic examinations in patients with diagnosis of neonatal bowel obstruction was performed at Kentucky Children's Hospital. Multiple examples of classical imaging findings were compiled and placed into a pictorial review.

Results: Neonatal intestinal obstruction generally presents with nonspecific symptoms such as abdominal distention, vomiting, or failure to pass meconium depending on the level of obstruction and time of occurrence of underlying congenital lesion/atresia in the intrauterine life. Initial plain radiographs of the abdomen reveal dilated bowel loops when obstruction is present. High intestinal obstruction is suspected when only few dilated loops are identified, while multiple dilated bowel loops are seen in low obstruction. Most cases of high obstruction may not need another diagnostic imaging test. All cases of distal intestinal obstruction require water soluble enema to identify the etiology of obstruction. In conditions like functional immaturity of the colon, and meconium ileus water soluble enema is therapeutic and thus surgery can be avoided in most cases. The objective of this presentation is to present an educational exhibit of classical imaging findings of various types of neonatal bowel obstructions, and how to differentiate between them.

Conclusions: Bowel obstruction is the most common abdominal emergency in the new born period. Most cases are secondary to a congenital surgical condition and early diagnosis and treatment significantly reduces mortality and morbidity. Radiographic evaluation plays a central role in the diagnosis and treatment of these conditions.

Poster #: EDU-017

3D T2-Weighted MRCP in the Pediatric Population—A Pictorial Review

Nathan Egbert, MBBS MPH, *University of Michigan, nathaneg@med.umich.edu*; Jonathan R. Dillman, Peter J. Strouse

Purpose or Case Report: To demonstrate the utility of 3D T2-weighted magnetic resonance cholangiopancreatography (MRCP) in the pediatric population, and to illustrate the MRCP findings of various conditions affecting in the pediatric pancreaticobiliary system.

Methods & Materials: We identified all MRCP exams performed on pediatric patients (< 18 years of age) from January 1, 2000 through August 1, 2011 by searching institutional electronic medical records. We then identified representative 3D T2-weighted MRCP images of various conditions affecting the pediatric pancreaticobiliary system.

Results: Representative 3D T2-weighted MRCP images (including source, maximum intensity projection, and volume rendered images) from the following conditions will be presented: abnormal biliary narrowing/stricture (including sclerosing cholangitis, anastomotic strictures following Kasai procedure & liver transplantation, and “pseudosticture”), biliary atresia, choledochal cyst (including various subtypes, based on Todani classification), choledocholithiasis & cholelithiasis, congenital anomalies of the pancreaticobiliary system (including pancreas divisum and anomalous pancreaticobiliary junction), pancreatobiliary system trauma (including main pancreatic duct transection), and other rare conditions affecting the pancreaticobiliary system (including rhabdomyosarcoma of the biliary tree).

Conclusions: 3D T2-weighted MRCP has become an extremely useful tool in the evaluation of children with suspected disorders of the pancreaticobiliary system. Since MRCP has distinct advantages over alternative diagnostic techniques, such as endoscopic retrograde cholangiopancreatography (ERCP) or percutaneous cholangiography, including lack of ionizing radiation and noninvasiveness, MRCP is a much preferred initial study for pediatric pancreaticobiliary imaging. This pictorial review is intended to highlight the 3D T2-weighted MRCP appearances of various pancreaticobiliary conditions occurring in the pediatric population.

Poster #: EDU-018

Role of MRI Diffusion-Weighted Imaging in Pediatric Inflammatory Bowel Disease: A Pictorial Review

Elon Granader, MD, *Division of Pediatric Radiology, University of Michigan Hospital and Health Systems, egranade@med.umich.edu;* Jonathan R. Dillman, Ajaykumar Morani, Kelly K. Horst, Mahmoud Al-Hawary, Peter J. Strouse

Purpose or Case Report: Magnetic resonance enterography (MRE) is rapidly emerging as an important imaging tool for the diagnosis and follow-up of inflammatory bowel disease (IBD). Its lack of ionizing radiation makes this imaging modality especially vital to the pediatric population. Using a case-based approach, we will demonstrate the usefulness of diffusion-weighted imaging (DWI) as part of a comprehensive MRE protocol for the assessment of IBD in children.

Methods & Materials: The basics of DWI will be discussed with particular attention to abdominopelvic techniques. The

role of MRE DWI for the evaluation of pediatric Crohn disease (CD) and ulcerative colitis (UC) will be reviewed using a case-based approach. Key images from pertinent imaging studies will be identified by searching institutional electronic medical records and presented with relevant clinical data.

Results: A review of pediatric MRE examinations suggests DWI can be used to detect the following: 1) small and large bowel segments affected by IBD (both CD and UC) 2) abdominopelvic abscesses (including within the mesentery, body wall, iliopsoas muscle, and liver) 3) abnormal lymph nodes 4) sacroiliitis 5) perianal disease (including abscesses and other penetrating complications).

Conclusions: DWI has the potential to play a very important role in the diagnosis and follow-up of pediatric IBD. This MRE technique is particularly useful for detecting a variety of disease-related complications. As the exact meaning of bowel wall restricted diffusion is poorly understood to date, continued investigation will be necessary to determine the clinical and histologic significance of this finding.

Poster #: EDU-019

Gastrointestinal Manifestations of Cystic Fibrosis in the Pediatric Patient: An Imaging Exhibit From the Fetus to The Young Adult

Lily Wang, MD, *Cincinnati Children's Hospital Medical Center, lily.wang@cchmc.org;* Arnold C. Merrow, Daniel J. Podberesky, Steven Kraus, Maria A. Calvo-Garcia

Purpose or Case Report: To review the spectrum of clinical and imaging manifestations of cystic fibrosis (CF) involving the pediatric gastrointestinal (GI) system.

Methods & Materials: Cases of CF involving the GI tract were collected from clinical workflow encounters of the authors and from the main hospital medical records database. Relevant imaging studies were reviewed for known GI manifestations of CF. These imaging studies were correlated with clinical histories and available intraoperative and pathologic findings.

Results: CF involvement of the GI tract presents over a wide range of ages, organs involved, and associated symptoms. These manifestations can generally be divided anatomically into those involving the alimentary tract, hepatobiliary system, and pancreas. Alimentary tract manifestations consist of meconium ileus in uncomplicated and complicated forms (with the latter including secondary intestinal atresia, volvulus, and perforation with meconium peritonitis/distal intestinal obstruction syndrome, constipation, rectal prolapse, duodenal fold thickening, and appendiceal dilation. Hepatobiliary disorders secondary to CF include microgallbladder, cholelithiasis, biliary ductal abnormalities, neonatal

hepatitis, and cirrhosis (including complications such as portal vein thrombosis and ascites). Pancreatic expressions of CF include fatty infiltration, calcifications, and cysts/cystosis, frequently in the setting of malnutrition and/or stooling abnormalities. This exhibit will demonstrate the spectrum of clinical and radiologic GI findings in this disease from the fetal and neonatal period through adolescence across a range of imaging modalities.

Conclusions: Gastrointestinal manifestations of cystic fibrosis occur frequently in the pediatric population and may be the earliest clinical expression of the disease. Familiarity with the variety of gastrointestinal imaging findings of cystic fibrosis can expedite appropriate diagnosis and therapy, particularly in those children in whom the primary disease is not clinically suspected.

Poster #: EDU-020

Beyond Acute Appendicitis: Imaging of Additional Pathologies of the Pediatric Appendix

Kelly Dietz, MD, Cincinnati Children's Hospital; Arnold C. Merrow, Daniel J. Podberesky, Alexander J. Towbin

Purpose or Case Report: Primary acute appendicitis (or appendiceal inflammation caused by a superimposed bacterial infection in the setting of appendiceal obstruction) is by far the most common pathology of the appendix, and imaging evaluations to exclude this diagnosis occur daily in the pediatric radiology setting. The clinical and imaging differential diagnosis in a patient with right lower quadrant pain and suspected appendicitis is a broad but well-recognized list that predominantly involves structures adjacent to the appendix including the ovaries, small and large bowel, and ureters. There are, however, less common pathologies primarily involving the appendix which can create an imaging diagnostic dilemma in the setting of right lower quadrant symptoms. Our goal is to review the imaging and clinical manifestations of these less commonly encountered appendiceal abnormalities.

Methods & Materials: Cases of appendices that were abnormal by imaging but ultimately determined not to be due to primary acute appendicitis were collected from clinical encounters by the authors as well as through a search of the radiology and pathology report databases. Clinical course, surgical findings, and pathology reports (if available) were subsequently reviewed through the main hospital medical records system.

Results: The collected cases demonstrate a wide range of additional pathologies of the appendix outside of primary acute appendicitis. A variety of imaging modalities were employed in the workup of these cases. Examples reviewed in this exhibit include Crohn's disease, ulcerative colitis,

cystic fibrosis, carcinoid tumor, inguinal hernia with incarceration, retained foreign body, pinworm infestation, and ileocolic intussusception.

Conclusions: Despite the frequency of primary acute appendicitis, there is a differential diagnosis when an abnormal appendix is found by imaging. Familiarity with these alternative diagnoses may be particularly helpful in guiding management of the patient whose clinical presentation is not typical for primary acute appendicitis.

Poster #: EDU-021

Abdominal Giants: More Than Wilms Tumor in Children with Beckwith-Wiedemann Syndrome

Lesli M. LeCompte, MD, Children's Hospital of Philadelphia, *lecomptel@email.chop.edu;* Lisa States

Purpose or Case Report: To review a variety of abdominal imaging findings in patients with Beckwith-Wiedemann syndrome (BWS), beyond Wilms tumor, including work-up for congenital hyperinsulinism given its close genetic association with BWS.

Methods & Materials: A hospital PACS database search from the past 10 years for patients with BWS. Selected cases, with multimodality imaging, were cross-referenced with pathology reports from patient records database.

Results: Intricate abdominal pathologies are depicted utilizing multimodality imaging, such as plain films, US, CT, MRI and PET/CT, and with pathologic correlation. Cases with highlight the following: Liver: hepatoblastoma, nonspecific hepatobiliary cysts, multiple hemangiomas mimicking metastatic disease; adrenal: dysplastic organomegaly mimicking neoplasm; pancreas: diffuse and focal hyperplasia in the setting of hyperinsulinism, organomegaly; renal: nephrocalcinosis, including medullary sponge kidney, nephroblastomatosis, organomegaly; adnexal: ectopic paraovarian adrenal tissue mimicking metastatic lymph node; urinary bladder: benign fibro-uroepithelial polyp.

Conclusions: Diagnosis of BWS can be difficult when the classic clinical and radiological findings are not present. These few cases highlight the unusual abdominal pathologies, so when detected, a radiologist can aid in the appropriate diagnosis and help guide therapy for these young patients. This poster will discuss pharmaceuticals the FDA considers investigational for their intended use.

Disclosure: Dr. LeCompte has indicated that she will discuss or describe, in the educational content, a use of a medical device or pharmaceutical that is classified by the Food and Drug Administration (FDA) as investigational for intended use.

Poster #: EDU-022**Radiologic-Pathologic Review of Pancreatic Masses Encountered at a Tertiary Pediatric Hospital Over a 10-Year Period**

No Kwak, MD, Radiology, Long Island Jewish Medical Center, kwak_nb@yahoo.com; Karen Naar, Jeanne Choi-Rosen, Lee Collins, Sukhjinder Singh, Anna Thomas

Purpose or Case Report: Review of pathologically proven pancreatic masses in pediatric patients encountered at a tertiary pediatric hospital over a 10-year period. Describe the key morphologic features and other pertinent findings using various imaging modalities. Correlate pathologic and radiologic findings.

Methods & Materials: Illustrate the various imaging characteristics of pathologically proven pancreatic masses including pseudocyst, pancreatoblastoma, solid pseudopapillary tumor, acinar cell carcinoma, ductal adenocarcinoma, lymphoma, pancreatic neuroblastoma, and inflammatory myofibroblastic tumor. Correlate pathologic and radiologic findings. Identify the key imaging features that allow narrower differential diagnosis.

Results: Pancreatoblastoma and solid pseudopapillary tumor are the more commonly encountered pediatric primary pancreatic tumors. Both are bulky and heterogeneously enhancing tumors with solid and cystic elements. Pancreatoblastoma occurs more commonly in young children. Internal hemorrhage and fibrous capsule favor solid pseudopapillary tumor which more commonly occurs in adolescent girls. Ductal adenocarcinoma, acinar cell carcinoma and an inflammatory myofibroblastic tumor, which were pathologically proven in our pediatric patients, are exceedingly rare entities. The imaging findings of these cases and their pathology when available will be presented, as well as a quick literature review of these rare tumors. Illustration and correlation of the pathologic and radiologic findings.

Conclusions: Pancreatic masses in children are rare but in general have a better prognosis than in adults. Salient imaging findings for the various tumors encountered at a tertiary care center with pathologic and radiologic correlation.

Poster #: EDU-023**Evaluation of Hepatoblastoma with Gadoxetate Disodium—Typical, Atypical, Pre and Post Treatment Evaluation**

Arthur B. Meyers, Radiology, Cincinnati Children's Hospital, arthurbmeyers@yahoo.com; Alexander J. Towbin, Daniel J. Podberesky

Purpose or Case Report: Gadoxetate disodium (Gd-EOB-DTPA) is a hepatobiliary MRI contrast agent that is widely

used in adults for characterization of liver tumors and is being increasingly used in pediatric patients. Hepatoblastoma is the most common primary hepatic malignancy of childhood. The purpose of this presentation is to describe our experience with the use of this agent in the MRI evaluation both before and after initiating therapy in patients with hepatoblastoma.

Methods & Materials: The radiology report system at our institution was queried for all patients with pathology proven hepatoblastomas who underwent a liver MR with administration of gadoxetate disodium between 8/1/10 and 2/28/2011. The MR imaging characteristics of the patient's primary hepatoblastoma pre- and post-therapy (when available) and post treatment findings (when available) were reviewed.

Results: 22 MRI studies in 9 different patients were reviewed. The patients ranged in age from 4 months to 12 years. 6 patients had pre and post treatment evaluation with Gd-EOB-DTPA enhanced MRI, 1 patient had only pretreatment evaluation and 2 patients had only post treatment evaluation. 6 of the hepatoblastomas did not take up Gd-EOB-DTPA during the hepatocyte phase and were therefore low signal intensity during the hepatocyte phase of imaging. This was useful in the pretreatment evaluation of hepatoblastoma, particularly in defining the relationship of the tumor to hepatic and portal veins. Post treatment Gd-EOB-DTPA imaging allowed characterization of the biliary anatomy and demonstrated the communication of a postoperative fluid collection with the biliary tree, consistent with biloma. 1 atypical hepatoblastoma showed uptake of Gd-EOB-DTPA on hepatocyte phase imaging, similar to what has been described in adults with atypical hepatocellular carcinoma.

Conclusions: Gadoxetate disodium enhanced MRI is useful in the imaging evaluation of hepatoblastoma, particularly in defining the relationship of tumor to vascular and biliary anatomy and in characterizing post-treatment complications.

Disclosure: Dr. Meyers has indicated that he will discuss or describe, in the educational content, a use of a medical device or pharmaceutical that is classified by the Food and Drug Administration (FDA) as investigational for intended use.

Poster #: EDU-024**Imaging of the Gallbladder and Biliary Tree in Pediatric Age Group**

Ihsan Mamoun, MD, Cleveland Clinic, ihsanmamoun@yahoo.com; S. Pinar Karakas, Unni Udayasankar, Neil Vachhani, Ellen Park

Purpose or Case Report: Interactive educational exhibit to illustrate the embryology, anatomical variants as well as

congenital and acquired diseases of the bile ducts and gallbladder in pediatric patients.

Methods & Materials: a)The embryology of the gallbladder and biliary tree will be demonstrated with diagrams. b) Imaging techniques for gallbladder and biliary tree including US, CT, MRI, ERCP and intraoperative cholangiogram will be discussed. c)Imaging findings of various lesions with special emphasis on key findings that can lead to accurate diagnosis will be discussed. d)An appropriate list of differential diagnosis will be provided. e)An algorithm for the assessment of suspected biliary pathology will be presented. f)The exhibit will be interactive and the reader will answer questions about the discussed entity, related imaging algorithm and management.

Results: a)Discuss congenital anomalies including duplicated and septated gallbladder, choledochal cyst, Caroli disease, situs abnormalities and biliary atresia. b)Discuss infectious and inflammatory conditions including cholecystitis, Kawasaki's disease, sclerosing cholangitis and hepatitis. c)Discuss iatrogenic complications including post transplant biliary stricture and leak. d)Discuss benign and malignant neoplasms involving the gallbladder including polyps, PTLD and rhabdomyosarcoma.

Conclusions: This exhibit will demonstrate a logical approach to imaging of the congenital and acquired diseases of the gallbladder and biliary tree based on the embryology and underlying pathology.

Poster #: EDU-025

Postnatal Work Up of Congenital Uronephropathies—A Pictorial Essay

Harigovinda R. Challa, *Radiology, University of Kentucky, hch229@uky.edu*

Purpose or Case Report: The use of obstetric ultrasound routinely in the prenatal care has lead to the discovery of many fetal anomalies. Uronephropathies in the newborn represent one of the largest groups of anomalies amenable to neonatal management. Since these uropathies are detected mostly in asymptomatic patients the treatment is mainly preventive. The pediatric radiologist has a key role in the post natal work up and management of these patients with prenatally diagnosed nephrouropathies and familiarity with the congenital urinary tract abnormalities is necessary.

Methods & Materials: A retrospective review of multiple radiographic, sonographic and fluoroscopic examinations performed in the newborn babies and infants with prenatal diagnosis of urinary tract abnormalities was performed at Kentucky Children's Hospital. Multiple examples of classical imaging findings were compiled and placed into a pictorial review.

Results: Numerous anomalies can be detected in utero, including anomalies of renal number, position, morphology, collecting system dilation and bladder, urethral abnormalities. Of these postnatal work of congenital hydronephrosis is the most common routinely encountered clinical entity. Renal ultrasound is the initial examination in the evaluation in all cases of prenatal hydronephrosis, which is best performed around postnatal day 5. If collecting system dilatation persists on postnatal ultrasound, further imaging work up with VCUG, radionuclide imaging may be required depending on degree of dilatation.

Conclusions: Uronephropathies are increasingly detected in the prenatal life with increasing use of obstetric ultrasound. The objective of this presentation is to demonstrate in a pictorial essay of different nephrouropathies and their work-up in newborns.

Poster #: EDU-026

Isolated Fallopian Tubal Torsion: Causes, Imaging Findings, and How to Suggest the Diagnosis

Jesse Courtier, MD, *UCSF Dept of Radiology, jesse.courtier@ucsf.edu*; Amaya M. Basta, Rebecca Maine, Pierre-Alain Cohen, Shinjiro Hirose, John D. MacKenzie

Purpose or Case Report: The purpose of this educational report is to describe the rare entity of isolated fallopian tubal torsion in the pediatric population and depict the cross sectional imaging findings that help make a diagnosis and guide management. The proposed pathophysiology, predisposing factors, and surgical management will be described. An illustrative case example of 12-year-old female patient will be provided with surgical correlation. The exhibit will review imaging findings on US, CT and MRI that help support the diagnosis including, dilated tubular structure in the pelvis, normal ovaries, and corkscrewing and beaking of the proximal fallopian tube. Isolated fallopian tubal torsion will be placed in the context of a differential diagnosis for girls presenting with pelvic pain and the imaging signs that help make a diagnosis of isolated tubal torsion and separate this entity from other causes of pediatric pelvic pain will be emphasized.

Poster #: EDU-027

Multimodality Imaging Characteristics of Genitourinary Rhabdomyosarcoma

Rhea Udyavar, MD, *George Washington University Medical Center, rudyavar@gwmail.gwu.edu*; Amir Noor, Pranav K. Vyas

Purpose or Case Report: In this pictorial essay, we will demonstrate salient imaging features of MR, US, and CT modalities for the diagnosis of genitourinary rhabdomyosarcoma in male ($N=4$) and female ($N=4$) children ages 2–14 years, evaluated at our institution over the past 6 years. Background information, including tumor biology, staging, and treatment will also be discussed.

Poster #: EDU-028

The Swollen Scrotum: Ultrasound Technique and Differential Diagnosis

Kelli R. Schmitz, MD, Oregon Health & Science University, schmitzk@ohsu.edu; Roya Sohaey

Purpose or Case Report: To review the ultrasound protocol for the performance of scrotal ultrasound and illustrate the ultrasound appearance of conditions resulting in scrotal swelling in pediatric patients.

Methods & Materials: A retrospective review of the imaging database at a tertiary pediatric referral center was performed to identify pediatric patients who presented with scrotal swelling and underwent diagnostic ultrasound. When available, surgical/pathologic correlation was obtained.

Results: A variety of pathologic processes result in scrotal swelling. Causes illustrated include: testicular torsion, epididymitis/orchitis, hydrocele, varicocele, inguinal hernia, trauma, adrenal rest, and testicular or paratesticular neoplasm.

Conclusions: The causes of scrotal swelling are myriad, including infectious/inflammatory, developmental, traumatic, and neoplastic etiologies. In children, the clinical presentation of a swollen scrotum is nonspecific, and ultrasound plays a key role in making the correct diagnosis.

Poster #: EDU-029

Experiences of Starting a Functional MR Urography Program at a University Hospital: Trials and Tribulations

Steven L. Blumer, BSc, Montefiore Medical Center/Albert Einstein College of Medicine, sblumer@montefiore.org; Ibrahim Tuna, Amanda North, Benjamin Taragin, Netta Blitman, Terry L. Levin

Purpose or Case Report: Starting a functional MRU program can be challenging as there are numerous potential hurdles to overcome. This presentation describes the process of starting a functional MR Urography (fMRU) program at a university hospital and discusses the difficulties encountered starting such a program. Selecting a sufficient patient referral base, resolving common and uncommon technological issues, and education of

clinicians, patients and technical staff are some of the challenges that will be discussed.

Conclusions: Awareness of the common pitfalls in fMRU imaging and close partnering with referring physicians can make establishing a functional MRU program easier. Despite many potential obstacles, the benefit of exquisite anatomical and functional information provided by fMRU in children, without exposure to ionizing radiation, greatly outweighs any challenges.

Disclosure: Dr. Blumer has indicated that he will discuss or describe, in the educational content, a use of a medical device or pharmaceutical that is classified by the Food and Drug Administration (FDA) as investigational for intended use.

Poster #: EDU-030

Pictorial Review of Ultrasound Findings in Boys Presenting to Emergency Department/Urology with Acute Scrotum

Teresa Liang, Faculty of Medicine, University of British Columbia, teresaliang86@gmail.com; Peter Metcalfe, William Sevcik, Michelle Noga

Purpose or Case Report: Testicular torsion is a common acute condition in adolescent boys. Rapid and accurate diagnosis is critical. Diagnosis is currently based on history, physical findings, and ultrasound (U/S) with Doppler. The objective of this poster is to demonstrate ultrasound findings from a retrospective review of acute scrotum over 3 years, and to demonstrate some pitfalls of the technique with regard to testicular torsion diagnosis.

Methods & Materials: We reviewed the U/S, surgical and ED records at the Stollery Children's Hospital for boys aged 1 month to 17 years, presenting with acute scrotum from July 1, 2008 to 2011. Age, demographics, clinical symptoms, and physical findings, U/S and surgical techniques, findings, diagnoses and follow-up were also recorded.

Results: 343 patients presented to UAH Stollery ED with acute scrotum: 35 were diagnosed with testicular torsion (2 inguinal torsion), 11 were suspected of a torsion-detorsion, 3 torsion of appendix testes, 135 epididymitis/orchitis, and 159 other diagnoses including hydroceles, varicoceles, epididymal cysts, abscesses, cellulitis and hematomas. For the 266 patients who had ultrasound, 100% sensitivity and 88% specificity for testicular torsion. The ultrasound findings including size, vascularity and echogenicity associated with both salvageable and necrotic testicles including use of color and pulse Doppler will be reviewed. The sonographic findings and pictorial examples associated with the more common acute scrotum etiologies will be presented. Sonographic findings from problematic cases (those with inconclusive ultrasound reports or false positive reports) will also be addressed.

Conclusions: Ultrasound imaging problem case examples and characteristic findings of common acute scrotum presentations at Stollery Hospital at the University of Alberta are reviewed in this poster.

Poster #: EDU-031

Primary and Secondary Amenorrhea in Pediatric Patients: From the Beginning to the End

Cesar Cortes, MD, *Miami Children's Hospital, n4c03@hotmail.com;* Yanerys Ramos, Ricardo Restrepo, Alejandro Diaz, Lorena Sequeira, Edward Lee

Purpose or Case Report: To describe the role of imaging in evaluating patients with primary and secondary amenorrhea and to illustrate the normal imaging findings of the reproductive organs in the pediatric population as well as the imaging findings of the different etiologies causing amenorrhea.

Methods & Materials: A search of the literature is done to determine the different etiologies of amenorrhea and the role of imaging in their evaluation. First, we will focus on the normal physiologic hormonal influence and changes of the girl's reproductive organs since birth until adolescence on ultrasound and MRI. Images of the normal appearance of the female reproductive organs as well as imaging findings of the different common and uncommon etiologies of amenorrhea will be shown. Then, specific reference will be made to crucial related concepts such as minipuberty of infancy, latest criteria for polycystic ovarian disease and ovarian failure syndrome among others. Finally, the treatment, either medical or surgical will be briefly discussed.

Results: Causes of amenorrhea in children range from disorders affecting the hypothalamus, pituitary gland, adrenal glands, and ovaries, as well as uterine and vaginal structural abnormalities. Even though history and clinical exam are essential in evaluating a patient with amenorrhea, the pediatric radiologist plays a pivotal role helping guide the area to be imaged and thus the modality that should be used. MRI and ultrasound are the main modalities in the evaluation of amenorrhea.

Conclusions: Ultrasound and MRI are the main imaging modalities used in the evaluation of amenorrhea in children and are usually part of the work up. Amenorrhea in children can have implications in girl's fertility allowing pediatric radiologists to play an important role in helping not only the patient but also their offspring.

Poster #: EDU-032

Imaging of Mullerian Duct Anomalies in Children

Kelly K. Horst, MD, *Radiology, University of Michigan, khorst@med.umich.edu;* Maryam Ghadimi Mahani, Deepa Pai, Jonathan R. Dillman, Peter J. Strouse

Purpose or Case Report: The purpose of this educational exhibit is to provide an up-to-date appraisal of Mullerian duct anomalies presenting in the pediatric population. The appearances of anatomic variants on ultrasound and MRI will be used to illustrate the strengths and potential pitfalls of these imaging modalities.

Methods & Materials: Patients who have previously undergone ultrasound and/or MRI in the course of their clinical workup within the University of Michigan Health System (UMHS) were identified using electronic medical records. Imaging reports were reviewed by a single author in order to identify relevant imaging findings (interesting anatomic variations, associated anomalies, etc.). Pertinent images from these imaging examinations were de-identified and saved to a secure hard drive. The medical record was accessed by a single researcher to obtain relevant information regarding the patients' clinical presentations. In cases of corrective surgery, pathology reports were reviewed, if available, for correlation with the imaging findings.

Results: Cases of Mullerian duct anomalies were reviewed within the pediatric population. Clinical manifestations were correlated with imaging appearances.

Conclusions: Mullerian duct anomalies represent a range of developmental variants. Although functioning ovaries and age-appropriate external genitalia are characteristic, there may be anomalies ranging from uterine and vaginal agenesis, to duplication of the uterus and vagina, to minor uterine cavity abnormalities. Müllerian malformations are frequently associated with abnormalities of the renal and axial skeletal systems, and pediatric patients in particular may present with these associated anomalies. Menstrual abnormalities may represent a more typical presentation in the adolescent age group. This is in contrast to the adult population, which may be more likely to present with infertility. The variation in clinical presentations make Mullerian duct anomalies difficult to diagnose and, because surgical techniques for correction and treatment depend on the underlying anatomy, understanding these variants in the context of imaging studies is important to their diagnosis and management.

Poster #: EDU-033**Neonatal Osteomyelitis: A Radiological Review**

Lucila A. Rosines, *New York Presbyterian Hospital—Morgan Stanley Children's Hospital of New York, Lm650@columbia.edu;*

Purpose or Case Report: 1. To review the causes, pathophysiology, treatments, and complications of neonatal osteomyelitis. 2. To review the appearance of neonatal osteomyelitis on multiple radiological modalities including radiographs, ultrasound, MRI and nuclear medicine.

Methods & Materials: Retrospective review of 6 medical charts and radiologic studies of neonatal osteomyelitis that were collected during my pediatric rotations.

Results: Patient 1 had osteomyelitis of the left humerus. Radiographs showed periosteal reaction along the left proximal humerus. Ultrasound revealed an irregular left humeral cortex. Patient 2 had radiographs which showed an irregular left humeral metaphysis with an associated fracture. Patient 3 had a 3 phase bone scan that showed slightly increased uptake on the angiographic and blood pool phases and increased activity on the delayed phase in the right femur. Radiographs showed a moth eaten appearance of the right femur with soft tissue swelling. Patient 4 had radiographs that showed periosteal reaction in the right tibia with an associated fracture. Patient 5, in addition to radiographs, had an MRI that showed osteomyelitis of the left humerus and scapula with an associated subperiosteal abscess. Patient 6 had multi focal osteomyelitis that was demonstrated on radiographs by irregular cortices and periosteal reaction involving the upper and lower extremities.

Conclusions: Neonatal osteomyelitis is an uncommon entity that can have severe complications if not diagnosis and treated promptly. It is important to review cases and to review the appearance of neonatal osteomyelitis on multiple modalities. Radiographs will usually demonstrate periosteal reaction and possibly soft tissue swelling. Additional studies may be obtained to evaluate for complications, such as abscesses or involvement of the joint space.

Poster #: EDU-034**Update on DDH (Developmental Dysplasia of the Hip) and the Role of MRI**

Sabah Servaes, MD, *Children's Hospital of Philadelphia, servaes@email.chop.edu*

Purpose or Case Report: Review the epidemiology of DDH. Describe the critical diagnostic imaging findings of DDH. Understand the role of imaging accompanying treatment.

Methods & Materials: Images including radiographs, ultrasound, CT and MRI will be used to demonstrate the current and historical role of imaging in caring for patients with DDH. Discussion of the importance of reducing radiation exposure when choosing imaging studies will be included.

Results: Radiographs and ultrasound are used primarily in making the diagnosis of DDH. Ultrasound and MRI are most often used during the course of treatment to assess its effectiveness. MRI is increasingly utilized without sedation for patients in spica cast.

Conclusions: Imaging is critical in the care of patients with DDH.

Poster #: EDU-035**Pediatric Musculoskeletal Ultrasound of the Proximal Lower Extremity (Pelvis to Thigh)**

Julia Rissmiller, MD, *Dept of Radiology, Children's Hospital Boston, julia.rissmiller@childrens.harvard.edu;* Howard Christianson, Michael J. Callahan

Purpose or Case Report: To review indications for ultrasound of the proximal lower extremity (pelvis, hip and thigh), and to illustrate the practical use of ultrasound in evaluation of the proximal lower extremity, emphasizing the sonographic appearance of various musculoskeletal disorders.

Methods & Materials: Ultrasound is a well-established modality for the evaluation of painful hip, developmental hip dysplasia, soft tissue infection, palpable masses, and foreign bodies in children. In general, ultrasound has a more limited role for the primary evaluation of other pediatric musculoskeletal disorders including trauma, articular and periarticular diseases and tumors or tumor-like processes. Advantages of ultrasound, a relatively non-invasive technique, include excellent spatial resolution, low cost, lack of ionizing radiation, lack of need for sedation, and the ability to image the patient in real-time. The major disadvantage of ultrasound is operator dependency, which is particularly evident in musculoskeletal applications. We present ultrasound examples of pathology involving the proximal lower extremity (pelvis, hip and thigh). Cases include developmental hip dysplasia, hip effusion, osseous metastasis to the iliac bone, osteomyelitis of the hip, femoral acetabular impingement, rectus femoris hernia, vascular malformation, Ewing's sarcoma and myositis ossificans.

Results: A range of images from pediatric diagnostic ultrasounds performed of the proximal lower extremity (pelvis to thigh) will be presented emphasizing the sonographic appearance of various musculoskeletal disorders.

Conclusions: Ultrasound is an excellent modality for evaluating the proximal lower extremity in children, beyond the current indications of painful hip, developmental hip dysplasia, soft tissue infection, palpable masses, and foreign bodies in children.

Poster #: EDU-036

A Multi-Modality Pictorial Review of Lesions of the Epiphysis in Infants and Children

Ernesto I. Blanco, MD, *St. Christopher's Hospital for Children, eiblanco74@gmail.com;* Jacqueline Urbine, Evan Geller, Peter Pizzutillo

Purpose or Case Report: To review the imaging spectrum of epiphyseal lesions in infants and children.

Methods & Materials: A retrospective review of our imaging database was performed to identify studies with either primary lesions of the epiphysis or processes that affect the epiphysis.

Results: Multiple epiphyseal lesions were elucidated primarily by radiography, with cross-sectional imaging included where clinically necessary. Congenital lesions include the epiphyseal dysplasias represented here by chondrodysplasia punctata. Epiphyseal infarction may be due to multiple etiologies including slipped capital femoral epiphysis, developmental dysplasia of the hip, sickle cell disease, or idiopathic reasons. Neoplasms may occur in the epiphysis, including chondroblastoma and histiocytosis. Traumatic lesions include fracture and avulsion. Osteomyelitis can occur in the epiphysis as well. Pseudolesions that mimic pathology will also be reviewed. Other pathologies that can affect the epiphysis include juvenile idiopathic arthritis and hemophilia.

Conclusions: A wide spectrum of congenital and acquired pathologies may affect the epiphysis in the infant and child. Plain radiography, computed tomography, and magnetic resonance imaging all contribute to the diagnosis of these varied lesions.

Poster #: EDU-037

Pediatric Hip Disorders: A Systematic Approach

Sumit Singh, MD, *Radiology, Children's Hospital of Wisconsin, sumitsingh78@yahoo.com;* Tushar Chandra, Ibrahim S. Tuna, Carla Quijano

Purpose or Case Report: We aim to present the spectrum of common and uncommon hip disorders in pediatric population. We will formulate a systematic approach and present a flowchart to workup and characterize hip diseases.

Methods & Materials: Relevant imaging appearances of normal as well as pathological hip will be presented. Normal hip anatomy will be discussed through anatomic drawings and radiological images (plain radiographs, CT, USG, and MRI). We will illustrate the various anatomic landmarks, measurements and lines on plain radiographs and ultrasound of hip.

Results: Evaluation of limp and hip pain in the pediatric population has undergone rapid evolution. Surgical treatment for these disorders continues to be refined, and our ability to identify patients along the spectrum of disease continues to improve. Yet, despite our advances, obtaining an accurate diagnosis can remain challenging, especially in the setting of mild structural abnormalities. Many imaging studies can be used to evaluate the bones and soft tissues, but conventional radiography is the primary imaging modality for most clinical conditions. Plain radiographs usually are obtained first because they are sensitive and specific for a wide range of bone pathology. More sophisticated imaging modalities including radionuclide scintigraphy (bone scan), ultrasonography (USG), computed tomography (CT) and magnetic resonance imaging (MRI) are reserved for specific clinical situations. Each of these imaging modalities has specific advantages and disadvantages. It is the aim of this review to guide in selecting and interpreting the appropriate imaging modality for a variety of common disorders. This exhibit will illustrate imaging features of developmental dysplasia of hip, Perthes disease, Slipped Capital femoral epiphyses, hip malformations in syndromes, femoral acetabular impingement, labral disorders, septic arthritis and other disorders. The role of various imaging modalities in evaluation of these disorders will be discussed, along with common imaging pearls and pitfalls.

Conclusions: A systematic approach is necessary for evaluation of pediatric hip disorders. Familiarity with normal appearances, pitfalls and specific imaging of these entities is essential for proper diagnosis and management.

Poster #: EDU-038

Osteoid Osteomas: A Pain in the “Night” Diagnosis

Nancy K. Laurence, MD, *The Children's Hospital of Philadelphia, nkang26@gmail.com;* Monica Epelman, Richard Markowitz, Camilo Jaimes, Diego Jaramillo, Nancy Chauvin

Purpose or Case Report: A common benign bone-forming lesion, osteoid osteoma comprises approximately 12% of all

benign bone tumors. The tumor is composed of a nidus of vascular osteoid tissue and woven bone lined by osteoblasts, frequently with considerable surrounding inflammation. The radiolucent nidus surrounded by variable degrees of reactive sclerosis usually leads to a straightforward diagnosis; however, sometimes the diagnosis of osteoid osteoma can be challenging, as it may have a non-specific and misleading appearance on different imaging modalities, particularly on MRI. The purpose of this exhibit is to review the typical and atypical features of osteoid osteomas on different imaging modalities. We present diagnostic dilemmas of osteoid osteomas from our institution and how imaging characteristics can aid in diagnosis.

Methods & Materials: We performed a retrospective review of our imaging database to identify cases of typical and atypical osteoid osteomas, with special emphasis on cases which posed a diagnostic dilemma on imaging.

Results: When osteoid osteomas occur in atypical locations the diagnosis can be elusive. When located in the intraarticular space there is often minimal or absent cortical thickening and there may be a joint effusion with synovial hypertrophy. Phalangeal lesions may cause extensive bone marrow edema and surrounding soft tissue swelling. Both of these types of osteoid osteomas can be mistaken for infection. The recently described “CT vessel” or “vascular groove” sign, a low density vascular groove adjacent to the nidus, is highly specific for osteoid osteoma. In the authors’ experience, a rim of sclerosis surrounding the nidus may aid in diagnosis on MRI and can be identified as an outer hypointense halo on all sequences. We illustrate the findings in cases of atypical osteoid osteomas which may be difficult to diagnose including intraarticular, phalangeal, and vertebral osteoid osteomas. We also show examples of the newly described sign which has high specificity for osteoid osteoma.

Conclusions: Imaging findings in osteoid osteomas can be misleading and cause misdiagnosis, especially in atypical cases. Knowledge of their appearance in atypical locations and specific findings can aid in the correct diagnosis.

Poster #: EDU-039

Ultrasound of Normal Enteses in the Growing Skeleton
Nancy Chauvin, MD, *Department of Radiology, The Children's Hospital of Philadelphia, chauvinn@email.chop.edu*; Pamela F. Weiss, Monica Epelman, Diego Jaramillo

Purpose or Case Report: Ultrasound is an underutilized modality in the evaluation of the pediatric musculoskeletal system. Evaluation of tendon insertions about the elbow, knee and foot can be easily performed with ultrasonography. A good knowledge of the age dependent normal ultrasound

appearance of the enteses is crucial in order to evaluate for pathology, such as trauma or enthesitis-related arthritis. This exhibit will serve to provide the reader with a practical approach to imaging when assessing tendon insertions. Optimal patient positioning and transducer selection will be discussed. In addition, important anatomic landmarks will be described to allow for reproducibility and avoiding pitfalls.

Methods & Materials: Transverse and longitudinal ultrasound images of 12 enteseal insertion sites were performed on 20 healthy girls and boys between the ages of 5 and 17 years. Ultrasound of the elbow was performed while in full extension and the insertions of the common flexor and common extensor tendons were evaluated. The quadriceps and patellar insertions were imaged with patients in the supine position, with the knees flexed at 30 degrees. The Achilles tendon and plantar fascia insertion were evaluated with the patient prone, with the feet hanging off the edge of the table.

Results: Tendons demonstrated the expected fibrillar pattern with parallel echogenic lines. The appearance of the enteses changed as the insertion matured from sonolucent cartilage to echogenic bone.

Conclusions: Using a systematic approach and knowledge of the normal anatomy, sonography of the tendons of the elbow, knee and foot can easily be performed in children.

Poster #: EDU-040

Pediatric Musculoskeletal Ultrasound of the Distal Lower Extremity (Knee to Ankle)

Howard Christianson, MD, *Radiology, Children's Hospital Boston, howard.christianson@childrens.harvard.edu*; Julia Rissmiller, Michael J. Callahan

Purpose or Case Report: Ultrasound is a well-established technique in children for evaluation of the painful hip, developmental dysplasia of the hip, soft tissue infection, palpable masses and foreign bodies. In general, ultrasound has a somewhat more limited role for the primary evaluation of several other pediatric musculoskeletal disorders in the setting of trauma, articular and periarticular diseases and tumors and tumor-like conditions. Inherent advantages of ultrasound include excellent spatial resolution, a lack of ionizing radiation, a relatively non-invasive technique and lack of a need for sedation. Real-time imaging allows problem solving not available with other modalities which is well suited for musculoskeletal applications, particularly in the setting of trauma. The major disadvantage of ultrasound is operator dependency, which is particularly evident in musculoskeletal applications. The purpose of this study is to illustrate the practical use of ultrasound in the evaluation of

the distal lower extremity (knee to ankle) emphasizing the sonographic appearance of various musculoskeletal disorders. Examples include: 1) Cystic lesions around the joints: Baker's cyst, synovial cyst, ganglion cyst and suprapatellar bursitis; 2) Infectious processes: pretibial, subperiosteal and intramuscular abscess; 3) Tumor and tumor like lesions: nerve sheath tumor, tumoral calcinosis; 4) Trauma related injuries: Sinding Larsen Johansson, tibialis anterior muscle herniation, hematoma.

Methods & Materials: Cases selected for presentation from a series of diagnostic musculoskeletal ultrasounds performed at our institution.

Results: A range of images from diagnostic ultrasounds performed of the distal lower extremity (knee to ankle) will be presented emphasizing the sonographic appearance of various musculoskeletal disorders.

Conclusions: Selected musculoskeletal ultrasounds of the distal lower extremity are presented to familiarize the audience with the sonographic appearance of various musculoskeletal disorders and to highlight the tremendous potential of ultrasound in evaluating musculoskeletal disease in children and adolescents.

Poster #: EDU-041

Role of Conventional and Dynamic Contrast Enhanced Magnetic Resonance Imaging in Diagnosis of Hemihypertrophy Syndromes in Children

Shrey K. Thawait, MD, PhD, *Radiology, Yale University—Bridgeport Hospital, sthawait2@jhmi.edu*; Gaurav K. Thawait, Sally E. Mitchell, Laura M. Fayad, John A. Carrino, Kate Puttgen

Purpose or Case Report: Hemihypertrophy syndromes in children are complex and there is some overlap among these conditions. Hence, establishing a diagnosis can be challenging. Identification of the correct vascular anomaly associated with these overgrowth disorders helps to correctly classify the disease into one of the several syndromes, which in turn guides management. In this educational poster, we will review the definition, clinical presentation, conventional Magnetic Resonance Imaging (MRI) and contrast enhanced Magnetic Resonance Angiography and Venography (MRA / MRV) features of hemihypertrophy syndromes in children.

Methods & Materials: 1. Learn the diagnostic criteria for overgrowth syndromes in children such as Klippel-Trenaunay Syndrome (KTS) and Parkes Weber Syndrome (PWS) with special emphasis on associated vascular anomalies. 2. Gain knowledge of high resolution MRI technique for evaluation of vascular anomalies associated with the hemihypertrophy syndromes. 3. Understand the additional

value of dynamic contrast enhanced MRA / MRV in the differentiation of the hemihypertrophy syndromes in the pediatric age group.

Results: 1. MRI technique for a dedicated "vascular anomaly protocol" consisting of fat saturated T2 weighted, pre contrast axial T1 weighted, and post contrast triplanar T1 weighted fat saturated imaging will be described. 2. Special emphasis will be provided on dynamic contrast enhanced MRA/MRV. 3. Conventional and dynamic MRI features of clinically proven cases of hemihypertrophy syndromes will be demonstrated.

Conclusions: Systematic MRI interpretation utilizing a dedicated vascular anomaly protocol enables the radiologist to correctly identify the hemihypertrophy syndrome, and provide detailed extent of disease.

Poster #: EDU-042

Correlative Ultrasound, MRI Imaging and Physical Examination of Elbows in Hemophilic Children

Andrea S. Doria, MD, *The Hospital for Sick Children—Diagnostic Imaging, andrea.doria@sickkids.ca*; Frederico Xavier, Arun Mohanta, Carina Man, Ningning Zhang, Pamela Hilliard

Purpose or Case Report: 1. To report a systematic ultrasound (US) protocol for assessment of hemophilic elbows. 2. To discuss advantages and disadvantages of US and MRI for evaluating hemophilic elbows in comparison with physical examination. 3. To illustrate US and MRI findings and associated pitfalls in hemophilic joints. Background: The value of physical examination for assessment of early arthropathic changes in hemophilic joints is unknown. US does not require sedation in young children, but involves operator training and standardized technique. MRI is the reference standard imaging modality for assessment of pathology in hemophilic joints. Standardization of a systematic protocol for data acquisition and interpretation of US findings and understanding of the correlation of findings between physical examination, US and MRI in hemophilic elbows is essential for the use US as an outcome measure both in clinical practice and research. So far such information is not available for growing elbow joints.

Methods & Materials: Eight hemophilic boys (age range/median, 7–17/13 years) with a history of prior elbow bleeds underwent US and MR imaging, and physical examination on the same day. Corresponding images on US and MRI were highlighted to illustrate abnormalities and pitfalls. Soft tissues (effusion/hemarthrosis, synovial hypertrophy, hemosiderin deposition) changes were characterized as small, moderate, or large. Erosions, cartilage and subchondral

abnormalities were graded based on depth or extent of articular changes.

Results: 1. US is helpful for discriminating synovial hypertrophy, joint effusion/hemarthrosis, and large hemosiderin deposition which otherwise generates susceptibility artifacts on gradient-echo MRI obscuring adjacent tissues. 2. US can visualize erosions, cartilage and subchondral abnormalities at the joint periphery. However, differentiation between subchondral cysts and erosions is usually unfeasible by US. 3. Prior knowledge of the degree of joint maturation is essential for an accurate evaluation of cartilage loss by US. 4. Physical examination has limitations for assessment of early joint changes in contrast to US.

Conclusions: US can be useful for assessing hemophilic elbows, with advantages over MRI in the evaluation of soft tissues. Further development of an US-MRI atlas on normal cartilage in growing joints is needed for definition of the value of US in the assessment of minimal osteochondral abnormalities.

Poster #: EDU-043

Digital Atlas of Skeletal Surveys of Common Skeletal Dysplasias

Shawn Parnell, MBBS, MD, DNB, Radiology, Seattle Children's Hospital, shawn.parnell@seattlechildrens.org; Corey Wall, Edward Weinberger

Purpose or Case Report: Skeletal dysplasias are conditions of abnormal bone and cartilage growth which result in short stature. Developing expertise in the radiographic evaluation of skeletal dysplasias can be difficult, as more than 250 dysplasias exist. Exhaustive description of individual dysplasias can be found in hard copy textbooks, without the ability to compare individual dysplasias side by side. By providing radiographic images and descriptive text of thirteen common skeletal dysplasias and two comparative normal skeletal surveys, we aim to facilitate understanding of the terminology and highlight the differences in imaging appearances one may commonly encounter in interpreting skeletal dysplasias.

Methods & Materials: Initial skeletal surveys and/or follow up radiographs obtained for evaluation of skeletal dysplasias at our institution from 2005 to 2011 were compiled and reviewed for best quality images. Selected images for each case were labeled according to body part and view, to include AP and lateral views of the spine and skull and AP views of the extremities and pelvis. For neonates, AP and lateral babygram images were used. The software program used for viewing the atlas, written in C#, may be freely downloaded. It permits linked scrolling and resizing of the

images, and simultaneous comparison of different cases is available. Cases may be viewed as unknowns or in a self-teaching mode.

Results: Radiographic images for thirteen common skeletal dysplasias and two comparative normal skeletons (neonate and child) are provided within an interactive digital atlas. Cases include achondroplasia, pseudoachondroplasia, cleidocranial dysplasia, thanatophoric dysplasia, diaphyseal dysplasia, multiple epiphyseal dysplasia, osteopetrosis, osteogenesis imperfecta, multiple hereditary exostoses, dysostosis multiplex, fibrous dysplasia, asphyxiating thoracic dysplasia (Jeune syndrome), and spondyloepiphyseal dysplasia.

Conclusions: By displaying radiographic images of several common skeletal dysplasias in an interactive and comparative format with descriptive text, understanding of basic radiographic terminology and appearances will be facilitated.

Poster #: EDU-044

Pediatric Musculoskeletal (MSK) Soft Tissue Masses

Ajaykumar C. Morani, MBBS, Department of Radiology, University of Michigan, ajaycmorani@gmail.com; Ramon Sanchez, Ethan A. Smith, Maria Ladino-Torres, Peter J. Strouse

Purpose or Case Report: 1. To classify various pediatric MSK soft tissue masses 2. To describe pathogenesis, imaging appearances and differential diagnosis of these lesions

Methods & Materials: Radiology and clinical medical records were reviewed and pediatric patients with musculoskeletal soft tissue masses were identified. Representative images were collected as examples of each lesion. The lesions were then classified into different groups based on the similar pathology and etiology. Brief discussion is done for each of these masses with their multimodality imaging appearances.

Results: The search yielded pediatric soft tissue masses of multiple different etiologies, including post-traumatic (hematoma, fat necrosis, fibromatosis coli, myositis ossificans), inflammatory or infectious (cellulitis, abscess, granuloma annulare, retained foreign bodies), pseudotumors (synovial cysts, ganglion cysts, vascular malformations) and neoplastic lesions (fatty, vascular, neural, fibrous, muscular). Multiple different imaging modalities were used to evaluate these masses, including ultrasound, CT and MRI. Representative examples of different lesions and their appearances on different imaging modalities will be presented and an organized approach to the diagnosis of these lesions will be discussed.

Conclusions: Musculoskeletal soft tissue masses are relatively common in children. Majority of these are benign;

however, up to 6% of these lesions can be malignant “sarcomas”. Multiple different imaging modalities often provide complimentary information in the work-up of these lesions. Despite multimodality imaging approach, tissue diagnosis or short interval follow-up is still often required when the mass does not show typical features of a benign etiology. Pediatric radiologists should be familiar with various pediatric MSK soft tissue masses and their imaging appearances, and should be able to guide appropriate management.

Poster #: EDU-045

MRI Findings in a Pediatric Cohort Presenting with Elbow Instability

Michael Guandalini, MD, *Royal Children's Hospital*; Murray Bartlett

Purpose or Case Report: To describe and illustrate the elbow findings identified by MRI performed in a cohort of pediatric patients with the clinical presentation elbow instability.

Methods & Materials: Retrospective review of MRI elbow studies performed at The Royal Children's Hospital, Melbourne between 2003 and 2011. The studies were reviewed by a Pediatric Musculoskeletal Radiologist and Pediatric Radiology Fellow with patient demographics, clinical indication, findings and images recorded.

Results: 199 elbow MRI examinations were reviewed on children aged 4 months to 18 years with 28 (14%) of these investigating clinical instability in 25 children. Mechanism of injuries included congenital dislocation 10 (36%), traumatic dislocation 13 (46%), fracture or avulsion 2 (7%) and other injuries 3 (11%). The patient's with congenital elbow dislocations most commonly presented with radial head dislocation and associated dysplasia or flattening, effusion and less frequently dysplasia of the olecranon or capitellum. Patient's with traumatic dislocations were frequently associated with ligamentous or capsular disruption, bone oedema and epicondylar avulsion with effusion, loose osseous bodies and fractures less often. The epicondylar avulsions and ligamentous or tendon injuries occurred equally often in those few patients with unspecified injury mechanism.

Conclusions: A number of the bony, ligamentous, articular and developmental anomalies evident on elbow MRI have been illustrated highlighting the importance of careful and systematic review of all elbow structures when presented with a child with elbow instability. Accurate identification of these abnormalities is vital to facilitate their appropriate management.

Poster #: EDU-046

Dynamic Ultrasound Study in Evaluation of Infants with Vertical or Oblique Talus Deformities

Nucharin Supakul, MD, *Radiology, Riley Hospital for Children*, *tanyasupakul@yahoo.com*; Boaz Karmazyn

Purpose or Case Report: To summarize our experience with the use of ultrasonography (US) for evaluation of vertical or oblique talus deformities in infants.

Methods & Materials: From our computerized radiology information system, we retrieved all patients that have foot ultrasound for evaluation of vertical or oblique talus deformities in the last 6 years (10/2005-10/2011). The US was performed by a pediatric radiologist using a high resolution linear and tight convex curve probes with foot in neutral, plantar flexion and dorsiflexion. All medical charts, ultrasound scans and foot radiographs were reviewed by a pediatric radiologist.

Results: We identified nine patients' with foot deformities who were suspected of vertical or oblique talus and were evaluated by ultrasound. Seven patients are male; two of them had initial foot radiographs that were not diagnostic. Two female patients had unilateral oblique talus deformity. There were 7 patients with vertical talus deformity; three of them had bilateral deformities.

Conclusions: US can directly visualize the unossified navicular, the talar cartilage and their alignment. Dynamic US can.

Poster #: EDU-047

Ultrasound Evaluation of Costal Chondral Pathologies in Children Presented as Anterior Chest Wall Mass or Pain

Nucharin Supakul, MD, *Radiology, Riley Hospital for Children*, *tanyasupakul@yahoo.com*; Boaz Karmazyn

Purpose or Case Report: To summarize our experience with the use of ultrasonography (US) for evaluation of costal cartilage pathology presented as anterior chest wall mass.

Methods & Materials: From our computerized radiology information system, we retrieved all patients that have chest wall ultrasound for evaluation of a mass in the last 4.5 years (4/2007–8/2011). The US was performed by a pediatric radiologist using a localized scan with high resolution linear probe. All medical charts, pathology results, ultrasound scans and other imaging studies were reviewed by a pediatric radiologist.

Results: Ten patients were found with costal chondral pathologies. Nine patients presented with anterior chest wall mass

and one with chest wall pain. Eight patients had angular deformity of a single costal cartilage and one patient had biopsy proven osteochondroma, presented with anterior chest wall mass. One patient had a non-union fracture after motor vehicle accident, presented with anterior chest wall pain. In patients with rib deformity, the mass was non-tender. Nine patients had prior imaging study including chest x-rays ($n=8$), CT scan ($n=2$), breast MR ($n=1$). All these studies were negative.

Conclusions: US optimally demonstrated costal cartilage abnormalities. Chest radiographs and cross sectional studies were negative. We therefore recommend using high resolution chest wall US in children with negative chest radiograph and anterior hard chest wall mass.

Poster #: EDU-048

Challenges in Pediatric Marrow Imaging—Boning Up on Current MR Techniques

Srikala Narayanan, MD, *Division of radiology, Children's National Medical Center, snarayan@childrensnational.org*; Neha Kwatra, Nabile Safdar

Purpose or Case Report: A wide range of pathologies demonstrate similar findings when imaged using conventional MR sequences. However, pediatric musculoskeletal imagers are increasingly leveraging newer techniques to add specificity to their diagnoses when abnormal marrow signal is detected. The purpose of this educational exhibit is to review the application of current MR techniques to pediatric marrow imaging across the spectrum of normal, variant, and pathologic processes.

Methods & Materials: Cases with potentially overlapping imaging appearances on conventional MR sequences, including hematopoietic marrow, sickle cell disease, osteomyelitis, chronic recurrent multifocal osteomyelitis, and infiltrative neoplasms, will be presented. The basis of various MR techniques including chemical shift imaging, “whole body” marrow imaging, diffusion weighted imaging, and fat-water separation techniques such as Dixon or IDEAL (GE) will be reviewed. The strengths and weaknesses of such techniques in differentiating between infection, neoplasm, and normal variation will be emphasized through the case examples. Challenges and pitfalls in the imaging of these pathologies using such techniques will be discussed.

Results: Current MR imaging techniques add specificity to diagnoses of marrow pathology which are otherwise difficult to differentiate using traditional sequences alone. The use of opposed phase imaging can be helpful in differentiate hematopoietic marrow or infection from infiltrative and neoplastic conditions. “Whole body” marrow imaging may serve as an alternative to other modalities which involve significant

radiation exposure. The use of diffusion weighted imaging is a promising, but developing, technique being applied to marrow pathology.

Conclusions: Pediatric bone marrow MR imaging is a challenging area for a vast majority of the radiologists. Understanding normal developmental bone marrow changes and being aware of the pitfalls is crucial to render accurate diagnosis. Current techniques such as IDEAL, chemical shift imaging, and “whole body” MRI have a potentially important role in further characterization of marrow abnormalities.

Poster #: EDU-049

Radiologists Beware: Unusual Imaging Manifestations in Child Abuse

Eglal Shalaby-Rana, MBBS (Hons), *Children's National Medical Center, erana@childrensnational.org*; Allison M. Jackson, Tanya Hinds, Katherine Deye

Purpose or Case Report: To present less common imaging manifestations of injuries in child abuse that may not be readily recognized as possibly abusive injury.

Methods & Materials: Through bi-monthly review of cases with the child protection team over a period of 12 years, the imaging studies of patients with suspected non-accidental trauma were recorded. Of the 654 pts with suspected non-accidental trauma, outcomes were available in 599 patients. The child protection team concluded 254 (43%) were cases of non-accidental trauma with reasonable medical certainty. This data base was reviewed for less common injuries that were found in these medically confirmed cases of child abuse.

Results: Less common manifestations of abuse identified by radiographs included Salter-Harris injuries in the proximal humerus, and proximal femur. Pelvic fractures were rare and when present were associated with sexual abuse. Severe chest wall injury, with associated rib fractures, causing complete or near-complete white-out of the chest was occasionally encountered. Soft tissue injuries, such as hematomas were found in various locations in the body including the buttocks and anterior abdominal wall, were imaged on ultrasound and CT. Para- or prevertebral injuries, with or without associated bone injury were identified; one infant presented with retropharyngeal soft tissue swelling. MRI identified cervical spine injuries which included ligamentous injury and intrathecal hematomas.

Conclusions: While classic metaphyseal lesions and rib fractures are the most common, specific injuries documented by radiologic work up of suspected non-accidental trauma, less common injuries to the soft tissue and skeletal system may occur as a result of child abuse. The ability of the radiologist to recognize these uncommon manifestations of

abuse and offer potential mechanisms of injury may help make the diagnosis of child abuse.

Poster #: EDU-050

The Pediatric Elbow—MRI Findings with Multimodality Correlation

Michael Guandalini, MD, *Royal Children's Hospital*; Murray Bartlett

Purpose or Case Report: To describe and illustrate elbow abnormalities identified by MRI performed in a cohort of pediatric patients with multimodality correlation.

Methods & Materials: Retrospective review of MRI elbow studies performed at The Royal Children's Hospital, Melbourne between 2003 and 2011. The studies were reviewed by a Pediatric Musculoskeletal Radiologist and Pediatric Radiology Fellow with patient demographics, clinical indication, findings and selected images recorded.

Results: 199 elbow MRI examinations were reviewed on children aged 4 months to 18 years (123 boys, 76 girls) with equal numbers of left and right sides examined. Clinical indications included previous trauma in 147 cases (74%) and non-traumatic conditions in 52 (26%). The most common traumatic indication was suspected or confirmed fractures or avulsions (21%) followed by osteochondral or cartilage injuries (18%), growth arrest (16%), loose bodies (14%) and ligament injuries (10%). Hemophilia (38%) was the most frequent non-traumatic indication followed by neoplasm (17%). Mild to severe arthropathy, fractures, physal growth arrest, subluxations, osteochondral lesions and loose bodies were the most frequently demonstrated abnormalities. Ligament strains and tears, bone oedema, neuromuscular abnormalities, infections and several neoplasms including lipomas, vascular/lymphatic malformations and bone tumors also featured.

Conclusions: This pictorial review illustrates the broad range of abnormalities one might expect to encounter on pediatric elbow MRI studies, highlighting the major features and corresponding appearances on CT and plain X-ray.

Poster #: EDU-051

Spectrum of Patellar Tendon Avulsive Injury on MRI in Children: Differentiation Between Acute and Chronic Avulsive Injuries of the Inferior Patellar Pole and Tibial Tuberosity

Zeyad Metwalli, MD, *Baylor College of Medicine*, metwalli@bcm.edu; Herman Kan, Scott Rosenfeld, R. P. Guillerman

Purpose or Case Report: The extensor mechanism of the knee is an intricate component of the joint and is frequently

injured in pediatric athletes. Due to the strength of the patella tendon, trauma to the anterior knee is often manifested by avulsive injuries, which may occur on an acute or chronic repetitive basis. Purpose: This pictorial review will illustrate differentiating radiographic and MRI features of acute and chronic avulsive injuries of the pediatric knee. Outline: 1. Anatomy and physiology a. Discuss the anatomic differences of the pediatric and adult knee extensor mechanism b. Pathophysiology and biomechanical basis for chondro-osseous avulsion injuries versus tendon tears in the skeletally immature. 2. Inferior patellar pole avulsive injuries a. Illustrate radiographic and MRI examples of acute and healing inferior patellar sleeve fractures b. Illustrate radiographic and MRI examples of Sinding-Larsen-Johansson disease at various stages of healing c. Differentiating features of acute inferior patellar sleeve fractures and Sinding-Larsen-Johansson disease. d. Orthopaedic management of patellar sleeve fractures and Sinding-Larsen-Johansson disease. 3. Tibial tuberosity avulsive injuries a. Illustrate radiographic and MRI examples of acute and healing tibial tuberosity avulsion injuries. b. Illustrate radiographic and MRI examples of Osgood-Schlatter disease. c. Differentiating features of acute tibial tuberosity avulsion fractures and Osgood-Schlatter disease d. Orthopaedic management of tibial tuberosity avulsion fractures and Osgood-Schlatter disease. Conclusion: Acute and chronic patellar tendon avulsive injuries are frequently seen in children and have characteristic imaging features. Understanding the biomechanical basis of these avulsive injuries and orthopaedic management is important for radiologic interpretation of relevant imaging findings and effective communication to the treating physician.

Poster #: EDU-052

MRI Anatomy of the Hindfoot and Ankle Ligaments: An Interactive Review

Paul Thacker, MBBS, MD, DNB, *Children's Mercy Hospital*, pthacker@cmh.edu; Neil Mardis

Purpose or Case Report: The purpose of this educational exhibit is to demonstrate the magnetic resonance imaging (MRI) appearance of the ankle and hindfoot ligaments using an interactive approach.

Methods & Materials: A 3 Tesla Siemens MRI scanner with a multichannel ankle coil was utilized in the acquisition of images of ankle and hindfoot. Three dimensional volume acquisition proton density images will be used to demonstrate the ligamentous anatomy of the ankle and hindfoot in axial, axial oblique, coronal, and sagittal planes.

Results: The exhibit will begin with an interactive review of the ankle and hindfoot ligamentous anatomy with each ligament

demonstrated in axial, coronal, and sagittal planes. The ligament of interest will be denoted by arrows. At the conclusion of the anatomy section, there will be a self assessment exam. The participants then will be asked to identify the ligament. If answered correctly, a summary slide will be displayed and, if common, images of the relevant pathology will be demonstrated. If an incorrect answer is indicated, a slide will appear denoting the incorrect answer with explanation.

Conclusions: Hopefully, with review of this educational exhibit, the participant will have a better understanding of the relevant ligamentous anatomy of the ankle and hindfoot.

Poster #: EDU-053

Pediatric Ankle Ultrasound: Commonly Encountered Pathologies

Ajaykumar C. Morani, MD, *Department of Radiology, University of Michigan, ajaycmorani@gmail.com*; Deepa Pai, Ramon Sanchez, Michael Di Pietro, Jon Jacobson

Purpose or Case Report: The purpose of this educational exhibit is to demonstrate the pathologic sonographic findings, one might encounter in the pediatric ankle.

Methods & Materials: A systematic methodological approach including patient positioning, transducer orientation and sonographic technique are vital for ideal sonographic assessment of the pediatric ankle. Using a data search program from a large academic institution, pediatric ankle ultrasounds performed in the last 10 years were reviewed. Pathologies include trauma, inflammation/infection, masses and congenital abnormalities. Examples of normal anatomy will be included particularly when demonstrating ligament and tendon pathology. The normal side was often assessed for comparison purposes.

Results: Ankle sonography is a useful modality to evaluate commonly encountered pathologies in the pediatric ankle. Radiographically occult fractures may be discovered. Ligament and tendon pathology, such as tears of the anterior talofibular ligament, high ankle sprain and peroneus longus tendon tears, can be easily detected. Signs of infection that can be radiographically occult such as subtle periosteal reaction or fluid collections can be identified. Finally, “lumps and bumps” can be characterized. For example, one of the most commonly encountered masses in the pediatric ankle is a ganglion cyst which can be well characterized sonographically. Awareness of imaging pitfalls is also critical to avoid misdiagnosis and to guide appropriate management.

Conclusions: With basic ultrasound skills and knowledge of normal anatomy, sonography of the pediatric ankle is a useful modality to evaluate soft tissue structures and other pathologies. It is comparable to MRI and allows for dynamic evaluation without need for anesthesia.

Poster #: EDU-054

Maximizing Time Resolved MRA for Differentiation of Hemangiomas, Vascular Malformations, and Vascularized Tumors

Jane S. Kim, MD, *Children's Hospital at Montefiore, Montefiore Medical Center, janekim80@gmail.com*; Linda Y. Kao, Ross Borzykowski, Benjamin Taragin

Purpose or Case Report: Contrast-enhanced Magnetic Resonance Angiography (MRA) using time resolved imaging is a relatively new technique that has become increasingly utilized in the diagnosis of vascular anomalies. We will describe the technique used at our institution, Time Resolved Imaging of Contrast Kinetics (TRICKS, GE Healthcare, Milwaukee, WI), and the parameters that can be adjusted to optimize the exam. We will review key imaging features of hemangiomas and vascular malformations in various modalities, with a special emphasis on the TRICKS appearance.

Methods & Materials: We performed a retrospective review of all the TRICKS studies performed at our institution for suspected vascular anomalies. In addition to the MR imaging features, we specifically analyzed the T1 weighted with fat saturation post TRICKS enhancement and the temporal TRICKS enhancement pattern. We reviewed all additional imaging including plain film, ultrasound, and CT and correlated the radiographic imaging with the available clinical and histopathologic features.

Results: We present illustrative cases of hemangiomas, kaposiform hemangioendothelioma, venous malformations, arteriovenous malformations, lymphatic malformations, and other pitfall lesions. We propose a diagnostic algorithm that relies heavily on the post contrast T1 weighted with fat saturation post TRICKS enhancement pattern and the temporal TRICKS enhancement pattern.

Conclusions: Time resolved contrast-enhanced MRA has become an increasingly important adjunct in the diagnosis of vascular anomalies. Optimization of the exam technique and familiarity of the TRICKS imaging appearance is essential and can often assist in accurate lesion characterization.

Poster #: EDU-055

Vertical Expandable Prosthetic Titanium Rib (VEPTR): A Review of Indications, Normal Radiographic Appearance, and Complications

Grace S. Phillips, MD, *Department of Radiology, Seattle Children's Hospital, University of Washington, grace.phillips@seattlechildrens.org*; Shawn E. Parnell, Jonathan O. Swanson, Kit Song, Eric L. Effmann

Purpose or Case Report: Vertical Expandable Prosthetic Titanium Rib (VEPTR) is increasingly used in the treatment of thoracic insufficiency, scoliosis, and chest wall defects in children. In contrast to spinal fusion surgery, VEPTR allows for growth while stabilizing the deformity. We review the indications, pre-operative imaging, normal radiographic appearance, and complications of this device.

Methods & Materials: On review of the literature, the indications for VEPTR have expanded in the past several years to include thoracic insufficiency, idiopathic and neuromuscular scoliosis, and chest wall defects. We illustrate the normal radiographic appearance of the three common configurations of VEPTR (cradle-to-cradle assembly, cradle with lumbar extension assembly; cradle-to-ala hook assembly). We discuss the potential complications of VEPTR, including infection, rib fracture, dislodged hardware, and neurological injury, with an emphasis on imaging diagnosis.

Results: There is a relatively high rate of reported complications with VEPTR in the literature. Therefore, awareness of the growing number of indications, as well as the expected and unexpected appearance of this device, aids in radiographic diagnosis of complications.

Conclusions: Vertical Expandable Prosthetic Titanium Rib (VEPTR) is gaining acceptance in the treatment of thoracic insufficiency, scoliosis, and chest wall defects in children. Recognition of the indications, normal radiographic appearance, and complications of this device will facilitate timely and accurate diagnosis.

Disclosure: Dr. Philips has indicated that she will discuss or describe, in the educational content, a use of a medical device or pharmaceutical that is classified by the Food and Drug Administration (FDA) as investigational for intended use.

Poster #: EDU-056

Spectrum of Pediatric Spinal Neoplasms: An Interactive Tutorial

Benjamin T. Haverkamp, MD, *Radiology, University of Missouri—Kansas City, haverkampbt@umkc.edu; Salvador F. Iloreta, Maha Jarmakani, Lisa Lowe, Seth Gibson*

Purpose or Case Report: The objective of this educational electronic exhibit is to provide the radiologist with an approach to pediatric spinal neoplasms. Emphasis will be placed on narrowing the differential diagnosis using a combination of lesion location, characteristic imaging findings, relevant history, and associations.

Methods & Materials: The exhibit format will include a case-based review of various pediatric spinal neoplasms, radiologic-pathologic correlation, and a brief discussion of imaging findings useful in guiding surgical management. An interactive self-assessment exam will be presented at the end of the exhibit.

Results: A review of the specific etiologies will be presented with classification as intra- and extra-medullary and extradural lesions. Radiologic images will be related to gross and microscopic pathology.

Conclusions: After viewing this exhibit, the learner will be able to: 1. Recognize the clinical, imaging, and pathologic characteristics of pediatric spinal neoplasms. 2. Understand relevant imaging findings useful in surgical management. 3. Test their understanding of the presented material through an interactive exam.

Poster #: EDU-057

Craniosynostosis

Jason Tsai, MBChB, *Children's Hospital Boston, jason.tsai@childrens.harvard.edu; Diana P. Rodriguez*

Purpose or Case Report: To review the normal developmental appearance of the cranial sutures with computed tomography (CT) and to describe CT findings of the various forms of craniosynostoses.

Methods & Materials: In this IRB-approved retrospective study we reviewed CT images of subjects diagnosed with craniosynostosis between 2006 and September 2011. We included patients with single-suture synostosis, isolated bilateral coronal synostosis, pansynostosis, and combined craniosynostoses. Additionally, we identified individuals with normal appearing sutures from 0 to 5 years of age imaged with head CT to describe the pattern of normal development of the cranial sutures.

Results: A description of the normal developmental CT appearance of the cranial sutures using computed tomography has been provided. Of the group of patients with craniosynostosis the following variables were recorded: age at presentation, the pattern of sutural fusion, skull shape, presence of hydrocephalus, genetic testing, and types of surgical correction.

Conclusions: We have demonstrated the normal developmental CT appearance of the cranial sutures and the CT patterns of the various forms of craniosynostoses, with clinical, genetic and surgical correlation.

Poster #: EDU-058

Posterior Fossa Tumours: A Pictorial Review

Sam Byott, MD, *Manchester Children's Hospital, sambyott@hotmail.com; Neville Wright, Vivian Tang, Abdu Shabani, Stavros Stivaros*

Purpose or Case Report: Posterior fossa tumours account for 54–70% of childhood brain tumours. The most common differentials include pilocytic astrocytoma,

medulloblastoma and ependymoma. MR imaging is crucial to diagnosis, staging and identification of complications such as hydrocephalus and haemorrhage. Soft tissue characteristics alongside tumour location, invasion and clinical history facilitate radiological discrimination prior to surgery. However, there is significant clinical equipoise with regards to the imaging appearances in a significant proportion of cases making definite diagnosis difficult. The aim of this study is to evaluate the radiological findings and correlate with histological data. This will allow identification of the key morphological features that discriminate different tumours. These can then be presented to educate fellow radiologists.

Methods & Materials: Radiology PACS and patient notes were used to collate radiological, histological and clinical data.

Results: There were 27 patients presenting at our institution with posterior fossa tumours. 12 had pilocytic astrocytomas, 8 had medulloblastomas and 7 had ependymomas. One patient had an atypical teratoid rhabdoid tumour (ATRT). Traditional features alongside more advanced MR characteristics were correlated with histology, and the features allowing for discrimination of tumour types are presented in this pictorial review.

Conclusions: Posterior fossa tumours have a highly variable radiological appearance. We present a range of appearances and describe the important morphological features that allow radiological discrimination of tumour type.

Poster #: EDU-059

3DT1 Imaging of the Pediatric Spine

Teresa C. Gross Kelly, *Children's Hospital of Wisconsin, tkelly@chw.org*; **Ibrahim S. Tuna**, **Mia S. Kelly**, **Tushar Chandra**, **Sumit Singh**, **Mohit Maheshwari**, **Hervey D. Segall**

Purpose or Case Report: Some abnormalities of the pediatric spine can be challenging. We have discovered that in many such cases, diagnosis of spinal lesions can be facilitated by using the 3DT1 weighted sequence. The purpose of this educational poster is to demonstrate the remarkable usefulness of 3DT1 weighted images for delineating pathology of the pediatric spine.

Methods & Materials: Lesions of the spine that will be reviewed in this educational exhibit will be categorized as: (1) vascular (2) due to infection/inflammation (3) neoplastic/neurogenic (4) congenital (5) traumatic/iatrogenic (6) endocrine/metabolic. The imaging characteristics of lesions found in the pediatric spine will be described and the utility of 3D T1-weighted MR sequences for the evaluation of these lesions will be discussed. Finally the role of imaging in the

treatment planning of abnormalities of the pediatric spine will be addressed.

Results: This educational exhibit will provide numerous examples of how 3D T1-weighted imaging can elucidate diagnosis of lesions involving the spine. Examples include enhancement of the cauda equina in Guillain Barre syndrome, lipomatous malformations, spondylolysis in children with low back pain, thecal cysts, filar cysts, metastasis, hydromyelia and ventriculus terminalis.

Conclusions: 3D T1-weighted images of the spine performed in the sagittal plane with coronal and axial reformations, as well sagittal oblique reformations (scotty dog reformations) for evaluation of spondylolysis, can facilitate the evaluation of lesions involving the pediatric spine.

Poster #: EDU-060

The Normal Pediatric Spine: A Pictorial Review of MR Anatomy and Development in the Infant, Child and Adolescent

Ibrahim S. Tuna, MD, *Radiology, Children's Hospital of Wisconsin, dristuna@yahoo.com*; **Teresa C. Gross Kelly**, **Tushar Chandra**, **Mohit Maheshwari**, **Sumit Singh**, **Hervey D. Segall**

Purpose or Case Report: Radiological evaluation of the pediatric spine can be more challenging in child than in the adult patient due to the wide range of normal anatomic variants and synchondroses, combined with the unique effects of trauma in children. MRI is an excellent imaging modality for the evaluation of the pediatric spine. However, in order to provide an accurate interpretation of acute post-traumatic changes in the pediatric spine, particularly in the setting of abusive head trauma, a fundamental knowledge of normal anatomy, variants and pathology of the pediatric spine is required. The aim of this educational exhibit is to illustrate normal MRI anatomy of the spine in the infant, child and adolescent.

Methods & Materials: This exhibit will first describe basic spinal embryology and development of the vertebra and spinal cord, followed by MRI depiction of the developmental anatomy of the spine from infancy through adolescence. The changing appearance of the spinal canal, spinal cord and vertebral bodies with age will be illustrated using normal cases from the radiology database. Sagittal and transverse diameter of vertebral bodies, thickness of the dural thecal sac, dimensions of the spinal canal, normal bone marrow signal changes, vertebral body heights, level of conus medullaris, prevertebral and paraspinal soft tissues and epidural fat thickness will be described and changes according to age will be pointed out.

Results: In early life, the spinal cord extends to the inferior aspect of the bony spinal column. Because the vertebral bodies grow longitudinally faster than the spinal cord does, the conus medullaris may change. Ossification of the vertebral bodies and posterior elements is nearly complete by age 10, with a resultant decrease in the spinal canal diameter. The nucleus pulposus becomes smaller after 10 years and spans approximately half the disk space in the sagittal plane. The spinal cord is elliptical in cross section in the cervical spine and demonstrates a difference in signal between the normal gray and white matter of the spinal cord which should not be mistaken for intramedullary pathology.

Conclusions: A solid understanding of normal spine anatomy and embryological development is essential in evaluation of pediatric spine, mainly in the setting of trauma. Familiarity with normal anatomic variants is essential to provide an accurate interpretation of pathology in the pediatric spine.

Poster #: EDU-061

Spectrum of Intracranial Cystic Lesions in Infants and Children

Ernesto I. Blanco, MD, St. Christopher's Hospital for Children, eiblanco74@gmail.com; Eric Faerber

Purpose or Case Report: To review the imaging spectrum of intracranial cystic lesions in the pediatric population.

Methods & Materials: A retrospective review of our imaging database was performed to identify studies obtained in which the findings included intracranial cystic lesions.

Results: Multiple cystic lesions were elucidated primarily by computed tomography or magnetic resonance imaging. These lesions can be divided into nonneoplastic and nonneoplastic tumor-associated cysts. The nonneoplastic cysts, which is the largest group, include: cavum septi pellucidi and cavum veli interpositi, choroid plexus cyst, enlarged peri-vascular spaces, pineal cyst, the large spectrum of arachnoid cysts, colloid cyst, epidermoid cyst, Rathke cleft cyst, and porencephalic cyst. Nonneoplastic tumor-associated cysts include: craniopharyngioma, optic glioma, pilocytic astrocytoma, hemangioblastoma, and ganglioglioma.

Conclusions: Intracranial cystic lesions are relatively common entities in the pediatric population. A wide spectrum of nonneoplastic and nonneoplastic tumor associated pathologies are presented using both computed tomography and magnetic resonance imaging.

Poster #: EDU-062

Pediatric Spinal Cord Tumours: A Pictorial Overview

Tushar Chandra, MD, Children's Hospital of Wisconsin, dtusharchandra@gmail.com; Mohit Maheshwari, Teresa C. Gross Kelly, Sumit Singh, Ibrahim S. Tuna, Hervey D. Segall

Purpose or Case Report: The aim of this educational exhibit is to provide a comprehensive review of imaging features, classification and management of pediatric spinal cord tumors. We also aim to elicit the differences between pediatric spinal cord tumors and their adult counterparts. We will summarize the differences between the individual tumors based on histological cell types and the pertinent implications on management and outcome

Methods & Materials: This exhibit will provide an overview of the common as well as uncommon tumors of the pediatric spinal cord. Various classification systems for these tumors—anatomical as well as histological will be discussed. We will illustrate the relevant imaging findings that can help in differentiating these tumors.

Results: Pediatric spinal cord tumors account for 1% to 10% of all pediatric central nervous system tumors. MRI is the mainstay for the initial diagnosis as well as the post surgical evaluation and surveillance of these tumors. Pediatric and adult spinal cord tumours differ both in terms of anatomical location as well as histology. The disease and treatment related morbidities are also different in children as compared to adults. Astrocytomas, ependymomas, glioneural tumors and CSF metastasis represent the vast majority of cord neoplasms in the pediatric age group. Some of cord tumors may also be associated with inherited syndromes (like Neurofibromatosis type 2) or may have genetic predisposition. These would also be discussed. We will also illustrate and discuss common non neoplastic spinal masses that may mimic tumors.

Conclusions: Pediatric spinal cord tumors have varied clinical presentations, imaging appearance and outcome. This review would improve the understanding of these tumors thereby helping in diagnosis, management and follow up of these uncommon neoplasms.

Poster #: EDU-063

Multi-Modality Imaging of Pediatric Head and Neck Lesions

Jason Au, MD, Oklahoma University Health Sciences Center, jasonmau@gmail.com; Anthony Alleman, Mahmoud Elkaissi, Roy Jacob

Purpose or Case Report: The purpose of this study is to present a side by side comparison of the multi-modality imaging features of pediatric masses. Using cases that have been imaged with multiple modalities, the exhibit will delineate the sonographic, MR, and CT appearance of congenital, infectious, and neoplastic head and neck lesions in the pediatric population.

Methods & Materials: A retrospective search of PACS was performed on studies completed at the Oklahoma University Medical Center on the Oklahoma University Health Science Center Campus from January 2008 to the present. Ultrasound, CT, and MR examinations were selected that depicted relevant pediatric head and neck pathology. All studies were de-identified prior to image export.

Results: Over twenty representative cases of pediatric infections, fibrous tumors, cystic neoplasms, vascular malformation, bony tumors, developmental anomalies, and other neoplasms were selected for inclusion.

Conclusions: Familiarity with the imaging features of pediatric head and neck lesions facilitates clinical treatment planning. This exhibit is meant to concisely summarize the relevant imaging features of both common and uncommon clinical entities.

Poster #: EDU-064

Imaging of Congenital Spinal Malformations with MRI and Ultrasound, A Case-Based Review

Daniel A. Strauchler, *Jacobi Medical Center, dstrauchler@hotmail.com*; Einat Blumfield

Purpose or Case Report: 1. To discuss and review the classification of congenital spinal anomalies with emphasis on spinal dysraphism. 2. To review and compare imaging of spinal dysraphism with ultrasound and MRI in the neonatal period and discuss the advantages and disadvantages of each method. 3. Case based review of imaging findings of spinal dysraphism in ultrasound and MRI.

Methods & Materials: 1. Review of the classification and nomenclature of congenital spinal malformations including opened and closed spinal dysraphism and Chiari malformations. 2. Case-Based review, using representative and unique cases for illustration. 3. Discussion of imaging with ultrasound and MRI and review of advantages/disadvantages of each method.

Results: Pictorial review of cases including the following representative cases: myelomeningocele associated with Arnold Chiari malformation, lipomyelomeningocele, tethered cord with spinal lipoma/fibrofatty filum, tethered cord and

dermal sinus tract, and Chiari I with syringohydromyelia. Several unique cases including the following will be presented as well: thoracic meningocele with Arnold Chiari malformation, terminal myelocystocele, diastematomyelia, and myelomeningocele without Arnold Chiari malformation. While MRI demonstrates the cranio-cervical junction and the cervico-thoracic spinal cord better than ultrasound, ultrasound often allows for improved resolution of the distal spinal cord, lumbosacral spinal canal, and spinal dysraphism structures near the skin surface in the neonate.

Conclusions: Congenital spinal malformations are complex and variable in imaging appearance. It is important to understand the classification in order to determine the appropriate management and prognosis. In the neonatal period imaging should be performed with ultrasound and MRI studies, as they may provide different and complementary information.

Poster #: EDU-065

Hypoxic Ischemic Injury: An Overview of Clinical and Radiological Manifestations From Premie to Adult

Neal Desai, MD, *UMKC SOM, neal540@gmail.com*; Ramya Kollipara, Paul Thacker, Lisa H. Lowe

Purpose or Case Report: 1. To describe the molecular pathophysiology of Hypoxic Ischemic Injury (HII). 2. To describe the clinical signs and symptoms of HII occurring in each age group. 3. To discuss imaging modalities and age-related radiological findings for HII. 4. To give a brief discussion of MRI findings, and the timing of various findings. 5. To use this knowledge to help establish the diagnosis and reduce mortality.

Methods & Materials: 1. Pathophysiology of HII: • Types of Cell Death • Selective Vulnerability of Tissues 2. Signs and Symptoms of HII: • Preterm (< 36 wks) • Term (> 36 wks) • Postnatal- young kids (<2yo) • Older kids/Adults (>2yo) 3. Imaging Modalities & Age-related Radiological Manifestations of HII: • Ultrasound • Compute Tomography • Magnetic Resonance Imaging and Magnetic Resonance Spectroscopy, including timing of findings on various sequences 4. Making a Diagnosis: • Sample Cases • Review Questions

Conclusions: Hypoxic Ischemic Injury is a common condition resulting in a wide spectrum of severe neurological defects. While in the past treatment only consisted of supportive care for HII, recent advances have yielded promising treatment options if initiated within a limited time window. Thus due to the severity of the disease and the need for rapid

intervention, it is important to recognize radiological manifestations of HII along with its clinical signs and symptoms to offer a better prognosis to the patient.

Poster #: EDU-066

Craniosynostosis: Looking Beyond the Sutures

Tushar Chandra, MD, *Children's Hospital of Wisconsin, drtusharchandra@gmail.com*; Teresa C. Gross Kelly, Mohit Maheshwari, Sumit Singh, Ibrahim S. Tuna, Hervey D. Segall

Purpose or Case Report: The aim of this educational exhibit is to provide a framework upon which the diagnosis of the various types of craniosynostosis can be facilitated. Our goal is to provide an efficient way to evaluate craniosynostosis for the radiologist in clinical practice.

Methods & Materials: We plan to accomplish this goal by providing a succinct review of the sutures, an overview of the various classification schemes for craniosynostosis and potential complications associated with premature sutural closure. The role of imaging in the evaluation of craniosynostosis will be described and the features of craniosynostosis that are most important to the craniofacial surgeon will be elucidated. Finally, surgical strategies for the repair of craniosynostosis and postoperative findings will be described.

Results: Some of the forms of craniosynostosis may have a genetic basis, but many are spontaneous in nature. Untreated progressive craniosynostosis can lead to inhibition of brain growth, and an increase in intracranial pressure. MDCT with MIP and 3D surface reformations is the preferred modality for diagnostic evaluation of craniosynostosis. It is also a robust modality for post operative assessment and long-term follow up. MRI is a useful adjunct for assessment of associated intracranial anomalies and complications. Timely and appropriate imaging is essential to assess for potential complications of craniosynostosis which may include intracranial hypertension, anomalies of external and middle ear, hydrocephalus, chronic tonsillar herniation, cranial base deformity, impaired venous drainage, enlarged emissary foramina and veins and optic atrophy. On the other hand, positional plagiocephaly should not be misinterpreted as craniosynostosis. Surgical management is typical for non-syndromic craniosynostosis, which involves correction of craniosynostosis between three to six months of age. Conservative management is the mainstay for syndromic craniosynostosis. Postoperative follow up imaging for surveillance

for ventricular size and signs of raised intracranial pressure are necessary.

Conclusions: Craniosynostosis is a challenging area of pediatric neuroimaging. Knowledge of the sutural anatomy, an understanding of the potential intracranial complications caused by premature sutural closure, as well as the role that imaging plays in presurgical planning, can provide a practical way for the radiologist to evaluate craniosynostosis in a fast-paced clinical setting.

Poster #: EDU-067

The Perinatal Brain and Spinal Cord—Imaging Across a Life Border: A Case-Based Approach

Anand Dorai Raju, MD, *Radiology University of Tennessee, araju@uthsc.edu*; Harris L. Cohen, Matthew Whitehead, Asim Choudhri

Purpose or Case Report: To review normal and abnormal perinatal Ultrasound (US) and Magnetic Resonance (MR) imaging findings and note their significance for the analysis of the fetal and neonatal brain as well as spinal cord and vertebral column using a case based approach. To highlight US and MR capabilities in allowing correct perinatal diagnosis of congenital and acquired central nervous system abnormalities.

Methods & Materials: Cases will be shown of normal and abnormal anatomic findings in fetal and neonatal brain and spinal cord imaging. Key teaching points necessary for the diagnosis of such brain abnormalities as ventriculomegaly, Chiari malformations, holoprosencephaly, and agenesis of the corpus Callosum as well as Dandy Walker malformations and AVMs will be discussed. Intraventricular hemorrhage, periventricular leukomalacia, anoxic injuries and infectious abnormalities will be reviewed. Abnormal anatomic findings in fetal and neonatal spine evaluations for congenital and acquired abnormalities and key teaching points necessary for the accurate diagnosis of tethered cord, myelomeningocele, caudal regression syndrome, hydromyelia, diastomatomyelia and sacrococcygeal teratoma will be reviewed. Some diagnostic difficulties and controversies will be addressed.

Conclusions: Ultrasound aided by MRI can provide ready diagnosis to many central nervous system abnormalities involving fetuses and neonates. Ever improving perinatal imaging experience and technique allow for better prenatal as well as postnatal diagnosis. Cases showing such imaging and key points helping such imaging diagnoses will be reviewed.

Poster #: EDU-068**Overview of Imaging of Pediatric Extraocular Orbital Tumors**

Srikala Narayanan, MD, *Division of Radiology, Children's National Medical Center, snarayan@childrensnational.org*; Nadja Kadom, Gilbert L. Vezina

Purpose or Case Report: To show the spectrum of benign and malignant extraocular orbital tumors in children.

Methods & Materials: We reviewed the cross-sectional imaging of orbit (CT and MR) done in the last 5 years. Specific imaging signs of extraocular tumors including benign and malignant tumors such as hemangiomas, lymphangiomas, optic nerve glioma, optic nerve sheath meningioma, pseudotumors, rhabdomyosarcoma, orbital myofibroma, eosinophilic granuloma and neuroblastoma metastases will be shown. Important imaging features that should be considered when formulating a differential diagnosis will be described.

Conclusions: The spectrum of diseases affecting pediatric orbit is substantially different from what we see in the adults. It is not easy always to differentiate between different tumors. Important imaging characteristics will help us towards better differential diagnosis.

Poster #: EDU-069**Pediatric Spinal Ultrasound: Pearls and Pitfalls**

Tushar Chandra, MD, *Children's Hospital of Wisconsin, dtusharchandra@gmail.com*; Mohit Maheshwari, Teresa C. Gross Kelly, Sumit Singh, Ibrahim S. Tuna, Hervey D. Segall

Purpose or Case Report: The purpose of this exhibit is to review the technique, indications and limitations of neonatal spinal ultrasound with emphasis on normal variants and imaging pitfalls that may mimic disease processes.

Methods & Materials: In this exhibit, we will illustrate ultrasound anatomy of the neonatal spinal cord. Discussion of the normal anatomic variants and pathological conditions of the spinal cord will be provided. Representative images of a variety of common and uncommon pathological conditions of the spine will be presented to illustrate teaching points. In abnormal cases, follow up MRI images will also be illustrated for comparison.

Results: Ultrasound is a robust screening modality for evaluation of the lumbosacral spine in neonates. It is cheaper, readily available, safer first line imaging modality in neonates suspected to have spinal malformations. Under able

and well trained operator, diagnostic accuracy of spinal ultrasound approaches MRI. However, MRI remains the gold standard for imaging evaluation of spine. Normal variants that simulate disease processes like ventriculus terminalis, prominent filum terminale and central echo complex will be presented. Congenital malformations of the cord such as tethered cord, hydromyelia, lipoma, diastematomyelia, myelomeningocele, lateral meningocele and presacral masses will also be discussed.

Conclusions: Ultrasound is a very useful screening technique for evaluation of pathological conditions of lumbosacral spine in neonates. This review would improve the understanding of utility and limitations of ultrasound in evaluation of neonatal spinal malformations.

Poster #: EDU-070**Pediatric Brain PET-CT: An Atlas of Imaging Findings of C11 Methionine and F18 Deoxyglucose Studies for the Evaluation of Seizures and Brain Tumors**

Padmaja Naidu, MD, *Phoenix Children's Hospital, pnaidu@phoenixchildrens.com*; Jeff H. Miller, John Curran, John Egelhoff

Purpose or Case Report: Although MRI is the standard for detecting epilepsy and brain tumor abnormalities, PET-CT is performed to ascertain metabolism related to epileptogenic regions or characterize tumor metabolic activity. Asymmetric metabolism often correlates to structural abnormalities like cortical dysplasia. Metabolic activity often correlates with tumor aggressiveness or grade. FDG PET is commonly used to assess seizure and tumor metabolism. The lesser utilized amino acid PET tracers (C11 Methionine, FDOPA) show increasing value with lower grade tumors due to high tumor to normal tissue contrast. Literature is accumulating regarding C11 methionine (CMET) in the detection of lesions like cortical dysplasia and its ability to delineate low grade seizure related tumor lesions. Despite the established FDG and accumulating CMET literature, little information exists about the imaging seen with both in pediatrics. As these studies are increasingly viewed as part of fusion MRI images, there is more scrutiny of focal metabolism correlating with MRI findings and less interpretative reliance on abnormality based solely on asymmetry.

Methods & Materials: Review of 110 patients who underwent CMET and FDG brain PET-CT was performed. Each was imaged on a Philips scanner and had prior MRI. Studies demonstrating a variety of tumors, postoperative findings of residual or recurrent tumor, and pseudoprogression were

selected. Epilepsy cases with structural cortical abnormalities or seizure-associated tumors were also selected. CMET and FDG studies were analyzed by 3 pediatric neuroradiologists and the imaging findings correlated with prior MRI and any pathology or follow-up imaging. Pictorial galleries of the CMET and FDG imaging patterns were created.

Results: Pathologically proven low-grade glial tumors showed increased CMET uptake and no hypermetabolism on FDG. High-grade tumors showed increased uptake on CMET and hypermetabolism on FDG. Patients with residual or recurrent tumors showed uptake similar to their original tumor. Granulation tissue and pseudoprogression changes showed increased uptake on CMET and no hypermetabolism on FDG. Epilepsy surgery patients with cortical dysplasia or low grade glial tumors showed increased uptake on CMET and FDG hypometabolism.

Conclusions: This study illustrates the variety of findings on CMET and FDG PET-CT in pediatric patients clinically evaluated for brain tumor and epilepsy. This atlas provides readers with a guide to the appearance of these findings on an emerging imaging technique.

Poster #: EDU-071

Pediatric Head and Neck Neoplasms: A Multimodality Pictorial Review

Alok Jaju, MD, *Mallinckrodt Institute of Radiology, alokjaju@gmail.com*; Marilyn J. Siegel

Purpose or Case Report: Neck masses are common in children and most occur in the suprahyoid region. Knowledge of the fascial spaces involved in conjunction with imaging features can help in diagnosis. In this pictorial review, we present a multimodality imaging approach based on anatomy of the suprahyoid fascial spaces for evaluation of pediatric neck tumors.

Methods & Materials: Radiology information system (RIS) at our tertiary care children's hospital was queried to identify patients with suprahyoid neck masses who had imaging performed between July 2004 and present. A variety of conditions having congenital, inflammatory, neoplastic, or vascular origin were identified and the anatomic location in the neck as well as imaging and clinical findings were retrospectively reviewed.

Results: The imaging evaluation included ultrasound, CT and MRI. Lesions arose within the following fascial spaces of the suprahyoid neck: superficial, carotid, masticator, submandibular, sublingual, parotid, parapharyngeal, visceral, retropharyngeal and prevertebral. Key imaging features

important in diagnosis included lesion vascularity, calcification, necrosis and bone invasion. We discuss and illustrate these imaging findings and relate them to specific suprahyoid fascial spaces. Specific lesions include vascular and lymphatic malformations, teratoma, nerve sheath tumors, thyroglossal duct and branchial cleft cysts, pleomorphic adenoma, dermoid cyst, ranula, lymphadenopathy, abscess, lymphoma, rhabdomyosarcoma, neuroblastoma and nasopharyngeal carcinoma.

Conclusions: Knowledge of fascial spaces of the suprahyoid compartment and key imaging features on multiple modalities can aid in the diagnosis of pediatric neck masses.

Poster #: EDU-072

Pediatric Sinusitis: Spectrum of Imaging Findings with Clinicopathologic Correlation

Roy Jacob, MD, *University of Oklahoma, drjacobr@gmail.com*; Paul Digoy, Robert S. Glade, Anthony Alleman

Purpose or Case Report: The clinical spectrum of sinusitis in children can range from uncomplicated bacterial sinusitis to invasive fungal sinusitis. Most cases respond favorably to medical management. However, complications occasionally occur due to the spread to adjacent structures. Imaging plays an important role in characterizing the disease and guiding the clinical and surgical planning and treatment. This electronic presentation outlines the following—1. Review radiologic anatomy and unique characteristics of pediatric sinuses. 2. Review the clinical features, pathophysiology, and microbiology of sinusitis. 3. Review of CT and MRI imaging characteristics of sinusitis with representative cases such as complicated sinusitis and invasive fungal sinusitis. 4. Review the treatment approaches of sinusitis.

Methods & Materials: A retrospective search of PACS was performed on studies completed at the OU Children's Hospital in Oklahoma City for the last three years. CT and MR examinations were selected that depicted relevant disease processes. Corresponding nasal endoscopic pictures were obtained from cases which required surgical management. All studies were de-identified prior to image export.

Results: Over fifteen representative cases of the clinical spectrum of sinusitis and its complications were selected for inclusion.

Conclusions: This educational exhibit provides a concise review of imaging, clinical features, and treatment of pediatric sinusitis. Findings will be richly illustrated with radiological and clinical images.

Poster #: EDU-073**CNS Imaging Findings in Hemophagocytic Lymphohistiocytic Syndrome**

Rupa Radhakrishnan, MBBS, MD, DNB, Radiology, University of Cincinnati College of Medicine, radhakrp@ucmail.uc.edu; Marcia K. Kukreja, Alexandra Filipovich, Alexander J. Towbin

Purpose or Case Report: Hemophagocytic lymphohistiocytosis (HLH) is a rare, life threatening condition caused by an uncontrolled proliferation of activated lymphocytes and histiocytes with high levels of inflammatory cytokines. The organs most commonly involved in this disorder include the liver, spleen, lymph nodes, bone marrow and central nervous system (CNS). The purpose of this exhibit is to review the CNS imaging findings associated with HLH, its complications, and its management.

Methods & Materials: The published literature was reviewed to identify the potential imaging findings HLH. The electronic medical record system was then searched to find illustrative case examples from our institution. Cases demonstrating the primary imaging findings as well cases highlighting complications of the disease or its therapy were selected.

Results: CNS involvement is common in HLH with approximately 75% of patients demonstrating neurological symptoms. CT findings of CNS involvement include diffuse parenchymal atrophy, low attenuation lesions in the white matter and calcifications. MR findings include diffuse leptomeningeal and perivascular enhancement, T2 hyperintense lesions with nodular or rim enhancement as well as confluent white matter lesions, and diffuse parenchymal volume loss of the cerebrum and cerebellum. Restricted diffusion has been demonstrated in some lesions. Ring enhancing parenchymal lesions have been described representing active demyelination. Intracranial hemorrhage may occur as a result of thrombocytopenia and coagulation abnormalities. Sepsis with opportunistic organisms can involve the CNS and produce intracranial findings such as parenchymal abscesses. CNS changes, such as posterior reversible encephalopathy syndrome, are also seen with the commonly used immunomodulatory regimen used in the treatment of HLH.

Conclusions: This exhibit will aid the viewer in identifying the CNS imaging findings of HLH as well as the complications of the disease and its therapy. While the CNS imaging findings are not specific, they may help the radiologist formulate a diagnosis in association with the other clinical and imaging findings; furthermore, imaging can help the clinical team in managing the disease and its complications.

Poster #: EDU-074**Role of Ultrasound in the Evaluation of Palpable Head Lesions in Children: A Pictorial Review**

Ajaykumar C. Morani, MD, Department of Radiology, University of Michigan, ajaycmorani@gmail.com; Ramon Sanchez, Maria Ladino-Torres, Fransisco Rivas Rodriguez, Ramiro J. Hernandez

Purpose or Case Report: To illustrate the role of ultrasound (US) and correlation with other imaging modalities in the evaluation of palpable head lesions in children.

Methods & Materials: Medical records of our pediatric patients with palpable head masses over the last 5 years, were reviewed and images were collected. Correlation of US of these lesions with other imaging modalities and/or pathologic diagnosis was done.

Results: US appearances of various head masses including congenital/developmental (encephalocele, meningocele, dermoid, occipital protuberance), traumatic (cephalhematoma, subgaleal hematoma, calvarial fracture), inflammatory/infectious (sebaceous cyst, histiocytosis, dermatitis), vascular (malformations, pseudoaneurysm) and neoplastic (benign and malignant lesions including metastases) etiologies, will be illustrated with case based approach. MRI and/or CT or tissue diagnosis can be problem solving. Role of ultrasound guidance for percutaneous procedures (biopsy, sclerotherapy) will also be described.

Conclusions: Ultrasound can play an important role in the delineation, diagnosis and guiding further management of pediatric palpable head masses. US can differentiate various scalp lesions and suggest the underlying calvarial defect or involvement to some extent, helping to narrow the differential diagnosis for such lesions. Color doppler US can be useful to detect vascularity within the lesion or vascular lesions. Given that US is often requested for the evaluation of palpable head masses, pediatric radiologists should be familiar with their sonographic features.

Poster #: EDU-075**Posterior Fossa Malformations—A Pictorial Review**

Rui Santos, MD, BC Children's Hospital, ruiradiologia@gmail.com; Khalid Khashoggi, Angela T. Byrne

Purpose or Case Report: Posterior fossa malformations are a group of central nervous system anomalies that may be detected during pregnancy or present early infancy with features that include hypotonia, developmental delay,

microcephaly or hydrocephalus. Knowing the embryology of the cerebellum and 4th ventricle is important to perceive the development of posterior fossa malformations and to further understand the imaging findings. Several classifications schemes have been proposed from a pure embryologic to an imaging-based approach using some essential findings such as the size of the posterior fossa, the presence of CSF collection or expansion of CSF space, and the size and morphology of the cerebellum. MR is the gold-standard for adequately access and characterize the posterior fossa structures. This pictorial essay will review the MR findings of some of the most common posterior fossa malformations including Dandy-Walker malformation, persistent Blakes pouch, mega cisterna magna, arachnoid cyst, paleocerebellar hypoplasia, cerebellar agenesis, cerebellar and pontocerebellar hypoplasia, cerebellar cortical malformations, isolated brainstem hypoplasia/dysplasia and Chiari malformations. We will provide a practical approach to the MR findings of posterior fossa malformations in children.

Conclusions: MR plays a crucial role in identifying and characterizing malformations of the posterior fossa structures. It should give a logical approach to these complex malformations thus guiding the referring physician into the clinical approach and in determining further investigations.

Poster #: EDU-076

Imaging of Petrous Apex in Children: Variants, Pitfalls and Pathologic Conditions

Murat Kocaoglu, MD, *Radiology, Gulhane Military Medical School, kocaoglumurat@yahoo.com*; Bilal Battal, Emrah Ozcan, Alcin Bozkurt

Purpose or Case Report: Petrous apex lesions are rare; however a wide number of pathologies may be seen during radiologic studies of this region. The aims of this pictorial review are: 1. To describe the pseudolesions involving the petrous apex. 2. To classify the petrous apex pathologies. 3. To recognize the patterns and imaging features of diseases that may involve the petrous apex.

Methods & Materials: Plain radiography, high resolution computed tomography (HRCT) and magnetic resonance (MR) imaging with diffusion-weighted sequences can be used in the assessment of petrous apex.

Results: Many tumoral and nontumoral lesions can occur within this structure such as cholesterol granuloma, cholesteroloma, cephalocele, mucocele, apical petrositis, Langerhans cell histiocytosis and sarcomas. In addition to these lesions, a number of normal imaging variants may complicate the diagnosis.

Conclusions: An understanding of the patterns and extent of disease processes of the petrous apex facilitates diagnosis

and staging. HRCT, MR imaging including diffusion-weighted MR imaging allow detailed evaluation of petrous apex.

Poster #: EDU-077

Imaging of Bithalamic Lesions in the Pediatric Brain: Demystifying a Diagnostic Conundrum

Paritosh C. Khanna, *Radiology, Seattle Children's Hospital, pkhanna@uw.edu*; Apeksha Chaturvedi, Ramesh Iyer, Gisele Ishak, Dennis Shaw

Purpose or Case Report: 1. To review the imaging features of bilateral thalamic lesions in children. 2. To discuss differential diagnoses, including metabolic/toxic phenomena, demyelination, infection, vascular lesions and neoplastic entities. 3. To overview additional imaging sequences and techniques useful for determining the etiology of thalamic involvement.

Methods & Materials: 1. Description and classification of abnormal imaging appearances of the thalami. 2. Devising an approach to imaging diagnosis based on patient history, imaging appearances and presence or absence of extra-thalamic involvement. 3. Role of imaging towards formulating a management plan and in subsequent follow-up. 4. Artifacts and diagnostic pitfalls were noted.

Results: Neuroimaging features of abnormal thalami as encountered in the pediatric population were detailed, and wherever applicable, the relevance of additional MR imaging sequences and techniques to determine etiology was described. While there was considerable overlap in imaging appearances, making a precise diagnosis was found to be challenging in difficult cases, and by and large, a stepwise approach was successfully formulated and used to: 1. Diagnose the more emergent conditions and to 2. Devise a management algorithm for the less acute abnormalities.

Conclusions: Bilateral thalamic lesions are occasionally encountered in pediatric neuroimaging and have a limited differential; a good knowledge base and adequate technique are imperative to tease out the precise diagnosis and institute appropriate management.

Poster #: EDU-078

Cortical Developmental Abnormalities in Pediatric Seizure Patients

Ibrahim S. Tuna, MD, *Radiology, Children's Hospital of Wisconsin, dristuna@yahoo.com*; Mohit Maheshwari, Teresa C. Gross Kelly, Sumit Singh, Tushar Chandra, Hervey D. Segall

Purpose or Case Report: To describe various cortical malformations with illustrative examples. We will also briefly

discuss the embryology, genetic basis, classification schemes and characteristic imaging findings .

Methods & Materials: This exhibit will illustrate three main categories of cortical malformations: neuronal proliferation, migration and organization. Understanding of this complex topic would be facilitated by brief discussion on the embryological basis and proposed genetic causes of some of these cortical malformations. Classification schemes on embryology and imaging will be discussed. Characteristic imaging findings of these malformations will be discussed and examples from the authors database will be shown.

Results: Neuroimaging in pediatric seizures is challenging. MRI is considered the imaging modality of choice because of superior soft tissue contrast and better ability to characterize the pathologic process. We will also discuss the dedicated seizure protocol which is used in our institute. PET-CT imaging can also provides additional information in cases where MRI is negative, inconclusive or does not correlate with EEG/clinical findings. Brief discussion on advanced imaging techniques will also be presented. Malformations are frequently detected in infancy. However, if the initial MRI scan performed in infancy is negative, a repeat scan after 2 years of age may be helpful.

Conclusions: Evaluation of cortical malformation in seizure patients still remains a challenging area of pediatric neuroimaging. Reviewing of the embryological basis, classification schemes and characteristic imaging findings would improve the understanding the cortical malformations and interpreting the images.

Poster #: EDU-079 SPRS Best Poster 2011

Cystic Neonatal Lesions Associated with the Spinal Cord: Discussion and Differential Diagnosis for these Uncommon Lesions

Jacob Pirkle, MD, jpirkle@mc.utmck.edu, James Boyd, Brian Dupree

Purpose or Case Report: To review intradural cystic neonatal spine lesions and discuss the various causes and appearance of these lesions. This poster presentation provides a brief review of neonatal cystic spine lesions, including their etiologies, and presents the targeted audience (radiology residents, fellows, and practicing radiologists) a helpful differential diagnosis of these lesions based upon their imaging appearance.

Methods & Materials: A brief overview of neonatal cystic spine lesions, their etiology, and imaging appearance is presented in poster format utilizing both literature search and printed reference material. Images from several cases of cystic neonatal spine lesions are presented.

Results: A brief overview of neonatal cystic spine lesions, their etiology, and imaging appearance is presented in poster

format utilizing both literature search and printed reference material. Images from several cases of cystic neonatal spine lesions are presented.

Conclusions: Neonatal spine ultrasound is often performed to evaluate for abnormalities related to the presence of sacral dimples, cutaneous stigmata, skin tags, hairy tufts, during the evaluation of other congenital anomalies, or when prenatal ultrasound/MRI demonstrates an abnormality warranting postnatal follow-up. The identification of cystic spinal cord lesions is relatively rare in the neonate. However, the etiology of these lesions can often be deduced or surmised based upon the location and the imaging appearance of the lesion. The most common cause of a cystic intramedullary spinal lesion is ventriculus terminalis, with a reported incidence of 2.6%. Additional lesions include transient dilatation of the central canal, filar cyst, syringohydromyelia, intramedullary arachnoid cyst, and myelomalacia related to in utero/birth trauma. Extremely rare etiologies in the neonate include epidermoid/dermoid, cavernous malformation, intranatal cystic infections etiologies, neuroepithelial cysts, and cystic neoplasms. Mimics include diastematomyelia, spinal lipomas, and intramedullary hematomas. Numerous imaging examples of these lesions are provided in the accompanying poster.

Poster #: EDU-080

Brain MRI in Peroxisomal Disorders: A Pictorial Essay
Bruno P. Soares, MD, *Radiology and Biomedical Imaging, University of California at San Francisco, bruno.soares@ucsf.edu; Leonardo Vedolin, Guido Gonzalez*

Purpose or Case Report: Our presentation aims to illustrate the brain MRI patterns in peroxisomal disorders. Peroxisomes are intracellular organelles involved in important cellular processes including beta-oxidation of very-long-chain fatty acids and plasmalogen production. Peroxisomal disorders can be categorized into disorders of peroxisomal biogenesis, in which the peroxisomes are abnormally formed and several peroxisomal functions are deficient, and in defects involving a single peroxisomal function, in which the structure of the peroxisome is intact. Disorders of peroxisomal biogenesis include Zellweger syndrome, neonatal adrenoleukodystrophy, infantile Refsum disease and rhizomelic chondrodysplasia punctata. Numerous disorders are caused by loss of a single peroxisomal function including X-linked adrenoleukodystrophy and Acyl-coA oxidase deficiency. Clinical findings in peroxisomal disorders include dysmorphic features, hepatic dysfunction, neurodevelopmental delay, retinopathy and hearing impairment.

Methods & Materials: Pictorial essay illustrating brain MRI patterns in peroxisomal disorders, including disorders

of peroxisomal biogenesis and disorders with loss of a single peroxisomal function.

Results: Brain abnormalities in peroxisomal disorders have a wide spectrum of patterns. Neuronal migration disorders with abnormal myelination are typically seen in Zellweger disease and neonatal adrenoleukodystrophy. Specifically, the association of abnormal myelination with germinolytic cysts is suggestive of Zellweger syndrome. Classic X-linked adrenoleukodystrophy typically shows posterior central white matter involvement and symmetric demyelination also involving the corticospinal tracts and corpus callosum. A similar pattern of white matter involvement is seen in Acyl-coA oxidase deficiency and infantile Refsum disease.

Conclusions: Brain MRI helps narrow the differential diagnosis and guides subsequent evaluation in infants presenting with clinical features concerning for peroxisomal disorders. Therefore, knowledge of the brain MRI patterns in peroxisomal disorders is important for the radiologist interpreting neuroimaging studies.

Poster #: EDU-081

Clots in Tots: Role of Imaging in Diagnosis of Acute Stroke and its Causes in Children

Asif Abdullah, C.S. Mott Children's Hospital of The University of Michigan, asifa@med.umich.edu; Ellen Hoeffner, Augusto Elias

Purpose or Case Report: Stroke is a major cause of morbidity and mortality in children. Long-term neurologic deficits occur in 50% to 85% of infants and children after arterial ischemic stroke. Limited awareness regarding pediatric stroke among physicians and in general community is a major concern. Imaging plays crucial role in the diagnosis of pediatric stroke. The goal of this presentation is to provide awareness to the reader about the role of imaging in childhood stroke and its myriad causes in children.

Methods & Materials: We will provide a case based approach to imaging diagnosis of acute pediatric stroke based on three categories: (1) arterial ischemic stroke, (2) cerebral venous thrombosis, and (3) hemorrhagic. Arterial ischemic stroke (AIS) is classified according to the Pediatric Stroke Classification (PSC). PSC includes eight subtypes of AIS: (1) sickle cell disease, (2) cardioembolic disease, (3) Moyamoya syndrome, (4) cervical arterial dissection, (5) stenooclusive cerebral arteriopathy, (6) other determined etiology, (7) multiple probable etiologies, and (8) undetermined etiology. We will describe the role of computed tomography (CT) and magnetic resonance imaging including angiography (MRI/MRA) in identifying these causes in relation to available clinical data. The etiologies of cerebral venous thrombosis

related infarction would be discussed from an imaging perspective with a case-based approach with emphasis on MRV and SWI techniques. Finally, we will focus on hemorrhagic causes of childhood stroke such as vascular malformation, aneurysm, neurocutaneous disorders, coagulopathy, and a variety of other causes from an imaging standpoint. Perfusion imaging in pediatric stroke demonstrates flow within the brain and can detect areas that are at risk of ischemia; however, further studies in the pediatric population need to be validated for the role of this technique in pediatric stroke.

Results: The most important factors in the diagnosis of childhood stroke are causal investigation, appropriate laboratory tests, and imaging studies. Imaging is frequently the first step in the evaluation of an acutely ill child.

Conclusions: Pediatric stroke is a debilitating disease that requires urgent multidisciplinary approach for diagnosis and treatment. In cases of both ischemic and hemorrhagic origin, the radiological approach to be obtained in emergency setting leads to the initial screening and the first therapeutic possibility.

Poster #: EDU-082

Extracranial Head and Neck Vascular Malformations: Diagnosis and Management

Ibrahim S. Tuna, MD, Radiology, Children's Hospital of Wisconsin, dristuna@yahoo.com; Mohit Maheshwari, David Moe, Craig Johnson, Sumit Singh, Tushar Chandra, et al

Purpose or Case Report: To describe and review imaging findings of various extracranial head and neck vascular malformations and discuss the interventional treatment strategies for these lesions.

Methods & Materials: This exhibit will illustrate the characteristic imaging findings of vascular anomalies in the head and neck region. Vascular anomalies are divided into vascular tumors and vascular malformations which include slow flow malformations (capillary malformations, venous malformations, lymphatic malformations and their combinations) and high flow malformations (arteriovenous fistula and arteriovenous malformations). Complex malformations are also seen in several syndromes including Klippel-Trenaunay Syndrome, PHACE syndrome, etc. Cases from author's database will be used for illustration.

Results: A review of clinical manifestations, characteristic imaging findings and interventional treatment strategies in cases of head and neck vascular anomalies will be presented with pre and post treatment imaging features. Ultrasonography and MRI are the mainstay in diagnosis of these malformations. CT scan and catheter angiography may occasionally be needed for diagnosis and treatment planning. Various imaging findings and main treatment options will be listed.

Conclusions: Head and neck vascular malformations are common in pediatric population. Understanding the characteristic imaging findings and clinical presentation is essential in evaluating the vascular malformations. Interventional procedures are generally the preferred treatment modality, either alone or in association with surgery in majority of these cases.

Poster #: EDU-083

Isolated Cortical Diffusion Restriction in Pediatric Brain MRI

Ihsan Mamoun, MD, *Cleveland Clinic, ihsanmamoun@yahoo.com;* Sarah Stock, S. Pinar Karakas, Unni Udayasankar, Janet R. Reid

Purpose or Case Report: Diffusion-weighted imaging continues to emerge as a powerful neuroimaging tool. Isolated cortical restricted diffusion is a particularly striking pattern with specific differential in the pediatric population. We aim to review this specific imaging pattern supplemented by case examples and key physiologic and imaging concepts.

Methods & Materials: Review the concept of diffusion restriction A) Pathophysiology B) Specific imaging appearances Pictorial review of pediatric conditions that lead to cortical restricted diffusion: A) Post ictal change B) Infection—i. Meningoencephalitis ii. Herpes C) Hypoxic ischemic injury D) Infarct: venous and arterial E) Posterior reversible leukoencephalopathy F) Mitochondrial Cytopathy G) Metabolic: hypoglycemia. Discuss certain artifacts. Summary table and differential clues

Conclusions: The pattern of isolated cortical restricted diffusion has specific differential diagnosis in the pediatric population. The radiologist should be aware of this as use of DWI continues to grow. This exhibit with familiarize the reader with common conditions that specifically affect the cortex and produces true restricted diffusion.

Poster #: EDU-084

Inner Ear Malformations: Classification System and Embryologic Basis

Sumit Singh, MD, *Radiology, Children's Hospital of Wisconsin, sumitsingh78@yahoo.com;* Mohit Maheshwari, Teresa C. Gross Kelly, Robert H. Chun, Tushar Chandra, Ibrahim S. Tuna

Purpose or Case Report: The purpose of the exhibit is to discuss spectrum of Inner Ear malformations with illustrative examples. We would also discuss the new classification system of cochleovestibular malformations and their embryologic basis [1].

Methods & Materials: High resolution CT scan and MRI are mainstay of diagnosis and assessment in patients with sensorineural hearing loss. In this exhibit we will present a pictorial review of CT scan and MRI images of various causes of sensorineural hearing loss (SNHL) that are seen on imaging. Reviewing the embryologic basis of these anomalies would enable better understanding of this complex subject.

Results: The new system classifies these malformations according to descending order of severity into complete labyrinthine aplasia, cochlear aplasia, common cavity, cystic cochleovestibular malformation or incomplete partition- I (IP-I), cochleovestibular hypoplasia, and incomplete partition- II (IP-II). There is a lot of confusion in literature pertaining to Mondini deformity. The new classification divides incomplete partition into IP-I representing cystic cochleovestibular malformation and IP-II representing the classic Mondini deformity with three components (cystic cochlear apex, dilated vestibule, and large vestibular aqueduct). Recently a subclassification of IP-I and IP-II has been proposed (subdividing into typical and atypical subtypes)[2]. This will be discussed briefly. Isolated large vestibular aqueduct without associated cochlear abnormalities will also be discussed. We will discuss the relevant embryology with correlations of malformations to the timing of embryologic insult.

Conclusions: The new classification system provides precision in description of inner ear malformation. This also helps in providing a uniform scale for comparison of effectiveness of cochlear implant for different malformations. Bibliography: [1] A new classification for cochleovestibular malformations. *Laryngoscope.* 2002 Dec;112(12):2230–41. [2] Radiological diagnosis of incomplete partition type I versus type II: significance for cochlear implantation. *Eur Radiol.* 2011 Oct 1. [Epub ahead of print]

Poster #: EDU-085

Modern Imaging of Pediatric Hydrocephalus

Wendy D. Ellis, Monroe Carell Jr. Children's Hospital at Vanderbilt University; Sudha Singh, Sumit Pruthi

Purpose or Case Report: In recent years, there has been a revolution in the diagnosis and treatment of pediatric hydrocephalus. The evolution of MRI and the advent of new neurosurgical techniques have inspired renewed interest in this commonly encountered entity. This educational review will offer a new approach to better understand and optimally image pediatric hydrocephalus.

Methods & Materials: 1. Review pediatric hydrocephalus, including: classification, etiologies, and pathophysiology of obstructive and non-obstructive hydrocephalus. 2. Review the role of conventional imaging techniques in the evaluation of hydrocephalus. 3. Emphasize modern imaging techniques, adding

value and expertise to the clinical picture. 4. Discuss the preoperative and postoperative radiological assessment of hydrocephalus, and its complications. 5. Overview the neurosurgical perspective of imaging and address new surgical techniques.

Conclusions: This review will present an updated overview of pediatric hydrocephalus with an emphasis on recent progress and modern imaging techniques.

Poster #: EDU-086

Effective Imaging and Diagnosis of Congenital Cranial Nerve Anomalies: What Radiologists Should Know

Britton Bennett, *Arkansas Children's Hospital, bennettbrittonm@uams.edu*; Raghu H. Ramakrishnaiah, Chetan C. Shah, Charles M. Glasier

Purpose or Case Report: Congenital cranial nerve anomalies often present as sensory and/or motor deficits of unknown etiology in the pediatric age group. The early recognition of a definitive cranial nerve abnormality using high-resolution imaging can focus further clinical investigation and shorten the time to diagnosis.

Methods & Materials: To promote appropriate recognition of cranial nerve anomalies, we present the imaging findings of the most commonly affected cranial nerves and provide correlation with clinical presentation. All studies were performed on a 1.5 T magnet with dedicated high resolution imaging of cranial nerve exit zones.

Results: Ours is a tertiary care pediatric hospital with an extensive neuroimaging database. We intend to review all known cases of cranial nerve anomalies from the prior 5 years and present interesting and representative images including optic nerve hypoplasia as part of septo-optic dysplasia, Kallman syndrome, Duane retraction syndrome, and Mobius syndrome.

Conclusions: Congenital cranial nerve anomalies present with varied symptomatology including anosmia, impaired vision, oculomotor deficits, and hearing loss. Additionally, clinical manifestations of cranial nerve anomalies can be difficult to recognize in the pediatric age group. Effective imaging and prompt diagnosis is crucial to initiate appropriate clinical management.

Poster #: EDU-087

Pediatric Brain PET-CT Atlas and Technical Manual for Combination C11 Methionine and F18 Deoxyglucose Studies to Evaluate Seizures and Brain Tumors

Anne McLellan, *Radiology, Phoenix Children's Hospital, ayost@phoenixchildrens.com*; Jeff Miller, Richard Towbin, David Aria

Purpose or Case Report: MR is the standard for evaluation of tumors or epilepsy. PET-CT imaging is often performed to ascertain metabolic asymmetries related to epileptogenic regions or to better characterize the metabolic activity of tumors. A baseline for normals with PET-CT FDG-18 and C11 Methionine does not exist.

Methods & Materials: Retrospective review was performed of the 110 pediatric patients who underwent PET-CT with C11 Methionine and FDG. Representative studies were selected for patients imaged during infancy (<1 yr), early childhood (1–4), childhood (4–7), late childhood (7–12), teenage (13–18). C11 methionine and FDG studies were analyzed for normal patterns of uptake and any trends identified across the stratified age groups. Representative pictorial image galleries of the C11 methionine and FDG imaging patterns through development were created.

Results: The pattern of radiotracer uptake on C11 methionine differed from that of FDG. The C11 uptake remained low level throughout development compared to FDG uptake, which was robust in much of the cortex. The cortical FDG uptake within the frontal lobes progressively increased with age. The C11 uptake within the brainstem and thalamus was equal to cortex throughout development. The FDG uptake within the basal ganglia was equal to cortex while the brainstem and thalamic uptake was generally less than cortex. Several anatomic structures showed robust C11 uptake not seen on FDG. These included the lacrimal, submandibular and parotid glands. Incidentally, the pituitary gland and hippocampus consistently showed C11 uptake equal to cortex contrary to their appearance on FDG. Our institutional protocol regarding the performance of combination C11 methionine and FDG brain PET-CT studies is presented.

Conclusions: This study illustrated the normal appearance of brain PET-CT imaging performed with C11 methionine and FDG in a representative cohort of the pediatric patients through development. Normal variance imaging patterns and developmental trends seen with each radiotracer was demonstrated.

Poster #: EDU-088

The Pediatric Cerebellum: A Pictorial Review of Normal Anatomy using MRI and Diffusion Tensor Imaging

Ibrahim S. Tuna, MD, *Radiology, Children's Hospital of Wisconsin, dristuna@yahoo.com*; Sumit Singh, Teresa C. Gross Kelly, Mohit Maheshwari, Tushar Chandra, Hervey D. Segall

Purpose or Case Report: The aim of this educational exhibit is to illustrate normal anatomical and functional anatomy of the cerebellum in the pediatric patient. The cerebellum receives sensory input from the brain and spinal cord and integrates this information to coordinate motor

control. In addition, the cerebellum also plays a role in some cognitive functions such as attention and language. The first step toward understanding how cerebellar abnormalities can lead to neurological dysfunction, is to provide a solid understanding of the neuroanatomy and functional pathways of the cerebellum. We will describe basic cerebellar embryology, the various cell types and gross anatomy using MR images as well as DTI fiber tractography.

Methods & Materials: This exhibit will describe the microstructure, gross anatomy and functional pathways of the cerebellum through illustrations, MR images, diffusion tensor imaging (DTI) and pathological correlation. First embryology of the cerebellum will be described, followed by MRI depiction of the developmental anatomy of the cerebellum from infancy through adolescence. Finally DTI tractography images will be used to delineate functional pathways to and from, as well as within, the cerebellum. Pathological specimens will be photographed to further illustrate gross anatomy.

Results: Afferent white matter pathways travel mainly via the inferior and middle cerebellar peduncles. The main efferent cerebellar white matter pathway is through the superior cerebellar peduncle. Transverse fiber tracts are present in the vermis. There are mainly two main systems of cerebellar white matter fibers which are easily visualized with DTI color mapping; however more anterior components of DTI tracts are intermixed with afferent white matter projections following the middle cerebellar peduncle.

Conclusions: Knowledge of the precise neuroanatomy and white matter tracts of cerebellum may elucidate our ability to comprehend the clinical manifestations of cerebellar diseases in children. A solid understanding of normal cerebellar anatomy, development and functional fiber tracts in the pediatric patient can provide a baseline that may help predict the clinical outcome of various diseases or interventional procedures.

Poster #: EDU-089

Gastroesophageal Reflux Scintigraphy: A Low Radiation Alternative to GERD Evaluation in Children

Vikas Menghani, MD, *Pediatric Radiology, Women's and Children's Hospital, drvikasmenghani@gmail.com*; Feraas Jabi, Jan Najdzionek, Vaseem Iqbal

Purpose or Case Report: Gastroesophageal reflux disease (GERD) is among the common causes for failure to thrive, recurrent cough and aspiration in children. Early diagnosis of GERD is essential in avoiding long-term sequelae such as growth delay, chronic lung disease, esophageal stricture, and esophagitis. Gastroesophageal reflux scintigraphy, a non-invasive imaging modality, has been applied for detection of GERD and gastric emptying in children over the past few decades. The radiation burden is considerably small given that

a very low dose of radioactivity via a short half-life radioisotope like Technetium-99 m tagged to oral sulfur colloid is administered to a patient. This feature makes reflux scintigraphy especially attractive as the patient can be scanned for prolonged and delayed periods without increasing radiation dose permitting not only identification but also assessment of severity of GERD. Characterizing GERD severity is essential in determining how aggressive the pediatrician should be with therapy. Gastroesophageal reflux scintigraphy also allows a child to be fed their regular meal tagged to radiopharmaceutical without altering food taste. Qualitative and quantitative parameters like gastrointestinal transit and gastric emptying time can be measured, respectively. Scintigraphy is highly sensitive to low grade reflux making it very desirable for monitoring response to therapy. While scintigraphy like all other imaging modalities, has limitations, it continues to be an excellent technique for GERD identification and characterization as well as in monitoring response to GERD therapy.

Poster #: EDU-090

The Pediatric Kidney—A Review of Common and Uncommon Renal Anomalies

Ruby Lukse, *Staten Island University Hospital, drjosemorey@gmail.com*; José Morey, Jeremy Neuman, Arnold Brenner, Oren Herman, Adam Bernheim

Purpose or Case Report: Renal parenchymal imaging in nuclear medicine has long been performed with ^{99m}Tc-dimercaptosuccinic acid (DMSA) due to its sufficient binding to the renal tubules to permit renal cortical imaging. DMSA is of particular value when high-resolution images of the renal cortex are needed. This poster will be a pictorial review of common and uncommon congenital anomalies evaluated on DMSA imaging, such as horseshoe kidney, pelvic kidney, s-shaped kidney and crossed-fused ectopia. The poster will also correlate planar imaging findings with appropriate additional imaging including computed tomography (CT), magnetic resonance imaging (MRI), fluoroscopic imaging and plain film radiographs when clinically warranted and in keeping with the as low as reasonably achievable (ALARA) principle set forth by the American College of Radiology (ACR).

Poster #: EDU-091

Pediatric Hydronephrosis—The Utility of the Renal Scan in the Evaluation of Pediatric Hydronephrosis

David Krausz, *Staten Island University Hospital, drjosemorey@gmail.com*; José Morey, Jeremy Neuman, Arnold Brenner, Conor Lowry, Cyril Varghese

Purpose or Case Report: In this poster we will review the differential diagnoses of congenital anomalies that give the appearance of hydronephrosis on renal imaging of the pediatric patient. We will show a pictorial review of both common and uncommon congenital anomalies such as congenital megaureter, ureterocele, uretero-pelvic junction (UPJ) obstruction, uretero-vesicular junction (UVJ) obstruction and posterior urethral valves (PUV). We will also review common mimickers of hydronephrosis such as multicystic dysplastic kidney (MCDK) and pseudo-obstruction secondary to bladder overdistention. The poster will also correlate planar imaging finds with appropriate additional imaging including computed tomography (CT), magnetic resonance imaging (MRI), fluoroscopic imaging and plain film radiographs when clinically warranted and in keeping with the as low as reasonably achievable (ALARA) principle set forth by the American College of Radiology (ACR).

Poster #: EDU-092

The Pediatric Bone Scan—A Review of Neoplastic Pathology

Shrita Smith, *Staten Island University Hospital, drjosemorey@gmail.com*; José Morey, Jeremy Neuman, Arnold Brenner, Daniel Klein,

Purpose or Case Report: Bone imaging continues to be the second greatest-volume of nuclear imaging procedure performed today, offering the advantage of total body examination, low cost, and high sensitivity. The diagnostic utility, sensitivity, specificity and predictive value of 99 m-Tc bone imaging of malignant conditions have long been established. In fact, more than 3,450,000 bone scans were performed in the United States in 2005. In this poster we will review the current indications for planar bone imaging for the evaluation of malignant and benign neoplasms in the pediatric population, such as osteoid osteoma, Langerhan cell histiocytosis (LCH), osteoblastoma, Ewing's sarcoma, lymphoma, osteosarcoma and osseous/hepatic metastatic disease from neuroblastoma. The poster will also correlate planar and single-photon emission computed tomography (SPECT) imaging findings with appropriate additional imaging including computed tomography (CT), magnetic resonance imaging (MRI), positron emission tomography (PET), and plain film radiographs when clinically warranted and in keeping with the as low as reasonably achievable (ALARA) principle set forth by the American College of Radiology (ACR).

Poster #: EDU-093

The Many Faces of Duplex Kidneys on DMSA Scans—A Pictorial Essay

Neha Kwatra, *Children's National Medical Center, nskwatra@childrensnational.org*; Massoud Majd

Purpose or Case Report: Renal duplication is the most common malformation of the urinary tract and is often seen in children with urinary tract infections (UTI). The purpose of this study is to learn to recognize duplex kidneys on Dimercaptosuccinic acid (DMSA) scintigraphy, review their entire spectrum of findings and correlate with other imaging modalities.

Methods & Materials: DMSA scintigraphy is routinely performed in the nuclear medicine department with a single-head gamma camera (Siemens e.cam, Schaumburg, Illinois). About 1.5 h after injection of DMSA, posterior and posterior oblique images are obtained using parallel and pin hole collimators. Differential renal function is also calculated. DMSA scan reports containing the words “duplex” or “duplicated” from 2006–2011 were populated using a radiology search engine (Montage Health care Solutions Inc.). The images were then reviewed in PACS and representative examples were selected for the poster. The scans were evaluated for renal position, size, contour, any evidence of duplication and parenchymal damage.

Results: Patterns of duplication included non complicated duplex kidney recognized by asymmetric renal size and a prominent cortical bar separating the two moieties, complicated duplex systems with hydronephrosis, scarring or pyelonephritis of one or both moieties. A small non-functioning upper moiety was sometimes evidenced by just an indentation along the superomedial aspect of the larger lower moiety. Cases with bilateral duplex kidneys were also seen. Illustrative examples of each will be provided. Correlating findings on other imaging modalities will also be included.

Conclusions: Establishing the diagnosis of duplex kidney on a DMSA scan requires a careful systematic review of the images. The findings can be subtle and it is important for the radiologist to recognize them. Correlation with other modalities such as ultrasound or voiding cystogram can be complementary. The assessment of parenchymal function of the upper and lower moieties separately on DMSA scintigraphy can be of immense value in patient management and in choosing surgical options.

Poster #: EDU-094**18 F-FDG PET/CT Imaging of Pediatric Brain Tumors, Neurofibromatosis 1(NF1) and Non-Lymphomatous Head and Neck Tumors.****Lisa States, MD, Radiology, CHOP, states@email.chop.edu;**

Purpose or Case Report: This educational poster will review the current literature and summarize the value of 18 F-FDG PET/CT in standard clinical practice in the evaluation of pediatric brain tumors, NF1 plexiform neurofibromas and malignant peripheral nerve sheath tumors, and non-lymphomatous head and neck tumors. Normal variants and pitfalls will be reviewed. Comparison with other PET tracers will be briefly discussed.

Methods & Materials: Case examples will be used to illustrate the value of 18 F-FDG PET/CT in grading, staging, assessment of therapeutic response and detection of residual or recurrent disease in various pathologic entities.

Results: Examples of cases will include: benign brain tumor, residual brain tumor in the post-operative bed, brain metastasis, malignant peripheral nerve sheath tumor in NF1, head and neck rhabdomyosarcoma, mandibular osteosarcoma, and infection.

Conclusions: An understanding of the value of PET molecular imaging is essential to the success of the next phase of hybrid imaging with PET/MRI which has the potential to play an important role in the development of new diagnostic and therapeutic approaches for the treatment of pediatric brain tumors, NF1, and pediatric head and neck tumors.

Disclosure: Dr. States has indicated that she will discuss or describe, in the educational content, a use of a medical device or pharmaceutical that is classified by the Food and Drug Administration (FDA) as investigational for intended use.

Poster #: EDU-095**The Pediatric Bone Scan—A Review of Non-Malignant Pathology****José Morey, Staten Island University Hospital, drjosemorey@gmail.com;** Jeremy Neuman, Arnold Brenner, Vinh Phan, Cheryl Lin

Purpose or Case Report: Bone imaging continues to be the second most performed nuclear imaging procedure, offering the advantage of total body examination, low cost, and high sensitivity. The diagnostic utility, sensitivity, specificity and predictive value of 99 m-Tc bone imaging of benign conditions have long been established. In fact, more than 3,450,000 bone scans were performed in the United States in 2005. In this poster we will review the current indications for planar bone imaging for the evaluation of non-malignant diseases in the pediatric population, such as Acute Osteomyelitis secondary to Salmonella Enterobacteriaceae and tubercle bacillus (TB), chronic osteomyelitis, reflex sympathetic dystrophy, spondylolysis, bone infarcts in the setting of sickle cell disease, fractures (occult/stress), ankylosing spondylitis, dermatomyositis and non-accidental trauma. The poster will also correlate planar and single-photon emission computed tomography (SPECT) imaging findings with appropriate additional imaging including computed tomography (CT), magnetic resonance imaging (MRI), positron emission tomography (PET), and plain film radiographs when clinically warranted and in keeping with the as low as reasonably achievable (ALARA) principle set forth by the American College of Radiology (ACR).

Poster #: EDU-096

WITHDRAWN

Poster #: EDU-097**Diffusion-Weighted Imaging Features of Pediatric Abdominal Masses****Rakhee Gawande, MD, Stanford University School of Medicine, Department of Radiology, rakheegawande@yahoo.com;** Gabriel Gonzalez, Shreyas Vasanawala, Heike Daldrup-Link

Purpose or Case Report: The purpose of this educational exhibit is to provide an overview of imaging features of pediatric abdominal tumors on diffusion-weighted MRI (DWI) scans and apparent diffusion coefficient (ADC) maps.

Methods & Materials: The study was approved by the institutional review board. 68 pediatric patients with abdominal tumors underwent DWI scans. 39 of these patients were scanned on a 1.5 Tesla scanner with DWI 5250-7500/54-64/0, 500 (TR/TE/b-value) sequences and 29 of the patients underwent DWI 3500-4000/66-73/0, 500 sequences on a 3 T scanner. This exhibition will show typical DWI imaging characteristics of a variety of benign and malignant abdominal masses on DWI and ADC maps.

Results: Hepatoblastomas, hepatocellular carcinomas and liver metastases demonstrated restricted diffusion with ADC values of $<1.2 \times 10^{-3}$ mm

Poster #: EDU-098

Radiology of Diesel Exposure

David A. Mong, MD, Children's Hospital of Philadelphia, mong@email.chop.edu; Sabah Servaes, Ann Johnson

Purpose or Case Report: We review the radiologic features of pathologic conditions linked to diesel exposure. The hydraulic fracturing (“fracking”) technique is increasingly used in many areas of the country to extract natural gas from rock formations. Diesel fuel, or fluids containing diesel, are one component of fracking fluid and create a potential for ground water contamination and risk to air quality. The toxic effects of diesel exhaust are described in the literature, and include asthma, hydrocarbon pneumonitis, and leukemia. There are no scientific data currently available on the effects of chronic diesel ingestion.

Methods & Materials: Multi-modality examples of pathology were obtained from a radiology database at a tertiary care pediatric hospital. The specific cases displayed are not known to have diesel exposure, but are intended to serve as representative examples of the type of pathology that may be encountered in the setting of chronic diesel exposure.

Results: Imaging findings of asthma include hyperexpansion, atelectasis, peribronchial thickening, and air-trapping. Hydrocarbon pneumonitis may demonstrate low attenuation consolidation and subsequent pneumatoceles with CT. Leukemia may present on plain radiographs with lucent metaphyseal bands and with marrow infiltration on MRI.

Conclusions: In conjunction with other symptoms not necessarily evaluated in the radiology department, including rhinitis, laryngitis, acute coronary syndrome, and dementia, the radiologist may suggest the diagnosis of diesel toxicity, particularly in populations that may be at high risk of exposure.

Poster #: EDU-099

Pediatric Radiology in the Philadelphia Region: A Historical Review*

Richard Markowitz, MD, Children's Hospital of Philadelphia, markowitz@email.chop.edu

Purpose or Case Report: The specialty of pediatric radiology in the Philadelphia region has grown and evolved over the past eight decades originating from early “visiting” radiologists to Drs. Hope and Kirkpatrick, the “giants” of the 1950s and '60s, to over fifty practicing pediatric radiologists today. Clinical excellence, commitment to teaching, and advancement of knowledge through research remain the goals and ideals, much as they were many years ago. Philadelphia has been a fertile home and environment for this evolution, mostly because of outstanding leaders and role models who have trained and influenced generations of pediatric radiologists. Developments and leadership at the Children’s Hospital of Philadelphia, St. Christopher’s Hospital for Children, and A.I. duPont Institute are highlighted. The purpose of this poster is to tell the story of the growth and development of pediatric radiology in this area and to explore the intellectual origins, professional “genealogy,” and legacies left by those who created and those who have carried on this tradition. *Note: This material is based on a previously published article: *Pediatric Radiology* (2009) 39:969–981 and “Addendum” (*Pediatric Radiology* 2010: 1454–1455), but never presented at SPR.

Poster #: EDU-100

Superficial Lumps and Bumps

Henrietta K. Rosenberg, MD, Radiology, The Mt. Sinai Medical School, Henrietta.Rosenberg@mountsinai.org; Diane Belvin, Neil Lester

Purpose or Case Report: Superficial soft tissue masses in the pediatric age range can be quite challenging to the pediatrician and the imager. The purpose of this presentation is to demonstrate the efficacy of duplex/color Doppler ultrasound for the diagnosis and follow up of a large gamut of superficial lumps and bumps.

Methods & Materials: We reviewed our experience during the past 6 years using ultrasound to evaluate superficial soft tissue masses that had been encountered in many parts of the body, from the skull to the soles of the feet, in a large group of patients ranging in age from newborn to 21 years. All sonograms were performed after obtaining pertinent clinical information as well information regarding the clinical characteristics of each of the masses, e.g. location, consistency (firm [solid],

compressible [cystic]), fixed or easily movable, smooth or irregular surface, tenderness. The masses were palpated by the imaging team and duplex/color Doppler ultrasound was performed. Comparison sonographic views of the opposite side were obtained as needed. Clinical followup and surgical/pathological correlation was obtained in most of the patients.

Results: Most of the masses were benign and included a wide variety of etiologies. Most often, US was sufficient for assessment of soft tissue masses if the entire mass was included in the field of view. If the lesion was too large for the field of view or malignancy was suspected, CT/MRI were required preoperatively. Nuclear medicine studies are reserved for midline masses likely due to ectopic thyroid and PET was used for more complete evaluation of a lesion that was likely malignant.

Conclusions: Duplex/color Doppler ultrasound (US) is the modality of choice for evaluation of superficial lumps and bumps! This modality allows for rapid acquisition of information without the use of ionizing radiation, intravenous contrast material, or sedation/anesthesia. Reliable information can be rapidly acquired regarding the size, shape, borders, location, internal consistency, vascularity, vascular encasement/displacement. Correlation of the ultrasound and clinical findings helps narrow differential diagnosis. Sonography helps to determine what is the next best step: watchful waiting (clinical observation, follow-up US), surgical resection, or US guided interventional procedure.

Poster #: EDU-101

Present Day Imaging of Down Syndrome

Rupa Radhakrishnan, MD, Radiology, University of Cincinnati College of Medicine, radhakrp@ucmail.uc.edu; Alexander J. Towbin

Purpose or Case Report: Down syndrome is a common genetic condition characterized by unique physical traits and multisystem anomalies. The purpose of this exhibit is to portray the imaging findings of Down syndrome and discuss with illustrative examples, the use of imaging in multidisciplinary management.

Methods & Materials: Published literature was reviewed to identify the multisystem imaging findings in Down syndrome. The electronic medical record system was then searched to find illustrative case examples from our institution.

Results: In patients with Down syndrome, abnormalities can be found in the musculoskeletal, cardiovascular, respiratory, gastrointestinal, and central nervous systems. Abnormalities can range from emergent, life threatening conditions such as malrotation with midgut volvulus to chronic conditions such as scoliosis. Examples of abnormalities from each organ system and the modalities used for diagnosis and

management are described. Cardiovascular system: Echocardiogram and cardiac MRI and CT are useful in evaluating congenital heart disease associated with Down syndrome. Respiratory system: Micrognathia with macroglossia and hypotonia predisposes patients to sleep apnea which can be evaluated with dynamic MRI. Chest CT demonstrates subpleural cysts which are characteristic of this syndrome. Gastrointestinal system: Fluoroscopy and/or radiographs are the mainstay in diagnosing many gastrointestinal disorders including duodenal atresia, malrotation, annular pancreas, imperforate anus, and Hirschsprung disease. Central nervous system: Choroid plexus cysts may be identified on prenatal ultrasound in a fetus with Down syndrome. Imaging is used in the evaluation of epilepsy, hearing loss and Alzheimer disease that is more common in these individuals. Musculoskeletal system: Multiple skeletal anomalies can be present in patients with Down syndrome. Radiographs are often used as the method of identifying and, if needed, following the anomalies. Prenatal imaging: Increased nuchal translucency is the earliest imaging finding. Other features of Down syndrome can be identified on prenatal ultrasound or MRI. Prenatal imaging is helpful in determining the prognosis of the fetus and in guiding management.

Conclusions: Modern day multidisciplinary management has improved quality of life and survival in individuals with Down syndrome. Imaging plays a critical role in guiding management in these individuals.

Poster #: EDU-102

Imaging the Spectrum of Lymphatic Malformations in the Pediatric Patient

Andrew Schapiro, MD, Radiology, University of Wisconsin, ASchapiro@uwhealth.org; Kara Gill, Bradley Maxfield

Purpose or Case Report: Lymphatic malformations (LM) occur as a result of abnormal development of the lymphatic system during embryogenesis. As 90% of LM present by 2 years of age, these lesions represent an important pediatric entity. LM can often be suspected clinically in an infant with the classic presentation of an asymptomatic, soft mass in the head, neck, or axilla. However, myriad presentations are possible as LM occur in numerous other anatomic locations, can be multiple, and can be a component of mixed vascular malformations. In addition, the true extent of LM is often not apparent clinically. Given these considerations and the implications for proper management, imaging plays an important role in the assessment of LM. The purpose of this exhibit is to review the spectrum of radiographic, CT, sonographic, and MR imaging findings of a variety of LM presentations.

Methods & Materials: Cases of lymphatic malformation in pediatric patients identified at a single institution over the past ten years with available imaging were reviewed utilizing PACS.

Results: Images of LM involving the head and neck, chest, abdomen, retroperitoneum, extremities, and skeletal system were identified. In addition, cases of lymphangiomatosis and mixed venolymphatic malformation were identified. Various imaging modalities including radiography, CT, sonography, and MR were represented.

Conclusions: Adequate knowledge of the imaging characteristics of LM across multiple modalities enables proper diagnosis, assessment of disease extent, and guidance of appropriate therapy in pediatric patients.

Poster #: EDU-103

"You're so VEIN"—Unusual Causes and Complications of Abdominal and Pelvic Large Vein Thrombosis in Children and Adolescents

Anita Mehta, MD, Radiology, Montefiore Medical Center, anita.mehta5@gmail.com; Terry L. Levin, Benjamin Taragin, Seong Oh

Purpose or Case Report: To present a variety of unusual disease entities that may lead to thrombosis of large abdominal or pelvic veins and to discuss the pathogenesis and potential complications of each entity.

Methods & Materials: Clinical and imaging findings in children and adolescents with unusual causes of thrombosis of abdominal and/or pelvic veins are presented and discussed.

Results: CT and MR imaging findings in nine cases will be presented. They include 1) Congenital absence of the inferior vena cava with thrombosis of the external iliac vein secondary to venous stasis 2) Pyelophlebitis complicating ruptured appendicitis 3) Left iliac vein thrombosis in a patient with May-Thurner syndrome 4) Splenic vein thrombosis complicating pancreatitis 5) Splenic vein thrombosis following splenectomy 6) Renal vein thrombosis in an infant of a diabetic mother 7) Adrenal vein thrombosis as the presenting sign of antiphospholipid syndrome 8) Budd-Chiari syndrome associated with underlying myeloproliferative disease 9) Iliac vein thrombosis as a manifestation of Behcet's syndrome (Hughes-Stovin syndrome, a variant of Behcet's syndrome, which presents with systemic venous thrombosis and pulmonary artery aneurysms will also be discussed).

Conclusions: Thrombosis of large abdominal and pelvic veins in children and adolescents is uncommon. Certain conditions, both congenital and acquired, predispose to the development of venous thrombosis. CT/MR imaging defines the extent of thrombosis, and demonstrates additional findings that may elucidate the nature of the underlying condition leading to clot formation.

Poster #: EDU-104

Imaging Evaluation of Toddlers with Abnormal Gait

Jie C. Nguyen, MD, MS, Department of Radiology, University of Wisconsin Hospital and Clinics, jnguyen@uwhealth.org; Kara Gill, Bradley Maxfield, Kirkland Davis

Purpose or Case Report: Because abnormal gait in a young child has a wide range of causes, imaging plays a critical role in establishing the definitive diagnosis. The purpose of this exhibit is to review the clinical clues (age, duration, laboratory markers) and imaging findings of the causes of abnormal gait in a toddler and to assess the strengths and limitations of radiographs, ultrasound, magnetic resonance imaging (MRI), and computed tomography (CT).

Methods & Materials: Cases, from a single institution experience with various causes for abnormal gait in a toddler, are reviewed and categorized into congenital, traumatic, inflammatory, neoplastic, or neuromuscular etiologies.

Results: There are various causes of abnormal gait in a toddler. The congenital causes include spinal dysraphism, proximal and distal skeletal deformities and dysplasias. The traumatic causes include non-accidental trauma, toddler's fracture, foreign body, and soft tissue injuries. The inflammatory causes include juvenile idiopathic arthritis, transient synovitis, and infection, including osteomyelitis, septic arthritis, discitis, cellulitis, and abscess. The neoplastic causes include various neurogenic, bone, and soft tissue tumors. The neuromuscular causes include cerebral palsy and spinal bifida. The combination of clinical presentation, supporting laboratory findings, and classic imaging findings help to distinguish the possibilities and often allows confident diagnosis.

Conclusions: Knowledge of imaging findings and clinical factors can demystify the diagnosis of abnormal gait in a toddler. Familiarity with the clinical presentation can ensure the performance of the appropriate diagnostic studies, timely diagnosis, and effective treatment. Nonaccidental causes should never be overlooked. Ultrasonography has become an important tool in the radiologist's armamentarium, augmenting radiography, MRI, and CT.

Poster #: EDU-105

Use of MR and CT Contrast Media in Children: Indications, Injection Protocols and FDA Approval Status

Keerthana Bhat, Texas A&M Health Science Center College of Pharmacy, smithu_s@yahoo.com; Rajesh Krishnamurthy

Purpose or Case Report: To analyze indications, injection protocols and FDA approval status of MR and CT contrast agents in children

Methods & Materials: Approximately 20 different contrast agents for MRI and CT are now commercially available for use. Although most of them are FDA approved in adults, information on usage and safety in children is not readily available. The most important reason is lack of controlled studies in children, especially for the age of 0–2 years. However, the lack of FDA approval has not limited the use of these promising agents in children. In fact, there is widespread off-label use of these agents in most major pediatric hospitals in the country. Based on a review of relevant literature in children, and based on a survey of radiology faculty at major pediatric hospitals, this poster will address the gap between approved use and reality in the setting of pediatrics.

Results: Using a tabular format, this poster will provide a list of MR and CT contrast agents that are available for clinical use, their relevant clinical properties (ionic or non-ionic, viscosity, linear or macrocyclic, degree of relaxivity for MRI, iodine concentration for CT, cost, dosage, half-time, incidence of allergic reactions, nephrogenic systemic fibrosis and other adverse reactions), FDA approval status (for ages 0–30 days, 30 days–2 years, and 2–17 years), common pediatric applications, and contrast injection protocols for common applications.

Conclusions: To enlighten imaging personnel about usage and safety of contrast agents in children.

Disclosure: Dr. Krishnamurthy has indicated that he will discuss or describe, in the educational content, a use of a medical device or pharmaceutical that is classified by the Food and Drug Administration (FDA) as investigational for intended use.

Poster #: EDU-106

A Pictorial Essay and Literature Review of the Spleen in Sickle Cell Disease

David Hindson, MD, Boston Medical Center, david.hindson@bmc.org; Heather Imsande, Philippa Sprinz, Ilse Castro-Aragon

Purpose or Case Report: The morbidity and mortality of sickle cell disease (SCD) results from acute and chronic infarction events that affect almost every organ. Repeated infarction has some of its greatest visual and physiologic impact within the spleen. Continuous hemolysis, sequestration and vaso-occlusion within the spleen result in loss of splenic function early in life and frequently autosplenectomy thereafter. By 2 years of age, approximately

90% of children with hemoglobin SS disease will have diminished splenic function, putting them at increased risk for infections. Treatments for SCD have evolved over the last 20 years, and among others include penicillin prophylaxis and immunizations, Hydroxyurea and transfusion therapy (or hypertransfusion program). Imaging findings are a reflection of the different treatments and their efficacy.

Methods & Materials: Our institution cares for a large group of patients with Sickle Cell Disease, from birth to adulthood. This offers an unprecedented opportunity to document the imaging findings of the spleen with different treatment regimens, and over many years. The splenic size and morphology can be followed, by ultrasound, in a very straightforward way. We have compiled a pictorial essay of the various imaging characteristics of spleens from infants to adults. We also performed a literature review to compare and supplement the findings of our images.

Results: There is a spectrum of imaging findings in the spleen of patients with SCD that changes from birth to childhood. The findings range from the normal appearance of a spleen to a calcified spleen, and include regenerative nodules, fibrosis, altered parenchymal echotexture, increased echogenicity, and changes in size, including enlargement secondary to sequestration. The ultrasound characteristics not only change with advancing age, but also appear to depend on whether or not the patient has received specific treatments, and at what age treatment was initiated.

Conclusions: The ultrasound appearance of the spleen in patients with SCD is variable. Treatments such as blood transfusions and Hydroxyurea, patient compliance with therapy and type and severity of the disease are some of the factors that affect imaging characteristics.

Poster #: EDU-107

Cystic Fibrosis: Not Just for Children

Cindy Miller, MD, Radiology, Yale-New Haven Hospital, cindy.miller@yale.edu

Purpose or Case Report: Cystic fibrosis has been recognized for hundreds of years with the first descriptions of it including such anecdotes as mothers licking the foreheads of their children and knowing that if it tasted salty, an early death could be predicted. It was not until 1939 that the disease was first named by Dr. Dorothy Andersen, and for the following 50 years, treatment was largely supportive, and imaging was essentially done with plain films alone. In 1989 with the elucidation of the CFTR gene, there was an explosion of knowledge which included the range of

mutations responsible for the disease and proposals as to mechanism of action of the mutation with respect to disease manifestations. This preceded the development of hypotheses regarding the relationship between genotype and phenotype and the attempt to utilize imaging modalities that could better assess disease activity as it related to functional status. The purpose of this exhibit is to briefly review the history pre-1989 and to focus on the numerous ways in which the understanding has improved since that time.

Conclusions: 1. There are over 1000 different mutations of the CFTR gene responsible for cystic fibrosis with varying prevalence throughout the world. 2. The class of mutation often dictates its particular mechanism of action. 3. There is some relationship between genotype and phenotype—particularly with respect to pancreatic involvement. 4. Newer imaging modalities including CT and MRI with or without hyperpolarized helium are better predictors of disease severity than is plain film.

Poster #: EDU-108

Imaging Pulmonary Tuberculosis in Infants: What are the Most Useful Diagnostic Radiological Findings?

Handan Cakmakci, *Pediatric Radiology, Dokuz Eylul University Hospital, handancakmakci@gmail.com*; Nevin Uzun, Filiz Tetik

Purpose or Case Report: Early diagnosis and treatment are very important for infants with tuberculosis. Infantile pulmonary tuberculosis is more symptomatic, and the risk of severe and life-threatening complications such as tuberculous meningitis or miliary tuberculosis is higher. Bacteriologic confirmation of the disease in children is difficult and in younger infants (<3 months), the tuberculin skin test is frequently negative. Therefore, radiological findings play important role in diagnosing tuberculosis in infants. The purposes of this study are to identify chest x-ray and lung CT findings in pulmonary tuberculosis of infants and consider the most useful diagnostic findings of these age group patients.

Methods & Materials: Chest radiographs and chest CT images of 7 infants who were diagnosed in our hospital from 2005 to 2011 were retrospectively reviewed. The study group included 2 boys and 5 girls ranging in age from 2 to 12 months (mean age, 6 months). Chest x-ray and computed tomography images were analyzed considering air space consolidation, nodular lesions, cavitating lesions, mediastinal enlargement, hyperinflation, bronchial narrowing, atelectasis pleural effusion on plain radiography and additional mediastinal calcific or caseating lymph nodes on CT images.

Results: Air space consolidation was seen on 5 out of 7 chest x-ray and computed tomography images. Nodular lesions were seen 2 out of 7 chest x-ray and computed tomography images. Cavitating lesion was seen on 1 out of 7 chest x-ray and computed tomography images. Mediastinal enlargement suggesting lymph node was seen 5 out of 7 chest x-ray and computed tomography images. Hyperinflation, bronchial narrowing was seen 2 out of 7 chest x-ray and computed tomography images. Atelectasis, pleural effusion was seen 1 out of 7 chest x-ray and 2 out of 7 computed tomography images. Mediastinal caseating lymph nodes, mediastinal calcific lymph nodes were seen 3 out of 7 computed tomography images.

Conclusions: Frequent and the most useful diagnostic radiological findings of pulmonary tuberculosis in infants are mediastinal or hilar lymphadenopathy with central necrosis and air space consolidations. Disseminated nodules including miliary lesions and airway complications are also detected in this age group. CT can show detailed parenchymal lesions and tuberculous lymphnodes especially calcified ones.

Poster #: EDU-109

The Ductus Bump: Radiographic Findings of This Normal Variant and Differential Diagnoses

Anusuya Mokashi, *Staten Island University Hospital, anusuya.mokashi@gmail.com*; Jeremy Neuman, Cheryl Lin

Purpose or Case Report: The Ductus Bump: Review of radiographic findings, differential diagnoses and current controversies. The ductus bump was first described in 1965 by Berdon et al as a transient physiologic mass in the chest in newborn infants. Some controversy remains as to the exact etiology and clinical significance. Although initially thought to represent a dilated ductus arteriosus, recently it has been suggested that it actually represents a ductus arteriosus aneurysm that spontaneously resolves. Others contend it represents dilation of the infundibulum of the closing ductus. Regardless of etiology, the time of discovery, location, and rapid resolution are characteristic of this entity. In this presentation we will review the radiographic and echocardiogram findings of the ductus bump, as well as discuss the differential diagnosis. The frontal radiographic findings are a round mass to the left of the vertebral spine projecting from the mediastinum near the aortic arch. This mass does not indent the esophagus and it cannot be seen on the lateral view. It is classically said to resolve within the first few days of life. The controversy regarding the etiology has also led to some disagreement involving the clinical significance and appropriate follow up, which will also be discussed. After reviewing this educational poster, the reader will have

increased awareness and understanding of the suspected etiology, imaging findings and significance of the ductus bump.

Poster #: EDU-110

The Contribution of 3D Imaging for Evaluation of the Pediatric Central Airways

Jessica Kurian, MD, *The Children's Hospital of Philadelphia, kurianj@email.chop.edu*; Monica Epelman, David A. Mong

Purpose or Case Report: Evaluation of the central airways in children has historically been accomplished by flexible bronchoscopy, an invasive technique associated with inherent risks and complications. Multidetector CT (MDCT) with volume rendering offers a noninvasive alternative for airway evaluation. In this educational exhibit, we will review imaging techniques and clinical applications of MDCT for the assessment of large airway maladies in children.

Methods & Materials: MDCT imaging in children with a variety of tracheobronchial disorders is reviewed. For each entity, the characteristic clinical features are described, and key imaging features are illustrated. Emphasis is placed on the contribution of 3D techniques for characterizing complex airway anomalies. Dose reduction strategies are also highlighted.

Results: The entities reviewed in this exhibit include, but are not limited to, congenital anomalies of tracheobronchial branching, airway malformations associated with situs, and congenital or acquired airway compression and/or obstruction.

Conclusions: MDCT with volume visualization is a useful adjunct for evaluation of the pediatric central airways in a variety of pathologies. As a noninvasive technique, it avoids sedation risks and spare patients from complications associated with conventional flexible bronchoscopy. Low dose protocols should be used to minimize radiation exposure.

Poster #: EDU-111

Congenital Pulmonary Airway Malformation – Common and Uncommon Appearances Using a Multi-Modality Radiologic Approach

Kelly K. Horst, MD, *Radiology, University of Michigan, khorst@med.umich.edu*; Jonathan R. Dillman, Maria Ladino-Torres, George B. Mychaliska, Ethan A. Smith, Peter J. Strouse

Purpose or Case Report: Congenital Pulmonary Airway Malformations (CPAMs) represent a form of

bronchopulmonary foregut malformation that result from abnormal budding of the primitive foregut. Currently, many such anomalies are initially detected by prenatal ultrasound and are further delineated by fetal magnetic resonance imaging (MRI), while others may be incidentally detected on postnatal radiologic examinations or later in life in the setting recurrent pulmonary infection. Imaging plays a very important role in the diagnosis and characterization of these lesions and assists surgical planning. The purpose of our educational exhibit is to illustrate the common and uncommon radiologic appearances of CPAMs using various imaging modalities, including radiography, computed tomography, prenatal and postnatal ultrasound, and prenatal and postnatal MRI.

Methods & Materials: All pediatric and adult CPAM (including both sequestration and CCAM) patients were identified using electronic medical records. Pertinent imaging reports (including radiography, prenatal and postnatal ultrasound, CT, and prenatal and postnatal MRI) were reviewed by a single author in order to identify relevant imaging findings. Relevant images from these imaging examinations were de-identified and saved to a secure hard drive. Medical records were accessed by a single researcher to obtain relevant demographic information as well as data regarding the patients' clinical presentations. In cases of corrective surgery, operative and pathology reports were reviewed, if available, for correlation with the imaging findings.

Results: Cases of pediatric and adult CPAM were identified and presented in a variety of clinical contexts. Their appearances were reviewed through multiple imaging modalities.

Conclusions: Congenital pulmonary airway malformations are varied in their clinical presentation and imaging appearance. The purpose of this pictorial essay is to enhance understanding of their diagnosis and to use a multidisciplinary approach in order to highlight imaging aspects that may alter clinical management.

Disclosure: Dr. Horst has indicated that she will discuss or describe, in the educational content, a use of a medical device or pharmaceutical that is classified by the Food and Drug Administration (FDA) as investigational for intended use.

Poster #: EDU-112

The Imaging Evaluation of Cystic Lung Disease in Children: An Evidence-Based Approach

Jordan Caplan, MD, *Pediatric Radiology, Lucile Packard Children's Hospital, Stanford University, caplan@stanford.edu*; Beverley Newman

Purpose or Case Report: The goal of the poster is to provide a framework for use when confronted with cystic lung disease in a child.

Methods & Materials: The differential diagnosis for the types and causes of cystic lung disease in children will be presented using an evidence-based, age appropriate approach. Categories of disease discussed and illustrated with case examples will include: A. Congenital cystic bronchopulmonary malformations B. Infectious cysts C. Autoimmune/inflammatory/vasculitic disease with cavitating lesions D. Neoplastic conditions E. Collagen/soft tissue abnormalities F. Mimics of cystic lung disease

Results: The pathophysiology, imaging appearance, and demographics of the above entities will be reviewed with attention to relevant recent literature. Important educational points include the differentiation of bronchopulmonary malformations from neoplasm, notably pleuropulmonary blastoma (PPB), the relationship between lung cysts and PPB, and the management and surveillance of lung cysts in children.

Conclusions: An evidence-based approach to the broad spectrum of causes of cystic lung disease in children is a useful starting point in forming a concise and pertinent differential diagnosis. An understanding of the pathophysiology, imaging appearance, and demographics of these entities is essential in guiding patient management.

Poster #: EDU-113

Pediatric Interstitial Lung Disease (ILD): A Pictorial Review with Radiologic and Pathologic Correlation

Hollie West, MD, *Diagnostic Radiology, Vanderbilt University, hollie.c.west@Vanderbilt.edu*; **Melissa A. Hilmes, Sudha P. Singh, Jennifer Soares, Lisa Young**

Purpose or Case Report: While adult interstitial lung disease is a well-described and fairly well understood group of disease processes, pediatric interstitial lung disease (ILD) remains a subject of uncertainty and misunderstanding for many clinicians and radiologists. Confusion surrounding the phenomenon of pediatric ILD stems not only from the rarity of the disease, but also from the extensive list of disease entities that can produce ILD, the existence of certain patterns that are restricted to infants and children and the fact that patterns of ILD manifest differently in a child's developing lung than in an already developed adult lung. Imaging plays an important role in diagnostic work-up of this disease and can guide lung biopsy in specific patient populations.

Methods & Materials: The IRB approved retrospective study will show patients at our institution over a 10 year period diagnosed with various types of ILD, including pulmonary interstitial glycogenolysis (PIG), diffuse neuroendocrine cell hyperplasia (NEHI), surfactant deficiency

diseases, and lung diseases associated with other systemic processes such as Downs syndrome and inflammatory bowel disease. We will include patients with biopsy proven ILD and will provide examples of the major ILDs, including clinical, radiologic and pathologic correlation. Our pictorial review will describe the radiologic patterns associated with the different forms of ILD, emphasizing what the radiologist needs to know and how to be helpful to a multidisciplinary team in the diagnosis and treatment of these diseases.

Results: The study will report the frequency of ILD at our institution, including a breakdown of the various subtypes of ILD. We will show examples of the subtypes with correlative chest radiography, computed tomography, and pathology. We plan to highlight specific differentiating factors between the different diseases and demonstrate how a radiologist can be helpful in collaborating with clinicians in diagnosing and treating these diseases.

Conclusions: Pediatric ILD can be a confusing topic for radiologists. Increasing knowledge and awareness of these diseases, their clinical presentation, work up, and treatment is important for pediatric radiologists who work as part of a multidisciplinary team.

Poster #: SCI-001

CT Radiation Dose Delivered by Community Hospitals and Imaging Centers

Stephen Little, *Children's Healthcare of Atlanta, stephen.little@choa.org*; **Damien Grattan-Smith, Bonnie Johnson**

Purpose or Case Report: To evaluate and compare CT radiation dose for pediatric abdominal and cranial CT examinations performed by community hospitals and imaging centers.

Methods & Materials: 148 consecutive CT examinations (49 cranial, 99 abdominal) from 41 community hospitals and imaging centers were reviewed following transfer of care. The examinations were performed between January and July 2011. 433 consecutive CT examinations (241 cranial, 192 abdominal) performed at our own institution were also reviewed. CTDIVOL and DLP were obtained from the dose report for each examination (32 cm-phantom for abdominal exams, 16 cm-phantom for cranial exams). Patient age and weight were obtained from the medical record.

Results: Average CTDIVOL for abdominal CT performed by local community hospitals and imaging centers was 8.7 mGy, while average CTDIVOL was 4.3 mGy for abdominal CT performed at CHOA. There was a wide variation in CT radiation dose delivered. While some sites delivered a CT radiation dose comparable to our own, others delivered a substantially greater dose. In fact, 23% of pediatric abdominal CT exams performed by local community

hospitals and imaging centers exceeded the Notification Value recommended by the AAPM (10 mGy using the 32-cm phantom). Low kVp technique for imaging small children was infrequent. Multi-phase examinations were more often performed, resulting in additional elevation in CT radiation dose when DLP is considered. Average CTDIVOL delivered by local community hospitals and imaging centers for cranial CT was 44 mGy compared to a CTDIVOL of 30 mGy for cranial CT performed at CHOA. 8% of pediatric cranial CT exams performed by local community hospitals and imaging centers exceeded the Notification Value recommended by the AAPM (60 mGy for 2–5 years, 80 mGy for >5 years).

Conclusions: Despite ongoing efforts at education, there is wide variation in CT radiation dose delivered for pediatric abdominal and cranial CT examinations performed by local community hospitals and imaging centers. Appropriate use of dose check software on newer scanners may help reduce the number of children subjected to excessive CT radiation dose. Ultimately, each site performing pediatric CT must take responsibility for minimizing radiation dose while producing diagnostic quality exams.

Poster #: SCI-002

The Impact of Adaptive Statistical Iterative Reconstruction on CT Image Quality Parameters - A Phantom Study

Karen Thomas, MD, *Radiology, Hospital for Sick Children, karen.thomas@sickkids.ca*; Nancy Ford, Angjelina Protik, Paul Babyn

Purpose or Case Report: To quantify the effect of Adaptive Statistical Iterative Reconstruction (ASIR) on CT image quality parameters.

Methods & Materials: Phantom (Catphan 600) studies were performed on a GE HD750 64-slice scanner to investigate the impact of a) 50% ASIR compared to routine filtered back projection using variable kVp (80–140) and mAs (5–200), and b) incremental ASIR % (0, 30, 50, 70, 100%), scanning at 75mAs and variable kVp (80–120). Pitch, acquisition FOV and detector width were kept constant. Image noise, spatial and contrast resolution, contrast noise ratio (CNR) and Wiener spectrum analysis were performed on 0.625 mm Ax, 5 mm Ax MPR and 2 mm Cor MPR series.

Results: 50% ASIR resulted in a mean decrease in noise of 30% (0.625 mm Ax), 26% (Ax MPR) and 28% (Cor MPR) and improvement in CNR of 38–49%. Incremental advantage was seen with stepwise increase in ASIR %. However, application of ASIR was associated with a small reduction in spatial resolution (2–8% at 50% ASIR). Low contrast detectability (LCD) improved except at the smallest target lesion size. Image quality effects at very low mAs and at high ASIR % will be presented.

Conclusions: Image noise reduction and improvements in CNR and LCD with ASIR hold considerable potential for dose reduction in pediatric CT. This study provides quantitative data that may be used to design ASIR-enhanced protocols with consideration of diagnostic task, balancing image quality benefits and potential pitfalls.

Poster #: SCI-003

Pictorial Essay on Cardiac MR for Congenital Heart Disease on 3 T MR Scanner with RF Multi-Transmit Technology (Tx)

Taylor Chung, MD, *Diagnostic Imaging, Children's Hospital & Research Center Oakland, taylorchung12@gmail.com*

Purpose or Case Report: This is a pictorial essay (e-poster) to show artifacts on cine SSFP images pre-Tx and post-Tx upgrade on congenital heart disease cardiac MR; to illustrate methods prior to Tx-upgrade to minimize artifacts.

Disclosure: Dr. Chung has indicated that he will discuss or describe, in the educational content, a use of a medical device or pharmaceutical that is classified by the Food and Drug Administration (FDA) as investigational for intended use.

Poster #: SCI-004

Revisiting the Relationship Between Anthropometric Parameters and Left Ventricular Mass

Abdullahi Adamu, MD, PhD, *Ahmadu Bello University, scorpion68kd@yahoo.com*

Purpose or Case Report: The purpose of this study was to find the correlation between anthropometric parameters and left ventricular mass in normal adolescents and young adults.

Methods & Materials: 147 healthy individuals in the age range 17 to 23 years (73 males and 74 females) were included in this study. Anthropometry was performed with standard anthropometry kit and measurements of height, weight, Body Surface Area (BSA), upper arm circumference and upper hip circumference were taken. Echocardiography was performed and the American Society of Echocardiography (ASE)-recommended method was employed for calculation of left ventricular mass (LVM). Statistical analysis was performed using Statistica 6.0 (Stat Soft, USA).

Results: The mean value of LVM for all our subjects was found to be 124.53±2.79 g. There was significant correlation between LVM and height ($r=0.52$, $p<0.0001$), weight ($r=0.63$, $p<0.00001$) and BSA ($r=0.64$, $p<0.00001$). Correlation with upper arm circumference was moderate ($r=0.46$, $p<0.0001$), while it was found to be weak with upper hip circumference ($r=0.23$, $p<0.01$).

Conclusions: Anthropometric parameters are a strong determinant of LVM in healthy individuals. It will be logical to presume that body constitution will have a positive influence on cardiac size.

Poster #: SCI-005

Cardiac MRI in Pediatric Patients with Congenital Heart Disease: Comparison at 1.5 T and at 3.0 T

Kim-Lien Nguyen, MD, NHLBI, Laboratory of Cardiac Energetics, nguyenk2@mail.nih.gov; Sarah N. Khan, John Moriarty, Kiyarash Mohajer, Pierangelo Renella, Paul J. Finn

Purpose or Case Report: Despite theoretical advantages of higher field strength, widespread adoption of cardiac MR at 3.0 T has been slow. To the best of our knowledge, there have been no published reports on the use of 3.0 T for imaging in pediatric congenital heart disease (CHD). We sought to assess the feasibility of cardiac MR in pediatric patients with CHD at 3.0 T and to compare the technical and diagnostic performance with an age-matched and clinically comparable control group at 1.5 T.

Methods & Materials: 46 pediatric patients with suspected or known CHD were referred for MR evaluation. 23 underwent imaging at 1.5 T (age 1 day to 7.8 years, mean 28.7 ± 33 months) and 23 underwent imaging at 3.0 T (age 3 days to 8 years, mean 47.8 ± 31.4 months). SSFP cine imaging, time-resolved magnetic resonance angiography (TR-MRA), and high resolution contrast-enhanced MRA (CE-MRA) were performed. Two readers independently evaluated the data for image quality, vessel and cardiac chamber definition, and presence of artifacts. SNR and CNR were calculated.

Results: 95% of SSFP cine images at 3 T were rated as good or excellent quality with 73% having mild and 24% having moderate artifacts ($k=0.07$). SNR was 45.0 ± 22.3 (3.0 T) vs 19.0 ± 6.3 (1.5 T) ($P<0.01$); CNR was 25.7 ± 20.0 vs 7.8 ± 5.2 ($P<0.01$). 100% of arterial and venous phase CE-MRA images were considered good or excellent ($k=0.18$, $k=0.23$ respectively). SNR was 31.7 ± 10.9 vs 24.3 ± 11.9 ($P<0.01$); CNR was 25.2 ± 10.4 vs 18.4 ± 9.8 . Cardiac chamber definition was considered good or excellent in 95% of arterial and venous phase CE-MRA images ($k=0.08$). 100% CE-MRA images showed good or excellent definition of the thoraco-abdominal vessels ($k=0.08$). TR-MRA maximum enhancement factor was 2.3 ± 1.9 vs 1.7 ± 0.8 ($P<0.01$). On average, both readers scored cine SSFP images higher at 1.5 T and CEMRA images higher at 3.0 T. Overall diagnostic performance was high at both field strengths.

Conclusions: MRI of pediatric patients with CHD and vascular abnormalities at 3.0 T is feasible. Relative to 1.5 T, SNR and CNR are both improved at higher field strength and higher resolution CEMRA is achievable. Whereas SSFP artifacts at 3.0 T are more prevalent, they rarely render cine imaging non-

diagnostic. Both field strengths can be used successfully for cardiac and vascular imaging. The decision as to which to use is weighted by local availability and the relative requirement for detailed vascular vs intra-cardiac imaging.

Disclosure: Dr. Nguyen has indicated that she will discuss or describe, in the educational content, a use of a medical device or pharmaceutical that is classified by the Food and Drug Administration (FDA) as investigational for intended use.

Poster #: SCI-006

Color Coded 3D Cardiac CTA of Congenital Heart Disease: A Five Year Experience

Nhi Huynh, MD, Radiology, St. Joseph Hospital and Medical Center, e.nhihuynh@gmail.com; Randy Richardson

Purpose or Case Report: Post-processing of cardiac computed tomography angiograms can be performed on a commercially available workstation to create color coded 3D volume rendered images of the segmented heart and great vessel anatomy in patients with congenital heart disease. These studies optimally demonstrate complex anatomy, streamlining communication between members of the healthcare team and providing a tool for communicating complex anatomy and treatment options with families. These studies have been ordered with more frequency over the past five years. We retrospectively reviewed the types of congenital heart disease demonstrated by cardiac 3D CTA over the past five years at a congenital heart center.

Methods & Materials: Color coded cardiac CTA post-processing was performed from ECG gated prospective and retrospective CTA data on a commercially available workstation for 333/395 patients over the past three years. The anatomy was initially segmented and colored into individual parts of the anatomy of the heart and great vessels as follows RV = purple, LV = light red, aorta = red, pulmonary arteries = blue, systemic veins and right atrium = aqua, pulmonary veins and left atrium = pink, PDA or collaterals = green, airway = yellow, coronary arteries = neutral. The anatomy was then reassembled and images obtained every 3° in a 360° rotation for display.

Results: 3D color coded CTA images were used in the treatment and care of congenital heart patients for the following types of congenital heart diseases: 124 cases of complex anatomy (TGA, truncus arteriosus, HLHS, tricuspid atresia, TOF...), 67 coronary artery anomalies, 68 cases of pulmonary atresia or stenosis, 44 cases of systemic and venous anomalies, 40 cases of coarctation or interruption of the aortic arch, and 56 tracheobronchial tree anomalies.

Conclusions: Color coded cardiac CTA post-processing is an effective and viable method for demonstrating anatomy in complex congenital heart patients. It is an excellent tool for

demonstrating anatomy which is difficult to see by echocardiography such as: coronary artery anomalies, pulmonic atresia, aortic arch coarctation or interruption, and tracheo-bronchial anomalies and/or stenosis.

Poster #: SCI-007

Neuroimaging in the Evaluation of HIE in Term Neonates Post Hypothermia Therapy

Julio M. Araque, MD, *Radiology, Medical College of Georgia, jaraque@georgiahealth.edu*; Jatinder Bhatia, Leann VanLandingham

Purpose or Case Report: To illustrate and review the potential utility of brain MRI, CT and ultrasound in hypoxic ischemic encephalopathy in newborns treated with hypothermia.

Methods & Materials: Neuroimaging studies including brain ultrasound, CT and MRI of fifteen term newborns treated in our institution with therapeutic hypothermia, since April 2010 were evaluated retrospectively. More relevant lesions are depicted and the diagnostic and prognostic value of the findings is discussed and compared with a review of the literature.

Results: Recent studies showed that patients treated with cooling had a more favorable prognosis than was suggested by the clinical grade of encephalopathy compared with infants treated with standard care. Our institutional protocol includes the performance of MRI, and Ultrasound. CT is performed when is a clinical impossibility of perform MRI. Brain ultrasound was performed in all the 15 patients. MRI scans were obtained in 11 neonates. CT was obtained in 3 patients. All MRI studies included DWI. The utility of DWI and ADC maps as an aid in diagnosis of non-ischemic lesions is becoming increasingly established. MRI evidence of brain injury was visible on basal ganglia in 8 cases with negative ultrasound. Abnormal signal intensity in the posterior limb of the internal capsule coexists with lesions in the basal ganglia and thalami have been associated with abnormal motor outcome. The remaining 3 newborns did not develop significant MRI evidence of brain injury. It has been suggested that the ability of MRI to predict subsequent neurological impairment is unaltered by therapeutic hypothermia. Further research is needed for defining the relation between MRI findings and cooling. It is possible that imaging findings might be delayed in cooled infants.

Conclusions: MRI offers the highest sensitivity in detecting anoxic injury of the neonatal brain. MR biomarkers in combination with clinical markers may identify patients with adverse outcome with therapeutic implications.

Disclosure: Dr. Araque has indicated that he will discuss or describe, in the educational content, a use of a medical device or pharmaceutical that is classified by the Food and Drug Administration (FDA) as investigational for intended use.

Poster #: SCI-008

Prenatal Evaluation of Limb Body Wall Complex with Emphasis on MRI

Elisa Aguirre-Pascual, *Radiology, Hospital Universitario de Getafe, elisa.aguirre.pascual@gmail.com*; Teresa Victoria, Ann Johnson, Nancy Chauvin, Beverly Coleman, Monica Epelman

Purpose or Case Report: Limb body wall complex (LBWC), a universally fatal condition, is defined by presence of two of three manifestations: 1) Ventral wall anomaly, 2) limb defect & 3) Craniofacial defects. Its prevalence is 1/10,000 -1/40,000 births. The prenatal diagnosis of LBWC and its differentiation from other treatable abdominal wall defects is crucial. The goal of our study is to describe the MR features of LBWC with emphasis on ventral wall defects, spinal and limb anomalies.

Methods & Materials: We performed a retrospective review of all fetal MRI exams dating from 2001 to 2011. Inclusion criteria included: presence of thoracoabdominal wall defects, spinal abnormalities or limb anomalies (the MRIs were not tailored for detecting craniofacial defects). Exclusion criteria were lack of correlating US or follow up information. Two pediatric radiologists blinded to US findings reviewed the MR images and analyzed the contents of abdominal wall defect, organ location and attachment; spine anomalies; umbilical cord and limb anomalies.

Results: Our search yielded 16 patients. All fetuses had ventral wall defects, small thorax and eviscerated liver and bowel. In two cases kidneys were in extracorporeal location. In 12/16 there was no membrane covering extruded organs. In five MR showed organs attached to the placenta or uterine wall (mainly bowel and liver). Ectopia cordis was present in 3. Thoracolumbar scoliosis was present in 14/16 cases and 5 had spinal dysraphism. Eight cases had a short, uncoiled cord. Limb anomalies present in $n=8$, including: absent extremities, amputated foot, shortened bones and abnormal limb articulation. In 2/16 amniotic bands were present.

Conclusions: We illustrate the common fetal MR findings of LBWC. Awareness and early, accurate recognition of this entity will help differentiate it from other more benign conditions and provide guidance for genetic counseling.

Poster #: SCI-009

Diffusion-Weighted Imaging in Pediatric Small Bowel Crohn Disease: MRI and Clinical Correlation

Justin Ream, *Radiology, University of Michigan, justinre@med.umich.edu*; Jonathan R. Dillman, Jeremy Adler, Shokoufeh Khalatbari, Peter J. Strouse, Mahmoud Al-Hawary

Purpose or Case Report: To correlate bowel wall diffusion-weighted imaging (DWI) apparent diffusion coefficient (ADC) values with multiple MR enterography (MRE) and clinical findings in pediatric small bowel Crohn disease.

Methods & Materials: 54 pediatric Crohn disease patients with MRE exams containing diffusion-weighted imaging and demonstrating terminal ileitis were identified. Minimum bowel wall ADC values were tested for correlation/association with other MRI findings and clinical parameters (including laboratory values).

Results: There is negative correlation between ADC value and degree of bowel wall thickening ($R=(-)0.27$; $p=0.048$). Lower ADC values were significantly associated with striated pattern of arterial phase postcontrast enhancement ($p=0.007$), greater degree of arterial phase postcontrast enhancement ($p=0.006$), and presence of stricture ($p=0.005$). ADC values were not associated with diseased bowel length, degree/pattern of delayed postcontrast enhancement, degree of mesenteric inflammation or fibrofatty proliferation, or clinical markers of inflammation.

Conclusions: Restricted diffusion in pediatric small bowel Crohn disease is associated with other MRI findings of that are suggestive of active disease, including degree of bowel wall thickening and degree and pattern of arterial phase postcontrast enhancement. Our data also suggests that DWI may be useful when attempting to characterize small bowel strictures as either predominantly inflammatory or fibrotic, although further investigation is needed.

Poster #: SCI-010

Quantification of Blood Flow Into and Out of the Liver with 4 d Phase Contrast MRI in the Pediatric Patient

Binh Huynh, MD, Radiology, Stanford, bhuynh@stanford.edu; Shreyas Vasanawala, Albert Hsiao

Purpose or Case Report: The ability to probe blood flow dynamics in the liver may aid management of children with liver disease, including shunt fractions in portal hypertension and arterial flow fraction in diffuse liver disease. The purpose of this study is to evaluate the ability to measure blood flow into and out of the liver with time resolved volumetric (4D) phase contrast MRI in the pediatric patient.

Methods & Materials: Nineteen consecutive patients were retrospectively identified who underwent 4D flow imaging through the level of the hepatic vessels on 1.5 T and 3 T magnets. A software enabling 4D flow program was utilized to first assess for the feasibility of measurement of flow in the hepatic artery (HA), portal vein (PV), splenic vein (SPV), superior mesenteric vein (SMV), supra (SIVC) and infrahepatic (IIVC) inferior vena cava. If measurable, calculations were performed to evaluate for internal consistency

by comparing the sum of SMV and SPV flow to PV flow. Calculations were then performed to compare hepatic inflow (PV+HA) to hepatic outflow (SIVC-IIVC) and for the percentage of PV and HA contribution to hepatic inflow.

Results: Of the nineteen patients, all of the above mentioned six vessels were visualized and measurable in two patients, both of which were imaged on the 1.5 T magnet. In the remaining patients, flow measurements were limited by respiratory motion artifacts obscuring the smaller vessels, and severe eddy currents, particularly in patients imaged with the 3 T magnet. The evaluation for internal consistency demonstrated an average of 1.2% (0.06% & -1.5%) difference between SMV+SPV and PV flow. Hepatic inflow was found to closely match the measured hepatic outflow with an average difference of 11.1% (19.1% & 3.1%). The portal vein was found to contribute 82.9% and 87.3% to hepatic inflow, while the hepatic artery contributed 17.1% and 12.7%.

Conclusions: Measurement of hepatic flow with phase contrast MRI is more challenging than assessment of thoracic flow. When respiratory artifacts are minimal, vessels can be identified and measurements have internal consistency and good agreement between hepatic inflow and outflow at 1.5 T. Conversely, flow measurements were limited at 3 T by eddy currents. Thus, ongoing efforts are aimed at mitigating respiratory motion artifacts at 1.5 T.

Poster #: SCI-011

MRI Findings in Post-Fontan Hepatopathy

Adina Alazraki, MD, Radiology, Emory University/Children's Healthcare of Atlanta, adina.alazraki@choa.org; Pinar Bulut, Kiery Braithwaite, Miriam Vos, Rene Romero, Nitika A. Gupta

Purpose or Case Report: As advances in congenital heart disease continue to improve both mortality and quality of life, associated complications are becoming more prevalent. Amongst patients who have had Fontan repair for hypoplastic left heart syndrome, tricuspid atresia, or other right heart dysfunction, it is well known that liver disease is a complication. We describe the MRI findings in post-Fontan patients and propose MRI as a useful tool to the hepatologist's evaluation of these patients.

Methods & Materials: IRB approval was obtained for a retrospective review of 29 patients who underwent Fontan repair and were subsequently referred for hepatology evaluation between 2010–2011. All but one patient was scanned on a Siemens Trio Trim 3 T magnet; one patient was scanned on a GE Twinspeed 1.5 T magnet with an equivalent protocol due to orthodontics. A standardized departmental protocol was utilized. MRI findings were correlated with age at surgery and years since surgery. MR images were reviewed

independently by 2 pediatric radiologists and compared with the dictated report in the patients record.

Results: 17 patients underwent MRI of the abdomen. 4 patients had MRI incompatible hardware and 8 patients were not scanned secondary to insurance denial. Patients were divided into 4 groups based on elapsed time since surgery: less than 5 years, 5–10 years, 10–15 years, and greater than 15 years. (table 1) MR images were evaluated for the presence of fibrosis, congestion and any other hepatic abnormalities. Fibrosis was determined based on a specific pattern of delayed reticular enhancement in combination with liver morphology. Congestion was deemed present if there was increased T2 signal in the liver parenchyma or periportal regions in combination with cloud-like enhancement on dynamic post-contrast images. All patients demonstrated morphologic changes in the liver with varying degrees of hepatic fibrosis and hepatic congestion. Fibrotic changes were often non-uniform, and thus could be underdiagnosed by biopsy. Interestingly, 4 patients, 24%, had focal arterially enhancing lesions speculated to represent vascular proliferative lesions, however, none warranted biopsy.

Conclusions: It is established that patients who undergo Fontan develop hepatic abnormalities. MRI is a reliable, non invasive technique that accurately demonstrates these findings. MRI may be a more sensitive method to evaluate the etiology and full extent of hepatic disease.

Poster #: SCI-012

WITHDRAWN

Poster #: SCI-013

Complications Within the Interventional Radiology Division of a Tertiary Care Children's Hospital: Initiatives for Ongoing Quality and Practice Improvement

Brian Dillon, *Children's Hospital Boston*, brian.dillon@childrens.harvard.edu; Pamela Sanborn, Yolanda Milliman-Richard, Darren Orbach, Stephan Voss

Purpose or Case Report: Between 2004 and 2010, procedure-related complications occurring within the division of interventional radiology at our institution were recorded and classified according to level of severity. The goals of this study were to determine rates of procedure-based complications based on severity, to establish thresholds for complications, and to determine whether measurable trends in complications over time were evident.

Methods & Materials: Between 2004 and 2010, 14,042 interventional procedures were performed within the

division of interventional radiology at our institution. Adverse events were characterized both according to level of severity (using an institutional 5 point severity scale), and with brief descriptions of individual events. Adverse events were reviewed monthly at the division's morbidity and mortality conference, with respect to procedure type and operator. Based on review of our interventional radiology data and benchmarks rates used for diagnostic errors, threshold complication rates were established by consensus between the department quality improvement committee and the division of interventional radiology. For severe events (Level 4 and 5) there is no allowable threshold; all such events were subjected to both internal and institutional review.

Results: The overall complication rate was less than 1% for all procedures performed. The complication rates for the respective severity levels were: Level 1 (0.235), Level 2 (0.3), Level 3 (0.1), Level 4 (0.249), and Level 5 (0.028). The severity of a given complication was not associated with procedural complexity. No operator-specific trends were identified.

Conclusions: Since 2003, the Society of Interventional Radiology has offered guidelines and strategies for improving safety and quality in interventional radiology. However, no specific benchmark data or procedural recommendations are available for pediatric interventional procedures. Our results demonstrate rates of complications well below published overall complication rates for interventional radiologic procedures. This database of procedure-based complications serves as a foundation for a quality improvement program that allows review of complications with respect to specific procedure types, individual operators, and procedural complexity, in an effort to institute an ongoing and continuous process of quality improvement within interventional radiology.

Poster #: SCI-014

Dysosteosclerosis Presents as an "Osteoclast-Poor" Form of Osteopetrosis: Comprehensive Investigation of a 3-Year-Old Girl

William H. McAlister, MD, *Mallinckrodt Institute of Radiology, Washington University Medical School*, mcalisterw@mir.wustl.edu; Michael Whyte, Deborah Wenkert, Deborah Novack, Angie Nenninger, Xiafant Zhang

Purpose or Case Report: Dysosteosclerosis (DSS), an extremely rare dense bone disease, features short stature and fractures and sometimes optic atrophy, cranial nerve palsy, developmental delay, and failure of tooth eruption in infancy or early childhood consistent with osteopetrosis (OPT). Bone histology during childhood shows unresorbed primary spongiosa from deficient osteoclast action. Additionally, there is remarkable progressive flattening of all vertebrae

and, by adolescence, paradoxical metaphyseal osteopenia with thin cortical bone. Reports of consanguinity indicate autosomal recessive inheritance, yet more affected males than females suggest X-linked recessive inheritance.

Methods & Materials: We investigated a non-consanguineous girl with DSS by a number of methods including radiographically, biochemically and genetically.

Results: Generalized osteosclerosis was discovered at age 7 mo. Our studies, spanning ages 11–44 mo, showed weight ~50%, but length diminishing from ~30% to -2.3 SD. Head circumference was +4 SD. She had frontal bossing, blue sclera, normal teeth, genu valgum, and unremarkable joints. Radiographs showed orbital and facial sclerosis, basilar thickening, "bone-in-bone" appearance in the pelvis, sclerotic long bone ends, and fractures of ribs and extremities. Progressive metaphyseal widening occurred as vertebrae changed from ovoid to flattened and became beaked anteriorly. Consistent with OPT, serum PTH concentrations reflected dietary calcium levels. Serum bone alkaline phosphatase, osteocalcin, and TRAP5b were sub-normal. Iliac crest contained excessive primary spongiosa and no osteoclasts. Splice sites and exons were intact for the genes encoding cholride channel 7, T-cell immune regulator 1, OPT-associated transmembrane protein 1, M-CSF and its receptor C-FMS, ANKH, OPG, RANK, and RANKL. Microarray was unrevealing.

Conclusions: DSS is a distinctive OPT of unknown etiology featuring osteoclast deficiency during early childhood.

Poster #: SCI-015

Anomalous Cervical Arteries in Chondrodysplasia Punctata Brachytelephalangi Type

Mari Okabe, *Dept of Radiology, National Center for Child Health and Development, okabe-m@ncchd.go.jp*; Osamu Miyazaki, Shunsuke Nosaka, Mikiko Miyasaka, Nobuhito Morota, Gen Nishimura

Purpose or Case Report: Chondrodysplasia punctata brachytelephalangi type (CDP-BT) is an X-linked recessive disorder caused by a mutation or a deletion of aryl sulfate E gene (ARSE). The hallmarks include stippled epiphyses, nasal hypoplasia, and hypoplastic distal phalanges and developmental delay. Punctate calcifications are seen not only in the epiphyses but also in the paravertebral regions. Paravertebral puncta are commonly associated with defective ossifications in the cervical spine. The malformation of the cervical spine causes spinal canal stenosis and instability, which occasionally necessitate surgical intervention. In the preoperative spinal imaging of the affected patients, the presence of anomalous cervical arteries came to attention. This observation led us to this study on the

prevalence and radiological manifestations of this vascular malformation in this disorder. Objective: To determine the characteristics in the imaging of vertebral and carotid arteries in CDP-BT.

Methods & Materials: Subjects were five children with CDP-BT (mean age: 1.1 years; range: 1 month – 2 years), who underwent contrast enhanced CT and MRI for preoperative planning of cervical spinal fusion. The images were retrospectively reviewed, focusing on the presence of luminal narrowing and/or tortuosity of vertebral arteries (VA), common carotid arteries (CCA), external carotid arteries (ECA) and internal carotid arteries (ICA). Presence of collateral arteries and brain infarction were also reviewed.

Results: All cases showed spiral tortuosity of the VA. Four out of five had luminal narrowing of the vertebral arteries and 3 out of 5 had collateral arteries. Spiral tortuosity of the carotid arteries was not identified; yet, acute-angled elongation was found in CCA ($n=1$), ECA ($n=3$), and ICA ($n=4$). None of the cases had brain infarction.

Conclusions: Tortuosity and luminal narrowing of the cervical arteries is a common finding in CDP-BT. This previously unknown malformation is an important factor to discriminate patients at increased risk of cerebral ischemia, particularly in patients undergoing surgical intervention.

Disclosure: Dr. Okabe has indicated that she will discuss or describe, in the educational content, a use of a medical device or pharmaceutical that is classified by the Food and Drug Administration (FDA) as investigational for intended use.

Poster #: SCI-016

Severe Skeletal Toxicity from Prolonged Etidronate Therapy for Generalized Arterial Calcification of Infancy

William H. McAlister, MD, *Mallinckrodt Institute of Radiology, Washington University Medical School, mcalisterw@mir.wustl.edu*; Jesse Otero, Gary Gottesman, Steven Mumm, Katherine Madson, Campbell Sheen

Purpose or Case Report: Generalized Arterial Calcification of Infancy (GACI) is an autosomal recessive disorder caused by deactivating mutations within the gene for ectonucleotide pyrophosphatase phosphodiesterase-1 (ENPP1). ENPP1 on osteoblasts, chondrocytes, and vascular smooth muscle cells hydrolyzes nucleotide triphosphates to nucleotide monophosphates and inorganic pyrophosphate (PPi). PPi potently inhibits mineralization. In GACI, low extracellular levels of PPi promote hydroxyapatite crystal deposition in elastic fibers of arteries. Untreated, ~85% of patients die by age six months from cardiac ischemia and congestive heart failure. Etidronate (EHDP), inhibits bone resorption but can

mimic PPI blocking mineralization. During EHDP treatment for GACI, In our patient prolonged high dose EHDP resulted in severe skeletal deformity resembling hypophosphatasia which was reversible with drug stoppage.

Methods & Materials: A 7-year-old boy with GACI referred for profound, acquired, progressive skeletal deformity. He was receiving 200 mg/day of EHDP and was wheelchair bound. We studied him and his response to stopping EHDP.

Results: Skeletal radiographic findings resembled pediatric hypophosphatasia with pancranial synostosis, widened physes with metaphyseal osteosclerosis, "tongues" of radiolucency, along with cupping and fraying, and long-bone bowing. In addition there were large intra and extraarticular calcifications. Radiographic features of BP-induced OPT included femoral Erlenmeyer flask deformity and osteosclerosis (lumbar sine DXA z-score +5.7). Biochemical parameters of mineral homeostasis were essentially normal although serum osteocalcin was low and he had markedly elevated serum levels of creatine kinase and TRAP-5b consistent with osteopetrosis (OPT). After stopping EHDP, he improved quickly with remarkable healing of his rachitic appearing skeleton and decreased joint calcifications.

Conclusions: Our patient with GACI had profound skeletal deformities from high-dose EHDP therapy that significantly improved with drug stoppage.

Poster #: SCI-017

Magnetic Resonance Imaging in the Evaluation of Infants with Hypoxic Ischemic Encephalopathy

Julio M. Araque, MD, Radiology, Medical College of Georgia, jaraque@georgiahealth.edu

Purpose or Case Report: To illustrate and review a spectrum of brain abnormalities of infants with HIE. Defining the most useful approaches and MRI sequences, to facilitate identification and early diagnosis of lesions with the potential to predict outcome and abnormal neurodevelopment.

Methods & Materials: Reviewed available evidence on MRI strategies for evaluating infants with Hypoxic ischemic encephalopathy. Different cases illustrating lesions are presented and discussed for proper diagnosis correlating physiopathology and imaging appearance. More relevant findings are depicted with didactic illustrations. Identifying studies where new techniques such as DWI, ADC, DTI, SWI, or MRS adds significant diagnostic value to the overall interpretation.

Results: MRI is routinely performed as a very sensitive method for detection of HIE lesions. Advanced MR techniques, such as DTI, DWI, ADC, MRS, SWI offer the possibility of detecting injuries at a time when intervention is theoretically possible. The understanding of the physiopathology allows for prediction of the location and extent of

lesions, facilitating identification and appropriate classification. The identification of infants with potentially abnormal neurodevelopment, offers the opportunity to provide therapeutic neurodevelopmental interventions in early childhood. MRS is the best MR biomarker to predict neurodevelopmental outcome in asphyxiated full-term neonates. Brain metabolite ratios and regional ADC values may vary between MR systems and coils. Development of normal values for each institution is required, and support of physicists is mandatory.

Conclusions: MRI continues to evolve as a valuable adjunctive tool routinely obtained in nearly all cases of HIE. Advanced MRI techniques increase sensitivity of conventional T1 and T2-W images and outperform computer tomography and ultrasound for confirming the diagnosis of hypoxic-ischemic brain injury or providing prognostic information for the care of patient with HIE.

Disclosure: Dr. Araque has indicated that he will discuss or describe, in the educational content, a use of a medical device or pharmaceutical that is classified by the Food and Drug Administration (FDA) as investigational for intended use.

Poster #: SCI-018

Posterior Fossa Abnormalities in Children

Amit Gupta, MBBS, Radiodiagnosis, R.N.T. Medical College, Udaipur, Rajasthan, India, amitsensation@yahoo.co.in

Purpose or Case Report: The aim of this exhibit is to demonstrate various conditions involving the posterior fossa in children with emphasis on importance of embryologic development of cerebellum in reaching a correct diagnosis.

Methods & Materials: This pictographic presentation displays the imaging features of cases encountered in our clinical practice on 1.5 Tesla magnetic resonance (MR) imaging.

Results: With the advent of MR imaging, there has been a revolution in identification and characterization of malformations of the brain. This is especially true in posterior fossa, where the sensitivity and specificity of MR imaging with its multidimensional imaging capability are far superior to those of computed tomography (CT) in the detection of subtle morphologic abnormalities. However, there is still a great deal of confusion regarding their classification, terminology, and spectrum of expression and this is where neuroembryology is of great help. This exhibit demonstrates : 1) Review of embryology and normal anatomy of cerebellum. 2) MR appearance of spectrum of conditions involving posterior fossa in children which includes developmental abnormalities (Dandy-Walker complex, Arnold Chiari malformations, cerebellar dysplasia/hypoplasia, Joubert's syndrome, etc.), cysts (arachnoid cyst, giant cisterna magna etc.), tumours (medulloblastoma, ependymoma, hemangioblastoma etc.) and miscellaneous conditions.

Conclusions: Abnormalities of the posterior fossa are often difficult to differentiate solely on the basis of their radiologic appearances alone. However, an accurate diagnosis is essential for proper treatment planning and genetic counselling. Therefore it is imperative for radiologists to be well versed with the normal anatomy and development of cerebellum so as to correctly diagnose the various posterior fossa abnormalities.

Poster #: SCI-019

Imaging of Oculoauriculofrontonasal Syndrome with Low-Dose 3-Dimensional Computed Tomography

Paritosh C. Khanna, MD, Radiology, Seattle Children's Hospital, pkhanna@uw.edu; Kelly Evans, Gisele Ishak, Joseph Gruss, Michael Cunningham, Anne Hing

Purpose or Case Report: Oculoauriculofrontonasal syndrome (OAFNS) combines elements of abnormal morphology of the frontonasal and maxillary processes of the face. The aim of our exhibit is to demonstrate the low-dose Computed Tomography (CT) features of this syndrome, in seven patients who have been followed at Seattle Children's Hospital (SCH) over 18 years. We underscore the imaging features of this condition, and describe additional features including bony nasal abnormalities not previously described in the literature, to improve imaging recognition of this spectrum.

Methods & Materials: We present 3D CT imaging features of a series of eight patients with OAFNS. In keeping with the ALARA (As Low As Reasonably Achievable) concept and the Image Gently recommendations (www.imagegently.org), CT head and face studies were obtained on six of eight patients at SCH, while two had prior exams at outside institutions. Using a 64-slice multidetector CT scanner (GE LightSpeed VCT, Waukesha WI), low-dose CT (120 kV, 150 mAs or lower depending on age) of the head and face was obtained. Planar bone window and 3D surface rendered images were analyzed.

Results: Our series of patients demonstrated bifid nasal bones, uni- or bilateral mandibular hypoplasia, temporomandibular and zygomatic dysplasia and bony external auditory canal abnormalities. One patient had an interfrontal bone with a frontal bony defect that was contiguous with the metopic suture. We describe additional previously unidentified CT anomalies of the nasal bones, anterior nasal spine and nasal septum. These structures are involved in all patients who had CT imaging available, although unique features are present in each case.

Conclusions: CT is the mainstay of imaging of craniofacial anomalies in the post-natal period, both pre- and post-operatively. In addition to our low-dose CT imaging findings of OAFNS, novel nasal bone anomalies identified by our

group serve to identify a new subset of patients with this syndrome and may help refine the phenotype of the OAFNS spectrum.

Poster #: SCI-020

Can Time-Resolved Contrast-Enhanced MRA (TWIST) Classify Soft Tissue Vascular Anomalies in the Head and Neck in Children Accurately?

Aylin Tekes, MD, Radiology, JHH, atekes1@jhmi.edu; Asim Esenkaya, Clifford Weiss, Sumera Ali, Sally E. Mitchell, Thierry A. Huisman

Purpose or Case Report: Soft tissue vascular anomalies (VA) commonly present in the head and neck in children. Accurate classification is crucial since treatment and morbidity changes significantly between vascular tumors and vascular malformations. Further classification of vascular malformations is critical as the treatment method and agents are different for slow and fast flow vascular malformations. Conventional MRI with contrast is routinely performed for diagnosis and follow-up of VA. Our objective is to evaluate accuracy of time resolved dynamic contrast enhanced MRA (TWIST) against conventional MRI with contrast in classification of soft tissue vascular anomalies in the head and neck in children.

Methods & Materials: Children with suspected diagnosis of VA in the head and neck were referred for MRI from 2008 to 2011. 28 children from 0–17 years of age were enrolled. TWIST and conventional MRI was performed (Triplanar T2-Weighted [T2-W] imaging with fat saturation, pre-contrast axial T1-Weighted [T1-W] imaging, and post contrast triplanar fat-suppressed T1-W imaging). TWIST was performed in coronal plane using blood-pool MR contrast agent (Ablavar-Lantheus) to enhance image quality and spatial resolution of MRA. Two pediatric neuroradiologists evaluated all patients in two different sessions, 15 days apart: one session conventional MRI with contrast was evaluated, in the second session TWIST was evaluated. Clinical evaluation and/or percutaneous venogram/lymphogram data were the gold standard.

Results: Our patients had diagnosis of infantile hemangioma ($n=4$), venous malformation ($n=12$), and lymphatic malformation ($n=12$). TWIST alone could accurately classify 26/28, conventional MRI with contrast could accurately classify 22/28. Conventional MRI with contrast combined with TWIST could accurately classify all cases.

Conclusions: TWIST offers high temporal resolution in the order of seconds, and provides functional data about the dynamics of contrast enhancement comprising the arterial, venous and delayed venous phases, which reflects the nature of the vascular anomaly. MRI of soft tissue VA in the head and neck would be incomplete without TWIST. Use of Ablavar

significantly reduces dose (1/3 of other gadolinium based contrast agents), and doesn't require trigger imaging. Conventional MRI provides important information regarding the anatomical extent, size, and relation to critical anatomical structures thus when combined with TWIST, MRI provides the best information without use of radiation in children.

Poster #: SCI-021

Functional Connectivity MRI in Pediatric Brain Tumor Patients with and without Epilepsy

Andrew V. Poliakov, PhD, *Radiology, Seattle Children's Hospital*; David Bauer, Edward Novotny, Seth D. Friedman, Dennis Shaw, Jeff Ojemann

Purpose or Case Report: Functional connectivity MRI (fcMRI) is a way to evaluate cortical networks across different modalities such as motor, sensory, vision, and the default mode network using functional Magnetic Resonance Imaging. fcMRI relies on correlation in fMRI image intensity that occurs between functionally connected regions. This effect can be seen in awake as well as anesthetized patients. We evaluated these pathways in pediatric patients with brain tumors.

Methods & Materials: Patients were randomly selected from our tumor database. Inclusion criteria included age less than 18, history of brain tumor resection, and complete fcMRI data. Imaging was performed on a 3 T Siemens Trio system. Functional MRI data were acquired as part of a clinical imaging protocol over 6.5–8 min using a gradient echo, echo-planar sequence. Preprocessing of fMRI data followed by Independent Component Analysis (ICA) was performed using FSL software. Functional connectivity analysis was performed using software provided by 1000 Functional Connectomes Project, based on AFNI and FSL software packages. Correlation maps were produced by extracting the BOLD time course from a seed region, computing the correlation coefficient between that time course and the time course from all other brain voxels, correcting for multiple sampling and degrees of freedom and thresholded at a z value of 3.0.

Results: Fourteen patients were included in the study, eight female and six male. Tumor types include ganglioglioma (5), pleomorphic xanthoastrocytoma (2), juvenile pilocytic astrocytoma (2), ependymoma (1), anaplastic astrocytoma (1), glioblastoma multiforme (2), and primitive neuroectodermal tumor (1). Seven patients had tumor-associated epilepsy, and seven patients did not. The figure shows connectivity patterns in the motor network in patients without (A) and with (B) epilepsy. In the patients without epilepsy, functional connectivity was often displaced but not decreased or absent. In the patients with epilepsy, we observed decreased or absent

functional connectivity. Similar results were found for default mode network: connectivity was diminished or absent in the patients affected by epilepsy.

Conclusions: fcMRI is a novel technique that may prove useful for evaluation and presurgical planning by giving us insight into how tumors disrupt function. Functional connectivity was often displaced but relatively preserved in the patients without epilepsy. It was disrupted or absent in the patients with epilepsy.

Poster #: SCI-022

Corpus Callosum DTI Measurements in Neurofibromatosis Type 1 and Normal Controls

Nadja Kadom, MD, *Radiology, Children's National Medical Center*, nkadom@childrensnational.org; Amir Noor, Rhea Udyavar, Marine Bouyssi-Kobar, Iordanis Evangelou, Maria T. Acosta

Purpose or Case Report: Many patients with Neurofibromatosis type 1 (NF1) have corpus callosum enlargement; pathogenesis and underlying pathophysiology are unclear. The goal of our study is to investigate the pathophysiological basis of corpus callosum enlargement in NF1 patients through MRI diffusion tensor (DTI) measurements.

Methods & Materials: Retrospective study, IRB approved. Patients consecutively selected from institutional data base; inclusion criteria: established diagnosis of NF1, brain imaging with DTI sequence, abnormally high corpus callosum to skull ratio; excluded were patients with complications of NF1 that could affect size of the corpus callosum. Age and gender matched normal controls were randomly selected from the radiology data base. ROI were placed manually over the corpus callosum for DTI measurements using DTI-Studio by two independent researchers, one blinded to diagnosis.

Results: Fifteen NF1 patients and matched controls were analyzed. The corpus callosum to skull ratio was found to be significantly different between the experimental and control group ($p=0.0001$). For NF1 patients we found: a trend to lower apparent diffusion coefficient (ADC, $p=0.067$), significantly higher radial diffusivity ($p=0.023$), significantly lower axial diffusivity ($p=0.0002$), and significantly lower fractional anisotropy (FA, $p=0.0012$).

Conclusions: The significantly lower axial diffusivity in NF1 can indicate that there are more crossing fibers in the corpus callosum of NF1 patients than in normal controls. Further studies using comparative DTI tractography may be helpful in further investigating this stipulation. The significant increase in radial diffusivity can be explained by a variety of factors, including thinner myelin sheaths, increased interstitial

fluid, smaller axons, or a combination thereof. The trend of lower ADC may indicate low axonal diameter, as ADC has been shown to more strongly correlate with axonal diameter without the myelin sheath. In future studies we will correlate abnormal corpus callosum DTI markers with cognitive functions in NF1 patients to see if relationships exist that can be used as predictors of cognitive deficits in NF1 patients.

Poster #: SCI-023

Screening for Vitamin D Deficiency in Children with Suspected Non-Accidental Fracture

Conor Kain, MD, *Tripler Army Medical Center*; Veronica Rooks, Laura Keller, Jordan Pinsker, Allyson Cordoni, Sarah Frioux

Purpose or Case Report: Determine if routine screening of vitamin D levels after suspected non-accidental fracture detects vitamin D deficiency and changes clinical outcomes.

Methods & Materials: After IRB approval we reviewed all skeletal surveys performed at Tripler Army Medical Center (TAMC) in the last 10 years and selected the children who were evaluated for suspected non-accidental fracture. We determined if 25-hydroxyvitamin D [25(OH)D] level was requested for these patients and characterized the provider's clinical suspicion of vitamin D deficiency as high or low. Per the 2010 Institute of Medicine Report and 2011 Endocrine Society Guidelines we defined vitamin D deficiency as a 25(OH)D level of less than 20 ng/mL. We calculated the prevalence of children with low 25(OH)D levels whose providers had low clinical suspicion for vitamin D deficiency.

Results: 396 skeletal surveys were done at TAMC from November 2000 to July 2011. 99 were performed after identifying a suspected non-accidental fracture. Of these patients 11 children from ages 1 to 7 months had 25(OH)D levels requested. For children whose providers had a low pre-test suspicion for vitamin D deficiency, the prevalence of vitamin D deficiency was 12.5% (95% binomial CI 0.003–0.524, 1 of 8 cases). These results indicate that at least one out of every three hundred children evaluated for non-accidental fracture could have vitamin D deficiency despite a low clinical suspicion by their provider, although the actual rate is likely much higher given that we found one in eight cases. The child we identified with a low Vitamin D level whose provider had no suspicion for rickets was treated with Ergocalciferol and continued to be evaluated for abuse.

Conclusions: Routine vitamin D level screening after non-accidental fracture may detect vitamin D deficiency in children for whom there is low clinical suspicion. As our population resides at a low latitude and receives greater than

average sun exposure, the rate of deficiency in children with suspected non-accidental fracture may be much greater in other areas.

Poster #: SCI-024

Comet Tails and Dirty Shadows: The Secrets Behind Artifacts in Pediatric Ultrasound

Adam Edelstein, *Pediatric Radiology, Massachusetts General Hospital*; Anuradha Shenoy-Bhangle, Katherine Nimkin

Purpose or Case Report: To review common ultrasonographic artifacts, explain what causes them, and show how they can be used to aid in diagnosis in a variety of pediatric conditions, including less common entities.

Methods & Materials: Ultrasonographic images in patients less than 18 years of age were reviewed. Cases were selected that showed classic artifacts which helped with the diagnosis of a variety of entities.

Results: Ultrasound artifacts include comet tail, reverberation, ring down and “dirty” shadowing. These can be used to help characterize a variety of pediatric conditions including gossypiboma, bezoar, subcutaneous foreign body, complications of NEC, and staghorn calculus. Artifacts can also be used to confirm the presence of stool or bowel gas.

Conclusions: Familiarity with ultrasonographic artifacts is critical for tissue characterization and can help narrow the differential diagnosis in difficult pediatric cases.

Poster #: SCI-025

Cardiac CTA: Non-Vascular Ring Tracheobronchial Compression Secondary To Enlarged Patent Ductus Arteriosus in Infants with Congenital Heart Disease.

Nhi Huynh, MD, *Radiology, St. Joseph Hospital and Medical Center*; *e.nhihuynh@gmail.com*; Todd Chapman, Randy Richardson

Purpose or Case Report: Tracheobronchial compression or narrowing secondary to a vascular ring has been well documented. The purpose of this study is to describe the frequency of airway compression secondary to an enlarged patent ductus arteriosus detected by CCTA without the presence of a vascular ring.

Methods & Materials: A retrospective study of 282 CCTA exams in infants was performed over the period between 03/28/2007 and 09/28/2011. CCTA was performed with a 64-slice

MDCT, with EKG gating, followed by three-dimensional reformations.

Results: Of the 282 congenital heart disease infant patients, there are 49 patients with tracheobronchial compression or narrowing. Of these 49 patients, 20 patients reported to have patent ductus arteriosus as the primary cause of tracheobronchial compression or narrowing. Approximately 41% of patients with airway compression in patients with congenital heart disease are secondary to an enlarged and/or tortuous patent ductus arteriosus. None of these cases were due to a vascular ring. Of these 20 patients, 10, 6, and 4 patients demonstrated to have mild, moderate, and severe airway compression respectively.

Conclusions: Tracheobronchial compression or narrowing secondary to vascular ring with a patent ductus arteriosus has been well documented. In this study, we demonstrate that a significant percentage of airway compression in patients with congenital heart disease without a vascular ring is due to a tortuous enlarged patent ductus arteriosus. Cardiac CTA is uniquely equipped to evaluate airway compression due to an enlarged patent ductus arteriosus and can help improve patient care in congenital heart disease patients with respiratory symptomatology.

Poster #: SCI-026

Pediatric Liver MR Elastography: A Primer

Suraj Serai, PhD, CCHMC, suraj.serai@cchmc.org;
Daniel J. Podberesky, Alexander J. Towbin

Purpose or Case Report: A wide variety of pediatric liver disorders may be complicated by the development of liver fibrosis and ultimately cirrhosis. With early interventions, the progression to hepatic fibrosis can be slowed, halted, and in some cases reversed. Liver biopsy has long been considered the gold standard for assessing the presence and degree of liver fibrosis. However, liver biopsy has disadvantages, due to its potential sampling error, risk of complications, relatively high cost, intra- and inter-observer variability, and, in general, poor acceptance by pediatric patients and their parents. MR elastography (MRE) is a relatively new, non-invasive technique that provides a safe, rapid and cost-effective method for objectively evaluating a wide variety of hepatic diseases by quantitative stiffness evaluation of the liver-parenchyma. The purpose of this exhibit is to review our clinical experience with this technique and illustrate the application of liver MRE in the pediatric population at our medical center.

Methods & Materials: A review of pathogenesis and staging of liver fibrosis in children and current methods available for assessing liver fibrosis will be provided. A review of

MRE physics and technique, including the specific liver MRE protocol used at our institution will be illustrated. We will review widely-used and emerging clinical indications for liver MRE, as well as benefits and limitations to the technique, supported by brief literature review.

Results: In addition to sharing our liver MRE technique, we will illustrate clinical case examples from our institution of a variety of liver disorders including non-alcoholic fatty liver disease, non-alcoholic steatohepatitis, storage disorders, cardiac disease, and idiopathic elevated liver enzymes.

Conclusions: This educational exhibit will review our experience with liver MRE, a safe, newly available technique which will play an increasingly important role in the non-invasive evaluation of pediatric liver disease.

Poster #: SCI-027

Spectrum of Tuberculosis in Children

Amit Gupta, MBBS, Radiodiagnosis, R.N.T. Medical College, Udaipur, Rajasthan, India, amitsensation@yahoo.co.in

Purpose or Case Report: The aim of this exhibit is to present a spectrum of tuberculosis (TB) in the human body which commonly involves pulmonary, nervous, musculoskeletal, gastrointestinal and genitourinary systems.

Methods & Materials: This pictographic presentation displays the imaging features of TB cases encountered in our clinical practice with reference to plain X-rays, CT and MRI as appropriate.

Results: With the advent of the newer modalities, the utility of the plain skaiogram has been largely limited a initial screening tool only. Whereas CT scores over MRI in pulmonary TB (parenchymal disease, lymphadenopathy, pleural effusion, empyema, miliary disease) and abdominal TB (spectrum from mesenteric lymphadenitis to visceral involvement), the magnetic resonance (MR) imaging is much better in diagnosing CNS TB (tuberculoma, abscess, meningitis, subdural empyema and myelitis). In musculoskeletal and genitourinary TB, CT and MR imaging may be preferred based on the stage of disease and the character of the lesion. Cardiac involvement (pericarditis) is among the less common affections of TB.

Conclusions: Tuberculosis is a multisystem disease that can affect virtually any part of the body from head to toe. TB demonstrates a variety of clinical and radiologic findings and has a known propensity for dissemination from its primary site and therefore can mimic numerous other disease entities. Hence it is imperative for radiologists to understand the typical disease distribution, patterns and imaging manifestations of TB.

AUTHOR INDEX

Abbara, Suhny	PA-112	Armstrong-Wells, Jennifer	CR-21
Abdeen, Nishard	PA-139	Atweh, Lamy A.	PA-059, PA-126
Abdulhadi, Mike	PA-105	Au, Jason	EDU-63
Abdullah, Asif	CR-15, CR-20, EDU-81	Au Yong, Kong Jung	PA-016
Acosta, Maria T.	SCI-22, PA-071	Aukland, Stein Magnus	PA-056
Adamu, Abdullahi	SCI-4	Aw, Jessie	PA-018
Adeb, Melkamu	PA-085	Ayyala, Rama	PA-065
Adler, Brent	CR-18	Babb, James	PA-007
Adler, Jeremy	SCI-9, PA-050	Babcock, Evelyn	PA-023
Agarwal, Prachi	PA-030	Babic, Drazenko	PA-087
Aguirre-Pascual, Elisa	SCI-8	Babikian, Sarkis	PA-041
Ahlawat, Shivani	CR-27	Babyn, Paul	SCI-2
Aksoy, Murat	PA-021	Badea, Cristian	PA-066
Al-Hawary, Mahmoud	SCI-9, EDU-18	Bagade, Swapnil	EDU-15
Al-Qassabi, Badriya	PA-144	Bagrosky, Brian M.	PA-001
Alasti, Fatemoh	PA-075	Bailey, Smita S.	PA-003
Alazraki, Adina	CR-8, SCI-11	Bajaj, Lalit	PA-010
Alboliras, Ernerio	PA-035	Ballisty, Marianne M.	EDU-14
Alexander, Allyson	PA-012	Bammer, Roland	PA-021
Ali, Sumera	SCI-20	Bandarkar, Anjum N.	PA-080
Alleman, Anthony	EDU-63, EDU-72	Bardo, Dianna M.	PA-094, PA-121
Alley, Marcus	PA-025	Barlev, Dan	CR-14
Altaye, Mekibib	PA-146	Barnes, Patrick	PA-012, PA-014, PA-017, PA-054, PA-070, PA-076
Altinok, Deniz	PA-145	Barth, Richard A.	PA-100, PA-118, PA-120
Altinok, Gulcin	PA-145	Bartlett, Murray	EDU-45, EDU-50
Amaral, Joao	CR-13, PA-159	Bartz, Brett	PA-099
Amin, Raouf S.	PA-064	Baskin, Kevin	PA-088
Amirabadi, Afsaneh	PA-127, PA-136	Basta, Amaya M.	EDU-8, EDU-26
Amundson, Per	EDU-9	Battal, Bilal	EDU-76
Andrew, Watt	PA-097	Bauer, David	SCI-21
Angels, Erin	PA-096	Beaumont, Claire B.	CR-4
Annapragada, Ananth	PA-066, PA-067, PA-068	Bell, Robert	PA-068
Anooshiravani, Mehrak	PA-077	Bellah, Richard	CR-12, EDU-12
Anton, Christopher G.	PA-152	Belvin, Diane	EDU-100
Anupindi, Sudha A.	PA-065	Bennett, Britton	EDU-86
Aouthmany, Ahmad	CR-15, CR-20	Benya, Ellen	PA-046
Applegate, Kimberly	CR-2	Bernard, Timothy J.	PA-051, PA-053, CR-21
Araque, Julio M.	SCI-7, SCI-17	Bernheim, Adam	EDU-90
Araujo, M.	PA-024		
Aria, David	EDU-87		

Bhargava, Ravi	PA-016	Burrowes, Delilah	PA-018
Bhat, Keerthana	EDU-105	Bushur, Katie	PA-037
Bhatia, Jatinder	SCI-7	Byott, Sam	EDU-58
Billups, Catherine	PA-002	Byrne, Angela T.	EDU-13, EDU-75
Bisset, George S.	PA-135	Cahill, Anne Marie	PA-086
Bissler, John	PA-157	Cakmakci, Handan	EDU-108
Bittman, Mark	PA-045	Calhoon, Meghan J.	PA-051
Bixby, Sarah	PA-154	Callahan, Michael J.	EDU-35, EDU-40, PA-045, PA-092
Blanchette, Victor	PA-128	Calvo-Garcia, Maria A.	EDU-19
Blanco, Ernesto I.	EDU-36, EDU-61	Campen, Cynthia	PA-070
Blask, Anna	PA-101	Caplan, Jordan	EDU-112
Blitman, Netta	EDU-29	Capocelli, Kelley	PA-049
Blomqvist, Lennart	PA-048	Carpineta, Lucia	PA-117, PA-144
Blumenstein, Marilyn	PA-086	Carrico, Caroline W.	PA-099
Blumer, Steven L.	EDU-29	Carrino, John A.	EDU-41
Blumfield, Einat	EDU-64	Carroll, Elizabeth	PA-051
Bodmer, Nicholas	PA-081	Casale, Pasquale	PA-085
Boe, Justin	PA-069, PA-100, PA-140	Castro, Denise	CR-22
Boechat, Ines	PA-026, PA-031	Castro-Aragon, Ilse	EDU-106
Bogale, Savivek	PA-033	Cavanaugh, Beth Anne	PA-006
Boiselle, Phillip M.	PA-060, PA-061	Cecil, Kim M.	PA-146, PA-149
Bonner, Earic	CR-1	Cerwinka, Wolfgang	PA-084
Borzykowski, Ross	EDU-54	Ceschin, Rafael	PA-123
Boue, Daniel	CR-23	Cha, Sang Hoon	PA-011
Bouyssi-Kobar, Marine	SCI-22	Challa, Harigovinda R.	EDU-16, EDU-25
Bowers, Daniel C.	PA-015	Chan, Frandics	PA-069
Boyd, James	EDU-79	Chan, Michael W.	PA-127
Boyd, Kevin P.	PA-046	Chandra, Tushar	EDU-7, EDU-37, EDU-59, EDU-60, EDU-62, EDU-66, EDU-69, EDU-78, EDU-82, EDU-84, EDU-88
Boylan, Emma	PA-018, PA-028	Chang, Franklin	PA-001
Bozkurt, Yalcin	EDU-76	Chapman, Teresa	PA-081
Braithwaite, Kiery	CR-2, SCI-11, EDU-14	Chapman, Todd	SCI-25
Brandon, Jonathan L.	PA-049	Chaturvedi, Apeksha	EDU-77
Bravo, Monica	PA-024	Chau, Cam	PA-035
Bravo, Paco E.	PA-004	Chauvin, Nancy	SCI-8, EDU-38, EDU-39, PA-129
Bray, Heather	EDU-13	Chen, Yi-Fang	CR-11
Brenner, Arnold	EDU-90, EDU-91, EDU-92, EDU-95	Chetty, Shilpa	PA-118
Brody, Alan S.	PA-058	Choi, Byung Min	PA-011
Browne, Lorna	PA-033	Choi-Rosen, Jeanne	EDU-22
Bulas, Dorothy	PA-054, PA-080, PA-101		
Bulut, Pinar	SCI-11		
Buonomo, Carlo	PA-154		

Chong, W K Kling	PA-056	Darling, Stephen	PA-151
Choudhri, Asim	EDU-67	Davis, Carl	PA-097
Chouthai, Nitin	PA-145	Davis, Kirkland	EDU-104
Chow, Jeanne S.	PA-043	Davis, Richard	PA-107
Chowdhury, Shilpy	PA-044, PA-082	Deakayne, Sara	PA-010
Christianson, Howard	EDU-35, EDU-40	Deloney, Linda A.	PA-036
Christianson, Olav	PA-115	Dent, Carly M.	CR-19, PA-052
Chun, Robert H.	EDU-84	Deoliveira, Vicente	CR-13
Chung, Taylor	SCI-3, PA-029	Desai, Neal	EDU-4, EDU-65
Ciccarone, Antonio	PA-019	Desilet-Dobbs, Debbie	CR-24
Cilento, Bartley	PA-043	Deye, Katherine	EDU-49, PA-142, PA-155
Clark, Joseph F.	PA-149	Dhanantwari, Amar C.	PA-121
Clayton, Barbara	PA-123	Di Pietro, Michael	EDU-53
Coakley, Fergus V.	EDU-8	Diab, Karim	PA-035
Cohen, Harris L.	EDU-67	Diaz, Alejandro	EDU-31
Cohen, Ira	CR-26	Dickson, Paula	EDU-14
Cohen, Mervyn	PA-095	Dietz, Kelly	EDU-20
Cohen, Pierre-Alain	EDU-26	Digoy, Paul	EDU-72
Colantoni, William	PA-053	Dillman, Jonathan R.	SCI-9, EDU-17, EDU-18, EDU-32, EDU-111, PA-050
Coleman, Beverly	SCI-8	Dillon, Brian	SCI-13
Coleman, Lee T.	PA-016	DiPietro, Michael	PA-160
Collado, I.	PA-024	Ditchfield, Michael R.	PA-016
Collins, Lee	EDU-22	Divekar, Abhay	PA-067
Connolly, Bairbre	CR-13, PA-159	Dobbs, Matthew D.	CR-9
Coombs, Laura	PA-092, PA-114	Dome, M.D., PhD, Jeffrey	PA-083
Cooper, David	PA-004	Domina, Jason G.	PA-050
Cope-Yokoyama, Sandy	CR-25	Don, Steven	PA-093
Cordoni, Allyson	SCI-23	Donald, Tracy A.	PA-060
Cortes, Cesar	EDU-31	Done, Stephen	EDU-1, PA-151
Cotten, Michael C.	PA-099	Dorai Raju, Anand	EDU-67
Courtier, Jesse	EDU-8, EDU-26	Dorfman, Adam	PA-030, PA-050
Crapp, Seth	CR-1	Doria, Andrea S.	EDU-42, PA-127, PA-128, PA-136
Crowe, James E.	PA-135	Doshi, Taral	PA-107
Crowley, John	PA-091, PA-088	Dubois, Josée	PA-133
Cunningham, Michael	SCI-19	Dumoulin, Charles	PA-098, PA-130
Curran, John	EDU-70	Dupree, Brian S.	EDU-79
Dajani, Nafisa K.	CR-4	Edelstein, Adam	SCI-24
Daldrup-Link, Heike	EDU-97, PA-137, PA-140	Edwards, Michael	PA-012, PA-014, PA-017
Daneman, Alan	PA-119	Effmann, Eric L.	EDU-55
Daniel, Michael E.	CR-25	Egbert, Nathan	EDU-17
Dardanelli, E.	PA-024		
Darge, Kassa	EDU-6, PA-040, PA-085, PA-092, PA-114		

Egelhoff, John	EDU-70	Fonda, Claudio	PA-019
Egloff, Alexia	PA-101	Forbes, Peter	PA-154
Ehrlich, M.D., Peter	PA-083	Ford, Nancy	SCI-2
Eide, Geir Egil	PA-056	Fox, Ira	PA-088
El Jalbout, Ramy	CR-17	Freiman, Moti	PA-045
Elgen, Irene B.	PA-056	Friedman, Seth D.	SCI-21, PA-055, PA-057, PA-072, PA-151
Elias, Augusto	EDU-81	Frioux, Sarah	SCI-23
Elkaissi, Mahmoud	EDU-63	Frischer, Jason S.	CR-6
Elliott, Martin J.	PA-156	Frush, Donald	PA-092, PA-108, PA-110, PA-114, PA-115
Ellis, Wendy D.	EDU-85	Frush, Donald P.	PA-096
Emery, Kathleen	PA-130, PA-152	Furey, Beth	PA-089
Epelman, Monica	EDU-6, SCI-8, EDU-38, EDU-39, EDU-110, PA-065, PA-105, PA-119, PA-122	Furuta, Glenn	PA-049
Esenkaya, Asim	SCI-20	Gargan, Lynn	PA-015
Eslamy, Hedieh K.	PA-120	Garnet, Daniel	CR-14
Espinosa, Gabriela	PA-068	Gawande, Rakhee	EDU-97, PA-137, PA-140
Estroff, Judy A.	PA-116	Gebhard, Robyn	PA-109
Evangelou, Iordanis	SCI-22	Geller, Evan	EDU-36
Evangelou, Vangelis	PA-040	Ghadimi Mahani, Maryam	EDU-32, PA-030
Evans, Kelly	SCI-19	Ghaghada, Ketan	PA-066, PA-067
Ey, Elizabeth	PA-108	Giaquinto, Randy	PA-130
Faerber, Eric	EDU-61, PA-108	Gibson, Seth	EDU-56
Fagen, Kimberly	CR-26	Gill, Kara	EDU-102, EDU-104
Fagerberg, Ulrika	PA-048	Ginsberg, Jill P.	CR-12
Fairman, Ron	PA-086	Glade, Robert S.	EDU-72
Fayad, Laura M.	EDU-41	Glasier, Charles M.	EDU-86, PA-036, PA-147
Fefferman, Nancy	PA-007	Gongidi, Preetam	CR-3
Feinstein, Kate	PA-107	Gonzalez, Gabriel	EDU-97, PA-137
Feldman, Kenneth W.	PA-150, PA-151	Gonzalez, Guido	EDU-80
Fenton, Laura Z.	PA-051, PA-053, PA-001, PA-013, PA-049	Goske, Marilyn J.	A-092, PA-093, PA-108, PA-109, PA-113, PA-114
Ferguson, Mark R.	PA-057	Gottesman, Gary	SCI-16
Fernandes, Neil J.	CR-25	Gourdazi, Behnaz	PA-004
Fierke, Shelby	PA-008	Granader, Elon	EDU-18
Filipovich, Alexandra	EDU-73	Grattan-Smith, Damien	PA-084, SCI-1
Finn, Paul J.	SCI-5, PA-026, PA-031	Greenberg, S Bruce	EDU-5, PA-036, PA-111
Fitz, Charles	PA-088	Gross Kelly, Teresa C.	EDU-7, EDU-59, EDU-60, EDU-62, EDU-66, EDU-69, EDU-78, EDU-84, EDU-88
Fleck, Robert J.	PA-063, PA-064		
Fluss, Joël	PA-077		
Foley, Paul	PA-086		

Gruss, Joseph	SCI-19	Hoffer, Fredric A.	PA-083
Gu, Jeffrey	PA-102	Hoffman, Eric	PA-066, PA-067
Guandalini, Michael	EDU-45, EDU-50	Hogestad, Neta	PA-037
Guevara, Carlos J.	PA-099	Holdsworth, Samantha J.	PA-021
Guillermo, R. P.	EDU-51, PA-058, PA-059, PA-066, PA-126, PA-131, PA-141	Hollingsworth, Caroline L.	PA-099
		Holshouser, Barbara	PA-023
		Hopkins, Katharine	PA-094, PA-121
Gupta, Amit	SCI-18, SCI-27	Hoppel, Bernice	PA-122
Gupta, Ayushi	EDU-4	Horst, Kelly K.	EDU-18, EDU-32, EDU-111
Gupta, Nitika A.	SCI-11		
Gupta, Puneet	CR-5	Hsiao, Albert	SCI-10, PA-025
Gutmark, Ephraim	PA-064	Huang, Chun-Chao	CR-11
Hai, Nabila	PA-071	Huang, Hao	PA-023
Hales, Jasmine	PA-087	Hubbel, Marius	EDU-4
Hall, Seth	PA-113, PA-138	Huda, Walter	PA-020
Hanquinet, Sylviane	PA-077	Hudgins, Louanne	PA-120
Hargreaves, Brian A.	PA-082	Huisman, Thierry A.	SCI-20
Haroyan, Harut	PA-145	Hulett, Rebecca	EDU-15
Hater, Dianne	PA-109	Hunter, Jill V.	PA-039
Haverkamp, Benjamin T.	EDU-56	Huynh, Binh	SCI-10
Hayes, Kari	PA-001	Huynh, Nhi	SCI-6, SCI-25
Hayes, Laura L.	PA-074	Iloreta, Salvador F.	EDU-56
Hegde, Shilpa V.	EDU-5	Imsande, Heather	EDU-106
Hellinger, Jeffrey	EDU-6, PA-105, PA-122	Iqbal, Vaseem	CR-5, CR-10, EDU-89
Hellström, Per	PA-048	Ishak, Gisele	SCI-19, EDU-77
Hendriks, Benno	PA-087	Islam, Omar	CR-22
Herliczek, Thaddeus W.	PA-009	Ismail, Ameera	PA-075
Herman, Oren	EDU-90	Iyer, Ramesh	EDU-77
Hernandez, Ramiro J.	EDU-74	Jabi, Feraas	EDU-89
Higgins, Rosemary	PA-054, PA-076	Jackson, Allison M.	EDU-49, PA-142, PA-155
Hildebrand, Hans	PA-048		
Hilliard, Pamela	EDU-42, PA-128	Jacob, Roy	EDU-63, EDU-72
Hilmes, Melissa A.	EDU-113	Jacobson, Jon	EDU-53
Hilpipre, Nicholas	PA-028	Jaimes, Camilo	CR-12, EDU-38, PA-129
Hinds, Tanya	EDU-49, PA-142, PA-155		
		Jaju, Alok	EDU-9, EDU-71, PA-047
Hindson, David	EDU-106		
Hing, Anne	SCI-19	Jamieson, Douglas	EDU-13, EDU-96
Hingorani, Sangeeta	PA-081	Jans, Lennart	PA-016
Hintz, Susan	PA-054, PA-076	Jaramillo, Diego	EDU-38, EDU-39, PA-129
Hirose, Shinjiro	EDU-26		
Ho-Fung, Victor	PA-129	Jaremko, Jacob L.	PA-016
Hoeffner, Ellen	EDU-81	Jarmakani, Maha	EDU-56

Je, Bo-Kyung	PA-011	Kim, Jane S.	EDU-54
John, Philip	PA-159	Kim, Myung-Joon	PA-042, PA-106
Johnson, Ann	SCI-8, EDU-11, EDU-98	Kim, Sung-Bum	PA-011
Johnson, Bonnie	SCI-1	Kirsch, Andrew	PA-084
Johnson, Craig	EDU-7, EDU-82	Kis, Antonella	PA-127
Johnson, Peter	PA-095	Kitazono, Mary	EDU-12
Johnson, Victor M.	PA-060	Klein, Daniel	EDU-92
Johnston, Jennifer H.	PA-096, PA-124	Kleinman, Patricia L.	PA-153
Jones, Richard A.	PA-074, PA-084	Kleinman, Paul K.	PA-153, PA-154
Jubang, Michael	CR-16	Kline-Fath, Beth M.	PA-098
Jung, Dorothy	PA-063	Kocaoglu, Murat	EDU-76
Kaczka, David	PA-066	Kollipara, Ramya	EDU-65
Kadom, Nadja	SCI-22, CR-26, EDU-68, PA-071, PA-142, PA-148	Koral, Korgun	PA-015
Kain, Conor	SCI-23	Kramer, Sandra S.	EDU-11
Kalinkin, Olga	PA-035	Krane, Elliot	PA-062
Kalra, Mannudeep	PA-112	Kraus, Steven J.	PA-006, PA-109, EDU-19
Kamholz, John	PA-073	Krausz, David	EDU-91
Kan, Herman	EDU-51, PA-126, PA-131	Krishnamurthy, Rajesh	EDU-105, PA-032, PA-033, PA-067, PA-068
Kao, Jeffrey S.	CR-24	Kruse, Travis D.	CR-7
Kao, Linda Y.	EDU-54	Kudlas, Myke	PA-108
Kaplan, Bernard	CR-12	Kukreja, Marcia K.	EDU-73
Karakas, S. Pinar	EDU-24, EDU-83	Kumpe, David	PA-053
Karmazyn, Boaz	EDU-46, EDU-47, PA-095	Kunkel, Samuel	PA-138
Kaser, Keith	PA-095	Kurhanewicz, John	PA-102
Kasper, Kelly	PA-037, PA-038	Kurian, Jessica	EDU-6, EDU-110
Kathryn, Fowler	PA-047	Kwak, No B.	EDU-22
Kaufman, Robert	PA-002	Kwatra, Neha	EDU-48, EDU-93
Kedia, Sita	CR-21	Ladenson, Paul	PA-004
Keller, Laura	SCI-23	Ladino-Torres, Maria	EDU-44, EDU-74, EDU-111
Khademian, Zarir P.	PA-142	Lala, Shailee	PA-007
Khalatbari, Shokoufeh	SCI-9, PA-050	Lambert, Sarah	PA-085
Khan, Sarah N.	SCI-5, PA-031	Laor, Tal	PA-124, PA-125
Khanna, Geetika	EDU-15, PA-047, PA-083	Laptook, Abbot	PA-076
Khanna, Paritosh C.	SCI-19, EDU-77	Larson, David B.	PA-008, PA-113
Khashoggi, Khalid	EDU-13, EDU-75, EDU-96	Laukka, Jeremy J.	PA-073
Khrichenko, Dmitry	PA-085	Laurence, Nancy K.	EDU-38
Kim, Eugene S.	PA-141	Leach, James L.	PA-146
Kim, Hee K.	PA-124, PA-125	LeCompte, Lesli M.	EDU-21, PA-085
		Lee, Edward Y.	PA-058, PA-060, PA-061, EDU-31

Lee, Joshua	PA-140	Mahmoud, Mohamed	PA-063, PA-064
Lee, Ki Yeol	PA-011	Maine, Rebecca	EDU-26
Lee, Mi-Jung	PA-042, PA-106	Majd, Massoud	EDU-93
Lensing, Shelly	PA-036	Makris, Joseph	PA-153
Lentle, Brian	PA-133	Malarik, Remo	PA-113
Leopard, Catherine	PA-109	Malone, William J.	CR-16
Lester, Neil	EDU-100, PA-132	Maloney, John A.	CR-21, PA-013
Levin, Terry L.	EDU-29, EDU-103	Mamoun, Ihsan	EDU-24, EDU-83
Levsky, Jeffrey	PA-104	Man, Carina	EDU-42, PA-128
Li, Xinhua	PA-112	Mandal, Soma	PA-027
Li, Yu	PA-098	Mandell, Gerald A.	PA-003
Liang, Teresa	EDU-30, PA-079	Mardis, Neil	EDU-52
Liang, Yun	PA-095	Marina, Neyssa	PA-140
Ligouri, Andrew	PA-034	Markowitz, Richard	EDU-38, EDU-99
Lin, Cheryl	EDU-95, EDU-109	Martin, Lisa	CR-23
Linam, Leann E.	CR-4, PA-111	Masand, Prakash	PA-032, PA-033, PA-067
Lindquist, Diana M.	PA-149		
Lipsich, J.	PA-024	Masterson, Joanne	PA-049
Little, Stephen	SCI-1, PA-084, PA-134	Mather, Richard	PA-122
		Matzinger, Mary Ann E.	PA-133
Liu, Bob	PA-112	Maugans, Todd A.	PA-146
Liu, Jimmy C.	PA-030	Maxfield, Bradley	EDU-102, EDU-104
Lober, Robert	PA-012, PA-014, PA-017	Maxfield, Charles M.	PA-099
		McAlister, William H.	SCI-14, SCI-16
Loewen, Jonathan	CR-8	McBride, Kim L.	CR-19
Long, Frederick R.	PA-058	McCarville, Beth	PA-002
Lopez Bueno, Javier A.	PA-139	McConnell, Keith	PA-064
Love, Terri L.	CR-7	McDonald, Scott	PA-076
Lowe, Lisa H.	EDU-56, EDU-65	McKinstry, Robert	EDU-10
Lowry, Conor	EDU-91	McLaren, Clare	PA-156
Loyd, Andre M.	PA-143	McLellan, Anne	EDU-87
Lucky, Anne W.	CR-6	McMann, Leah P.	PA-041
Lukse, Ruby	EDU-90	Meehan, Conor P.	PA-031
Lustik, Michael B.	PA-041	Mehta, Anita	EDU-103
MacKenzie, John D.	EDU-8, EDU-26, PA-102	Menghani, Vikas	CR-5, CR-10, EDU-89
Mackenzie, Tippi	EDU-8	Merlini, Laura	PA-077
MacMahon, Heber	PA-107	Merrow, Arnold C.	CR-6, EDU-19, EDU-20, PA-103, PA-124, PA-125
Madan, Shobhit	PA-027		
Madson, Katherine	SCI-16	Metcalfe, Peter	EDU-30, PA-079
Maheshwari, Mohit	EDU-7, EDU-59, EDU-60, EDU-62, EDU-66, EDU-69, EDU-78, EDU-82, EDU-84, EDU-88	Metwalli, Zeyad	EDU-51, PA-141
		Meyers, Arthur B.	EDU-23
		Meyers, Kevin E.	CR-12
		Mhlanga, Joyce C.	PA-004

Miller, Cindy	EDU-107	Nael, Kambiz	PA-026
Miller, Jeff	EDU-87	Nagaraj, Usha D.	CR-18, CR-19, CR-23
Miller, Jeff H.	EDU-70	Naidu, Padmaja	EDU-70
Milliman-Richard, Yolanda	SCI-13	Najdzionek, Jan	CR-5, CR-10, EDU-89
Mills, Thalia T.	PA-093	Naranjo, Arlene	PA-083
Minhas, Anum S.	PA-110	Narayanam, Surendra	CR-13
Mirenda, William	CR-16	Narayanan, Srikala	EDU-48, EDU-68, PA-080, PA-148
Mitchell, Ian	EDU-22	Naveed, Muhammad A.	PA-020
Mitchell, Mark	CR-3	Nelson, Caleb	PA-043
Mitchell, Sally E.	SCI-20, EDU-41	Nenninger, Angie	SCI-14
Miyasaka, Mikiko	SCI-15	Neuman, Jeremy	EDU-90, EDU-91, EDU-92, EDU-95, EDU-109
Miyazaki, Osamu	SCI-15	Newman, Beverley	EDU-112, PA-062, PA-069, PA-100
Moe, David	EDU-82	Nguyen, Jie C.	EDU-104
Moguillansky, S.	PA-024	Nguyen, Kim-Lien	SCI-5
Mohajer, Kiyarash	SCI-5	Nguyen, Lily H P.	PA-144
Mohanta, Arun	EDU-42	Nguyen, Linda	PA-102
Moineddin, Rahim	PA-127	Nijs, Els	EDU-6
Mokashi, Anusuya	EDU-109	Nimkin, Katherine	SCI-24
Moles, Rebecca L.	PA-153	Nishimura, Gen	SCI-15
Mong, David A.	EDU-11, EDU-98, EDU-110	Noga, Michelle	EDU-30, PA-079
Montgomery, Paul	CR-10	Noor, Amir	SCI-22, EDU-27, PA-071
Moore, Aideen M.	PA-119	North, Amanda	EDU-29
Moorjani, Vijay	CR-17	Norton, Mary E.	PA-118
Morag, Iris	PA-119	Nosaka, Shunsuke	EDU-2, SCI-15
Morani, Ajaykumar C.	EDU-18, EDU-44, EDU-53, EDU-74, PA-030	Novack, Deborah	SCI-14
Morey, Jose	EDU-90, EDU-91, EDU-92, EDU-95	Novotny, Edward	SCI-21, PA-055
Moriarty, John	SCI-5, PA-026	Ntoulia, Katerina	PA-040
Morota, Nobuhito	SCI-15	Obi, Chrystal	PA-086
Morris, Nicole B.	PA-153	Oh, Seong	EDU-103
Morrison, Gregory	PA-108	Ojemann, Jeff	SCI-21, PA-055
Mortilla, Marzia	PA-019	Okabe, Mari	SCI-15
Mosse, Yael P.	CR-12	Ong, Seng	PA-107
Mulla, Wadia	CR-3	Orbach, Darren	SCI-13
Mumm, Steven	SCI-16	Orth, Robert C.	PA-059, PA-126, PA-131
Munden, Marthe	PA-039, PA-078	Otero, Jesse	SCI-16
Murati, Michael A.	PA-103	Otto, Randolph	PA-057
Mychaliska, George B.	EDU-111		
Naar, Karen	EDU-22		
Nachabe, Rami	PA-087		
Nadel, Helen R.	EDU-13, PA-133		

Oviedo, Angelica	EDU-96	Qandeel, Monther	PA-013
Ozcan, Emrah	EDU-76	Quijano, Carla	EDU-37
Pai, Deepa	EDU-32, EDU-53	Racadio, John M.	PA-087, PA-157
Palasis, Susan	PA-074	Radhakrishnan, Rupa	EDU-73, EDU-101
Panigrahy, Ashok	PA-023, PA-123	Raffini, Leslie	PA-086
Papadopoulou, Frederica	PA-040	Ralhan, Taruna	PA-034
Parad, Richard B.	PA-116	Rama, Jennifer A.	PA-058
Parisi, Marguerite	PA-081	Ramakrishnaiah, Raghu H.	EDU-86, PA-036, PA-147
Park, Ellen	EDU-24	Ramos, Yanerys	EDU-31
Parnell, Shawn	EDU-43, EDU-55	Rao, Anil G.	PA-020
Parra, David	CR-1	Rasalingham, Pam	CR-22
Parra, Dimitri	CR-13, PA-159	Raver, Emma K.	PA-090
Patel, Amish	PA-132	Ream, Justin	SCI-9
Patel, Manish	PA-103	Reavey, Hamilton E.	CR-2
Patel, Neel	PA-107	Reemtsen, Brian	PA-026
Patel, Neil	PA-097	Reid, Janet R.	EDU-83
Patel, Suchit	EDU-4	Renella, Pierangelo	SCI-5
Patel, Tanmay	EDU-16	Restrepo, Ricardo	EDU-31
Patino, Mario	PA-063	Rhee, Robert	PA-091
Perez Rossello, Jeannette	PA-045	Ricafort, Rosanna	PA-104
Perlman, Elizabeth	PA-083	Richards, Allyson	PA-015
Petit, Christopher	PA-068	Richardson, Randy	SCI-6, SCI-25, PA-034, PA-035
Pettersson, David	PA-094, PA-121	Richer, Edward	CR-8
Phan, Vinh	EDU-95	Rigsby, Cynthia K.	PA-028, PA-046
Phelps, Andrew	EDU-3	Rink, Britton	PA-120
Philips, Paul H.	PA-147	Rissmiller, Julia	EDU-35, EDU-40
Phillips, Grace S.	EDU-55	Rivard, Doug	EDU-4
Pinkney, Lynne	PA-007	Rivas Rodriguez, Fransisco	EDU-74
Pinsker, Jordan	SCI-23	Robinson, Terry E.	PA-062
Pirkle, Jacob	EDU-79	Rodriguez, Diana P.	EDU-57
Pizzutillo, Peter	EDU-36	Rodriguez, Gail	PA-093
Podberesky, Daniel J.	EDU-19, EDU-20, EDU-23, SCI-26, PA-096, PA-113	Roebuck, Derek J.	PA-156
Poletto, Erica	EDU-11	Rollins, Nancy	PA-023
Poliachik, Sandra L.	PA-072	Romero, Rene	SCI-11
Poliakov, Andrew V.	SCI-21, PA-055, PA-072	Rooks, Veronica	SCI-23, PA-041
Ponisio, Maria R.	EDU-10	Rosenberg, Henrietta K.	EDU-100, PA-132
Pratt, Ron G.	PA-098	Rosenblum, Jeremy	PA-104
Protik, Angjelina	SCI-2	Rosendahl, Karen	PA-056
Pruthi, Sumit	CR-9, EDU-85	Rosenfeld, Scott	EDU-51
Puttgen, Kate	EDU-41	Rosines, Lucila A.	EDU-33
Pyne-Geithman, Gail J.	PA-149	Rosoklija, Iliana	PA-043
		Routh, Jonathan	PA-043

Rubesova, Erika	PA-100, PA-118, PA-120	Shah, Prakesh S.	PA-119
Rubio, Eva I.	PA-101	Shalaby-Rana, Eglal	EDU-49, PA-142, PA-155
Ruess, Lynne	CR-19, PA-052	Shankaran, Seetha	PA-076
Rusin, Jerome	CR-19, PA-052	Shaw, Dennis	SCI-21, EDU-77, PA-055, PA-072
Russell, Heidi V.	PA-141	Shaw, Peter	PA-091
Safdar, Nabile	EDU-48	Sheen, Campbell	SCI-16
Salisbury, Sheilia	PA-008, PA-109	Shenouda, Nazih	PA-133
Salisbury, Shelia	PA-063	Shenoy-Bhangle, Anuradha	SCI-24
Samei, Ehsan	PA-115	Shiels, William E.	PA-090, PA-158
Sanborn, Pamela	SCI-13	Shih, Shin-Lin	CR-11
Sanchez, Ramon	EDU-44, EDU-53, EDU-74	Shimony, Joshua	EDU-9
Santos, Rui	EDU-13, EDU-75, EDU-96	Shochat, Stephen	PA-002
Saranathan, Manojkumar	PA-082	Shott, Sally R.	PA-064
Sato, T. Shawn	PA-075	Shulkin, Barry	PA-002
Sato, Yutaka	PA-075	Siegel, Marilyn J.	EDU-71
Savelli, Sara	PA-019	Simpson, Judith	PA-097
Schapiro, Andrew	EDU-102	Singh, Sudha	EDU-85
Scherz, Hal	PA-084	Singh, Sudha P.	EDU-113
Schierling, Ross	PA-087	Singh, Sumit	EDU-7, EDU-37, EDU-59, EDU-60, EDU-62, EDU-66, EDU-69, EDU-78, EDU-82, EDU-84, EDU-88
Schmit, Pierre	PA-089	Skare, Stefan	PA-021
Schmitz, Kelli R.	EDU-28	Skelton, Matthew R.	PA-149
Schoeneman, Samantha	PA-018	Slovis, Thomas	PA-054
Schrader, Tim	PA-134	Smith, Ethan A.	EDU-44, EDU-111
Schroeder, Shauna	PA-049	Smith, Richard	PA-075
Schubert, Johanna	CR-7	Smith, Shrita	EDU-92
Sedaghat, Farzad	CR-16	Soares, Bruno P.	EDU-80
Segall, Hervey D.	EDU-59, EDU-60, EDU-62, EDU-66, EDU-69, EDU-78, EDU-88	Soares, Jennifer	EDU-113
Seghers, Victor	PA-059	Soboleski, Don	CR-22
Seinfeld, Joshua	PA-053	Sohaey, Roya	EDU-28
Sequeira, Lorena	EDU-31	Soltys, Kyle	PA-088
Serai, Suraj	SCI-26, PA-124, PA-125, PA-130	Soman, Salil	PA-022
Servaes, Sabah	EDU-34, EDU-98, PA-105	Song, Kit	EDU-55
Sevcik, William	EDU-30, PA-079	Spelic, David C.	PA-093
Shabani, Abdu	EDU-58	Spinning, Kristopher	PA-094
Shafer, Grant J.	PA-157	Spottswood, Stephanie E.	CR-9
Shah, Chetan C.	PA-147, EDU-86, PA-036, PA-111	Sprinz, Philippa	EDU-106
Shah, Jay	PA-145	Stain, Ann Marie	PA-128
		Stanescu, Luana	EDU-1

States, Lisa	EDU-21, EDU-94	Torabi, Bahar	PA-144
Stence, Nicholas V.	CR-21, PA-013, PA-038, PA-051, PA-053	Torkzad, Michael	PA-048
Stenhouse, Emily	PA-097	Towbin, Alexander J.	EDU-20, EDU-23, SCI-26, EDU-73, EDU-101, PA-008, PA-113, PA-138
Stevens, Donna M.	PA-121	Towbin, Richard	EDU-87
Stivaros, Stavros	EDU-58	Tracy, Donald A.	PA-061
Stock, Sarah	EDU-83	Traipe, Elfrides	PA-039
Strain, John	PA-010, PA-013, PA-037, PA-038, PA-051	Tsai, Jason	EDU-57, PA-061
Strauchler, Daniel A.	EDU-64	Tse, Sunny K.	PA-060
Strauss, Keith	PA-092, PA-114	Tuna, Ibrahim S.	EDU-29, EDU-59, EDU-7, EDU-37, EDU-60, EDU-62, EDU-66, EDU-69, EDU-78, EDU-82, EDU-84, EDU-88, PA-104
Strouse, Peter J.	SCI-9, EDU-17, EDU-18, EDU-32, EDU-44, EDU-111, PA-050	Udayasankar, Unni	EDU-24, EDU-83
Strubel, Naomi	PA-007	Udyavar, Rhea	SCI-22, EDU-27, PA-071
Sun, Binjian	PA-074	Ullberg, Ulla	PA-048
Sung, Kyung	PA-082	Urbine, Jacqueline	EDU-36
Supakul, Nucharin	EDU-46, EDU-47	Uzenoff, Robert A.	PA-093
Sutcavage, Thomas	PA-123	Uzuner, Nevin	EDU-108
Sutton, Lisa	CR-25	Vachha, Behroze	PA-116
Swanson, Jonathan O.	EDU-55	Vachhani, Neil	EDU-24
Swenson, David	PA-009	Van, Anh	PA-021
Tacy, Theresa	PA-100	VanLandingham, Leann	SCI-7
Tadros, Sameh	PA-027	Varghese, Cyril	EDU-91
Tang, Vivian	EDU-58	Vasanawala, Shreyas	SCI-10, EDU-97, PA-025, PA-044, PA-069, PA-082, PA-100, PA-118, PA-137
Taragin, Benjamin	EDU-29, EDU-54, EDU-103, PA-104	Vedolin, Leonardo	EDU-80
Tariq, Umar	PA-025	Vezina, Gilbert L.	EDU-68, PA-071
Tekes, Aylin	SCI-20	Victoria, Teresa	SCI-8, EDU-11
Temple, Michael	PA-159	Villa, Christopher	PA-098
Tetik, Filiz	EDU-108	Vorona, Gregory	PA-123
Teubner, Gordon	PA-038	Vos, Miriam	SCI-11
Thacker, Paul	EDU-52, EDU-65	Voss, Stephan	SCI-13
Thawait, Gaurav K.	EDU-41	Vossough, Arastoo	PA-105
Thawait, Shrey K.	EDU-41	Vyas, Pranav K.	EDU-27
Thomas, Anna	EDU-22	Wahl, Richard	PA-004
Thomas, Karen	SCI-2	Walker, Gregor	PA-097
Thomas, Richard	CR-5		
Tkach, Jean A.	PA-098		
Toh, Luke	CR-13		
Tomlinson, Christopher	PA-136		
Toncheva, Greta	PA-096		

Walker, Marc R.	PA-041
Wall, Corey	EDU-43
Walters, Michele	PA-154
Walters, Shannon	PA-082
Wang, Kuan-Chieh J.	PA-136
Wang, Lily	EDU-19, PA-125
Wang, Zhiyue W.	PA-023
Warfield, Simon	PA-045
Weinberger, Edward	EDU-43
Weiss, Clifford	SCI-20
Weiss, Pamela F.	EDU-39
Wendel, John D.	CR-7
Wenkert, Deborah	SCI-14
West, Hollie	EDU-113
Westra, Sjirk	PA-112, PA-114
Wheelock, Lisa M.	CR-7
Whitehead, Matthew	EDU-67
Whyte, Michael	SCI-14
Williams, Jennifer L.	PA-078
Williams, Joseph	PA-134
Winfeld, Matthew	PA-007
Wong, Brenda	PA-125
Wong, Brenda L.	PA-124
Wong, Lincoln M.	CR-7
Wrage, Lisa	PA-054
Wright, Linda	PA-037
Wright, Neville	EDU-58
Wu, George	CR-16
Wu, Jianrong	PA-002
Wu, Yen-Ying	PA-131
Xavier, Frederico	EDU-42
Yang, Fei-Shih	CR-11
Yang, Lynda	PA-160
Yanof, Jeff	PA-121
Yen, Yi-Fen	PA-102
Yeom, Kristen	PA-012, PA-014, PA-017, PA-021, PA-070
Yilmaz, Sabri	PA-091
Yoshida, Michelle A.	PA-052
Yoshizumi, Terry T.	PA-096
Young, Lisa	EDU-113
Youssfi, Mostafa	PA-005
Ywakim, Rania	PA-144

Zakhari, Andrew M.	PA-144
Zhang, Gang	PA-028
Zhang, Ningning	EDU-42, PA-128
Zhang, Wei	PA-058, PA-059, PA-126, PA-131
Zhang, Xiafant	SCI-14
Zhong, Anguo	PA-127, PA-136
Zingula, Shannon N.	PA-152
Ziniel, Sonja	PA-043
Zuccoli, Giulio	PA-123
Zucker, Evan J.	PA-061
Zurakowski, David	PA-060, PA-061

KEYWORD INDEX

24 hour delayed imaging	PA-003
3D MRI	CR-22
3DT1	EDU-59
Abdominal MRI	CR-8
Abdominal tumors	EDU-97
abnormal gait	EDU-104
Abuse	SCI-23, EDU-49, PA-151, PA-155
Acute pelvic pain	PA-080
acute testicular pain	PA-079
Advanced MR techniques	SCI-17
airway	EDU-101
airway compression	SCI-25
airway obstruction	PA-064
ALARA	EDU-2, PA-050, PA-093, PA-094, PA-107, PA-123
anamolies	SCI-18
anatomy	EDU-60, EDU-88
anesthesia	PA-063
anesthesiology consultation	CR-26
Ankle	EDU-52
anomalies	EDU-1
Anterior Chest Wall Mass	EDU-47

Apert	PA-101	Cartilage	PA-128
apparent diffusion coefficient	SCI-17	catheter directed thrombolysis	PA-086
appendiceal diameter	PA-008	CCAM	EDU-111
appendicitis	PA-009	CCHD	PA-039
Appropriateness criteria	PA-038	cerebellum	SCI-18, EDU-88
arachnoid cyst	PA-018		
ARFI	PA-106	cerebral blood flow	PA-146
ARFI elastography	PA-042	cerebral infarction	PA-052
Arteriovenous malformation	EDU-41	cerebral palsy	PA-054, PA-076
Arthritis	PA-136		
arthrogryposis	PA-120	Cerebral perfusion	PA-012
ASIR	SCI-2	cervical spine	PA-142
asthma	EDU-98	CFTR gene	EDU-107
Astrocystoma	EDU-56	Chemical Shift imaging	EDU-48
Bankart lesion	PA-129	child	CR-25
Beckwith-Wiedemann Syndrome	EDU-21	child abuse	PA-142, PA-150, PA-154
Biliary tree	EDU-24		
biphosphonate	SCI-16	chylothorax	CR-27
blood oxygen level dependent	PA-127	Cingulate gyrus	PA-071
body constitution	SCI-4	Clinical guidelines	PA-010
bone dysplasia	SCI-14	Clinical Protocols	PA-153
bone lesions	PA-132	Cochleovestibular malformations	EDU-84
Bone Mineral Density	PA-133	coil	PA-130
bone tumor	EDU-38	complications	PA-044
Bony abnormality	CR-16	complications of sinusitis	EDU-72
bowel obstruction	EDU-16, PA-118	Computed Tomography	PA-122
		cone beam CT	PA-087
brachial plexus	PA-160	congenital aortic	EDU-1
brain tumor	PA-013, PA-014, PA-015	Congenital Diaphragmatic Hernia	PA-097
		congenital heart disease	CR-2, SCI-5, EDU-5, SCI-6, PA-035
Brain tumors	PA-017		
Brain tumours	PA-016		
brain ventricles	PA-018		
bronchomalacia	EDU-5	contrast agents	EDU-105
C11-Methionine for Tumors	EDU-87	contrast enema	PA-006
cancer	PA-138	Contrast study	CR-14
Cardiac CT	PA-033	Corpus callosum	SCI-22
cardiac cta	SCI-6, PA-035	correlative multi modality imaging	EDU-63
		cortical malformation	EDU-78
cardiac embryology	EDU-3	Cortical restricted diffusion	EDU-83
cardiac fibroma	CR-1	cortical scar	EDU-93
cardiac magnetic resonance imaging	SCI-5	Cranial Ultrasound	CR-5, EDU-10
cardiovascular	PA-025		
cardiovascular MRI	CR-1	Craniofacial Imaging	SCI-19

craniosynostosis	EDU-57, EDU-66	drop metastases DTI	PA-015 PA-023, PA-077
Crohn disease	SCI-9		
Crohn's	PA-045	Duane syndrome	EDU-86
Crohn's Disease	EDU-20	Duchenne muscular dystrophy	PA-125
CT	EDU-2	dwarfism	EDU-43
CT and MR of Orbit	EDU-68	DWI	PA-137
CT angiography	EDU-6, SCI-15, PA-112	Dynamic MR venography echocardiography	PA-032 SCI-4
CT Contrast agent	PA-067	ectopic calcification	SCI-16
CT dose optimization	PA-092, PA-114	Education effective dose	PA-036 PA-096
CT dosimetry	PA-112	EKG	PA-033
CT image quality	PA-113	elastography	SCI-26
CT radiation dose	PA-113	elbow dislocation	EDU-45
CT scan parameters	PA-121	Encephalocele, neck masses	EDU-9
CT technologists	PA-108	endovascular therapy	PA-053
CTA	PA-034, PA-105	enhancement	PA-013, PA-103
CTDI	SCI-1	Ependymoma	EDU-56, EDU-58
CTDI (CT Dose Index)	PA-095		
CTV	PA-065	Epididymitis orchitis	EDU-30
Cyst	EDU-79	Epilepsy	EDU-70
cystic kidney disease	CR-12	Epiphysis	EDU-36
cytotoxic edema	CR-21	equivocal	PA-008
De Morsier's Syndrome	PA-147	Extrahepatic Portal Vein obstruction	PA-065
developmental anatomy of sinuses	EDU-72	F18 Deoxyglucose for Eleptogenic evaluation	EDU-87
Diagnostic Algorithm	EDU-54	Fallopian tube	PA-080
diagnostic reference levels	PA-092	fallopian tube torsion	EDU-26
diffuse lung disease	PA-058	fetal	EDU-19, PA-101, PA-116
diffusion	EDU-73		
diffusion tensor imaging	PA-072		
Diffusion weighted imaging	SCI-9, PA-047	fetal abnormalities fetal craniopharyngioma	SCI-8 CR-3
diffusion-weighted imaging	PA-021	fetal gastric outlet obstruction	CR-6
Digital Radiography	PA-093	Fetal head and neck masses/vascular anomalies	EDU-7
dissection	PA-053	fetal MR	EDU-11, PA-097
diuresis renogram	PA-041		
dose creep	PA-107	Fetal MRI	EDU-7, EDU-9, EDU-12, PA-117, PA-118, PA-120
Dose length product	PA-020		
dose reduction	SCI-2, PA-068		
Dose Reduction in Pediatric Patients	PA-095		
doxycycline	PA-090	Fontan	SCI-11

fracture	EDU-50, PA-143	imaging	EDU-66, EDU-108
fractures	PA-135	Imaging economics	PA-010
Fractures, Bone/*radiography	PA-153	imaging information	PA-110
functional magnetic resonance imaging	PA-127	Impact	PA-117
functional MR Urography (fMRU)	PA-085	indication	PA-111
gadoxetate disodium	EDU-23	Infarct	CR-18
Gallbladder	EDU-24	inflammatory bowel disease	PA-046
gastrostomy	CR-13	Internal Auditory Canal	CR-20
genetics	PA-075	interventional	PA-157
genito-urinary imaging	PA-043	interventional radiology	PA-089
genitourinary	EDU-28, PA-157	intestinal obstruction	EDU-14
genitourinary.	CR-10	Intima-Media Thickness	PA-024
gonadal shielding	PA-007	Intracranial cysts	EDU-61
head and neck	EDU-82	Intussusception	PA-011
head ultrasound	PA-099	Intussusception, therapy	PA-011
healthcare	SCI-13	investigative radiology	PA-087
healthy children	PA-106	Isolated cortical restricted diffusion	EDU-83
Hematoma	PA-145	Iterative Reconstruction	PA-094
hemiplegic migraine	CR-21	Labral injury	PA-129
hemophilia	EDU-50	language	PA-074
Hemophilic elbows	EDU-42	late effects	PA-138
Hepatobiliary	PA-003	leukemia	EDU-98
Hepatoblastoma	EDU-23	Leukodystrophy	PA-073
hepatocellular carcinoma	CR-9	ligament injury	EDU-45
hepatocyte	PA-088	liver transplant	PA-044
Heterotopia	CR-23	Liver transplant complications	CR-8
HIE	PA-145	Loeys-Dietz	EDU-4
High temporal and spatial resolution	PA-032	Low Birth Weight	PA-056
hindbrain malformations	PA-077	lung malformation	EDU-8
Hindfoot	EDU-52	lung mass	PA-116
Hip	EDU-37, PA-134	lung recruitment	PA-062
History	EDU-99, PA-111	lymphangiomatosis	EDU-102
Hybrid Imaging	EDU-94	lymphoma surveillance	PA-139
Hydrocephalus	EDU-85	lytic bone lesions	CR-27
hydronephrosis	EDU-14, EDU-29, PA-042	magnetic resonance cholangiopancreatography	EDU-17
hyperinsulinism	EDU-21	Magnetic Resonance Imaging	EDU-77, EDU-80, EDU-81, PA-102
Hypoxic Ischemic Encephalopathy	EDU-65	malformations	EDU-75
Hypoxic Ischemic Injury	EDU-65	malignancy	CR-10
		Malrotation	CR-7
		Margin definition	PA-103

masses	EDU-44	nanoparticle	PA-066,
medical education	PA-108		PA-067,
medical literacy	PA-109		PA-068
medulloblastoma	EDU-58	NAT	CR-24
menses	EDU-31	NEC-related stricture	PA-006
mental retardation	PA-149	neck masses	EDU-71
mesenchymal neoplasm	CR-25	neck spaces	EDU-71
metabolic disorders	EDU-80	neonatal	EDU-16,
Midgut volvulus	PA-005		EDU-33,
mitochondrial disease	PA-072		PA-054,
MOSFET	PA-096	Neonatal brain spine	PA-076
MR enterography	EDU-20,	Neonatal brain.	EDU-67
	PA-047	Neonatal Hypoxia Ischemia	SCI-7
MR Sedation	PA-037	neonatal MRA	EDU-10
MR urography	PA-084	Neonate	PA-026
MR-Guided intervention	PA-159	Neoplasm	PA-098
MR-Guided procedures	PA-159	neuroanatomy	EDU-68
MRA	PA-031	neuroblastoma	CR-22
MRI	SCI-11,		CR-12,
	CR-18,	Neurocutaneous Syndrome	PA-141
	CR-23,	Neuroradiology	CR-5
	EDU-34,		EDU-64,
	EDU-85,	neurosensory hearing loss	PA-016
	EDU-96,	New classification	PA-075
	EDU-97,	NF1	EDU-84
	PA-009,		SCI-22,
	PA-021,	Non-accidental Trauma	PA-071
	PA-045,	Noncardiac findings	PA-154
	PA-046,	Nuclear Medicine	PA-030
	PA-050,		EDU-70,
	PA-057		EDU-89
MRI and CT	EDU-105	Omphalocele	CR-7
MRI Biomarkers	SCI-7	Oncologic	EDU-96
MRU	EDU-29	Oncology	EDU-27,
MSK	EDU-40,		PA-137
	PA-132	Optic nerve hypoplasia	EDU-86
Mullerian duct	EDU-32	Orbits	PA-014,
Multidetector computed tomography	EDU-110		PA-017
Multidetector CT	PA-060,	Order Entry	PA-038
	PA-061	Osgood-Schlatter	EDU-51
Musculoskeletal	CR-16,	osteoclast deficiency	SCI-14
	CR-17,	Osteomyelitis	EDU-33,
	EDU-34,		PA-001
	EDU-43,	Osteoporosis	PA-133
	EDU-48	pancreaticobiliary system	EDU-17
myocardial strain	PA-027	parent education	PA-109
NAA	PA-146		

partial iterative reconstruction	PA-123	preterm	PA-099
pda	SCI-25, PA-034	process improvement	PA-037
pediatric	SCI-26, EDU-36, EDU-61, EDU-67, EDU-112, PA-143	protocol development	PA-051
		proximal femur physis	PA-155
		pulmonary	SCI-27
		pulmonary angiography	PA-066
		Pulmonary Embolism	PA-060, PA-061
pediatric ankle	EDU-53	pulmonary nodules	PA-002
Pediatric bilateral thalamic lesions	EDU-77	pulmonary vasculature	PA-026
pediatric brain MRI	PA-019	pyelonephritis	EDU-93
pediatric cardiac MRI	PA-030	pyeloplasty	PA-084
pediatric ct radiation dose	SCI-1	QA	PA-089
pediatric elbow	PA-130	quality	PA-062
pediatric functional MRI	PA-074	Quantitative MRI	PA-128
Pediatric GI	EDU-89	QUS	PA-136
pediatric head	EDU-74	Radiation	PA-115
Pediatric Head and Neck Imaging	SCI-19	radiation dose	PA-139
pediatric head and neck masses	EDU-63	Radiation Safety	PA-122
pediatric MRI	PA-082	radiation safety resources	PA-110
pediatric neuroimaging	PA-022	relaxometry	PA-057
pediatric normal variant	EDU-109	remnant	EDU-15
Pediatric Radiology	EDU-99	Renal anomaly	PA-039
pediatric stroke	EDU-81	renal function	PA-082
Pelizaeus-Merzbacher disease	PA-073	renovascular hypertension	EDU-6
Pelvic masses	EDU-27	Resident	PA-036
Pelvicalyceal Dilation	PA-085	resuscitation	PA-064
PET	EDU-13, PA-104	retention anchor suture	CR-13
		retroperitoneum	CR-15
Petrous apex	EDU-76	Risk	PA-115
PFIC	CR-9	safety	SCI-13, PA-098
Phantom studies	PA-023	salivary gland ablation	PA-158
phase contrast	PA-025	sedation	PA-063
physics of CT	PA-121	seizure	EDU-78
plagiocephaly	EDU-57	Septo Optic Dysplasia	PA-147
Plain films, USG and MRI	EDU-37	sequestration	EDU-111
polycystic ovarian disease	EDU-31	Shunt malposition	PA-148
Portal vein thrombosis	PA-119	sialorrhea	PA-158
positron emission tomography	PA-002	Sinding-Larsen-Johansson	EDU-51
post-operative complication	PA-141	Skeletal surveys of contacts	PA-150
posterior fossa	EDU-75	skeltal dysplasia	SCI-15
prenatal	EDU-8, EDU-101	Slow-flow Vascular malformation	EDU-41
PRES	EDU-73	soft tissue	EDU-44

sonography	CR-3, EDU-40	trauma	PA-135, PA-144, PA-151, PA-152
sonography superficial soft tissue masses	EDU-100		
spectroscopy	PA-149		
spinal	EDU-69	tubal	EDU-26
spinal cord	EDU-62	tubercular	SCI-27
spinal dysraphism	EDU-64	tuberculosis	EDU-108
spinal rods	PA-001	tumor	PA-104
spine	EDU-60, EDU-79	tumor ablation	PA-090
		Tumor rupture	PA-083
splenic	EDU-106	tumours	EDU-62
spondylolysis	EDU-59	TWIST, ablavar	SCI-20
stenosis	PA-156	Ultrasound	EDU-25, EDU-42, EDU-46, EDU-47, EDU-53, EDU-69, EDU-74, EDU-104, EDU-106, PA-005, PA-041, PA-079
stent migration	CR-2		
Stomach	EDU-13		
superficial soft tissue masses	EDU-100		
surfactant	PA-058		
survey	PA-043		
susceptibility weighted imaging	PA-019, PA-022		
synovial sarcoma	CR-15		
T2 mapping	PA-125		
T2*	PA-027	ultrasound contrast agent	PA-040
teaching	EDU-3	Umbilicus	EDU-15
Temporal Bone	CR-20, PA-144	unusual	EDU-49
		upper extremity deep venous thrombosis	PA-086
Tendon insertion	EDU-39	Urea Cycle Disorder	CR-19
Tendon thickness	EDU-39	US	PA-119
testicular abscess	EDU-30	Vascular	PA-105
testicular pseudomass	PA-078	vascular anomalies	SCI-20
testicular vascular bundle	PA-078	vascular anomaly	EDU-109
thoracic	EDU-11, EDU-112	vascular groove sign	EDU-38
		vascular malformation	EDU-82
Thoracic Insufficiency	EDU-55	VCUG	EDU-25
Thrombolysis	PA-091	Venous anomalies	CR-14
Thyroglobulin	PA-004	Venous Infarct	CR-19
Thyroidectomy	PA-004	venous thrombosis	EDU-103
Time Resolved Imaging of Contrast Kinetics	EDU-54	ventral abdominal wall defect	SCI-8
Titanium Rib	EDU-55	Ventricular dilatation	PA-056
Tortuosity	EDU-4	Ventricular Shunts	PA-148
trachea	PA-156	version	PA-134
tracheobronchial tree	EDU-110	Vertical or oblique talus	EDU-46
traction neuroma	PA-160	vesicoureteric reflux	PA-040
transplant	PA-031, PA-088	volume CT dose index (CTDIvol)	PA-020
		Wilms tumor	PA-083